

NASA

Earth Resources
A Continuing
Bibliography
with Indexes

NASA SP-7041 (59)
November 1988

National Aeronautics and
Space Administration

**es Earth Resource
s Earth Resource
Earth Resources
th Resources Ea
Resources Earth
Resources Earth
resources Earth D.**

ACCESSION NUMBER RANGES

Accession numbers cited in this Supplement fall within the following ranges.

STAR (N-10000 Series) N88-20254 — N88-25430

IAA (A-10000 Series) A88-32797 — A88-45806

EARTH RESOURCES

A CONTINUING BIBLIOGRAPHY WITH INDEXES

Issue 59

A selection of annotated references to unclassified reports and journal articles that were introduced into the NASA scientific and technical information system and announced between July 1 and September 30 in

- *Scientific and Technical Aerospace Reports (STAR)*
- *International Aerospace Abstracts (IAA).*



Scientific and Technical Information Division 1988
National Aeronautics and Space Administration
Washington, DC

This supplement is available from the National Technical Information Service (NTIS), Springfield, Virginia 22161, price code A07.

INTRODUCTION

The technical literature described in this continuing bibliography may be helpful to researchers in numerous disciplines such as agriculture and forestry, geography and cartography, geology and mining, oceanography and fishing, environmental control, and many others. Until recently it was impossible for anyone to examine more than a minute fraction of the Earth's surface continuously. Now vast areas can be observed synoptically, and changes noted in both the Earth's lands and waters, by sensing instrumentation on orbiting spacecraft or on aircraft.

This literature survey lists 518 reports, articles, and other documents announced between July 1 and September 30, 1988 in *Scientific and Technical Aerospace Reports (STAR)*, and *International Aerospace Abstracts (IAA)*.

The coverage includes documents related to the identification and evaluation by means of sensors in spacecraft and aircraft of vegetation, minerals, and other natural resources, and the techniques and potentialities of surveying and keeping up-to-date inventories of such riches. It encompasses studies of such natural phenomena as earthquakes, volcanoes, ocean currents, and magnetic fields; and such cultural phenomena as cities, transportation networks, and irrigation systems. Descriptions of the components and use of remote sensing and geophysical instrumentation, their subsystems, observational procedures, signature and analyses and interpretive techniques for gathering data are also included. All reports generated under NASA's Earth Resources Survey Program for the time period covered in this bibliography are also included. The bibliography does not contain citations to documents dealing mainly with satellites or satellite equipment used in navigation or communication systems, nor with instrumentation not used aboard aerospace vehicles.

The selected items are grouped in nine categories. These are listed in the Table of Contents with notes regarding the scope of each category. These categories were especially chosen for this publication, and differ from those found in *STAR* and *IAA*.

Each entry consists of a standard bibliographic citation accompanied by an abstract. The citations include the original accession numbers from the respective announcement journals.

Under each of the nine categories, the entries are presented in one of two groups that appear in the following order:

- IAA* entries identified by accession number series A88-10,000 in ascending accession number order;

- STAR* entries identified by accession number series N88-10,000 in ascending accession number order.

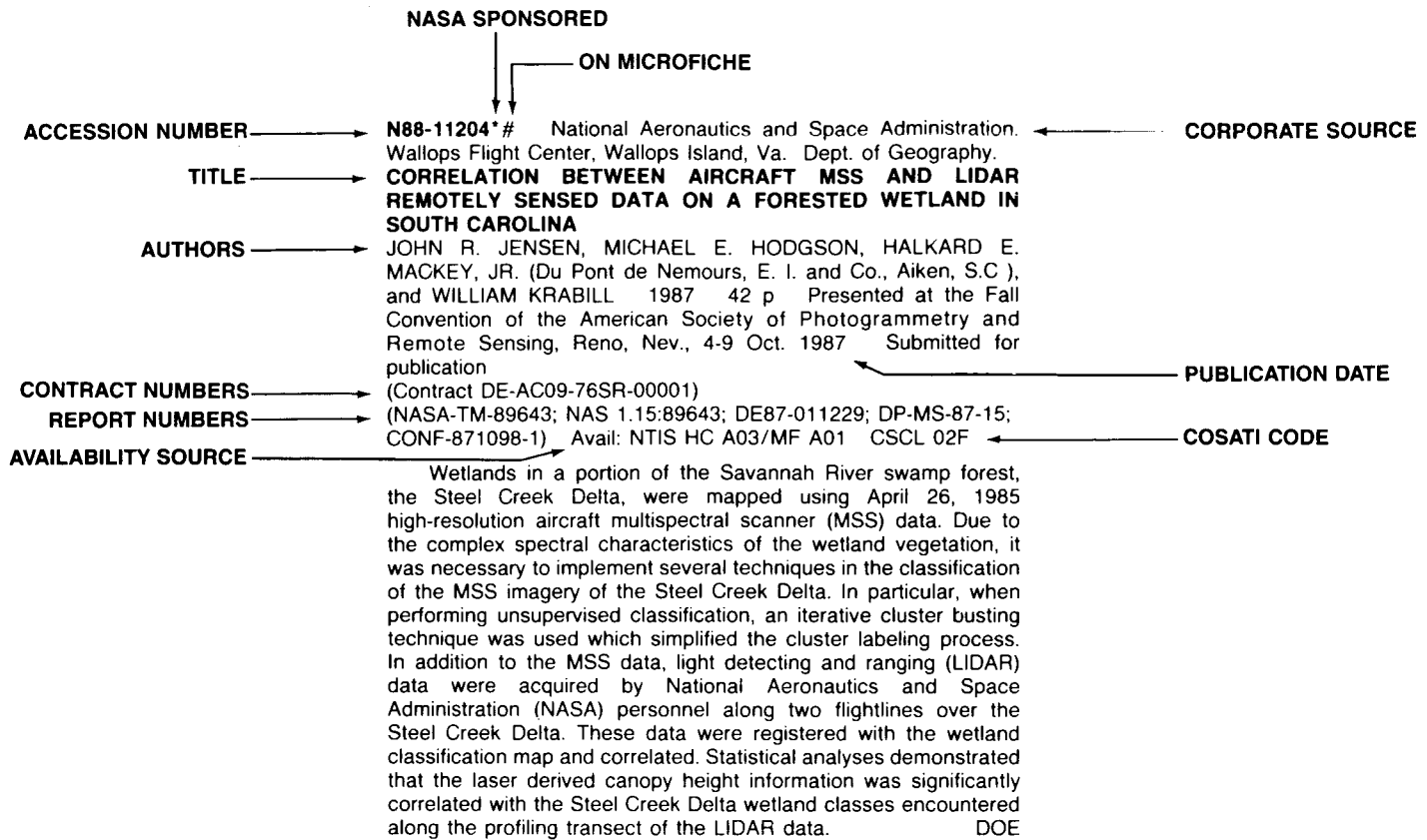
After the abstract section, there are seven indexes:

- subject, personal author, corporate source, foreign technology, contract number, report/ accession number, and accession number.

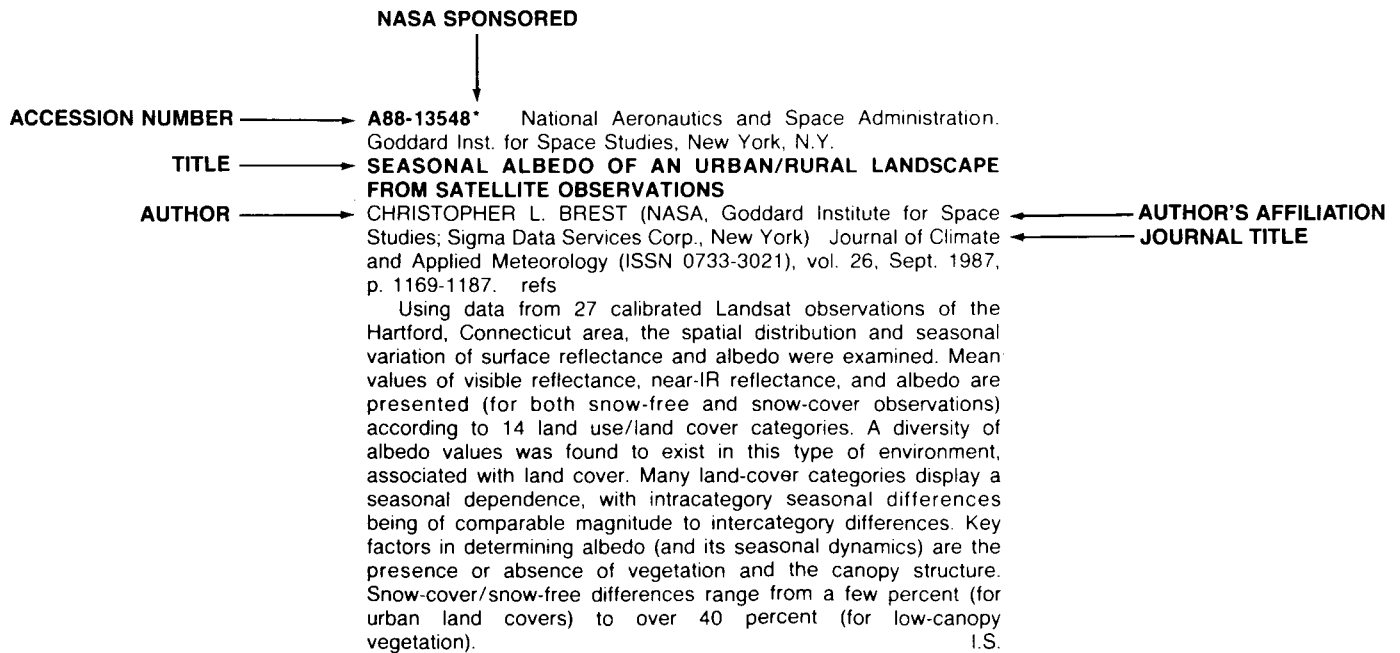
TABLE OF CONTENTS

	Page
Category 01 Agriculture and Forestry Includes crop forecasts, crop signature analysis, soil identification, disease detection, harvest estimates, range resources, timber inventory, forest fire detection, and wildlife migration patterns.	1
Category 02 Environmental Changes and Cultural Resources Includes land use analysis, urban and metropolitan studies, environmental impact, air and water pollution, geographic information systems, and geographic analysis.	18
Category 03 Geodesy and Cartography Includes mapping and topography.	24
Category 04 Geology and Mineral Resources Includes mineral deposits, petroleum deposits, spectral properties of rocks, geological exploration, and lithology.	25
Category 05 Oceanography and Marine Resources Includes sea-surface temperature, ocean bottom surveying imagery, drift rates, sea ice and icebergs, sea state, fish location.	39
Category 06 Hydrology and Water Management Includes snow cover and water runoff in rivers and glaciers, saline intrusion, drainage analysis, geomorphology of river basins, land uses, and estuarine studies.	50
Category 07 Data Processing and Distribution Systems Includes film processing, computer technology, satellite and aircraft hardware, and imagery.	57
Category 08 Instrumentation and Sensors Includes data acquisition and camera systems and remote sensors.	68
Category 09 General Includes economic analysis.	77
Subject Index	A-1
Personal Author Index	B-1
Corporate Source Index	C-1
Foreign Technology Index	D-1
Contract Number Index	E-1
Report Number Index	F-1
Accession Number Index	G-1

TYPICAL REPORT CITATION AND ABSTRACT



TYPICAL JOURNAL ARTICLE CITATION AND ABSTRACT



EARTH RESOURCES

A Continuing Bibliography (Issue 59)

NOVEMBER 1988

01

AGRICULTURE AND FORESTRY

Includes crop forecasts, crop signature analysis, soil identification, disease detection, harvest estimates, range resources, timber inventory, forest fire detection, and wildlife migration patterns.

A88-32909*# Geological Survey, Reston, Va.
PRELIMINARY MEASUREMENTS OF SPECTRAL SIGNATURES OF TROPICAL AND TEMPERATE PLANTS IN THE THERMAL INFRARED

JOHN W. SALISBURY and N. M. MILTON (USGS, Reston, VA)
IN: Thematic Conference on Remote Sensing for Exploration Geology, 5th, Reno, NV, Sept. 29-Oct. 2, 1986, Proceedings. Volume 1. Ann Arbor, MI, Environmental Research Institute of Michigan, 1987, p. 131-143. NASA-supported research. refs

Spectral reflectance measurements of seven tropical species and six deciduous species were carried out in thermal infrared to establish the species-dependent spectral characteristics and to investigate the effect on spectral signatures of environmental variables, such as leaf maturity, drought, and metal stress. Seasonal variations of spectral signatures occurred between spring and summer leaves, but such variations were minimal during summer and early fall. Overall reflectance of senescent leaves was higher than that of young leaves, as was the reflectance of leaves from trees growing in metal-enriched soils, as compared with leaves from the control area. However, the characteristic spectral features were not changed in either case. It was also found that water stress did not have any effect on the infrared signatures: trees grown during a drought season maintained their characteristic spectral signatures. I.S.

A88-32910*# Jet Propulsion Lab., California Inst. of Tech., Pasadena.

A NEAR INFRARED VEGETATION INDEX FORMED WITH AIRBORNE MULTISPECTRAL SCANNER DATA

CHRISTOPHER D. ELVIDGE and BARRETT N. ROCK (California Institute of Technology, Jet Propulsion Laboratory, Pasadena) IN: Thematic Conference on Remote Sensing for Exploration Geology, 5th, Reno, NV, Sept. 29-Oct. 2, 1986, Proceedings. Volume 1. Ann Arbor, MI, Environmental Research Institute of Michigan, 1987, p. 147-159. refs

A near infrared vegetation index (NIVI) has been formed with the 1.24 and 1.65 micron bands on the NS001 Thematic Mapper Simulator. The NIVI was compared to the more traditional Perpendicular Vegetation Index (PVI) formed with the 0.66 and 0.83 micron bands. The PVI was found to be less susceptible to problems with rock and soil spectral variations than the VIVI.

Author

A88-32911#
PRELIMINARY EVALUATION OF REMOTE SENSING DATA FOR DETECTION OF VEGETATION STRESS RELATED TO HYDROCARBON MICROSEEPAGE - MIST GAS FIELD, OREGON

MICHAEL F. CRAWFORD (ARCO Oil and Gas Co., Plano, TX)
IN: Thematic Conference on Remote Sensing for Exploration

Geology, 5th, Reno, NV, Sept. 29-Oct. 2, 1986, Proceedings. Volume 1. Ann Arbor, MI, Environmental Research Institute of Michigan, 1987, p. 161-177. refs

A88-32921#
PROCESSING OF MULTIDATE LANDSAT TM DATA TO MAP SOIL COLOR VARIATIONS RELATED TO HYDROCARBON MICROSEEPAGE IN A CROPLAND SETTING - CEMENT, OKLAHOMA TEST SITE

JOHN B. MCKEON and MARK SETTLE (ARCO Oil and Gas Co., Plano, TX) IN: Thematic Conference on Remote Sensing for Exploration Geology, 5th, Reno, NV, Sept. 29-Oct. 2, 1986, Proceedings. Volume 1. Ann Arbor, MI, Environmental Research Institute of Michigan, 1987, p. 347-361. refs

A88-32928#
SHIFT IN SPECTRAL RESPONSE OF NICKEL-LOADED AND CONTROL SHOOTS OF WHITE BIRCH

G. M. COURTIN, P. J. BECKETT, and G. O. TAPPER (Sudbury, Laurentian University, Canada) IN: Thematic Conference on Remote Sensing for Exploration Geology, 5th, Reno, NV, Sept. 29-Oct. 2, 1986, Proceedings. Volume 1. Ann Arbor, MI, Environmental Research Institute of Michigan, 1987, p. 441-449. refs

A88-32930#
EFFECTS OF HEAVY METAL INDUCED CANOPY STRUCTURAL CHANGES ON FOREST CANOPY REFLECTANCE

C. BANNINGER (Graz, Technische Universitaet und Forschungszentrum, Austria) IN: Thematic Conference on Remote Sensing for Exploration Geology, 5th, Reno, NV, Sept. 29-Oct. 2, 1986, Proceedings. Volume 2. Ann Arbor, MI, Environmental Research Institute of Michigan, 1987, p. 465-469. Research supported by the Scientific Research Office of Syria and BMFWF. refs

Relationships derived between canopy structure, soil metal content, and canopy reflectance of a spruce tree stand show a good correspondence between an increase in soil copper-lead-zinc content and a decrease in leaf density and Landsat Thematic Mapper (TM) canopy radiance values. The high correlation values obtained for TM bands 4 and 5 and the transformations employing these bands and the absence of visible stress symptoms in the canopy indicate a predominately morphological rather than a physiological basis of the changes in canopy spectral reflectance in response to heavy metal stress. Author

A88-32935#
SURROGATE SPECTRAL REFLECTANCES OF VEGETATION APPLIED TO GEBOTANICAL REMOTE SENSING

G. O. TAPPER, G. M. COURTIN, and P. J. BECKETT (Sudbury, Laurentian University, Canada) IN: Thematic Conference on Remote Sensing for Exploration Geology, 5th, Reno, NV, Sept. 29-Oct. 2, 1986, Proceedings. Volume 2. Ann Arbor, MI, Environmental Research Institute of Michigan, 1987, p. 545-554. refs

The paper reviews the methodology for measuring spectral reflectance of vegetation targets using handheld spectroradiometers. The objective was to measure the spectral reflectance of: (1) intact vegetation canopies; (2) the canopy of

felled trees; and (3) samples of clipped branches from within the canopy. This was done for samples of white birch, a species of extensive land cover throughout the boreal forest of northern Ontario. The spectral reflectances of samples were measured in situ and in the laboratory. The results indicate spectral response differences between different sample configurations of the birch samples. It is the aim of this work to improve the technique and field measurement of vegetation spectral response, and to allow increased accuracy to be obtained for the analysis and interpretation of remotely sensed data applied to geobotanical mineral exploration, as well as the ultimate detection of subsurface mineralization in the heavily forested Canadian Shield region of northern Ontario. Author

A88-35161
REGIONAL CROP-FORECASTING WITH LANDSAT - A FARMER'S EXPERIENCE

FRANK G. LAMB (Eastern Oregon Farming Co., Irrigon, OR) IN: Aerospace century XXI: Space sciences, applications, and commercial developments; *Proceedings of the Thirty-third Annual AAS International Conference*, Boulder, CO, Oct. 26-29, 1986. San Diego, CA, Univelt, Inc., 1987, p. 1713-1723. (AAS PAPER 86-401)

This paper describes how a potato farmer uses Landsat data and a microprocessor-based image processing system as a management tool in his business, and how this technique has been applied to larger-scale agricultural efforts. The use of Landsat data in an information system which could be used to expand the potato crop in the Columbia Basin is described. The application of these techniques to crops other than potatoes is discussed. C.D.

A88-35194* National Aeronautics and Space Administration. Ames Research Center, Moffett Field, Calif.

THERMAL ANALYSIS OF WILDFIRES AND EFFECTS ON GLOBAL ECOSYSTEM CYCLING

VINCENT G. AMBROSIA and JAMES A. BRASS (NASA, Ames Research Center, Moffett Field, CA) *Geocarto International* (ISSN 1010-6049), vol. 3, March 1988, p. 29-39. refs

Biomass combustion plays an important role in the earth's biogeochemical cycling. The monitoring of wildfires and their associated variables at global scales is feasible and can lead to predictions of the influence of combustion on biogeochemical cycling and tropospheric chemistry. Remote sensing data collected during the 1985 California wildfire season indicate that the information content of key thermal and infrared/thermal wave band channels centered at 11.5 microns, 3.8 microns, and 2.25 microns are invaluable for discriminating and calculating fire related variables. These variables include fire intensity, rate-of-spread, soil cooling recovery behind the fire front, and plume structure. Coinciding Advanced Very High Resolution Radiometer (AVHRR) data provided information regarding temperature estimations and the movement of the smoke plume from one wildfire into the Los Angeles basin. Author

A88-35195
REMOTE SENSING FOR WILDLIFE MANAGEMENT - GIANT PANDA HABITAT MAPPING FROM LANDSAT MSS IMAGES

ROBERT R. DE WULF, ROLAND E. GOOSSENS (Gent, Rijksuniversiteit, Ghent, Belgium), JOHN R. MACKINNON (World Wide Fund for Nature, Gland, Switzerland), and WU SHEN CAI (Sichuan Forestry Bureau, Chengdu, People's Republic of China) *Geocarto International* (ISSN 1010-6049), vol. 3, March 1988, p. 41-50. refs

A88-35397
INFLUENCE OF TOPOGRAPHY ON FOREST REFLECTANCE USING LANDSAT THEMATIC MAPPER AND DIGITAL TERRAIN DATA

C. E. LEPRIEUR, J. M. DURAND (CNES, Laboratoire d'Etudes et de Recherches en Teledetection Spatiale, Toulouse, France), and J. L. PEYRON (Ecole Nationale du Genie Rural et des Eaux et

Forets, Nancy, France) *Photogrammetric Engineering and Remote Sensing* (ISSN 0099-1112), vol. 54, April 1988, p. 491-496. refs (Contract CNES-85-1257; CNRS-508533)

The relationship between forestry variables and the response of Thematic Mapper bands is analyzed over selected mountainous forest sites with a view to improving current models. Forestry stand species and age information was collected for 250 sites in a region with slopes up to 35 degrees and a variety of aspects. Spring and summer Thematic Mapper imagery over the area were used; these data contain a wealth of information related to species and age, and topography. A digital elevation model was compiled with a resolution of 30 meters in order to study the relationship between reflectance, the variable of interest, and the local sun/surface/sensor geometry. Site radiance is dependent on illumination effects and directional effects. The distribution of apparent reflectances versus topographic parameters for each forestry class and each spectral band helped characterize species by their reflective properties. The influence of the age on the apparent reflectance distribution is analyzed: reflectance globally decreases with stand age, especially for TM4, TM5, and TM7. Author

A88-35398
CANOPY REFLECTANCE OF SOYBEAN AS AFFECTED BY CHRONIC DOSES OF OZONE IN OPEN-TOP FIELD CHAMBERS

WILLIAM W. CURE (North Carolina State University, Raleigh), SARAH M. NUSSER (Iowa State University, Ames), and ALLEN S. HEAGLE (USDA, Agriculture Research Service; North Carolina State University, Raleigh) *Photogrammetric Engineering and Remote Sensing* (ISSN 0099-1112), vol. 54, April 1988, p. 499-504. refs

The relationship between canopy reflectance and ozone (O₃) treatment was investigated in a field experiment with soybean growing in 3-m diameter, 2.4-m high open-top exposure chambers. The objectives were to develop an understanding of the pattern of reflectance changes induced by this air pollutant and to investigate how these changes might ultimately be related to yield. Correlations were obtained between the reflectance data and visual estimates of non-green leaf area, a widely-used technique for rating pollutant injury. Analysis of reflectance spectra taken in early September, early October, and mid October showed O₃ treatments to be highly correlated with reflectances at visible wavelengths and at near-infrared wavelengths up to about 720 nm. Early leaf senescence caused by O₃ was easily measured by reflectance changes. As this would reduce the time during which the plants could produce photosynthate needed for seed development, we hypothesize that multitemporal reflectance data could be used to estimate a rate of senescence that would relate to yield. Correlations between the reflectance data and visual estimates of non-green leaf area were high, indicating that rates of senescence could be estimated by either means. Author

A88-36164
REMOTE-SENSING METHODS FOR THE MONITORING AND FORECASTING OF THE ENTOMOLOGICAL CONDITION OF TAIGA FORESTS [DISTANTSIONNYE METODY KONTROLIA I PROGNOZA LESOENTOMOLOGICHESKOGO SOSTOIANIIA TAEZHNYKH TERRITORII]

A. S. ISAEV and V. IA. RIAPOLOV (AN SSSR, Institut Lesa i Drevesiny, Krasnoyarsk, USSR) *Issledovanie Zemli iz Kosmosa* (ISSN 0205-9614), Jan.-Feb. 1988, p. 48-55. In Russian. refs

A88-36165
INVESTIGATION AND MAPPING OF FORESTS USING SPACE SCANNER IMAGERY OBTAINED IN WINTER [IZUCHENIE I KARTOGRAFIROVANIE LESOV PO MATERIALAM ZIMNEI SKANERNOI S'EMKI IZ KOSMOSA]

V. I. KRAVTSOVA and E. P. SALAKHETDINOVA (Moskovskii Gosudarstvennyi Universitet, Moscow, USSR) *Issledovanie Zemli iz Kosmosa* (ISSN 0205-9614), Jan.-Feb. 1988, p. 56-65. In Russian. refs

Boundaries of forest regions and felled areas were identified

on Meteor-30 Fragment scanner imagery obtained over the Kostroma region in the winter of 1984. In terms of optical density, the forests in this area belong to four categories with different coniferous/deciduous ratios. The data obtained are compared with old maps in order to trace patterns of forest-land percentage, forest border lengths, and overall changes in forests over 40 years. B.J.

A88-36170
LINEAR COMBINATIONS OF SPECTRAL REFLECTANCES IN CROP ANALYSES [LINEINYE KOMBINATSII KOEFFITSIENTOV SPEKTRAL'NOI IARKOSTI PRI ANALIZE SEL'SKOKHOZIAISTVENNOI RASTITEL'NOSTI]

T. A. NIL'SON (AN ESSR, Institut Astrofiziki i Fiziki Atmosfery, Tartu, Estonian SSR) Issledovanie Zemli iz Kosmosa (ISSN 0205-9614), Jan.-Feb. 1988, p. 95-103. In Russian. refs

A88-37370* Massachusetts Inst. of Tech., Cambridge.
IDENTIFICATION OF TERRAIN COVER USING THE OPTIMUM POLARIMETRIC CLASSIFIER

J. A. KONG, A. A. SWARTZ, H. A. YUEH (MIT, Cambridge, MA), L. M. NOVAK, and R. T. SHIN (MIT, Lexington, MA) Journal of Electromagnetic Waves and Applications (ISSN 0920-5071), vol. 2, no. 2, 1988, p. 171-194. DARPA-sponsored research. refs

A systematic approach for the identification of terrain media such as vegetation canopy, forest, and snow-covered fields is developed using the optimum polarimetric classifier. The covariance matrices for various terrain cover are computed from theoretical models of random medium by evaluating the scattering matrix elements. The optimal classification scheme makes use of a quadratic distance measure and is applied to classify a vegetation canopy consisting of both trees and grass. Experimentally measured data are used to validate the classification scheme. Analytical and Monte Carlo simulated classification errors using the fully polarimetric feature vector are compared with classification based on single features which include the phase difference between the VV and HH polarization returns. It is shown that the full polarimetric results are optimal and provide better classification performance than single feature measurements. Author

A88-37415* California Univ., Berkeley.
A METHODOLOGY FOR MAPPING FOREST LATENT HEAT FLUX DENSITIES USING REMOTE SENSING

LARS L. PIERCE and RUSSELL G. CONGALTON (California, University, Berkeley) Remote Sensing of Environment (ISSN 0034-4257), vol. 24, April 1988, p. 405-418. Research supported by the University of California. refs
 (Contract NCA2-13B)

Surface temperatures and reflectances of an upper elevation Sierran mixed conifer forest were monitored using the Thematic Mapper Simulator sensor during the summer of 1985 in order to explore the possibility of using remote sensing to determine the distribution of solar energy on forested watersheds. The results show that the method is capable of quantifying the relative energy allocation relationships between the two cover types defined in the study. It is noted that the method also has the potential to map forest latent heat flux densities. R.R.

A88-37418* Kansas State Univ., Manhattan.
RADIATIVE SURFACE TEMPERATURES OF THE BURNED AND UNBURNED AREAS IN A TALLGRASS PRAIRIE

G. ASPAR, T. R. HARRIS, R. L. LAPITAN (Kansas State University, Manhattan), and D. I. COOPER (Arizona, University, Tucson) Remote Sensing of Environment (ISSN 0034-4257), vol. 24, April 1988, p. 447-457. refs
 (Contract NAG5-389; NGT-17-002-801)

This study was conducted in a natural tallgrass prairie area in the Flint Hills of Kansas. The objective was to evaluate the surface radiative temperatures of burned and unburned treatments of the grassland as a means of delineating the areas covered by each treatment. Burning is used to remove the senescent vegetation resulting from the previous year's growth. Surface temperatures were obtained in situ and by an airborne scanner. Burned and

unburned grass canopies had distinctly different diurnal surface radiative temperatures. Measurements of surface energy balance components revealed a difference in partitioning of the available energy between the two canopies, which resulted in the difference in their measured surface temperatures. The magnitude of this difference is dependent on the time of measurements and topographic conditions. Author

A88-38373#
VEGETATION INDICES AND OTHER VEGETATION PARAMETERS - EXAMPLES, INTERPRETATION AND PROBLEMS

K. BLUEMEL and W. TONN (Berlin, Freie Universitaet, Federal Republic of Germany) Rivista di Meteorologia Aeronautica (ISSN 0035-6328), vol. 47, Apr.-June 1987, p. 135-150. refs

NOAA-AVHRR multichannel data have been received since 1982 and are used for deriving vegetation indices. There exist several types of indices which depend on atmospheric influences, viewing geometry, surface topography and vegetation density in different ways. Here, results for the most significant indices are presented. Bidimensional frequency distributions of spectral channel are performed in different regions of Central Europe and North Africa for vegetation-type analysis. The interpretation of the normalized vegetation index (NVI) as a measure of leaf area index, biomass, canopy resistance, and biomass productivity is also discussed. Finally, vegetation index grain production, and weather conditions in the FRG in 1983-1984 are compared, and the correlation of NVI and radiation temperature of the ground is investigated. Author

A88-38805* National Aeronautics and Space Administration. Langley Research Center, Hampton, Va.
PARTICULATE EMISSIONS FROM A MID-LATITUDE PRESCRIBED CHAPARRAL FIRE

WESLEY R. COFER, III, JOEL S. LEVINE, DANIEL I. SEBACHER (NASA, Langley Research Center, Hampton, VA), EDWARD L. WINSTEAD (ST Systems Corp., Hampton, VA), PHILIP J. RIGGIN (USDA, Forest Service, Riverside, CA), JAMES A. BRASS, and VINCENT G. AMBROSIA (NASA, Ames Research Center, Moffett Field, CA) Journal of Geophysical Research (ISSN 0148-0227), vol. 93, May 20, 1988, p. 5207-5212. refs

Particulate emission from a 400-acre prescribed chaparral fire in the San Dimas Experimental Forest was investigated by collecting smoke aerosol on Teflon and glass-fiber filters from a helicopter, and using SEM and EDAX to study the features of the particles. Aerosol particles ranged in size from about 0.1 to 100 microns, with carbon, oxygen, magnesium, aluminum, silicon, calcium, and iron as the primary elements. The results of ion chromatographic analysis of aerosol-particle extracts (in water-methanol) revealed the presence of significant levels of NO₂(-), NO₃(-), SO₄(2-), Cl(-), PO₄(3-), C₂O₄(2-), Na(+), NH₄(+), and K(+). The soluble ionic portion of the aerosol was estimated to be about 2 percent by weight. I.S.

A88-39082* Delaware Univ., Newark.
REMOTE SENSING OF BIOMASS OF SALT MARSH VEGETATION IN FRANCE

M. F. GROSS, V. KLEMAS (Delaware, University, Newark), and J. E. LEVASSEUR (Rennes I, Universite, France) International Journal of Remote Sensing (ISSN 0143-1161), vol. 9, March 1988, p. 397-408. Research supported by the University of Delaware; Centre National pour l'Exploitation des Oceans. refs
 (Contract CNEOX-83/7202; NAGW-374)

Spectral data (gathered using a hand-held radiometer) and harvest data were collected from four salt marsh vegetation types in Brittany, France, to develop equations predicting live aerial biomass from spectral measurements. Remote sensing estimates of biomass of the general salt marsh community (GSM) and of *Spartina alterniflora* can be obtained throughout the growing season if separate biomass prediction equations are formulated for different species mixtures (for the GSM) and for different canopy types (for *S. alterniflora*). Results suggest that remote sensing will not

be useful for predicting *Halimione portulacoides* biomass, but can be used to estimate *Puccinellia maritima* biomass early in the growing season. Author

A88-39090
FLOOD DAMAGE ANALYSIS USING MULTITEMPORAL LANDSAT THEMATIC MAPPER DATA

YOSHIKI YAMAGATA and TSUYOSHI AKIYAMA (National Institute of Agro-Environmental Sciences, Tsukuba, Japan) International Journal of Remote Sensing (ISSN 0143-1161), vol. 9, March 1988, p. 503-514. refs

The paddy rice damage caused by a flood in the Kanto district in Japan has been analyzed using multitemporal Landsat-5 Thematic Mapper images. The image acquired immediately after the flood showed the spread of turbid water over the paddy fields and the image acquired 1 month after the flood showed the paddy rice damage in the inundated areas. The flood damage assessment was undertaken using several multivariate analyses: (1) the correlation analysis revealed that the turbidity level of flood water was related to the rice damage; (2) the decrease of the rice yield was estimated from both images by multiple regression models; and (3) the flood damage relationship was determined by a cluster analysis using the higher-order principal components of the multitemporal image. Based on the results of these analyses, distribution maps of the rice yield levels were estimated at each date and a classification of the flood damage pattern was obtained. Author

A88-40352#
SIR-B EXPERIMENTS IN JAPAN. II - RICE CROP EXPERIMENT

TAKESHI SUITZ, SHIN YOSHIKADO, MASARU ICHINOSE, YOSHIMATSU ECHIZENYA, MITSUHIRO KAMATA et al. Radio Research Laboratory, Journal (ISSN 0033-8001), vol. 35, March 1988, p. 29-37.

This paper describes ground activities, including ground truth measurements made for a rice crop experiment as a part of SIR-B experiment proposal submitted by the Radio Research Laboratory to NASA. The main objective was to study the potential of remote sensing of rice crop conditions and of vegetation classification. The condition of the test site and rice crops and the results of field investigations for vegetation classification study are described. Descriptions are also made for an in-situ microwave backscatter measurement which was made as a part of the rice crop truth data collection. Author

A88-40355#
SIR-B EXPERIMENTS IN JAPAN. V.

SHIN YOSHIKADO, MASARU ICHINOSE, and MAKOTO SATAKE Radio Research Laboratory, Journal (ISSN 0033-8001), vol. 35, March 1988, p. 77-84. refs

Remote sensing of rice fields in Japan was executed using a microwave imaging radar in the SIR-B experiments. Imaging data taken over the Ohgata-mura test site were analyzed to study the microwave backscattering characteristics of rice plants and crop classification. There was a difference in image intensity between the rice fields and the surrounding area. However, no meaningful difference in the image intensity of the rice fields before and after harvest was found. Also, the correlation between the image intensity and the rice plant conditions was not clear. The investigation of crop classification also gave no significant results. The present results may be mainly attributed to the delay of the experimental term from August to October. Other possible explanations for the results are discussed. Author

A88-40784*# Oregon State Univ., Corvallis.
REMOTE SENSING OF LEAF WATER STATUS

WILLIAM J. RIPPLE and BARRY J. SCHRUMPF (Oregon State University, Corvallis) International Conference on Measurement of Soil and Plant Water Status, Utah State University, Logan, July 6-10, 1987, Paper. 8 p. refs (Contract NAGW-924)

Relative water content (RWC) measurements were made

concurrently with spectral reflectance measurements from individual snapbean leaves. The relationships between spectra and RWC were described using second order polynomial equations. The middle infrared bands most sensitive to changes in leaf RWC also had the highest water absorption coefficients, as published by Curcio Petty (1951). The relationship between reflectance at 2100nm and total water potential for a single leaf was found to be linear. Author

A88-41028*# National Aeronautics and Space Administration. Goddard Space Flight Center, Greenbelt, Md.

A FOUR-LAYER MODEL FOR THE HEAT BUDGET OF HOMOGENEOUS LAND SURFACES

B. J. CHOUDHURY and J. L. MONTEITH (NASA, Goddard Space Flight Center, Greenbelt, MD) Royal Meteorological Society, Quarterly Journal (ISSN 0035-9009), vol. 114, Jan. 1988, p. 373-398. refs

The present model envisions the heat balance of a homogeneous land surface in terms of available energy, a set of driving potentials, and parameters for the physical state of the soil and vegetation. Two unique features of the model are: (1) the expression of the interaction of evaporation from the soil and from foliage by changes in the value of the saturation vapor pressure deficit of air in the canopy (the conclusions of this interaction being consistent with field observations); and (2) the treatment of sensible and latent heat exchange between the atmosphere and a soil consisting of two discrete layers. O.C.

A88-41055
MAPPING FROST-SENSITIVE AREAS WITH A THREE-DIMENSIONAL LOCAL-SCALE NUMERICAL MODEL. I - PHYSICAL AND NUMERICAL ASPECTS

R. AVISSAR (Colorado State University, Fort Collins) and Y. MAHRER (Jerusalem, Hebrew University, Rehovot, Israel) Journal of Applied Meteorology (ISSN 0894-8763), vol. 27, April 1988, p. 400-413. Research supported by the Israel Academy of Sciences and Humanities. refs (Contract NSF ATM-84-14181; NSF ATM-86-16662)

A88-41947* National Aeronautics and Space Administration. John C. Stennis Space Center, Bay Saint Louis, Miss.
PRELIMINARY INVESTIGATION OF LARGE FORMAT CAMERA PHOTOGRAPHY UTILITY IN SOIL MAPPING AND RELATED AGRICULTURAL APPLICATIONS

R. E. PELLETIER (NASA, National Space Technology Laboratories, Bay Saint Louis, MS) and W. H. HUDNALL (Louisiana State University, Baton Rouge) IN: American Society for Photogrammetry and Remote Sensing and ACSM, Fall Convention, Reno, NV, Oct. 4-9, 1987, ASPRS Technical Papers. Falls Church, VA, American Society for Photogrammetry and Remote Sensing, 1987, p. 55-64. refs

The use of Space Shuttle Large Format Camera (LFC) color, IR/color, and B&W images in large-scale soil mapping is discussed and illustrated with sample photographs from STS 41-6 (October 1984). Consideration is given to the characteristics of the film types used; the photographic scales available; geometric and stereoscopic factors; and image interpretation and classification for soil-type mapping (detecting both sharp and gradual boundaries), soil parent material topographic and hydrologic assessment, natural-resources inventory, crop-type identification, and stress analysis. It is suggested that LFC photography can play an important role, filling the gap between aerial and satellite remote sensing. T.K.

A88-41948
ECONOMIC POTENTIAL OF LANDSAT THEMATIC MAPPER DATA FOR CROP CONDITION ASSESSMENT OF WINTER WHEAT

WARREN THETFORD and GEORGE MAY (Space Remote Sensing Center, Bay Saint Louis, MS) IN: American Society for Photogrammetry and Remote Sensing and ACSM, Fall Convention, Reno, NV, Oct. 4-9, 1987, ASPRS Technical Papers. Falls Church,

VA, American Society for Photogrammetry and Remote Sensing, 1987, p. 65-72. refs

April, 1986 Landsat Thematic Mapper data were used in an attempt to estimate crop condition of winter wheat (*Triticum aestivum* L.) fields in Calloway County, Kentucky. It was hoped that information of some potential financial benefit to Hutson Company, Inc., a regional fertilizer distributor, might be extracted through analysis of the data. A total of 24,387 acres of wheat were classified and mapped. A method of estimating nitrogen deficiency was derived and implemented to provide Hutson with acreage and supplemental nitrogen need figures for the study area. The use of the Thematic Mapper data was found to have at best, marginal financial potential for Hutson in Calloway County alone. However, the prospect of applying similar techniques on a quarter scene or whole scene basis appears promising. Based on a quarter scene, profits from additional nitrogen sales ranged from \$21,000 to \$23,400 which could exceed imagery, processing, and analysis costs. Author

A88-41951* South Carolina Univ., Columbia.
**CORRELATION BETWEEN AIRCRAFT MSS AND LIDAR
 REMOTELY SENSED DATA ON A FORESTED WETLAND IN
 SOUTH CAROLINA**

JOHN R. JENSEN (South Carolina, University, Columbia), MICHAEL E. HODGSON (Colorado, University, Boulder), HALKARD E. MACKEY, JR. (Savannah River Laboratory, Aiken, SC), and WILLIAM KRABILL (NASA, Wallops Flight Facility, Wallops Island, VA) IN: American Society for Photogrammetry and Remote Sensing and ACSM, Fall Convention, Reno, NV, Oct. 4-9, 1987, ASPRS Technical Papers. Falls Church, VA, American Society for Photogrammetry and Remote Sensing, 1987, p. 136-149. Previously announced in STAR as N88-11204. refs
 (Contract DE-AC09-76SR-00001)

Wetlands in a portion of the Savannah River swamp forest, the Steel Creek Delta, were mapped using April 26, 1985 high-resolution aircraft multispectral scanner (MSS) data. Due to the complex spectral characteristics of the wetland vegetation, it was necessary to implement several techniques in the classification of the MSS imagery of the Steel Creek Delta. In particular, when performing unsupervised classification, an iterative cluster busting technique was used which simplified the cluster labeling process. In addition to the MSS data, light detecting and ranging (LIDAR) data were acquired by National Aeronautics and Space Administration (NASA) personnel along two flightlines over the Steel Creek Delta. These data were registered with the wetland classification map and correlated. Statistical analyses demonstrated that the laser derived canopy height information was significantly correlated with the Steel Creek Delta wetland classes encountered along the profiling transect of the LIDAR data. Author

A88-41952* Science Applications Research, Lanham, Md.
**OBTAINING SPECTRAL REFLECTANCE FACTOR
 MEASUREMENTS OF STRESSED FOREST VEGETATION**
 DAVID W. CASE (Science Applications Research, Lanham, MD) and DARREL L. WILLIAMS (NASA, Goddard Space Flight Center, Greenbelt, MD) IN: American Society for Photogrammetry and Remote Sensing and ACSM, Fall Convention, Reno, NV, Oct. 4-9, 1987, ASPRS Technical Papers. Falls Church, VA, American Society for Photogrammetry and Remote Sensing, 1987, p. 150-160. refs

Techniques and instruments used to collect spectral reflectance data on Vermont spruce and fir stands subjected to stress (due to acid rain and ozone) are described and illustrated. The healthy and stressed sites selected are characterized; the data-quality requirements are indicated; and particular attention is given to (1) a helicopter-mounted instrument package (radiometer, spectrometer, cameras, and video camera) for canopy-level remote sensing of reflectance and (2) a portable hemispherical light source for use in taking laboratory reflectance measurements from branches or needles. Typical data are presented in graphs and briefly discussed. T.K.

A88-41954
**REMOTE SENSING AND THE ROLE OF TERRESTRIAL
 VEGETATION IN THE GLOBAL CARBON CYCLE**

LAWRENCE FOX, III and JOHN D. STUART (Humboldt State University, Arcata, CA) IN: American Society for Photogrammetry and Remote Sensing and ACSM, Fall Convention, Reno, NV, Oct. 4-9, 1987, ASPRS Technical Papers. Falls Church, VA, American Society for Photogrammetry and Remote Sensing, 1987, p. 191-196. refs

A88-41963
**DIGITAL PROCESSING OF AIRBORNE MSS DATA FOR
 FOREST COVER TYPES CLASSIFICATION**

KUO-MU CHIAO, YEONG-KUAN CHEN, and HANN-CHIN SHIEH (National Taiwan University, Taipei, Republic of China) IN: Remote sensing for resources development and environmental management; Proceedings of the Seventh International Symposium, Enschede, Netherlands, Aug. 25-29, 1986. Volume 1. Rotterdam, A. A. Balkema, 1986, p. 15-18. Research supported by the Council of Agriculture of the Republic of China.

The purpose of this study is to find optimal band combinations of airborne MSS data for forest cover types classification. An eleven-channel airborne multispectral scanner was used to collect data. Processing of the MSS data was achieved through the use of the Interactive Digital Image Manipulation System (IDIMS). Forest cover types were interpreted with a hybrid supervised/unsupervised approach. Eight original bands of airborne MSS data and enhanced data such as principal component transformations, ratio images, spatial filtering data, resampling data and mixed bands were subjected to standard clustering and classification techniques. Among the numerous band combinations of MSS data, forty-seven best band combinations with highest values of average divergence and minimum divergence were selected, and classified on IDIMS by the maximum likelihood classifier. Findings of this study are summarized as follows: (1) the best band combination is the combination which contains more bands; (2) resampling and spatial filtering techniques increase 7-10 percent classification accuracy; and (3) because of the inherent property, the principal component transformations, ratio images and mixed bands are insufficient to improve the classification accuracy. Author

A88-41971
**DIGITAL CLASSIFICATION OF FORESTED AREAS USING
 SIMULATED TM- AND SPOT- AND LANDSAT 5/TM-DATA**

H.-J. STIBIG (Freiburg, Universitaet, Freiburg im Breisgau, Federal Republic of Germany) and M. SCHARDT (DFVLR, Cologne, Federal Republic of Germany) IN: Remote sensing for resources development and environmental management; Proceedings of the Seventh International Symposium, Enschede, Netherlands, Aug. 25-29, 1986. Volume 1. Rotterdam, A. A. Balkema, 1986, p. 79-85.

In the following piece of research both SPOT- and TM-images, as well as true Landsat 5/TM data have been digitally classified. The results show information about the possibilities of recognizing different types and age classes of trees, together with a high resolution of the classified forest units. Using both TM- and SPOT-data it is possible to differentiate between at least three age classes in forest stands. As well as distinguishing between coniferous and deciduous trees, it is possible to recognize certain tree types in pure crop stands within these classes, depending on the time of year. The correctly classified forest unit is influenced by the form and size of the stands, but generally stands larger than an hectare can be recognized. The classification of the Landat 5/TM scenes was improved by taking into account topographical information and by using multitemporal data. Author

A88-41984
**RELATING L-BAND SCATTEROMETER DATA WITH SOIL
 MOISTURE CONTENT AND ROUGHNESS**

P. J. F. SWART (Delft, Technische Hogeschool, Netherlands) IN: Remote sensing for resources development and environmental management; Proceedings of the Seventh International Symposium,

01 AGRICULTURE AND FORESTRY

Enschede, Netherlands, Aug. 25-29, 1986. Volume 1. Rotterdam, A. A. Balkema, 1986, p. 183-186. refs

Preliminary results are reported of the analysis of L-band airborne radar backscatter data from large homogeneous agricultural fields. Examples are given of the calculated normalized radar cross section versus incidence angle. The main theme of discussion will be this angular dependency and its relation with measured soil moisture content and roughness. Author

A88-41986

RELATIONSHIP BETWEEN SOIL AND LEAF METAL CONTENT AND LANDSAT MSS AND TM ACQUIRED CANOPY REFLECTANCE DATA

C. BANNINGER (Graz, Forschungszentrum, Austria) IN: Remote sensing for resources development and environmental management; Proceedings of the Seventh International Symposium, Enschede, Netherlands, Aug. 25-29, 1986. Volume 1. Rotterdam, A. A. Balkema, 1986, p. 195-200. Research supported by the Science Research Office of Styria and BMFWF. refs

The presence of high concentrations of copper, lead, and zinc in the soils underlying a spruce tree stand is not mirrored in the metal content of the spruce needles, except for zinc. A much stronger correlation exists between Landsat canopy reflectance data and soil metal content than with spruce needle metal content. This implies that the toxic effects of the heavy metals on the spruce trees are centered in the root systems rather than in the foliar parts of the trees. Author

A88-41987

THE DERIVATION OF A SIMPLIFIED REFLECTANCE MODEL FOR THE ESTIMATION OF LAI

J. G. P. W. CLEVERS (Landbouwhogeschool, Wageningen, Netherlands) IN: Remote sensing for resources development and environmental management; Proceedings of the Seventh International Symposium, Enschede, Netherlands, Aug. 25-29, 1986. Volume 1. Rotterdam, A. A. Balkema, 1986, p. 215-220. refs

A simplified crop reflectance model for the estimation of leaf area index (LAI) which makes corrections for background caused by soil reflectance is presented. The model works by defining an apparent soil cover and then calculating a corrected infrared reflectance by subtracting the contribution of the soil from the measured reflectance. It is assumed that there is a constant ratio between the reflectances of bare soil in different spectral bands, independent of soil moisture content, enabling the corrected infrared reflectance to be calculated without knowing soil reflectance. Simulations with the SAIL model (Verhoef, 1984) are used to confirm this semi-empirical model's potential for estimating LAI. R.B.

A88-41988

THE APPLICATION OF A VEGETATION INDEX IN CORRECTING THE INFRARED REFLECTANCE FOR SOIL BACKGROUND

J. G. P. W. CLEVERS (Landbouwhogeschool, Wageningen, Netherlands) IN: Remote sensing for resources development and environmental management; Proceedings of the Seventh International Symposium, Enschede, Netherlands, Aug. 25-29, 1986. Volume 1. Rotterdam, A. A. Balkema, 1986, p. 221-226. refs

A88-41989

MULTITEMPORAL ANALYSIS OF THEMATIC MAPPER DATA FOR SOIL SURVEY IN SOUTHERN TUNISIA

G. F. EPEMA (Landbouwhogeschool, Wageningen, Netherlands) IN: Remote sensing for resources development and environmental management; Proceedings of the Seventh International Symposium, Enschede, Netherlands, Aug. 25-29, 1986. Volume 1. Rotterdam, A. A. Balkema, 1986, p. 245-249. refs

A88-41991

SPECTRAL SIGNATURE OF RICE FIELDS USING LANDSAT-5 TM IN THE MEDITERRANEAN COAST OF SPAIN

S. GANDIA, V. CASELLES, A. GILABERT, and J. MELIA (Valencia, Universidad, Spain) IN: Remote sensing for resources development and environmental management; Proceedings of the Seventh International Symposium, Enschede, Netherlands, Aug. 25-29, 1986. Volume 1. Rotterdam, A. A. Balkema, 1986, p. 257-259. refs

This work gives the first results of a study carried out in an agricultural area of the Spanish Mediterranean coast using Thematic Mapper images. Three cover types, rice, critic - vegetable orchard and urban area are classified in the zone by using a vegetation index. Bands 4 and 5 seem to be more suitable for a possible classification of two varieties of rice. Author

A88-41993

DETERMINATION OF SPECTRAL SIGNATURES OF DIFFERENT FOREST DAMAGES FROM VARYING ALTITUDES OF MULTISPECTRAL SCANNER DATA

A. KADRO (Freiburg, Universitaet, Freiburg im Breisgau, Federal Republic of Germany) IN: Remote sensing for resources development and environmental management; Proceedings of the Seventh International Symposium, Enschede, Netherlands, Aug. 25-29, 1986. Volume 1. Rotterdam, A. A. Balkema, 1986, p. 281-284. refs

Within the scope of the project 'forest damage inventory with multispectral scanner data' at the Department of Remote Sensing at the University of Freiburg, thematic mapper simulation data of different altitudes was acquired. Five test areas which differ in morphology, forest types and forest damage degree were sensed. For the investigation of the spectral signatures, reference panels were placed along the flying strip (size ca. 200 sqm) for the determination of the global radiation. The data were obtained from three altitudes (300, 1000, 3000 m) so that the spectral signatures could be determined in relation to the flight altitude. The scanner data of 300 m altitude enables the investigation of single trees. The data of higher altitudes only permit the investigation of trees or stands because of the larger pixel size. The same test areas have been used also for the investigation of spectral signatures of Landsat (TM) data. In this paper the results of the investigation are presented and discussed. Author

A88-41994

MULTITEMPORAL ANALYSIS OF LANDSAT MULTISPECTRAL SCANNER (MSS) AND THEMATIC MAPPER (TM) DATA TO MAP CROPS IN THE PO VALLEY (ITALY) AND IN MENDOZA (ARGENTINA)

M. MENENTI, S. AZZALI (Instituut voor Cultuurtechniek en Waterhuishouding, Wageningen, Netherlands), D. A. COLLADO, and S. LEGUIZAMON (Instituto de Investigaciones Aplicadas en Ciencias Espaciales, Mendoza, Argentina) IN: Remote sensing for resources development and environmental management; Proceedings of the Seventh International Symposium, Enschede, Netherlands, Aug. 25-29, 1986. Volume 1. Rotterdam, A. A. Balkema, 1986, p. 293-299. refs

A88-41997

SPECTRAL SIGNATURES OF SOILS AND TERRAIN CONDITIONS USING LASERS AND SPECTROMETERS

H. SCHREIER (British Columbia, University, Vancouver, Canada) IN: Remote sensing for resources development and environmental management; Proceedings of the Seventh International Symposium, Enschede, Netherlands, Aug. 25-29, 1986. Volume 1. Rotterdam, A. A. Balkema, 1986, p. 311-315. refs

This paper presents the results of two studies. In the first, the results of airborne laser test flights were documented, demonstrating that high-resolution data on the terrain and vegetation heights and on the surface reflection can be obtained simultaneously. In the second study, conducted to explore the possibilities of ground-based multispectral laser measurements, ground-based reflection measurements (at 550, 630, and 1600 nm) done by a spectrometer were correlated with the contents of C, Fe, and sand, respectively, in different sets of soil samples. The relationships obtained were not universal, and were only applicable on a site-specific basis. For instance, organic carbon

could only be predicted with confidence in soils originating from a field where the organic C content was highly variable and greater than 2 percent, and the percent sand could be predicted accurately in samples with organic carbon below 2 percent. I.S.

A88-41998**RELATION BETWEEN SPECTRAL REFLECTANCE AND VEGETATION INDEX**

S. M. SINGH (Reading, University, England) IN: Remote sensing for resources development and environmental management; Proceedings of the Seventh International Symposium, Enschede, Netherlands, Aug. 25-29, 1986. Volume 1. Rotterdam, A. A. Balkema, 1986, p. 317-319. refs
(Contract NERC-F60/G6/12)

Atmospheric corrections are applied to the Advanced Very High Resolution Radiometer (AVHRR) channel-1 and channel-2 data. Both raw and atmospherically corrected Normalized Difference Vegetation Indices (NDVIs) are calculated. A comparison between them shows a contrast enhancement by a factor of at least two when atmospheric corrections are applied. Spectral reflectances and atmospherically corrected NDVI are partially correlated indicating a possibility of improving surface cover classification using NDVI and spectral reflectances instead of NDVI values alone. Raw NDVI and atmospherically corrected NDVI do not have a unique relationship but are highly correlated. This indicates that atmospheric corrections be applied to each scene of interest.

Author

A88-41999**LANDSAT TEMPORAL-SPECTRAL PROFILES OF CROPS ON THE SOUTH AFRICAN HIGHVELD**

B. TURNER (National Physical Research Laboratory, Pretoria, Republic of South Africa) IN: Remote sensing for resources development and environmental management; Proceedings of the Seventh International Symposium, Enschede, Netherlands, Aug. 25-29, 1986. Volume 1. Rotterdam, A. A. Balkema, 1986, p. 325-330. refs

Landsat MSS data were standardized for variations in digital count coding between different receiving stations, satellite sensor response and solar illumination of the scene. The Kauth and Thomas approach has been used to obtain the independent variables of soil brightness, greenness and yellowness. The coefficients of the rotation matrix were modified to suit local conditions. Three vegetation indices, the vegetation ratio, the normalized vegetation index and the greenness index have been determined on a field-by-field basis using data recorded on sixteen overpasses within thirteen months. An intercomparison of the spectral-temporal profiles for a variety of crops is in progress. A correlation between the spectral profiles and a ground reference set consisting of detailed information on planting, growth and environmental conditions is to be undertaken. The spectral separability of the crops in terms of the vegetation indices and the field conditions is being evaluated.

Author

A88-42002**OPTIMAL THEMATIC MAPPER BANDS AND TRANSFORMATIONS FOR DISCERNING METAL STRESS IN CONIFEROUS TREE CANOPIES**

C. BANNINGER (Graz, Forschungszentrum, Austria) IN: Remote sensing for resources development and environmental management; Proceedings of the Seventh International Symposium, Enschede, Netherlands, Aug. 25-29, 1986. Volume 1. Rotterdam, A. A. Balkema, 1986, p. 371-374. refs

A statistical analysis of multitemporal Landsat Thematic Mapper (TM) data acquired from a pine and a spruce tree stand growing in copper-lead-zinc enriched soils helped define the TM spectral bands and transformations best suited for detecting metal stress in coniferous tree canopies. Based on four Landsat TM scene dates, the first principal component (PC1) and the band difference (BD1) rank the highest of thirty-one single and transformed TM bands examined, followed by the TM brightness index (TMB) and Thematic Mapper bands 5 and 7.

Author

A88-42003**THE USE OF MULTITEMPORAL LANDSAT DATA FOR IMPROVING CROP MAPPING ACCURACY**

ALAN S. BELWARD and JOHN C. TAYLOR (Cranfield Institute of Technology, England) IN: Remote sensing for resources development and environmental management; Proceedings of the Seventh International Symposium, Enschede, Netherlands, Aug. 25-29, 1986. Volume 1. Rotterdam, A. A. Balkema, 1986, p. 381-386. refs

The value of using multitemporal Landsat MSS data to improve classification accuracy in an area of diverse crop production was investigated using a 625-sq km area centered on Framingham, England, as a test site. Six scenes from between October 1979 and August 1980 were located, and the data were matched to 2000 hectares of ground information giving the crop type and field boundaries for the 1979-1980 growing season. Ten cover classes were identified: winter wheat, winter barley, spring barley, oilseed rape, grassland, sugar beet, peas, beans, and deciduous and coniferous woodland. It was found that multitemporal data gave better overall classification accuracies than the single date images. The best results were from a spring/early summer combination, with a mean classification accuracy of 70 percent. This is a 6-percent increase over the best single-date classification from May, and 46 percent better than the worst from February.

I.S.

A88-42004**INVENTORY OF DECLINE AND MORTALITY IN SPRUCE-FIR FORESTS OF THE EASTERN U.S. WITH CIR PHOTOS**

W. M. CIESLA, C. W. DULL, L. R. MCCREERY, and M. E. MIELKE (USDA, Forest Service, Fort Collins, CO) IN: Remote sensing for resources development and environmental management; Proceedings of the Seventh International Symposium, Enschede, Netherlands, Aug. 25-29, 1986. Volume 1. Rotterdam, A. A. Balkema, 1986, p. 391-396. refs

An accelerated decline and mortality of several commercially important trees, including red spruce, *Picea rubens*, has recently been reported in the eastern United States. The causal agents responsible for this syndrome are not yet fully known. This has led to a concern that some form of anthropogenic pollution may be involved. Beginning in 1984, a series of special inventories were conducted by the Forest Pest Management organization of the USDA Forest Service to quantify the status of red spruce decline and mortality throughout its natural range. Color infrared aerial photography was used as an integral stage of these surveys. Photographic parameters and survey design approaches are described, and examples of survey results are presented. Resultant data are being stored in geographic information systems to facilitate integration with other resource information and research data. Survey designs currently used in the United States are compared to European approaches for assessment of similar types of damage.

Author

A88-42005**A REMOTE SENSING AIDED INVENTORY OF FUELWOOD VOLUMES IN THE SAHEL REGION OF WEST AFRICA - A CASE STUDY OF FIVE URBAN ZONES IN THE REPUBLIC OF NIGER**

STEVEN J. DAUS, MAMANE GUERO (Forestry and Land Use Planning, Niamey, Niger), and LAWALLY ADA (Niamey, University, Niger) IN: Remote sensing for resources development and environmental management; Proceedings of the Seventh International Symposium, Enschede, Netherlands, Aug. 25-29, 1986. Volume 1. Rotterdam, A. A. Balkema, 1986, p. 403-408. Research supported by the U.S. Agency for International Development.

A88-42006**THE USE OF SPOT SIMULATION DATA IN FORESTRY MAPPING**

S. J. DURY, W. G. COLLINS, and P. D. HEDGES (Aston, University, Birmingham, England) IN: Remote sensing for resources development and environmental management; Proceedings of the

01 AGRICULTURE AND FORESTRY

Seventh International Symposium, Enschede, Netherlands, Aug. 25-29, 1986. Volume 1. Rotterdam, A. A. Balkema, 1986, p. 425-428. refs

The potential usefulness of the SPOT satellite for providing data for forestry management was investigated, comparing satellite data with the ground data on a test area located within the Forest of Dean, England. Several digital enhancement techniques were applied to SPOT simulation imagery and were visually assessed to give the best discrimination of the tree types; a maximum likelihood classification was then performed on suitably enhanced images. The results indicate that SPOT images can be used not only for distinguishing different tree species but also different age classes of certain species. A major source of error resulted from the high spectral variance of urban areas within the forest. Methods for overcoming this problem are proposed. I.S.

A88-42007

SPRUCE BUDWORM INFESTATION DETECTION USING AN AIRBORNE PUSHBROOM SCANNER AND THEMATIC MAPPER DATA

H. EPP (Canada Centre for Remote Sensing, Ottawa) and R. REED (Saskatchewan Parks and Renewable Resources, Prince Albert, Canada) IN: Remote sensing for resources development and environmental management; Proceedings of the Seventh International Symposium, Enschede, Netherlands, Aug. 25-29, 1986. Volume 1. Rotterdam, A. A. Balkema, 1986, p. 429-434. refs

The potentials of high-resolution MEIS-II pushbroom scanner and Thematic Mapper data for detecting spruce budworm infestation were investigated. Data were acquired in the summer of 1985 on a test site in east-central Saskatchewan, Canada. The results showed that it is possible to identify areas of spruce budworm damage using areal photography and natural color images obtained from the pushbroom scanner data; one level of budworm infestation, with indications of a second level, was detected by the scanner. The lower-resolution Thematic Mapper data could only be used to identify the severely affected spruce budworm areas. I.S.

A88-42008

CONTRIBUTION OF REMOTE SENSING TO FOOD SECURITY AND EARLY WARNING SYSTEMS IN DROUGHT AFFECTED COUNTRIES IN AFRICA

ABDISHAKOUR A. GULAIID (Berlin, Technische Universitaet, Federal Republic of Germany) IN: Remote sensing for resources development and environmental management; Proceedings of the Seventh International Symposium, Enschede, Netherlands, Aug. 25-29, 1986. Volume 1. Rotterdam, A. A. Balkema, 1986, p. 457-460. refs

As a result of the disastrous drought that affected many countries in the Sahel Zone in 1973/74, the international community has been looking for means of obtaining immediate and reliable information on the potential causes of this terrible danger that threatens millions of human and animal lives. The Food and Agricultural Organization of the United Nations (FAO), for example, has established an early warning system for predicting food shortages in many developing countries. The United Nations Environmental Program (UNEP) installed a global environmental monitoring program (GEMS). Many developing countries have set up their own food security and early warning systems with the help of multilateral or bilateral technical cooperation projects. The common aim of these programs is the collection, processing and analysis of relevant data with the help of one or several methods, and the subsequent presentation of the derived information to the planners and decision-makers in order to take appropriate measures in time. This paper assesses the role of remote sensing in the existing and the future food security programs and early warning systems in developing countries with particular emphasis on the drought affected countries in Africa. Author

A88-42009

DOUBLE SAMPLING FOR RICE IN BANGLADESH USING LANDSAT MSS DATA

BARRY N. HAACK (George Mason University, Fairfax, VA) IN: Remote sensing for resources development and environmental management; Proceedings of the Seventh International Symposium, Enschede, Netherlands, Aug. 25-29, 1986. Volume 1. Rotterdam, A. A. Balkema, 1986, p. 461-464. refs

Landsat Multispectral Scanner (MSS) data were utilized to assess the location and area of the winter or boro rice crop for a study site in Bangladesh. Both digital classifications and visual interpretations of the Landsat data were conducted using a double sampling between the Landsat analyses and governmental reported acreages for ten administrative units. The digital data were classified using a table look-up of MSS Bands 5 and 7 and the visual analysis conducted with an enlarged false color composite subscene and a rearview projector. Both techniques located about one-half of the reported acreage but had correlations between the reported and Landsat data for the ten units of over 0.90. This study indicates that double sampling with Landsat data can be an effective technique for the inventory of renewable resources in rural areas. Author

A88-42010

EXPERIENCES IN APPLICATION OF MULTISPECTRAL SCANNER-DATA FOR FOREST DAMAGE INVENTORY

A. KADRO and S. KUNTZ (Freiburg, Universitaet, Freiburg im Breisgau, Federal Republic of Germany) IN: Remote sensing for resources development and environmental management; Proceedings of the Seventh International Symposium, Enschede, Netherlands, Aug. 25-29, 1986. Volume 1. Rotterdam, A. A. Balkema, 1986, p. 469-472. refs

For testing the potential use of multispectral scanner data for the inventory of forest damages in large areas five test sites in southwest Germany were sensed at three flight altitudes with an 11-channel scanner. At the same time, ground truth information in these test sites were obtained and the actual state of the forest stands was documented with color infrared (CIR) aerial photographs. The test sites differ in morphology, forest types and degree of the actual forest damage. The acquired data were evaluated with a computer aided supervised classification using the maximum-likelihood method. For verification of the classification results for both single trees and stands, the terrestrial ground truth and the CIR-photographs were used. This paper presents the classification results and discusses the problems of a computer aided forest damage inventory. Author

A88-42011

APPLICATION OF MULTISPECTRAL SCANNING REMOTE SENSING IN AGRICULTURAL WATER MANAGEMENT PROBLEMS

G. J. A. NIEUWENHUIS (Instituut voor Cultuurtechniek en Waterhuishouding, Wageningen, Netherlands) and J. M. M. BOUWMANS (Landinrichtingsdienst, Utrecht, Netherlands) IN: Remote sensing for resources development and environmental management; Proceedings of the Seventh International Symposium, Enschede, Netherlands, Aug. 25-29, 1986. Volume 1. Rotterdam, A. A. Balkema, 1986, p. 489-494. refs

A method has been developed for the automatical mapping of evapotranspiration from digitally taken reflection and thermal images. This method has been tested in combination with field measurements and agrohydrological model calculations. An important improvement of the hydrological description of an area can be achieved by combining the remote sensing approach with conventional methods. Especially the spatial variation in soil physical characteristics can be determined more accurately by applying remote sensing techniques. Satellite and airplane images acquired after a dry period supply information about the occurrence of drought damage. Because of the fast changing weather conditions in humid areas like the Netherlands remote sensing in water management will mainly depend on scanning techniques from airplanes. Author

A88-42012

GLOBAL VEGETATION MONITORING USING NOAA GAC DATA

H. SHIMODA, K. FUKUE, T. HOSOMURA, and T. SAKATA (Tokai University, Tokyo, Japan) IN: Remote sensing for resources development and environmental management; Proceedings of the Seventh International Symposium, Enschede, Netherlands, Aug. 25-29, 1986. Volume 1. Rotterdam, A. A. Balkema, 1986, p. 505-508.

In the last decade, the necessity of global monitoring of vegetations or bio-mass has become a more urgent matter. In order to prevent the large disaster which may be caused by vegetation decrease, accurate conditions or stage of the world vegetation should be monitored. The only satellite system and observation data which can be used for the purpose is TIROS/NOAA system and Vegetation Index Data (VID) made of AVHRR, respectively. The purpose of this study is to establish the method to derive a global vegetation map from a VID set. One data set was used in this study. Large shading effects mainly caused by sun angle deviations were first eliminated. The classification was done using a maximum likelihood method with four channels of VID. Training data composed of 67 categories were chosen according to the World Vegetation Map made by Preston James et al. After the classification, these 67 categories were unified to 17 categories. Then the classified images were transformed to longitude and latitude coordinates. As a result of this study, NOAA Vegetation Index Data were proved to be a suitable data for worldwide vegetation monitorings. Author

A88-42013**CLASSIFICATION OF THE RIVERINA FORESTS OF SOUTH EAST AUSTRALIA USING CO-REGISTERED LANDSAT MSS AND SIR-B RADAR DATA**

A. K. SKIDMORE, P. W. WOODGATE, and J. A. RICHARDS (New South Wales, University, Kensington, Australia) IN: Remote sensing for resources development and environmental management; Proceedings of the Seventh International Symposium, Enschede, Netherlands, Aug. 25-29, 1986. Volume 1. Rotterdam, A. A. Balkema, 1986, p. 517-519. refs

A88-42014**COMPARISON OF SPOT-SIMULATED AND LANDSAT 5 TM IMAGERY IN VEGETATION MAPPING**

H. TOMMERVIK (Tromsø, Universitetet, Norway) IN: Remote sensing for resources development and environmental management; Proceedings of the Seventh International Symposium, Enschede, Netherlands, Aug. 25-29, 1986. Volume 1. Rotterdam, A. A. Balkema, 1986, p. 525-529. refs

Results from work done on both SPOT-simulated imagery and Landsat 5 TM imagery are presented. The test area is situated in Central Troms, Northern Norway, and has a fairly wide variation in ecological niches and comprises both forest landscape and mountain areas (Arctic alpine vegetation). The ground truth program did include both a traditional vegetation mapping program and a test-site program. Digital image processing was carried out both on the SPOT-simulated imagery and the Landsat imageries, but the scenes were taken too early in the spring or too late in the autumn to give a sufficient basis for a good classification. The investigation has shown that the Landsat scene from the springtime almost had the same accuracy by supervised classification as the SPOT-simulated imagery, due to the better radiometric resolution for the TM-sensor compared to the simulated HRV-sensor on the SPOT satellite. But classification on the SPOT-simulated imagery showed that the vegetation units within small areas, were better picked out due to the better spatial resolution, compared to the TM-sensor on the Landsat 5 satellite. Visual interpretation on the autumn-scene of Landsat 5 TM-sensor gave a successful detection of swamp forests at the riverbanks by using the channel combinations of CH 456 and CH 543. Author

A88-42015**MULTI-TEMPORAL LANDSAT FOR LAND UNIT MAPPING ON PROJECT SCALE OF THE SUDD-FLOODPLAIN, SOUTHERN SUDAN**

Y. A. YATH (Jonglei Executive Organ, Karthoem, Sudan) and H. A. M. J. VAN GILS (International Institute for Aerospace Survey

and Earth Sciences, Enschede, Netherlands) IN: Remote sensing for resources development and environmental management; Proceedings of the Seventh International Symposium, Enschede, Netherlands, Aug. 25-29, 1986. Volume 1. Rotterdam, A. A. Balkema, 1986, p. 531, 532.

The Sudd floodplain is extremely flat, covered mainly by grasslands, only locally interrupted by clusters of fields and seasonally flooded by rain and/or river water. Since photo-interpretation is based on relief, vegetation structure and field pattern, such technique is not satisfying for the Sudd floodplain. Moreover, the most important environmental component - the flooding - can be assessed only on sequential series of photographs. Studies of the Sudd-floodplain on regional scale have been carried out as environmental impact study for the Jonglei Canal project. However, such information proved of limited value on project scale. For the latter a combination of Landsat, aerial photography and field survey has been tried and proven successful. The methodology, results and limitations are outlined for application in similar floodplain areas as there are the Llanos in Southern America, Zambesi floodplain, Kafue flats and the Okavango swamps in Africa. Author

A88-42024**THEMATIC MAPPING FROM AERIAL PHOTOGRAPHS FOR KANDI WATERSHED AND AREA DEVELOPMENT PROJECT, PUNJAB (INDIA)**

B. DIDAR SINGH and KANWARJIT SINGH (Planning and Design State Directorate, Chandigarh, India) IN: Remote sensing for resources development and environmental management; Proceedings of the Seventh International Symposium, Enschede, Netherlands, Aug. 25-29, 1986. Volume 2. Rotterdam, A. A. Balkema, 1986, p. 595-598.

A88-42035**SMALL SCALE EROSION HAZARD MAPPING USING LANDSAT INFORMATION IN THE NORTHWEST OF ARGENTINA**

JOSE MANUEL SAYAGO IN: Remote sensing for resources development and environmental management; Proceedings of the Seventh International Symposium, Enschede, Netherlands, Aug. 25-29, 1986. Volume 2. Rotterdam, A. A. Balkema, 1986, p. 669-674. refs

A88-42060**HOW FEW DATA DO WE NEED - SOME RADICAL THOUGHTS ON RENEWABLE NATURAL RESOURCES SURVEYS**

J. A. ALLAN (London, University, England) IN: Remote sensing for resources development and environmental management; Proceedings of the Seventh International Symposium, Enschede, Netherlands, Aug. 25-29, 1986. Volume 2. Rotterdam, A. A. Balkema, 1986, p. 901-906. refs

The use of remote sensing in renewable natural resources surveys is discussed, emphasizing the economics of monitoring and predicting agricultural change and production. It is argued that remote sensing specialists should identify economic activities which attract returns to institutions which will benefit by advance warning of agricultural performance at the regional level, and then determine the minimum level of sample coverage and frequency necessary to provide predictive information at a price which the economic activities will bear. It is concluded that any economically viable operational system will require economies in spatial cover through sampling. Principles according to which such economies might be decided are suggested, discussing the implications for sensor design and data processing. R.B.

A88-42061**THE POTENTIAL OF NUMERICAL AGRONOMIC SIMULATION MODELS IN REMOTE SENSING**

J. A. A. BERKHOUT (Centre for World Food Studies, Wageningen, Netherlands) IN: Remote sensing for resources development and environmental management; Proceedings of the Seventh International Symposium, Enschede, Netherlands, Aug. 25-29,

01 AGRICULTURE AND FORESTRY

1986. Volume 2. Rotterdam, A. A. Balkema, 1986, p. 907-911. refs

The possible use of remote sensing in a Geographic Information System (GIS) including crop growth models and the possible use of GIS as a partial substitute for ground truth in remote sensing analysis are discussed. Remote sensing can provide information required for successful implementation of an agricultural GIS early warning system, such as additional knowledge of the actual land use pattern, synoptic time series of the actual weather, and detailed knowledge on the physiography including soil characteristics and hydrology. Although it is felt that extensive field observations will continue to be required to quantify the combined effect of all land entities and farm practices on the cultivation of specific crops, the number of observations could be reduced with the introduction of numerical simulation models. R.B.

A88-42538

DETECTION OF ENVIRONMENTAL NOISES BETWEEN A VEGETATION CANOPY AND A RADIOMETRIC SENSOR

M. C. MUEKSCH (Saarland, Universitaet, Herrenberg, Federal Republic of Germany) IN: Optoelectronic technologies for remote sensing from space; Proceedings of the Meeting, Cannes, France, Nov. 19, 20, 1987. Bellingham, WA, Society of Photo-Optical Instrumentation Engineers, 1988, p. 81-85. refs

A method to determine environmental noises between a radiometric sensor and a vegetation canopy is described. The noises are the differences between the incoming radiation and a synthetic radiation, computed by a radiation model in which the local climatological data are introduced over the evapotranspiration component. Climatological data are simultaneously collected by sensors in the station and target area over a local area network (LAN), controlled by a master station in the radiometer standpoint. The LAN can quickly be rearranged in the observation area to get the actual amount of local environmental noises which then can be taken into consideration as corrections at the observed canopy reflectances. The method is primarily designed for remote sensing ground control. Author

A88-42545

IN FLIGHT CALIBRATION FOR THE IMAGING INSTRUMENT OF VEGETATION PAYLOAD (SPOT 4)

R. KRAWCZYK and G. CERUTTI-MAORI (Aerospatiale, Cannes, France) IN: Optoelectronic technologies for remote sensing from space; Proceedings of the Meeting, Cannes, France, Nov. 19, 20, 1987. Bellingham, WA, Society of Photo-Optical Instrumentation Engineers, 1988, p. 126-133. CNES-supported research.

'Vegetation' is a payload that will be carried by the earth-observation satellite SPOT 4 when it is launched in 1992; it is primarily aimed at conducting a global survey of vegetation cover in order to forecast agricultural yields and assist in environmental studies. The payload is secondarily concerned with the observation of oceanic areas. Of the five spectral bands used, three are in the visible, one is in the near-IR, and the last is in the mid-IR. The pushbroom imaging used employs a CCD focal plane array, and capitalizes on the trajectory's perpendicularity to the CCD array to furnish 1.165-km sampling on the ground. O.C.

A88-42760

A VHF RADAR TO MAKE TERRAIN ELEVATION MODELS THROUGH TROPICAL JUNGLE

ROGER S. VICKERS (SRI International, Menlo Park, CA), RAYMOND T. LOWRY, and ARLEN D. SCHMIDT (Intera Technologies, Ltd., Calgary, Canada) IN: IEEE National Radar Conference, 3rd, Ann Arbor, MI, Apr. 20, 21, 1988, Proceedings. New York, Institute of Electrical and Electronics Engineers, Inc., 1988, p. 44-49. refs

A radar system is described, operating at 200-400 MHz, which produces profiles of the ground in the presence of dense tropical forest cover. The profiles can be assembled to construct a contour map of the terrain at scales as large as 1:10,000. The radar uses a 5-ns pulsewidth, and has achieved a total system accuracy of 2.5 m (vertical). A brief description is given of each of the major features of the radar system, including antennas, processor, and

radio frequency design. Examples are given of mapping products from a recent survey in Indonesia. Possible future improvements involving the use of the Global Positioning System are mentioned. I.E.

A88-43220

CROP CLASSIFICATION FROM AIRBORNE SYNTHETIC APERTURE RADAR DATA

G. M. FOODY (Kingston Polytechnic, Kingston upon Thames, England) International Journal of Remote Sensing (ISSN 0143-1161), vol. 9, April 1988, p. 655-668. refs

The ability of radar systems to record useful data independently of the prevailing weather conditions and the future increase in radar data availability is likely to result in their increased utilization for crop classification. However, a variety of factors relating to the quantity and quality of the data will influence the accuracy with which these data can be classified. This paper aims to illustrate the effect of some of these factors on crop classification accuracy from a multi-feature synthetic aperture radar data base. The results show that in addition to the number of data channels available for a classification, the method of radiometric correction applied to the data and the use of data from different look directions can have significant effects on the classification accuracy. The use of a multi-feature data base, however, was found to enable accurate discrimination of a variety of crop types. Author

A88-43221

USE OF DIGITAL TERRAIN DATA IN THE INTERPRETATION OF SPOT-1 HRV MULTISPECTRAL IMAGERY

A. R. JONES, B. K. WYATT (NERC, Institute of Terrestrial Ecology, Bangor, Wales), and J. J. SETTLE (NERC, Unit for Thematic Information Systems, Reading, England) International Journal of Remote Sensing (ISSN 0143-1161), vol. 9, April 1988, p. 669-682. refs

This paper describes the complementary use of digital terrain information and SPOT-1 HRV multispectral imagery for the study and mapping of semi-natural upland vegetation. A digital terrain model was derived for a 10 by 10 km study area in southern Snowdonia, Wales, and was used to generate slope and aspect images. A model was developed as a first-order approximation of changes in radiance with local topography, assuming Lambertian behavior of vegetation canopies. The model was implemented for the study area to assess its use in suppressing the effects of relief on scene radiance. Subsequently the model was refined to describe non-Lambertian reflectance. Author

A88-43222

POTATO CROP DISTRIBUTION AND SUBDIVISION ON SOIL TYPE AND POTENTIAL WATER DEFICIT - AN INTEGRATION OF SATELLITE IMAGERY AND ENVIRONMENTAL SPATIAL DATABASE

G. G. WRIGHT and J. G. MORRICE (The Macaulay Land Use Research Institute, Aberdeen, Scotland) International Journal of Remote Sensing (ISSN 0143-1161), vol. 9, April 1988, p. 683-699. refs

A88-43670

TAKING THE EFFECT OF VEGETATION INTO ACCOUNT IN THE MICROWAVE-RADIOMETER REMOTE SENSING OF THE EARTH SURFACE ON THE RESULTS OF REMOTE SOUNDING OF THE EARTH SURFACE BY MICROWAVE RADIOMETRY [OB UCHETE VLIANIYA RASTITEL'NOSTI PRI DISTANTSIONNOM SVCH-RADIOMETRICHESKOM ZONDIROVANII ZEMNYKH POKROVOV]

A. A. CHUKHLANTSEV and A. M. SHUTKO (AN SSSR, Institut Radiotekhniki i Elektroniki, Moscow, USSR) Issledovanie Zemli iz Kosmosa (ISSN 0205-9614), Mar.-Apr. 1988, p. 67-72. In Russian. refs

This paper describes a method for estimating the effect of vegetation on the characteristics of soil moisture content obtained by remote microwave radiometry. The method, based on the procedure of Kurdiashev and Chukhlantsev (1979) developed originally for single-wave measurements and a priori knowledge of

the vegetation transfer coefficient, uses spectral measurements and makes it possible to determine the moisture content without a priori information. Using both methods, it was shown that the moisture content of soil under vegetative cover with a mass of 200-300 centners/hectare could be obtained with errors that are about 10-30 percent higher than errors for an open surface. The errors obtained with the spectral-measurement method do not exceed the errors obtained with single-wave measurements. I.S.

A88-43671

CONTRAST ENHANCEMENT OF AEROSPACE SCANNER IMAGERY OF CROP FIELDS [POVYSHENIE KONTRASTNOSTI SKANERNYKH AEROKOSMICHESKIKH IZOBRAZHENI SEL'SKOKHOZIAISTVENNYKH POLEI]

A. S. BARYKIN and V. P. POPOV (Vsesoiuznyi Nauchno-Issledovatel'skii Tsentr AIUS-Agroresursy; Moscow, USSR) *Issledovanie Zemli iz Kosmosa* (ISSN 0205-9614), Mar.-Apr. 1988, p. 73-82. In Russian.

This paper presents a novel digital method that uses a moving contrast operator, which emphasizes intrafield brightness contrasts on aerospace scanner images of crop fields and makes it possible to restore smooth margins of the fields. The method increases crop classification distinctions and yields high-accuracy results on the phytopathological analysis of crops. Examples are presented using Landsat scanner images. I.S.

A88-43864

A SECOND GENERATION LUNAR AGRICULTURAL SYSTEM

JUDITH FIELDER and NICKOLAUS LEGGETT British Interplanetary Society, *Journal* (ISSN 0007-084X), vol. 41, June 1988, p. 263-268. refs

This paper presents a soil-based system of agriculture for use at a second generation lunar base. Enriched lunar regolith is used to grow food crops in pressurized agricultural modules. Estimated physical requirements and agricultural practices for a self-sustaining system are discussed. This agricultural system is designed to supplement and perhaps supplant hydroponic agricultural systems used for first generation applications. Author

A88-44116* Texas Univ., Arlington.

AN EMPIRICAL MODEL FOR POLARIZED AND CROSS-POLARIZED SCATTERING FROM A VEGETATION LAYER

H. L. LIU and A. K. FUNG (Texas, University, Arlington) *Remote Sensing of Environment* (ISSN 0034-4257), vol. 25, June 1988, p. 23-36. refs
(Contract NAG9-115)

An empirical model for scattering from a vegetation layer above an irregular ground surface is developed in terms of the first-order solution for like-polarized scattering and the second-order solution for cross-polarized scattering. The effects of multiple scattering within the layer and at the surface-volume boundary are compensated by using a correction factor based on the matrix doubling method. The major feature of this model is that all parameters in the model are physical parameters of the vegetation medium. There are no regression parameters. Comparisons of this empirical model with theoretical matrix-doubling method and radar measurements indicate good agreements in polarization, angular trends, and k sub a up to 4, where k is the wave number and a is the disk radius. The computational time is shortened by a factor of 8, relative to the theoretical model calculation. Author

A88-44117

THE EFFECT OF ATMOSPHERIC CORRECTION ON THE INTERPRETATION OF MULTITEMPORAL AVHRR-DERIVED VEGETATION INDEX DYNAMICS

S. M. SINGH (NERC, Unit for Thematic Information Systems, Reading, England) and R. J. SAULL (Reading, University, England) *Remote Sensing of Environment* (ISSN 0034-4257), vol. 25, June 1988, p. 37-51. refs
(Contract NERC-F60/G6/12)

The actual evapotranspiration and potential evapotranspiration data for the 1984 vegetation season over the United Kingdom

supplied by the UK Meteorological Office Rainfall and Evapotranspiration Calculation System are used to indicate moisture stress variation on the vegetation canopy. Raw and atmospherically corrected normalized difference vegetation indices (NDVIs) for the same period are calculated from 10 images obtained from the AVHRR in order to test the effect of the atmosphere on the NDVI dynamics interpretation. Comparison of the NDVI seasonal cycle (for various surface-cover types) with the moisture stress variation shows that: (1) there is a marked improvement in the understanding of the vegetation dynamics if remotely sensed data are corrected for atmospheric effects and (2) the relationship between the NDVI and moisture stress seems to depend on the type of vegetation present in the area in question. Author

A88-44119

SOIL AND ATMOSPHERE INFLUENCES ON THE SPECTRA OF PARTIAL CANOPIES

A. R. HUETE (Arizona, University, Tucson) and R. D. JACKSON (USDA, Water Conservation Laboratory, Phoenix, AZ) *Remote Sensing of Environment* (ISSN 0034-4257), vol. 25, June 1988, p. 89-105. refs

Ground-measured radiances over partially vegetated canopies with their simulated responses at the top of a clear 100 km meteorological range and a turbid 10 km atmosphere are compared using an atmospheric radiant transfer model. Atmospheric influences on the spectra of partial canopies were found to be dependent on the brightness of the underlying soil. Both increasing soil brightness and atmospheric turbidity lower the ratio vegetation index (RVI) and normalized difference vegetation index (NDVI) values. Atmospheric-induced RVI and NDVI degradation were greatest over canopies with darker soils and were not detectable over canopies with light-colored soils, whereas soil and atmospheric effects on the perpendicular vegetation index were independent with atmosphere degradation being similar across all soil backgrounds. R.B.

A88-44307

RADAR BACKSCATTER CHARACTERISTICS OF TREES AT 215 GHZ

RAM MOHAN NARAYANAN, CHRISTOPH C. BOREL, and ROBERT E. MCINTOSH (Massachusetts, University, Amherst) *IEEE Transactions on Geoscience and Remote Sensing* (ISSN 0196-2892), vol. 26, May 1988, p. 217-228. refs
(Contract DAAG29-85-K-0227)

Millimeter-wave backscatter measurements are presented for various tree types taken during the 1987 growing season at Amherst, Massachusetts. These measurements were taken with a 215-GHz radar system that is capable of measuring backscatter for the VV (vertical transmit, vertical received), HH (horizontal transmit, horizontal received), VH, and HV polarizations. Geometrical optics modeling was used for the normalized radar cross section (RCS) of deciduous trees and the backscatter is shown to be characterized in terms of gravimetric leaf water content, the leaf area, and the foliage crown cover. Data are also provided for coniferous trees, although the geometrical optics model is not applicable in those cases. I.E.

A88-44308

MILLIMETER-WAVE BISTATIC SCATTERING FROM GROUND AND VEGETATION TARGETS

FAWWAZ T. ULABY, TAHERA E. VAN DEVENTER, JACK R. EAST, THOMAS F. HADDOCK, and MICHAEL EUGENE COLUZZI (Michigan, University, Ann Arbor) *IEEE Transactions on Geoscience and Remote Sensing* (ISSN 0196-2892), vol. 26, May 1988, p. 229-243. refs

A 35-GHz bistatic radar system was used to measure the attenuation through trees and the bistatic scattering pattern of tree foliage. The data were found to be in good agreement with a first-order multiple scattering model. Measurements were also made to study the angular vibration of the bistatic scattering coefficient of a smooth sand surface, a rough sand surface, and a gravel surface. The measurements, which were made for HH, HV (horizontal transmit, vertical receive), and VV polarization

01 AGRICULTURE AND FORESTRY

configurations over a wide range of the azimuth angle and the scattering angle, provide a quantitative reference for the design and use of millimeter-wave bistatic radar systems. I.E.

A88-44319#

MILLIMETER-WAVE PROPAGATION IN VEGETATION: EXPERIMENTS AND THEORY

FELIX K. SCHWERING (U.S. Army, Communications Electronics Command, Fort Monmouth, NJ), EDMOND J. VIOLETTE, and RICHARD H. ESPELAND (National Telecommunications and Information Administration, Institute for Telecommunication Sciences, Boulder, CO) IEEE Transactions on Geoscience and Remote Sensing (ISSN 0196-2892), vol. 26, May 1988, p. 355-367. refs

Microwave/millimeter-wave propagation in woods and forests was investigated at 9.6, 28.8, and 57.6 GHz. The experiments were repeated over the same transmission paths, under both summer and winter conditions, i.e., with tree in leaf and without leaves. Of particular interest were the range dependence, beam broadening, and depolarization of millimeter-wave beams in vegetation and frequency dependence of these effects. The experiments have shown, in particular, that the range dependence is characterized by a high attenuation rate at short vegetation depths and a reduced attenuation rate at large depth. For trees fully in leaf, the transition between the two regimes can be abrupt and the change in attenuation rate substantial. Just after the transition significant beam broadening (and depolarization) occurs. A theory of millimeter-wave propagation in vegetation was derived using transport theory. Theoretical and experimental results are in good qualitative agreement; both show the same trends. The theory explains these trends in terms of the interplay between the coherent (direct path) field component and the incoherent (multiscattered) field component. Good quantitative agreement will require further refinement of the theory. I.E.

A88-44521 Thessaloniki Univ. (Greece).

MANUAL INTERPRETATION OF SMALL FORESTLANDS ON LANDSAT MSS DATA

MICHAEL A. KARTERIS (Salonika, University, Greece) Photogrammetric Engineering and Remote Sensing (ISSN 0099-1112), vol. 54, June 1988, p. 751-755. Research supported by the Michigan Department of Natural Resources and NASA. refs

The use and potential of Landsat MSS images for interpretation and mapping small scattered forestlands were evaluated in this study. Four images - two from late winter (a black-and-white band 5 and a color composite) - and two from early fall (a color composite and a diazo-enhanced color composite) - were tested. Forestlands were interpreted and mapped from each Landsat image and the resulting maps were compared with various other sources. The detected interpretation errors were categorized as commission and omission, and were further classified into errors of boundary placement (over 85 percent of the cases) and errors of identification. Over 55 percent of all errors were less than 2.0 hectares in size. The most frequently misclassified areas were agricultural lands, treed-bogs, brushlands, lowland hardwoods, and mixed hardwoods. Oak-hickory was the most accurately interpreted forest type category. The overall interpretation performance, which was expressed by two types of accuracy (identification and mapping), ranged between 74 and 95 percent. The best results were obtained from the interpretation of the winter color composite with snow on the ground. Author

A88-44643* California Univ., Santa Barbara.

SIMULATION OF L-BAND AND HH MICROWAVE BACKSCATTERING FROM CONIFEROUS FOREST STANDS - A COMPARISON WITH SIR-B DATA

GUO-QING SUN and DAVID S. SIMONETT (California, University, Santa Barbara) International Journal of Remote Sensing (ISSN 0143-1161), vol. 9, May 1988, p. 907-925. refs (Contract JPL-956887)

SIR-B images of the Mt. Shasta region of northern California are used to evaluate a composite L-band HH backscattering model

of coniferous forest stands. It is found that both SIR-B and simulated backscattering coefficients for eight stands studied have similar trends and relations to average tree height and average number of trees per pixel. Also, the dispersion and distribution of simulated backscattering coefficients from each stand broadly match SIR-B data from the same stand. Although the limited quality and quantity of experimental data makes it difficult to draw any strong conclusions, the comparisons indicate that a stand-based L-band HH composite model seems promising for explaining backscattering features. R.B.

A88-44644* Jet Propulsion Lab., California Inst. of Tech., Pasadena.

SHUTTLE RADAR MAPPING WITH DIVERSE INCIDENCE ANGLES IN THE RAINFOREST OF BORNEO

J. P. FORD and D. J. CASEY (California Institute of Technology, Jet Propulsion Laboratory, Pasadena) International Journal of Remote Sensing (ISSN 0143-1161), vol. 9, May 1988, p. 927-943. refs

N88-20711*# Massachusetts Inst. of Tech., Cambridge. Research Lab. of Electronics.

REMOTE SENSING OF EARTH TERRAIN Semiannual Report, 1 Sep. 1987 - 29 Feb. 1988

J. A. KONG 28 Apr. 1988 17 p

(Contract NAG5-270)

(NASA-CR-182677; NAS 1.26:182677) Avail: NTIS HC A03/MF A01 CSCL 08B

A systematic approach for the identification of terrain media such as vegetation canopy, forest, and snow covered fields is developed using the optimum polarimetric classifier. The covariance matrices for the various terrain covers are computed from the theoretical models of random medium by evaluating the full polarimetric scattering matrix elements. The optimal classification scheme makes use of a quadratic distance measure and is applied to classify a vegetation canopy consisting of both trees and grass. Experimentally measured data are used to validate the classification scheme. Theoretical probability of classification error using the full polarimetric matrix are compared with classification based on single features including the phase difference between the VV and HH polarization returns. It is shown that the full polarimetric results are optimal and provide better classification performance than single feature measurements. A systematic approach is presented for obtaining the optimal polarimetric matched filter which produces maximum contrast between two scattering classes, each represented by its respective covariance matrix. Author

N88-21553 Institut National de la Recherche Agronomique, Paris (France).

MODELING SURFACE EXCHANGES: THE SOIL-VEGETATION-ATMOSPHERE CONTINUUM [MODELISATION DES ECHANGES DE SURFACE: CONTINUUM SOL-PLANTE-ATMOSPHERE]

A. D. PERRIER In CNES, Climatology and Space Observations p 423-456 Sep. 1987 In FRENCH

Avail: CEPADUES-Editions, 111 rue Nicolas-Vauquelin, 31100 Toulouse, France

The basic processes regulating the exchange of climatic factors are described in order to calculate climatic balances. The application of notions such as flow resistance and surface potential is suggested. It is shown that the soil-vegetation-atmosphere complex may be treated in space diversity as a single entity. The adopted method is based on the linearization of the temperature gradients. The applications discussed include a model of soil surface, a vegetation model, and equilibrium temperature determination. ESA

N88-22448# Environmental Protection Agency, Research Triangle Park, N.C. Atmospheric Sciences Research Lab.

ASSESSMENT OF CROP LOSS FROM AIR POLLUTANTS: METEOROLOGY-ATMOSPHERIC CHEMISTRY AND LONG RANGE TRANSPORT

A. P. ALTSULLER Dec. 1987 49 p
(PB88-146857; EPA-600/D-87-366) Avail: NTIS HC A03/MF
A01 CSCL 02C

The scales of intermediate and longer range transport influencing the atmospheric distribution of O₃ are discussed. Atmospheric concentrations of O₃ can vary substantially during each day, from day to day, and with the season of the year as well as with geographical location. In contrast to ozone, sulfur dioxide is a primary pollutant. Both the sources of SO₂ and its mechanisms of removal can be much different than for ozone. Sulfur dioxide exposures tend to be of concern on a local rather than a regional scale. Author

N88-22452*# Alabama A & M Univ., Huntsville. Center for Application of Remote Sensing.

DEVELOPMENT OF REMOTE SENSING TECHNIQUES CAPABLE OF DELINEATING SOILS AS AN AID TO SOIL SURVEY Final Report, 1 Oct. 1984 - 1 Mar. 1986

T. L. COLEMAN and O. L. MONTGOMERY 12 Apr. 1988 28 p
(Contract NAG13-3)
(NASA-CR-182610; NAS 1.26:182610; ACARS-123187) Avail:
NTIS HC A03/MF A01 CSCL 08M

Eighty-one benchmark soils from Alabama, Georgia, Florida, Tennessee, and Mississippi were evaluated to determine the feasibility of spectrally differentiating among soil categories. Relationships among spectral properties that occur between soils and within soils were examined, using discriminant analysis. Soil spectral data were obtained from air-dried samples using an Exotech Model 20C field spectroradiometer (0.37 to 2.36 microns). Differentiating among the orders, suborders, great groups, and subgroups using reflectance spectra achieved varying percentages of accuracy. Six distinct reflectance curve forms were developed from the air-dried samples based on the shape and presence or absence of adsorption bands. Iron oxide and organic matter content were the dominant soil parameters affecting the spectral characteristics for differentiating among and between these soils. Author

N88-23315# Instituto de Pesquisas Espaciais, Sao Jose dos Campos (Brazil).

USE OF ENERGY EMISSION FOR DETECTING THE NECESSITY OF IRRIGATION IN WHEAT IN FIELD CONDITIONS M.S. Thesis [USO DE ENERGIA EMITIDA, PARA DETECTAR NE CESSIDADE DE IRRIGACAO EM TRIGO, EM CONDICAOES DE CERRADO]

RUBENS AUGUSTO CAMARGOLAMPARELLI Apr. 1988 99 p
In PORTUGUESE; ENGLISH summary
(INPE-4461-TDL/318) Avail: NTIS HC A05/MF A01

Through the utilization of plant parameters (radiometric canopy temperature, T sub d, aerodynamic and canopy resistances) and meteorological data (air temperature, T sub A, global net radiation, R sub n, vapor pressure deficit in air, delta e), which are components of the Index (CWSI), the utility of this methodology is demonstrated to identify the plant water status and detect irrigation necessity. The objectives of this methodology were to: observe the T sub d behavior with irrigation levels; verify cloud and wind influences in the T sub d; and to observe the index (CWSI) behavior, as an indicative irrigation necessity. That experiment was performed in the Centro de Pesquisas Agropecuarias dos Cerrados (CPAC) and consists of three parcels with the following treatments: daily irrigation; irrigation (day 50 after the seedling growth); two irrigations (days 50 and 60 after seedling growth), in the booting period. At thirty-day intervals, T sub A, T sub d, R sub n, wind velocity, soil water potential data and plant parameters were collected daily. The results showed that the radiometric canopy temperature and the index (CWSI) had a relationship according to the treatments verified through the data. The wind influence was only observed in radiometric canopy temperature and cloud appearance provoked changes in the radiometric canopy temperature as well as in the index (CWSI). The qualitative analysis was possible only because of the small sensibility of some systems of measurement. Author

N88-23322# Instituto de Pesquisas Espaciais, Sao Jose dos Campos (Brazil).

DETECTION, MONITORING AND ANALYSIS OF SOME ENVIRONMENTAL EFFECTS OF FIRES IN THE AMAZON REGION THROUGH UTILIZATION OF NOAA AND LANDSAT SATELLITE IMAGERY AND AIRCRAFT DATA M.S. Thesis [DETECCAO, MONITORAMENTO E ANALISE DE ALGUNS EFEITOS AMBIENTAIS DE QUEIMADAS NA AMAZONIA ATRAVES DA UTILIZACAO DE IMAGENS DOS SATELITES NOAA E LANDSAT, E DADOS DE AERONAVE]

MARCOS DACOSTAPEREIRA 1987 258 p In PORTUGUESE; ENGLISH summary
(INPE-4503-TDL/326) Avail: NTIS HC A12/MF A01

The purpose is to analyze, using orbital remote sensing as a main tool, some of the environment effects caused by combustion of large amounts of biomass in the Amazon forest. During the GTE/ABLE-2A, an experiment to measure trace gases and aerosols in the Amazon troposphere from July 19 to August 8, 1985, twenty-five images of the NOAA-8 and 9 satellites were recorded, in which many smoke plumes and fires of large dimensions were detected. After locating the areas most affected by the fires, LANDSAT/TM images of the same place were processed and the spectral characteristics of the fires and burned sites were studied with both satellites. With radiosounding data a trajectory analysis of the emissions were performed in order to study the long-range transport of pollutants. Based on aircraft sampling data from GTE/ABLE-2A an estimate was performed of the amounts of gases and aerosols produced by regional and global effects. Author

N88-24015*# Jet Propulsion Lab., California Inst. of Tech., Pasadena.

RADAR PENETRATION IN THE AMAZONIAN RAIN FOREST

Abstract Only

ROBERTO PEREIRADACUNHA (Instituto de Pesquisas Espaciais, Sao Jose dos Campos, Brazil) and JOHN FORD In INPE, Latin American Symposium on Remote Sensing. 4th Brazilian Remote Sensing Symposium and 6th SELPER Plenary Meeting, Volume 1 p 58 1986

Avail: NTIS HC A99/MF E03

Radar return from vegetation covered terrains is due to three components: the scattering resulting from the top surface of the vegetation canopy (surface scattering); the scattering which occurs within the vegetation layer (volume scattering); and the scattering which takes place at the surface below the vegetation canopy (ground scattering). Through the studies of selected areas in the Amazon Region a case is presented where most of the radar returns observed in radar imagery results from the scattering at the surface below vegetation layer (ground scattering). Thus, radar penetration occurred. Author

N88-24016# Instituto de Pesquisas Espaciais, Sao Jose dos Campos (Brazil).

A PROPOSAL FOR A PROJECT ENTITLED ASSESSMENT OF FOREST RESOURCES IN URUGUAY SUBMITTED TO THE UNITED NATIONS INDUSTRIAL DEVELOPMENT ORGANIZATION (UNIDO) Abstract Only

RENE ANTONIO NOVAES, DAVID CHUNG LIANG LEE, PEDRO HERNANDEZ FILHO, ARMANDO PACHECODOSSANTOS, and FLAVIO JORGE PONZONI In its Latin American Symposium on Remote Sensing. 4th Brazilian Remote Sensing Symposium and 6th SELPER Plenary Meeting, Volume 1 p 59 1986

Avail: NTIS HC A99/MF E03

The main objective of this project is to collect basic forest information for the development, promotion, and utilization of alternative sources of energy through the use of national resources, and to determine the value of LANDSAT-TM data as an aid in efficient management of Uruguay's plantations. An additional objective is to train a Uruguayan technical team. Indications are given as to how each task will be accomplished and what techniques will be employed in performing main tasks such as: forest mapping and development of the map legends; map accuracy assessment and forest area correction; stand timber volume

01 AGRICULTURE AND FORESTRY

evaluation; and field sampling and mensuration procedures. In addition, information was included concerning: project flow diagram; activity bar diagrams; and equipment required for task accomplishment. The required specific results of maps and timber volumes were mentioned. Author

N88-24023# Silsoe Coll., Bedford (England).
MAPPING SOIL AND ROCK VARIATION FROM SATELLITE IMAGES IN THE SAHEL Abstract Only

JOHN TAYLOR, ALAN BELWARD, DAVID HEWITT, and BARRY WYATT /n INPE, Latin American Symposium on Remote Sensing. 4th Brazilian Remote Sensing Symposium and 6th SELPER Plenary Meeting, Volume 1 p 131 1986
Avail: NTIS HC A99/MF E03

The use of the Soil Brightness Index (SBI) for mapping soil and rock variation in arid and semi-arid conditions with partial vegetation cover was investigated. The test site was near Kao in the Sahelian pasturelands of the Republic of Niger. Field visits were undertaken to characterize the range of cover types in the study area and to establish training areas which could be located on LANDSAT 5 MSS imagery. The main rock types were laterites in easily identifiable outcrops. Soils consisted of fractured laterite close to the outcrops progressing through various mixtures of clay outwash with laterite gravel to clay outwash furtherest from the outcrop. Spectral reflectance measurements of surface soils, rocks, and vegetation were made in the field using a portable seven-band radiometer. The relationship between reflectances of the bare soil and rock categories in the red and infrared wavebands was determined by linear regression. The equation of the soil line for the MSS image was used to calculate a transform equation to calculate the value of the SBI for each pixel of the Kao test area. Author

N88-24030# Paraiba Univ., Joao Pessoa (Brazil).
IDENTIFICATION OF SHALLOW GROUNDWATER REGIONS IN SEMI-ARID BRAZIL BY REMOTE SENSING METHODS Abstract Only

S. V. KAMESWARA SARMA /n INPE, Latin American Symposium on Remote Sensing. 4th Brazilian Remote Sensing Symposium and 6th SELPER Plenary Meeting, Volume 1 p257 1986
Avail: NTIS HC A99/MF E03

Employing remote sensing techniques for identifying regions with shallow groundwater depths is a recent advance reported by Menenti (1984). In semi-arid and arid regions, the evaporation can be reliably determined by soil balance methods. A rugged crust overlying a 20 cm deep groundwater table or a smooth hard, very dry soil surface overlying a 1 m deep water table are examples that can be cited to establish the efficacy of this method. However, initial calibration by a thermal infrared radiometer or a neutron probe of ground reference points would be necessary to establish the required relationships for the interpretation of the data. The field data from observed piezometric heads would help in finding the detailed groundwater flow pattern. The large daily amplitudes of surface temperatures observed in soft friable surfaces where groundwater discharge occurs is taken advantage of in predicting the shallow groundwater regions. Using the soil water flow simulation model SWATR, relationships between shallow groundwater depth and ratio of actual to potential evaporation could be obtained. The potentially useful role of remotely sensed data to study the soil layering, surface energy balance, and evaporation of semi-arid and arid regions of north-east Brazil is stressed. Author

N88-24036# Sociedad Colombiana de Fotogrametria y Percepcion Remota, Bogota.

THE USE OF SLAR AND SIRA IMAGENES FOR THE CLASSIFICATION OF FOREST TYPEN IN TROPICAL RAIN FORESTS Abstract Only

LUIS CARLOS MOLINAMARINO /n INPE, Latin American Symposium on Remote Sensing. 4th Brazilian Remote Sensing Symposium and 6th SELPER Plenary Meeting, Volume 1 p 323 1986
Avail: NTIS HC A99/MF E03

The use of the three radar systems, two airborne (Westinghouse and Goodyear) and one spaceborne (SIR-A) for delineation and classification of biomass, ecosystem, and forest types in different ecological conditions of tropical rain forest in Columbia are described. The results are shown in a comparative form with respect to its use. The reflection of vegetation is analyzed in a comparative form with its advantages and limitations. Furthermore, this work presents the classification systems for tropical rain forests utilizing remote sensing imagery. Author

N88-24041# Universidad Nacional de Lujan (Argentina).
ESTIMATION OF AN AREA CULTIVATED WITH WHEAT FROM LANDSAT DATA THROUGH A TWO-PHASE SAMPLING METHOD Abstract Only [ESTIMACION DEL AREA CULTIVADA CON TRIGO A PARTIR DE DATOS LANDSAT MEDIANTE EL METODO DE MUESTREO EN DOS FASES]

CARLOS A. CAPPELLETTI and MARIA C. SERAFINI /n INPE, Latin American Symposium on Remote Sensing. 4th Brazilian Remote Sensing Symposium and 6th SELPER Plenary Meeting, Volume 1 p 357-360 1986 In SPANISH; ENGLISH summary
Avail: NTIS HC A99/MF E03

The objective is to estimate the cultivated area of wheat using combined ground and LANDSAT data through a two-phase sampling system with estimation of regression, fixed error rate, and minimum cost. The result obtained was 92.217 ha with a coefficient of variation of 8.93 percent. The results compared with the simulated system by a Monte Carlo technique presented an error (relative difference) of 1.73 percent. Author

N88-24042# Sao Paulo Univ. (Brazil). Escola Superior de Agricultura.

UTILIZATION OF TM/LANDSAT IMAGES IN THE IMPLANTED FORESTS MAPPING IN THE MOGI-GUACU REGION (SP-BRAZIL) [UTILIZACAO DE IMAGENS TM/LANDSAT NO Mapeamento de Florestas Implantadas na Regiao de Mogi-Guacu (SP-Brazil)]

CARLOS A. VETTORAZZI and HILTON T. Z. DOCOUTO /n INPE, Latin American Symposium on Remote Sensing. 4th Brazilian Remote Sensing Symposium and 6th SELPER Plenary Meeting, Volume 1 p 361-365 1986 In PORTUGUESE; ENGLISH summary
Avail: NTIS HC A99/MF E03

Through the visual interpretation of TM/LANDSAT images and field checking, the forest cover mapping was made of the Horto Mogi-Guacu (Mogi-Guacu-SP). The analysis of the obtained results led to the conclusion that the utilization of images from the spectral bands 3, 4, and 5 were efficient for the forest cover mapping, allowing the discrimination of seven different classes of occupation of the stands: stands being reformed; various native species; angico (*Piptadenia* spp); tropical pine; eucalypts up to one year old; eucalypts between one and two years old; and eucalypts over two years old. Author

N88-24043# Instituto de Pesquisas Espaciais, Sao Jose dos Campos (Brazil).

ANOMALIES IN THE VEGETATION IN THE ALTO XINGU - MT [ANOMALIAS DE VEGETACAO NO ALTO XINGU - MT]
MARIA DELOURDESBUENOTRINDADE, ROBERTO PEREIR-ADACUNHA, and PEDRO HERNANDEZ FILHO /n its Latin American Symposium on Remote Sensing 4th Brazilian Remote Sensing Symposium and 6th SELPER Plenary Meeting, Volume 1 p 366-372 1986 In PORTUGUESE; ENGLISH summary
Avail: NTIS HC A99/MF E03

The MSS and TM LANDSAT data showed anomalies in the vegetal cover in the transition between Amazonian rain forests and cerrado, Brazilian tropical savannah. The study was carried out in the Alto Xingu region (Mato Grosso state, Brazil). Through visual interpretation a map was made showing the spatial distribution of the anomalies in the study area. In order to do the multitemporal monitoring of the anomalies, a test area was selected and MSS images of two different dates were visually interpreted. Within the tests area, for these two dates, a thematic classification

through digital analysis was also carried out on the I-100 Image Analyzer. The auxiliary data used were color infrared photographs (scale 1:15,000) and field information. Author

N88-24044*# Jet Propulsion Lab., California Inst. of Tech., Pasadena.

RADAR PENETRATION IN THE AMAZONIAN RAIN FOREST

ROBERTO PEREIRADACUNHA (Instituto de Pesquisas Espaciais, Sao Jose dos Campos, Brazil) and JOHN P. FORD *In its* Latin American Symposium on Remote Sensing. 4th Brazilian Remote Sensing Symposium and 6th SELPER Plenary Meeting, Volume 1 p 373-374 1986
Avail: NTIS HC A99/MF E03

Radar return from vegetation covered terrains is due to three components: the scattering resulting from the top surface of the vegetation canopy (surface scattering); the scattering which occurs within the vegetation layer (volume scattering); and the scattering which takes place at the surface below the vegetation canopy (ground scattering). Through the studies of selected areas a case is presented where most of the radar return observed in radar imageries results from the scattering at the surface below the vegetation layer (ground scattering). Author

N88-24045# Instituto de Pesquisas Espaciais, Sao Jose dos Campos (Brazil).

REMOTE SENSING TECHNIQUES IN THE ESTIMATION OF THE AREA CULTIVATED WITH BEANS, CORN, AND CASTOR BEANS IN THE IRECE COUNTY (BAHIA STATE)
[SENSORIAMENTO REMOTO NA ESTIMATIVA DA AREA PLANTADA COM FEIJAO, MILHO E MAMONA NO MUNICIPIO DE IRECE]

BERNARDO F. T. RUDORFF and THELMA KRUG *In its* Latin American Symposium on Remote Sensing. 4th Brazilian Remote Sensing Symposium and 6th SELPER Plenary Meeting, Volume 1 p 380-384 1986 In PORTUGUESE; ENGLISH summary
Avail: NTIS HC A99/MF E03

The objective was to obtain an estimation of the areas cultivated with beans, corn, and castor beans in the Irece county (Bahia State) using statistical and remote sensing techniques. Using a topographic chart at a scale of 1:100,000 the county area was divided into approximately 2000 segments of 2 x 1 km. A random sample of 97 segments (corresponding to 5 percent of the target area) was considered. Over these segments aerial vertical photographs were obtained in the approximate scale of 1:40,000 by means of a 35 mm camera with a wide-angle of 28 mm focal length lens aboard a Cherokee-six aircraft. The projection of the aerial color photographs over 1:5000 cadastral maps available in the region made it possible to extract the thematic information of the planted areas of interest. Subsequently an evaluation of the area cultivated with beans, corn, and castor beans was made. From the results the estimates (punctual and by interval) were obtained and the following results encountered: 87,759 ha with beans, 76,519 ha with castor beans, and 10,550 ha with corn. Author

N88-24046# Instituto de Pesquisas Espaciais, Sao Jose dos Campos (Brazil).

CANASATE: SUGAR CANE MAPPING BY SATELLITE
[CANASATE - MAPEAMENTO DA CANA-DE-ACUCAR POR SATELLITE]

FRANCISCO JOSE MENDONCA *In its* Latin American Symposium on Remote Sensing. 4th Brazilian Remote Sensing Symposium and 6th SELPER Plenary Meeting, Volume 1 p 385-393 1986 In PORTUGUESE; ENGLISH summary
Avail: NTIS HC A99/MF E03

The CANASATE Project, sugarcane mapping by satellite, has the objective of obtaining the spatial distribution and area estimation of sugarcane plantations, at national level, using remote sensing techniques. To achieve this objective, Brazil was divided into three areas: Area 1, which includes Rio de Janeiro, Sao Paulo, and Parana states; Area 2, which includes Alagoas, Pernambuco, Paraiba, and Rio Grande do Norte states; and Area 3, which includes Minas Gerais, Espirito Santo, Goias, and Mato Grosso

do Sul states. The results show that Area 1 represents approximately 60 percent of the national sugarcane plantations. Twenty-three thematic maps on the scale of 1:250,000 were obtained using LANDSAT MSS or TM images of 1983 and 1984. The results were: 236,635 ha in Rio de Janeiro state; 2,158,000 ha in Sao Paulo state; and 135,859 ha in Parana state. The overall average accuracy on the estimation was 91 percent. Author

N88-24047# Instituto de Pesquisas Espaciais, Sao Jose dos Campos (Brazil).

SPECTRAL BEHAVIOR OF CROPS THROUGH ANALYSIS OF LANDSAT-TM DATA [COMPORTAMENTO ESPECTRAL DE CULTURAS A PARTIR DA ANALISE DE DADOS DO LANDSAT TM]

SHERRY CHOU CHEN, JEAN FRANCOIS DALLEMAND, and DANIEL ALFREDO ROSENTHAL *In its* Latin American Symposium on Remote Sensing. 4th Brazilian Remote Sensing Symposium and 6th SELPER Plenary Meeting, Volume 1 p 394-401 1986 In PORTUGUESE; ENGLISH summary
Avail: NTIS HC A99/MF E03

The LANDSAT-TM digital data of January 19, 1985, were requested for a 15 x 15 km area near Maringa, Parana State to study spectral response of agricultural crops of soybeans, corn, and sugarcane. Study results show that correlations were found between spectral data of visible bands (band 1, 2, and 3) and infrared bands (band 4 vs 5 and band 5 vs 7). Among the six TM bands analyzed, bands 4 and 5 contained more information than the others. For crop discrimination using single TM bands, band 4 was the best even though differentiations of soybeans from non-soybeans was possible in bands 5 and 7. These preliminary results indicate not only the potential of LANDSAT-TM data for crop discrimination, but also differentiations of sugarcane varieties and the soybean biomass. Author

N88-24048# Empresa Brasileiro de Pesquisa Agropecuaria, Planaltina.

IDENTIFICATION OF AREAS CULTIVATED WITH SOYBEANS IN THE CERRADOS REGIONS, THROUGH DIGITAL PROCESSING OF SATELLITE IMAGES: A METHODOLOGICAL APPROACH [IDENTIFICACAO DE AREAS CULTIVADAS COM SOJA NOS CERRADOS, ATRAVES DO PROCESSAMENTO DIGITAL DE IMAGENS DE SATELITE: UM APORTE METODOLOGICO]

PAULO JORGE ROSACARNEIRO *In its* Latin American Symposium on Remote Sensing. 4th Brazilian Remote Sensing Symposium and 6th SELPER Plenary Meeting, Volume 1 p 402-417 1986 In PORTUGUESE; ENGLISH summary
Avail: NTIS HC A99/MF E03

Soybean growing recently introduced in the cerrado region, has shown exceptional growth in areal extent every year. Digital processing of LANDSAT images makes it possible to accompany this evolution with efficiency, providing precise data such as area planted and expected yield, of great use in planning actions necessary for strengthening this sector. Author

N88-24049# Instituto de Pesquisas Espaciais, Sao Jose dos Campos (Brazil).

STRUCTURE AND DYNAMICS OF VEGETATION IN THE MIDDLE SEMI-ARID TROPICS. QUIXABA'S CAATINGA (PE): TERRAIN ANALYSIS OF MSS/LANDSAT DATA [ESTRUTURA E DINAMICA DA VEGETACAO EM MEIO TROPICAL SEMI-ARIDO. A CAATINGA DE QUIXABA (PE): DO TERRENO A ANALISE DE DADOS MSS/LANDSAT]

VITOR CELSODECARVALHO *In its* Latin American Symposium on Remote Sensing. 4th Brazilian Remote Sensing Symposium and 6th SELPER Plenary Meeting, Volume 1 p 418-426 1986 In PORTUGUESE; ENGLISH summary
Avail: NTIS HC A99/MF E03

Estimation of practicability and limits of MSS/LANDSAT data for monitoring and the control of the tropical semi-arid ecosystems from a test region of Brazilian Nordeste, north of Petrolina-PE (Quixaba) and their vegetal cover are presented. A structural classification of the vegetation is developed and applied. Then, a

01 AGRICULTURE AND FORESTRY

1:100,000 scale structural mapping, drawn from the 1955, 1965, and 1983 aerial photographs, allows structural characterization and dynamic evaluation of the Quixabas Caatinga. The power discrimination of the images from four MSS/LANDSAT scenes (1973, 1974, and 1983-2) numerical processing, are estimated, by comparison to vegetation structure maps: while in these maps, 15 thematic classes are distinguished, only 7 are available on the classified picture (maximum). Author

N88-24072# Instituto de Pesquisas Espaciais, Sao Jose dos Campos (Brazil).

INTERPRETATION OF MSS/LANDSAT DATA FOR EVALUATION OF PHYSICAL DISTRIBUTION OF MANGROVES IN CANANEIA-IGUAPE (SP) [INTERPRETACAO DE DADOS MSS/LANDSAT PARA AVALIAR A DISTRIBUICAO FISICA DOS MANGUEZAIS DE CANANEIA-IGUAPE (SP)]

CARMEN REGINA SILVEIRAESPINDOLA *In its* Latin American Symposium on Remote Sensing. 4th Brazilian Remote Sensing Symposium and 6th SELPER Plenary Meeting, Volume 1 p 604-614 1986 In PORTUGUESE; ENGLISH summary
Avail: NTIS HC A99/MF E03

Mangrove is considered responsible for the high productivity of biological and ecological coastal systems. However, it is unknown and strongly destroyed, requiring appropriate research techniques to provide fast and cheap procedures for its identification. Remote sensing techniques using digitally processed satellite data, were found to be valuable not only for its low cost, but also for its overall view. The objective is to evaluate the physical distribution of Cananeia-Iguape mangroves using MSS-LANDSAT image processing and correlate it with radar images and aerial photographs. A statistical classification performed by algorithms used by the Multispectral Interactive Image Analyzing System (IMAGE-100) provided a thematic map with 13 mangrove units from which areas were calculated and correlated with areas obtained from panchromatic aerial photographs and from radar images. The results indicate very high linear correlation coefficients ($r = 0.99$) which showed that the use of MSS-LANDSAT products are good enough to spectrally separate mangroves from other soil cover types. Author

N88-24075# Instituto de Pesquisas Espaciais, Sao Jose dos Campos (Brazil).

EVALUATION OF AN ESTIMATION SYSTEM FOR AN IRRIGATED AREA IN A TROPICAL REGION THROUGH TM-LANDSAT IMAGERY [AVALIACAO DE UM SISTEMA DE ESTIMATIVA DE AREA IRRIGADA EM REGIAO TROPICAL ATRAVES DE IMAGENS TM-LANDSAT]

SHERRY C. CHEN, EVELYN M. LEO NOVO, SERGIO DOSANJOS F. PINTO, MARIO VALERIO FILHO, and ROBERTO ROSA (Universidade Federal de Uberlandia, Brazil) *In its* Latin American Symposium on Remote Sensing. 4th Brazilian Remote Sensing Symposium and 6th SELPER Plenary Meeting, Volume 1 p 630-637 1986 In PORTUGUESE; ENGLISH summary
Avail: NTIS HC A99/MF E03

A joint project of the Sao Paulo State Department of Water and Energy (DAEE) and INPE was performed to evaluate the possibility of using LANDSAT-TM imagery for irrigated area estimation in the water basin of Piracicaba. Successful studies were reported in the semi-arid region where the identification of irrigated areas using remotely sensed data obtained during the dry season is relatively trivial due to the presence of green biomass. However, in the tropical environment, there is no well defined dry period and the cropping and irrigation systems are diversified, these factors make the task of estimating irrigated areas difficult. Two methods were proposed to estimate irrigated areas: direct expansion of field information collected in sampled segments when LANDSAT data are not available and regression estimation using ground-gathered data of sampled segments and multitemporal LANDSAT false color images. Study results show that when the LANDSAT data were used and incorporated to ground information of the randomly selected segments, a reduction of 94.02 percent in variance of the estimated acreage was achieved compared to

that obtained using the approach of direct expansion. The advantages and limitations of using LANDSAT data to estimate irrigated areas in tropical climates are also presented. Author

N88-24086# Instituto de Pesquisas Espaciais, Sao Jose dos Campos (Brazil).

EVALUATION OF THE MANGROVE AREA AT THE PIAUI RIVER (SE) THROUGH REMOTE SENSING [AVALIACAO DAS AREAS DE MANGUEZAL DO RIO PIAUI (SE) ATRAVES DE SENSORIAMENTO REMOTO]

MYRIAN DEMOURAABDON, CARMEN REGINA S. ESPINDOLA, DALTON DEM. VALERIANO, ERNESTO GETULIOMVIEIRA, ALBERTO W. SETZER, AUXILIADORA MARIA SANTOS, and YARA SCHAEFFER NOVELLI (Sao Paulo Univ., Brazil) *In its* Latin American Symposium on Remote Sensing. 4th Brazilian Remote Sensing Symposium and 6th SELPER Plenary Meeting, Volume 1 p 710-713 1986 In PORTUGUESE; ENGLISH summary
Avail: NTIS HC A99/MF E03

The purpose is to estimate the areas of mangroves at the estuary of the River Piaui (SE) with remote sensing techniques, and also to evaluate any degradation of these areas associated with the growing industrialization in the region. Aerial panchromatic photos in the 1:25,000 scale from December 20, 1984, were used to produce a ground truth map where mangrove areas were identified from other ground cover features. Digital multispectral and multitemporal analysis of MSS/LANDSAT (March 26, 1979) and TM/LANDSAT (July 19, 1984) imagery produced thematic maps of the region, which showed that no significant clearing occurred in the mangrove areas for the 1979 and 1984 period. Author

N88-24087# Universidade Federal de Parana, Curitiba (Brazil).

THE 35 MM VERTICAL AERIAL PHOTOGRAPHS FOR MAPPING STANDS OF BRACATINGA IN DIFFERENT AGE CLASSES [FOTOGRAFIAS AERAS VERTICAIS 35 MM PARA MAPEAR POVOAMENTOS DE BRACATINGA EM DIFERENTES IDADES]

ATTILIO ANTONIO DISPERATI, NELSON CARLOS ROSOT, and JOAO ROBERTODOSSANTOS *In* INPE, Latin American Symposium on Remote Sensing. 4th Brazilian Remote Sensing Symposium and 6th SELPER Plenary Meeting, Volume 1 p 716-723 1986 In PORTUGUESE; ENGLISH summary
Avail: NTIS HC A99/MF E03

The value of 35 mm vertical aerial photographs used to identify and map *Mimosa scabrella* Benth (bracatinga) in different age classes is shown. It was possible to differentiate three age classes of bracatinga using the elements of image interpretation. Complemented by field work and dendrometric measurements on the stands, it was possible to discriminate on the photographs of all seven of the different ages of stands in the area. From the resulting photointerpretation map, the area of bracatinga stands in the study area was found. For comparison, the number of bracatinga crowns in plots on 1:3,000 aerial photographs were counted and compared with the data collected in the field. The best results were found for the stands between four to six years of age. Author

N88-24089# Universidad Nacional de San Juan (Argentina).

THE BROKEN ANTICLINES, CUESTA AND CREST HOMOCLINES, ORTOCLINAL VALLEYS, AND OTHER FORMS OF RELIEF OUTCROPS DELINEATED WITH THE HELP OF REMOTE SENSING IMAGERY [ANTICLINALES APORTILLADOS, CUESTAS Y CRESIAS HOMOCLINALES, VALLES ORIOCLINALES Y OTRAS FORMAS DE RELIEVES PLEGADOS DELIMITADOS CON AYUDA DE IMAGENS DE SENSORES REMOTOS]

GRACIELA M. SUIVRES *In* INPE, Latin American Symposium on Remote Sensing. 4th Brazilian Remote Sensing Symposium and 6th SELPER Plenary Meeting, Volume 1 p 733-738 1986 In SPANISH; ENGLISH summary
Avail: NTIS HC A99/MF E03

A regional geomorphological map was obtained, in the scale

of 1:250,000 from analysis and interpretation of satellite imagery. This map shows many landscapes of relief elaborated over folded outcrops. The Broken anticlines of Guayaguas-Catantã and Las Quijadas, cuesta and crest homoclinal, orthoclinal, and transversal valley are the main landforms. Author

N88-24091# Universidade Federal de Parana, Curitiba (Brazil). Departamento de Silvicultura e Manejo.

STEREOSCOPIC PHOTOGRAPHS, GROUND AND AERIAL, OF TREES USED IN THE ARBORIZATION OF CURITIBA (PR) [FOTOGRAFIAS ESTEROSCOPICAS, TERRESTRES E AEREAS, DE ARVORES UTILIZADAS NA ARBORIZACAO DE CURITIBA - PR]

ATTILIO ANTONIO DISPERATI and CARLOS VELLOZO RODERJAN *In* INPE, Latin American Symposium on Remote Sensing. 4th Brazilian Remote Sensing Symposium and 6th SELPER Plenary Meeting, Volume 1 p 757-763 1986 *In* PORTUGUESE; ENGLISH summary
Avail: NTIS HC A99/MF E03

This paper deals with the acquisition of 35 mm ground stereo photographs using one camera. The usual trees in the arborization of Curitiba were photographed in two different seasons of the year. Technical and practical aspects related with the acquisition and stereo observation are discussed. The ground stereo-pairs and aerial stereo-pairs, recently acquired from a photogrammetry survey, were introduced in the practical classes of Forest Photointerpretation and Dendrology and the reactions of the students were extremely favorable. Author

N88-24092# Instituto de Pesquisas Espaciais, Sao Jose dos Campos (Brazil).

MAPPING OF PLANT ASSOCIATIONS AND THE VARIATION OF SURFACE WATER IN THE PANTANAL MATO-GROSSENSE NATIONAL PARK, THROUGH REMOTE SENSING TECHNIQUES [MAPEAMENTO DAS FORMACOES VEGETAIS E DA VARIACAO DA LAMINA D'AGUA NO PARQUE NACIONAL DO PANTANAL MATO GROSSENSE, ATRAVES DE TECNICAS DE SENSORIAMENTO REMOTO]

DAGOBERTO SILVA and HERMANN J. H. KUX *In its* Latin American Symposium on Remote Sensing. 4th Brazilian Remote Sensing Symposium and 6th SELPER Plenary Meeting, Volume 1 p 764-771 1986 *In* PORTUGUESE; ENGLISH summary
Avail: NTIS HC A99/MF E03

The objective was to map the plant associations and the variation of the water surface in the Pantanal Mato-grossense National Park, using remote sensing techniques. Color infrared aerial photographs and MSS-LANDSAT digital data were used. Using aerial photographic interpretation techniques, the following vegetation units were identified: semideciduous seasonal alluvial forest, vegetation of transition, and seasonally flooded grasslands. During the digital processing (supervised classification) of the MSS-LANDSAT data, the seasonally flooded grasslands unit was considered as two under classes, due to the relationship between spectral response and soil moisture. The utilization of a SLICER algorithm at the MSS-LANDSAT 7 band allowed mapping of the area covered with water in flooded and dry seasons. Author

N88-24093# Instituto de Pesquisas Espaciais, Sao Jose dos Campos (Brazil).

PRELIMINARY STUDY ON THE APPLICATION OF DIGITAL PROCESSING OF TM-LANDSAT DATA IN THE MAPPING OF APPLE ORCHARDS IN FRAIBURGO (SC) [ESTUDO PRELIMINAR SOBRE A APLICACAO DE PROCESSAMENTO DIGITAL DE DADOS TM-LANDSAT NO MAPEAMENTO DE POMARES DE MACA EM FRAIBURGO, SC]

JOSE ROBERTO PROVESI, DALTON DEMORISSON VALERIANO, and THELMA KRUG *In its* Latin American Symposium on Remote Sensing. 4th Brazilian Remote Sensing Symposium and 6th SELPER Plenary Meeting, Volume 1 p 772-784 1986 *In* PORTUGUESE; ENGLISH summary
Avail: NTIS HC A99/MF E03

An evaluation of the discriminability of apple orchards from other land uses in the county of Fraiburgo, SC, was attempted

through digital analysis of TM-LANDSAT data. The ground truth was a panchromatic aerial survey acquired in September, 1979 (1:20,000) and a ground verification realized in January, 1986; the TM-LANDSAT data (221/79A, December, 1984, bands TM: 2, 3, 4, and 7) were analyzed in the Image-100 System (1:25,000). A hybrid digital classification was employed in the study area. Eight spectral classes were obtained through the K-Means algorithm (non-supervised). These were further divided into eighteen supervised classes by the MAXVER algorithm, comprising eight informative classes: pinus, forest, apple, prepared soil, pasture, water, wetlands, and urban areas. The analysis of the classes localized in the space of attributes TM-3 x TM-4 indicated that the three supervised classes for apple overlapped with the forest, pasture, and wetlands classes. These confusions were attributed to differences in the management of the orchards and the age of the apple parcels (from 5 to 20 years). A multitemporal approach, which better explores the phenological characteristics of apple is suggested so as to better discriminate this class from other land uses. Author

N88-24095# Sao Paulo Univ. (Brazil). Escola Superior de Agricultura.

CHARACTERISTICS OF DRAINAGE DETERMINATIONS IN AERIAL PHOTOGRAPHS AND RELIEF DETERMINATION ON DIFFERENT SCALES PLANIALTIMETRIC CHARTS FOR THREE SOILS IN THE STATE OF SAO PAULO [CARACTERISTICAS DA DRENAGEM DETERMINADAS EM FOTOGRAFIAS AEREAS DO RELEVO DETERMINADAS EM CARTAS PLANIALTIMETRICAS DE ESCALAS DIFERENTES PARA TRES SOLOS DO ESTADO DE SAO PAULO]

R. ANGULOFILHO, V. A. DEMETRIO, and G. V. DEFRANCA *In* INPE, Latin American Symposium on Remote Sensing. 4th Brazilian Remote Sensing Symposium and 6th SELPER Plenary Meeting, Volume 1 p 792-798 1986 *In* PORTUGUESE; ENGLISH summary
Avail: NTIS HC A99/MF E03

Based on the interpretation of vertical aerial photographs on a 1:35,000 scale, the characterization was made of the drainage standards from three different soils of the State of Sao Paulo (red-yellow latosol, red-yellow podzol, and litosol) and the variation was determined for the relief indices obtained from planialtimetric charts on different scales. Each soil unit was represented by three circular samples of 10 sq km. From tracing the drainage networks on the vertical aerial photographs, quantitative indices for the drainage standards were determined for the circular samples. The relief indices were obtained from the circular samples traced on the different scales planialtimetric charts (1:10,000 and 1:50,000). Subsequently, the values for the relief indices obtained from the two charts were compared to determine their variation. Author

N88-24096# Instituto de Pesquisas Espaciais, Sao Jose dos Campos (Brazil).

EVALUATION OF TM FALSE COLOR COMPOSITES FOR CROP DISCRIMINATION [AVALIACAO DE COMPOSICOES COLIDAS TM FALSA COR PARA A DISCRIMINACAO DE CULTURAS]

CHOU CHEN SHERRY and ANGELA MARIA DELIMA *In its* Latin American Symposium on Remote Sensing. 4th Brazilian Remote Sensing Symposium and 6th SELPER Plenary Meeting, Volume 1 p 799-804 1986 *In* PORTUGUESE; ENGLISH summary
Avail: NTIS HC A99/MF E03

Visual interpretation of LANDSAT imagery is frequently used in natural resources studies instead of the sophisticated digital analysis which is more expensive and requires expertise. To form false color composites, three LANDSAT bands are needed, generally bands 4, 5, and 7 are used for the 4 band LANDSAT-MSS data. However, the selection of three bands from the available 7 TM bands is not an easy task; because there are 210 possible combinations of the selected three bands with the three prime colors. In this study three different criteria for band selection: entropy, the optimum index factor, and the principal component were used. After band selection, color composites were compared

visually to verify discrimination of soybeans, corn, and sugar cane. Study results show that there was no apparent superiorities of visual differentiation among crop types for the color composites selected by any of the studied criteria over the conventional composites using bands 2, 3, and 4. It is concluded that the conventional false color composite should be used for crop discrimination, because no additional training of photointerpreter on the color-surface target relationship is needed. Author

N88-24109*# Pennsylvania State Univ., University Park. Dept. of Meteorology.

AN UPDATE ON REMOTE MEASUREMENT OF SOIL MOISTURE OVER VEGETATION USING INFRARED TEMPERATURE MEASUREMENTS: A FIFE PERSPECTIVE
Semiannual Status Report, Mar. 1987 - Mar. 1988

TOBY N. CARLSON Jun. 1988 29 p

(Contract NAG5-919)

(NASA-CR-182926; NAS 1.26:182926) Avail: NTIS HC A03/MF A01 CSCL 08B

Using model development, image analysis and micro-meteorological measurements, the object is to push beyond the present limitations of using the infrared temperature method for remotely determining surface energy fluxes and soil moisture over vegetation. Model development consists of three aspects: (1) a more complex vegetation formulation which is more flexible and realistic; (2) a method for modeling the fluxes over patchy vegetation cover; and (3) a method for inferring a two-layer soil vertical moisture gradient from analyses of horizontal variations in surface temperatures. HAPEX and FIFE satellite data will be used along with aircraft thermal infrared and solar images as input for the models. To test the models, moisture availability and bulk canopy resistances will be calculated from data collected locally at the Rock Springs experimental field site and, eventually, from the FIFE project. Author

N88-25134*# National Aeronautics and Space Administration. John F. Kennedy Space Center, Cocoa Beach, Fla.

HISTORY OF WILDLAND FIRES ON VANDENBERG AIR FORCE BASE, CALIFORNIA

DIANA E. HICKSON (Bionetics Corp., Cocoa Beach, Fla.) Mar. 1988 39 p

(Contract NAS10-10285)

(NASA-TM-100983; BIO-1; NAS 1.15:100983) Avail: NTIS HC A03/MF A01 CSCL 06C

The fire history of the past 50 years for Vandenberg AFB, California was determined using aerial photography, field investigation, and historical and current written records. This constitutes a record of the vegetation age classes for the entire base. The location, cause, and fuel type for sixty fires from this time period were determined. The fires were mapped and entered into a geographic information system (GIS) for Vandenberg. Fire history maps derived from this GIS were printed at 1:9600 scale and are on deposit at the Vandenberg Environmental Task Force Office. Although some ecologically significant plant communities on Vandenberg are adapted to fire, no natural fire frequency could be determined, since only one fire possibly caused by lightning occurred in the area now within the base since 1937. Observations made during this study suggest that burning may encourage the invasion of exotic species into chaparral, in particular Burton Mesa or sandhill chaparral, an unusual and geographically limited form of chaparral found on the base. Author

ENVIRONMENTAL CHANGES AND CULTURAL RESOURCES

Includes land use analysis, urban and metropolitan studies, environmental impact, air and water pollution, geographic information systems, and geographic analysis.

A88-33770* National Aeronautics and Space Administration. Ames Research Center, Moffett Field, Calif.

MONITORING THE ENVIRONMENT BY REMOTE SENSING

WALTER E. WESTMAN (NASA, Ames Research Center, Moffett Field; California, University, Berkeley) Trends in Ecology and Evolution (ISSN 0169-5347), vol. 2, Nov. 1987, p. 333-337. refs

Structural features of ecosystems, such as leaf area index, phytomass and canopy chemical contents, are beginning to be estimated from remotely sensed data. This development, in combination with ecological modeling, is permitting the estimation of functional features of ecosystems including primary productivity and nutrient cycling. Such techniques are also being applied to the problem of monitoring the effects of air or water pollutants on biota. Sensors that obtain data at a coarse spatial scale (1 km² or more) are also permitting the observation of biospheric patterns at a large regional or global scale for the first time. When coupled with atmospheric measurements, field data and simulation models, such data may serve to address ecological processes, including pollution effects, at large regional or global scales. Author

A88-36243#

LONG-TERM AIR QUALITY MONITORING AT THE SOUTH POLE BY THE NOAA PROGRAM GEOPHYSICAL MONITORING FOR CLIMATIC CHANGE

E. ROBINSON (Mauna Loa Observatory, Hilo, HI), B. A. RODHAINE, W. D. KOMHYR, S. J. OLTMANS (NOAA, Air Resources Laboratory, Boulder, CO), L. P. STEELE (Cooperative Institute for Research in Environmental Sciences, Boulder, CO) et al. Reviews of Geophysics (ISSN 8755-1209), vol. 26, Feb. 1988, p. 63-80. refs

The objectives of the NOAA program of Geophysical Monitoring for Climatic Change (GMCC) for the South Pole include measurements of atmospheric changes which can potentially impact climate. This paper discusses the long-term GMCC South Pole air chemistry data for carbon dioxide, total ozone, surface ozone, methane, halocarbons, nitrous oxide, and aerosol concentrations, comparing the findings with GMCC data for other regions. Special consideration is given to the results of recent GMCC ozonesonde operations and to an assessment of Dobson ozone spectrophotometer data taken at South Pole by NOAA since 1964. Data are discussed in the framework of Antarctic 'ozone hole' phenomenon. I.S.

A88-39094

URBANIZATION AND LANDSAT MSS ALBEDO CHANGE IN THE WINDSOR-QUEBEC CORRIDOR SINCE 1972

ALAIN ROYER, LISE CHARBONNEAU, and FERDINAND BONN (Sherbrooke, Universite, Canada) International Journal of Remote Sensing (ISSN 0143-1161), vol. 9, March 1988, p. 555-566. Research supported by the Ministere de l'Education du Quebec. refs

(Contract NSERC-A-8643; NSERC-A-5252)

A88-41961

REMOTE SENSING FOR RESOURCES DEVELOPMENT AND ENVIRONMENTAL MANAGEMENT; PROCEEDINGS OF THE SEVENTH INTERNATIONAL SYMPOSIUM, ENSCHEDE, NETHERLANDS, AUG. 25-29, 1986. VOLUMES 1, 2, & 3

M. C. J. DAMEN, ED., G. SICCO SMIT, ED., and H. TH. VERSTAPPEN, ED. (International Institute for Aerospace Survey and Earth Sciences, Enschede, Netherlands) Symposium sponsored by the International Society of Photogrammetry and

02 ENVIRONMENTAL CHANGES AND CULTURAL RESOURCES

Remote Sensing (Commission VII) and Netherlands Remote Sensing Board. Rotterdam, A. A. Balkema, 1986, p. Vol. 1, 562 p.; vol. 2, 414 p.; vol. 3, 115 p. For individual items see A88-41962 to A88-42070.

Papers and working group conclusions and recommendations are presented concerning the use of remote sensing for resources development and environmental management in the fields of visible and infrared data, microwave data, spectral signatures of objects, renewable resources in rural areas, nonrenewable resources, hydrology, human settlements, and geoinformation systems. Topics covered include methods of image and data processing and classification, the use of remote sensing for geological analysis, satellite mapping of vegetation, forestry, agriculture, soil survey, and land and water use. The use of remote sensing in geomorphology, oceanography and engineering projects, satellite observation of surface water, coastal zones, ice and snow, and remote sensing for urban surveys, human settlement analysis, and archeology, and the analysis of data obtained by Landsat, SIR-A, SIR-B, SLAR, and SPOT systems are also discussed. R.B.

A88-41972 CLASSIFICATION OF LAND FEATURES, USING LANDSAT MSS DATA IN A MOUNTAINOUS TERRAIN

H. TAHERKIA and W. G. COLLINS (Aston, University, Birmingham, England) IN: Remote sensing for resources development and environmental management; Proceedings of the Seventh International Symposium, Enschede, Netherlands, Aug. 25-29, 1986. Volume 1. Rotterdam, A. A. Balkema, 1986, p. 87-91.

This paper evaluates Landsat MSS data in a hostile terrain located in central Alborz, north of Iran. Correlation of the Three bands of the image were evaluated, and separation of different ground features was examined. Training areas of different categories were located on the image using field work. Data from the training areas then were manipulated to eliminate unwanted pixels. Mean and standard deviation of the categories were calculated and data which fell in the range of three standard deviations was selected. For the execution of the training areas a selected subscene was chosen and then classified. Author

A88-42000 MONITORING OF RENEWABLE RESOURCES IN EQUATORIAL COUNTRIES

R. VAN KONIJNENBURG (Nederlands Instituut voor Vliegtuigontwikkeling en Ruimtevaart, Delft, Netherlands) and MAHSUM IRSYAM (Indonesian National Institute of Aeronautics and Space, Jakarta, Indonesia) IN: Remote sensing for resources development and environmental management; Proceedings of the Seventh International Symposium, Enschede, Netherlands, Aug. 25-29, 1986. Volume 1. Rotterdam, A. A. Balkema, 1986, p. 335-340. refs

Studies have been conducted on the feasibility of a joint Indonesian-Netherlands project for the development and operation of a dedicated Tropical Earth Resources Satellite (TERS) system. The studies confirm the need for an earth-observation system with a high temporal and geometric resolution to provide the capability of monitoring the renewable resources in equatorial countries. The result of cloud studies indicates that the requirement for a high temporal resolution cannot be met by a satellite in polar orbit. An equatorial orbit, however, can meet this requirement. In the course of the studies the user requirements for such a tropical earth-observation satellite were elaborated. Based on these requirements a baseline design was conceived. 'Key applications' have been identified, which would typically need a TERS system and which are of sufficient importance from a benefits point of view. The two most important fields of application are agriculture and forestry. Analysis of these key applications indicate profits in excess of yearly cost. It has been recognized that it will be necessary to ascertain that by the time TERS becomes operational an adequate infrastructure for the utilization of such a system will be available. For that purpose the preliminary outlines of a rice production monitoring system and of a TERS utilization preparation plan have been established. Author

A88-42018 OPERATIONAL SATELLITE DATA ASSESSMENT FOR DROUGHT/DISASTER EARLY WARNING IN AFRICA - COMMENTS ON GIS REQUIREMENTS

HUBERTUS L. BLOEMER, SCOTT E. NEEDHAM (Ohio University, Athens), and LOUIS T. STEYAERT (NOAA, National Environmental Satellite Data and Information Service, Columbia, MO) IN: Remote sensing for resources development and environmental management; Proceedings of the Seventh International Symposium, Enschede, Netherlands, Aug. 25-29, 1986. Volume 2. Rotterdam, A. A. Balkema, 1986, p. 561-568. refs

An operational climate impact assessment system for improved drought/disaster early warning in semi-arid regions of Africa using daily NOAA polar orbiting AVHRR satellite data in combination with ten-day rainfall reports from ground stations throughout the region has been developed. Assessments are prepared using a 'light table' Geographic Information System (GIS) approach for map/image overlay and statistical time series analysis. The assessment process and hardware and software considerations to meet the needs of the spatial analyst are discussed. Remote sensing data processing and GIS capabilities are assessed according to various data handling proficiency and applicability of data, including available computer systems. R.B.

A88-42020 GLOBAL DISTRIBUTIVE COMPUTER PROCESSING SYSTEMS FOR ENVIRONMENTAL MONITORING, ANALYSIS AND TREND MODELING IN EARLY WARNING AND NATURAL DISASTER MITIGATION

J. O. BRUMFIELD (Marshall University, Huntington, WV) and H. L. BLOEMER (Ohio University, Athens) IN: Remote sensing for resources development and environmental management; Proceedings of the Seventh International Symposium, Enschede, Netherlands, Aug. 25-29, 1986. Volume 2. Rotterdam, A. A. Balkema, 1986, p. 573-577. refs

Hierarchical levels of environmental data availability and processing capabilities are discussed and illustrated for the following global configuration of components based on experimental design results: (1) national analysis and early warning workstations, (2) international regional processing nodes, (3) international data and processing facilities, and (4) global telecommunication networking for computers and early warning systems. Inasmuch as the components of computer hardware/software systems and source data are spatially distributed on a global scale, workstations and nodes must be able to communicate effectively (analog and/or digital) to maximize information exchange and decision making potential on a national or regional basis. Further information/data from global data bases are often necessary to supplement or augment locally or regionally derived information (e.g., climate data from NOAA and NASA and WMO and AVHRR and/or GOES data from NOAA. Author

A88-42031 REMOTE SENSING ASSESSMENT OF ENVIRONMENTAL IMPACTS CAUSED BY PHOSPHAT INDUSTRY DESTRUCTIVE INFLUENCE

S. C. MULARZ (Akademia Gornicza-Hutnicza, Krakow, Poland) IN: Remote sensing for resources development and environmental management; Proceedings of the Seventh International Symposium, Enschede, Netherlands, Aug. 25-29, 1986. Volume 2. Rotterdam, A. A. Balkema, 1986, p. 639-644. refs

A number of remote sensing techniques, such as color aerial photography, black and white aerial photography and thermal imaging have been used to detect adverse environmental impacts associated with the location of the phosphogypsum dump area. As an effect of processing and interpreting remotely sensed data, assessments of water pollution, solid waste disposal impacts on toe-failure deformation zones and the degree of vegetation cover damages, have been specified. Results of experiments indicate that remote sensing methods are an irreplaceable tool to solve environmental monitoring, as well as planning problems. Wide-area repetitive coverage by remote sensors provides information which

02 ENVIRONMENTAL CHANGES AND CULTURAL RESOURCES

is not readily available by conventional measuring techniques.

Author

A88-42032

REMOTE SENSING FOR SURVEY OF MATERIAL RESOURCES OF HIGHWAY ENGINEERING PROJECTS IN DEVELOPING COUNTRIES

R. L. NANDA (Nigerian Building and Road Research Institute, Lagos) IN: Remote sensing for resources development and environmental management; Proceedings of the Seventh International Symposium, Enschede, Netherlands, Aug. 25-29, 1986. Volume 2. Rotterdam, A. A. Balkema, 1986, p. 645-650. refs

The use of remote sensing techniques for highway engineering projects in developing countries for determining route location and highway pavement performance and for survey of material resources, especially sub-surface calcrete, is discussed. In India and Nigeria, remote sensing techniques have been limited to black and white aerial photographs, SLAR imagery, and Landsat imagery. It is found that air photo interpretation provides an accurate and expeditious means of conducting survey of highway material resources, even if the region is inaccessible, although both SLAR and Landsat imageries lack the three-dimensional view of terrain essential for the interpretation of sub-surface calcrete. R.B.

A88-42056

AN ANALYSIS OF REMOTE SENSING FOR MONITORING URBAN DERELICT LAND

E. C. HYATT, J. L. GRAY, and W. G. COLLINS (Aston, University, Birmingham, England) IN: Remote sensing for resources development and environmental management; Proceedings of the Seventh International Symposium, Enschede, Netherlands, Aug. 25-29, 1986. Volume 2. Rotterdam, A. A. Balkema, 1986, p. 817-822. refs

The use of aerial photography and the potential of Thematic Mapper satellite imagery for monitoring urban derelict land areas are considered. Aerial photography is revealed to be an accurate assessor of derelict and waste land sites at a mapping scale of 1: 10,000, comparing favorably, and being compatible with trends determined by local authorities. The role of satellite data and their problems and prospects are reviewed in the context of urban area studies. Author

A88-42057

HUMAN SETTLEMENT ANALYSIS USING SHUTTLE IMAGING RADAR-A DATA - AN EVALUATION

C. P. LO (Georgia, University, Athens) IN: Remote sensing for resources development and environmental management; Proceedings of the Seventh International Symposium, Enschede, Netherlands, Aug. 25-29, 1986. Volume 2. Rotterdam, A. A. Balkema, 1986, p. 841-845. refs

The detectability of human settlements from Shuttle Imaging Radar-A images was determined with reference to the radar system geometry and physical and cultural characteristics of the environment in four specific geographic regions of the United States represented in five strips of images. The usefulness of the settlement area data directly measured from the images for population estimation was also evaluated. It was concluded that Shuttle Imaging Radar-A data could produce accurate population estimates of individual settlements and complement other forms of high-resolution space data in human settlement analysis. Author

A88-42058* Lockheed Missiles and Space Co., Sunnyvale, Calif.

SPATIAL RESOLUTION REQUIREMENTS FOR URBAN LAND COVER MAPPING FROM SPACE

WILLIAM J. TODD (Lockheed Missiles and Space Co., Inc., Sunnyvale, CA) and ROBERT C. WRIGLEY (NASA, Ames Research Center, Moffett Field, CA) IN: Remote sensing for resources development and environmental management; Proceedings of the Seventh International Symposium, Enschede, Netherlands, Aug.

25-29, 1986. Volume 2. Rotterdam, A. A. Balkema, 1986, p. 881-886. refs

Very low resolution (VLR) satellite data (Advanced Very High Resolution Radiometer, DMSP Operational Linescan System), low resolution (LR) data (Landsat MSS), medium resolution (MR) data (Landsat TM), and high resolution (HR) satellite data (Spot HRV, Large Format Camera) were evaluated and compared for interpretability at differing spatial resolutions. VLR data (500 m - 1.0 km) is useful for Level 1 (urban/rural distinction) mapping at 1:1,000,000 scale. Feature tone/color is utilized to distinguish generalized urban land cover using LR data (80 m) for 1:250,000 scale mapping. Advancing to MR data (30 m) and 1:100,000 scale mapping, confidence in land cover mapping is greatly increased, owing to the element of texture/pattern which is now evident in the imagery. Shape and shadow contribute to detailed Level II/III urban land use mapping possible if the interpreter can use HR (10-15 m) satellite data; mapping scales can be 1:25,000 - 1:50,000. Author

A88-42059

SPECTRAL CHARACTERIZATION OF URBAN LAND COVERS FROM THEMATIC MAPPER DATA

DOUGLAS J. WHEELER (Utah State University, Logan) IN: Remote sensing for resources development and environmental management; Proceedings of the Seventh International Symposium, Enschede, Netherlands, Aug. 25-29, 1986. Volume 2. Rotterdam, A. A. Balkema, 1986, p. 893-898. refs

Using Salt Lake City, Utah, as a test case, this study evaluates the capabilities of Landsat 5 Thematic Mapper (TM) digital data for distinguishing urban land cover materials. This was accomplished by using a newly developed hierarchical clustering algorithm which statistically derived spectral classes from TM channels 2, 3, 4, and 5 (visible, near infrared and middle infrared). The relationships between spectral groups were further analyzed using three statistical evaluations: principal components analysis, cluster analysis, and discriminant analysis. Through the use of component scores, cluster linkage diagrams, and canonical discriminant function scatter plots; as well as TM spectral curves, aerial photography, and ground investigation; the spectral classes were grouped into twelve predetermined land cover categories. The accuracy of classification was assessed at approximately 80 percent (0.05 significance level). A significant improvement in classification accuracy (91.5 percent) was achieved by stratifying the multispectral classification with thresholds from the TM thermal channel introduced as ancillary data. Author

A88-42062

RECORDING RESOURCES IN RURAL AREAS

RICHARD K. BULLARD (National Remote Sensing Centre, Chelmsford, England) IN: Remote sensing for resources development and environmental management; Proceedings of the Seventh International Symposium, Enschede, Netherlands, Aug. 25-29, 1986. Volume 2. Rotterdam, A. A. Balkema, 1986, p. 913-916.

The use of high resolution satellite imagery in conjunction with conventional imagery to record resources in rural areas for use in multipurpose cadastre (MPC) is discussed. The use of the DTM allows the resources of a land parcel to be considered in three-dimensions. Satellite imagery can be used to detect resources both above and below ground. The MPC can serve as a data base for storing rural resources, aiding in reapportionment and development of rural areas. R.B.

A88-42063

EVALUATION OF REGIONAL LAND RESOURCES USING GEOGRAPHIC INFORMATION SYSTEMS BASED ON LINEAR QUADRICS

JAMES HOGG, MARK GAHEGAN, and NEIL STUART (Leeds University, England) IN: Remote sensing for resources development and environmental management; Proceedings of the Seventh International Symposium, Enschede, Netherlands, Aug. 25-29, 1986. Volume 2. Rotterdam, A. A. Balkema, 1986, p. 917-925. Research supported by the University of Leeds. refs

02 ENVIRONMENTAL CHANGES AND CULTURAL RESOURCES

Evaluation of regional land resources involves the integration and analysis of geographic data which comes from a variety of different sources and in many different forms. This paper describes results of a pilot study using a computerized geographic information system (GIS) based on linear quadtrees to integrate and analyze geographic data for evaluation of regional land resources near Matlock in the Peak District Derbyshire, England. Results are presented which show the response to queries involving set logic operations on binary raster images and are discussed in relation to methods of regional land resources evaluation. The paper concludes that GIS based on linear quadtrees provide a flexible, powerful analytical tool for geographical research involving integration of geographic data from various sources, including remote sensing. Author

A88-42064 A COMPREHENSIVE LRIS OF THE KANANASKIS VALLEY USING LANDSAT DATA

G. D. LODWICK, S. H. PAINE, M. P. MEPHAM, and A. W. COLIJN (Calgary, University, Canada) IN: Remote sensing for resources development and environmental management; Proceedings of the Seventh International Symposium, Enschede, Netherlands, Aug. 25-29, 1986. Volume 2. Rotterdam, A. A. Balkema, 1986, p. 927-932. refs

This paper describes the design and development of a general land-related information system (LRIS) covering the upper Kananaskis Valley of south western Alberta. Landsat data provide information on surface cover, principally vegetation, as well as on land use. In addition, a range of overlays of thematic data obtained from conventional sources, such as geology, topography, snow-cover, hydrology and pedology, is being added to the LRIS. The land information is stored on a VAX 11/750 computer system using VAX/DBMS a CODASYL compliant network data base system. The primary key is the position-based data defined by the geographic coordinates of the various data types. Information retrieval by various secondary keys is possible. As well, topological relationships have been incorporated into the LRIS design allowing data retrieval in both graphical and tabular form. Author

A88-42065 LAND RESOURCE USE MONITORING IN ROMANIA, USING AERIAL AND SPACE DATA

N. ZEGHERU (Institute of Geodesy, Photogrammetry, Cartography and Land Management, Bucharest, Rumania) IN: Remote sensing for resources development and environmental management; Proceedings of the Seventh International Symposium, Enschede, Netherlands, Aug. 25-29, 1986. Volume 2. Rotterdam, A. A. Balkema, 1986, p. 953-956. refs

A88-42069 THE INTEGRATION OF REMOTE SENSING AND GEOGRAPHIC INFORMATION SYSTEMS

DAVID G. GOODENOUGH (Canada Centre for Remote Sensing, Ottawa) IN: Remote sensing for resources development and environmental management; Proceedings of the Seventh International Symposium, Enschede, Netherlands, Aug. 25-29, 1986. Volume 3. Rotterdam, A. A. Balkema, 1986, p. 1015-1028. refs

The integration of remote sensing and geographic information systems is essential for effective resource management. The volume of remote sensing imagery for managing a provincial resource, such as forestry, is such that one must use digital image analysis systems. By combining remote sensing image analysis and geographic information systems, resource managers can have timely and accurate knowledge of a renewable resource. There are, however, several scientific and technical problems that reduce the success of this integration. This paper describes several integration problems and the LANDSAT Digital Image Analysis System (LDIAS) used at the Canada Center for Remote Sensing (CCRS). Experiments have been conducted integrating a forestry geographic information system for the province of British Columbia with LDIAS. Some of the difficulties encountered require the use

of non-algorithmic solutions which use symbolic reasoning. A brief description of expert systems for this integration is given. Several key issues for the future are raised for consideration. Author

A88-42070 MONITORING ENVIRONMENTAL RESOURCES THROUGH NOAA'S POLAR ORBITING SATELLITES

JOAN C. HOCK (NOAA, Assessment and Information Services Center, Washington, DC) IN: Remote sensing for resources development and environmental management; Proceedings of the Seventh International Symposium, Enschede, Netherlands, Aug. 25-29, 1986. Volume 3. Rotterdam, A. A. Balkema, 1986, p. 1029-1032.

Satellite imagery in combination with surface weather observations can provide a potential tool for evaluating ground and water conditions throughout the world. In order to monitor the economic impacts of anomalous weather, the Assessment and Information Services Center (AISC), of the National Environmental Satellite, Data, and Information Service (NESDIS), National Oceanic and Atmospheric Administration (NOAA) integrates satellite data, geographic information, agronomic, and economic models to monitor both land and marine resources. Such assessments can provide government officials with an early warning of crop failure in order to mitigate potential climate impacts and reduce climate vulnerability. Author

A88-44446 THE USE OF METRIC MULTISPECTRAL PHOTOGRAPHY IN ENVIRONMENTAL AND RESOURCE EXPLORATION

KARL-HEINZ MAREK, KARL-HEINZ JOHN (Akademie der Wissenschaften der DDR, Zentralinstitut fuer Physik der Erde, Potsdam, German Democratic Republic), and SIGMUND JAEHN (Jena Review (ISSN 0448-9497), vol. 32, no. 4, 1987, p. 160-163. refs

The application of high-resolution metric multispectral photography (MMP) to perform thematic, topographic, geologic, and land use maps, detect and localize depression zones, and perform shallow water bathymetry is examined. MMP can produce topographic maps with scales between 1:50,000 and 1:100,000. Advantages of the MMP system include recording earth surface images and extracting information from them more easily and economically efficiently than digital recording systems and producing images suitable for topographic and thematic mapping at low cost. R.B.

N88-22453# Instituto de Pesquisas Espaciais, Sao Jose dos Campos (Brazil).

UPDATING OF THE MUNICIPAL OFFICIAL REGISTER OF REAL ESTATE THROUGH A GEOGRAPHICAL INFORMATION SYSTEM [ATUALIZACAO DO CADASTRO IMOBILIARIO MUNICIPAL ATRAVES DE UM SISTEMA DE INFORMACOES GEOGRAFICAS]

ADRIANA ABRAHAO and MOACIR GODOYJUNIOR Dec. 1987 18 p In PORTUGUESE; ENGLISH summary Presented at the 1st National Meeting on Applied Remote Sensing for Municipal Planning, 22-23 Oct. 1987 (INPE-4459-PRE/1238) Avail: NTIS HC A03/MF A01

The objective of this work is to demonstrate the feasibility of automating the municipal land register by using the geographical information system now being developed at INPE. The test area was Jambouro city located in the Vale do Paraiba region, Sao Paulo state. The pilot program to update maps and taxes were developed with the municipal land register in mind. Author

N88-22456# Instituto de Pesquisas Espaciais, Sao Jose dos Campos (Brazil).

COMPARATIVE UTILIZATION OF ANALOG AND DIGITAL PROCESSES IN THE TREATMENT OF MSS-LANDSAT DATA FOR STUDYING THE NATIONAL PARKS OF BRAZIL M.S. Thesis

JOAQUIM HENRIQUE DURANPINTO Oct. 1986 184 p In PORTUGUESE; ENGLISH summary Original contains color

02 ENVIRONMENTAL CHANGES AND CULTURAL RESOURCES

illustrations

(INPE-4011-TDL/240) Avail: NTIS HC A09/MF A01

Three MSS-LANDSAT data interpretation methods are presented in a comparative form: visual interpretation using multispectral images of channel 5 and 7 at the 1:250,000 scale; visual interpretation using positive transparencies of the four channels at the 1:3,704,000 scale through a Color Additive Viewer; and digital analysis of compatible computer tapes (CCT) by means of the Image-100 System. The study areas comprise three modules of 400 sq km in the regions of Araguaia, Emas, and Iguacu National Parks. Qualitative, quantitative, and cost evaluations were made in the comparison of the three methods. This work also presents an analysis of land use in the regions around the parks. The results of this comparative study led to the following conclusions: the utilization of the color composite obtained by the Color Additive Viewer presented the best visualization of the classes, with clearly defined limits; visual interpretation through a Color Additive Viewer presented the lowest cost per square kilometer mapped, but it was the most-time consuming; on the other hand, the sophisticated digital analysis was the fastest with the highest cost, and generally, the resulted maps of the three interpretative methods showed that there was no significant differences in terms of area, form, and classes spatial distribution, when compared to ground information. Author

N88-22833# Instituto de Pesquisas Espaciais, Sao Jose dos Campos (Brazil).

ORBITAL REMOTE SENSING: AN INSTRUMENT FOR MONITORING URBAN GROWTH

MARIA DELOURDESN.O.KURKDJIAN Apr. 1988 7 p In PORTUGUESE; ENGLISH summary Presented at the National Meeting of the Study on Urban Growth, 5-9 Oct. 1987, Recife, Brazil

(INPE-4456-PRE/1287) Avail: NTIS HC A02/MF A01

The principal advantages in using orbital remote sensing data as an auxiliary instrument for urban growth monitoring are examined. Author

N88-23692# Instituto de Pesquisas Espaciais, Sao Jose dos Campos (Brazil).

APPLICATIONS OF MULTITEMPORAL COMPOSITIONS OBTAINED FROM LANDSAT DATA IN THE STUDY OF URBAN GROWTH [APLICACOES DE COMPOSICOES MULTITEMPORAIS OBTIDAS A PARTIR DE DADOS LANDSAT NO ESTUDO DE CRESCIMENTO URBANO]

MADALENA NIEROPEREIRA, MARIA DELOURDESNEVES-DEO.KURKDJIAN, CELINA FORESTI, and UBIRAJARA MAURICIO BARSOTTIDELIMA Mar. 1988 19 p In PORTUGUESE; ENGLISH summary Presented at the 3rd Brazilian Symposium on Remote Sensing, Rio de Janeiro, Brazil, 1984

(INPE-4480-PRE/1246) Avail: NTIS HC A03/MF A01

Urban growth has developed in an accelerated and disorganized manner in most Brazilian cities. One of the factors influencing the monitoring and control of urban growth is the lack of precise and updated information. Through the use of satellite remote sensing it is possible to obtain a repetitive covering of the target area showing the different tendencies of urban growth. Thus, the objective of this study is to analyze urban growth in the city of Sao Jose dos Campos during the past six years, using automatic digital processing of LANDSAT data. The algorithm Image Registration was used as implemented on the Image-100 System, which correlates image registration of LANDSAT data for different dates. Multitemporal color compositions using colored filters (blue, green, and red) were obtained. The analysis of the composites permitted the evaluation of the urban growth of Sao Jose dos Campos and showed the intense process of construction in isolated residential areas resulting from the redistribution of rural land into parcels or lots. Author

N88-23693# Instituto de Pesquisas Espaciais, Sao Jose dos Campos (Brazil).

UPDATING LAND-USE OF THE SAO JOSE DOS CAMPOS MUNICIPALITY THROUGH REMOTE SENSING DATA [ATUALIZACAO DO USO DA TERRA DO MUNICIPIO DE SAO JOSE DOS CAMPOS ATRAVES DE DADOS DE SENSORIAMENTO REMOTO]

MADALENA NIEROPEREIRA, EVELYN MARCIA LEAODEMORAESNOVO, MARIA DELOURDESN.DEO.KURKDJIAN, JULIO CESAR LIMADALGE, and TERESA GALLOTTIFLORENZANO Mar. 1988 66 p In PORTUGUESE; ENGLISH summary (INPE-4479-RPE/562) Avail: NTIS HC A04/MF A01

The land-use survey of Sao Jose dos Campos municipality using black and white aerial photographs is related to LANDSAT TM imagery. This work was carried out in a joint-cooperation with the local municipal administration according to the agreement that INPE provides the technical support to the local agency. The project included: (1) the developing of data interpretation methodology for LANDSAT-TM data and aerial photographs; (2) the evaluation of TM imagery for land-use mapping and monitoring; (3) the technology transfer of the developed methodology to the local agency through training courses; and (4) technical advice on the process of mapping the whole municipality using aerial photographs on the scale of 1:25,000. Land use maps on the scales of 1:25,000 and 1:100,000 based on aerial photographs and LANDSAT-TM imagery were produced. The mapping accuracy of the land use map obtained by using the LANDSAT-TM imagery is 85 percent at the 95 percent confidence level. The results demonstrate the adequacy of TM data for land-use mapping. Author

N88-24034# Gregory Geoscience Ltd., Ottawa (Ontario).

REMOTE SENSING AND DATA INTEGRATION: PRACTICAL SOLUTIONS FOR RESOURCE MANAGERS Abstract Only

JACQUES GUERETTE and BILL BRUCE (Canada Centre for Remote Sensing, Ottawa, Ontario) In INPE, Latin American Symposium on Remote Sensing. 4th Brazilian Remote Sensing Symposium and 6th SELPER Plenary Meeting, Volume 1 1986 Avail: NTIS HC A99/MF E03

Augmenting data bases, even in data scarce areas, is only one requirement for improved resource management decision making. Equally important is the ability to compile and integrate the particular data sets most appropriate for the resolution of an individual resource problem. This integration must furthermore be accomplished in a fashion which yields effective results within a specific set of time, cost and performance constraints. For many applications computer-based geographical information systems can provide a desirable solution. For many operational resource management agencies, the cost prevents development and support. Attention is being focused on finding practical solutions to the common data integration and update problems faced by such agencies. In Canada, practical needs have contributed to the development of data integration methodologies which are a blend of digital and analog technologies. A system now in use in Canada is described. Applications of this system are presented under the constraints of operational mapping programs in agriculture, forestry, geology, and in map revision. Author

N88-24063# Toulouse Univ. (France).

THE SAGE GEOGRAPHIC ANALYSIS SYSTEM

R. CAUBET and A. HAMEURLAIN In INPE, Latin American Symposium on Remote Sensing. 4th Brazilian Remote Sensing Symposium and 6th SELPER Plenary Meeting, Volume 1 p 541-547 1986

Avail: NTIS HC A99/MF E03

The design and implementation of a geographic analysis system, SAGE, is described. A classification of geographic analysis database queries and two geographic data manipulation modes are presented. Then, after establishing a database model for geographic charts, integrity constraints are specified for the time and space elements of the geographic database and a means of ensuring the structural coherence of geographic objects is discussed. Author

N88-24071# BP Mineracao Ltda., Rio de Janeiro (Brazil).
TORNADO TRACKS IN SOUTHWESTERN BRAZIL, EASTERN PARAGUAY, AND NORTHWESTERN ARGENTINA [RASTROS DE TORNADOS NO SUDOESTE DO BRASIL, LESTE DO PARAGUAI E NORDESTE DA ARGENTINA]

ROBERT C. DYER *In* INPE, Latin American Symposium on Remote Sensing. 4th Brazilian Remote Sensing Symposium and 6th SELPER Plenary Meeting, Volume 1 p 589-603 1986 In PORTUGUESE; ENGLISH summary
 Avail: NTIS HC A99/MF E03

A series of tornado tracks which were identified in a region that encompasses part of eastern Paraguay, southwestern Brazil, and northeastern Argentina is described. The tracks are clearly observable on 1965 black-and-white photographs (1:60,000) and on some of the early 1970 LANDSAT imagery. The multitemporal assessment of different photocoverages and LANDSAT imagery pertaining to the depicted region, showed that most of those tornadoes struck the region sometime between June 1964 and July 1965; a few tracks were determined to belong to tornadoes that hit the region in earlier years and one, in later years. The most extensive trajectories are 70 km long, and the widest, around 2 km. The severe deforestation that took place in the region in the late 1960s obliterated almost completely the tornado scars on more recent remote sensing products. A scan of the literature pertaining to the region under investigation resulted in the gathering of some interesting information on damages caused by the effect of such tornadoes. Author

N88-24074# Instituto de Pesquisas Espaciais, Sao Jose dos Campos (Brazil).

LOW ALTITUDE REMOTE SENSING DATA IN THE IMPLEMENTATION OF A MATHEMATICAL MODEL FOR THE PLANNING OF URBAN EQUIPMENT NETWORKS [DADOS DE SENSORIAMENTO REMOTO A BAIXA ALTITUDE NA IMPLIMENTACAO DE UM MODELO MATEMATICO PARA O PLANEJAMENTO DE REDES DE EQUIPAMENTOS URBANOS]

MARIA DELOUDESNEVESDEOLIVEIRAKURKDJIAN, MARIA SUELENA SANTIADOBARRAS, HORACIO HIDEKIYANASSE, ACIOLI ANTONIODEOLIVO, and NANDAMUDI LANKALAPAL VIJAYKUMAR *In its* Latin American Symposium on Remote Sensing. 4th Brazilian Remote Sensing Symposium and 6th SELPER Plenary Meeting, Volume 1 p 622-629 1986 In PORTUGUESE; ENGLISH summary
 Avail: NTIS HC A99/MF E03

This work is mainly directed to urban planners involved in solving local social use equipment location problems. Such equipment is generated as an extension of the residential function and, therefore, their location in the urban structure must follow the distribution of the different population segments in the city. Photointerpretation data is used to supply the lack of urban information, a common fact observed in the municipal administration in Brazil. The aerial photographic data are used to locate, quantify, and give priority to the equipment demand, being the last aspect function of the socio-economic conditions of the several groups of households. The data from the photointerpretation are used to model the system as a network in order to rationalize the urban equipment location. This methodology was applied using as a test area Sao Jose dos Campos, SP, where the best location for a network of urban health equipment for local use was indicated. Author

N88-24085# Instituto de Pesquisas Espaciais, Sao Jose dos Campos (Brazil).

DETECTION OF BIOMASS BURNING AND SMOKE PLUMES IN THE AMAZON REGION THROUGH NOAA SATELLITE IMAGERY [DETECCAO DE QUEIMADAS E PLUMAS DE FUMACA NA AMAZONIA ATRAVES DE IMAGENS DOS SATELLITES NOAA]

M. C. PEREIRA and A. W. SETZER *In its* Latin American Symposium on Remote Sensing. 4th Brazilian Remote Sensing Symposium and 6th SELPER Plenary Meeting, Volume 1 p 701-709 1986 In PORTUGUESE; ENGLISH summary
 Avail: NTIS HC A99/MF E03

Twenty-five NOAA-8 and 9 satellite images covering the Amazon

region were recorded from July 19th to August 9th, 1985 and analyzed along with the GTE/ABLE-2A field measurements. The objective was the detection of biomass burnings and smoke plumes to assess the environmental impact caused by their emissions in the atmosphere. The area covered by the smoke varied from 2,800 to 90,000 sq km as the dry season progressed. Maps and slides show the areas affected by the burnings. The methodology proved to be adequate to the detection of large biomass burnings. Author

N88-24101*# Kansas Univ., Lawrence. Space Technology Center.

RESEARCH ON ENHANCING THE UTILIZATION OF DIGITAL MULTISPECTRAL DATA AND GEOGRAPHIC INFORMATION SYSTEMS IN GLOBAL HABITABILITY STUDIES Final Report, 1986-1987

EDWARD A. MARTINKO and JAMES W. MERCHANT Apr. 1988 138 p
 (Contract NGL-17-004-024)
 (NASA-CR-182799; NAS 1.26:182799) Avail: NTIS HC A07/MF A01 CSCL 08B

During 1986 to 1987, the Kansas Applied Remote Sensing (KARS) Program continued to build upon long-term research efforts oriented towards enhancement and development of technologies for using remote sensing in the inventory and evaluation of land use and renewable resources (both natural and agricultural). These research efforts directly addressed needs and objectives of NASA's Land-Related Global Habitability Program as well as needs of and interests of public agencies and private firms. The KARS Program placed particular emphasis on two major areas: development of intelligent algorithms to improve automated classification of digital multispectral data; and integrating and merging digital multispectral data with ancillary data in spatial modes. B.G.

N88-24104# Technische Hogeschool, Delft (Netherlands). Dept. of Geodesy.

COUPLING OF SATELLITE REMOTE SENSING TO DIGITIZED TOPOGRAPHIC MAP TO DETECT CHANGES IN LAND USE Thesis [HET KOPPELEN VAN SATELLIET REMOTE SENSING GEGEVENS AAN EEN GEDIGITALISEERDE TOPOGRAFISCHE KAART OM VERANDERINGEN IN GRONDGEBRUIK TE DEKTEREN]

L. F. VERHEIJ Nov. 1987 65 p In DUTCH; ENGLISH summary
 (B8735129; ETN-88-92418) Avail: NTIS HC A04/MF A01

Images from LANDSAT Thematic Mapper were coupled to a 1:25,000 map to aid planning and environment management. By digitizing the analog map, a vector-file is created which consists of closed polygons. The lines of a polygon represent edges of roads and waterways, boundaries of urban areas, and boundaries of parcels in rural areas. Within one polygon the land use is homogeneous. Land use, as drawn in the map, is added to this file. A database is set up to record the relationship between the land use and the polygons. The vector file is projected on the satellite image by a similarity-transformation, after which for each polygon the class which is most represented by the labelled pixels is computed. Based upon decision rules, this class describes the actual land use. The coupling is executed and the found modifications of the land use are recorded in the database. The combination of the digital map and the satellite image assures good geometry with up to date thematic content. It can be regarded as a base for a geographic information system, although for this the geometry and the precision of the classification of satellite imagery need to be improved. ESA

N88-24844*# National Aeronautics and Space Administration. Goddard Space Flight Center, Greenbelt, Md.

THE ROLE OF SPACE BORNE IMAGING RADARS IN ENVIRONMENTAL MONITORING: SOME SHUTTLE IMAGING RADAR RESULTS IN ASIA

MARC L. IMHOFF and C. H. VERMILLION Nov. 1986 23 p
 (NASA-TM-101178; NAS 1.15:101178) Avail: NTIS HC A03/MF A01 CSCL 171

The synoptic view afforded by orbiting Earth sensors can be extremely valuable for resource evaluation, environmental monitoring and development planning. For many regions of the world, however, cloud cover has prevented the acquisition of remotely sensed data during the most environmentally stressful periods of the year. How synthetic aperture imaging radar can be used to provide valuable data about the condition of the Earth's surface during periods of bad weather is discussed. Examples are given of applications using data from the Shuttle Imaging Radars (SIR) A and B for agricultural land use and crop condition assessment, monsoon flood boundary and flood damage assessment, water resource monitoring and terrain modeling, coastal forest mapping and vegetation penetration, and coastal development monitoring. Recent SIR-B results in Bangladesh are emphasized, radar system basics are reviewed and future SAR systems are discussed. Author

N88-25020# Technische Hogeschool, Eindhoven (Netherlands).
THE APPLICATION OF SATELLITES IN CONNECTION WITH THE ENVIRONMENT

HERMANN BONDI 1986 13 p Presented at the Holst Memorial Lecture, Eindhoven, Netherlands, 3 Dec. 1986 (ETN-88-92474) Avail: NTIS HC A03/MF A01

Satellite observation for geology, crop monitoring, environmental monitoring, resources management, pest control, and oceanography is discussed. ESA

03

GEODESY AND CARTOGRAPHY

Includes mapping and topography.

A88-35156* Colorado Univ., Boulder.
SPACE GEODESY AND EARTHQUAKE PREDICTION

ROGER BILHAM (Colorado, University, Boulder; Lamont Doherty Geological Observatory, Palisades, NY) IN: Aerospace century XXI: Space sciences, applications, and commercial developments; Proceedings of the Thirty-third Annual AAS International Conference, Boulder, CO, Oct. 26-29, 1986. San Diego, CA, Univelt, Inc., 1987, p. 1637-1659. refs (Contract NSF EAR-86-10036; NAG5-799) (AAS PAPER 86-307)

Earthquake prediction is discussed from the point of view of a new development in geodesy known as space geodesy, which involves the use of extraterrestrial sources or reflectors to measure earth-based distances. Space geodesy is explained, and its relation to terrestrial geodesy is examined. The characteristics of earthquakes are reviewed, and the ways that they can be exploited by space geodesy to predict earthquakes is demonstrated. C.D.

A88-38023
GEOID ANOMALIES ACROSS PACIFIC FRACTURE ZONES

JEAN-CHARLES MARTY, ANNY CAZENAVE, and BERNARD LAGO (CNES, Toulouse, France) Geophysical Journal (ISSN 0952-4592), vol. 93, April 1988, p. 1-23. CNES-supported research. refs

Geoid step estimates have been obtained along altimeter profiles of the Seasat satellite across five fracture zones (FZs) of the NE Pacific. The geoid offset to age offset ratio $\Delta h / \Delta t$ is determined as a function of age, and for four of the FZs studied this dependence is found to be different than that predicted by conductive cooling models. Large fluctuations in the $\Delta h / \Delta t$ -age relationship are noted along three of the FZs, suggesting that the thermal structure of the oceanic lithosphere under a FZ is more complex than is to be expected from conductive cooling alone. R.R.

A88-38024* Stanford Univ., Calif.
THE EFFECT OF A SHALLOW LOW-VISCOSITY ZONE ON THE MANTLE FLOW, THE GEOID ANOMALIES AND THE GEOID AND DEPTH-AGE RELATIONSHIPS AT FRACTURE ZONES

ELIZABETH M. ROBINSON (Stanford University, CA), BARRY PARSONS (Oxford University, England), and MAVIS DRISCOLL (Analytic Sciences Corp., Reading, MA) Geophysical Journal (ISSN 0952-4592), vol. 93, April 1988, p. 25-43. refs (Contract NAG5-415; NSF EAR-83-06349)

A two-dimensional FEM is used to investigate the flow driven by the horizontal temperature gradient at a fracture zone and to calculate the resulting geoid and topography anomalies. Using a three-layered viscosity structure for the upper mantle, results are presented for the effects of varying: (1) the viscosity contrast between the fluid layers; (2) the Rayleigh number based on the viscosity of the bottom layer; and (3) the thickness of the low-viscosity channel. Good agreement is obtained with the results of geoid anomalies over the Udintsev fracture zone when the viscosity of the top layer is greater than one order of magnitude less than post-glacial rebound values. R.R.

A88-38902
EVIDENCE FROM GEOID DATA OF A HOTSPOT ORIGIN FOR THE SOUTHERN MASCARENE PLATEAU AND MASCARENE ISLANDS (INDIAN OCEAN)

ALAIN BONNEVILLE (CNRS, Centre de Recherches Volcanologiques, Clermont-Ferrand, France), JEAN PIERRE BARRIOT, and ROGER BAYER (Montpellier II, Universite, France) Journal of Geophysical Research (ISSN 0148-0227), vol. 93, May 10, 1988, p. 4199-4212. CNRS-supported research. refs

A high-resolution geoid map of the Madagascar and Mascarene basins is constructed from GEOS 3 and Seasat satellite altimetric data with an accuracy of 0.7 m. Large positive anomalies are due to topographic highs and their regional compensation. The deflection of the lithosphere under volcanic loads and its effect on the geoid are modeled for the Southern Mascarene Plateau, Mauritius, Reunion, and Rodriguez islands. Assuming a purely elastic lithospheric model, the effective flexural rigidity is estimated for the four zones. The highest rigidity occurs under Reunion Island and suggests a recent origin for the volcanism (3-5 Ma). The Southern Mascarene Plateau shows the lowest rigidity, suggesting a near-ridge origin; Rodriguez Island shows the same trend but in another tectonic framework. The topographic and geoid swell is studied as an effect of a thermal mantle plume. Using a conductive model of lithospheric heating, the assumption of 'hotspot migration' for the origin of the Southern Mascarene Plateau and the Mascarene Islands is confirmed. Author

A88-39518#
SATELLITE OBSERVATION OF SURFACE ALBEDO OVER THE QINGHAI-XINZANG PLATEAU REGION

QIANG ZHONG and YINHAI LI (Chinese Academy of Sciences, Lanzhou Institute of Plateau Atmospheric Physics, People's Republic of China) Advances in Atmospheric Sciences (ISSN 0256-1530), vol. 5, no. 1, 1988, p. 57-65. refs

A method to determine the surface albedo over the Qinghai-Xizang plateau region from NOAA polar orbiter AVHRR data is investigated, analyzing several measurements obtained between September and November 1985. The study of the empirical relationship between clear-sky planetary and surface albedos allows for the estimation of surface albedo given only the planetary albedo and vice versa. Estimated surface albedos are compared to observed albedos. The results show that the method used is suitable for detecting the spatial and temporal variation of surface albedo and is relevant for climatological studies. R.B.

A88-40688
GEOID ROUGHNESS AND LONG-WAVELENGTH SEGMENTATION OF THE SOUTH ATLANTIC SPREADING RIDGE

DOMINIQUE GIBERT (Institut Francais de Recherches pour l'Exploitation de la Mer, Centre de Brest, France) and VINCENT COURTILOT (Paris VI, Universite, France) *Nature* (ISSN 0028-0836), vol. 333, May 19, 1988, p. 255-258. CNRS-supported research. refs

The short wavelength part of the Seasat altimetry data set is used to derive a map of the 'geoid roughness' in the South Atlantic between 1° N and 39° S. This map reflects changes in the local amplitude of the geoid signal primarily associated with topography. Zones of high roughness correlate with major fracture zones, aseismic ridges and the Mid-Atlantic Ridge. The most remarkable feature is that the roughness is not uniform along the ridge but displays quasi-periodic variations with a wavelength of about 400 km, a segmentation an order of magnitude larger than described so far, which has persisted for at least 60 Myr. This segmentation may reflect either fabric generated at the ridge by normal plate tectonic processes or small-scale convective instabilities rising from a region of the upper mantle about 80 km deep. C.D.

A88-41835* Jet Propulsion Lab., California Inst. of Tech., Pasadena.

EFFECT OF WET TROPOSPHERIC PATH DELAYS ON ESTIMATION OF GEODETIC BASELINES IN THE GULF OF CALIFORNIA USING THE GLOBAL POSITIONING SYSTEM

DAVID M. TRALLI, TIMOTHY H. DIXON, and SCOTT A. STEPHENS (California Institute of Technology, Jet Propulsion Laboratory, Pasadena) *Journal of Geophysical Research* (ISSN 0148-0227), vol. 93, June 10, 1988, p. 6545-6557. refs

Surface Meteorological (SM) and Water Vapor Radiometer (WVR) measurements are used to provide an independent means of calibrating the GPS signal for the wet tropospheric path delay in a study of geodetic baseline measurements in the Gulf of California using GPS in which high tropospheric water vapor content yielded wet path delays in excess of 20 cm at zenith. Residual wet delays at zenith are estimated as constants and as first-order exponentially correlated stochastic processes. Calibration with WVR data is found to yield the best repeatabilities, with improved results possible if combined carrier phase and pseudorange data are used. Although SM measurements can introduce significant errors in baseline solutions if used with a simple atmospheric model and estimation of residual zenith delays as constants, SM calibration and stochastic estimation for residual zenith wet delays may be adequate for precise estimation of GPS baselines. For dry locations, WVRs may not be required to accurately model tropospheric effects on GPS baselines. R.B.

A88-41969

BASE MAP PRODUCTION FROM GEOCODED IMAGERY

DENNIS ROSS ROSE, IAN LAVERTY (MacDonald Dettwiler and Associates, Ltd., Richmond, Canada), and MARK SONDEHEIM (British Columbia Ministry of Environment, Surveys and Resource Mapping Branch, Victoria, Canada) *IN: Remote sensing for resources development and environmental management; Proceedings of the Seventh International Symposium, Enschede, Netherlands, Aug. 25-29, 1986. Volume 1. Rotterdam, A. A. Balkema, 1986, p. 67-71. refs*

Processes, such as feature extraction, thematic classification, and elevation derivation, used in producing maps from geocoded imagery are discussed. Resultant map accuracies are examined and a sample 1:50,000 scale base map derived entirely from Landsat TM imagery is presented and evaluated. Computerized production of a map based solely on satellite imagery can take less than 24 hours, including input, correction, geocoding of the imagery, and extraction of elevation, planimetric, and thematic data. The cost of this type of map production, which varies according to the type of terrain being mapped, is also examined. R.B.

N88-20713*# Ohio State Univ., Columbus. Dept. of Geodetic Science and Surveying.

DETERMINATION OF EARTH ROTATION BY THE COMBINATION OF DATA FROM DIFFERENT SPACE GEODETIC SYSTEMS

BRENT ALLEN ARCHINAL Feb. 1987 104 p

(Contract NSG-5265)

(NASA-CR-181388; NAS 1.26:181388; REPT-375) Avail: NTIS HC A06/MF A01 CSCL 08E

Formerly, Earth Rotation Parameters (ERP), i.e., polar motion and UTI-UTC values, have been determined using data from only one observational system at a time, or by the combination of parameters previously obtained in such determinations. The question arises as to whether a simultaneous solution using data from several sources would provide an improved determination of such parameters. To pursue this reasoning, fifteen days of observations have been simulated using realistic networks of Lunar Laser Ranging (LLR), Satellite Laser Ranging (SLR) to Lageos, and Very Long Baseline Interferometry (VLBI) stations. A comparison has been done of the accuracy and precision of the ERP obtained from: (1) the individual system solutions, (2) the weighted means of those values, (3) all of the data by means of the combination of the normal equations obtained in 1, and (4) a grand solution with all the data. These simulations show that solutions done by the normal equation combination and grand solution methods provide the best or nearly the best ERP for all the periods considered, but that weighted mean solutions provide nearly the same accuracy and precision. VLBI solutions also provide similar accuracies. Author

N88-23279# Institut fuer Angewandte Geodaesie, Frankfurt am Main (West Germany).

CONTRIBUTIONS TO GEODESY, PHOTOGRAMMETRY AND CARTOGRAPHY. SERIES 1, NUMBER 46

1987 235 p Presented at the 13th International Cartographic Association (ICA) Conference on Cartography, Morelia, Mexico, 1987 Original contains color illustrations Maps as supplement (ISSN-0469-4244; ETN-88-92386) Avail: NTIS HC A11/MF A01

Cartography as a management and planning tool; cartography as a communication process; cartographic technology, map compilation and revision; education in cartography; thematic and resources mapping; tourism; urban cartography; and maps for the blind are discussed. ESA

04

GEOLOGY AND MINERAL RESOURCES

Includes mineral deposits, petroleum deposits, spectral properties of rocks, geological exploration, and lithology.

A88-32831* Massachusetts Inst. of Tech., Cambridge.

GEODETIC MEASUREMENT OF DEFORMATION EAST OF THE SAN ANDREAS FAULT IN CENTRAL CALIFORNIA

JEANNE SAUBER, SEAN C. SOLOMON (MIT, Cambridge, MA), and MICHAEL LISOWSKI (USGS, Menlo Park, CA) *IN: Slow deformation and transmission of stress in the earth. Washington, DC, American Geophysical Union, 1988, 39 p. USGS-supported research. refs* (Contract NAG5-814)

The shear strain rates in the Diablo Range of California have been calculated, and the slip rate along the Calaveras and Paicines faults in Central California have been estimated, on the basis of triangulation and trilateration data from two geodetic networks located between the western edge of the Great Valley and the San Andreas Fault. The orientation of the principal compressive strain predicted from the azimuth of the major structures in the region is N 25 deg E, leading to an average shear strain value that corresponds to a relative shortening rate of 4.5 + or - 2.4 mm/yr. It is inferred that the measured strain is due to compression across the fold of this area. The hypothesized uniform, fault-normal compression within the Coast Ranges is not supported by these results. O.C.

A88-32901

THEMATIC CONFERENCE ON REMOTE SENSING FOR EXPLORATION GEOLOGY, 5TH, RENO, NV, SEPT. 29-OCT. 2, 1986, PROCEEDINGS. VOLUMES 1 & 2

Conference organized by the Environmental Research Institute of Michigan; Sponsored by ARCO Exploration and Technology Co., Exxon Production Research Co., Phillips Petroleum Co., et al. Ann Arbor, MI, Environmental Research Institute of Michigan, 1987, p. Vol. 1, 443 p.; vol. 2, 378 p. For individual items see A88-32902 to A88-32957.

This symposium includes papers on digital terrain model and image integration for geologic interpretation, mapping the Oman ophiolite using TM data, integration of SIR-B imagery with geological and geophysical data in Australia, developing petroleum exploration targets in south-central Texas through digital data integration, and the contribution of Landsat to a geologic expedition in the desert of north-central Sudan, Africa. Consideration is also given to the application of remote sensing to tectonic and metallogenic studies in NE Africa, the use of calibration targets in the measurement of 2.22-micron mineral absorption features in TM data, a geobotanical investigation of an exploration-sized territory, and the remote sensing of geological structure in temperate agriculture terrains. Additional papers are on the identification of clay minerals by feature coding of near-IR spectra, the detection of geologic features in Landsat TM imagery not revealed in Landsat MSS imagery, the remote compositional mapping of rocks using reflected and emitted radiance, and earth observations opportunities from Space Station. I.S.

A88-32902#

APPLICATION OF SYNTHETIC APERTURE RADAR (SAR) TO SOUTHERN PAPUA NEW GUINEA FOLD BELT EXPLORATION

JAMES M. ELLIS and FRANK D. PRUETT (Chevron Overseas Petroleum, Inc., San Ramon, CA) IN: Thematic Conference on Remote Sensing for Exploration Geology, 5th, Reno, NV, Sept. 29-Oct. 2, 1986, Proceedings. Volume 1. Ann Arbor, MI, Environmental Research Institute of Michigan, 1987, p. 15-34. refs

Synthetic-aperture radar (SAR) imagery acquired over an area within the southern Papuan Basin fold and thrust belt was used to construct surface-structure and stratigraphic maps for a hydrocarbon exploration program. Stereoscopic analysis of SAR provided essential geologic information that was used to guide the ongoing field work, to model subsurface structures, and to select well locations. SAR imagery revealed significant mass wasting that led to reevaluation of previously acquired field data. The reprocessing and contrast stretching of the digital radar imagery made it possible to extract additional geologic information from the survey in oversaturated (bright) or flared zones. I.S.

A88-32903#

LANDSAT STRUCTURAL ANALYSIS OF THE RHINE VALLEY AND THE JURA MOUNTAIN AREA, WESTERN EUROPE

Z. BERGER and F. V. CORONA (Exxon Production Research Co., Houston, TX) IN: Thematic Conference on Remote Sensing for Exploration Geology, 5th, Reno, NV, Sept. 29-Oct. 2, 1986, Proceedings. Volume 1. Ann Arbor, MI, Environmental Research Institute of Michigan, 1987, p. 35-48. refs

The results of the Landsat imagery analysis of the structural styles, trends, and timing of deformation of exposed and buried structures in the regions of the Rhine Valley, the Jura Mountain, and the Molasse basin are discussed. The Rhine Valley was found to display structural characteristics of an extensional fault-block regime, whereas the Jura Mountains were shown to be a detached fold-and-thrust belt consisting of thrust faults that have irregular to sinuous fault-line traces, elongated folds that are almost parallel to the exposed thrust faults, and strike-slip faults that occur obliquely to the thrust faults. Detailed analysis of the imagery revealed three different types of topographic expressions in the exposed fault systems of the Rhine Graben region: (1) NNE trending strike-slip faults related to the 'wrench-fault' deformation associated with the Hercynian orogenic event; (2) N- to NNE-trending normal faults associated with an Eocene to Pliocene extensional fault-block

events; and (3) possible Hercynian strike-slip faults that were activated as normal faults by the Eocene-Pliocene extensional event. I.S.

A88-32904#

DIGITAL TERRAIN MODEL AND IMAGE INTEGRATION FOR GEOLOGIC INTERPRETATION

R. SIMARD (Canada Centre for Remote Sensing, Ottawa) and R. SLANEY (Geological Survey of Canada, Ottawa) IN: Thematic Conference on Remote Sensing for Exploration Geology, 5th, Reno, NV, Sept. 29-Oct. 2, 1986, Proceedings. Volume 1. Ann Arbor, MI, Environmental Research Institute of Michigan, 1987, p. 49-60. refs

Automatic digital correlation techniques were used to construct an elevation model from two Landsat-5 TM images taken over the Kananaskis Valley, Alberta, Canada, from adjacent orbits with 50 percent overlap. The geology of the valley was taken from a detailed (1 in/2 miles) map and a 16-class geology theme map. The maps were traced manually and digitized, and both sets of TM and geology images were precisely coregistered in the UTM coordinate system with 25 x 25 meter pixels. A series of image products obtained by combining elements from the TM-digital elevation model-geology data sets include an orthographic 'image map', a stereomodel which combines an orthoimage and a synthetic stereomate with geological boundaries, and a geology map. Finally, a series of perspective views was prepared from the TM scene using the geology overlay and the thematic geology map. I.S.

A88-32905#

TARGETING EPITHERMAL ALTERATION AND GOSSANS IN WEATHERED AND VEGETATED TERRAINS USING AIRCRAFT SCANNERS - SUCCESSFUL AUSTRALIAN CASE HISTORIES

S. J. FRASER, A. R. GABELL, A. A. GREEN, and J. F. HUNTINGTON (CSIRO, Div. of Mineral Physics and Mineralogy, North Ryde, Australia) IN: Thematic Conference on Remote Sensing for Exploration Geology, 5th, Reno, NV, Sept. 29-Oct. 2, 1986, Proceedings. Volume 1. Ann Arbor, MI, Environmental Research Institute of Michigan, 1987, p. 63-84. Research sponsored by the Australian Mineral Industries Research Association. refs

Using data from the MEIS-II and Daedalus 1268 ATM scanners, goethitic and hematitic iron-oxide species over gossanous outcrops were mapped, and hydrothermal 'clay' alteration were detected in deeply weathered and vegetated terrains in Queensland, Australia. New processing techniques were developed to complement the improved spectral and radiometric sensitivity of these scanners. 'Image logarithmic residuals' allow interpretation in terms of known reflectivity relationships, by removing pixel-to-pixel brightness variation. 'Directed principal components' and 'least-squares residuals' separate the confusing effects of vegetation and 'clays' in mixed pixels in the 2.2-micron ATM bandpass. The MEIS iron-oxide study revealed that goethitic anomalies occurred at Loch Ness, Lady Annie, and Crystal Creek. Although vegetation can severely restrict the potential of the 2.2-micron ATM bandpass to detect clay alteration, using the above techniques it was possible to separate 'clay' from vegetation responses in mixed pixels at each of our test sites. Author

A88-32906# Jet Propulsion Lab., California Inst. of Tech., Pasadena.

MAPPING THE OMAN OPHIOLITE USING TM DATA

MICHAEL ABRAMS (California Institute of Technology, Jet Propulsion Laboratory, Pasadena) IN: Thematic Conference on Remote Sensing for Exploration Geology, 5th, Reno, NV, Sept. 29-Oct. 2, 1986, Proceedings. Volume 1. Ann Arbor, MI, Environmental Research Institute of Michigan, 1987, p. 85-95. refs

Ophiolite terrains, considered to be the onland occurrences of oceanic crust, host a number of types of mineral deposits: volcanogenic massive sulfides, podiform chromite, and asbestos. Thematic Mapper data for the Semail Ophiolite in Oman were used to separate and map ultramafic lithologies hosting these deposits, including identification of the components of the extrusive volcanic sequence, mapping of serpentinization due to various

tectonic processes, and direct identification of gossans. Thematic Mapper data were found to be extremely effective for mapping in this terrain due to the excellent spatial resolution and the presence of spectral bands which allow separation of the pertinent mineralogically caused spectral features associated with the rock types of interest. Author

A88-32907#

DISCRIMINATION OF LITHOLOGIC UNITS, ALTERATION PATTERNS AND MAJOR STRUCTURAL BLOCKS IN THE TONOPAH, NEVADA AREA USING THEMATIC MAPPER DATA
JOHN C. KEPPER, THOMAS P. LUGASKI (Nevada, University, Reno), and JOHN S. MACDONALD (MacDonald Dettwiler and Associates, Richmond, Canada) IN: Thematic Conference on Remote Sensing for Exploration Geology, 5th, Reno, NV, Sept. 29-Oct. 2, 1986, Proceedings. Volume 1. Ann Arbor, MI, Environmental Research Institute of Michigan, 1987, p. 97-115. refs

A88-32908#

ASSOCIATIONS AMONG LINEAMENTS, SUBSURFACE FRACTURES, HYDROCARBON MICROSEEPAGE, AND PRODUCTION IN THE UINTA BASIN, UTAH
ROGER MCCOY, STEPHEN YOUNG (Utah, University, Salt Lake City), MICHAEL J. HAVERTZ (Satellite Exploration Consultants, Inc., Midland, TX), KEITH CLEM, and CYNTHIA BRANDT (Utah Geological and Mineral Survey, Salt Lake City) IN: Thematic Conference on Remote Sensing for Exploration Geology, 5th, Reno, NV, Sept. 29-Oct. 2, 1986, Proceedings. Volume 1. Ann Arbor, MI, Environmental Research Institute of Michigan, 1987, p. 117-130. refs

Two oil fields in the Uinta Basin of Utah were studied for relationships among lineaments, hydrocarbon gas flux, and rates of production. The Monument Butte Field, with production from 3500 to 5800 feet, showed a strong positive relationship among lineament density, near-surface gas flux, and production rates. In contrast, the Altamont-Bluebell Field has much deeper production, 8000-16,000 feet, and the relationship between lineament density and production was weak. Greater promise is shown in the Altamont-Bluebell for the analysis of intersections between lineament sets, particularly E-W lineaments with other sets. It is concluded that the combination of lineament analysis and geochemical surveys can be a successful exploration tool in both the shallow reservoir of the Monument Butte Field, and deep reservoir of the Altamont-Bluebell Field. Author

A88-32912#

INTEGRATION OF SIR-B IMAGERY WITH GEOLOGICAL AND GEOPHYSICAL DATA IN AUSTRALIA
G. J. LYNNE and G. R. TAYLOR (New South Wales, University, Sydney, Australia) IN: Thematic Conference on Remote Sensing for Exploration Geology, 5th, Reno, NV, Sept. 29-Oct. 2, 1986, Proceedings. Volume 1. Ann Arbor, MI, Environmental Research Institute of Michigan, 1987, p. 179-191. refs

SIR-B imagery of the arid region of central Australia is integrated with co-registered Landsat MSS and TMS thermal data. Multi-band and color ratio composites of SIR-B and TMS imagery are found to enhance different geological information. The relative abilities of SIR-B and airphotos to discern lineaments are compared, and SIR-B is found to enhance lineaments perpendicular to the look direction and suppress those that are parallel. Lineaments digitized directly from a 1:100,000 print of the SIR-B Amadeus scene are processed to produce a contour plot of fracture density values. Lineament density contours integrated with geological and geophysical data define structural regions in both basement rocks and overlying sediments. Multiple SIR-B imagery acquired over South Australia clearly shows the dependence of radar backscatter on incidence angle. Low incidence angles define topographic variations, while backscatter response at medium to high incidence angles is dependent on surface roughness. Author

A88-32913#**FRACTURE PATTERNS AND PRODUCTION TRENDS, BIG SANDY FIELD, EASTERN KENTUCKY**

ROBERT J. PAUKEN (Mobil Exploration and Production Services, Inc., Dallas, TX), J. H. GRIFFITH, and J. H. HALSEY IN: Thematic Conference on Remote Sensing for Exploration Geology, 5th, Reno, NV, Sept. 29-Oct. 2, 1986, Proceedings. Volume 1. Ann Arbor, MI, Environmental Research Institute of Michigan, 1987, p. 193-216. refs

The major directions of natural fractures were identified and correlated with the production trends in the Big Sandy Gas Field in eastern Kentucky using a broad spectrum of data and types of technology. The initial production values for over 7000 wells were mapped to determine productivity trends; in order to perform the trend analysis, well locations, initial production volumes, and producing horizons were digitized into a computer-accessible database. The photolineaments (most of which were segments of stream valleys or alignments of notches in the interstream divides) were measured on Landsat and airborne SLR imagery. The results of the analysis show a consistent set of fracture trends which appear to be uniform over much of the Appalachian Basin. The calculated productivity trends were found to correspond on a one-to-one basis with the fracture trends, indicating that the photolineament pattern is reflecting the orientation of subsurface fractures which are controlling gas production. I.S.

A88-32914#**ROCK DISCRIMINATION AND ALTERATION MAPPING FOR MINERAL EXPLORATION USING THE CARR BOYD/GEOSCAN AIRBORNE MULTISPECTRAL SCANNER**

F. R. HONEY (Geoscan Pty., Ltd., Perth, Australia) and J. L. DANIELS (Carr Boyd Minerals, Ltd., Perth, Australia) IN: Thematic Conference on Remote Sensing for Exploration Geology, 5th, Reno, NV, Sept. 29-Oct. 2, 1986, Proceedings. Volume 1. Ann Arbor, MI, Environmental Research Institute of Michigan, 1987, p. 267-278.

A88-32915*# Nevada Univ., Reno.**CORRELATION BETWEEN HIGH RESOLUTION REMOTE SENSING IMAGERY AND HYDROTHERMAL ALTERATION, TYBO MINING DISTRICT, NEVADA**

S. C. FELDMAN and J. V. TARANIK (Nevada, University, Reno) IN: Thematic Conference on Remote Sensing for Exploration Geology, 5th, Reno, NV, Sept. 29-Oct. 2, 1986, Proceedings. Volume 1. Ann Arbor, MI, Environmental Research Institute of Michigan, 1987, p. 279-297. Research supported by ARCO Exploration and Technology Co. refs (Contract NASW-4050)

A88-32916#**CONTRIBUTION OF LANDSAT TO A GEOLOGIC EXPEDITION IN THE DESERT OF NORTH CENTRAL SUDAN, AFRICA**

CLAUDE M. FROIDEVAUX (Phillips Petroleum Co., Bartlesville, OK) and STEVEN J. TKACH (Phillips Petroleum Co., Denver, CO) IN: Thematic Conference on Remote Sensing for Exploration Geology, 5th, Reno, NV, Sept. 29-Oct. 2, 1986, Proceedings. Volume 1. Ann Arbor, MI, Environmental Research Institute of Michigan, 1987, p. 299-305.

A88-32917*#

Jet Propulsion Lab., California Inst. of Tech., Pasadena.

SATELLITE RADARS FOR GEOLOGIC MAPPING IN TROPICAL REGIONS

J. P. FORD (California Institute of Technology, Jet Propulsion Laboratory, Pasadena) and F. F. SABINS (Chevron Oil Field Research Co., La Habra, CA) IN: Thematic Conference on Remote Sensing for Exploration Geology, 5th, Reno, NV, Sept. 29-Oct. 2, 1986, Proceedings. Volume 1. Ann Arbor, MI, Environmental Research Institute of Michigan, 1987, p. 307-316. refs

This paper presents interpretations of the satellite radar images of cloud-covered portions of Indonesia and Amazonia obtained from NASA's Shuttle imaging radar experiments in 1981 (SIR-A) and 1984 (SIR-B). It was found that different terrain categories

04 GEOLOGY AND MINERAL RESOURCES

observed from distinctive image textures correlate well with major lithologic associations. The images show geologic structures at regional and local scales. The SIR-B images of East Kalimantan, Indonesia, reveal structural features and terrain distributions that had been overlooked or not perceived in previous surface mapping. Variability in radar response from the vegetation cover is interpretable only in coastal areas or alluvial areas that are relatively level. I.S.

A88-32918#

AFTER EXPLORATION, WHAT? - CASE HISTORIES OF SEVEN DIVERSE PRODUCTION, DEVELOPMENT AND DISTRIBUTION APPLICATIONS OF REMOTE SENSING

ALLEN M. FEDER, CYNTHIA A. SHEEHAN, and DARCY L. VIXO (Western Geophysical Company of America, Houston, TX) IN: Thematic Conference on Remote Sensing for Exploration Geology, 5th, Reno, NV, Sept. 29-Oct. 2, 1986, Proceedings. Volume 1. Ann Arbor, MI, Environmental Research Institute of Michigan, 1987, p. 317-324.

The paper describes seven diverse case histories in successful postexploration applications of remote sensing. The first three case histories involve 8-14-micrometer remote sensing for locating groundwater for drilling, for determining geologic conditions suitable for drilling-waste disposal, and for mapping the advance of a steam-flood front in secondary recovery. The fourth case history involves aeromagnetometry for the measure of the areal extent of a reservoir, and 'stepping-off' production from producing fields. The next two case histories center on Landsat imagery processing and interpretation for pipeline routing in Arctic permafrost and humid tropics terrains. The last case history returns to 8-14 micrometer scanning for efficacious pipeline leak detection. As a suite, these case histories provide examples of innovative applications of remote sensing, with its unique advantages, that make it possible to bridge the critical activities between exploration and final marketing. Author

A88-32920#

LINEAMENTS OF THE NORTHERN DENVER BASIN AND THEIR PALEOTECTONIC AND HYDROCARBON SIGNIFICANCE

S. L. PERRY (Barringer Geoservices, Inc., Golden, CO) and KEENAN LEE (Colorado School of Mines, Golden) IN: Thematic Conference on Remote Sensing for Exploration Geology, 5th, Reno, NV, Sept. 29-Oct. 2, 1986, Proceedings. Volume 1. Ann Arbor, MI, Environmental Research Institute of Michigan, 1987, p. 335-346. refs

Twenty four lineaments in the northern Denver Basin were interpreted using a statistical analysis of mapped linear features from edge-enhanced Landsat MSS imagery (bands 7, 5, and 4), and their paleotectonic and hydrocarbon significance is discussed. In the northern Denver Basin, lineaments trend predominately northeast and northwest and are divided into mountain-flank and basin-interior groups. Several lineaments show relationships to known hydrocarbon accumulations, by paralleling production trends and bounding production domains. I.S.

A88-32922#

GEOLOGIC INTERPRETATION OF AIR PHOTOS AND RADAR IMAGERY FOR HYDROELECTRIC POWER PROJECTS IN UPPER UCAYALI JUNGLE REGION OF PERU

EPIFANIO SUYO RIVERA (Electroperu, S.A., Peru) IN: Thematic Conference on Remote Sensing for Exploration Geology, 5th, Reno, NV, Sept. 29-Oct. 2, 1986, Proceedings. Volume 1. Ann Arbor, MI, Environmental Research Institute of Michigan, 1987, p. 363-371. refs

A88-32923#

THEMATIC MAPPER DATA APPLIED TO MAPPING HYDROTHERMAL ALTERATION IN SOUTH WEST NEW MEXICO

ROBERT W. MAGEE, JOHN MCMAHON MOORE, and JAKE BRUNNER (Imperial College of Science and Technology, London, England) IN: Thematic Conference on Remote Sensing for

Exploration Geology, 5th, Reno, NV, Sept. 29-Oct. 2, 1986, Proceedings. Volume 1. Ann Arbor, MI, Environmental Research Institute of Michigan, 1987, p. 373-382. refs

This study evaluates the value of the TM 5/7 clay ratio (which allows the detection of silicic, advanced argillic, and sericitic hydrothermal alteration) and the limonite-sensitive ratios TM 5/1, TM 5/4, TM 3/2, and TM 3/1 as an aid to prospecting for epithermal mineral deposits. In the Summit Mountains used as a test site, all these bands successfully showed the alterations. These ratios were used to produce an alteration map of the Blue Creek Basin of southwest New Mexico, comparable to the map obtained from conventional field mapping methods. The performance of all the ratios was found to be affected by the presence of vegetation. A vegetation masking technique, using TM bands 4, 3, and 2 transformed to the hue saturation and the intensity values, was applied to the band ratios to remove spurious targets, thus making it possible to recognize in the Blue Creek Basin several previously unrecorded localities with the spectral characteristics of hydrothermal alteration. I.S.

A88-32924#

APPLICATION OF REMOTE SENSING TO TECTONIC AND METALLOGENIC STUDIES IN NE AFRICA

SEIFE M. BERHE (Open University, Milton Keynes, England) IN: Thematic Conference on Remote Sensing for Exploration Geology, 5th, Reno, NV, Sept. 29-Oct. 2, 1986, Proceedings. Volume 1. Ann Arbor, MI, Environmental Research Institute of Michigan, 1987, p. 383-391. Sponsorship: Research supported by the World University Service. refs

A model for the regional framework of NE Africa was developed initially using field traverses and bulk processed black and white Landsat MSS images at a scale of 1:500,000. From this broad perspective, interactive digital processing was carried out on selected areas in W Ethiopia, SE Sudan, and N Kenya. Principal component analysis decorrelation stretching and box-car filtering were used to delineate major lithologic and crustal lineaments. Based on this study it was possible to trace five ophiolitic belts, and to subdivide NE Africa into three structurally distinct areas: (1) in NE Sudan-Eritrea there is a complex interaction of northeasterly and northwesterly structures; (2) in W Ethiopia the structural trends are dominantly N-S to northeasterly; (3) in S Ethiopia, Uganda and N Kenya the structural trend is northwesterly, which is a consequence of shearing along northwesterly trending faults. W Ethiopia has been taken as a case study and guidelines for future mineral exploration are discussed. From consideration of the geographical distribution of orefields, geochemical anomalies and lineament maps, it is shown that lineaments may have influenced localization of several ore deposits in this region. Author

A88-32925#

IMPORTANCE OF FAULT MAPPING TO MINERAL/GEOTHERMAL EXPLORATION: RELATIONSHIP TO FLUID MIGRATION AND ORE FORMATION - NORTHWEST WASHINGTON

LOWELL E. BOGART (Geological and Exploration Associates, Port Townsend, WA) and LEIGH A. READDY (Geological and Exploration Associates, Kirkland, WA) IN: Thematic Conference on Remote Sensing for Exploration Geology, 5th, Reno, NV, Sept. 29-Oct. 2, 1986, Proceedings. Volume 1. Ann Arbor, MI, Environmental Research Institute of Michigan, 1987, p. 395-404. refs

A88-32926#

SPECTRAL DISCRIMINATION OF ZEOLITES AND DIOCTAHEDRAL CLAYS IN THE NEAR-INFRARED

WILLIAM J. EHMANN and NORMA VERGO (USGS, Reston, VA) IN: Thematic Conference on Remote Sensing for Exploration Geology, 5th, Reno, NV, Sept. 29-Oct. 2, 1986, Proceedings. Volume 1. Ann Arbor, MI, Environmental Research Institute of Michigan, 1987, p. 417-425. refs

Analysis of laboratory near-infrared spectra of zeolites and dioctahedral clays suggests a means for discriminating between

the two mineral groups. From 0.4-0.7 micron, the spectral curves of both zeolites and dioctahedral clays show increasing reflectance values, with high reflectance values from 0.7-2.5 microns, punctuated by intense molecular water absorptions at 1.41 and 1.90 microns. However, at 2.20 microns, dioctahedral clays show a moderately strong absorption feature due to overtones of the Al-OH bending mode, whereas most zeolites have a local reflectance maximum in this region. Natrolite and analcime are unusual in that they exhibit additional well-defined absorption features in the 2.0-2.5 micron region that probably result from water occupying different molecular sites. Although the spectral difference between the zeolites and clays at 2.20 microns is not resolvable using the Thematic Mapper, it should be apparent when using higher resolution sensors such as the Airborne Imaging Spectrometer.

Author

A88-32927*# Jet Propulsion Lab., California Inst. of Tech., Pasadena.

USE OF CALIBRATION TARGETS IN THE MEASUREMENT OF 2.22-MICRON MINERAL ABSORPTION FEATURES IN THEMATIC MAPPER DATA

CHRISTOPHER D. ELVIDGE (California Institute of Technology, Jet Propulsion Laboratory, Pasadena) IN: Thematic Conference on Remote Sensing for Exploration Geology, 5th, Reno, NV, Sept. 29-Oct. 2, 1986, Proceedings. Volume 1. Ann Arbor, MI, Environmental Research Institute of Michigan, 1987, p. 427-438. refs

A mineral absorption index (MAI) has been developed to separate leaf water and mineral absorption in the 2.22-micron Thematic Mapper band. The MAI uses three baselines to estimate and subtract the absorption attributable to vegetation. Digital number data from calibration targets devoid of vegetation are used to establish the positions of the baselines in Thematic Mapper data.

Author

A88-32929#
SURFACE EXPRESSION OF SUBSURFACE STRUCTURES IN THE MICHIGAN BASIN

JOHN D. HERMAN and JANE E. WAITES (GeoSpectra Corp., Ann Arbor, MI) IN: Thematic Conference on Remote Sensing for Exploration Geology, 5th, Reno, NV, Sept. 29-Oct. 2, 1986, Proceedings. Volume 2. Ann Arbor, MI, Environmental Research Institute of Michigan, 1987, p. 451-461. refs

Consideration is given to the surface features over subsurface structures associated with selected known oil and gas fields in the Michigan Basin including the Boyd-Peters field in southern St. Clair County, the Rich oil and gas field in northern Lapeer County, the Albion-Scipio field in Calhoun, Jackson, and Hillsdale Counties, and the Stoney Point field in Jackson and Hillsdale Counties. Comparisons were made between bedrock surface contour maps and glacial drift thickness and lithology maps, subsurface structure maps, plots of Landsat lineaments and circular features, Landsat lineament density contour maps automatically produced by computer software, and shaded relief maps derived from digital terrain data tapes by computer software. It is shown that subsurface structures on the southern rim of the Michigan Basin are associated with detectable surface expressions in the form of lineaments and oval features even though these structures are covered by glacial drift.

K.K.

A88-32931#
A GEOBOTANICAL INVESTIGATION OF AN EXPLORATION-SIZED TERRITORY

MATHEW R. SCHWALLER (EOSAT Co., Lanham, MD) and STEVEN J. TKACH (Phillips Petroleum Co., Denver, CO) IN: Thematic Conference on Remote Sensing for Exploration Geology, 5th, Reno, NV, Sept. 29-Oct. 2, 1986, Proceedings. Volume 2. Ann Arbor, MI, Environmental Research Institute of Michigan, 1987, p. 483-489. refs

This paper summarizes the final results from a series of geobotanical investigations conducted on Michigan's Keweenaw Peninsula. The investigations were conducted in an area of copper sulfide mineralization covered by deciduous forest. This area was

chosen because a 30,000 sample soil geochemical survey covering 20 sq km was available for comparison with airborne Thematic Mapper Simulator (TMS) imagery. Linear discriminant analysis revealed that the TMS thermal channel (10.32-12.33 microns) contributed most, while TMS bands 2 (0.53-0.60 micron), 3 (0.63-0.69 micron), and 5 (1.53-1.73 anomalous and background sites micron) contributed somewhat more modestly to separation of geochemically anomalous and background sites imaged by the TMS. Geobotanical indices based on these bands identified candidate areas that contained elevated concentrations of soil copper at a rate up to 8 times higher than expected by random or systematic sampling.

Author

A88-32934#
SPECTRAL GEOBOTANICAL INVESTIGATION OF MINERALIZED TILL SITES

V. SINGHROY (Ontario Centre for Remote Sensing, Toronto, Canada), R. STANTON-GRAY (Perceptron Computing, Inc., Toronto, Canada), and J. SPRINGER (Ontario Geological Survey, Sudbury, Canada) IN: Thematic Conference on Remote Sensing for Exploration Geology, 5th, Reno, NV, Sept. 29-Oct. 2, 1986, Proceedings. Volume 2. Ann Arbor, MI, Environmental Research Institute of Michigan, 1987, p. 523-543. refs

The spectral response of conifers and deciduous tree species growing on three mineralized sites in glaciated and vegetated terrains (a site near White Lake site in Northern Manitoba, a site near Natal Lake in Northern Ontario, and a site near Arnprior in Eastern Ontario) is studied. The till of the White Lake site contains 150 to 3,000 ppm of Zn-Cu-Pb whereas the geochemical values at the Natal Lake and Arnprior sites vary from 60 to 1,500 ppm of Zn-Cu-Pb in the rock in soil. It is shown that, when MEIS II bands are matched to reliable spectral signatures, the data they produce are capable of revealing geochemically stressed vegetation.

K.K.

A88-32936#
A COMPARISON OF LINEAMENTS INTERPRETED FROM REMOTELY SENSED DATA AND AIRBORNE MAGNETICS AND THEIR RELATIONSHIP TO GOLD DEPOSITS IN CENTRAL NOVA SCOTIA

J. HARRIS (F. G. Bercha and Associates, Ltd.; Canada Centre for Remote Sensing, Ottawa) IN: Thematic Conference on Remote Sensing for Exploration Geology, 5th, Reno, NV, Sept. 29-Oct. 2, 1986, Proceedings. Volume 2. Ann Arbor, MI, Environmental Research Institute of Michigan, 1987, p. 557-576. refs

A88-32937#
CONFIRMATION OF QUANTITATIVE MORPHOSTRUCTURAL ANALYSIS BY SEISMIC, AEROMAGNETIC AND GEOCHEMICAL DATA IN THE AMAZON BASIN, BRAZIL
FERNANDO PELLON DE MIRANDA and NELSON ADAO BABINSKI (PETROBRAS, Centro de Pesquisas e Desenvolvimento, Rio de Janeiro, Brazil) IN: Thematic Conference on Remote Sensing for Exploration Geology, 5th, Reno, NV, Sept. 29-Oct. 2, 1986, Proceedings. Volume 2. Ann Arbor, MI, Environmental Research Institute of Michigan, 1987, p. 579-587. refs

A88-32938#
THEMATIC MAPPER APPLIED TO ALTERATION ZONE MAPPING FOR GOLD EXPLORATION IN SOUTH-EAST SPAIN
J. A. HUCKERBY, R. MAGEE, J. MCM. MOORE (Imperial College of Science and Technology, London, England), and D. COATES IN: Thematic Conference on Remote Sensing for Exploration Geology, 5th, Reno, NV, Sept. 29-Oct. 2, 1986, Proceedings. Volume 2. Ann Arbor, MI, Environmental Research Institute of Michigan, 1987, p. 591-599.

A88-32939#
EXPLORATION FOR MERCURY AND LEAD-ZINC-SILVER USING THE AIRBORNE THEMATIC MAPPER, ALMADEN AREA, SPAIN
A. E. HARDING, G. R. GARRARD (Hunting Geology and Geophysics, Ltd., Borehamwood, England), and E. ORTEGA

04 GEOLOGY AND MINERAL RESOURCES

GIRONES (Minas de Almaden y Attayanes, S.A., Spain) IN: Thematic Conference on Remote Sensing for Exploration Geology, 5th, Reno, NV, Sept. 29-Oct. 2, 1986, Proceedings. Volume 2. Ann Arbor, MI, Environmental Research Institute of Michigan, 1987, p. 601-606. refs

A88-32940#

THE USE OF THEMATIC MAPPER IMAGERY FOR MINERAL EXPLORATION IN THE SEDIMENTARY TERRAIN OF THE SPRING MOUNTAINS, NEVADA

DAVID W. BRICKEY (USGS, Reston, VA) IN: Thematic Conference on Remote Sensing for Exploration Geology, 5th, Reno, NV, Sept. 29-Oct. 2, 1986, Proceedings. Volume 2. Ann Arbor, MI, Environmental Research Institute of Michigan, 1987, p. 607-613. refs

This study reports on an assessment of the mineral potential of the sedimentary rocks in a part of the Spring Mountains of southern Nevada. The mountains are comprised of Precambrian to Jurassic sedimentary rocks of predominately carbonate composition. Known mineralization occurs primarily as vein and replacement ores of base and precious metals in Paleozoic dolomitized limestones, and in Precambrian clastic and carbonate rocks. A color-ratio-composite (CRC) image of Landsat Thematic Mapper (TM) band ratios 5/7, 5/4, and 3/1 was used to locate potentially hydrothermally altered rocks associated with these mineralization types. Subsequent field checking of the TM-defined anomalies located four altered areas in clastic rocks and one in carbonate rocks. TM anomalies caused by unaltered carbonate rocks could be distinguished from altered rocks only with field work. A digital classification of hydrothermally altered rocks was made by using the CRC image. Author

A88-32941*# Nevada Univ., Reno.

AN INTEGRATED APPROACH TO THE USE OF LANDSAT TM DATA FOR GOLD EXPLORATION IN WEST CENTRAL NEVADA

D. A. MOUAT (Nevada, University, Reno), J. S. MYERS (NASA, Ames Research Center, Moffett Field, CA), and N. L. MILLER (Advanced Exploration Technologies, Vancouver, Canada) IN: Thematic Conference on Remote Sensing for Exploration Geology, 5th, Reno, NV, Sept. 29-Oct. 2, 1986, Proceedings. Volume 2. Ann Arbor, MI, Environmental Research Institute of Michigan, 1987, p. 615-626. refs

This paper represents an integration of several Landsat TM image processing techniques with other data to discriminate the lithologies and associated areas of hydrothermal alteration in the vicinity of the Paradise Peak gold mine in west central Nevada. A microprocessor-based image processing system and an IDIMS system were used to analyze data from a 512 X 512 window of a Landsat-5 TM scene collected on June 30, 1984. Image processing techniques included simple band composites, band ratio composites, principal components composites, and baseline-based composites. These techniques were chosen based on their ability to discriminate the spectral characteristics of the products of hydrothermal alteration as well as of the associated regional lithologies. The simple band composite, ratio composite, two principal components composites, and the baseline-based composites separately can define the principal areas of alteration. Combined, they provide a very powerful exploration tool. Author

A88-32942#

IDENTIFICATION OF CLAY MINERALS BY FEATURE CODING OF NEAR-INFRARED SPECTRA

YASUSHI YAMAGUCHI and RONALD J. P. LYON (Stanford University, CA) IN: Thematic Conference on Remote Sensing for Exploration Geology, 5th, Reno, NV, Sept. 29-Oct. 2, 1986, Proceedings. Volume 2. Ann Arbor, MI, Environmental Research Institute of Michigan, 1987, p. 627-636. refs

A88-32944#

DETECTION OF GEOLOGIC FEATURES IN LANDSAT TM IMAGERY NOT REVEALED IN LANDSAT MSS IMAGERY

T. E. TOWNSEND (Exxon Production Research Co., Houston, TX)

IN: Thematic Conference on Remote Sensing for Exploration Geology, 5th, Reno, NV, Sept. 29-Oct. 2, 1986, Proceedings. Volume 2. Ann Arbor, MI, Environmental Research Institute of Michigan, 1987, p. 651-654.

Landsat Thematic Mapper (TM) data are significantly better than Landsat Multispectral Scanner (MSS) data for exploration applications because TM data provide geologic information not previously available. Landsat-4 MSS imagery of Death Valley, California, was compared with simultaneously acquired TM imagery of the same area to determine how the geologic interpretability of the data was enhanced by its greater spatial, spectral, and radiometric resolution. The greater spatial resolution of the TM allowed faults and folds to be interpreted more reliably and allowed secondary features associated with them to be recognized that were not detectable on the MSS imagery. Furthermore, oxidation of basalts was detected because of the better spectral resolution of the system. The additional structural and lithologic information available from TM data promotes improved geologic mapping, which can often be critical to exploration applications. Author

A88-32945#

SPECTRAL REFLECTANCE FROM LICHENS TREATED WITH COPPER

P. J. BECKETT and G. M. COURTIN (Sudbury, Laurentian University, Canada) IN: Thematic Conference on Remote Sensing for Exploration Geology, 5th, Reno, NV, Sept. 29-Oct. 2, 1986, Proceedings. Volume 2. Ann Arbor, MI, Environmental Research Institute of Michigan, 1987, p. 661-666. Research supported by the Laurentian University of Sudbury and Ontario Geoscience Research Grant Program. refs

Reflectance spectra were measured on 'Caribou Lichen' before, and following exposure to copper sulphate solutions. The copper treatment produced shift changes in the visible and 0.75-1.0 micron portions of the spectrum. Metal extraction techniques indicated that about 90 percent of the copper taken up by the lichen was located outside the algal cells and fungal hyphae. The spectral changes in the visible wavelengths correlate with the destruction of algal chlorophyll by the copper taken into the cells. Author

A88-32946#

USE OF DIGITALLY PROCESSED LABORATORY REFLECTANCE SPECTRA FOR THE DEFINITION OF PROBABLE MICROSEEPAGE - INDUCED MINERALOGIC VARIATIONS, LISBON VALLEY, UTAH

DONALD B. SEGAL, IRA S. MERIN, and MICHAEL C. PLACE (Earth Satellite Corp., Chevy Chase, MD) IN: Thematic Conference on Remote Sensing for Exploration Geology, 5th, Reno, NV, Sept. 29-Oct. 2, 1986, Proceedings. Volume 2. Ann Arbor, MI, Environmental Research Institute of Michigan, 1987, p. 667-676. refs

A88-32947#

GEOLOGIC SPATIAL ANALYSIS - A NEW MULTIPLE DATA SOURCE EXPLORATION TOOL

JAY R. ELIASON (Battelle Pacific Northwest Laboratories, Richland, WA) and RICHARD L. THIESSEN (Washington State University, Pullman) IN: Thematic Conference on Remote Sensing for Exploration Geology, 5th, Reno, NV, Sept. 29-Oct. 2, 1986, Proceedings. Volume 2. Ann Arbor, MI, Environmental Research Institute of Michigan, 1987, p. 677-692. refs (Contract DE-AC06-76RL-01830)

A research program has been initiated at the DOE Pacific Northwest Laboratory to develop quantitative and predictive spatial analysis techniques for determining the relationships between geological, geophysical, and geochemical structures in the solid earth. The geologic spatial analysis (GSA) program involves the development of digitized structural geologic analysis techniques to quantitatively analyze three-dimensional geologic data sets. Applying GSA to specific data sets makes it possible to: (1) evaluate oil and natural gas resources as well as geothermal fluid migration paths, (2) locate and assess mineral deposits, and (3) model ground-water flow systems. K.K.

A88-32948* # Cornell Univ., Ithaca, N.Y.

DISCRIMINATION AND SUPERVISED CLASSIFICATION OF VOLCANIC FLOWS OF THE PUNA-ALTIPLANO, CENTRAL ANDES MOUNTAINS USING LANDSAT TM DATA

J. H. MCBRIDE, E. J. FIELDING, and B. L. ISACKS (Cornell University, Ithaca, NY) IN: Thematic Conference on Remote Sensing for Exploration Geology, 5th, Reno, NV, Sept. 29-Oct. 2, 1986, Proceedings. Volume 2. Ann Arbor, MI, Environmental Research Institute of Michigan, 1987, p. 693-702. refs (Contract NAS5-28767)

Landsat Thematic Mapper (TM) images of portions of the Central Andean Puna-Altiplano volcanic belt have been tested for the feasibility of discriminating individual volcanic flows using supervised classifications. This technique distinguishes volcanic rock classes as well as individual phases (i.e., relative age groups) within each class. The spectral signature of a volcanic rock class appears to depend on original texture and composition and on the degree of erosion, weathering, and chemical alteration. Basalts and basaltic andesite stand out as a clearly distinguishable class. The age dependent degree of weathering of these generally dark volcanic rocks can be correlated with reflectance: older rocks have a higher reflectance. On the basis of this relationship, basaltic lava flows can be separated into several subclasses. These individual subclasses would correspond to mappable geologic units on the ground at a reconnaissance scale. The supervised classification maps are therefore useful for establishing a general stratigraphic framework for later detailed surface mapping of volcanic sequences. Author

A88-32949#

ASSESSMENT OF DIGITAL ENHANCEMENT TECHNIQUES USING LANDSAT TM DATA IN MAPPING GEOLOGIC LINEAMENTS, WITH APPLICATION TO THE MACTAQUAC HEADPOND AREA, SOUTHERN NEW BRUNSWICK

R. YAZDANI, E. DERENYI, J. J. CHANDRA, and G. GOUCHER (New Brunswick University, Fredericton, Canada) IN: Thematic Conference on Remote Sensing for Exploration Geology, 5th, Reno, NV, Sept. 29-Oct. 2, 1986, Proceedings. Volume 2. Ann Arbor, MI, Environmental Research Institute of Michigan, 1987, p. 707-712. refs

A88-32950#

LANDSAT TM DATA AS AN AID IN PLANNING AND INTERPRETATION OF REGIONAL GEOCHEMICAL SURVEYS IN THE CANADIAN SHIELD

JOHN A. C. FORTESCUE (Ontario Geological Survey, Toronto, Canada), VERN H. SINGHROY (Ontario Centre for Remote Sensing, Toronto, Canada), and ROBERTA STANTON-GRAY (PCI, Ltd., Toronto, Canada) IN: Thematic Conference on Remote Sensing for Exploration Geology, 5th, Reno, NV, Sept. 29-Oct. 2, 1986, Proceedings. Volume 2. Ann Arbor, MI, Environmental Research Institute of Michigan, 1987, p. 715-721.

The feasibility of using Landsat TM data to plan and interpret regional geochemical surveys in the Canadian Shield based on lake waters and sediments is assessed. A 112.2 x 15 km area in the District of Algoma was chosen for study; the geological map of the sampled area includes areas of granitic terrain, metavolcanics, and metasediments. It is concluded that Landsat TM data may be of considerable importance to the methodology of regional and geochemical surveying. K.K.

A88-32951* # Dartmouth Coll., Hanover, N.H.

REMOTE SENSING OF GEBOTANICAL ASSOCIATIONS IN CLASTIC SEDIMENTARY TERRANE

N. J. DEFEO, R. W. BIRNIE (Dartmouth College, Hanover, NH), and K. G. MILLER (Pennsylvania, Millersville University, Millersville) IN: Thematic Conference on Remote Sensing for Exploration Geology, 5th, Reno, NV, Sept. 29-Oct. 2, 1986, Proceedings. Volume 2. Ann Arbor, MI, Environmental Research Institute of Michigan, 1987, p. 723-732. refs (Contract NASW-4049; JPL-956937)

Landsat Thematic Mapper data have been used to map lithologic units in the heavily forested Ridge and Valley Province,

Pennsylvania. This region provides an excellent study area because there is a north-south replication of lithologic units, each with varying slope, aspect, and geobotanical associations. Each of four possible combinations of lithology (sandstone and shale) and aspect (north and south) was found to support a unique forest association. In addition, each of the four lithologic/aspect units has a unique TM spectral signature. A maximum likelihood classification algorithm produced a map that correlates well with the known lithology of the study area. The first principal component of the TM data correlates highly with illumination. The second principal component of the TM data correlates highly with latitude and may reflect senescence changes in this fall scene. Author

A88-32952#

INTEGRATION OF REMOTE SENSING AND OTHER GEO-DATA FOR ORE EXPLORATION - A SW-IBERIAN CASE STUDY

P. VOLK, R. HAYDN (Gesellschaft fuer angewandte Fernerkundung mbH, Munich, Federal Republic of Germany), and J. BODECHTEL (Muenchen, Universitaet, Munich, Federal Republic of Germany) IN: Thematic Conference on Remote Sensing for Exploration Geology, 5th, Reno, NV, Sept. 29-Oct. 2, 1986, Proceedings. Volume 2. Ann Arbor, MI, Environmental Research Institute of Michigan, 1987, p. 733-744. refs (Contract BMFT-01-QS-0730)

An area in the heart of the Southwest Iberian pyrite belt with potential for unexplored polymetallic pyrite ore (Rio Tinto-Tharsis type) has been the subject of a research project at the Institute for General and Applied Geology. An attempt was made to establish an effective exploration strategy by integrated survey techniques, based on the ore-genetical conditions and the lithological environment. Indirect and direct hints to ore facies were among the two types of thematic information extracted. K.K.

A88-32953#

REMOTE SENSING AND SURFACE GEOCHEMICAL STUDY OF RAILROAD VALLEY, NYE COUNTY, NEVADA - DETAILED GRID STUDY

S. G. BURTELL, V. T. JONES (Exploration Technologies, Inc., Houston, TX), R. A. HODGSON (Geologic Consulting Services, Jamestown, PA), K. OKADA, and T. OHHASHI (Japex Geoscience Institute, Inc., Tokyo, Japan) IN: Thematic Conference on Remote Sensing for Exploration Geology, 5th, Reno, NV, Sept. 29-Oct. 2, 1986, Proceedings. Volume 2. Ann Arbor, MI, Environmental Research Institute of Michigan, 1987, p. 745-759. refs

A two-year combined remote sensing and soil-gas geochemical study conducted in Railroad Valley, Nevada is described. Soil-gas compositional subdivisions subdivide the Currant area into two compositionally different anomalies which are located northwest and southeast of the Currant Creek regional lineament. Near-surface light hydrocarbon data in the Grant Canyon detail area reveal a series of anomalous zones which reflect the updip migration of gases from the Grant Canyon producing area along the valley boundary fault. K.K.

A88-32954#

PYROPHYLLITE AND KAOLINITE ALTERATION - MINERAL DISCRIMINATION BY SAMPLE REFLECTANCE MEASUREMENT

PAUL M. LAWRENCE, RAYMOND E. LETT, NORMAN GROSKOPF (Barringer Research, Ltd., Rexdale, Canada), and GEORGE CARGILL (Utah Mines, Ltd., Toronto, Canada) IN: Thematic Conference on Remote Sensing for Exploration Geology, 5th, Reno, NV, Sept. 29-Oct. 2, 1986, Proceedings. Volume 2. Ann Arbor, MI, Environmental Research Institute of Michigan, 1987, p. 775-784. refs

A88-32956#

PATTERN RECOGNITION AND GEOLOGICAL INTERPRETATION OF SIR-B IMAGES OF CENTRAL AUSTRALIA

G. R. TAYLOR and G. J. LYNNE (New South Wales, University, Sydney, Australia) IN: Thematic Conference on Remote Sensing

04 GEOLOGY AND MINERAL RESOURCES

for Exploration Geology, 5th, Reno, NV, Sept. 29-Oct. 2, 1986, Proceedings. Volume 2. Ann Arbor, MI, Environmental Research Institute of Michigan, 1987, p. 799-809. refs

A test area of the northern margin of the Simpson Desert was chosen for study because of the availability of planned SIR-B orbits, its petroleum potential, and the normally arid nature of the region. The application of various preprocessing and pattern recognition filters designed to facilitate geological discrimination is described. It is concluded that the use of SIR-B variance images for pattern recognition provides an objective machine-assisted technique for radar image interpretation that is particularly valid for remote areas where detailed topographic contour data are not available. K.K.

A88-32957# DISCRIMINATION OF GEBOTANICAL ANOMALIES IN RUGGED ALPINE TERRAIN USING LANDSAT THEMATIC MAPPER DATA

C. BANNINGER (Graz, Technische Universitaet und Forschungszentrum, Austria) IN: Thematic Conference on Remote Sensing for Exploration Geology, 5th, Reno, NV, Sept. 29-Oct. 2, 1986, Proceedings. Volume 2. Ann Arbor, MI, Environmental Research Institute of Michigan, 1987, p. 813-816.

A88-35160 APPLICATION OF AEROSPACE REMOTE SENSING TO GEOLOGICAL INVESTIGATIONS IN NEVADA AND CALIFORNIA

JAMES V. TARANIK (Nevada, University, Reno) IN: Aerospace century XXI: Space sciences, applications, and commercial developments; Proceedings of the Thirty-third Annual AAS International Conference, Boulder, CO, Oct. 26-29, 1986. San Diego, CA, Univelt, Inc., 1987, p. 1695-1711. refs (AAS PAPER 86-400)

The current state and future developments of technology in geological remote sensing are discussed. The Landsat satellite is described, and applications of its data to mineral exploration are considered. The airborne Thematic Mapper, Spot satellite, Large Format Camera, Collins Airborne Radiometer and Imaging Spectrometer, and Side-Looking Airborne Radar (SLAR) and their geological remote sensing applications are addressed. Experimental remote sensing techniques with potential for application to geological investigation in Nevada and California are examined, including the Airborne Imaging Spectrometer, Advanced Visible and Infrared Imaging Spectrometer, Spaceborne Imaging Spectrometer, Thermal Infrared Multispectral Scanner, and Spaceborne Imaging Radar. C.D.

A88-35192 POTENTIAL OF LANDSAT THEMATIC MAPPER IMAGE FOR CRYSTALLINE ROCK TYPE DISCRIMINATION - GREGORY RIFT, KENYA

ALESSANDRO TIBALDI and MASSIMO FERRARI (Milano, Universita, Milan, Italy) Geocarto International (ISSN 1010-6049), vol. 3, March 1988, p. 3-12. refs

In order to test the full potential of the computer-enhanced image of original Landsat Thematic Mapper data, the semiarid area of the Gregory Rift Valley (Kenya) was selected. The aim is to estimate the capability of false partially color composite in bands one, three, and four to discriminate among metamorphic and various volcanic rock types. Furthermore signal reflectance differences among rocks of various ages but equal chemical characteristics were evaluated. Field surveys of the authors and published geological data made it possible to gather a great amount of ground truth. Comparison of satellite image interpretation and field geological data has demonstrated the validity of this TM image enhancement in lithotype discrimination, but also has led to better definition of the spatial distribution of the various rock types in the area. Author

A88-35193

COMPUTER PROCESSING OF SATELLITE DATA FOR GEOSTRUCTURAL ZONING OF A COLLISIONAL BOUNDARY, SIGNIFICANCE AND FIELD CHECKS - THE EXAMPLE OF TUNISIA

CARLO MARIA MARINO and ALESSANDRO TIBALDI (Milano, Universita, Milan, Italy) Geocarto International (ISSN 1010-6049), vol. 3, March 1988, p. 13-28. refs

A88-36161

THE USE OF SPACE DATA TO STUDY PRECAMBRIAN STRUCTURES [ISPOL'ZOVANIE KOSMICHESKOI INFORMATSII PRI IZUCHENII DOKEMBRIISKIKH STRUKTUR] L. N. UIMANOVA (Vsesoiuznyi Nauchno-Issledovatel'skii Institut Geologii Zarubezhnykh Stran, Moscow, USSR) Issledovanie Zemli iz Kosmosa (ISSN 0205-9614), Jan.-Feb. 1988, p. 30-36. In Russian.

The possibility of using space photographic data to identify and study the development of Precambrian structures is assessed on the example of Central East Africa. As a rule, these are deep-seated structures which have been repeatedly activated during tectonic-magmatic cycles up to the period of recent riftingogenesis. B.J.

A88-36162

THE SOUTH ALAMURYNIAN RING STRUCTURE - A NEW PROMISING AREA TO SEARCH FOR HYDROCARBON DEPOSITS [IUZHNO-ALAMURYNSKAIA KOL'TSEVAIA STRUKTURA-NOVYI VOZMOZHNYI OB'EKT POISKOV ZALEZHEI UGLEVODORODOV]

V. I. POPKOV and A. A. RABINOVICH (Kazakhskii Gosudarstvennyi Nauchno-Issledovatel'skii i Proektnyi Institut Neftianoi Promyshlennosti, Shevchenko, Ukrainian SSR) Issledovanie Zemli iz Kosmosa (ISSN 0205-9614), Jan.-Feb. 1988, p. 37-41. In Russian.

Several ring structures were identified on space photographs of Mangyshlak. It is suggested that the South Alamurynian ring structure situated in the northwest Kara Bogaz Gol region may be a promising area for oil and gas exploration. B.J.

A88-36163

QUANTITATIVE ANALYSIS OF A NETWORK OF FAULTS RECOGNIZED ON REMOTE-SENSING IMAGES OF THE MUSHUGAI AREA IN MONGOLIA [OPYT KOLICHESTVENNOGO ANALIZA SETI RAZLOMOV, VYIAVLENNYKH PO AEROKOSMICHESKIM SNIMKAM V MUSHUGAISKOM RAIONE MNR]

ZH. GAN-OCHIR, M. GANZORIG, and Z. ARIUNAA (AN MNR, Institut Fiziki i Tekhniki, Ulan-Bator, Mongolian People's Republic) Issledovanie Zemli iz Kosmosa (ISSN 0205-9614), Jan.-Feb. 1988, p. 42-47. In Russian. refs

A88-36172

REMOTE SENSING OF THE EARTH'S SURFACE IN THE ULTRAVIOLET RANGE [DISTANSSIONOE ZONDIROVANIE ZEMNOI POVERKHNOSTI V UL'TRAIOLETOVOM DIAPAZONE]

V. A. SELIVANOV (Moskovskii Elektrotekhnicheskii Institut Sviazi, Moscow, USSR) Issledovanie Zemli iz Kosmosa (ISSN 0205-9614), Jan.-Feb. 1988, p. 111-120. In Russian. refs

The published literature on the remote sensing of the earth's surface in the UV range is reviewed. Particular consideration is given to the history of the question, the reflective properties of natural formations in the UV range, the observation conditions, and UV imaging techniques. It is concluded that UV sensing can provide information in various areas (geology, environment protection, etc.) that does not duplicate information obtainable in the visible range. B.J.

A88-41945

INFLUENCE OF MINERAL COATINGS AND VEGETATION ON TM IMAGERY OVER TERTIARY CALDERA LITHOLOGIES BASIN AND RANGE PROVINCE, WESTERN U.S.

D. M. SPATZ, J. V. TARANIK, and L. C. HSU (Nevada, University, Reno) IN: American Society for Photogrammetry and Remote Sensing and ACSM, Fall Convention, Reno, NV, Oct. 4-9, 1987, ASPRS Technical Papers. Falls Church, VA, American Society for Photogrammetry and Remote Sensing, 1987, p. 13-25. refs

A88-41955* National Aeronautics and Space Administration, Goddard Space Flight Center, Greenbelt, Md.

MULTISPECTRAL GEOLOGIC REMOTE SENSING OF A SUSPECTED IMPACT CRATER NEAR AL MADAFI, SAUDI ARABIA

J. B. GARVIN and H. W. BLODGET (NASA, Goddard Space Flight Center, Greenbelt, MD) IN: American Society for Photogrammetry and Remote Sensing and ACSM, Fall Convention, Reno, NV, Oct. 4-9, 1987, ASPRS Technical Papers. Falls Church, VA, American Society for Photogrammetry and Remote Sensing, 1987, p. 317-323. refs

A multispectral Landsat TM image of a 6-km-diameter circular formation at Al Madafi in NW Saudi Arabia is interpreted by means of color-band composites, band ratios, and principal-components analysis to determine the nature of this feature. The geological characteristics of impact craters are discussed, and the satellite-image analysis techniques are described. Disruptions in the pattern of spectral signatures are seen in the Al Madafi formation and shown to be consistent with an impact origin. T.K.

A88-41975

SYNTHETIC GEOLOGICAL MAP OBTAINED BY REMOTE SENSING - AN APPLICATION TO PALAWAN ISLAND

F. BENARD and C. MULLER (Institut Francais du Petrole, Rueil-Malmaison, France) IN: Remote sensing for resources development and environmental management; Proceedings of the Seventh International Symposium, Enschede, Netherlands, Aug. 25-29, 1986. Volume 1. Rotterdam, A. A. Balkema, 1986, p. 103-109. refs

A88-41978

SHUTTLE IMAGING RADAR RESPONSE FROM SAND DUNES AND SUBSURFACE ROCKS OF ALASHAN PLATEAU IN NORTH-CENTRAL CHINA

HUADONG GUO (Chinese Academy of Sciences, Institute of Remote Sensing Application, Beijing, People's Republic of China), G. G. SCHABER, C. S. BREED (USGS, Flagstaff, AZ), and A. J. LEWIS (Oregon State University, Corvallis) IN: Remote sensing for resources development and environmental management; Proceedings of the Seventh International Symposium, Enschede, Netherlands, Aug. 25-29, 1986. Volume 1. Rotterdam, A. A. Balkema, 1986, p. 137-143. refs

SIR-A and SIR-B images of three sand dunes and two bedrock regions in Alashan Plateau of north-central China have been studied and compared to Landsat imagery and field investigation data. The results of the study show that radar illumination direction is an important factor which results in the echo strength change for the same type and size of sand dunes. The sand dunes in which the slipfaces are oriented to radar beam have a bright-point response and the dunes in which the gentle slopes face the radar beam have a dark signature on the radar image. Two Precambrian metamorphic rockbodies buried beneath the thin layer of alluvial material or aeolian sand have been detected by using these two radar images. Author

A88-41979

DETECTION BY SIDE-LOOKING RADAR OF GEOLOGICAL STRUCTURES UNDER THIN COVER SANDS IN ARID AREAS

B. N. KOOPMANS (International Institute for Aerospace Survey and Earth Sciences, Enschede, Netherlands) IN: Remote sensing for resources development and environmental management; Proceedings of the Seventh International Symposium, Enschede, Netherlands, Aug. 25-29, 1986. Volume 1. Rotterdam, A. A. Balkema, 1986, p. 149-156. refs

Images of SIR-A and SIR-B shuttle radar have been studied for penetration capability of the microwaves in arid areas. In the Red Sea hills (Sudan), the radar information was compared with

Landsat Images and Large Format Camera (LFC) photos. Particularly on the latter, much detail could be obtained through stereo analysis. A radar strip over the central Iranian desert was compared with hand-held shuttle photography. In both Sudan and Iran it appeared that the radar images revealed some information of the bedrock in the sandy areas otherwise not visible on the images obtained in the visible or near infrared part of the spectrum, indicating a certain penetration capability of microwaves through thin cover sands. The differences between 'dike lineament' interpretation on radar image and LFC photos are not so much influenced by the penetration capability of microwaves, but much more by the influence radar look direction has on the enhancement or depreciation of lineaments. Author

A88-41980

GEOLOGICAL ANALYSIS OF SEASAT SAR AND SIR-B DATA IN HAITI

PH. REBILLARD (Societe Europeenne de Propulsion, Division de Traitement d'Images, Puteaux, France) and B. MERCIER DE L'EPINAY (Paris VI, Universite, France) IN: Remote sensing for resources development and environmental management; Proceedings of the Seventh International Symposium, Enschede, Netherlands, Aug. 25-29, 1986. Volume 1. Rotterdam, A. A. Balkema, 1986, p. 157-160. refs

Synthetic Aperture Radar data obtained by Seasat in 1978 and by SIR-B in 1984 were registered to the corresponding Landsat MSS data over the Western part of Haiti. Two areas were studied: the island of La Gonave and the Miragoane area. Seasat SAR data were registered to the Landsat data over the island of La Gonave and both Seasat and SIR-B data were compared over the Miragoane area. In both cases, difficulties occurred in the interpretation due to the relief which distorted the radar data, particularly the Seasat data for which the radar incidence angle was 20 degrees; furthermore, on the Miragoane area difficulties occurred using the SIR-B data due to low radar signal. Structural lines and lithological boundaries were pointed out thanks to the compositional and textual informations provided by the radar and MSS data. Geological interpretation maps of La Gonave and the Miragoane area were drawn: boundaries between rocks Eocene of age and rough basalts were precise as well as (1) domes, (2) ancient faults oriented NE-SW, (3) faults oriented NW-SE linked to the La Gonave anticline and (4) faults oriented E-W integrated in the tectonic model of the Caribbean plate. Author

A88-41983

EVALUATION OF DIGITALLY PROCESSED LANDSAT IMAGERY AND SIR-A IMAGERY FOR GEOLOGICAL ANALYSIS OF WEST JAVA REGION, INDONESIA

INDROYONO SOESILO and RICHARD A. HOPPIN (Iowa, University, Iowa City) IN: Remote sensing for resources development and environmental management; Proceedings of the Seventh International Symposium, Enschede, Netherlands, Aug. 25-29, 1986. Volume 1. Rotterdam, A. A. Balkema, 1986, p. 173-182. Research supported by the Indonesian Cultural Foundation. refs

A88-41992

THE USE OF THEMATIC MAPPER IMAGERY FOR GEOMORPHOLOGICAL MAPPING IN ARID AND SEMI-ARID ENVIRONMENTS

A. R. JONES (Reading, University, England) IN: Remote sensing for resources development and environmental management; Proceedings of the Seventh International Symposium, Enschede, Netherlands, Aug. 25-29, 1986. Volume 1. Rotterdam, A. A. Balkema, 1986, p. 273-280. refs

The evaluation of satellite obtained imagery for geomorphological mapping is discussed with emphasis on the main advantages of such data: a synoptic overview, multi-date coverage, multispectral imagery and digital format which allows the user to employ computer-assisted image processing. The Thematic Mapper (TM) sensor of the Landsat satellites is better suited for geoscientific applications than the earlier Multispectral scanner (MSS) system. This is due to improved spatial and spectral

characteristics. Examples are given, using a test site in southern Tunisia, of the value of TM imagery for geomorphological investigations. To effectively employ such data for such studies, digital image processing must be utilized to extract the necessary information. Examples of techniques such as contrast stretching, image convolution, band ratioing, principal component analysis and unsupervised classification are discussed. Author

A88-42017
REGIONAL GEOLOGIC MAPPING OF DIGITALLY ENHANCED LANDSAT IMAGERY IN THE SOUTHCENTRAL ALBORZ MOUNTAINS OF NORTHERN IRAN

SIMA BAGHERI (New Jersey Institute of Technology, Newark) and RALPH W. KIEFER (Wisconsin, University, Madison) IN: Remote sensing for resources development and environmental management; Proceedings of the Seventh International Symposium, Enschede, Netherlands, Aug. 25-29, 1986. Volume 2. Rotterdam, A. A. Balkema, 1986, p. 555-559. refs

This study evaluates the utility of using Landsat MSS data in regional geologic mapping of lineaments. Both conventional image interpretation techniques and digital enhancement techniques were utilized. The presence and orientation of lineaments can have great structural significance and a correlation may exist between them and zones of weakness characterized by seismic activity and mineral concentrations. The lineaments detected on computer-enhanced imagery of the study area exhibited definite trends providing a regional view of the geological 'grain' of the area. When lineament alignments located by Landsat image analysis were plotted, a correlation was found between lineaments detected on the enhanced scene and earthquake epicenters, as well as the mapped location of phosphate deposits of the study area. Author

A88-42019
COMPARISON BETWEEN INTERPRETATION OF IMAGES OF DIFFERENT NATURE

G. BOLLETTINARI (Morfogeo, Ferrara, Italy) and F. MANTOVANI (Ferrara, Università, Italy) IN: Remote sensing for resources development and environmental management; Proceedings of the Seventh International Symposium, Enschede, Netherlands, Aug. 25-29, 1986. Volume 2. Rotterdam, A. A. Balkema, 1986, p. 569-571.

Band 7 and FCC Landsat images and SLAR and panchromatic black and white photomosaic images are analyzed to identify and interpret geomorphological and neotectonic features of central and northern Peru. The process used to interpret images and the morphoneotectonics classification used are analyzed, giving the advantages and disadvantages of each type of image and indicating limitations to their interpretation. It is concluded that both small and large scale resolution images are required for this type of regional study. R.B.

A88-42021
GEOLOGICAL ANALYSIS OF THE SATELLITE LINEAMENTS OF THE VISTULA DELTA PLAIN, ZULAWY WISLANE, POLAND

BARBARA DANIEL DANIELSKA, STANISLAW KIBITLEWSKI (Instytut Geologiczny, Warsaw, Poland), and ANDRZEJ SADURSKI (Gdansk, Politechnika, Poland) IN: Remote sensing for resources development and environmental management; Proceedings of the Seventh International Symposium, Enschede, Netherlands, Aug. 25-29, 1986. Volume 2. Rotterdam, A. A. Balkema, 1986, p. 579-584. refs

A88-42022
ANALYSIS OF LINEAMENTS AND MAJOR FRACTURES IN XICHANG-DUKOU AREA, SICHUAN PROVINCE AS INTERPRETED FROM LANDSAT IMAGES

DEFU LU, WENHUA ZHANG, BINGGUANG LIU (Chinese Academy of Geological Sciences, Institute of Geology, Beijing, People's Republic of China), RUISONG XU, and BAOLIN JANG (Chinese Academy of Sciences, Institute of Geologic Technology, Guangzhou, People's Republic of China) IN: Remote sensing for

resources development and environmental management; Proceedings of the Seventh International Symposium, Enschede, Netherlands, Aug. 25-29, 1986. Volume 2. Rotterdam, A. A. Balkema, 1986, p. 585-588.

A88-42023
APPLICATION OF REMOTE SENSING IN THE FIELD OF EXPERIMENTAL TECTONICS

J. DEHANDSCHUTTER (Museum Royal de l'Afrique Centrale, Tervuren, Belgium) IN: Remote sensing for resources development and environmental management; Proceedings of the Seventh International Symposium, Enschede, Netherlands, Aug. 25-29, 1986. Volume 2. Rotterdam, A. A. Balkema, 1986, p. 589-594. refs

A framework of transverse lineaments visible in Landsat MSS imagery of brittle and ductile tectonic domains in the Andes and Central Africa is used to study geological structures indicative of the orientation of the paleo-stress field in which they were created, including tensional joints, vertical faults, quartz dykes and sedimentary basins of pull-apart origin. Various classes of geological structures are shown to repeatedly occupy the same position inside a basic rhomb configuration. Photoelastic stress analyses show the elastic properties of homogenous plates cut by vertical discontinuities to be different from those in the interior of the plate, suggesting that several factors, including the rhombic pattern determine the geometric position of lineaments and structures. Directions of vertical faulting inside the blocks and oblique-slip rotational strain inside the lineaments are predicted. R.B.

A88-42027
APPLICATION OF MEIS-II MULTISPECTRAL AIRBORNE DATA AND CIR PHOTOGRAPHY FOR THE MAPPING OF SURFICIAL GEOLOGY AND GEOMORPHOLOGY IN THE CHATHAM AREA, SOUTHWEST ONTARIO, CANADA

A. B. KESIK, H. GEORGE, and M. M. DUSSEAULT (Waterloo, University, Canada) IN: Remote sensing for resources development and environmental management; Proceedings of the Seventh International Symposium, Enschede, Netherlands, Aug. 25-29, 1986. Volume 2. Rotterdam, A. A. Balkema, 1986, p. 615-617.

A88-42028
REMOTE SENSING METHODS IN GEOLOGICAL RESEARCH OF THE LUBLIN COAL BASIN, SE POLAND

STANISLAW KIBITLEWSKI and BARBARA DANIEL DANIELSKA (Instytut Geologiczny, Warsaw, Poland) IN: Remote sensing for resources development and environmental management; Proceedings of the Seventh International Symposium, Enschede, Netherlands, Aug. 25-29, 1986. Volume 2. Rotterdam, A. A. Balkema, 1986, p. 619-624. refs

A88-42029
PHOTO-INTERPRETATION OF LANDFORMS AND THE HYDROGEOLOGIC BEARING IN HIGHLY DEFORMED AREAS, NW OF THE GULF OF SUEZ, EGYPT

E. A. KORANY (University of Qatar, Doha) and L. L. ISKANDAR (Secondary Schools, Cairo, Egypt) IN: Remote sensing for resources development and environmental management; Proceedings of the Seventh International Symposium, Enschede, Netherlands, Aug. 25-29, 1986. Volume 2. Rotterdam, A. A. Balkema, 1986, p. 625-630. refs

A88-42030
MONITORING GEOMORPHOLOGICAL PROCESSES IN DESERT MARGINAL ENVIRONMENTS USING MULTITEMPORAL SATELLITE IMAGERY

A. C. MILLINGTON, A. R. JONES (Reading, University, England), N. QUARMBY, and J. R. G. TOWNSHEND (NERC, Unit for Thematic Information Services, Reading, England) IN: Remote sensing for resources development and environmental management; Proceedings of the Seventh International Symposium,

Enschede, Netherlands, Aug. 25-29, 1986. Volume 2. Rotterdam, A. A. Balkema, 1986, p. 631-637. refs

Methods for geomorphological process monitoring and change detection using digitally processed multitemporal Landsat TM and MSS imagery are evaluated in south-central Tunisia. Three categories of changes are detected - subsampling unit, seasonal and long-term changes. Hydrological and geomorphological changes in Tunisian playas are examined within these categories. Both surface water and groundwater are important in determining salt and sediment budgets on these playas. Author

A88-42033

DETECTING AND MAPPING OF DIFFERENT VOLCANIC STAGES AND OTHER GEOMORPHIC FEATURES BY LANDSAT IMAGES IN 'KATAKEKAUMENE', WESTERN TURKEY

F. SANCAR OZANER (Mineral Research and Exploration Institute, Ankara, Turkey) IN: Remote sensing for resources development and environmental management; Proceedings of the Seventh International Symposium, Enschede, Netherlands, Aug. 25-29, 1986. Volume 2. Rotterdam, A. A. Balkema, 1986, p. 653-656. refs

A88-42034

A REMOTE SENSING METHODOLOGICAL APPROACH FOR APPLIED GEOMORPHOLOGY MAPPING IN PLAIN AREAS

ELISEO POPOLIZIO (Universidad Nacional del Nordeste, Corrientes, Argentina) and CARLOS CANOBA (Rosario, Universidad Nacional, Argentina) IN: Remote sensing for resources development and environmental management; Proceedings of the Seventh International Symposium, Enschede, Netherlands, Aug. 25-29, 1986. Volume 2. Rotterdam, A. A. Balkema, 1986, p. 657-663. refs

A88-42036

AN EVALUATION OF POTENTIAL URANIUM DEPOSIT AREA BY LANDSAT DATA ANALYSIS IN OFFICER BASIN, SOUTH-WESTERN PART OF AUSTRALIA

H. WADA, K. KOIDE (Power Reactor and Nuclear Fuel Development Corp., Tokyo, Japan), Y. MARUYAMA, and M. NASU (Asia Air Survey Co., Ltd., Tokyo, Japan) IN: Remote sensing for resources development and environmental management; Proceedings of the Seventh International Symposium, Enschede, Netherlands, Aug. 25-29, 1986. Volume 2. Rotterdam, A. A. Balkema, 1986, p. 679-683. refs

A88-42049

ANALYSIS OF LANDSAT MULTISPECTRAL-MULTITEMPORAL IMAGES FOR GEOLOGIC-LITHOLOGIC MAP OF THE BANGLADESH DELTA

A. SESOREN (International Institute for Aerospace Survey and Earth Sciences, Enschede, Netherlands) IN: Remote sensing for resources development and environmental management; Proceedings of the Seventh International Symposium, Enschede, Netherlands, Aug. 25-29, 1986. Volume 2. Rotterdam, A. A. Balkema, 1986, p. 759-764. refs

A88-42068* Jet Propulsion Lab., California Inst. of Tech., Pasadena.

REMOTE SENSING FOR NON-RENEWABLE RESOURCES - SATELLITE AND AIRBORNE MULTIBAND SCANNERS FOR MINERAL EXPLORATION

ALEXANDER F. H. GOETZ (California Institute of Technology, Jet Propulsion Laboratory, Pasadena; Colorado, University, Boulder) IN: Remote sensing for resources development and environmental management; Proceedings of the Seventh International Symposium, Enschede, Netherlands, Aug. 25-29, 1986. Volume 3. Rotterdam, A. A. Balkema, 1986, p. 1009-1014. refs

The application of remote sensing techniques to mineral exploration involves the use of both spatial (morphological) as well as spectral information. This paper is directed toward a discussion of the uses of spectral image information and

emphasizes the newest airborne and spaceborne sensor developments involving imaging spectrometers. Author

A88-44646*

STRUCTURAL GEOLOGY AND REGIONAL TECTONICS OF THE MINERAL COUNTY AREA, NEVADA, USING SHUTTLE IMAGING RADAR-B AND DIGITAL AEROMAGNETIC DATA

MARCUS X. BORENGASSER and JAMES V. TARANIK (Cooperative Institute for Aerospace Science and Terrestrial Applications, Reno, Nevada) International Journal of Remote Sensing (ISSN 0143-1161), vol. 9, May 1988, p. 967-980. refs (Contract NASA ORDER L-61130-C)

SIR-B and aeromagnetic lineaments show a correlation with known faults within the Walker Lane of the western Basin and Range Province. Walker Lane faults can be extended based on SIR-B data and unmapped Walker Lane features are identified. South of the Pancake Range lineament, Walker Lane faults are seldom recognized but SIR-B data have the potential for delineating structural features in this area. Earthquake hypocenter distribution in profiles across a SIR-B lineament is consistent with that expected from a vertical fault. Field examination indicates that the lineament is an unmapped neotectonic Walker Lane feature. Author

A88-44647

A COMPARATIVE ANALYSIS OF DYKE LINEAMENTS MAPPED FROM SHUTTLE IMAGING RADAR AND LARGE FORMAT CAMERA PHOTOGRAPHY IN HYPERARID AREAS OF THE EASTERN DESERT, EGYPT, AND RED SEA HILLS, SUDAN

B. N. KOOPMANS (International Institute for Aerospace Survey and Earth Sciences, Enschede, Netherlands) International Journal of Remote Sensing (ISSN 0143-1161), vol. 9, May 1988, p. 981-995. refs

A88-45634

GEOTECHNICAL APPLICATIONS OF REMOTE SENSING AND REMOTE DATA TRANSMISSION; PROCEEDINGS OF THE SYMPOSIUM, COCOA BEACH, FL, JAN. 31-FEB. 1, 1988

A. I. JOHNSON, ED. (International Committee on Remote Sensing and Data Transmission, Arvada, CO) and C. B. PETERSSON, ED. (Brown and Root, Inc., Houston, TX) Symposium sponsored by ASTM, Philadelphia, PA, American Society for Testing and Materials, 1988, 286 p. For individual items see A88-45635 to A88-45643.

Papers and discussions concerning the geotechnical applications of remote sensing and remote data transmission, sources of remotely sensed data, and glossaries of remote sensing and remote data transmission terms, acronyms, and abbreviations are presented. Aspects of remote sensing use covered include the significance of lineaments and their effects on ground-water systems, waste-site use and geotechnical characterization, the estimation of reservoir submerging losses using CIR aerial photographs, and satellite-based investigation of the significance of surficial deposits for surface mining operations. Other topics presented include the location of potential ground subsidence and collapse features in soluble carbonate rock, optical Fourier analysis of surface features of interest in geotechnical engineering, geotechnical applications of U.S. Government remote sensing programs, updating the data base for a Geographic Information System, the joint NASA/Geosat Test Case Project, the selection of remote data telemetry methods for geotechnical applications, the standardization of remote sensing data collection and transmission, and a comparison of airborne Goodyear electronic mapping system/SAR with satelliteborne Seasat/SAR radar imagery. R.B.

A88-45635

CASE STUDIES ON THE APPLICATION OF REMOTE SENSING DATA TO GEOTECHNICAL INVESTIGATIONS IN ONTARIO, CANADA

VERNON H. SINGHROY (Ontario Centre for Remote Sensing, Toronto, Canada) IN: Geotechnical applications of remote sensing

04 GEOLOGY AND MINERAL RESOURCES

and remote data transmission; Proceedings of the Symposium, Cocoa Beach, FL, Jan. 31-Feb. 1, 1986. Philadelphia, PA, American Society for Testing and Materials, 1988, p. 9-45. refs

The contribution and limitations of remote sensing data to the planning and construction of cross-country natural gas pipelines, the search for suitable near-surface construction materials, the evaluation of sites for the disposal of hazardous water, and the identification of conditions likely to give rise to mine roof instabilities, are examined, using Landsat TM and Seasat SAR data taken before, during, and after construction of pipelines in southern Ontario. Airborne thermography was used to delineate an area of near-surface aggregate overlain by a layer of sand-silt till 3 to 7 mm thick. Infrared and geophysical data were used for mapping a potential nuclear waste disposal site, identifying dikes and faults and delineating surficial materials. Visible infrared and thermal data were used to detect areas of instability in the roof of a gypsum mine. It is concluded that the amount of moisture retained within the soil and in fractures at the time of data acquisition is a main link between remote sensing and geotechnical investigations.

R.B.

A88-45638

A SATELLITE-BASED INVESTIGATION OF THE SIGNIFICANCE OF SURFICIAL DEPOSITS FOR SURFACE MINING OPERATIONS

JOSEPH H. J. LEACH and C. W. MALLETT (CSIRO, Div. of Geomechanics, Indooroopilly, Australia) IN: Geotechnical applications of remote sensing and remote data transmission; Proceedings of the Symposium, Cocoa Beach, FL, Jan. 31-Feb. 1, 1986. Philadelphia, PA, American Society for Testing and Materials, 1988, p. 122-137. refs

The use of NOAA-AVHRR, Landsat MSS, and SIR imagery to determine the distribution, structure, and form of surficial deposits in the vicinity of large-scale mining operations in the Bowen Basin of Queensland, Australia is examined, pointing out the capabilities and limitations of geotechnical applications of remote sensing and discussing possible future developments in satellite systems. The use of satellite imagery to obtain data on structural lineaments and the location and variation within surficial deposits is discussed. The use of TM and SPOT systems for geotechnical applications is examined, and it is suggested that a potential comprehensive geotechnical remote sensing system should be able to generate stereoscopic images in the visible to midinfrared spectrum with a ground resolution of 20 m or less, be able to image in the thermal IR with a ground resolution of about 80 m and to generate day/night pairs from this imagery, and include a multiband radar imaging system with a variable look angle and an effective ground resolution comparable to that of the visible imaging system.

R.B.

A88-45641

GEO TECHNICAL APPLICATIONS OF THREE NEW U.S. GOVERNMENT REMOTE SENSING PROGRAMS

BRUCE F. MOLNIA (National Academy of Sciences, Washington, DC) IN: Geotechnical applications of remote sensing and remote data transmission; Proceedings of the Symposium, Cocoa Beach, FL, Jan. 31-Feb. 1, 1986. Philadelphia, PA, American Society for Testing and Materials, 1988, p. 183-189; Discussion, p. 190, 191. refs

The geotechnical data provided by the USGS's National High-Altitude Photography Program (NHAP) and Side-Looking Airborne Radar (SLAR) Program, and NASA's Shuttle Imaging Radar (SIR) Program are discussed. Applications of data from these programs include regional structural interpretation, delineation of drainage characteristics, evaluation of surface wetness characteristics, and assessment of rock and soil surface texture and grain size. The NHAP provides black and white and color infrared imagery at a nominal scale of 1:80,000, and enlargements at a scale of 1:24,000, covering 95 percent of the U.S. The SLAR has mapped 27 percent of the conterminous U.S. and 23 percent of Alaska, providing strip data at a scale of 1:250,000 and historic data at a scale of 1:400,000. The SIR-A imagery taken from the Shuttle covers 10 to the 7th sq km, at an incidence angle of 47

deg and a resolution of 40 m. The SIR-B provided images of 8 X 10 to the 6th sq km at a resolution of 20 m with an incidence angle of 47 deg.

R.B.

A88-45642

THE JOINT NASA/GEOSAT TEST CASE PROJECT

IN: Geotechnical applications of remote sensing and remote data transmission; Proceedings of the Symposium, Cocoa Beach, FL, Jan. 31-Feb. 1, 1986. Philadelphia, PA, American Society for Testing and Materials, 1988, p. 197-200.

A summary of a report on the Joint NASA/Geosat Test Case Project which analyzes Landsat MSS digital and photographic data to evaluate the geological usefulness of remote sensing technology, especially for mineral and petroleum exploration, is presented. Images were with a ground resolution of about 80 m in four spectral bands of eight test sites in the semiarid portions of the western US and the Appalachian mountains. Ground-based measurements were taken to determine the reflectance properties of rocks, soils, and natural vegetation, showing that rocks of similar lithology can exhibit different reflectance properties at different sites. It was found that such ground-based measurements are required for effective lithographic mapping.

R.B.

A88-45771

AIRBORNE RESISTIVITY MAPPING

ALEX BECKER (California, University, Berkeley) IEEE Transactions on Antennas and Propagation (ISSN 0018-926X), vol. 36, April 1988, p. 557-562. refs

A brief overview is presented of the theory and techniques for mapping the electrical resistivity of surficial formations by interpreting airborne electromagnetic induction data. Although the method has not yet reached its full potential, useful information can be obtained on the thickness, the conductivity, and the depth below the surface of any conductive unconsolidated material. Practical applications of this geophysical method include the mapping of aquifers, the delineation of salt-water intrusions, and the estimation of the depth of valley fill material. The instrumentation is described and both time- and frequency-domain systems are discussed. Methods and examples of automated data interpretation are given. On the basis of the results available to date it is concluded that with present equipment and using the limited methods of interpretation described, one can map the thickness of the uppermost layer (be it conductive or resistive) to a depth somewhat greater than 50 m with an accuracy of about 10-20 m.

I.E.

N88-20754*# Massachusetts Inst. of Tech., Cambridge. GEODETIC MEASUREMENT OF DEFORMATION EAST OF THE SAN ANDREAS FAULT IN CENTRAL CALIFORNIA

JEANNE M. SAUBER, MICHAEL LISOWSKI, and SEAN C. SOLOMON 1988 39 p Prepared in cooperation with Geological Survey, Menlo Park, Calif.

(Contract NAG5-814; NGT5-0103)

(NASA-CR-182709; NAS 1.26:182709) Avail: NTIS HC A03/MF A01 CSCL 08E

Triangulation and trilateration data from two geodetic networks located between the western edge of the Great Valley and the San Andreas fault have been used to calculate shear strain rates in the Diablo Range and to estimate the slip rate along the Calaveras and Paicines faults in Central California. Within the Diablo Range the average shear strain rate was determined for the time period between 1962 and 1982 to be 0.15 + or - 0.08 microrad/yr, with the orientation of the most compressive strain at N 16 deg E + or - 14 deg. The orientation of the principal compressive strain predicted from the azimuth of the major structures in the region is N 25 deg E. It is inferred that the measured strain is due to compression across the folds of this area: the average shear straining corresponds to a relative shortening rate of 4.5 + or - 2.4 mm/yr. From an examination of wellbore breakout orientations and the azimuths of P-axes from earthquake focal mechanisms the inferred orientation of maximum compressive stress was found to be similar to the direction of maximum compressive strain implied by the trend of local fold structures. Results do not support the

hypothesis of uniform fault-normal compression within the Coast Ranges. From trilateration measurements made between 1972 and 1987 on lines that are within 10 km of the San Andreas fault, a slip rate of 10 to 12 mm/yr was calculated for the Calaveras-Paicines fault south of Hollister. The slip rate of the Paicines fault decreases to 4 mm/yr near Bitter. Author

N88-22847*# University of Southern Illinois, Carbondale. Surficial Processes Research Group.

GROUNDWATER SAPPING VALLEYS: EXPERIMENTAL STUDIES, GEOLOGICAL CONTROLS AND IMPLICATIONS TO THE INTERPRETATION OF VALLEY NETWORKS ON MARS

Final Contractor's Report, 1 Feb. 1985 - 31 Jan. 1988

R. CRAIG KOCHER 15 May 1988 77 p

(Contract NAGW-707)

(NASA-CR-182718; NAS 1.26:182718) Avail: NTIS HC A05/MF A01 CSCL 03B

An integrated approach using experimental laboratory models, field studies of terrestrial analogs, and remote studies of terrestrial field sites were applied to the goals of understanding the nature and morphology of valley networks formed by groundwater sapping. In spite of problems with scaling, the experimental studies provide valuable insights into concepts relating to the initiation, development, and evolution of valleys by groundwater sapping. These investigations are also aimed at developing geomorphic criteria for distinguishing valleys formed by surface runoff from those formed by groundwater sapping processes. Channels that were field classified as sapping vs. runoff were successfully distinguished using statistical analysis of their respective morphologies; therefore, it may be possible to use similar techniques to interpret channel genesis on Mars. The terrestrial and flume studies provide the ground truth dataset which can be used (and will be during the present year) to help interpret the genesis of valley networks on Mars. Author

N88-24021*# Jet Propulsion Lab., California Inst. of Tech., Pasadena.

AIRBORNE AND SPACEBORNE RADAR IMAGES FOR GEOLOGIC AND ENVIRONMENTAL MAPPING IN THE AMAZON RAIN FOREST, BRAZIL Abstract Only

JOHN P. FORD and JAMES J. HURTAK (Technological Marketing Analysis Corp., San Francisco, Calif.) *In* INPE, Latin American Symposium on Remote Sensing. 4th Brazilian Remote Sensing Symposium and 6th SELPER Plenary Meeting, Volume 1, p 129 1986

Avail: NTIS HC A99/MF E03

Spaceborne and airborne radar image of portions of the Middle and Upper Amazon basin in the state of Amazonas and the Territory of Roraima are compared for purposes of geological and environmental mapping. The contrasted illumination geometries and imaging parameters are related to terrain slope and surface roughness characteristics for corresponding areas that were covered by each of the radar imaging systems. Landforms range from deeply dissected mountain and plateau with relief up to 500 m in Roraima, revealing ancient layered rocks through folded residual mountains to deeply beveled pediplain in Amazonas. Geomorphic features provide distinct textural signatures that are characteristic of different rock associations. The principle drainages in the areas covered are the Rio Negro, Rio Branco, and the Rio Japura. Shadowing effects and low radar sensitivity to subtle linear fractures that are aligned parallel or nearly parallel to the direction of radar illumination illustrate the need to obtain multiple coverage with viewing directions about 90 degrees. Perception of standing water and alluvial forest in floodplains varies with incident angle and with season. Multitemporal data sets acquired over periods of years provide an ideal method of monitoring environmental changes. Author

N88-24022# Technological Marketing Analysis Corp., San Francisco, Calif.

SUBSURFACE MORPHOLOGY AND GEOARCHAEOLOGY REVEALED BY SPACEBORNE AND AIRBORNE RADAR Abstract Only

J. J. HURTAK *In* INPE, Latin American Symposium on Remote Sensing. 4th Brazilian Remote Sensing Symposium and 6th SELPER Plenary Meeting, Volume 1, p 130 1986
Avail: NTIS HC A99/MF E03

The Shuttle Imaging Radar (SIR-A) aboard the Space Shuttle Columbia penetrated the extremely dry deserts of the eastern Sahara, revealing previously unknown buried valleys, geologic structures, and possible Stone Age occupation sites, not detectable by LANDSAT. Radar responses from bedrock and gravel surfaces were also able to provide information in areas covered by very dry sand up to a depth of six meters. The enhancement of many geologic structures and the delineation of adjunct units partly mantled by sand, make the SIR-A a valuable adjunct of conventional geographic mapping tools. The use of radar imaging to determine the subsurface fluvial features in southern Egypt and Sudan is compared with the detection of subsurface stream canals in the tropical terrain of Guatemala-Belize. Radar penetration of tropical vegetation and soil varies with the wavelength of the incident signals. Subsurface features with potential tectonic or geomorphic significance may also be revealed in other orbital radar. The CV 990 imaging of tropical terrain detected the presence of an extensive canal drainage network beneath the jungle cover of Guatemala, providing the specific geologic locations of landforms which were sites of episodic human habitation. Radar imagery represents a large-scale of perspective of providing extensive information improving both the quality and quantity of subsurface morphology and geoarchaeology targets through penetration of foliage, silt, and root cover to map ancient man-made roads, causeways, and natural signatures disclosing the larger environmental design. Author

N88-24031# Purdue Univ., West Lafayette, Ind. Dept. of Geosciences.

AN INTEGRATED STUDY OF THE ALTO PARANAIBA KIMBERLITE PROVINCE, MINAS GERAIS, BRAZIL: A POSSIBLE TOOL FOR DIAMOND EXPLORATION Abstract Only

ARVIND CHATURVEDI *In* INPE, Latin American Symposium on Remote Sensing. 4th Brazilian Remote Sensing Symposium and 6th SELPER Plenary Meeting, Volume 1 p 258-259 1986
Avail: NTIS HC A99/MF E03

The initial results from an integrated study of the Alto Paranaiba area utilizing remote sensing, geophysical, and geological data are presented. The Alto Paranaiba area is economically important due to the local occurrences of kimberlite and diamonds. Kimberlites in the area are confined to a narrow NW-SE oriented strip of Precambrian metasediments and occur as diatremes and dikes. Visual interpretation of LANDSAT MSS imagery permits the delineation of the regional geology and structure of the Alto Paranaiba area. The Precambrian metasediments are easily distinguished from each other based on photo-recognition criteria. Analysis of an X-band SLAR mosaic facilitates a more detailed interpretation of the geology and structure in the vicinities of Coromandel, Monte Carmelo, and Patrocinio where most of the known kimberlites appear to be concentrated. Subtle linear and circular features, not seen on LANDSAT MSS imagery, are expressed clearly on the SLAR mosaic because of the increased resolution, look direction, and larger scale. Initial results indicate that some circular and linear features appear to be related to the known kimberlites in the area. However, several circular features, located near fractures and or fracture intersections, are not shown on previously published geological maps of the area and need to be investigated in greater detail. Author

N88-24050# Instituto de Pesquisas Espaciais, Sao Jose dos Campos (Brazil).

REMOTE SENSING AND STRUCTURAL RUPTURE: APPLICATION EXAMPLES IN THE STUDY OF TECTONICS [O SENSORIAMENTO REMOTO E A ESTRUTURA RUPTIL: EXEMPLOS DE APLICACOES EM ESTUDOS TECTONICOS]

ATHOS RIBEIRODOSSANTOS *In its* Latin American Symposium on Remote Sensing. 4th Brazilian Remote Sensing Symposium

04 GEOLOGY AND MINERAL RESOURCES

and 6th SELPER Plenary Meeting, Volume 1 p 429-434 1986
In PORTUGUESE; ENGLISH summary
Avail: NTIS HC A99/MF E03

The regional distribution of the linear structural features is best characterized in small scale remote sensing products. The development of structural studies utilizing remote sensing data has provided a systematic procedure of photointerpretation with the purpose of the extraction of structural information in a regional scale. Some of these procedural methodology, potentiality, limitations, and results are shown and discussed. The remote sensing techniques contribute good results in the regional tectonic studies. With these techniques, both brittle and brittle-ductile tectonics can be deduced. Author

N88-24051# Rio Grande do Sul Univ., Porto Alegre (Brazil).
ANALYSIS AND INTERPRETATION OF IMAGE LITHOSTRUCTURE: AN APPLICATION OF THE MULTICONCEPT IN THE METAMORPHIC BELT OF SUL DE SANTANA DA BOA VISTA (RS) [ANALISE E INTERPRETACAO LITOSTRUTURAL DE IMAGENS. UMA APLICACAO DO CONCEITO MULTI NA FAIXA METAMORFICA AO SUL DE SANTANA DA BOA VISTA - RS]
MARISA T. G. DEOLIVEIRASCHUCK, NELSON AMORETTILIS-BOA, and NILO CLEMENTEICK *In* INPE, Latin American Symposium on Remote Sensing. 4th Brazilian Remote Sensing Symposium and 6th SELPER Plenary Meeting, Volume 1 p 435-446 1986 In PORTUGUESE; ENGLISH summary
Avail: NTIS HC A99/MF E03

A belt of metamorphic rocks was analyzed through the visual interpretation of radar and photographic images, applying the multiconcept. On the radar images part of a big folded structure, of the antiformal type, which is fractured by faulting, was regionally defined. On the aerial photography a detail was worked through the litho and structural photoanalysis and photointerpretation; and seven photogeologic units could be defined. By means of photogeologic criteria the kind of faulting as well as the relative block movement was qualitatively defined in some cases. A lot of geologic information could be obtained comparing these different images. A possible sequence of geologic events, which have caused the actual rock spatial position, could be established. Author

N88-24052# Instituto de Economia e Pesquisas, Aracaju (Brazil).
STUDY OF FRACTURING FOR GROUNDWATER RESEARCH IN THE SERGIPE STATE WITH REMOTE SENSING PRODUCTS [ESTUDOS DE FRATURAMENTOS PARA PESQUISA DE AGUA SUBTERRANEA NO ESTADO DE SERGIPE COM PRODUTOS DE SENSORIAMENTO REMOTO]
OSVALDO SOUZASAMPAIO, JUERCIO TAVARESDEMATOS, and PAULO VENEZIANI (Instituto de Pesquisas Espaciais, Sao Jose dos Campos, Brazil) *In its* Latin American Symposium on Remote Sensing. 4th Brazilian Remote Sensing Symposium and 6th SELPER Plenary Meeting, Volume 1 p 447-452 1986 In PORTUGUESE; ENGLISH summary
Avail: NTIS HC A99/MF E03

For groundwater prospecting in Sergipe Crystalline Complex, a systematic interpretation of the remote sensing data was conducted and enabled the delineation of some potential areas for groundwater exploration in the future. The method used includes the analysis of terrain relief and drainage for delineating the principal joint and fault systems and characterizing the favorable morphostructures. Owing to the fact that the Precambrian complex is extremely compact and impermeable, the only groundwater reservoirs occur in the fractured zones in the crystalline rocks, so that morphostructure mapping is the way for groundwater prospecting. Author

N88-24069# Instituto de Pesquisas Espaciais, Sao Jose dos Campos (Brazil).

UTILIZATION OF LANDSAT-TM, FOR AIDING IN THE LOCALIZATION OF ARCHEOLOGICAL SITES IN THE STATE OF SAO PAULO [UTILIZACAO DE IMAGENS LANDSAT/TM, PARA AUXILIAR NA LOCALIZACAO DE SITIOS ARQUEOLOGICOS NO ESTADO DE SAO PAULO]
VITALINA PAGLIUCA CICIVIZZO (Sao Paulo Univ., Brazil) and TANIA MARIA SAUSEN *In its* Latin American Symposium on Remote Sensing. 4th Brazilian Remote Sensing Symposium and 6th SELPER Plenary Meeting, Volume 1 p 579-582 1986 In PORTUGUESE; ENGLISH summary
Avail: NTIS HC A99/MF E03

A methodology for TM/LANDSAT images, for the identification of geomorphological forms and spectral patterns that may serve as indicators for the localization of archaeological sites was developed. As a result, maps with the identification of the possible localization of archaeological sites will be developed as well as the characterization of spectral and geomorphological patterns that prompt the identification of such sites. Author

N88-24088# Universidad Nacional de San Juan (Argentina).
DUNE FIELDS IN CENTRAL WESTERN ARGENTINA [CAMPOS DE DUNAS EN EL CENTRO-OESTE ARGENTINO]
GRACIELA M. SUVIREZ *In* INPE, Latin American Symposium on Remote Sensing. 4th Brazilian Remote Sensing Symposium and 6th SELPER Plenary Meeting, Volume 1 p 724-732 1986 In SPANISH; ENGLISH summary
Avail: NTIS HC A99/MF E03

Important accumulations of wind blown sands extend over some sections of plains and pediments. The three dune fields existing in the area are called: Medanos Grandes (great dunes) in the south end of Pie de Palo range between 660 to 750 masl; Las Chacras dune to the southwestern end of Valle Fertil range between 690 to 800 masl; and Mascasin dunes between 450 to 550 masl. These dune fields contain longitudinal, transverse, parabolic, and barchanoid sand dunes with interdune basins. Author

N88-24097# Mineracao Taboca S.A., Manaus (Brazil).
CRITERIA FOR PLANIMETRIC AND ALTIMETRIC CORRECTION OF MAPS RESTITUTED FROM AERIAL PHOTOGRAPHS IN 1:100,000 SCALE [CRITERIOS PARA CORRECAO PLANIMETRICA E ALTIMETRICA DE MAPAS RESTITUIDOS A PARTIR DE FOTOGRAFIAS AEREAS EM ESCALA 1:100000]
FRANCISCO A. DUPAS *In* INPE, Latin American Symposium on Remote Sensing. 4th Brazilian Remote Sensing Symposium and 6th SELPER Plenary Meeting, Volume 1 p 807-811 1986 In PORTUGUESE; ENGLISH summary
Avail: NTIS HC A99/MF E03

The aim is to introduce a simple method for correcting the scale of level curve charts restituted from aerial photographs in a 1:100,000 approximate scale used for planning the Pitinga mine facilities. The mine is located some 250 km north of Manaus (AM-Brazil) and the region displays moderately undulated relief. Through prominences of the relief and geodesic points, topographic surveys are performed so as to allow the determination of the east and north scale of the restituted chart, that later may be amplified or reduced. With a corrected area of 3000 sq km, the drainage maps were already in use for three years and have demonstrated sufficient precision for the general planning of the mine. To trace the level curves a microcomputer and a plotter were used. The original program was in FORTRAN and adapted to BASIC. Author

N88-24098# Universidad Nacional de San Juan (Argentina).
GEOMORPHOLOGIC SECTOR MAPS OF NIQUIZANGA-MAYARES, PROVINCE OF SAN JUAN, ARGENTINA [MAPA GEOMORFOLOGICO SECTOR NIQUIZANGA-MAYARES, PROVINCIA DE SAN JUAN-ARGENTINA]
GRACIELA M. SUVIREZ *In* INPE, Latin American Symposium on Remote Sensing. 4th Brazilian Remote Sensing Symposium

and 6th SELPER Plenary Meeting, Volume 1 p 812-818 1986
In SPANISH; ENGLISH summary
Avail: NTIS HC A99/MF E03

In the investigated area, the plains of the San Juan and Bermejo Rivers are made up by extensive abandoned flood plains characterized by the abundance of winding channels and meanders. After this fluvial action wide extensions of the area were covered by thick aeolian deposits. The alluvial plain of Bermejo River is formed by smaller landforms. Author

N88-24100# IBGE/DRN/BA SEPLAN, Salvador (Brazil). LITHOSTRUCTURAL INTERPRETATION OF CHAPDA DO CACHIMBO (PA-AM-MT), BASED ON RADAR AND LANDSAT IMAGERY [INTERPRETACAO LITO-ESTRUTURAL DA CHAPADA DO CACHIMBO (PA-AM-MT), BASEADA EM IMAGENS DE RADAR E LANDSAT]

MARIO IVAN CARDOSODELIMA In INPE, Latin American Symposium on Remote Sensing. 4th Brazilian Remote Sensing Symposium and 6th SELPER Plenary Meeting, Volume 1 p 826-839 1986 In PORTUGUESE; ENGLISH summary
Avail: NTIS HC A99/MF E03

The Cachimbo Plateau is situated at the bordering zones of the states of Para, Amazonas, and Mato Grosso, in the Brazilian Amazon. By using radar (X-band) and MSS LANDSAT (bands 5 and 7) imagery, photogeologic interpretation of the region was performed, and the principal units were identified: metamorphic basement, sedimentary metavolcanic sequence, volcanic-plutonic suite, sedimentary sequence 1, sedimentary sequence 2, basic plutonic 1 and 2, and sedimentary sequence 3. The sedimentary sequence 1 covers do Cachimbo Plateau and was divided into 17 units. Psamitic types dominate the northern portion while in the southwestern sector psamitic-carbonatic ones occur. Regarding the structural aspects, the Cachimbo Plateau comprises a vast basin with WNW-ESE axis. The northern border of the basin is unwarped and presents cuesta features. Folds related to vertical and compressible movements are manifested at the southern sectors and expose interference models. The provisional metalogeny for the Cachimbo Plateau denotes potential deposits of Cu, Co, Ag, U, Fe, Mn, barite, magnesite, diamond, phosphate, limestone, coal, and bauxite. Moreover at the north and south it is limited by two important gold and tin provinces (Tapajos and Floresta-Juruena). Author

05

OCEANOGRAPHY AND MARINE RESOURCES

Includes sea-surface temperature, ocean bottom surveying imagery, drift rates, sea ice and icebergs, sea state, fish location.

A88-33694
DIAGNOSTIC STUDY OF THE FRAM STRAIT MARGINAL ICE ZONE DURING SUMMER FROM 1983 AND 1984 MARGINAL ICE ZONE EXPERIMENT LAGRANGIAN OBSERVATIONS
JEAN-CLAUDE GASCARD, PIERRE-FRANCOIS JEANNIN (Paris VI, Universite, Paris, France), CLAUDE KERGOMARD (Lille I, Universite, Villeneuve-d'Ascq, France), and MICHEL FILY (Grenoble I, Universite, Saint-Martin-d'Herès, France) Journal of Geophysical Research (ISSN 0148-0227), vol. 93, April 15, 1988, p. 3613-3641. Navy-supported research. refs
(Contract CNRS-ASP-PNEDC-950057; CNRS-ATP-85-430510; CNRS-ATP-86-430010; EEC-CLI-083-F)

A88-33695
RADAR SIGNATURES OF OIL FILMS FLOATING ON THE SEA SURFACE AND THE MARANGONI EFFECT
WERNER ALPERS (Bremen, Universitaet, Federal Republic of Germany) and HEINRICH HUEHNERFUSS (Hamburg, Universitaet, Federal Republic of Germany) Journal of Geophysical Research

(ISSN 0148-0227), vol. 93, April 15, 1988, p. 3642-3648. refs
(Contract DFG-WA-124/12-1; BMFT-01-QS-86174)

Airborne radar backscattering experiments carried out recently by Singh et al. (1986) over sea surfaces covered with mineral oil films show that the radar cross section depression has a maximum as a function of incidence angle. In this paper it is shown that Singh et al.'s measurements can be explained by the Marangoni effect if the assumption is made that the mineral oil spill contained surface active material as 'impurities'. The Marangoni effect causes a resonance-type wave damping in the short gravity wave region when the sea surface is covered with a viscoelastic film. Maximum wave damping was observed by Singh et al. at frequencies around 8 Hz. Marangoni theory predicts such a maximum for surface active compounds of medium to low wave damping ability with a dilational modulus of the order of 0.01 N/m¹. Furthermore, it is demonstrated that the Ku band and C band radar backscattering depression curves do not contradict each other. It is pointed out that when converting the radar data into information on depression of spectral energy density of short surface waves, one has to take into account that the radar backscattering at low incidence angles is dominated by specular reflection, while at intermediate incidence angles it is dominated by Bragg scattering. Author

A88-33920
RANGE VARIATIONS OF THE TROPOSPHERIC PROPAGATION OF ULTRASHORT RADIO WAVES ABOVE THE SEA [VARIATSII DAL'NOSTI TROPOSFERNOGO RASPROSTRANENIIA UK RADIOVOLN NAD MOREM]

A. R. GLINER, S. N. KRIVONOZHKIN, and B. M. SHEVTSOV (AN SSSR, Tikhookeanskii Okeanologicheskii Institut, Vladivostok, USSR) Radiofizika (ISSN 0021-3462), vol. 31, no. 2, 1988, p. 238-240. In Russian. refs

Tropospheric variations of the propagation range of ultrashort waves above the sea were studied experimentally using NOAA-satellite observations over the northern part of the Indian Ocean at frequencies of 137.5 and 137.62 MHz. Distributions of the number of range-variation measurements observed in May and in December are presented. The distributions are appreciably asymmetric and disclose a structure that may be connected with fluctuations of the field-attenuation function. B.J.

A88-34643#
NONLINEAR MULTICHANNEL ALGORITHMS FOR ESTIMATING SEA SURFACE TEMPERATURE WITH AVHRR SATELLITE DATA

CHARLES C. WALTON (NOAA, Washington, DC) Journal of Applied Meteorology (ISSN 0894-8763), vol. 27, Feb. 1988, p. 115-124. refs

The familiar linear multichannel sea surface temperature algorithms (MCSST) for estimating sea surface temperature with AVHRR satellite data describe the solution in terms of a constant gamma parameter multiplied by the measured brightness temperature difference of two of the window channels. A nonlinear algorithm is developed in this paper which is similar in form to the MCSST algorithm but with the gamma parameter having a specific two- or three-channel temperature dependence. Simulation studies show that the linear and nonlinear algorithms provide nearly identical accuracies for a wide range of atmospheric conditions if the satellite data are error free. When random or noncorrelative error sources are present in the multichannel AVHRR data, it is found that the nonlinear algorithms significantly reduce their effect upon the final solution relative to the linear MCSST solution. These results are verified with actual AVHRR data obtained in January-March 1982 and 1983. The algorithm estimates of surface temperature are compared with buoy measurements in the North Atlantic and North Pacific. Author

A88-35058
TOPEX/POSEIDON - A CONTRIBUTION TO THE WORLD CLIMATE RESEARCH PROGRAM
ROBERT H. STEWART (California, University, La Jolla) and MICHEL LEFEBVRE (CNES, Toulouse, France) IN: Aerospace century XXI: Space missions and policy; Proceedings of the

05 OCEANOGRAPHY AND MARINE RESOURCES

Thirty-third Annual AAS International Conference, Boulder, CO, Oct. 26-29, 1986. San Diego, CA, Univelt, Inc., 1987, p. 117-128. refs
(AAS PAPER 86-306)

NASA and France's CNES will conduct a joint tides-and-currents measurement program, using the Topex/Poseidon satellite mission. The satellite carries altimeters for measuring satellite altitudes above sea level, and is supported by a precision orbit-determination system, a data analysis/distribution system, and a Principal Investigator program for scientific studies based on the satellite observations. Launch of the satellite is scheduled for 1991, so that the data obtained will coincide with that from the U.S. Navy's Remote Ocean Sensing System and ESA's ERS-1. O.C.

A88-35153

MARINE OBSERVATION SATELLITE-1 (MOS-1) AND ITS SENSORS

YUJI MIYACHI, YASUSHI HORIKAWA (National Space Development Agency of Japan, Tokyo), and YOSHIKAZU KAMIYA (National Space Development Agency of Japan, Los Angeles, CA) IN: Aerospace century XXI: Space sciences, applications, and commercial developments; Proceedings of the Thirty-third Annual AAS International Conference, Boulder, CO, Oct. 26-29, 1986. San Diego, CA, Univelt, Inc., 1987, p. 1611-1621. (AAS PAPER 86-288)

The Japanese Marine Observation Satellite-1 (MOS-1), launched in 1987, initiated Japan's program of earth observation by remote sensing. In this paper, the mission objectives, spacecraft characteristics, and development status of the MOS-1 satellite are presented. The three on-board sensors are briefly described. C.D.

A88-35199* Colspan, Inc., Boulder, Colo.

PASSIVE MICROWAVE DATA FOR SNOW AND ICE RESEARCH - PLANNED PRODUCTS FROM THE DMSP SSM/I SYSTEM

RONALD WEAVER, ROGER G. BARRY (Cooperative Institute for Research in Environmental Science, Boulder, CO), and CHARLES MORRIS (California Institute of Technology, Jet Propulsion Laboratory, Pasadena, CA) EOS (ISSN 0096-3941), vol. 68, Sept. 29, 1987, p. 769, 776, 777. refs
(Contract NAGW-641)

Recommendations which have been made for processing and distributing passive microwave data for snow and ice research obtained with the Defense Meteorological Satellite Program (DMSP) Special Sensor Microwave Imager (SSM/I) are discussed. The general objectives for SSM/I data are reviewed, and the sensor and data flow are described. The SSM/I sea ice products are discussed, and algorithm/product validation is addressed. Proposed services and implementation after SSM/I launch are summarized. C.D.

A88-35986

A METHOD FOR CALCULATING THE EFFECTIVE EMISSIVITY OF A GROOVE STRUCTURE

ZHIMIN ZHANG (Oxford University, England) IN: Optical systems for space applications; Proceedings of the Meeting, The Hague, Netherlands, Mar. 30-Apr. 1, 1987. Bellingham, WA, Society of Photo-Optical Instrumentation Engineers, 1987, p. 270-277. refs

A method for accurately and simply calculating the effective emissivity of a grooved surface is described, and the uncertainties are analyzed. This method was used to calculate the directional and hemispheric emissivities of a grooved surface. The method also allows an accurate determination of the normal and hemispheric emissivity of a cylindrically baffled grooved plate source. It is concluded that the proposed approach can provide an accurate radiance calibration for the ATSR (Along Track Scanning Radiometer) in connection with the measurement of sea surface temperature. B.J.

A88-36159

SATELLITE OBSERVATIONS AND THE NUMERICAL SIMULATION OF THE INTERACTION BETWEEN A SYNOPTIC EDDY AND A FRONTAL ZONE IN THE OCEAN [SPUTNIKOVYE NABLIUDENIYA I CHISLENNOE MODELIROVANIE VZAIMODEISTVIA SINOPTICHESKOGO VIKHRIA S FRONTAL'NYM RAZDELOM V OKEANE]

V. B. LOBANOV and E. V. IAROSHCHUK (AN SSSR, Tikhookeanskii Okeanologicheskii Institut, Vladivostok, USSR) Issledovanie Zemli iz Kosmosa (ISSN 0205-9614), Jan.-Feb. 1988, p. 16-21. In Russian. refs

A88-36160

EVALUATION OF THE POSSIBILITY OF DETERMINING CONCENTRATIONS OF VARIABLE COMPONENTS OF OCEAN WATER FROM AVERAGED SPECTRA OF THE DIFFUSE OPTICAL REFLECTION COEFFICIENT [OTSENKA VOZMOZHNOСТИ VOSSTANOVLENIYA KONTSENTRATSII PEREMENNYKH KOMPONENTOV OKEANSKOI VODY PO USREDNENNYM SPEKTRAM KOEFFITSIENTA DIFFUZNOGO OTRAZHENIYA SVETA]

V. P. LEVENTUEV (Vsesoiuznyi Nauchno-Issledovatel'skii Institut Morskogo Rybnogo Khoziaistva i Okeanografii, Moscow, USSR) Issledovanie Zemli iz Kosmosa (ISSN 0205-9614), Jan.-Feb. 1988, p. 22-29. In Russian. refs

A88-36241*# National Aeronautics and Space Administration, Goddard Space Flight Center, Greenbelt, Md.

ASSESSMENT OF POLAR CLIMATE CHANGE USING SATELLITE TECHNOLOGY

DOROTHY K. HALL (NASA, Goddard Space Flight Center, Greenbelt, MD) Reviews of Geophysics (ISSN 8755-1209), vol. 26, Feb. 1988, p. 26-39. refs

Using results of selected studies, this paper highlights some of the problems that exist in the remote sensing of snow and ice, and demonstrates the importance of remote sensing for the study of snow and ice in determining the effect of temperature increase, due to the atmospheric CO₂ increase, on the cryospheric features. Evidence obtained from NOAA, Nimbus, and other satellites, that may already indicate a global or at least a regional warming, includes an increase in permafrost temperature in northern Alaska and the retreat of many of the world's small glaciers in the last 100 years. It is emphasized that remote sensing is of major importance as the method of obtaining data for monitoring future changes in cryospheric features. I.S.

A88-36841* National Center for Atmospheric Research, Boulder, Colo.

A SYSTEM FOR REMOTE MEASUREMENTS OF THE WIND STRESS OVER THE OCEAN

WILLIAM G. LARGE and J. A. BUSINGER (National Center for Atmospheric Research, Boulder, CO) Journal of Atmospheric and Oceanic Technology (ISSN 0739-0572), vol. 5, April 1988, p. 274-285. refs

(Contract NASA ORDER W-15969; N0014-85-F-031)

The DISSTRESS system for remote measurements of the surface wind stress over the ocean from ships and buoys is described. It is fully digital, utilizing the inertial dissipation technique. Parallel processing allows anemometer data to be filtered in natural frequency space; that is, the filter cutoffs shift linearly with the mean wind speed of the data to be filtered. The construction of the digital Butterworth bandpass filters is presented in detail. The performance of the system is evaluated by analyzing the results from 28 days of operation during the Frontal Air-Sea Interaction Experiment. The mean wind speed is checked, the anemometer response function is established, and drag coefficients are compared to previous studies. The capability of the system is demonstrated by continuous time series of the friction velocity computed every 20 min. The conclusion is that the surface wind stress can be measured more reliably and accurately (20 percent) with this system than from anemometer wind speeds and a bulk formula. Author

A88-36843

PROCESSING, COMPRESSION AND TRANSMISSION OF SATELLITE IR DATA FOR NEAR-REAL-TIME USE AT SEA

PETER CORNILLON, DAVID EVANS (Rhode Island, University, Kingston), OTIS B. BROWN, ROBERT EVANS, PAUL EDEN (Miami, University, FL) et al. *Journal of Atmospheric and Oceanic Technology* (ISSN 0739-0572), vol. 5, April 1988, p. 320-327. refs

(Contract N00014-81-C-0062)

A method for acquisition, processing, and analysis of digital, satellite-derived SST fields on a research vessel at sea in near-real-time (within 10 h of the satellite pass) is discussed. Such imagery provides a general view of the SST field over a large area (700 x 900 km) centered on a 128 x 128 pixel, full-resolution view of the study area. The ability to send these images to the research vessel in a reasonable amount of time (about 1 h, using ATS-3) was a result of a three-level approach to data compression. To perform data compression, first, the overall image was decimated by two while the central 128 x 128 pixel portion was retained in full resolution. Second, a 1-bit-deep cloud mask was derived from the image. Third, the remaining SST values were encoded as SST steps from the previous pixel on a given scan line. Overall, the data were reduced by 75-80 percent. An error-correcting protocol, KERMIT, was used to establish low error rate data communications through the ATS-3 VHF links. A moderate capability digital display unit facilitates display and manipulation of the resultant imagery. Author

A88-37143

THE OCEAN AND THE ATMOSPHERE

H. CHARNOCK (Southampton, University, England) IN: Remote sensing applications in meteorology and climatology; Proceedings of the NATO Advanced Study Institute, Dundee, Scotland, Aug. 17-Sept. 6, 1986. Dordrecht, D. Reidel Publishing Co., 1987, p. 321-326.

The use of satellite remote-sensing data in the construction of numerical models of the ocean-atmosphere (OA) system is briefly discussed. A general description of the oceans is given, with an emphasis on the features which can be characterized by remote sensing, and the treatment of the oceans as the lower boundary of the atmosphere in global climate models is outlined. It is suggested that the fully coupled OA models required to explain complex energy-transfer phenomena will require computer power much greater than that currently available. T.K.

A88-37144

REMOTE SENSING OF SEA-SURFACE WINDS

T. H. GUYMER (Institute of Oceanographic Sciences, Wormley, England) IN: Remote sensing applications in meteorology and climatology; Proceedings of the NATO Advanced Study Institute, Dundee, Scotland, Aug. 17-Sept. 6, 1986. Dordrecht, D. Reidel Publishing Co., 1987, p. 327-357. refs

The theoretical basis and practical implementation of satellite microwave remote-sensing techniques for sea-surface winds are reviewed and illustrated with diagrams and graphs, maps, and sample images based on Seasat data. Methods discussed include scatterometry, altimetry, SAR, and SMMR. The design and operation of the Seasat instruments are described, and data-reduction procedures are explained. Particular attention is given to the positioning of synoptic features, the time-averaged wind distribution, and wind stress curl. The instrumentation of current (Nimbus 7 and Geosat) and planned (ERS-1 and NROSS) oceanographic satellites is briefly considered, and the need for data of extremely high accuracy is stressed. T.K.

A88-37148

THE ALONG-TRACK SCANNING RADIOMETER WITH MICROWAVE SOUNDER

KEITH MUIRHEAD (ESA, Earthnet Programme Office, Frascati, Italy) and DAVE ECCLES (SERC, Rutherford Appleton Laboratory, Didcot, England) IN: Remote sensing applications in meteorology and climatology; Proceedings of the NATO Advanced Study

Institute, Dundee, Scotland, Aug. 17-Sept. 6, 1986. Dordrecht, D. Reidel Publishing Co., 1987, p. 411-423. refs

The design, operation, and projected performance of the Along-Track Scanning Radiometer with Microwave Sounder (ATSR/M) for the ERS-1 oceanographic remote-sensing satellite (scheduled for Ariane launch in 1989) are reviewed. The ATSR/M employs a multichannel IR radiometer, a circular scanning scheme providing two independent looks at each area, an active cooling system, and a nadir-pointing dual-channel microwave sounder; it is designed to provide sea-surface temperatures of 0.5-K accuracy (with 80-percent cloud cover) in 500-km swaths of 50-km sq resolution cells. Consideration is given to the ERS-1 platform and payload components, the ground segment and data-distribution system, the development history of ATSR/M, pixel formatting for the IR radiometer, general data-processing methods, and the specific ATSR/M data products. T.K.

A88-37149

PLANS FOR ERS-1 DATA ACQUISITION, PROCESSING AND DISTRIBUTION

D. A. BATEMAN and A. HASKELL (Royal Aircraft Establishment, Farnborough, England) IN: Remote sensing applications in meteorology and climatology; Proceedings of the NATO Advanced Study Institute, Dundee, Scotland, Aug. 17-Sept. 6, 1986. Dordrecht, D. Reidel Publishing Co., 1987, p. 425-439.

The scientific aims and instruments of the ERS-1 oceanographic remote-sensing satellite (scheduled for Ariane launch in 1989) are discussed, and the ground segment and data-distribution system are described in detail. The major payload components are an SAR operating in both wind and wave modes, a radar altimeter, the Along-Track Scanning Radiometer with Microwave Sounder, the Precise Range and Range-rate Equipment, and a laser retroreflector. The fast-delivery data products (available within 3 h of the observation) for each instrument are listed, and particular attention is given to the procedures and installations to be used at the UK Processing and Archiving Facility (at RAE Farnborough) to generate and distribute off-line SAR, altimeter, and wave-mode products. A drawing of the satellite and flow charts of the data-processing system are provided. T.K.

A88-37270#

OCEAN-ATMOSPHERE INTERACTIONS IN LOW LATITUDE AUSTRALASIA

R. J. ALLAN and M. WEGENER (South Australia, Flinders University, Bedford Park, Australia) IN: National Space Engineering Symposium, 3rd, Canberra, Australia, June 30-July 2, 1987, Preprints of Papers. Barton, Australia/Brookfield, VT, Institution of Engineers/Brookfield Publishing Co., 1987, p. 189-191. Research supported by the Australian Marine Sciences and Technologies Advisory Committee. refs

This paper illustrates the logistics involved in developing a project for integrating conventional meteorological and oceanographical data with remotely sensed Geosynchronous Meteorological Satellite (GMS) and National Oceanic and Atmospheric Administration (NOAA) polar-orbiting satellite imagery to investigate the dominant mechanisms influencing large-scale ocean-atmosphere interactions in low-latitude Australasia. The study aims to produce and interpret a comprehensive set of wind, cloudiness-convective, sea surface temperature (SST) and radiative flux fields over the region 10 deg N - 20 deg S, 115 deg E - 135 deg E, during the 1987 and 1988 summer (December-February) and winter (June-August) monsoon seasons. Author

A88-37679

ACTIVE TWO-ELEMENT MICROWAVE INTERFEROMETRY OF THE SEA SURFACE [AKTIVNAIA DVUKHELEMENTNAIA MIKROVOLNOVAIA INTERFEROMETRIIA MORSKOI POVERKHNOSTI]

A. V. IVANOV (AN SSSR, Institut Radiotekhniki i Elektroniki, Moscow, USSR) *Radiofizika* (ISSN 0021-3462), vol. 31, no. 3, 1988, p. 263-273. In Russian. refs

The paper presents a theoretical assessment of the feasibility of using active two-element interferometers to measure the

three-dimensional spatial-temporal spectral densities of both sea surface reflectance variations and the sea surface layer velocity field. An algorithm for the processing of scattering data is presented, and an analysis is made of the sensitivity and resolution of the proposed technique. B.J.

A88-37720
DISTRIBUTION AND CHEMISTRY OF SUSPENDED PARTICLES FROM AN ACTIVE HYDROTHERMAL VENT SITE ON THE MID-ATLANTIC RIDGE AT 26 DEG N

ROBERT P. TROCINE and JOHN H. TREFRY (Florida Institute of Technology, Melbourne) Earth and Planetary Science Letters (ISSN 0012-821X), vol. 88, no. 1-2, April 1988, p. 1-15. refs (Contract NOAA-NA-85WCC06144)

A88-38690* Jet Propulsion Lab., California Inst. of Tech., Pasadena.

SATELLITE DATA MANAGEMENT FOR EFFECTIVE DATA ACCESS

PATRICK D. HOGAN and THOMAS L. KOTLAREK (California Institute of Technology, Jet Propulsion Laboratory, Pasadena) IN: International Conference on Data Engineering, 3rd, Los Angeles, CA, Feb. 3-5, 1987, Proceedings. Washington, DC, IEEE Computer Society Press, 1987, p. 494-500.

The management of data generated from satellite missions has not always led to effective access of that data by the scientific community. NASA has tried to alleviate this problem for ocean scientists, by initiating a program, the NASA Ocean Data System (NODS). The menu-based user interface that NODS employs allows a user to make request and receive answers within a short time of accessing the system. A catalog system, which holds information about oceanographic data sets may be queried to determine the suitability of a particular data set. Once a candidate data set is found, the user is directed to the person or place which actually holds the data. NODS also has an archive system that holds data from ocean-observing satellites. The archive may be queried to obtain a manageable data subset that can be delivered in a useful form. Author

A88-38691* California Univ., La Jolla.
SNOW MELT ON SEA ICE SURFACES AS DETERMINED FROM PASSIVE MICROWAVE SATELLITE DATA

MARK R. ANDERSON (California, University, La Jolla) IN: Large scale effects of seasonal snow cover. Wallingford, England, International Association of Hydrological Sciences (IAHS Publication, No. 166), 1987, p. 329-342. Research supported by the Mellon Foundation. refs (Contract NAGW-1028)

SMMR data for the year 1979, 1980 and 1984 have been analyzed to determine the variability in the onset of melt for the Arctic seasonal sea ice zone. The results show melt commencing in either the Kara/Barents Seas or Chukchi Sea and progressing zonally towards the central Asian coast (Laptev Sea). Individual regions had interannual variations in melt onset in the 10-20 day range. To determine whether daily changes occur in the sea ice surface melt, the SMMR 18 and 37 GHz brightness temperature data are analyzed at day/night/twilight periods. Brightness temperatures illustrate diurnal variations in most regions during melt. In the East Siberian Sea, however, daily variations are observed in 1979, throughout the analysis period, well before any melt would usually have commenced. Understanding microwave responses to changing surface conditions during melt will perhaps give additional information about energy budgets during the winter to summer transition of sea ice. Author

A88-39079
COMPARISON OF UNIFIED FULL-WAVE SOLUTIONS FOR NORMAL INCIDENCE MICROWAVE BACKSCATTER FROM SEA WITH PHYSICAL OPTICS AND HYBRID SOLUTIONS

E. BAHAR, M. A. FITZWATER (Nebraska, University, Lincoln), and D. E. BARRICK (Ocean Surface Research, Inc., Boulder, CO) International Journal of Remote Sensing (ISSN 0143-1161), vol.

9, March 1988, p. 365-377. NOAA-supported research. refs (Contract N00014-87-K-0177)

The unified full-wave solution for electromagnetic wave scatter from a rough surface is expressed as an integral similar in form to physical optics solutions. However, it correctly predicts return for small and intermediate roughness scales where the physical optics approach fails. This full-wave solution is used here to evaluate microwave sea surface backscatter at normal incidence for both the like-polarized and cross-polarized linear components. Surface heights and slopes are assumed to be Gaussian, the sea is characterized by its surface height spectral density function, and both perfectly and finitely conducting surfaces are considered. Results from this complete full-wave evaluation are compared with approximations, involving single-scale (specular point) and two-scale models. For both of these models, however, it is necessary to assume a spectral wavenumber, $\nu(d)$, where spectral splitting between the large and the small scales of the rough surface occurs. The full-wave solution is used as a guide in the selection of $\nu(d)$ and to study the accuracy and sensitivity of the different approximations to $\nu(d)$. It is also shown that results for cross-polarized backscatter based on the physical optics or two-scale models are totally inadequate. Author

A88-39081
SATELLITE DETECTED CYANOBACTERIA BLOOM IN THE SOUTHWESTERN TROPICAL PACIFIC - IMPLICATION FOR OCEANIC NITROGEN FIXATION

CECILE DUPOUY (Office de la Recherche Scientifique et Technique d'Outre-Mer, Plouzane, France), MICHEL PETIT (Office de la Recherche Scientifique et Technique d'Outre-Mer, Montpellier, France), and YVES DANDONNEAU (Office de la Recherche Scientifique et Technique d'Outre-Mer, Noumea, New Caledonia) International Journal of Remote Sensing (ISSN 0143-1161), vol. 9, March 1988, p. 389-396. Research supported by the Office de la Recherche Scientifique et Technique d'Outre-Mer, CNRS, and CNES. refs

Tropical seas are major sites for extensive cyanobacterial (blue-green algal) developments. The oceanic nitrogen fixation caused by such blooms may be of relatively great importance in regard to the global nitrogen budget. A Nimbus-7 Coastal Zone Color Scanner (CZCS) image on January 4, 1982, shows a large phytoplankton bloom (90,000 sq/km) around New Caledonia and the Vanuatu archipelago, located east of Australia in the Coral Sea (165 deg E, 20 deg S). The bloom is caused by cyanobacteria, presumably Oscillatoria (Trichodesmium) spp., which occur systematically in this region. This assertion was not controlled by simultaneous sea-truths, but several indices and current knowledge of the region indicate that the hypothesis is reasonable. By using the CZCS image, an estimation is made for the nitrogen fixation of the bloom. It suggests that such a biological event plays a significant role in the global nitrogen oceanic budget. Author

A88-39083
SURFACE TEMPERATURES AND SEA ICE TYPING FOR NORTHERN BAFFIN BAY

KONRAD STEFFEN (Zuerich, Eidgenoessische Technische Hochschule, Zurich, Switzerland) and JOHN E. LEWIS (McGill University, Montreal, Canada) International Journal of Remote Sensing (ISSN 0143-1161), vol. 9, March 1988, p. 409-422. refs

The northern region of Baffin Bay (74-79 deg N and 70-78 deg W) is known as the North Water Polynya - a region of inhomogeneous ice cover during the winter and spring months. During the winters of 1978/79 and 1980/81, a series of low-level aircraft flights were conducted over the North Water covering a length of 2300 km. Surface thermal infrared (TIR) temperatures were measured and visual surface ice characteristics photographed with the aid of a searchlight attached to the aircraft. Corrections procedures were applied to the TIR data which produced a temperature accuracy of + or - 0.15 C. A matching was made between visual ice types and ice surface temperatures along with ice properties using the aircraft and ice/meteorological data collected at a base station near Resolute Bay, Northwest Territories. Also, surface temperatures outside the spatial extent

of the aircraft measurements were extrapolated by means of NOAA-VHRR TIR imagery. From the two sets of data, regional surface temperature maps were constructed. Results indicated that grey-white ice for thicknesses of 0.15-0.3 m was the dominant type of ice especially during January and February with a marked increase of white ice percentage toward the end of the ice season. Ice-free areas or warm water actually constituted only a very small percentage of the total area for both winter seasons. Author

A88-39084
METHODOLOGY FOR AN OPERATIONAL MONITORING OF REMOTELY-SENSED SEA SURFACE TEMPERATURES IN INDONESIA

J. P. GASTELLU-ETCHEGORRY (Gadjah Mada University, Yogyakarta, Indonesia) and T. BOELY (Office de la Recherche Scientifique et Technique d'Outre-Mer, Paris, France) International Journal of Remote Sensing (ISSN 0143-1161), vol. 9, March 1988, p. 423-438. refs

Operational SST monitoring was tested with the study of large-scale SST features in Indonesia from July 1981 to June 1985. Digital data were provided by digitizing 208 weekly SST charts of NOAA-NES. The pixel size corresponded to 1 deg 15 min longitude and latitude. These data displayed a 0.5 deg K rms error compared with 1985 in situ measurements. Iterative interactive factorial analyses combined with a parallelepiped classifier as a clustering technique enhanced the SST spatiotemporal features. The study area was divided into zones in which pixels had similar SST profiles, and dates of occurrence of thermal anomalies were pointed out. Sea fronts and upwellings were mapped through spatiotemporal analyses of thermal gradients. This study stresses the possibility of operational SST monitoring for Indonesia, allowing simple data manipulation with hardware easily maintained locally. Author

A88-39085
SURFACE CURRENTS OFF THE WEST COAST OF IRELAND STUDIED FROM SATELLITE IMAGES

A. P. CRACKNELL and W. G. HUANG (Dundee, University, Scotland) International Journal of Remote Sensing (ISSN 0143-1161), vol. 9, March 1988, p. 439-446. refs

The surface current in the spring of 1984 off the west coast of Ireland has been mapped from NOAA-8 thermal infrared images. The 'feature-tracking method' has been used to derive flow vectors from advective sea surface temperature feature displacements and elapsed time. This feature-tracking method has a great advantage which gives a synoptic and spatial view of the velocity distribution over in situ measurements. Sequential images obtained on orbits 5596, 5610 and 5627 during the period of April 25-27, 1984, have been used and geometrically corrected. With the 24 hours and 48 hours differences, the measurement accuracy achieved in the speed of sea features was + or - 1.8 cm/s. The surface current pattern agrees with the main current pattern obtained by ships and drift bottles. A cyclonic eddy centered at 57 deg 04 min N 10 deg 59 min W has been studied. A very pronounced feature recognized is the sea surface front between mixed coastal water and stratified Atlantic water along the whole west coast of Ireland. The front is characterized by cyclonic and anticyclonic eddies which have time scales of the order of 1 to 7 days and length scales of the order of 30 km. Author

A88-39284* Columbia Univ., New York, N.Y.

POLYNYAS IN THE SOUTHERN OCEAN

ARNOLD L. GORDON (Columbia University, NY) and JOSEFINO C. COMISO (NASA, Goddard Space Flight Center, Greenbelt, MD) Scientific American (ISSN 0036-8733), vol. 258, June 1988, p. 90-97.

The formation of large regions of open ocean in the pack ice near Antarctica called polynyas is discussed. The role of the meridional circulation pattern of the Southern Ocean, of buoyancy, and of wind in the formation of polynyas is shown. The different characteristics and causes of coastal and open-ocean polynyas are pointed out. C.D.

A88-39746#

AN EVALUATION OF THE PERFORMANCE OF THE ECMWF OPERATIONAL SYSTEM IN ANALYZING AND FORECASTING EASTERLY WAVE DISTURBANCES OVER AFRICA AND THE TROPICAL ATLANTIC

R. J. REED, A. HOLLINGSWORTH, W. A. HECKLEY, and F. DELSOL (European Centre for Medium Range Weather Forecasts, Reading, England) Monthly Weather Review (ISSN 0027-0644), vol. 116, April 1988, p. 824-865. NOAA-supported research. refs (Contract NSF ATM-84-21396)

A88-40059* Maryland Univ., Cambridge.
THE DISPERSAL OF THE AMAZON'S WATER

FRANK E. MULLER-KARGER (Maryland, University, Cambridge), CHARLES R. MCCLAIN (NASA, Goddard Space Flight Center, Greenbelt, MD), and PHILIP L. RICHARDSON (Woods Hole Oceanographic Institution, MA) Nature (ISSN 0028-0836), vol. 333, May 5, 1988, p. 56-59. NSF-supported research. refs

New information obtained with NASA's Coastal Zone Color Scanner and with drifting buoys reveals that the discharge of the Amazon is carried offshore around a retroflection of the North Brazil Current and into the North Equatorial Countercurrent towards Africa between June and January each year. From about February to May, the countercurrent and the retroflection weaken or vanish, and Amazon water flows northwestward toward the Caribbean Sea. C.D.

A88-40353#

SIR-B EXPERIMENTS IN JAPAN. III - OIL-POLLUTION EXPERIMENT

TOSHIYUKI OKUYAMA, HIDEYUKI INOMATA, HARUNOBU MASUKO, and KENJI NAKAMURA Radio Research Laboratory, Journal (ISSN 0033-8001), vol. 35, March 1988, p. 39-54. refs

Artificial oil slicks were produced in accordance with the scheduled Shuttle Imaging Radar (SIR-B) orbit. The purpose was to evaluate the ability of spaceborne Synthetic Aperture Radar (SAR) to monitor oil spills at sea. Oleyl alcohol was used to produce these slicks because its surface tension was very similar to that of crude oil. Techniques were established for producing such artificial slicks. The slicks were observed by SIR-B, by an airborne X-band/Ka-band scatterometer developed by RRL, and by an airborne Ocean Color Scanner chartered by Toba Merchant Marine College (TMMC). Sea-truth data such as surface wind speed and direction, sea current speed and direction, wave height, and so on were collected by the boat which produced the slicks, and by observation vessels. Author

A88-40356#

SIR-B EXPERIMENTS IN JAPAN. VI.

TOSHIO IGUCHI and HIDEYUKI INOMATA Radio Research Laboratory, Journal (ISSN 0033-8001), vol. 35, March 1988, p. 85-104. refs

During the Shuttle Imaging Radar (SIR-B) mission in October 1984, Synthetic Aperture Radar (SAR) images were taken off the coast of Japan. An artificial oil slick was produced within the SAR swath to investigate its effect on the backscattered signal. Not only the slick but also the long-wave pattern was visible in the images. Image data was analyzed to examine how well wave spectra could be deduced from it and how much the oil slick reduced the backscattered signal. Wave spectra derived from SIR-B images were compared with simultaneous wave-buoy observations. Waves at the time of flight were nearly perpendicular to the SAR flight direction and were composed of two major systems: a swell of about 200-m wavelength and wind waves with 70-m wavelength. Both the swell and wind-wave peaks were identifiable in the SAR image spectra after stationary response correction. The peak frequencies derived from SIR-B images and from the wave gauge agreed satisfactorily. The presence of oleyl alcohol on the ocean surface was found to reduce radar backscatter by about 1.4 dB. This was smaller than the modulation caused by the long-wave field in the images. Several filters were applied to the oil-slick image to suppress the long-wave pattern and to enhance the slick image. The resulting filtered images are shown. Author

A88-40834

THE DETERMINATION OF THE PARAMETERS OF THE DIURNAL THERMOCLINE USING SATELLITE AND SHIP-BASED MEASUREMENTS [OB OPREDELENIU PARAMETROV SUTOCHNOGO TERMOKLINA PO SPUTNIKOVYIM I POPUTNYM SUDOVYIM IZMERENIAMI]

K. N. FEDOROV and A. I. GINZBURG (AN SSSR, Institut Okeanologii, Moscow, USSR) *Meteorologiya i Gidrologiya* (ISSN 0130-2906), April 1988, p. 82-91. In Russian. refs

A88-41257

MAGNETIC LINEATIONS ON THE FLANKS OF THE MARQUESAS SWELL - IMPLICATIONS FOR THE AGE OF THE SEAFLOOR

SARAH E. KRUSE (MIT, Cambridge, MA) *Geophysical Research Letters* (ISSN 0094-8276), vol. 15, June 1988, p. 573-576. refs (Contract NSF OCE-86-09526)

A88-41398

POSSIBILITY OF REPLACING COMPLEX VALUES OF PERMITTIVITY WITH REAL VALUES [O VOZMOZHNOSTI ZAMENY KOMPLEKSNYKH ZNACHENII DIELEKTRICHESKOI PRONITSAEMOSTI VESHCHESTVENNYMI]

A. A. VLASOV *Radiotekhnika i Elektronika* (ISSN 0033-8494), vol. 33, May 1988, p. 1068-1071. In Russian. refs

It is shown that the application of a method which replaces complex values of permittivity with real values can reduce the number of unknowns in certain remote-sensing problems. The determination of the emissivity of the sea surface is mentioned as an example. B.J.

A88-42039

THE JRC PROGRAM FOR MARINE COASTAL MONITORING

J. A. BEKKERING (CEC, Joint Research Centre, Ispra, Italy) IN: Remote sensing for resources development and environmental management; Proceedings of the Seventh International Symposium, Enschede, Netherlands, Aug. 25-29, 1986. Volume 2. Rotterdam, A. A. Balkema, 1986, p. 699-702. refs

An overview of a project using remote sensing techniques, in situ measurements, and a computer-run model to study coastal transport of pollution in the northern Adriatic sea is given. The project is a collaborative effort of EEC member states to develop an operative system capable of monitoring and forecasting major marine events in coastal areas. Nimbus 7 CZCS, NOAA AVHRR, and Landsat TM imagery is used in research and new sensors are being investigated to enlarge the number of marine parameters detectable. Campaigns are undertaken to provide in situ biological, chemical, physical, atmospheric, under and over water optical measurements, and airborne sensor data. The computer model being developed should predict the propagation, transformation, and sedimentation of pollutants and nutrients. R.B.

A88-42047

SEA SURFACE TEMPERATURE STUDIES IN NORWEGIAN COASTAL AREAS USING AVHRR- AND TM THERMAL INFRARED DATA

J. P. PEDERSEN (Tromsø, Universitetet, Norway) IN: Remote sensing for resources development and environmental management; Proceedings of the Seventh International Symposium, Enschede, Netherlands, Aug. 25-29, 1986. Volume 2. Rotterdam, A. A. Balkema, 1986, p. 749-754. refs

This work presents an algorithm for deriving sea surface temperatures from infrared satellite data. The algorithm is based upon physical solution of the equation of radiative transfer. The theory for calculating the atmospheric transmittance and radiance is briefly discussed. Calculated transmittances are compared to values reported by others. Results from applications of the algorithm on NOAA/AVHRR-data are presented. Finally, sea surface temperature data derived from the Landsat/Thematic Mapper are presented. Due to lack of TM calibration data, the temperatures are derived from comparisons of digital values and in situ measured temperatures at known locations in the data set.

Author

A88-42050

DETERMINATION OF SPECTRAL SIGNATURE OF NATURAL WATER BY OPTICAL AIRBORNE AND SHIPBORNE INSTRUMENTS

D. SPITZER and M. R. WERNAND (Nederlands Instituut voor Onderzoek der Zee, Texel, Netherlands) IN: Remote sensing for resources development and environmental management; Proceedings of the Seventh International Symposium, Enschede, Netherlands, Aug. 25-29, 1986. Volume 2. Rotterdam, A. A. Balkema, 1986, p. 771-773.

The advanced spectral irradiance meter, the coastal optical remote sensing airborne radiometer, and the portable four channel radiometer were developed, calibrated, tested, and applied for numerous measurements in and above various coastal and oceanic regions to determine the temporally and locally dependent signatures of diverse water types. The Indonesian marine environments remote sensing experiments performed in the coastal waters northeast of Java, within the framework of the Snellius II expedition are discussed. Also, the spectral, spatial and time resolutions of these instruments and data acquisition systems are determined. R.B.

A88-42443

MESOSCALE VARIABILITY IN CURRENT METER MEASUREMENTS IN THE CALIFORNIA CURRENT SYSTEM OFF NORTHERN CALIFORNIA

MICHELE M. RIENECKER, CHRISTOPHER N. K. MOOERS (Institute for Naval Oceanography, Bay Saint Louis, MS), and ROBERT L. SMITH (Oregon State University, Corvallis) *Journal of Geophysical Research* (ISSN 0148-0227), vol. 93, June 15, 1988, p. 6711-6734. Navy-sponsored research. refs

Current meter data from the OPTOMA program moorings (deployed from October 1984 to July 1985), located on the continental rise offshore of Point Reyes-Point Arena and from a LLWOD program mooring (deployed from September 1982 to August 1983) located about 250 km offshore were analyzed for information regarding the mesoscale variability in the California Current system (CCS). In addition, the oceanic response to local wind forcing, eddies, and offshore jets was investigated. The results of the analysis revealed a remarkable horizontal inhomogeneity and nonstationarity of the CCS, suggesting that a more extensive current meter array is required to fully investigate the mesoscale variability in the region covered. I.S.

A88-42444

SEA SURFACE FLOW ESTIMATION FROM ADVANCED VERY HIGH RESOLUTION RADIOMETER AND COASTAL ZONE COLOR SCANNER SATELLITE IMAGERY - A VERIFICATION STUDY

JAN SVEJKOVSKY (California, University, La Jolla) *Journal of Geophysical Research* (ISSN 0148-0227), vol. 93, June 15, 1988, p. 6735-6743. refs (Contract NOAA-NA-80AAD00120)

A refined technique for estimating surface currents from the displacement of features in sequential advanced very high resolution radiometer (AVHRR) and coastal zone color scanner (CZCS) images is presented. It is used to calculate flow fields in two regions along the California coast, and the results are compared to concurrent drifter drogue observations. There is overall agreement to within approximately 6 cm/s, with somewhat better agreement at velocities less than 40 cm/s. The poorer performance of the technique at high velocities was due to difficulties in identifying and tracking features in areas of rapid flow. The accuracy of the measurements is primarily affected by the analyst's precision in tracking each feature which, in turn, depends on how well the 2- to 6-km features preserve their identity from one image to the next. A 12- to 24-hour interval yielded the best results in this study. The directional component of the satellite-derived flow field was representative of subsurface flow patterns down to at least 100 m. Although velocities obtained from AVHRR infrared and CZCS visible images may not always represent flow at the same depth, the measurements were practically identical with the data used. Author

A88-42445* Jet Propulsion Lab., California Inst. of Tech., Pasadena.

MOISTURE AND LATENT HEAT FLUX VARIABILITIES IN THE TROPICAL PACIFIC DERIVED FROM SATELLITE DATA

W. TIMOTHY LIU (California Institute of Technology, Jet Propulsion Laboratory, Pasadena) *Journal of Geophysical Research* (ISSN 0148-0227), vol. 93, June 15, 1988, p. 6749-6760. refs

This paper describes a method of determining latent heat flux and the ocean-atmosphere moisture from sea surface temperature, precipitable water, and surface wind speed data derived from 1980-1983 observations of SMMR aboard Nimbus 7 above tropical Pacific. The observation period included a very intense El Niño-Southern Oscillation (ENSO) episode. It was found that, during the early phase of the 1982-1983 ENSO, a surface convergence center moved east leading the anomalous equatorial westerlies. At this center, the low wind and high humidity caused negative (low) latent heat flux anomalies, despite anomalously high sea surface temperatures. Latent heat flux was found to play an important role in the seasonal cooling of the upper ocean, except in areas covered by major surface convergence zones and in areas of ocean upwelling. I.S.

A88-42446* Institute of Ocean Sciences, Sidney (British Columbia).

TIME EVOLUTION OF SURFACE CHLOROPHYLL PATTERNS FROM CROSS-SPECTRUM ANALYSIS OF SATELLITE COLOR IMAGES

KENNETH L. DENMAN (Department of Fisheries and Oceans, Institute of Ocean Sciences, Sidney, Canada) and MARK R. ABBOTT (California Institute of Technology, Jet Propulsion Laboratory, Pasadena; California, University, La Jolla) *Journal of Geophysical Research* (ISSN 0148-0227), vol. 93, June 15, 1988, p. 6789-6798. Research supported by the Department of Fisheries and Oceans of Canada. refs

The rate of decorrelation of surface chlorophyll patterns as a function of the time separation between pairs of images was determined from two sequences of CZCS images of the Pacific Ocean area adjacent to Vancouver Island, Canada; cloud-free subareas were selected that were common to several images separated in time by 1-17 days. Image pairs were subjected to two-dimensional autospectrum and cross-spectrum analysis in an array processor, and squared coherence estimates found for several wave bands were plotted against time separation, in analogy with a time-lagged cross correlation function. It was found that, for wavelengths of 50-150 km, significant coherence was lost after 7-10 days, while for wavelengths of 25-50 km, significant coherence was lost after only 5-7 days. In both cases, offshore regions maintained coherence longer than coastal regions. I.S.

A88-42447*# National Aeronautics and Space Administration, Goddard Space Flight Center, Greenbelt, Md.

SATELLITE AND AIRCRAFT PASSIVE MICROWAVE OBSERVATIONS DURING THE MARGINAL ICE ZONE EXPERIMENT IN 1984

PER GLOERSEN (NASA, Goddard Space Flight Center, Greenbelt, MD) and WILLIAM J. CAMPBELL (USGS, Tacoma, WA) *Journal of Geophysical Research* (ISSN 0148-0227), vol. 93, June 15, 1988, p. 6837-6846. NASA-Navy-ESA-supported research. refs

This paper compares satellite data on the marginal ice zone obtained during the Marginal Ice Zone Experiment in 1984 by Nimbus 7 with simultaneous mesoscale aircraft (in particular, the NASA CV-990 airborne laboratory) and surface observations. Total and multiyear sea ice concentrations calculated from the airborne multichannel microwave radiometer were found to agree well with similar calculations using the Nimbus SMMR data. The temperature dependence of the determination of multiyear sea-ice concentration near the melting point was found to be the same for both airborne and satellite data. It was found that low total ice concentrations and open-water storm effects near the ice edge could be reliably distinguished by means of spectral gradient ratio, using data from the 0.33-cm and the 1.55-cm radiometers. I.S.

A88-42448* Woods Hole Oceanographic Institution, Mass. **TEMPORAL VARIATIONS OF PARTICLE FLUXES IN THE DEEP SUBTROPICAL AND TROPICAL NORTH ATLANTIC - EULERIAN VERSUS LAGRANGIAN EFFECTS**

W. G. DEUSER (Woods Hole Oceanographic Institution, MA), F. E. MULLER-KARGER (Maryland, University, Cambridge), and C. HEMLEBEN (Tubingen, Universitat, Federal Republic of Germany) *Journal of Geophysical Research* (ISSN 0148-0227), vol. 93, June 15, 1988, p. 6857-6862. DFG-supported research. refs (Contract NGT-21-002-822; NSF OCE-76-21280; NSF OCE-78-19813; NSF OCE-80-24130; NSF OCE-81-17002; NSF OCE-82-19588; NSF OCE-84-17909; NSF OCE-85-01955)

The flux of particles measured by sediment traps in the deep water of the Sargasso Sea and western tropical North Atlantic undergoes pronounced temporal variation. In the Sargasso Sea the variability is largely due to seasonal changes in mixed-layer depth and attendant changes in primary productivity affecting a wide region. By contrast, the variability in the western tropical Atlantic appears to be caused by patches of elevated nutrient and pigment concentrations which have their origin in the plumes of the Amazon and Orinoco rivers. Coastal zone color scanner scenes demonstrate the great seasonal and interannual differences in the direction and dispersal patterns of the plumes. The river plumes break up into irregular patches which may pass through the catchment area of a sediment trap at varying rates, thereby creating the impression of almost random temporal flux variability at a fixed trap site. Author

A88-42449

EMPIRICAL ORTHOGONAL FUNCTION ANALYSIS OF ADVANCED VERY HIGH RESOLUTION RADIOMETER SURFACE TEMPERATURE PATTERNS IN SANTA BARBARA CHANNEL

GARY S. E. LAGERLOEF (Science Applications International Corp., Bellevue, WA) and ROBERT L. BERNSTEIN (SeaSpace, Inc., San Diego, CA) *Journal of Geophysical Research* (ISSN 0148-0227), vol. 93, June 15, 1988, p. 6863-6873. Research sponsored by the U.S. Department of the Interior, Science Applications International Corp., and U.S. Navy. refs

This paper demonstrates an application of empirical orthogonal function (EOF) analysis to oceanographic and meteorological data sets sampled over space and time. Using yearlong AVHRR sea-surface temperature data for the Santa Barbara Channel, the method is used to extract the dominant spatial and temporal variance modes. It was found that the heavily dominant first mode of spatial variance for Santa Barbara Channel is consistent with a quasi-permanent front and associated strong temperature contrast between the two predominant water masses in the channel. A second spatial variance mode was found to be consistent with recurring eddies in the west central part of the channel. In contrast with the spatial variance modes, the first mode of temporal variance was found to be overwhelmingly dominant and reflected the basin-wide annual temperature cycle, having little spatial structure. This mode lagged the first spatial mode by about 90 days, which suggests two decoupled spatial annual cycles. I.S.

A88-42450

SATELLITE OBSERVATIONS OF TIDAL UPWELLING AND MIXING IN THE ST. LAWRENCE ESTUARY

YVES GRATTON, GORDON MERTZ (Quebec, Universite, Rimouski, Canada), and JACQUES A. GAGNE (Department of Fisheries and Oceans, Institute Maurice Lamontagne, Mont-Joli, Canada) *Journal of Geophysical Research* (ISSN 0148-0227), vol. 93, June 15, 1988, p. 6947-6954. Research supported by the Department of Fisheries and Oceans of Canada, Universite du Quebec, and NSERC. refs

Satellite thermal images (NOAA 9) of the St. Lawrence estuary are used to confirm the existence of a persistent cold spot due to tidal upwelling at the head of the lower St. Lawrence estuary and to show that cold water may be found episodically up to 100 km downstream of the head. This extended cold anomaly may exist in two spatial configurations: one confined to near the south shore, the other being centered over midestuary. The various physical

agencies likely to contribute to the growth of this anomaly are discussed, and it is concluded that wind, internal tides, and advection of cold water from the head region are the most significant factors. Author

A88-43217

CIRCULATION PATTERNS IN AVHRR IMAGERY

R. A. VAUGHAN (Dundee, University, Scotland) and I. D. DOWNEY (Salford, University, England) International Journal of Remote Sensing (ISSN 0143-1161), vol. 9, April 1988, p. 597-600. refs

AVHRR sea surface temperature data acquired in April 1984 are used to study the development of circulation patterns in the northeast Atlantic and around the eastern coast of Scotland. The data indicate that mesoscale eddies dominate the mixing process within the Rockall Trough. The relative temperature gradients were determined from the satellite data following correction for atmospheric effects using multichannel split window algorithms. Sources of error responsible for the differences found between the satellite-derived and buoy temperatures are discussed. R.R.

A88-43218

A MODEL OF SATELLITE RADAR ALTIMETER RETURN FROM ICE SHEETS

J. K. RIDLEY and K. C. PARTINGTON (London, University College, Dorking, England) International Journal of Remote Sensing (ISSN 0143-1161), vol. 9, April 1988, p. 601-624. refs

A theoretical model of satellite radar altimeter return has been developed, with application to the measurement of the form and mass balance of polar ice sheets. Altimeter returns over three widely spaced regions of the ice-sheet are shown to be strongly influenced by volume scattering as well as surface scattering. The results suggest that careful retracking of waveform data should be performed in these regions, and that failure to account for the depth of radar penetration can result in estimated elevations up to 3.3 m lower than the actual elevation (depending on local conditions and retracking method). R.R.

A88-43226

THE EFFECT OF DISSOLVED 'YELLOW SUBSTANCE' ON THE QUANTITATIVE RETRIEVAL OF CHLOROPHYLL AND TOTAL SUSPENDED SEDIMENT CONCENTRATIONS FROM REMOTE MEASUREMENTS OF WATER COLOUR

S. TASSAN (CEC, Joint Research Centre, Ispra, Italy) International Journal of Remote Sensing (ISSN 0143-1161), vol. 9, April 1988, p. 787-797. refs

A88-43664

RADIOMETRIC INVESTIGATION OF THE SEA-WAVE BREAKING PROCESS [RADIODISTANTSIONNYE ISSLEDOVANIYA PROTSESSA OBRUSHENIYA MORSKOI VOLNY]

I. V. CHERNYI and E. A. SHARKOV (AN SSSR, Institut Kosmicheskikh Issledovaniy, Moscow, USSR) Issledovanie Zemli iz Kosmosa (ISSN 0205-9614), Mar.-Apr. 1988, p. 17-28. In Russian. refs

The interactions between electromagnetic radiation and the rough sea surface during the wave breaking cycle were investigated using photography and measurements carried out from an experimental vessel in the Indian Ocean with a radiometer and a scatterometer integrated with an analog magnetic recorder. Two wave-breaking cycle stages (spray and foam formation) could be identified. The results of an analysis of the high-frequency spectrum of the scatterometer signal suggest that the speckle structure of the scattered signal field (horizontal polarization) depends on spray formation over the rough sea surface. I.S.

A88-43665

PARAMETERS OF EDDY STRUCTURES AND MUSHROOM CURRENTS IN THE BALTIC SEA DERIVED FROM SATELLITE IMAGERY [PARAMETRY VIKHREVIKH STRUKTUR I GRIBOVIDNYKH TECHENII V BALTIISKOM MORE PO SPUTNIKOVYIM IZOBRAZHENIYAM]

I. A. BYCHKOVA and S. V. VIKTOROV (Gosudarstvennyi

Okeanograficheskii Institut, Leningrad, USSR) Issledovanie Zemli iz Kosmosa (ISSN 0205-9614), Mar.-Apr. 1988, p. 29-35. In Russian. refs

A88-43669

METHOD FOR RAPIDLY ESTIMATING GEOPHYSICAL PARAMETERS OF THE OCEAN-ATMOSPHERE SYSTEM FROM SATELLITE MICROWAVE RADIOMETRY [OPERATIVNYI METOD OTSENKI GEOFIZICHESKIKH PARAMETROV SISTEMY OKEAN-ATMOSFERA PO DANNYM SPUTNIKOVOGO SVCH-RADIOMETRICHESKOGO ZONIROVANIYA]

V. M. POLIAKOV and V. P. SAVORSKII (AN SSSR, Institut Radiotekhniki i Elektroniki, Moscow, USSR) Issledovanie Zemli iz Kosmosa (ISSN 0205-9614), Mar.-Apr. 1988, p. 58-66. In Russian. refs

This paper describes a method for rapidly estimating geophysical parameters of the atmosphere and the sea surface from measurements of satellite-borne microwave radiometers. The procedure relies on determining direct multivariate regression correlations between the radiometer output signals and the variations of spatial (latitudinal) distributions of various geophysical parameters, such as the sea surface temperature and the integral water vapor content of the atmosphere. The latitudinal SST profile obtained with radiometer signals from Cosmos-1151 and the regression correlation developed for the northern Atlantic Ocean agree with data yielded by the rigorous solution of the inverse problem. I.S.

A88-43835*

National Aeronautics and Space Administration. Goddard Inst. for Space Studies, New York, N.Y.

MASS EXTINCTIONS, ATMOSPHERIC SULPHUR AND CLIMATIC WARMING AT THE K/T BOUNDARY

MICHAEL R. RAMPINO (NASA, Goddard Institute for Space Studies, New York; New York University, NY) and TYLER VOLK (New York University, NY) Nature (ISSN 0028-0836), vol. 332, March 3, 1988, p. 63-65. Research supported by Columbia University and NASA. refs

The possible climatic effects of a drastic decrease in cloud condensation nuclei (CCN) associated with a severe reduction in the global marine phytoplankton abundance are investigated. Calculations suggest that a reduction in CCN of more than 80 percent and the resulting decrease in marine cloud albedo could have produced a rapid global warming of 6 C or more. Oxygen isotope analyses of marine sediments from many parts of the world have been interpreted as indicating a marked warming coincident with the demise of calcareous nannoplankton at the K/T boundary. Decreased marine cloud albedo and resulting high sea surface temperatures could have been a factor in the maintenance of low productivity in the 'Strangelove Ocean' period following the K/T extinctions. C.D.

A88-44005*#

National Aeronautics and Space Administration. John C. Stennis Space Center, Bay Saint Louis, Miss.

REMOTE SENSING TECHNOLOGY AND APPLICATIONS

C. F. SCHUELER (NASA, John C. Stennis Space Center, Bay Saint Louis, MS) IN: Advanced topics in manufacturing technology: Product design, bioengineering; Proceedings of the Symposium, ASME Winter Annual Meeting, Boston, MA, Dec. 13-18, 1987. New York, American Society of Mechanical Engineers, 1987, p. 79-84.

(Contract NAGW-814)

Electro-optical imaging sensors form the principal devices that are typically used to obtain images of earth from satellite platforms, and substantial improvements in optics, electro-optical detection devices, cooling subsystems and composite structures have enabled the high quality performance exhibited by the current instrumentation. This paper reviews the fundamentals of system design for imaging sensors such as the Thematic Mapper on board Landsat, points out the key areas of current R&D, and briefly alludes to some important applications. Author

N88-20676# Joint Publications Research Service, Arlington, Va.
SPECTRAL REFLECTIVE CHARACTERISTICS OF SEA SURFACE Abstract Only

V. V. KAZARYAN and V. P. KOROVIN *In its* JPRS Report: Science and Technology. USSR: Earth Sciences p 1-2 26 Feb. 1988 Transl. into ENGLISH from Vestnik Leningradskogo Universiteta, Seriya 7: Geologiya, Geografiya (Leningrad, USSR), no. 1, Mar. 1987 p 97-99
 Avail: NTIS HC A04/MF A01

A multichannel type SP-4 spectropolarimeter operating in the 400 to 760 nm band from an aircraft was used to measure the spectral brightness of the sea surface and study the brightness variation as a function of various hydrophysical characteristics. It was found that the spatial resolution of the instrument increased with decreasing measurement altitude, but that this increased dispersion and standard deviation of the measured values. The spectral distribution of sea surface brightness differed for various water areas. Over the ocean there was a characteristic maximum at 470 to 490 nm, in littoral waters it is shifted to 490 to 535 nm.

Author

N88-20678# Joint Publications Research Service, Arlington, Va.
MUSHROOM-SHAPED CURRENTS (EDDY DIPOLES) UNDER ROTATION AND STRATIFICATION CONDITIONS Abstract Only

A. I. GINZBURG, A. G. KOSTYANOY, A. M. PAVLOV, and K. N. FEDOROV *In its* JPRS Report: Science and Technology. USSR: Earth Sciences p 3 26 Feb. 1988 Transl. into ENGLISH from Doklady Akademii Nauk SSSR (Moscow, USSR), v. 292, no. 4, Feb. 1987 p 971-974

Avail: NTIS HC A04/MF A01

The mushroom shaped currents detected from satellite images are a combination of narrow jet flows and plane eddy dipoles. A study was made to clarify the following aspects of this phenomenon: behavior of eddy dipoles under different conditions related to the presence or absence of stratification and different methods for inducing a disturbance allowing the possibility of a change in the sign and intensity of a relative angular momentum locally introduced into a fluid rotating as a solid body. The experimental apparatus included a rotating platform and a cylindrical basin filled with fresh water or a two layer fluid which was spun in a clockwise direction until solid body rotation was attained. The experimental configuration corresponded to an f-plane for which the beta-effect due to parabolic level curvature is negligible. A dye was used to ease observation of disturbance development. Various means were used to generate disturbances. The experiments revealed that in a fluid rotating system it is possible to stimulate currents on the f-plane by any of the various types of local disturbance in either a uniform or stratified fluid resulting in the formation of eddy dipole(s).

Author

N88-20714*# National Aeronautics and Space Administration. Goddard Space Flight Center, Greenbelt, Md.

THE 1987 AIRBORNE ANTARCTIC OZONE EXPERIMENT: THE NIMBUS-7 TOMS DATA ATLAS

ARLIN J. KRUEGER, PHILIP E. ARDANUY, FRANK S. SECHRIST, LANNING M. PENN, DAVID E. LARKO, SCOTT D. DOIRON, and REGINALD N. GALIMORE (Science Applications Research, Lanham, Md.) Mar. 1988 246 p

(NASA-RP-1201; REPT-88B0107; NAS 1.61:1201) Avail: NTIS HC A11/MF A01 CSCL 04B

Total ozone data taken by the Nimbus-7 Total Ozone Mapping Spectrometer (TOMS) played a central role in the successful outcome of the 1987 Airborne Antarctic Ozone Experiment. The near-real-time TOMS total ozone observations were supplied within hours of real time to the operations center in Punta Arenas, Chile, over a telecommunications network designed specifically for this purpose. The TOMS data preparation and method of transfer over the telecommunications links are reviewed. This atlas includes a complete set of the near-real-time TOMS orbital overpass data over regions around the Palmer Peninsula of Antarctica for the period of August 8 through September 29, 1987. Also provided are daily polar orthographic projections of TOMS total ozone

measurements over the Southern Hemisphere from August through November 1987. In addition, a chronology of the salient points of the experiment, along with some latitudinal cross sections and time series at locations of interest of the TOMS total ozone observations are presented. The TOMS total ozone measurements are evaluated along the flight tracks of each of the ER-2 and DC-8 missions during the experiment. The ozone hole is shown here to develop in a monotonic progression throughout late August and September. The minimum total ozone amount was found on 5 October, when its all-time lowest value of 109 DU is recorded. The hole remains well defined, but fills gradually from mid-October through mid-November. The hole's dissolution is observed here to begin in mid-November, when it elongates and begins to rotate. By the end of November, the south pole is no longer located within the ozone hole.

Author

N88-20780*# National Aeronautics and Space Administration. Goddard Space Flight Center, Greenbelt, Md.

TIDAL ESTIMATION IN THE PACIFIC WITH APPLICATION TO SEASAT ALTIMETRY

BRAULIO V. SANCHEZ and DAVID E. CARTWRIGHT (National Academy of Sciences - National Research Council, Washington, D. C.) Dec. 1987 27 p

(NASA-TM-100694; REPT-88B0061; NAS 1.15:100694) Avail: NTIS HC A03/MF A01 CSCL 08C

The techniques for computing the eigenfunctions of the velocity potential (Proudman functions) set out in Sanchez, et al. (1986) in relation to the Atlantic-Indian Oceans are here applied to the Pacific Ocean, using a 6x6 degree grid of 510 points (455 points for the associated stream functions). Normal modes are computed from the first Proudman functions and have natural periods from 43.9h downward. Tidal syntheses are derived from these modes by direct application of the (frictionless) dynamic equations and by least-squares fitting of Proudman functions to the dynamically interpolated tide-gauge data of Schwiderski (1983). The modes contributing the most energy to the principal harmonic tidal constituents are different in the two computations: their natural periods are typically in the range of 9 to 16h for semidiurnal, and 14 to 43h for diurnal tides. The rms of fit for the Proudman functions is, in all cases, better than the corresponding value for the same number of spherical harmonics.

Author

N88-20800# Scripps Institution of Oceanography, La Jolla, Calif. Space Inst.

RADIATIVE PROCESSES AFFECTING OCEAN MIXED-LAYER HEAT CONTENT AND THEIR MONITORING FROM SATELLITE

CATHERINE GAUTIER *In* Hawaii Univ., Dynamics of the Oceanic Surface Mixed Layer p 229-247 1987

(Contract N00014-86-K-0752; NSF OCE-82-14791)

Avail: NTIS HC A14/MF A01 CSCL 08C

Radiation flux observations (satellite and surface) from various studies are examined to assess their possible roles in modifying the ocean's mixed layer heat content. Several processes are investigated. First, observations indicate that the magnitude and extent of sea surface temperature (SST) diurnal warming events (changes of up to 3 degrees C), which affect air-sea heat fluxes, can be effectively monitored by satellite. Second, although still not well understood, a mechanism is suggested that would involve convective lines in upper ocean turbulent mixing generation. The mechanism has a strong diurnal variability, resulting in nighttime cooling in bursts concurrent with wind stress bursts, and might generate bursts of turbulent mixing. Third, mixings effect on photosynthesis and the potential influence of photoplankton distribution on mixing and thermal stratification are discussed. Lastly, several satellite methods for computing net surface radiation flux are reviewed and assessed.

Author

N88-21567 Centre National d'Etudes Spatiales, Toulouse (France). Groupe de Recherches de Geodesie Spatiale.

STUDY OF THE DYNAMIC TOPOGRAPHY OF OCEANS BY MEANS OF SATELLITE ALTIMETRY [ETUDE DE LA TOPOGRAPHIE DYNAMIQUE DES OCEANS PAR ALTIMETRIE SATELLITAIRE]

05 OCEANOGRAPHY AND MARINE RESOURCES

J. F. MINSTER *In its* Climatology and Space Observations p 763-813 Sep. 1987 In FRENCH
Avail: CEPADUES-Editions, 111 rue Nicolas-Vauquelin, 31100 Toulouse, France

Measuring problems and the correction of altimetric data are reviewed. The analysis refers to the results obtained with Seasat and GEOS3. The different methods of signal processing to extract the variability due to the mesoscale dynamic topography are described. Observations at large wavelength including tidal waves are discussed. It is concluded that the necessary accuracy to assess the ocean climatic role is attainable if all aspects of measurement are optimized. ESA

N88-21568 Institut Francais de Recherche pour l'Exploitation de la Mer, Brest (France).

BASIC NETWORKS OF TOGA: DETERMINATION OF THERMAL PROFILES BY XBT AND OF SEA LEVEL BY TIDE GAGE

J. R. DONGUY *In* CNES, Climatology and Space Observations p 815-819 Sep. 1987 In FRENCH; ENGLISH summary
Avail: CEPADUES-Editions, 111 rue Nicolas-Vauquelin, 31100 Toulouse, France

French participation in TOGA is reviewed. It includes the extension of the Pacific XBT network to the Atlantic and Indian oceans. The good monitoring of thermal structure anomalies which was obtained with El Nino in 1982 to 1983 guided network extension. The comparison of the data from XBT network with the data from the tide-gage network reveals a good correlation in the equatorial area between the thermocline depth and the sea level. ESA

N88-21570 Scott Polar Research Inst., Cambridge (England).
THE ROLE OF REMOTE SENSING IN THE STUDY OF POLAR ICE SHEETS

DAVID J. DREWRY *In* CNES, Climatology and Space Observations p 835-847 Sep. 1987
Avail: CEPADUES-Editions, 111 rue Nicolas-Vauquelin, 31100 Toulouse, France

Remote sensing methods including radar and laser altimetry to observe the configuration of ice sheets; microwave radiometry to measure short term accumulation and ablation patterns; microwave and infrared radiometry from the surface temperature; and imaging techniques to measure a variety of parameters by using specific techniques are reviewed. The measurement of ice thickness, however, is a major problem, and airborne methods are indicated for the time being. ESA

N88-21571 Laboratoire d'Océanographie Dynamique et de Climatologie, Paris (France).

ELEMENTS OF SEA ICE DYNAMICS AND THERMODYNAMICS

J. C. GASCARD *In* CNES, Climatology and Space Observations p 849-884 Sep. 1987 In FRENCH; ENGLISH summary
Avail: CEPADUES-Editions, 111 rue Nicolas-Vauquelin, 31100 Toulouse, France

A classical thermodynamical model is described and compared with observational results related to Arctic conditions. Examples of sea ice dynamics and sea ice thickness distribution are described. Remote sensing is discussed and applications from the Seasat SAR and AVHRR/TQVS on NOAA are presented. ESA

N88-21572 Max-Planck-Inst. fuer Meteorologie, Hamburg (West Germany).

SEA ICE OBSERVATIONS AND MODELS

P. LEMKE *In* CNES, Climatology and Space Observations p 885-895 Sep. 1987
Avail: CEPADUES-Editions, 111 rue Nicolas-Vauquelin, 31100 Toulouse, France

The natural variability of sea ice is described and an attempt is made to describe sea ice fluctuations with simple thermodynamics. More advanced dynamic-thermodynamic models are also discussed. Sea ice anomalies are expected to appreciably affect the structure of the atmosphere and ocean circulations. In

view of the long relaxation time of these anomalies, they are of considerable interest for the problem of long term weather prediction and climatic change. ESA

N88-21575# Technische Hogeschool, Delft (Netherlands). Orbital Mechanics Section.

FROM SATELLITE ALTIMETRY TO OCEAN TOPOGRAPHY, A SURVEY OF DATA PROCESSING TECHNIQUES

K. F. WAKKER, R. C. A. ZANDBERGEN, G. H. M. VANGELDORP, and B. A. C. AMBROSIUS 1987 41 p Presented at the EARSeL Symposium on Remote Sensing Needs in the 1990's, Oceanography/Sea Ice Workshop, Noordwijkerhout, Netherlands, 4-8 May 1987 Revised Sponsored by ESA-ESOC, Darmstadt, Fed. Republic of Germany; The Netherlands Space Research Organisation, Utrecht, Netherlands; and Begeleidingscommissie Remote Sensing, Delft, Netherlands
(ETN-88-91841) Avail: NTIS HC A03/MF A01

Satellite altimetry missions and altimeter data processing are reviewed. Orbit computation accuracy is addressed. Examples of geophysical products obtained from Seasat altimeter measurements are discussed. ESA

N88-21625# Centre National d'Etudes Spatiales, Toulouse (France). Centre Spatial.

MARGINAL ICE ZONE EXPERIMENT (MIZEX) 1984 VARAN-S DATA SET

N. LANNELONGUE, D. VAILLANT, J. PERBOS, and W. J. CAMPBELL Nov. 1985 61 p

(ETN-88-92032) Avail: NTIS HC A04/MF A01

Side-looking airborne radar was installed in a B-17 aircraft to map ice, at 200 to 3000 m altitude with 20 km swath width. The X-band digital radar provided 5 mosaics of 100 km by 100 km. The long range and low speed of the B17 are highly advantageous for ice mapping. ESA

N88-22267# Centre National d'Etudes Spatiales, Toulouse (France). Centre Spatial.

DEFINITION AND IMPLEMENTATION STUDY FOR THE VARAN-S RADAR [ETUDE DE DEFINITION ET DE MISE EN OEUVRE DU RADAR VARAN-S]

N. LANNELONGUE and D. VAILLANT 1 Aug. 1985 178 p In FRENCH

(CNES-CT/DRT/TIT/RL-143-T; ETN-88-92030) Avail: NTIS HC A09/MF A01

The Varan-S side looking radar was developed to implement high resolution imagery for oceanographic applications. It works as a synthetic aperture radar. The technical parameters required for oceanographic utilization and the onboard equipment necessary to implement the radar system are described. The ground-based data processing is also discussed. The specifications are given. ESA

N88-22447*# Bohan (Walter A.) Co., Park Ridge, Ill.
NIMBUS-7 CZCS. COASTAL ZONE COLOR SCANNER IMAGERY FOR SELECTED COASTAL REGIONS. NORTH AMERICA - EUROPE. SOUTH AMERICA - AFRICA - ANTARCTICA. LEVEL 2 PHOTOGRAPHIC PRODUCT

1984 99 p Original contains color illustrations

(Contract NAS5-29079)

(NASA-CR-180755; NAS 1.26:180755) Avail: NTIS HC A05/MF A01 CSCL 08B

The Nimbus-7 Coastal Zone Color Scanner (CZCS) is the first spacecraft instrument devoted to the measurement of ocean color. Although instruments on other satellites have sensed ocean color, their spectral bands, spatial resolution, and dynamic range were optimized for geographical or meteorological use. In the CZCS, every parameter is optimized for use over water to the exclusion of any other type of sensing. The signal-to-noise ratios in the spectral channels sensing reflected solar radiance are higher than those required in the past. These ratios need to be high because the ocean is such a poor reflecting surface that the majority of the signal seen by the reflected energy channels at spacecraft altitudes is backscattered solar radiation from the atmosphere

rather than reflected solar energy from the ocean. The CZCS is a conventional multichannel scanning radiometer utilizing a rotating plane mirror at a 45 deg angle to the optic axis of a Cassegrain telescope. The mirror scans 360 deg; however, only 80 deg of data centered on the spacecraft nadir is collected for ocean color measurements. Spatial resolution at spacecraft nadir is 825x825 m with some degradation at the edges of the scan swath. The useful swath width from a spacecraft altitude of 955 km is 1600 km. Author

N88-22504# Pacific Northwest Labs., Richland, Wash.
OCEAN GENERAL CIRCULATION MODELS: REPORT ON PROCEEDINGS OF A MEETING OF OCEAN AND CLIMATE MODELERS

C. R. SHERWOOD and J. P. DOWNING Jan. 1988 101 p
 Presented at the Meeting on Ocean and Climate Modelers: Ocean General Circulation Models, Sequim, Wash., 30 Jul. 1987 (Contract DE-AC06-76RL-01830) (DE88-005530; PNL-SA-15557; CONF-8707147-SUMM) Avail: NTIS HC A06/MF A01

The proceedings of a meeting of ocean general circulation modelers and oceanographers are summarized. New developments in coupling ocean general circulation models and atmospheric general circulation models, improvements in the representation of mixed layer and sea ice processes, optimization of model codes for parallel processing on the next generation of supercomputers and ocean data sets and their limitations are among the topics discussed. Author

N88-22506# Naval Postgraduate School, Monterey, Calif.
HYDROGRAPHIC DATA FROM THE OPTOMA (OCEAN PREDICTION THROUGH OBSERVATION, MODELING AND ANALYSIS) PROGRAM: OPTOMA 23, 9-19 NOVEMBER 1986
Progress Report, Nov. 1986 - Sep. 1987

J. E. JOHNSON, PAUL A. WITTMANN, and CHRISTOPHER N. MOOERS 8 Jan. 1988 95 p
 (AD-A189868; NPS-68-88-001) Avail: NTIS HC A05/MF A01 CSDL 08C

The OPTOMA (Ocean Prediction Through Observation, Modeling and Analysis) program, seeks to understand the mesoscale (fronts, eddies, and jets) variability and dynamics of the California Current System (CCS) and to determine the scientific limits to practical mesoscale ocean forecasting. OPTOMA 23 is the last of the OPTOMA surveys and it is unique in that this was the first effort to integrate concurrent satellite, drifting buoy, ship, and aircraft data in a comprehensive oceanographic, meteorological, and acoustical study of the CCS. Specific goals of the airborne surveys were to: provide synoptic data for objective analysis of various parameters (e.g., SST from AXBT- and PRT-5, mixed layer depth, thermal structure); provide initialization, boundary condition updating, and verification fields for dynamical model forecasts; and coordinate the observational strategy of the R/V POINT SUR by using near real time analyses to vector the ship into areas of interesting mesoscale activity. GRA

N88-22508# Woods Hole Oceanographic Institution, Mass.
REAL-TIME ENVIRONMENTAL ARCTIC MONITORING (R-TEAM) Interim Technical Report

ALESSANDRO BOCCONCELLI Nov. 1987 83 p
 (Contract N00014-86-C-0135) (AD-A189948; WHOI-87-50) Avail: NTIS HC A05/MF A01 CSDL 08C

The R-TEAM mooring is designed to collect oceanic environmental data in Arctic regions and to transmit these data to shore on a daily basis via ARGOS satellite telemetry. An ascent module comes to the surface once a day and transmits directly to ARGOS (ice free surface). When not transmitting the module remains in its rest position most of the time, well away from the surface, thus diminishing the risks of damage at the ice interface. The R-TEAM's design life is one year in situ. The mooring must be capable of deployment in depths of up to 4500 and must be able to withstand a maximum current speed of 2 knots at the surface. At an early stage two different transit options were

considered. The variable ballast elevator seemed more directly compatible with our existing capabilities. UHF and MF transmitters, antennae, and associated electronic were designed and built to system specifications. The prototype mooring was deployed at 2700 m at 39 deg N, 30 deg W on June 2, 1987 and entirely recovered 62 days later. By and large this experimental deployment was very successful but the test also revealed two deficiencies which need to be corrected. GRA

N88-23357 Max-Planck-Inst. fuer Meteorologie, Hamburg (West Germany).
INVESTIGATION OF THE IMAGING OF OCEAN SURFACE WAVES USING A SYNTHETIC APERTURE RADAR [UNTERSUCHUNG DER ABBILDUNG VON OZEANOBERFLAECHEWELLEN DURCH EIN SYNTHETIC APERTURE RADAR]

CLAUS BRUENING 1987 98 p In GERMAN (SER-A-WISS-ABHANDL-84; ETN-88-91470) Avail: Fachinformationszentrum Karlsruhe, 7514 Eggenstein-Leopoldshafen 2, Fed. Republic of Germany, 20 DM

The imaging of long, wind-induced ocean waves by a SAR using a two-dimensional Monte Carlo simulation model was investigated. It is shown that the nonlinear distortions in the SAR-imaging are essentially due to phase modulation and Doppler broadening of the SAR-signal by the subscale orbital velocities of backscattered SAR-signal. The pronounced azimuthal decay of the spectral energy density in the SAR-variance spectrum is due to the Doppler-broadening-induced reduction of the azimuthal resolution, and limits the signal-to-noise ratio of the signal. The validity of the SAR-simulation model was demonstrated by comparison with SAR-variance spectra taken by the Shuttle Imaging Radar. ESA

N88-23358# World Climate Programme, Geneva (Switzerland).
THE WOCE CORE PROJECT PLANNING MEETING ON THE GYRE DYNAMICS EXPERIMENT

Sep. 1987 47 p Meeting held in London, United Kingdom, 2-5 Sep. 1986 (WCP-139; WMO/TD-192; ETN-88-92209) Avail: NTIS MF A01; print copy avail. at World Meteorological Organization, Case Postale No. 5, CH-1211 Geneva 20, Switzerland

Aspects which a study of ocean gyre dynamics should address were defined. The ocean surface layer, ocean interior, and deep circulation were discussed. Apart from a deep circulation experiment in the Brazil basin, the favored site is the North Atlantic. ESA

N88-24024# Instituto de Pesquisas Espaciais, Sao Jose dos Campos (Brazil).
COMPARISON OF SURFACE CURRENT DETERMINED FROM SATELLITE-TRACKED BUOY WITH SHIPBOARD WIND DATA DURING THE 4TH BRAZILIAN ANTARCTIC EXPEDITION, 10-14 MARCH, 1986

MERRITT R. STEVENSON, EDUARDO M. B. ALONSO, CARLOS L. DASILVA, JR., and REINALDO SOLEWICZ In its Latin American Symposium on Remote Sensing. 4th Brazilian Remote Sensing Symposium and 6th SEELPER Plenary Meeting, Volume 1 p 181 1986
 Avail: NTIS HC A99/MF E03

A drifting buoy developed by INPE was launched on the 10th of March and tracked by the system ARGOS, using NOAA-6 and NOAA-9 satellites until the 14th of March, when the buoy was recovered by the oceanographic support ship Barao de Teffe. After the launch of the buoy, a set of oceanographic stations was occupied at which time wind measurements were made from the ship. Other wind measurements were also made at hourly intervals, and combined with station winds to form a times series for the experiment. Prior to and at the time of buoy launch, the wind was from the SW and parallel to the axis of the Strait. During the following 8 hours, winds were weak or calm. Afterward the wind changed direction and blew from the NE with speeds increasing to more than 30 knots and gusts to 48 knots during the following day. Wind continued strong and generally from the NE and E

05 OCEANOGRAPHY AND MARINE RESOURCES

until the 14th of March when the buoy was recovered. During the experiment about 40 buoy positions were determined by service ARGOS in Toulouse, France. A comparison was made of the wind and buoy trajectories in terms of time lag. Author

N88-24058# Instituto de Pesquisas Espaciais, Sao Jose dos Campos (Brazil).

NEAR SURFACE CURRENT DETERMINED FROM INPE'S SATELLITE-TRACKED BUOY, DURING 6-26 NOVEMBER, 1985
MERRITT R. STEVENSON and EDUARDO M. B. ALONSO /in its Latin American Symposium on Remote Sensing. 4th Brazilian Remote Sensing Symposium and 6th SELPER Plenary Meeting, Volume 1 p 494-500 1986
Avail: NTIS HC A99/MF E03

A field experiment was made to test INPE's drifting, oceanographic buoy during the 6th through the 26th of November, 1985. Buoy measurements obtained during the 10th through the 20th of November were made from the Brazilian hydrographic ship *Alte*, Saldanha, near 24 deg 8 min S, 45 deg 13 min W. Within the buoy, a UHF transmitter compatible with the System ARGOS, transmitted sensor data via an omnidirectional antenna. The System ARGOS aboard polar orbiting satellites received, recorded, and retransmitted the buoy signals. Geographic fixes were determined from the Doppler frequency of the buoy transmissions, in combination with the known orbital characteristics of the satellite receiving the signals. Positional accuracy of the buoy was estimated by determining positional differences with respect to the five mean positions, and then combining these differences to make an overall estimate of the positional error. The experiment suggests that the INPE drifting buoy is capable of obtaining useful measurements of near surface currents.

Author

N88-24126*# Alaska Univ., Fairbanks. Geophysical Inst.
INFLUENCE OF THE YUKON RIVER ON THE BERING SEA
Final Report
KENNESON G. DEAN and C. PETER MCROY 1988 22 p
Original contains color illustrations
(Contract NAS5-28769)
(NASA-CR-182802; NAS 1.26:182802) Avail: NTIS HC A03/MF A01 CSCL 08C

Physical and biological oceanography of the northern Bering Sea including the influence of the Yukon River were studied. Satellite data acquired by the Advanced Very High Resolution Radiometer (AVHRR), the LANDSAT Multispectral Scanner (MSS) and the Thematic Mapper (TM) sensor were used to detect sea surface temperatures and suspended sediments. Shipboard measurements of temperature, salinity and nutrients were acquired through the Inner Shelf Transfer and Recycling (ISHTAR) project and were compared to digitally enhanced and historical satellite images. The satellite data reveal north-flowing, warm water along the Alaskan coast that is highly turbid with complex patterns of surface circulation near the Yukon River delta. To the west near the Soviet Union, cold water, derived from an upwelling, mixes with shelf water and also flows north. The cold and warm water coincide with the Anadyr, Bering Shelf and Alaskan coastal water masses. Generally, warm Alaskan coastal water forms near the coast and extends offshore as the summer progresses. Turbid water discharged by the Yukon River progresses in the same fashion but extends northward across the entrance to Norton Sound, attaining its maximum surface extent in October. The Anadyr water flows northward and around St. Lawrence Island, but its extent is highly variable and depends upon mesoscale pressure fields in the Arctic Ocean and the Bering Sea. Author

N88-24129# Science Applications International Corp., College Station, Tex.
EXAMPLES OF ICE PACK RIGIDITY AND MOBILITY CHARACTERISTICS DETERMINED FROM ICE MOTION
JAMES K. LEWIS, RONALD E. ENGLEBRETSON, and WARREN W. DENNER Jan. 1988 19 p
(Contract N00014-87-C-0173)

(AD-A191163; SAIC-87/1869) Avail: NTIS HC A03/MF A01 CSCL 08L

A method has been developed to determine ice pack rigidity and mobility using observed ice motion. With this method, one may determine how solidly the ice pack is frozen in near real-time. Spatial and temporal variations in the freezing and thawing of the ice pack can also be studied. This method was developed to study how well numerical ice modeling techniques were reproducing actual sea ice processes. The ice pack rigidity parameter is now being used to compare observed periods of ice pack thawing and freezing with models from the same regions and times. Various degrees of ice rigidity and mobility were studied using remotely-sensed ice motion data off the north coast of Alaska during 1975 and 1979. Characteristics of the time histories of pack ice speed were used to infer changes in the rigidity of pack ice. Summer-time ice rigidities were detected first in late June 1975 and lasted through September. However, in 1979 considerably higher rigidities were found in August while summer-like rigidities were detected into late November. Analyses of atmospheric pressure distributions suggest that less mechanical breakup occurred in the summer of 1979, resulting in the greater rigidities during August of that year. GRA

06

HYDROLOGY AND WATER MANAGEMENT

Includes snow cover and water runoff in rivers and glaciers, saline intrusion, drainage analysis, geomorphology of river basins, land uses, and estuarine studies.

A88-34674
PRINCIPLES OF THE REMOTE MONITORING OF FRESH-WATER QUALITY [PRINTSIPY AEROKOSMICHESKOGO MONITORINGA KACHESTVA POVERKHNOSTNYKH VOD SUSHI]

K. IA. KONDRAT'EV (AN SSSR, Institut Ozerovedeniia, Leningrad, USSR) and A. A. GITEL'SON (AN SSSR, Gidrokhimicheskii Institut, Rostov-on-Don, USSR) Akademiia Nauk SSSR, Doklady (ISSN 0021-3454), vol. 299, no. 3, 1988, p. 590-595. In Russian. refs

Principles for the monitoring of fresh-water quality on the basis of satellite multispectral observations are presented. The proposed approach makes it possible to determine such water characteristics as concentrations of chlorophyll, petroleum, and dissolved organic matter; temperature; mineralization; pH; turbidity; oxygen content; and electroconductivity. B.J.

A88-35196
QUANTITATIVE ANALYSIS OF DISTRIBUTION OF SUSPENDED SEDIMENTS IN THE YELLOW RIVER ESTUARY FROM MSS DATA

WEN-YAO LIU and V. KLEMAS (College of Marine Studies, Newark, DE) Geocarto International (ISSN 1010-6049), vol. 3, March 1988, p. 51-62. refs

A88-35198* National Aeronautics and Space Administration. Goddard Space Flight Center, Greenbelt, Md.
REMOTE SENSING OF SNOW

J. L. FOSTER, D. K. HALL, and A. T. C. CHANG (NASA, Goddard Space Flight Center, Greenbelt, Md) EOS (ISSN 0096-3941), vol. 68, Aug. 11, 1987, p. 682-684. refs

The snow parameters affecting sensor responses at different wavelengths are discussed. The effects of snow depth and background radiation on gamma ray sensors and of crystal size, contaminants, snow depth, liquid water, and surface roughness on visible and near-infrared sensors are considered. The influence of temperature, crystal size, and liquid water on thermal infrared sensors and of liquid water, crystal size, water equivalent depth, stratification, snow surface roughness, density, temperature, and soil condition on microwave sensors are addressed. C.D.

A88-35399

QUANTITATIVE DESCRIPTION AND CLASSIFICATION OF DRAINAGE PATTERNS

DEMETRE P. ARGIALAS (Louisiana State University, Baton Rouge), JOHN G. LYON (Ohio State University, Columbus), and OLIN W. MINTZER (U.S. Army, Engineer Topographic Laboratories, Fort Belvoir, VA) Photogrammetric Engineering and Remote Sensing (ISSN 0099-1112), vol. 54, April 1988, p. 505-509. Research supported by the Louisiana State University. refs

A structural pattern recognition methodology is presented for computer-assisted description and classification of drainage patterns. Eight patterns types were quantitatively described and classified. The methodology to classify these patterns consisted of drainage pattern models, hierarchical and relational models, attribute extraction, and classification strategies. The results indicated that a digital computer can assist human interpretation on such patterns. Author

A88-36166

SALINE SALT AND WATER SURFACE MAPPING ON THE BASIS OF DATA FROM THE GYUNESH-84 REMOTE-SENSING EXPERIMENT [KARTOGRAFIROVANIE ZASOLENNYKH ZEMEL' I VODNOI POVERKHNOSTI PO REZUL'TATAM KOMPLESKNOGO AEROKOSMICHESKOGO EKSPERIMENTA 'GIUNESH-84']

A. SH. MEKHTIEV, P. IU. NAGIEV, E. M. DZHAFAROV, B. IA. DOLGOPOLOV, and E. A. MAMEDOV (AN ASSR, Nauchno-Proizvodstvennoe Ob'edinenie Kosmicheskikh Issledovaniy, Baku, Azerbaidzhan SSR) Issledovanie Zemli iz Kosmosa (ISSN 0205-9614), Jan.-Feb. 1988, p. 66-74. In Russian. refs

A88-37136

USE OF RADAR AND SATELLITE IMAGERY FOR THE MEASUREMENT AND SHORT-TERM PREDICTION OF RAINFALL IN THE UNITED KINGDOM

K. A. BROWNING (Meteorological Office, Bracknell, England) IN: Remote sensing applications in meteorology and climatology; Proceedings of the NATO Advanced Study Institute, Dundee, Scotland, Aug. 17-Sept. 6, 1986. Dordrecht, D. Reidel Publishing Co., 1987, p. 189-208. refs

The techniques and hardware being developed at the UK Meteorological Office to process radar data and satellite imagery for use in numerical rainfall prediction are discussed. The major components of the system include multiple unmanned radar sites with on-site minicomputers, a central network computer to combine the radar data and generate integrated rainfall maps, a ground station to receive and preprocess cloud images from GEO satellites, automatic forecasting algorithms based on simple extrapolation, interactive image-display terminals for comparison of satellite and radar data, and automated tailoring and distribution of rainfall measurements and predictions. The operation of these components is described in detail and illustrated with diagrams, maps, and sample images. T.K.

A88-37414

SATELLITE DETECTION OF BLOOM AND PIGMENT DISTRIBUTIONS IN ESTUARIES

RICHARD P. STUMPF (NOAA, Assessment and Information Services Center, Washington, DC) and MARY A. TYLER (Versar, Inc., Columbia, MD) Remote Sensing of Environment (ISSN 0034-4257), vol. 24, April 1988, p. 385-404. refs (Contract NSF OCE-81-09928; NSF OCE-83-10407)

A technique to obtain estimates of relative chlorophyll concentration in turbid water using satellite spectral data is described. The method is capable of identifying chlorophyll blooms in estuaries where the reflectance is between 0.01 and 0.07. With a simple uniform atmospheric correction to AVHRR and CZCS satellite data, maps of the vector orientation in bands j and i are used to show the location of blooms in the Chesapeake Bay in the springs of 1981 and 1982. With some calibration, the method may provide estimates of chlorophyll for concentrations greater than 5 microg/l. R.R.

A88-39078 San Diego State Univ., Calif.

REMOTE SENSING AND IMAGE PROCESSING REQUIREMENTS FOR EULERIAN FLOW FIELD ESTIMATIONS

DOUGLAS A. STOW (San Diego State University, CA) International Journal of Remote Sensing (ISSN 0143-1161), vol. 9, March 1988, p. 351-364. Research sponsored by the University of California and NASA. refs

The application of remote sensing and image processing to the development of numerical models for deriving estimates of a hydrodynamic surface flow field is considered. Remote sensing and image processing provide time-sequential tracer distribution information over a water surface as input to the flow estimating numerical model. Technical and scientific aspects of remote sensing tracers, platforms, and sensors are discussed, in addition to image processing procedures related to atmospheric corrections, geometric/radiometric processing, and spatial aggregation. R.R.

A88-39080

COMPARISON OF MEASURED SUSPENDED SEDIMENT CONCENTRATIONS WITH SUSPENDED SEDIMENT CONCENTRATIONS ESTIMATED FROM LANDSAT MSS DATA

JERRY C. RITCHIE (USDA, Hydrology Laboratory, Beltsville, MD) and CHARLES M. COOPER (USDA, Sedimentation Laboratory, Oxford, MS) International Journal of Remote Sensing (ISSN 0143-1161), vol. 9, March 1988, p. 379-387. refs

Landsat MSS data for 27 days between January 1983 and June 1985 for Moon Lake, Mississippi were analyzed as a means of determining the suspended sediment concentrations of lake surface water. Pixel values and radiance and reflectance measurements from Landsat data for 14 of the scenes were used to develop simple and multiple regression equations. The coefficient of determination for the relationship between measured and estimated suspended sediment concentrations was found to be greater than 0.80. The best estimates were obtained in the 50-250 mg/l concentration range. R.R.

A88-39089

RANGELAND RUNOFF CURVE NUMBERS AS DETERMINED FROM LANDSAT MSS DATA

A. W. ZEVENBERGEN (Landbouwhogeschool, Wageningen, Netherlands), A. RANGO, J. C. RITCHIE, E. T. ENGMAN (USDA, Hydrology Laboratory, Beltsville, MD), and R. H. HAWKINS (Utah State University, Logan) International Journal of Remote Sensing (ISSN 0143-1161), vol. 9, March 1988, p. 495-502. refs

A relationship has been found between satellite data and hydrologically defined runoff curve numbers (CN) for a limited number of watersheds. Watershed CNs calculated from rainfall-runoff data on small range land basins were correlated with Landsat multispectral scanner data transformed into 19 reflectance index models (RIM). In this study, nine small watersheds were found where sufficient CN and Landsat data were available. After eliminating the redundant or poorly correlated RIMs, five significant and highly correlated RIM versus CN regression relationships were selected as promising for use in rangeland studies. More testing should be done to validate the approach; however, the results indicate that satellite data may eventually be employed to directly and efficiently estimate rangeland CNs. This empirical approach has potential for use in planning studies and comprehensive range resources models. Author

A88-41946

APPLICATION OF LANDSAT THEMATIC MAPPER DATA TO ASSESS SUSPENDED SEDIMENT DISPERSION IN A COASTAL LAGOON

JOHN R. JENSEN, ELIJAH W. RAMSEY, III, BJORN KJERFVE, KAREN MAGILL, and JIM SNEED (South Carolina, University, Columbia) IN: American Society for Photogrammetry and Remote Sensing and ACSM, Fall Convention, Reno, NV, Oct. 4-9, 1987, ASPRS Technical Papers. Falls Church, VA, American Society for Photogrammetry and Remote Sensing, 1987, p. 26-35. refs

The techniques used to estimate the suspended sediment content of water in the Laguna de Terminos (Mexico) and adjacent coastal areas from a Landsat-5 TM image obtained on November

25, 1984 under cloud-free conditions are described. The steps applied include conversion of digital data to radiance values and bandwidth normalization, correction for atmospheric scattering and radiative transfer, application of a chromaticity-transform algorithm, and principal-component analysis. The results are presented in tables, graphs, and maps and briefly characterized, with reference to the predictions of a numerical model of sediment circulation in the lagoon. The highest correlation ($r = -0.61$) with predicted sediment concentration is found for the atmospherically corrected chromaticity level related to TM band 2. T.K.

A88-41949* National Aeronautics and Space Administration. John C. Stennis Space Center, Bay Saint Louis, Miss.

A GRIDDING APPROACH TO DETECT PATTERNS OF CHANGE IN COASTAL WETLANDS FROM DIGITAL DATA

R. E. PELLETIER and D. D. DOW (NASA, National Space Technology Laboratories, Bay Saint Louis, MS) IN: American Society for Photogrammetry and Remote Sensing and ACSM, Fall Convention, Reno, NV, Oct. 4-9, 1987, ASPRS Technical Papers. Falls Church, VA, American Society for Photogrammetry and Remote Sensing, 1987, p. 119-128. refs

The conversion of land to water or water to land in the Grand Bayou wetlands area from 1972 to 1981 is evaluated on the basis of Landsat MSS band 2 and 4 images. A postclassification (land vs water) procedure is employed, and grids 1, 5, 10, 25, and 50 pixels square are superimposed on the classified data in an effort to reduce the effects of poor georegistration of the images (simulated by shifting one set of grids two pixels vertically and horizontally). The results are presented in tables, maps, and sample images and characterized in detail. Grids 5 or 10 pixels square are found to give percentage land/water change values and locations similar to those obtained in pixel-by-pixel analysis of nearly perfectly matched images. T.K.

A88-41950 USING LANDSAT TO DERIVE CURVE NUMBERS FOR HYDROLOGIC MODELS

KENT M. MCGREGOR (North Texas State University, Denton, TX) IN: American Society for Photogrammetry and Remote Sensing and ACSM, Fall Convention, Reno, NV, Oct. 4-9, 1987, ASPRS Technical Papers. Falls Church, VA, American Society for Photogrammetry and Remote Sensing, 1987, p. 129-135. refs

As a watershed becomes more urbanized, floods occur more frequently. Cities are structurally complex, so it is difficult to monitor changes in urban land use/cover which affect streamflow. Computer processing of data from LANDSAT or similar sensors can potentially provide fast and accurate determination of the surface character for input into hydrological models. Experiments conducted on the eight square mile Cottonwood Creek drainage in Dallas, Texas indicated good agreement between predicted runoff using the Soil Conservation TR-20 hydrologic model and actual streamflow measured at gauging stations. Author

A88-41957 TOWARD AN INTEGRATED SYSTEM FOR SATELLITE REMOTE SENSING OF WATER QUALITY IN THE GREAT LAKES

THOMAS M. LILLESAND, RICHARD G. LATHROP, JR., and JOHN R. VANDE CASTLE (Wisconsin, University, Madison) IN: American Society for Photogrammetry and Remote Sensing and ACSM, Fall Convention, Reno, NV, Oct. 4-9, 1987, ASPRS Technical Papers. Falls Church, VA, American Society for Photogrammetry and Remote Sensing, 1987, p. 342-347. Research supported by the University of Wisconsin and William and Flora Hewlett Foundation. (Contract NOAA-NA-84AAD00065)

Water quality in the Great Lakes is a highly dynamic phenomenon that varies widely over both time and space. Monitoring requirements range from those involving small areas and short timeframes, to those involving the entire Great Lakes system and the identification of long-term trends. No single operational satellite system is optimal for meeting all of these requirements. However, data from the SPOT high resolution visible

(HRV) sensors, the Landsat Thematic Mapper (TM), and the NOAA Advanced Very High Resolution Radiometer (AVHRR) can all play a potentially important role in the overall monitoring process. The calibration and integration of the different spatial resolutions, spectral resolutions, and spatial and temporal coverage patterns provide a framework for an operational monitoring system for the Great Lakes. Author

A88-42026 SPRING MOUND AND AIOUN MAPPING FROM LANDSAT TM IMAGERY IN SOUTH-CENTRAL TUNISIA

ARWYN RHYS JONES and ANDREW MILLINGTON (Reading, University, England) IN: Remote sensing for resources development and environmental management; Proceedings of the Seventh International Symposium, Enschede, Netherlands, Aug. 25-29, 1986. Volume 2. Rotterdam, A. A. Balkema, 1986, p. 607-613. refs

Spring mounds and aioun, two rare geomorphological expressions of groundwater upwelling on playas in south-central Tunisia are studied through lineament analysis of Landsat TM imagery. The hydrogeology of the region, the identification of features on satellite imagery, and the digital processing of MSS and TM imagery of playa facies are discussed. Lineament directional trends are identified and analyzed, showing strong underlying hydrogeological controls on spring mounds and aioun related to Alpine folding and associated faulting and jointing. It is concluded that the detection of these features using remotely sensed imagery has many advantages over conventional ground survey. R.B.

A88-42038 A METHODOLOGY FOR INTEGRATING SATELLITE IMAGERY AND FIELD OBSERVATIONS FOR HYDROLOGICAL REGIONALISATION IN ALPINE CATCHMENTS

R. ALLEWIJN (Vrije Universiteit, Amsterdam, Netherlands) IN: Remote sensing for resources development and environmental management; Proceedings of the Seventh International Symposium, Enschede, Netherlands, Aug. 25-29, 1986. Volume 2. Rotterdam, A. A. Balkema, 1986, p. 693-697. refs

A88-42040 SIMPLE CLASSIFIERS OF SATELLITE DATA FOR HYDROLOGIC MODELLING

R. S. DRAYTON (Cardiff, University College, Wales), T. R. E. CHIDLEY, and W. C. COLLINS (Aston, University, Birmingham, England) IN: Remote sensing for resources development and environmental management; Proceedings of the Seventh International Symposium, Enschede, Netherlands, Aug. 25-29, 1986. Volume 2. Rotterdam, A. A. Balkema, 1986, p. 709-711.

Hydrological models are normally based on parameters extracted from conventional maps such as drainage density and land cover. In this paper the use of parameters derived from thematic classifications of satellite imagery is examined. The advantage of this technique is that the satellite image becomes an up-to-date, easily managed source of data for monitoring of water resources. The methods of classification range from simple density slicing to supervised classification. A model was constructed in which run-off characteristics were regressed on thematic classifications. The problem of achieving sufficient variance in the hydrological parameters within one satellite image are discussed, and recommendations for distributed modeling are made. Author

A88-42041 A HYDROLOGICAL COMPARISON OF LANDSAT TM, LANDSAT MSS AND BLACK AND WHITE AERIAL PHOTOGRAPHY

M. J. FRANCE and P. D. HEDGES (Aston, University, Birmingham, England) IN: Remote sensing for resources development and environmental management; Proceedings of the Seventh International Symposium, Enschede, Netherlands, Aug. 25-29, 1986. Volume 2. Rotterdam, A. A. Balkema, 1986, p. 717-720. refs

Landsat TM is evaluated for its accuracy in delineating, mapping

and measuring, water bodies, drainage networks, catchment areas and landcover. A comparison is made with results from Landsat MSS imagery and 1:50000 scale black and white aerial photography, for the same area in North Wales, UK. Landsat TM is found to have significant advantages over Landsat MSS for recording drainage network information. Lakes as small as 0.6 hectares can be identified using Landsat TM imagery and the delineation of small streams aids in accurately defining catchment boundaries.

Author

A88-42042

APPLICATION OF REMOTE SENSING IN HYDROMORPHOLOGY FOR THIRD WORLD DEVELOPMENT - A RESOURCE DEVELOPMENT STUDY IN PARTS OF HARYANA (INDIA)

A. S. JADHAV (Department of Geography, Kolhapur, India) IN: Remote sensing for resources development and environmental management; Proceedings of the Seventh International Symposium, Enschede, Netherlands, Aug. 25-29, 1986. Volume 2. Rotterdam, A. A. Balkema, 1986, p. 721-724.

A88-42043

REMOTE SENSING OF FLOW CHARACTERISTICS OF THE STRAIT OF ORESUND

L. JONSSON (Lund, Universitet, Sweden) IN: Remote sensing for resources development and environmental management; Proceedings of the Seventh International Symposium, Enschede, Netherlands, Aug. 25-29, 1986. Volume 2. Rotterdam, A. A. Balkema, 1986, p. 725-729.

The results of the use of NOAA and Landsat imagery of the strait of Oresund for extracting information on the large-scale flow pattern and for possibly distinguishing certain flow phenomena are examined. The hydrography of the region is discussed, pointing out the need for investigating interferences with coastal waters due to the heavy demand for using the coastal waters for different purposes. Remotely sensed data on large-scale water circulation is used in connection with numerical flow models to increase knowledge of hydrodynamic processes and circulation patterns in coastal waters.

R.B.

A88-42044

THE QUANTIFICATION OF FLOODPLAIN INUNDATION BY THE USE OF LANDSAT AND METRIC CAMERA INFORMATION, BELIZE, CENTRAL AMERICA

S. T. MILLER (Aston, University, Birmingham, England) IN: Remote sensing for resources development and environmental management; Proceedings of the Seventh International Symposium, Enschede, Netherlands, Aug. 25-29, 1986. Volume 2. Rotterdam, A. A. Balkema, 1986, p. 733-738. refs

A88-42045

REMOTE SENSING AS A TOOL FOR ASSESSING ENVIRONMENTAL EFFECTS OF HYDROELECTRIC DEVELOPMENT IN A REMOTE RIVER BASIN

W. MURRAY PATERSON and STEWART K. SEARS (Ontario Hydro, Toronto, Canada) IN: Remote sensing for resources development and environmental management; Proceedings of the Seventh International Symposium, Enschede, Netherlands, Aug. 25-29, 1986. Volume 2. Rotterdam, A. A. Balkema, 1986, p. 739-744. refs

The development of new hydroelectric generation projects in Ontario (Canada) requires environmental studies to be carried out at various stages in the project life cycle. The feasibility of using remotely-sensed Landsat satellite data to assist in these studies is assessed based on a pilot project carried out in a remote northern Ontario river basin. Results suggest that remote sensing technology offers a potentially effective and economical means of collecting, interpreting and presenting environmental information for studies related to broad level river basin planning, conceptual assessments, project scoping, impact assessment, and postdevelopment project follow-up and monitoring.

A88-42046

ENVIRONMENTAL ASSESSMENT FOR LARGE SCALE CIVIL ENGINEERING PROJECTS WITH DATA OF DTM AND REMOTE SENSING

TAICHI OSHIMA, ATSUSHI RIKIMARU (Hosei University, Tokyo, Japan), YUICHI KATO, and MASAHARU NAKAMURA (Pasco Corp., Tokyo, Japan) IN: Remote sensing for resources development and environmental management; Proceedings of the Seventh International Symposium, Enschede, Netherlands, Aug. 25-29, 1986. Volume 2. Rotterdam, A. A. Balkema, 1986, p. 745-748.

A study in which Digital Terrain Model (DTM) and remote sensing data were used to evaluate the danger of landslides at a dam reservoir construction site in the mountain region of Japan is discussed. Conditions such as topography, geology, vegetation and water resources were used in connection with DTM and Landsat MSS data to map grades of weathered granite and landslide danger. The site proposed for development was selected from ground investigation and results of photointerpretation.

R.B.

A88-42048*

Jet Propulsion Lab., California Inst. of Tech., Pasadena.

SATELLITE DATA IN AQUATIC AREA RESEARCH - SOME IDEAS FOR FUTURE STUDIES

JOUKO T. RAITALA (California Institute of Technology, Jet Propulsion Laboratory, Pasadena) IN: Remote sensing for resources development and environmental management; Proceedings of the Seventh International Symposium, Enschede, Netherlands, Aug. 25-29, 1986. Volume 2. Rotterdam, A. A. Balkema, 1986, p. 755-758. refs

Attempts to apply aquatic remote sensing to the preparation of parametric map-like presentations, quantitative evaluations and time-related investigations in various water areas in Finland are presented. The potential use of Landsat MSS data in aquatic area studies, including limnology, aquatic botany, geomorphology and engineering is evaluated using computer-aided digital remote sensing techniques. MSS data may provide information about depth, Secchi disc values, humus content in water, and productivity. Aquatic vegetation classification using MSS is possible only where vegetation units are large enough in respect to the 0.5 hectares ground resolution. Multitemporal satellite imagery has been used to evaluate alterations in the littoral areas of some Finnish water reservoirs between successive periods of high water. It is concluded that although MSS data can be of use in aquatic studies, it should be used in connection with field data and/or TM and SPOT data.

R.B.

A88-42051

CLASSIFICATION OF BOTTOM COMPOSITION AND BATHYMETRY OF SHALLOW WATERS BY PASSIVE REMOTE SENSING

D. SPITZER and R. W. J. DIRKS (Nederlands Instituut voor Onderzoek der Zee, Texel, Netherlands) IN: Remote sensing for resources development and environmental management; Proceedings of the Seventh International Symposium, Enschede, Netherlands, Aug. 25-29, 1986. Volume 2. Rotterdam, A. A. Balkema, 1986, p. 775-777.

The use of remote sensing data in the development of algorithms to remove the influence of the watercolumn on upwelling optical signals when mapping the bottom depth and composition in shallow waters. Calculations relating the reflectance spectra to the parameters of the watercolumn and the diverse bottom types are performed and measurements of the underwater reflection coefficient of sandy, mud, and vegetation-type seabottoms are taken. The two-flow radiative transfer model is used. Reflectances within the spectral bands of the Landsat MSS, the Landsat TM, SPOT HVR, and the TIROS-N series AVHRR were computed in order to develop appropriate algorithms suitable for the bottom depth and type mapping. Bottom depth and features appear to be observable down to 3-20 m depending on the water composition and bottom type.

R.B.

A88-42053

A STUDY WITH NOAA-7 AVHRR-IMAGERY IN MONITORING EPHEMERAL STREAMS IN THE LOWER CATCHMENT AREA OF THE TANA RIVER, KENYA

J. W. VAN DEN BRINK (DHV Consulting Engineers, Amersfoort, Netherlands) IN: Remote sensing for resources development and environmental management; Proceedings of the Seventh International Symposium, Enschede, Netherlands, Aug. 25-29, 1986. Volume 2. Rotterdam, A. A. Balkema, 1986, p. 783-785. refs

A88-43666

STATISTICAL ANALYSIS OF THE NEAR-SURFACE DISTRIBUTIONS OF CHLOROPHYLL AND TEMPERATURE FIELDS ON THE BASIS OF REMOTE IMAGERY FROM CZCS AND AVHRR SCANNERS [STATISTICHESKII ANALIZ PRIPOVERKHNOSTNYKH RASPREDELENII POLEI KHLOROFILLA I TEMPERATURY PO SPUTNIKOVYM IZOBRAZHENIAMI SKANEROV CZCS I AVHRR]

M. M. KAHRU (AN ESSR, Institut Termofiziki i Elektrofiziki, Tallinn, Estonian SSR) Issledovanie Zemli iz Kosmosa (ISSN 0205-9614), Mar.-Apr. 1988, p. 36-43. In Russian. refs

Remote images obtained by CZCS and AVHRR scanners were used to analyze distributions of the near-surface phytoplankton pigment concentration (PPC) and sea-surface temperature (SST) near the California coast. The spectra of spatial variability and rms coherence in the 2-100-km wavelength interval were estimated. It was found that the PPC spectra are more variable than the SST spectra and are less steep. Two patterns of variability were observed for the PPC and SST fields in the California Current, corresponding to the presence or the absence of pronounced transverse currents from the upwelling zone. I.S.

A88-43673

A COMPARATIVE ANALYSIS OF METHODS FOR COMPRESSING SPECTROPHOTOMETRIC DATA IN THE ESTIMATION OF HYDROLOGICAL PARAMETERS [SRAVNITEL'NYI ANALIZ METODOV SZHATIIA SPEKTROFOTOMETRICHESKOI INFORMATSII PRI OTSENKE gidrologicheskikh parametrov]

T. FARAGO (Baja Csillagvizsgalo Intezet, Budapest, Hungary) Issledovanie Zemli iz Kosmosa (ISSN 0205-9614), Mar.-Apr. 1988, p. 90-98. In Russian. refs

Several data-compression algorithms applied to remote spectrophotometry data on inland water bodies are discussed. Special consideration is given to methods for determining high-information-content spectral bands and integral signatures, such as color coordinates and principal-component expansion coefficients. Three feature-selection methods were compared in the analysis of chlorophyll concentration, concentration of suspended matter, and concentrations of suspended organic and mineral components in the Svir' Bay of Ladoga Lake and in adjacent regions of the lake, using spectrophotometric data obtained aboard experimental aircraft. I.S.

A88-44120

DETERMINATIONS OF SUSPENDED SEDIMENT CONCENTRATIONS FROM MULTIPLE DAY LANDSAT AND AVHRR DATA

JOHN G. LYON, KEITH W. BEDFORD, CHIEH-CHENG J. YEN (Ohio State University, Columbus), DEBORAH H. LEE (U.S. Army, Corps of Engineers, Detroit, MI), and DAVID J. MARK (U.S. Army, Corps of Engineers, Vicksburg, MS) Remote Sensing of Environment (ISSN 0034-4257), vol. 25, June 1988, p. 107-115. Research supported by Ohio State University. refs (Contract NOAA-NA-81AAD00095; NOAA-NA-84AAD00079)

A combination of satellite data, on-site sampling, and hydrodynamic and water quality model simulations was used to evaluate surface sediment concentrations in Sandusky Bay, Lake Erie. Both satellite brightness values and categorizations of total suspended sediment concentrations from Landsat and AVHRR data were evaluated for the period of June 10-28, 1981. The satellite data products displayed many of the trends in concentration

recorded by the on-site data, and were similar to the results of hydrodynamic and water quality (HWQ) model simulations reported elsewhere. Author

A88-44311#

MILLIMETER-WAVE MULTIPATH MEASUREMENTS ON SNOW COVER

UVE H. W. LAMMERS, DALLAS T. HAYES, and RICHARD A. MARR (USAF, Rome Air Development Center, Hanscom AFB, MA) IEEE Transactions on Geoscience and Remote Sensing (ISSN 0196-2892), vol. 26, May 1988, p. 259-267. refs

Multipath data were obtained at frequencies of 35.1, 98.1, and 140.1 GHz over a pathlength of 179.5 m by measuring height-gain patterns between 0.2 and 4.0 m with a vertically moving receiving antenna. Grazing angles from this geometry range between 0.5 and 2 deg measured interference patterns between direct and snow-reflected rays were generally coherent in appearance and on occasion exhibited cancellation depths greater than 20 dB. A computer program models the reflection as a coherent process, with the underlying snow surface represented by a series of linear sloping segments derived from actual terrain heights. The reflection coefficient near a 2-deg grazing angle ranged from 0.53 to 0.20 over matted grass, from 0.66 to 0.34 over freshly fallen snow, and from 0.85 to 0.71 over old snow. The higher numbers correspond to 35.1 GHz, the lower numbers correspond to 140.1 GHz. I.E.

A88-44447

COASTAL MONITORING BY REMOTE SENSING

THOMAS VOIGT (Department of Remote Sensing, Berlin, German Democratic Republic) and DIETRICH WEISS (Coastal Water Management, Stralsund; Department of Coastal Research, Rostock-Warnemuende, German Democratic Republic) Jena Review (ISSN 0448-9497), vol. 32, no. 4, 1987, p. 164-167. refs

The use of remote sensing for coastal monitoring in the interest of environmental protection and water management is discussed. An example of monitoring the coast of the Fischland peninsula in the GDR is presented. Properties of radiation behaviour in coastal water which influence the suitability of a remote sensing method are examined, including the spectral distribution of light extinction in the water, the directionality of reflectance of the water body, and the spectral distribution of the light reflected by the sea floor. Flight planning and photography and the quantitative restitution for bathymetry and depth mapping are also discussed. R.B.

A88-45115

THE 'TSUKUSYS' IMAGE PROCESSING SYSTEM AND ITS UTILIZATION IN THEMATIC MAPPER INVESTIGATIONS OF WATER QUALITY CONDITIONS

TAKASHI HOSHI (Tsukuba, University, Japan), KIYOSHI TORII (Kyoto University, Japan), and TOMOYUKI ISHIDA (Iwate University, Japan) Geocarto International (ISSN 1010-6049), vol. 3, June 1988, p. 27-36. refs

The 'Tsukusys' image processing system has been developed to analyze remote sensing data, particularly Landsat Multispectral Scanner (MSS) imagery. As Thematic Mapper (TM) data have only been available in Japan since 1985, that imagery was acquired to test the extension of 'Tsukusys' to improved spatial and spectral resolution data. The TM data were used to analyze water quality condition in and around the Kojima Bay, Japan where water pollution is an extremely important issue. The results of this endeavor indicate that the 'Tsukusys' image processing system can be utilized successfully for the analysis of TM data with some minor modifications to software processing. Author

A88-45116

ON THE REGIONAL CHARACTERISTICS OF ACTUAL EVAPOTRANSPIRATION DERIVED FROM LANDSAT MSS AND ELEVATION DATA

SATOSHI UCHIDA and TAKASHI HOSHI (Tsukuba, University, Ibaraki, Japan) Geocarto International (ISSN 1010-6049), vol. 3, June 1988, p. 57-66. refs

The system to estimate actual evapotranspiration (ET) over

wide area has been developed. The method of estimation is based on modified Penman's method and utilized Landsat MSS, elevation and ground observed meteorological data. The distinctive feature of this system is that it estimates ET not by directly using spectral data but by combining empirical parameters. Therefore once landuse data are produced from Landsat MSS data, various climatic condition can be applied to calculation. To examine the regional characteristics of ET, several watershed areas are selected in Japan. Then both local characteristics of landuse and topography and regional characteristics of climate are found to be equally influencing the amount of ET. Moreover, the calculation in the case of occurring landuse conversion according to land grading is executed. Its result has given the possibility to parameterize the amount of ET using a few parameters, that is the regional averaged value of albedo and/or soil heat flux constant. Author

A88-45636
LINEAMENTS: SIGNIFICANCE, CRITERIA FOR DETERMINATION, AND VARIED EFFECTS ON GROUND-WATER SYSTEMS - A CASE HISTORY IN THE USE OF REMOTE SENSING

KATHY D. PETER (USGS, Albuquerque, NM), KENNETH E. KOLM (Colorado School of Mines, Golden), JOE S. DOWNEY, and THOMAS C. NICHOLS, JR. (USGS, Denver, CO) IN: Geotechnical applications of remote sensing and remote data transmission; Proceedings of the Symposium, Cocoa Beach, FL, Jan. 31-Feb. 1, 1986. Philadelphia, PA, American Society for Testing and Materials, 1988, p. 46-68. refs

A88-45637
ESTIMATION OF RESERVOIR SUBMERGING LOSSES USING CIR AERIAL PHOTOGRAPHS - EXAMPLE OF THE ERTAN HYDROPOWER STATION ON THE YALONG RIVER IN SOUTHWEST CHINA

HUI LIN (Chinese Academy of Sciences, Institute of Geography, Beijing, People's Republic of China) IN: Geotechnical applications of remote sensing and remote data transmission; Proceedings of the Symposium, Cocoa Beach, FL, Jan. 31-Feb. 1, 1986. Philadelphia, PA, American Society for Testing and Materials, 1988, p. 89-98.

A88-45643
OVERVIEW OF REMOTE DATA TRANSMISSION SYSTEMS
 RICHARD W. PAULSON (USGS, Reston, VA) IN: Geotechnical applications of remote sensing and remote data transmission; Proceedings of the Symposium, Cocoa Beach, FL, Jan. 31-Feb. 1, 1986. Philadelphia, PA, American Society for Testing and Materials, 1988, p. 203-212.

Remote data transmission systems for monitoring the environment are reviewed, including the Argos system, geostationary meteorological satellite systems, and the meteorburst technique which relies on micrometeor trails in the atmosphere to reflect radio messages between a hydrologic station and an interrogation site. The snow telemetry hydrologic data collection system, Landsat series of satellites, synchronous meteorological and geostationary operational environmental satellites are discussed. Specific elements of these systems are examined and major operators and users of the systems are identified. R.B.

N88-21561 Centre National d'Etudes des Telecommunications, Issy-les-Moulineaux (France).
MEASUREMENT OF THE WATER CONTENT OF SOIL FROM SPACE AND APPLICATION TO THE REGIONAL WATER BALANCE [MESURES DU CONTENU EN EAU DES SOLS DEPUIS L'ESPACE ET APPLICATION AU BILAN HYDRIQUE REGIONAL]

DANIEL VIDAL-MADJAR In CNES, Climatology and Space Observations p 609-628 Sep. 1987 In FRENCH; ENGLISH summary
 Avail: CEPADUES-Editions, 111 rue Nicolas-Vauquelin, 31100 Toulouse, France

Work done to measure the regional soil water budget is described. The parameters which are measurable are identified

and it is possible to define strategies for applications to climatology. It is shown that measurement from space of soil moisture is possible either by infrared thermal radiation measurement or by radar measurements. Advantages of each method are discussed. ESA

N88-22455# Instituto de Pesquisas Espaciais, Sao Jose dos Campos (Brazil).

PROJECT CODEAMA/FUNCATE (TEST-AREA OF BARREIRINHA-AM): FIELD REPORT

TOMOYUKI OHARA, PAULO ROBERTO MARTINI, SERGIO DOSANJOSFERREIRAPINTO, and NELIO NOGUEIRADONAS-CIMENTO Mar. 1988 55 p In PORTUGUESE; ENGLISH summary
 (INPE-4500-RPE/563) Avail: NTIS HC A04/MF A01

The places studied during the multidisciplinary survey realized in the test-area of Barreirinha - Amazon State (CODEAMA Project), with the purpose of testing the use of MSS/LANDSAT images and checking the accuracy of the information obtained and incorporated in geomorphological and hydric system (inundation areas) maps, in the scale of 1:100,000 are described. The multidisciplinary survey was carried out from January 30 to February 14, 1985, investigating nearly 360 kilometers of fluvial and/or terrestrial survey, from which 64 places were described. The Appendix presents the map of localization of the places studied, in the scale of 1:250,000, which holds all the studied places.

Author

N88-22466# Dornier-Werke G.m.b.H., Friedrichshafen (West Germany).

FEASIBILITY STUDY FOR A 2ND GENERATION SYSTEM FOR AIRBORNE MARITIME POLLUTION SURVEILLANCE Final Report, 12 Dec. 1987

JOERG KOEPP and JOSEF SCHOBBER Bonn, Federal Republic of Germany BMFT 30 Apr. 1987 739 p Party in ENGLISH and GERMAN Sponsored by BMFT
 (ETN-88-92108) Avail: NTIS HC A99/MF E03

The feasibility of a sensor system for maritime pollution monitoring was established. Operational requirements for a sensor system, the technical description of possible mission equipment, and proposals for an optimal sensor-package are presented. Planning data for development and costs are given. ESA

N88-23303# Begeleidingscommissie Remote Sensing, Delft (Netherlands).

TURBIDITY PATTERNS IN THE DELTA WATERS OF SOUTHWEST NETHERLANDS ON THEMATIC MAPPER (TM) AND MULTISPECTRAL SCANNER (MSS) SATELLITE IMAGES [TROEBELHEIDSPATRONEN IN DE DELTAWATEREN VAN ZW NEDERLAND OP TM EN MSS SATELLIETBEELDEN]

J. STRONKHORST 1986 26 p In DUTCH
 (BCRS-86-06; GWWS-405; ETN-88-91553) Avail: NTIS HC A03/MF A01

Operational water quality measuring using LANDSAT Thematic Mapper (TM) and Multispectral Scanner (MS) is discussed. Image processing using the Remote Sensing Data processing system RESEDA is presented. The turbidity pattern in the Fore-delta, the Eastern Scheldt and the Western Scheldt (Netherlands) are discussed. The results show the limitations of LANDSAT that was designed for remote sensing of land, for water quality control in the delta waters with respect to spectral, radiometric, as well as spatial resolution. For the time being LANDSAT TM and MSS cannot be used for an operational water quality measuring system. ESA

N88-23359# National Marine Fisheries Service, Monterey, Calif. Fisheries Environmental Group.

HYDROGRAPHIC OBSERVATIONS IN THE NORTHWESTERN WEDDELL SEA MARGINAL ICE ZONE DURING MARCH 1986

D. M. HUSBY and R. D. MUENCH Jan. 1988 39 p Prepared in cooperation with Science Applications International Corp., Bellevue, Wash.
 (PB88-173240; NOAA-TM-NMFS-SWFC-106) Avail: NTIS HC A03/MF A01 CSCL 08C

06 HYDROLOGY AND WATER MANAGEMENT

Temperature and salinity observations were made from the surface down to 1500 m, in the central northwestern Weddell Sea, during March 1986. These observations sampled the three water masses characterizing the region. The uppermost, Surface Water, layer extended down to 30-50 m, had temperature from near freezing (-1.8 C) up to about 0 C and salinities of 33-34 ppt. A layer of Weddell Winter Water underlay the Surface Water, extending down to about 100 m, and had temperatures of -1.5 to -1.7 C and a salinity of about 34.46 ppt. The Weddell Warm Deep Water extended from the bottom of the Winter Water down to more than 1500 m, displaying temperature increasing with depth to a maximum of about 0.5 C near 500 m then decreasing down to 1500 m. The temperature maximum region within the Warm Deep Water decreased in depth eastward, toward the center of the gyre, within the core. The baroclinic circulation, expressed as dynamic topography of the surface relative to the 1500 db level, was insignificant throughout the region. GRA

N88-24032# Silsoe Coll., Bedford (England).
**SATELLITE REMOTE SENSING OF TURBIDITY AND
SEDIMENT CONCENTRATION IN LAGOA DOS PATOS**

Abstract Only

JOHN TAYLOR, VIPUL PATEL, ALAN BELWARD, LAWSON BELTRAME, and MARLEY GONCALVES (Rio Grande do Sul Univ., Porto Alegre, Brazil) *In* INPE, Latin American Symposium on Remote Sensing. 4th Brazilian Remote Sensing Symposium and 6th SELPER Plenary Meeting, Volume 1 p 279 1986
Avail: NTIS HC A99/MF E03

The use of LANDSAT Multispectral Scanner (MSS) digital imagery for mapping water turbidity and suspended sediment in Lagoa dos Patos, Rio Grande do Sul was investigated. Field measurements were taken from vessels in a test area, Saco De Tapes when there was a satellite overpass. Sample site locations were determined from shore-based fixes on the boats at the time of each reading. The satellite image was geometrically corrected and the sampling sites were located on it. Regression models were developed between LANDSAT digital data and field measurements. The results indicated that turbidity was linearly related to the spectral responses in MSS bands 1 and 2. The best relationship for the available data was with band 2. Suspended sediment concentration and turbidity were also linearly related using data from additional sampling data. Land and water features on the image were separated by masking. Band 2 of the satellite image of water surfaces was digitally smoothed to remove noise and then interactively density sliced. The regression equations were applied to determine the turbidity and suspended sediment levels for each slice. The results encourage the belief that satellite images can be used to quantitatively map the spatial distribution of turbidity and suspended sediment in Lagoa dos Patos. It was possible to identify as sources of clear or turbid water all of the streams flowing into the test area. Author

N88-24033# Indian Association for the Cultivation of Science, Calcutta.

**LANDUSE AND LANDFORM STUDIES OF THE MAHANADI
RIVER DELTA WITH THE HELP OF SATELLITE MSS BAND**

Abstract Only

RANJIT KUMAR BANERJEE *In* INPE, Latin American Symposium on Remote Sensing. 4th Brazilian Remote Sensing Symposium and 6th SELPER Plenary Meeting, Volume 1 p 291 1986
Avail: NTIS HC A99/MF E03

The present study is confined to the lower course of the Mahanadi River after the Satkosia Gorge. The Mahanadi River is one of the major rivers of the northern peninsular India which drains into the Bay of Bengal. Four major landforms are identified: residual hill termed highlands; intermediate lands; lowlands; and flood plains. The area is under the influence of deltaic environment and coastal vegetation is confined to the swampy areas with a big lake nearby known as Chilka Lake. Transport facility is meager in comparison with the industrial region near Cuttack and Bhubaneswar. Author

N88-24076# Instituto de Pesquisas Espaciais, Sao Jose dos Campos (Brazil).

**STUDY OF RESERVOIR WATER QUALITY UTILIZING
REMOTE SENSING TECHNIQUES: METHODOLOGICAL
CONCEPTS [ESTUDO DE QUALIDADE DA GUA DE
RESERVATORIOS, UTILIZANDO TECNICAS DE
SENSORIAMENTO REMOTO: CONCEITOS METODOLOGICOS]**
TANIA MARIA SAUSEN and MARISA DANTASBITEN-COURTPEREIRA (Sao Paulo Univ., Brazil) *In* its Latin American Symposium on Remote Sensing. 4th Brazilian Remote Sensing Symposium and 6th SELPER Plenary Meeting, Volume 1 p 638-644 1986 *In* PORTUGUESE; ENGLISH summary
Avail: NTIS HC A99/MF E03

The objective is to inform the public and the scientific community about the importance of an efficient methodology for monitoring artificially accumulated water and the uselessness of the remote sensing techniques as a practical and economic alternative to minimize the field trip work wherever water quality parameters are to be investigated. In order to achieve these aims, a bibliographic study of this subject was done through the main papers for the last two decades. Methodological topics are shown taking into account the spectral response of water (with and without sediments) and techniques to analyze remote sensing data. Author

N88-24077# THEMAG Engenharia Ltda., Sao Paulo (Brazil).
**UTILIZATION OF LANDSAT-TM IMAGERY IN THE
HYDROENERGETIC INVENTORY OF THE PARAIBA DE SUL
RIVER BASIN [UTILIZACAO DE IMAGENS LANDSAT TM NO
INVENTARIO HIDROENERGETICO DA BASIA DO RIO
PARAIBA DO SUL]**

AUGUSTO PAIVA FILHO, CARLOS BIANCO, and TANIA MARIA SAUSEN (Instituto de Pesquisas Espaciais, Sao Jose dos Campos, Brazil) *In* INPE, Latin American Symposium on Remote Sensing. 4th Brazilian Remote Sensing Symposium and 6th SELPER Plenary Meeting, Volume 1 p 645-653 1986 *In* PORTUGUESE; ENGLISH summary
Avail: NTIS HC A99/MF E03

The THEMAG Engenharia Ltda developed a power study in an inventory level in the Paraiba Basin, Sub-basin 2. The aim of this study was to establish in the Paraiba do Sul River and its afluentes (mainly the Sao Manoel, Sopoto, and Novo Rivers) alternatives for power plant schemes in a suitable profile. The TM digital products of the land use studies performed over the planned reservoirs and the surrounding areas were used. The CCT TM Quadrant Digital Products with the desired spectral band selected for this purpose were useful in identifying and surveying land use categories: urban areas, agricultural areas, forest areas, grazing areas, and drainage. Author

N88-24078# Instituto de Pesquisas Espaciais, Sao Jose dos Campos (Brazil).

**EVALUATION OF THE FLOODABLE AREA OF THE CANAL OF
SAO GONCALO THROUGH TM-LANDSAT 5 IMAGERY
[AVALIACAO DA AREA DE INUNDACAO DO CANAL DE SAO
GONCALO ATRAVES IMAGENS TM-LANDSAT 5]**

C. HARTMANN, R. A. C. LAMPARELLI, R. ROSA, and E. E. SANO *In* its Latin American Symposium on Remote Sensing. 4th Brazilian Remote Sensing Symposium and 6th SELPER Plenary Meeting, Volume 1 p 654-659 1986 *In* PORTUGUESE; ENGLISH summary Prepared in cooperation with Fundacao Univ. do Rio Grande (Brazil).
Avail: NTIS HC A99/MF E03

Two LANDSAT TM images were digitally processed on the I-100 Image Analyzer of INPE Sao Jose dos Campos, Sao Paulo). The floodable area of the canal de Sao Goncalo was studied. One image associated with exceptional high inundation (June 11, 1984) and one image associated with normal water level (December 4, 1984) were compared. The digital classification (1:50,000 scale) led to a map (1:100,000 scale) showing the limits of the flooding. This work demonstrated the usefulness of remote sensing techniques to demilitate and identify floodable areas. Author

N88-25018# Army Cold Regions Research and Engineering Lab., Hanover, N.H.

ICE CONDITIONS ALONG THE OHIO RIVER AS OBSERVED ON LANDSAT IMAGES, 1972-1985

LAWRENCE W. GATTO Jan. 1988 168 p (AD-A191172; CRREL-SR-88-1) Avail: NTIS HC A08/MF A01 CSCL 08L

Landsat images were used to map ice distributions along the Ohio River. Ice conditions were inferred based on image grey tones interpreted using conventional photointerpretation techniques. Portions of the river that appeared black were considered ice-free. Grey tones were interpreted as ice that varied from patches of thin, snow-free solid or fragmented ice, sometimes with open areas, to floes, pans and slush. A white tone represented thick ice or snow-covered ice with few interspersed open areas. Ice that produced grey tones on the images occurred most frequently. Ice typically forms in late December or early January on the Ohio River and is gone by mid to late February. Ice was observed on the upstream section of the river from Pittsburgh to Greenup Dam during 7 of the 13 winters from 1972 to 1985, on the middle section from Greenup Dam to Cannelton Dam during 3 winters, and on the downstream section from Cannelton Dam to the Mississippi River during 4 winters. The most severe and long-lasting ice conditions occurred during the 1976-77 winter when ice covered 65 percent of the upstream section, 56 percent of the middle section, and 78 percent of the downstream section.

GRA

07

DATA PROCESSING AND DISTRIBUTION SYSTEMS

Includes film processing, computer technology, satellite and aircraft hardware, and imagery.

A88-32932#
COLOR SPACE MAPPING USING TERNARY/CHROMATICITY DIAGRAMS - A TECHNIQUE FOR COMPOSITE IMAGE INTERPRETATION

VINCENT J. REALMUTO (Arizona, University, Tucson) and THOMAS A. KING IN: Thematic Conference on Remote Sensing for Exploration Geology, 5th, Reno, NV, Sept. 29-Oct. 2, 1986, Proceedings. Volume 2. Ann Arbor, MI, Environmental Research Institute of Michigan, 1987, p. 491-500. Research supported by the University of Arizona.

A method has been developed to map spectral signatures of lithologic units into color space for rapid composite image interpretation. The method requires use of in situ spectral reflectance data, ratios, normalized ratio values, ternary diagrams and chromaticity diagrams. The analyst can design an analysis program to optimize spectral separability of materials by plotting normalized ratio values in the feature space of a ternary diagram. Then, through a color space mapping process, involving the transformation of a ternary diagram into a chromaticity diagram, one can determine the color of each lithologic field sample as it will appear in a color composite image. The project consisted of combining multispectral data sets for detection of hydrothermal alteration zones in the Silver Bell mining district. Five three-ratio combinations were analyzed, and the best combination correlated to the ternary diagram that showed the best data spread in the feature space. Also, color designations for lithologies, as plotted in the color space of a chromaticity diagram, matched the colors for each unit in the composite image. Author

A88-32933#
RESTORATION TECHNIQUES FOR SIR-B DIGITAL RADAR IMAGES

PAT S. CHAVEZ, JR. (USGS, Flagstaff, AZ) and GRAYDON L.

BERLIN (Northern Arizona University, Flagstaff, AZ; King Abdulaziz University, Riyadh, Saudi Arabia) IN: Thematic Conference on Remote Sensing for Exploration Geology, 5th, Reno, NV, Sept. 29-Oct. 2, 1986, Proceedings. Volume 2. Ann Arbor, MI, Environmental Research Institute of Michigan, 1987, p. 501-511. refs

The performance of special algorithms designed to suppress SIR-B radiometric and speckle noise is evaluated. The following geological environments in Saudi Arabia served as test areas: (1) the Tihamat coastal plain and Hijaz mountainous zone bordering the Red Sea, and (2) the sedimentary terrane of the Arabian shelf near the oasis city of Buraydah. A special algorithm incorporating nine across-track multiplicative coefficients proved capable of suppressing the radiometric noise component in images representing different geologic terrains and SIR-B system parameters. In an attempt to reduce speckle contrast, five different spatial-filter operations were implemented on the radiometrically corrected images; the best results were obtained with 3- by 3-pixel median and 2- by 2-pixel mean filter operations. K.K.

A88-32943#
QUANTITATIVE PROCEDURE FOR PRODUCING COLOR-CALIBRATED THEMATIC MAPPER NATURAL-COLOR IMAGES

GRAYDON L. BERLIN (Northern Arizona University, Flagstaff, AZ) and PAT S. CHAVEZ, JR. (USGS, Flagstaff, AZ) IN: Thematic Conference on Remote Sensing for Exploration Geology, 5th, Reno, NV, Sept. 29-Oct. 2, 1986, Proceedings. Volume 2. Ann Arbor, MI, Environmental Research Institute of Michigan, 1987, p. 639-648.

A two-staged quantitative correction procedure for Thematic Mapper bands 1-3 effectively suppresses atmospheric haze and increases scene brightness or contrast while maintaining band-to-band color balance. The procedure computes MIN/MAX contrast-stretch parameters, with gain, offset, and atmospheric-scattering normalization, for each of the three bands. To date, Thematic Mapper natural-color images have been produced of three different geologic environments (Arizona, California, and Saudi Arabia) wherein the image colors closely match those of the terrain. Author

A88-33377
THE PRODUCTION OF DISTORTION FREE SAR IMAGERY

J. W. WOOD (Royal Signals and Radar Establishment, Malvern, England) IN: Radar - 87; Proceedings of the International Conference, London, England, Oct. 19-21, 1987. London and New York, Institution of Electrical Engineers, 1987, p. 471-473.

A method of removing geometric errors in SAR imagery has been developed and is shown to remove distortions to the theoretical limit. The procedure enables azimuth distortion-free SAR imagery to be produced routinely and automatically. The restrictions on the SAR system for the method to be applied are that all motion errors should be restricted to the across-track direction. The measurement accuracy requirements for this motion are described, showing that autofocus measurements satisfy them. The update time between autofocus measurements and the maximum length of flight that can be processed for given aircraft dynamics are derived. C.D.

A88-33774
THE USE OF MULTISPECTRAL SPACE PHOTOGRAPHS TO DRAW UP A MAP OF LAND USE IN WESTERN SLOVAKIA

J. FERANEC, J. OTAHEL (Slovenska Akademia Vied, Geograficky Ustav, Bratislava, Czechoslovakia), M. HAJEK (Slovenska Vysoka Skola Technicka, Bratislava, Czechoslovakia), S. SLOBODA (Geodesy and Cartography Research Institute, Bratislava, Czechoslovakia), and J. SAFAR (Slovenska Kartografia, Bratislava, Czechoslovakia) Photogrammetria (ISSN 0031-8663), vol. 42, March 1988, p. 157-162. refs

07 DATA PROCESSING AND DISTRIBUTION SYSTEMS

A88-36171

NEW ASPECTS OF THE INTERPRETATION OF SPACE RADAR IMAGES [O NOVYKH ASPEKTAKH INTERPRETATSII RADIOLOKATSIONNYKH KOSMICHESKIKH IZOBRAZHENIИ]

T. KH. GEOKHLANIAN and G. V. BUGAEVA (Gosudarstvennyi Nauchno-Issledovatel'skii Tsentr Izucheniia Prirodnykh Resursov, Moscow, USSR) Issledovanie Zemli iz Kosmosa (ISSN 0205-9614), Jan.-Feb. 1988, p. 104-110. In Russian.

High-level radar echoes were measured over land regions with a dense network of synoptic and aerological stations as well as over inland bodies of water. Particular emphasis is placed on Cosmos-1500 sidelooking-radar data. It is shown that such high-level radar signals are observed in regions of high atmospheric activity throughout the troposphere and lower stratosphere. B.J.

A88-37123

FACTORS AFFECTING FEATURE DIFFERENTIATION - THE IMPACT AND SOURCE OF VARIANCE IN THE UPWELLING RADIANCE FIELD

M. J. DUGGIN (New York, State University, Syracuse) IN: Remote sensing applications in meteorology and climatology; Proceedings of the NATO Advanced Study Institute, Dundee, Scotland, Aug. 17-Sept. 6, 1986. Dordrecht, D. Reidel Publishing Co., 1987, p. 19-31. refs

Problems in discriminating ground features or cloud formations in satellite remote-sensing images are examined in an analytical review, with a focus on the principal IR bands at 0.4-2.0, 3.5-4.2, and 8-12 microns. The sources of systematic and random error are listed in extensive flow charts, and their effects on discrimination are quantified in empirical formulas. Techniques for reducing and comparing multichannel image data obtained with different sensors on different dates are briefly considered. T.K.

A88-37131

DATA RECEPTION, ARCHIVING AND DISTRIBUTION

P. E. BAYLIS (Dundee, University, Scotland) IN: Remote sensing applications in meteorology and climatology; Proceedings of the NATO Advanced Study Institute, Dundee, Scotland, Aug. 17-Sept. 6, 1986. Dordrecht, D. Reidel Publishing Co., 1987, p. 69-86.

Technological aspects of the transmission, reception, and storage of satellite remote-sensing data are summarized in a series of diagrams and briefly reviewed, with an emphasis on the NOAA AVHRR system. Particular attention is given to the instrument parameters influencing the data rate, data encoding and modulation, antenna characteristics and performance, the optimization of the (receiver gain)/(system noise temperature) ratio, receiver antenna mounting, tracking control, the principal receiver components, magnetic-tape storage systems, error-detection techniques, and optical disk storage. T.K.

A88-37147

SURFACE ENERGY BUDGET, SURFACE TEMPERATURE AND THERMAL INERTIA

H. MANNSTEIN (DFVLR, Institut fuer Physik der Atmosphaere, Wessling, Federal Republic of Germany) IN: Remote sensing applications in meteorology and climatology; Proceedings of the NATO Advanced Study Institute, Dundee, Scotland, Aug. 17-Sept. 6, 1986. Dordrecht, D. Reidel Publishing Co., 1987, p. 391-410. refs

A technique for thermal-inertia (TI) mapping of land surfaces on the basis of satellite remote-sensing data is described and demonstrated. The derivation of the method from surface energy budgets and an atmospheric radiative-transfer model is explained in detail; the empirical data used in constructing practical models are characterized; the mapping of apparent TI on dry surfaces, heat capacity, and soil moisture is discussed; and sample results from studies of alpine thermally induced circulation are presented graphically. It was found that direct atmospheric warming by sensible heat flux on a cloudless late-summer day was due mainly to the sun-exposed slopes at elevation 2000-3000 m. T.K.

A88-37287#

IMAGE PROCESSING FOR EARTH REMOTE SENSING

RUDOLPH FIEDLER Dornier-Post (English Edition) (ISSN

0012-5563), no. 1, 1988, p. 19-23.

An account is given of the specialized and complex signal processing procedures required by imaging radars in such earth sensing applications as the ERS-1 satellite. The ERS-1 SAR is capable of a 30-m geometrical resolution, comparable to those of Landsat and SPOT and fruitfully applicable to oceanography, snow hydrology, and glacial geology. Attention is presently given to the DIPIDOS modular interactive image processing system, which has been designed in order to furnish both monospectral and multispectral data formats with high radiometric resolution, and geometrical resolution and/or image sizes from one image point to several thousand lines and columns. The software used allows interactive display handling as well as image filtering and scenery analysis. O.C.

A88-37417

INTERANNUAL LANDSAT-MSS REFLECTANCE VARIATION IN AN URBANIZED TEMPERATE ZONE

ALAIN ROYER, LISE CHARBONNEAU (Sherbrooke, Universite, Canada), and PHILIPPE M. TEILLET (Canada Centre for Remote Sensing, Ottawa, Canada) Remote Sensing of Environment (ISSN 0034-4257), vol. 24, April 1988, p. 423-446. Research supported by the Ministere de l'Education du Quebec. refs (Contract NSERC-A-8643; NSERC-A-5252)

Short-term and long-term variations in land-surface parameters are studied based on a chronological time series of 40 Landsat-MSS images over southeastern Canada for the 1972-1984 period. The data were processed for radiometric correction and atmospheric correction, and background contamination effects were taken into account. The results indicate that for the Montreal area the yearly mean albedo showed a decreasing trend of -0.05 since 1972 due to urbanization, deforestation, and decreasing farmland. The year-to-year normalized vegetation index fluctuations are found to correlate with the cumulative amount of summer precipitation, which in turn is related to the mean summer evapotranspiration and global solar radiation. R.R.

A88-37421

THE SEMIVARIOGRAM IN REMOTE SENSING - AN INTRODUCTION

PAUL J. CURRAN (Sheffield, University, England) Remote Sensing of Environment (ISSN 0034-4257), vol. 24, April 1988, p. 493-507. refs

(Contract NERC-GR/3/5096)

The earth's surface and remotely sensed imagery contain spatial information that, if quantified, could be used to optimize many sampling procedures in remote sensing. Until recently a suitable and simple technique for the spatial characterization of surfaces was not readily available. Now, thanks to the development of regionalized variable theory there is a near-ideal tool, the semivariogram. The semivariogram is a function that relates semivariance to sampling lag. This function can be estimated using remotely sensed data or ground data and represented as a plot that gives a picture of the spatial dependence of each point on its neighbor. This paper provides an introduction to the semivariogram and indicates how it could be employed in remote sensing research. Author

A88-39095

TRANSFORMATION OF GLOBAL VEGETATION INDEX (GVI) DATA FROM THE POLAR STEREOGRAPHIC PROJECTION TO AN EQUATORIAL CYLINDRICAL PROJECTION

J. R. HARDY, S. M. SINGH, and A. S. NARRACOTT (Reading, University, England) International Journal of Remote Sensing (ISSN 0143-1161), vol. 9, March 1988, p. 583-589. refs (Contract NERC-F60/G6/12)

A88-39097

USING SPATIAL AUTOCORRELATION ANALYSIS TO EXPLORE THE ERRORS IN MAPS GENERATED FROM REMOTELY SENSED DATA

RUSSELL G. CONGALTON (California, University, Berkeley) Photogrammetric Engineering and Remote Sensing (ISSN 0099-1112), vol. 54, May 1988, p. 587-592. Research supported by the Nationwide Forestry Applications Program and McIntire-Stennis Project. refs

Three data sets of varying spatial complexity, including an agricultural area, a range area, and a forest area, were chosen for investigation in this study. A difference image was generated for each data set by comparing a Landsat classification with an assumed correct reference classification and noting the agreement and disagreement. Visual inspection and spatial autocorrelation analysis were used to identify and quantify the patterns of error within each difference image. This information is very important when land cover maps generated from remotely sensed data are sampled for accuracy assessment. Author

A88-39098

A COMPARISON OF SAMPLING SCHEMES USED IN GENERATING ERROR MATRICES FOR ASSESSING THE ACCURACY OF MAPS GENERATED FROM REMOTELY SENSED DATA

RUSSELL G. CONGALTON (California, University, Berkeley) Photogrammetric Engineering and Remote Sensing (ISSN 0099-1112), vol. 54, May 1988, p. 593-600. Research supported by the Nationwide Forestry Applications Program and McIntire-Stennis Project. refs

A88-39099

DIFFERENTIATION OF ECOLOGICAL ZONES IN THE OKAVANGO DELTA, BOTSWANA BY CLASSIFICATION AND CONTEXTUAL ANALYSES OF LANDSAT MSS DATA

SUSAN RINGROSE (University of Botswana, Gaborone), WILMA MATHESON (Gaborone Secondary School, Botswana), and TIMOTHY BOYLE (Satellite Remote Sensing Centre, Johannesburg, Republic of South Africa) Photogrammetric Engineering and Remote Sensing (ISSN 0099-1112), vol. 54, May 1988, p. 601-608. Research supported by the Ministry of Mineral Resources and Water Affairs of Botswana. refs

A88-41298

ALTERNATIVES FOR MAPPING FROM SATELLITE IMAGERY

G. KONECNY (Hannover, Universitaet, Hanover, Federal Republic of Germany) (IAF, International Astronautical Congress, 37th, Innsbruck, Austria, Oct. 4-11, 1986) Acta Astronautica (ISSN 0094-5765), vol. 17, March 1988, p. 355-358. (IAF PAPER 86-76)

The paper discusses the alternatives for mapping the earth surface using remote-sensing satellite imagery by Landsat- MSS and-TM and by sensors of cartographic satellites, such as the European Spacelab-1' and SPOT sensors. The quality of these images are compared with images obtained by the MKF-6 camera system aboard Soyuz-Salyut missions and by the KATE 140,200 and the KFT 1000. Special attention is given to the question of cost of satellite imagery, with comparisons presented for the price per image and per million pixel for various sensors. I.S.

A88-41944

A COMPARISON BETWEEN CLASSIFICATION DIFFERENCING AND IMAGE DIFFERENCING FOR LAND COVER TYPE CHANGE DETECTION

KUO-MU CHIAO, YEONG-KUAN CHEN, and CHAO-FU CHOW (National Taiwan University, Taipei, Republic of China) IN: American Society for Photogrammetry and Remote Sensing and ACSM, Fall Convention, Reno, NV, Oct. 4-9, 1987, ASPRS Technical Papers. Falls Church, VA, American Society for Photogrammetry and Remote Sensing, 1987, p. 1-12. Research supported by the Council of Agriculture of the Republic of China.

The effectiveness of two differencing methods in identifying changes in land use (from agricultural or forest to urban) is investigated in trial analyses of a region near Taipei, Taiwan. The techniques evaluated are described in detail, and the results are presented in extensive tables. An image-differencing scheme, in which the Landsat MSS band 5 values for each pixel of an image

are subtracted from those obtained on a different date and the pixels with nonzero differences are marked as areas of land-use change, is found to be more accurate than a classification-differencing scheme, in which independent classifications (to five ground-cover types) for each date are compared. T.K.

A88-41958

ENHANCEMENT OF SPOT IMAGE RESOLUTION USING AN INTENSITY-HUE-SATURATION TRANSFORMATION

W. JOSEPH CARPER, RALPH W. KIEFER, and THOMAS M. LILLESAND (Wisconsin, University, Madison) IN: American Society for Photogrammetry and Remote Sensing and ACSM, Fall Convention, Reno, NV, Oct. 4-9, 1987, ASPRS Technical Papers. Falls Church, VA, American Society for Photogrammetry and Remote Sensing, 1987, p. 348-361. refs

Techniques for merging SPOT 10 m resolution panchromatic and 20 m resolution multispectral data for enhanced image interpretability have recently been developed. The effectively 10 m resolution multispectral images produced using these procedures contain the high resolution information of the panchromatic image while maintaining the basic color content of the multispectral data. A method for merging the two data sets, which utilizes an intensity, hue and saturation transformation, is described. The effects of this merger on the spectral characteristics of the data are analyzed, along with those of two other techniques. Author

A88-41962

STRUCTURAL INFORMATION OF THE LANDSCAPE AS GROUND TRUTH FOR THE INTERPRETATION OF SATELLITE IMAGERY

M. ANTROP (Gent, Rijksuniversiteit, Ghent, Belgium) IN: Remote sensing for resources development and environmental management; Proceedings of the Seventh International Symposium, Enschede, Netherlands, Aug. 25-29, 1986. Volume 1. Rotterdam, A. A. Balkema, 1986, p. 3-8. refs

The possibilities for a detailed and accurate land use interpretation using satellite imagery, depend for a great part upon the landscape structure. The selection of the training sites for image classification should follow a stratified scheme based upon a landscape classification which uses structural indicators. An analysis is made of the landscapes of Flanders based upon such indicators. An estimation of the occurrence of pure pixels (TM size) for different landscape components and types is given, as well as the compactness of the field shapes and their orientation in relation to the pixel size and scan direction. Author

A88-41964

IMAGE OPTIMIZATION VERSUS CLASSIFICATION - AN APPLICATION ORIENTED COMPARISON OF DIFFERENT METHODS BY USE OF THEMATIC MAPPER DATA

HERMANN KAUFMANN and BERTHOLD PFEIFFER (Karlsruhe, Universitaet, Federal Republic of Germany) IN: Remote sensing for resources development and environmental management; Proceedings of the Seventh International Symposium, Enschede, Netherlands, Aug. 25-29, 1986. Volume 1. Rotterdam, A. A. Balkema, 1986, p. 31-35. refs

A88-41965

COMPARISON OF CLASSIFICATION RESULTS OF ORIGINAL AND PREPROCESSED SATELLITE DATA

BARBARA KUGLER and RUEDIGER TAUCH (Berlin, Technische Universitaet, Federal Republic of Germany) IN: Remote sensing for resources development and environmental management; Proceedings of the Seventh International Symposium, Enschede, Netherlands, Aug. 25-29, 1986. Volume 1. Rotterdam, A. A. Balkema, 1986, p. 41-45.

The production of satellite image maps is one of various objectives of image processing. Satellite image maps are very important tools as orientation maps in regions, where other topographic maps are either not available or out of date. They may also serve as basic information for thematic maps for landuse, geological and ecological purposes. The methods of multispectral

classification are applied to obtain landuse maps from satellite image data. These methods are based on the characteristic spectral reflectance of objects that enables to extract feature sets for different classes. By means of the feature sets it is possible to assign every picture element (pixel) to one of the various classes. For digital image classification the spectral signatures are the substantial source of information. Therefore usually roughly preprocessed data are used. The classification of preprocessed data offers advantages if the concerned area is covered by several satellite image scenes. In this case the data undergo radiometrical and geometrical processing before classification takes place. The purpose of this paper is to investigate digitally classified original and preprocessed data. The classification results of the two data types are compared. Author

A88-41966
AIRPHOTO MAP CONTROL WITH LANDSAT - AN
ALTERNATIVE TO THE SLOTTED TEMPLLET METHOD

W. D. LANGERAAR (Euroconsult, Arnhem, Netherlands) IN: Remote sensing for resources development and environmental management; Proceedings of the Seventh International Symposium, Enschede, Netherlands, Aug. 25-29, 1986. Volume 1. Rotterdam, A. A. Balkema, 1986, p. 47-50.

The use of Landsat imagery for cartographic control in the production of geographic basemaps produced by assembling tilted airphotos with varying scales is discussed. Use of this method to map southeastern Irian Java produced basemaps with a mean accuracy of 1.5 mm on a photo scale of 1/20,000. Airphoto map control using Landsat is compared to the slotted templet method, showing that the method using Landsat has several advantages. With this method, photo tilt and scale variations do not alter map accuracy and no ground control is required prior to flying. It is found that Landsat control allows for production of more accurate maps in a shorter amount of time. R.B.

A88-41967
SPACE PHOTOMAPS - THEIR COMPILATION AND
PPECULARITIES OF GEOGRAPHICAL APPLICATION

B. A. NOVAKOVSKII (Moskovskii Gosudarstvennyi Universitet, Moscow, USSR) IN: Remote sensing for resources development and environmental management; Proceedings of the Seventh International Symposium, Enschede, Netherlands, Aug. 25-29, 1986. Volume 1. Rotterdam, A. A. Balkema, 1986, p. 59-62. refs

The use of satellite images in cartography is discussed, focusing on the creation of photomaps by converting space photographs into orthophotoimages through optomechanical analog or electronic-digital orthophotographic equipment. The method used to process stereoscopic photographs is presented, using a 1:500,000 photomap made from images of the Pamiro-Alay region of the Soviet Union taken by the Soyuz-22 multispectral MKF-6 camera as an example. The use of hypsometric pictures to compile maps of morphoisoline, horizontal, and vertical relief dissection, erosion networks, and lineaments is discussed. Also, the combination of cartometry, morphometry, quantitative interpretation, and mathematical-cartographical modeling is examined. R.B.

A88-41968
PROCESSING OF RAW DIGITAL NOAA-AVHRR DATA FOR
SEA- AND LAND APPLICATIONS

G. J. PRANGSMA and J. N. ROOZEKRANS (Koninklijk Nederlands Meteorologisch Instituut, De Bilt, Netherlands) IN: Remote sensing for resources development and environmental management; Proceedings of the Seventh International Symposium, Enschede, Netherlands, Aug. 25-29, 1986. Volume 1. Rotterdam, A. A. Balkema, 1986, p. 63-66. refs

A project has been started at the KNMI to develop algorithms for digital processing of data of the Advanced Very High Resolution Radiometer (AVHRR) in an automatic way. Digital processing gives the opportunity to obtain quantitative data of the Earth-surface. For the conversion of the raw AVHRR-data into true parameters of the Earth-surface many steps have to be taken. The processing scheme is presented and the results of verification studies are discussed. Author

A88-41970
PER-FIELD CLASSIFICATION OF A SEGMENTED SPOT
SIMULATED IMAGE

J. H. T. STAKENBORG (CEC, Joint Research Centre, Ispra, Italy) IN: Remote sensing for resources development and environmental management; Proceedings of the Seventh International Symposium, Enschede, Netherlands, Aug. 25-29, 1986. Volume 1. Rotterdam, A. A. Balkema, 1986, p. 73-78. refs

A per-field classification has been applied to a SPOT simulated image of an area in southern France with mainly agricultural landuse. Using edge preserving smoothing, edge extraction, and edge tracking techniques the field boundaries are derived from the panchromatic channel. The segmented image is replaced by a property table in which the spectral signatures, position, and simple form describing factors of all segments are stored. Author

A88-41973
THEMATIC MAPPING BY SATELLITE - A NEW TOOL FOR
PLANNING AND MANAGEMENT

J. W. VAN DEN BRINK, R. BECK (DHV Consulting Engineers, Amersfoort, Netherlands), and H. RIJKS (Delft, Technische Hogeschool, Netherlands) IN: Remote sensing for resources development and environmental management; Proceedings of the Seventh International Symposium, Enschede, Netherlands, Aug. 25-29, 1986. Volume 1. Rotterdam, A. A. Balkema, 1986, p. 93-95. refs

The new generation of 'high-resolution' remote sensing satellites will increase the number of applications drastically. It is believed that the imagery of these new satellite systems will play a substantial role in the planning and management practices of land and water. Even in countries where a well-developed structure for geo-data processing exists such as the Netherlands, satellite remote sensing forms an important additional source of information in planning and management. This latter statement is also supported by the encouraging results of the case study presented in this article. The objective of the study was to evaluate the possibilities of the new satellite imagery and to present the obtained information in a way accessible to planners, etc. Therefore the concept of the 'Satellite Thematic Map' was adopted as a user-friendly endproduct useful for a large user community. In the article, characteristics of the Satellite Thematic Map for the 'Kromme Rijn' Area in the Netherlands are discussed. Author

A88-41974
SPATIAL FEATURE EXTRACTION FROM RADAR IMAGERY

G. BELLAVIA and J. ELGY (Aston, University, Birmingham, England) IN: Remote sensing for resources development and environmental management; Proceedings of the Seventh International Symposium, Enschede, Netherlands, Aug. 25-29, 1986. Volume 1. Rotterdam, A. A. Balkema, 1986, p. 99-102. refs

It is accepted that the major role of remote sensing as an information source will be in its contribution to geographical information systems. With the advances in remote sensing, images are being created at an increasing rate. The extraction of information from such data is traditionally done manually and is thus costly in both time and money. Therefore techniques need to be developed which automatically extract information from remotely sensed images. This paper considers the extraction of thin line features such as forest rides, dykes and streams from active microwave imagery. Because radar images are coherently created speckle is produced which renders traditional feature extraction methods virtually useless. It is assumed that global techniques such as generalized rough transforms or intelligent graph searching will be more successful than simple local methods. Author

A88-41981
DIGITAL ELEVATION MODELING WITH STEREO SIR-B IMAGE
DATA

R. SIMARD (Canada Centre for Remote Sensing, Ottawa), F. PLOURDE, and T. TOUTIN (DIGIM /1983/, Inc., Montreal,

Canada) IN: Remote sensing for resources development and environmental management; Proceedings of the Seventh International Symposium, Enschede, Netherlands, Aug. 25-29, 1986. Volume 1. Rotterdam, A. A. Balkema, 1986, p. 161-166. refs

A stereo SIR-B image data set has been used to produce a digital elevation model (DEM) for a test site located in the Mount Shasta area in California. The stereo pair was formed with images acquired at 53 and 29 degree incidence angles, both on the same side. A digital method has been developed for the extraction of differential parallaxes which relies mainly on a hierarchical nested zoomed correlation procedure. The efficiency of the proposed method for automatic production of DEM is investigated in relation to terrain and SAR parameters. Author

A88-41982

EARTHSCAN - A RANGE OF REMOTE SENSING SYSTEMS

D. R. SLOGGETT and C. MCGEACHY (Software Sciences, Ltd., Environmental and Space Systems Group, Farnborough, England) IN: Remote sensing for resources development and environmental management; Proceedings of the Seventh International Symposium, Enschede, Netherlands, Aug. 25-29, 1986. Volume 1. Rotterdam, A. A. Balkema, 1986, p. 167-171. Research supported by the National Remote Sensing Centre of England. refs

The Earthscan range of remote sensing systems designed around a core set of image processing and image manipulation routines to provide a building block on which operational remote sensing and research work may be carried out is discussed. The system design is modular, making it portable between host computer systems. The system displays images on an associated workstation and incorporates Geographic Information System capability. The architecture of the systems and their associated baseline image processing functions and the adaptation of the system in order to generate new products, enhance the catalogue, and add new image processing routines are examined. The range of systems may be applied to hydrology, agriculture, geology, environmental monitoring, oceanography, and land use surveys. R.B.

A88-42001

VISUAL INTERPRETATION OF MSS-FCC MANUAL CARTOGRAPHIC INTEGRATION OF DATA

E. AMAMOO-OTCHERE (ECA, Regional Centre for Training in Aerial Surveys, Ile-Ife, Nigeria) IN: Remote sensing for resources development and environmental management; Proceedings of the Seventh International Symposium, Enschede, Netherlands, Aug. 25-29, 1986. Volume 1. Rotterdam, A. A. Balkema, 1986, p. 359-369. refs

The objective was to use the holistic and synoptic qualities of Landsat 2 MSS-FCC taken in 1975 to reorganize from an existing stock of scattered data, a relevant description of aspects of renewable resources development situation in which the fiscal decision makers and development planners have shown keen interest. The cartographic projection from the FCC interpretation was to illustrate the kind of information obtainable with simple techniques, but which data has so much been in short supply in the African resources development arena. The study purposefully selected 'frontier development' problem because it is an important development issue in Ghana. The themes chosen and visually interpreted from the FCC, and the manual cartographic integration of the information illustrate some aspects of the ways for closing the cooperation gap between mapping authorities and the national fiscal authorities. The latter, because of partly tight money situation and partly for lack of appreciation of the role of mapping, usually accord low priority to the former's needs. The study area was in northern Ghana. Author

A88-42016

ASSESSMENT OF TM THERMAL INFRARED BAND CONTRIBUTION IN LAND COVER/LAND USE MULTISPECTRAL CLASSIFICATION

JOSE A. VALDES ALATAMIRA (ICI, Mexico), MARION F. BAUMGARDNER (Purdue University, West Lafayette, IN), and

CARLOS R. VALENZUELA (International Institute for Aerospace Survey and Earth Sciences, Enschede, Netherlands) IN: Remote sensing for resources development and environmental management; Proceedings of the Seventh International Symposium, Enschede, Netherlands, Aug. 25-29, 1986. Volume 1. Rotterdam, A. A. Balkema, 1986, p. 533-539. refs

Thermal data from Landsat 4 TM were used in conjunction with the six reflective TM bands to assess the contribution of the thermal band in eight multispectral classifications using four different data sets. Despite its coarse resolution and differences in radiometric measurements, the thermal data provided an additional informational plane in the generation principal components. This informational plane did not appear when the thermal band was excluded from the linear transformation. The use of all seven TM bands for cluster statistics generation provided greater statistically separability between pairs of spectral classes than when only reflective bands were used. Classification with subsets of selected bands gave better results than classification performed without the use of the thermal band for statistics generation. Classifications with principal components reduced the number of spectrally separable classes, but with a significant reduction in computer time. Author

A88-42025

ASSESSMENT OF DESERTIFICATION IN THE LOWER NILE VALLEY (EGYPT) BY AN INTERPRETATION OF LANDSAT MSS COLOUR COMPOSITES AND AERIAL PHOTOGRAPHS

A. GAD and L. DAELS (Gent, Rijksuniversiteit, Ghent, Belgium) IN: Remote sensing for resources development and environmental management; Proceedings of the Seventh International Symposium, Enschede, Netherlands, Aug. 25-29, 1986. Volume 2. Rotterdam, A. A. Balkema, 1986, p. 599-605. refs

A88-42037

DIGITAL ANALYSIS OF STEREO PAIRS FOR THE DETECTION OF ANOMALOUS SIGNATURES IN GEOTHERMAL FIELDS

E. ZILIOLO, P. A. BRIVIO, M. A. GOMARASCA, and R. TOMASONI (CNR, Istituto per la Geofisica della Litosfera, Milan, Italy) IN: Remote sensing for resources development and environmental management; Proceedings of the Seventh International Symposium, Enschede, Netherlands, Aug. 25-29, 1986. Volume 2. Rotterdam, A. A. Balkema, 1986, p. 685-690. refs

A88-42052

SATELLITE REMOTE SENSING OF THE COASTAL ENVIRONMENT OF BOMBAY

V. SUBRAMANYAN (Indian Institute of Technology, Bombay, India) IN: Remote sensing for resources development and environmental management; Proceedings of the Seventh International Symposium, Enschede, Netherlands, Aug. 25-29, 1986. Volume 2. Rotterdam, A. A. Balkema, 1986, p. 779-781. refs

Landsat imagery is used to trace the development and evolution of the Bombay coast. Geological and geomorphological field traverses and maps, including topographical maps on the scale of 1:63,360 are used with black and white MSS band 6 Landsat imagery on the scale of 1:250,000 and false-color MSS bands 4,5, and 7 imagery on the scale of 1:500,000. An attempt is made to reconstruct the initial configuration of the region, where specific geological and geomorphological features of the region are indicated and discussed, and future changes in the coastal area are predicted. R.B.

A88-42054

A SIMPLE ATMOSPHERIC CORRECTION ALGORITHM FOR LANDSAT THEMATIC MAPPER SATELLITE IMAGES

P. I. G. M. VANOUPLINES (Museum Royal de l'Afrique Centrale, Tervuren, Belgium) IN: Remote sensing for resources development and environmental management; Proceedings of the Seventh International Symposium, Enschede, Netherlands, Aug. 25-29, 1986. Volume 2. Rotterdam, A. A. Balkema, 1986, p. 787-791. refs

An atmospheric correction algorithm for Landsat Thematic

Mapping which uses the horizontal visibility or meteorological range as its only meteorological variable is presented. The algorithm is based on Sturm's (1981) correction for oceanographic applications using the Nimbus-7 CZCS. Because the horizontal visibility can be retrieved from meteorological time series, the algorithm can be applied to images months or even years after they were taken. The algorithm is tested with a sensitivity analysis and is shown to be applicable in regions where atmospheric conditions are stable and well measured. For water quality applications it may be necessary to cluster 4 X 4 pixels to increase the signal to noise ratios, allowing for a resolution of 120 m. R.B.

**A88-42055
EVALUATION OF COMBINED MULTIPLE INCIDENT ANGLE
SIR-B DIGITAL DATA AND LANDSAT MSS DATA OVER AN
URBAN COMPLEX**

B. C. FORSTER (New South Wales, University, Sydney, Australia) IN: Remote sensing for resources development and environmental management; Proceedings of the Seventh International Symposium, Enschede, Netherlands, Aug. 25-29, 1986. Volume 2. Rotterdam, A. A. Balkema, 1986, p. 813-816.

As part of the NASA sponsored SIR-B experiment, digital data with incident angles of 17, 36 and 43 deg were recorded over Sydney, Australia, and have been used in a study of radar imagery for urban purposes. The effect on radar backscatter of the multifaceted and oriented features found in urban regions has been examined as a means for improving urban discrimination when combined with Landsat multispectral data. Imagery at different incidence angles were registered to each other and to Landsat data and analyzed using an image analysis computer system. While systematic interpretation of the radar imagery is complicated by the high response from urban features aligned at right angles to the incident radiation, the combined radar and Landsat images are shown to give good discrimination between sites cleared for development and those heavily urbanized. These areas show a similar Landsat response but are markedly different in radar. Moreover in older residential areas, with significant tree cover, the Landsat response is dominated by the vegetation signature, while radar is shown to provide an increased response from the underlying buildings. Author

**A88-42771
A STATISTICAL MODEL FOR PREDICTION OF PRECISION
AND ACCURACIES OF RADAR SCATTERING COEFFICIENT
MEASUREMENTS DERIVED FROM SAR DATA**

ERIC S. KASISCHKE, GARY W. FOWLER, and CHRISTOPHER C. WACKERMAN (Michigan, Environmental Research Institute, Ann Arbor) IN: IEEE National Radar Conference, 3rd, Ann Arbor, MI, Apr. 20, 21, 1988, Proceedings. New York, Institute of Electrical and Electronics Engineers, Inc., 1988, p. 111-117. refs

A model is presented to estimate a relative error-bound associated with radiometric calibration of the scattering coefficient derived from synthetic-aperture radar (SAR) data. This error bound is based on a statistical coefficient-of-variation error model. The error model was exercised parametrically to determine what factors most significantly influence radiometric errors from SAR systems. It was found that errors in the measurement of the antenna elevation gain-pattern resulted in the most dramatic increases in the statistical error bound. The results from this analysis can be utilized in both the design of SAR systems and measurements programs needed to calibrate SAR systems to minimize the error bounds associated with radiometric calibration. I.E.

**A88-43223
RADIOMETRIC CORRECTION FOR ATMOSPHERIC AND
TOPOGRAPHIC EFFECTS ON LANDSAT MSS IMAGES**
YOSHIYUKI KAWATA, SUEO UENO, and TAKASHI KUSAKA (Kanazawa Institute of Technology, Nonoichi, Japan) International Journal of Remote Sensing (ISSN 0143-1161), vol. 9, April 1988, p. 729-748. refs
(Contract MOESC-60129032)

Raw radiance data measured by a Landsat satellite includes undesirable atmospheric and topographic effects. The correction

to allow for these effects is important in order to increase the accuracy of classification. In this paper it is shown how these effects on the Landsat MSS data are estimated, allowing for the transfer theory of radiation in the atmosphere-ground system. First, the theoretical basis of the atmospheric effect correction system (AECS), which corrects for atmospheric effects on the Landsat MSS data over a flat terrain, is presented. Then a simple radiometric correction method which can remove both the atmospheric and topographic effects from the Landsat MSS data over a rugged terrain is proposed. It is applied to a mountainous test area with known digital terrain data, and satisfactory results are obtained. In the present analyses, the values of relevant atmospheric parameters such as the optical thickness, the single scattering albedo, and the turbidity factor of the atmosphere were adopted from either an Elterman's (1968) model atmosphere or a model atmosphere given by the Lowtran 5 code in the evaluation of scattering and transmission functions. Lambert's law was assumed as a bidirectional reflection at the ground surface. Author

A88-43224* Jet Propulsion Lab., California Inst. of Tech., Pasadena.

**DIRECTED BAND RATIOING FOR THE RETENTION OF
PERCEPTUALLY-INDEPENDENT TOPOGRAPHIC EXPRESSION
IN CHROMATICITY-ENHANCED IMAGERY**

ROBERT E. CRIPPEN, RONALD G. BLOM, and JAN R. HEYADA (California Institute of Technology, Jet Propulsion Laboratory, Pasadena) International Journal of Remote Sensing (ISSN 0143-1161), vol. 9, April 1988, p. 749-765. refs

A band ratioing method is developed which directs the retention of topographic expression and albedo information so that they remain depicted as prominent variations in image intensity. Band data are adjusted so that ratio values for each surface material coherently increase with increasing pixel bispectral radiance for all three ratios of the color composite. The retained topographic expression and albedo information do not significantly distort the ratio-enhanced band-variant reflectance information, and the resultant images are similar to chromaticity-enhanced band composite images, but require only simple arithmetic processing steps. R.R.

A88-43225* Jet Propulsion Lab., California Inst. of Tech., Pasadena.

**THE DANGERS OF UNDERESTIMATING THE IMPORTANCE
OF DATA ADJUSTMENTS IN BAND RATIOING**

ROBERT E. CRIPPEN (California Institute of Technology, Jet Propulsion Laboratory, Pasadena; California, University, Santa Barbara) International Journal of Remote Sensing (ISSN 0143-1161), vol. 9, April 1988, p. 767-776. refs
(Contract NAG5-177; NAGW-455)

The practical importance of simple data adjustments for path (atmospheric) radiance and sensor calibration offsets prior to band ratioing has often been overlooked or misjudged. This paper describes and demonstrates the critical nature of data adjustments for the production of useful ratio images, including ratio images derived solely from long wavelength bands. A simple bispectral graphic model is used for illustrating and evaluating the impact of data offsets upon ratio images. Orthogonal indices, used as alternatives to band ratios, are shown to be sometimes less sensitive to topographic influences than ratios of unadjusted data but not less sensitive than ratios of properly adjusted data. Author

**A88-43672
CORRECTION OF SPATIAL AND TEMPORAL DISTORTIONS
IN THE PHOTOGRAPHIC IMAGE INPUT INTO AN
INTERACTIVE PROCESSING SYSTEM [KORREKTSIIA
PROSTRANSTVENNO-VREMENNYKH ISKAZHENII VVODA
FOTOIZOBRAZHENII V SISTEMU INTERAKTIVNOI
OBRABOTKI]**

S. A. BARTALEV and M. D. BREIDO (Vsesoiuznoe Aerofotosoustroitel'noe Ob'edinenie Lesproekt, Moscow, USSR) Issledovanie Zemli iz Kosmosa (ISSN 0205-9614), Mar.-Apr. 1988, p. 83-89. In Russian.

This paper describes a method for correcting spatial and temporal distortions in photographic images, which makes it possible to generate digital imagery invariant to the input conditions in an interactive processing system. The efficiency of the method was evaluated using real black-and-white images of an area covered with saxaul bushes for the determination of crown diameters and of the number of bushes. I.S.

A88-44517
OBJECT-SPACE LEAST-SQUARES CORRELATION

U. V. HELAVA (Helava Associates, Inc., Southfield, MI) Photogrammetric Engineering and Remote Sensing (ISSN 0099-1112), vol. 54, June 1988, p. 711-714. refs

A variation of the least-squares correlation, called least-squares groundel correlation (LSGC), which is performed in object space by matching densities assigned to ground elements (groundels) is presented. LSGC is used for refining results obtained using conventional methods, processing each groundel individually, accommodating multiple images, and employing mathematical processing to sharpen automatic measurements. The application of LSCS to the measurement of point elevations and tie points for aerial triangulation are discussed. It is expected that LSCS may be a means of eventually merging automatic correlation and feature extraction into one integrated process. R.B.

A88-44532
THEORETICAL BASIS FOR MULTISPECTRAL IMAGING SIMULATION

K. Q. LAO and G. R. LOEFER (Lockheed-Georgia Co., Marietta, GA) IN: Infrared image processing and enhancement; Proceedings of the Meeting, Orlando, FL, May 20, 21, 1987. Bellingham, WA, Society of Photo-Optical Instrumentation Engineers, 1987, p. 33-39. refs

Layered weather models are presently used to compute the spectral irradiance and attenuation experienced by simulated multispectral imagers due to atmospheric constituents along the propagation path. In the case of FLIR imagery, the IR spectral band is divided into subbands; for each of these, a set of effective temperatures must be computed in order to supplant the physical temperature of the emission sources. A common algorithm can be used to simulate both IR and mm-wave passive imagery. O.C.

A88-44534
THERMAL MODELING AND IR SCENE GENERATION

RANDY K. SCOGGINS (U.S. Army, Engineer Waterways Experiment Station, Vicksburg, MS) IN: Infrared image processing and enhancement; Proceedings of the Meeting, Orlando, FL, May 20, 21, 1987. Bellingham, WA, Society of Photo-Optical Instrumentation Engineers, 1987, p. 50-57. Army-supported research. refs

Numerical models have been developed for the simulation of terrain surface temperatures for such geographic constituents as grasslands, deserts, and forested regions, using semiempirical techniques and local surface meteorology and material thermal properties as inputs. Attention is presently given to the temperature modeling approach used, the structuring of the codes in the requisite form for scene generation, and the data required by the models. Approaches to accounting for the effects of atmospheric contaminants are noted. O.C.

A88-44540
INTEGRATION OF LANDSAT, DTED, AND DFAD

NICKOLAS L. FAUST (Georgia Institute of Technology, Atlanta) IN: Infrared image processing and enhancement; Proceedings of the Meeting, Orlando, FL, May 20, 21, 1987. Bellingham, WA, Society of Photo-Optical Instrumentation Engineers, 1987, p. 106-115.

Procedures for the integration of Landsat Thematic Mapper digital data with DMA provided DTED and DFAD data sets are presented. Geometric correction issues in the merging of the data sets are addressed and examples are given. Presentation of the

results of a data merge are displayed using a licensed perspective sceneration program GTVISIT. Author

A88-44641* Georgia Univ., Athens.
CARTOGRAPHIC FEATURE EXTRACTION WITH INTEGRATED SIR-B AND LANDSAT TM IMAGES

R. WELCH and MANFRED EHLERS (Georgia, University, Athens) International Journal of Remote Sensing (ISSN 0143-1161), vol. 9, May 1988, p. 873-889. refs
(Contract JPL-957516)

A digital cartographic multisensor image database of excellent geometry and improved resolution was created by registering SIR-B images to a rectified Landsat TM reference image and applying intensity-hue-saturation enhancement techniques. When evaluated against geodetic control, RMSE(XY) values of approximately + or - 20 m were noted for the composite SIR-B/TM images. The completeness of cartographic features extracted from the composite images exceeded those obtained from separate SIR-B and TM image data sets by approximately 10 and 25 percent, respectively, indicating that the composite images may prove suitable for planimetric mapping at a scale of 1:100,000 or smaller. At present, the most effective method for extracting cartographic information involves digitizing features directly from the image processing display screen. Author

A88-44648* Vexcel Corp., Boulder, Colo.
SIR-B STEREO-RADARGRAMMETRY OF AUSTRALIA

F. LEBERL, W. MAYR, G. DOMIK (Vexcel Corp., Boulder, CO), and M. KOBRICK (California Institute of Technology, Jet Propulsion Laboratory, Pasadena) International Journal of Remote Sensing (ISSN 0143-1161), vol. 9, May 1988, p. 997-1011. refs
(Contract JPL-957549)

Results are reported from an ongoing program of radargrammetric experimentation with SIR-B data. Six stereo models of orbits over Australia were processed in an analytical stereo plotter. Height accuracies were up to + or - 25 m or 1.8 times the range resolution. This is better than in previous SIR-B stereo work, probably due to better image quality. Some inconsistencies were encountered between look angle geometries and height measurement accuracies. While general observations about earlier SIR-B stereo results were confirmed, inconsistencies with theoretical expectations could not be fully explained. Author

A88-44649* Vexcel Corp., Boulder, Colo.
DEPENDENCE OF IMAGE GREY VALUES ON TOPOGRAPHY IN SIR-B IMAGES

G. DOMIK, F. LEBERL (Vexcel Corp., Boulder, CO), and J. CIMINO (California Institute of Technology, Jet Propulsion Laboratory, Pasadena) International Journal of Remote Sensing (ISSN 0143-1161), vol. 9, May 1988, p. 1013-1022. refs
(Contract JPL-957549)

This paper focuses on the use of a high resolution digital elevation model (DEM) to aid in rectifying and enhancing synthetic aperture radar images. Using a synthetic backscatter image, the SIR-B images are manually rectified and resampled to remove geometric distortions caused by topography. In a second step, an improved reflectance function of incidence angle is derived from the DEM and the rectified image and this function is used to reduce radiometric effects of topography yielding an albedo image which clearly shows the thematic, as opposed to topographic content of the image. The procedure is tested on four SIR-B images of a scene in Argentina (crossover point) that is imaged under different azimuth and incidence angles. The similarity of the resulting images indicates that the procedure effectively reduces artefacts from the images that are dependent on topography. Author

A88-44650* Cornell Univ., Ithaca, N.Y.
A DEMONSTRATION OF STEREOGRAMMETRY WITH COMBINED SIR-B AND LANDSAT TM IMAGES

ARTHUR L. BLOOM, ERIC J. FIELDING, and XIU-YEN FU (Cornell University, Ithaca, NY) International Journal of Remote Sensing

(ISSN 0143-1161), vol. 9, May 1988, p. 1023-1038. refs
(Contract JPL-956926; NAS5-28767; NGT-33-010-801)

Shuttle Imaging Radar-B (SIR-B) and Landsat Thematic Mapper (TM) images can be viewed stereoscopically if the illumination geometries are compatible. To create the stereoscopic effect points must be coregistered. Simplified stereophotogrammetric equations permit the height of an object above a reference plane to be crudely calculated from the target offset toward the SIR-B radar antenna with reference to its position on a TM image. Precision is limited by pixel resolution and target correlation. Future spaceborne imaging radar missions will offer the potential for topographic mapping in many areas where TM coverage is available. Author

**A88-44651
AN EFFECT OF COHERENT SCATTERING IN SPACEBORNE
AND AIRBORNE SAR IMAGES**

R. K. RANEY (Radarsat Project Office, Ottawa, Canada), A. L. GRAY, and J. G. PRINCZ (Canada Centre for Remote Sensing, Ottawa) International Journal of Remote Sensing (ISSN 0143-1161), vol. 9, May 1988, p. 1039-1049. refs

Radar imagery obtained by the Shuttle Imaging Radar-B (SIR-B) is compared to high resolution aircraft imagery of the same urban and agricultural areas close to the city of Montreal, Canada. It is clear that the SIR-B radar is more sensitive than the aircraft radar to reflections from extended, along-track radar targets. The effect is evident for both urban and agricultural areas in which the street or field orientation is near parallel to the radar azimuth direction. It is likely that such reflectivity enhancement is due to coherent combination of the scattered field from appropriate scattering centers. The paper considers the observed phenomena and probes potential scattering models to explain the results. Author

**A88-45116
EVALUATIONS OF UNSUPERVISED METHODS FOR
LAND-COVER/USE CLASSIFICATIONS OF LANDSAT TM
DATA**

KIYONARI FUKUE, HARUHISA SHIMODA, YOSHIKI MATUMAE, RYUJI YAMAGUCHI, and TOSHIBUMI SAKATA (Tokai University, Japan) Geocarto International (ISSN 1010-6049), vol. 3, June 1988, p. 37-44.

Classification accuracies of unsupervised classification methods for Landsat TM data are estimated using land-cover/use test site data, evaluated, and compared to a conventional supervised maximum likelihood classification. The unsupervised classification methods are six kinds of hierarchical clustering and a minimum residual clustering. The nearest neighbor, farthest neighbor, and median methods show classification accuracies lower than the maximum likelihood method because the distance measures used are not weighted by numbers of elements within clusters. The Ward method, group average method, and minimal residual group clustering show accuracies 6 to 7 percent higher than the maximum likelihood method. R.B.

**A88-45639
APPLICATION OF SPATIAL STATISTICS TO ANALYZING
MULTIPLE REMOTE SENSING DATA SETS**

CHARLES E. GLASS, HSIEN-MIN YANG, DONALD E. MYERS (Arizona, University, Tucson), and JAMES R. CARR (Nevada, University, Reno) IN: Geotechnical applications of remote sensing and remote data transmission; Proceedings of the Symposium, Cocoa Beach, FL, Jan. 31-Feb. 1, 1986. Philadelphia, PA, American Society for Testing and Materials, 1988, p. 138-150. refs

The results of research using image spatial statistics to improve the resolution of low-resolution digital images are presented. Two digital images in adjacent spectral bands are degraded to simulate a low-resolution image. New samples within the sparse, low-resolution images are estimated using the spatial characteristics displayed in a variogram function and an estimation process known as cokriging. The resulting high-resolution estimation is compared with the original undegraded image to check accuracy. Accuracy improves from a mean square error of 826 for sample replication to 56 for cokriging. It is concluded that cokriging is an accurate

and flexible estimation technique, which could possibly be used for future automated image interpretation and feature extraction algorithms. R.B.

**A88-45640* Geological Survey, Baton Rouge, La.
A COMPARISON OF AIRBORNE GEMS/SAR WITH
SATELLITE-BORNE SEASAT/SAR RADAR IMAGERY - THE
VALUE OF ARCHIVED MULTIPLE DATA SETS**

BRADFORD C. HANSON (Louisiana Geological Survey, Baton Rouge) and LOUIS F. DELLWIG (Kansas, University, Lawrence) IN: Geotechnical applications of remote sensing and remote data transmission; Proceedings of the Symposium, Cocoa Beach, FL, Jan. 31-Feb. 1, 1986. Philadelphia, PA, American Society for Testing and Materials, 1988, p. 163-179; Discussion, p. 179-182. Research supported by the Phillips Petroleum Co. refs
(Contract JPL-954946)

In a study concerning the value of using radar imagery from systems with diverse parameters, X-band images of the Northern Louisiana Salt dome area generated by the airborne Goodyear electronic mapping system (GEMS) are analyzed in conjunction with imagery generated by the satelliteborne Seasat/SAR. The GEMS operated with an incidence angle of 75 to 85 deg and a resolution of 12 m, whereas the Seasat/SAR operated with an incidence angle of 23 deg and a resolution of 25 m. It is found that otherwise unattainable data on land management activities, improved delineation of the drainage net, better definition of surface roughness in cleared areas, and swamp identification, became accessible when adjustments for the time lapse between the two missions were made and supporting ground data concerning the physical and vegetative characteristics of the terrain were acquired. R.B.

N88-20712# Instituto de Pesquisas Espaciais, Sao Jose dos Campos (Brazil).

**RESTORATION TECHNIQUES FOR REDISPLAY OF
LANDSAT-5 SATELLITE IMAGERY [TECNICAS DE
RESTAURACAO PARA REAMOSTRAGEM DE IMAGENS DO
SATELITE LANDSAT-5]**

LEILA MARIA GARCIA FONSECA, NELSON DELFINO DAVIL MASCARENHAS, and GERALD JEAN FRANCIS BANON Jun. 1987 14 p In PORTUGUESE Presented at the 5th Brazilian Symposium of Telecommunication Campinas, Brazil, 8-10 Sep. 1987

(INPE-4189-PRE/1076) Avail: NTIS HC A03/MF A01

Some results are shown of restoration for redisplayed images of the Thematic Mapper, utilizing Fourier domain techniques. A restored image is compared to the redisplayed image with cubic convolution interpolation. The comparison is done visually and through radiometric profile of the line imagery. Author

N88-22450# Northwest Research Associates, Inc., Bellevue, Wash.

**GEOMETRIC RESTORATION OF SATELLITE IMAGE DATA
Scientific Report No. 3, 20 Feb. - 30 Sep. 1987**

R. D. LUCAS and ROBERT E. ROBINS 15 Oct. 1987 31 p
(Contract F19628-87-C-0003)

(AD-A190462; NWRA-CR-R019; AFGL-TR-87-0270) Avail: NTIS HC A03/MF A01 CSCL 08B

We describe an approach for projecting satellite image data onto arbitrary map coordinates. This transformation removes distortions caused by the basic geometry of cross-track scanners and by spacecraft pitch, roll, and yaw. Geometrically restored images are useful for morphological analyses and correlative studies involving concurrent data from multiple sensors. It is possible, for example, to present AIRS passes from distinct receivers, all-sky camera images, radar data, and other relevant spatial measurements on one map in geographic coordinates. Out approach is rigorous in that arbitrary satellite motions are accounted for and exact principles of geometry are used throughout. The floating-point intensive geometry calculations are performed on an arbitrary (adjustable) reference grid, which can be coarse for quick-look purposes, or fine for highest accuracy. Concurrent images for distinct wavelengths can be efficiently projected without

redundant geometry calculations. An IBM PC/AT compatible implementation for Polar BEAR AIRS image data is described. Results are presented for two data sets representing moderate and severe platform motions. GRA

N88-22451# Northwest Research Associates, Inc., Bellevue, Wash.

SATELLITE UV IMAGE PROCESSING Scientific Report No. 4, 1 Jul. - 10 Sep. 1987

NORMAN ROSENBERG 9 Oct. 1987 56 p

(Contract F19628-87-C-0003)

(AD-A190466; NWRA-CR-87-R016; AFGL-TR-87-0271) Avail:

NTIS HC A04/MF A01 CSCL 17E

The overall objective of the computer program is the photometric and geometric processing of UV satellite images. The data source is the AIRS scanning UV spectrometer aboard the POLAR BEAR satellite. The processing is designed to provide geographic-mapped images which describe the spatial and temporal variability of airglow and aurora of emitting species. The AIRS data stream provided simultaneous records from 3 detectors received at several ground stations from several passes per day. These total about 1500 useful images from launch to Feb. 1987. The major progress during the report period has been development of programs to accomplish the following: (1) Statistical filtering of low-count images to provide meaningful brightness estimates; (2) Use of observed limb locations to provide attitude correction in daylit images and attitude estimation in night images to provide accurate ground positions; (3) Normalization of airglow based on column path length and solar flux which allows separation of aurora from airglow portions of the images; (4) Multi-band presentation of auroral features which clearly define differences between the location of emitting species. GRA

N88-22454# Instituto de Pesquisas Espaciais, Sao Jose dos Campos (Brazil).

METHOD FOR RESTORATION AND RESAMPLING OF TM SENSOR IMAGERY [METODO PARA RESTAURACAO E REAMOSTRAGEM DE IMAGENS DO SENSOR TM]

LEILA MARIA GARCIAFONSECA and NELSON DELFINODA-VILAMASCARENHAS Mar. 1988 16 p In PORTUGUESE; ENGLISH summary Presented at the 2nd Latin American Symposium on Remote Sensing, Bogota, Colombia, Nov. 1987 (INPE-4491-PRE/1255) Avail: NTIS HC A03/MF A01

Some results obtained with the restoration for resampling TM images using techniques designed in the Fourier domain and implemented in the spatial domain are presented. The main idea is to obtain a good approximation for the original image over a finer grid, by substituting conventional interpolation techniques by the restoration technique. Therefore, image data with slightly better spatial and radiometric quality than the raw data can be synthesized with the resampling process. The work involves the design of a linear restoration filter with input and output defined on different sampling grids. The filter is designed in the Fourier domain by using the technique of compensation of the transfer function. Subsequently, a linear operator in the spatial domain is derived to be applied in the image restoration process. The restoration filter is applied to resample images from the TM sensor of the LANDSAT-5 on a 15 m sampling grid. These restored images are compared to the images that were resampled with the parametric cubic convolution. The comparison is made in visual terms, through the radiometric profile along on image line, through the difference between the images and through statistical measures, indicating better results with the proposed method. Author

N88-22485# Instituto de Pesquisas Espaciais, Sao Jose dos Campos (Brazil).

CALIBRATION AND PROCESSING OF AVHRR DATA FOR TEMPERATURE ESTIMATION [CALIBRACAO E PROCESSAMENTO DOS DADOS DE AVHRR PARA ESTIMATIVA DE TEMPERATURA]

KEIKO TANAKA, CARLOS HO SHIH NING, YOSHIHIRO YAMAZAKI, and VALDER MATOSDEMEDEIROS Mar. 1988 25

p In PORTUGUESE; ENGLISH summary Presented at the SELPER/86, Gramado/RS, Brazil, 10-15 Aug. 1986 (INPE-4493-PRE/1257) Avail: NTIS HC A03/MF A01

The results of a quantitative analysis of the thermal channels of the NOAA-9 satellite Advanced Very High Resolution Radiometer (AVHRR) scanning radiometer digital data, recorded on a CCT magnetic tape, are presented. The calibration coefficients derived from the reference parameters contain information on the following telemetry data: the energy levels detected by the AVHRR sensor during space view and the internal calibration target for each thermal channel and each scanning. The linearization functions are found by taking, for each channel, the radiometric mean of 10 samples of space view and internal target data. The linear radiance was produced by taking the average of 50 scan data. These linear functions give the sensor radiance variations for each target scanned, and were used to convert the digital image data into radiance, and consequently, into temperature values using the inverse Planck function. The main results of the April 18th, 1986 image processed, applying the navigation system, for an area of 256 x 256 pixels are presented. Author

N88-23300# Begeleidingscommissie Remote Sensing, Delft (Netherlands).

PROPOSALS FOR THE PRE-OPERATIONAL USE OF DATA FROM THE EUROPEAN REMOTE SENSING SATELLITE ERS-1 [VOORSTEL VOOR HET PRE-OPERATIONELE GEBRUIK VAN ERS-1 GEGEVENS]

J. REIFF (Royal Netherlands Meteorological Inst., De Bilt.) 1986 57 p In DUTCH

(BCRS-86-02; ETN-88-91549) Avail: NTIS HC A04/MF A01

Payload and time planning of ERS-1, and comparable satellites are discussed. The deduction of geophysical parameters from ERS-1 data is explained. The international data flow and data management, data management in the Netherlands, and mission operations plan are outlined. Finance, national and international cooperation, and commercialization possibilities are discussed. ESA

N88-23302# Begeleidingscommissie Remote Sensing, Delft (Netherlands).

INVESTIGATION OF THE USEFULNESS OF SPECKLE ANALYSIS IN IMAGING RADAR SYSTEMS [ONDERZOEK NAAR DE BRUIKBARHEID VAN SPECKLE-ANALYSIS IN BEELDVOORMENDE RADARSYSTEMEN]

A. H. J. M. PELLEMANS (Technische Hogeschool, Delft, Netherlands) Oct. 1986 72 p In DUTCH

(BCRS-86-05; ETN-88-91552) Avail: NTIS HC A04/MF A01

The usefulness of speckle analysis in imaging side looking airborne radar systems was investigated. The speckle-analysis model, and the programs developed for simulations are explained. The imaging of periodic objects is presented. If the object consists of a grid of equidistant point targets, it is possible to determine periodicities in the object with repetition distances smaller than the resolution using the power density spectrum in the azimuthal direction. The model cannot be applied for sea wave observation. Decorrelation calculations give a decorrelation distance of 0.5 to 0.6 m above sea, which is smaller than half the antenna length (1.25 m). ESA

N88-23304# Begeleidingscommissie Remote Sensing, Delft (Netherlands).

RESULTS OF THE TESTING OF THE SEGMENTATION PROGRAM ON RESEDA [RESULTATEN VAN DE BEPROEVING VAN HET SEGMENTATIEPROGRAMMA OP RESEDA]

G. J. L. NOOREN (National Aerospace Lab., Amsterdam, Netherlands) and D. H. HOEKMAN 1987 38 p In DUTCH (BCRS-87-01; NLR-TR-86104-L; ETN-88-91554) Avail: NTIS HC A03/MF A01

A segmentation program was tested using images of agriculture and forestry areas from side looking airborne radar as well as from Seasat synthetic aperture radar. Segmentation following the method of Gerbrands, and the implementation of the segmentation

algorithm in the Remote Sensing Data processing system RESEDA are explained. The experiments show that the accuracy of surface determination and field average estimate is determined by the segmentation without postprocessing. The (positive) effect of the segmentation on the classification is determined. ESA

N88-23309# Begeleidingscommissie Remote Sensing, Delft (Netherlands).

STUDY OF THE PLAN FOR A NATIONAL DATA CENTER FOR THE EUROPEAN REMOTE SENSING SATELLITE ERS-1 [STUDIE NAAR DE OPZET VAN EEN NATIONAAL ERS-1 DATACENTRUM]

R. W. VANSWOL (National Aerospace Lab., Amsterdam, Netherlands) Jul. 1987 80 p In DUTCH (BCRS-87-11; NLR-TR-87055-L; ETN-88-91560) Avail: NTIS HC A05/MF A01

The way to receive and distribute in the Netherlands the data of ERS-1 was studied. It was investigated which data will come from ERS-1, which data products will be deduced by ESA, how ESA will distribute these products, and who will be the Dutch users. The investigation shows that for the Netherlands the real-time use of ERS-1 data in regional weather and wave prediction models will be the most important operational application of the data. In that respect, proposals for the practical use of the data are given. ESA

N88-24017# Societe Europeenne de Propulsion, Bordeaux (France). Image Processing Div.

THE GEOMETRIC WORKSTATION, A NEW APPROACH FOR GEOMETRIC CORRECTIONS OF REMOTELY SENSED DATA Abstract Only

P. N. PASCAUD and PH. REBILLARD In INPE, Latin American Symposium on Remote Sensing. 4th Brazilian Remote Sensing Symposium and 6th SELPER Plenary Meeting, Volume 1 p 69 1986

Avail: NTIS HC A99/MF E03

Accurate registration of image data to maps or image-to-image is mandatory for both cartographic and multitemporal or multisensor studies. The auxiliary data provide with the images do not allow a satisfactory precision level in the image production. The magnitude of the errors vary with the sensors and can be greater than a hundred pixels. If a better precision is needed, additional information such as pairs of ground control points (GCP) must be introduced. Acquisition of such sets of control points is usually a difficult and tiresome repetitive task. The geometric workstation overpasses some typical limitations of existing methods. An interactive software was designed in order to improve efficiency of the operators. The systematic access to the map sheet was suppressed by digitally storing the maps and retrieving them using a cartographic data base service. An automatic recognition of the GCP is provided by the data base. A sophisticated signal processing was implemented in order to improve the quality of the auxiliary data. The combination of all these features allows the geometric workstation to perform quick and efficient geometric corrections. This improved precision is fully exploited by the accurate algorithm used for geometric precision modeling. Author

N88-24018# MacDonald, Dettwiler and Associates Ltd., Richmond (British Columbia).

MAPPING FROM LANDSAT AND SPOT SATELLITE IMAGERY Abstract Only

IAN LAVERTY In INPE, Latin American Symposium on Remote Sensing. 4th Brazilian Remote Sensing Symposium and 6th SELPER Plenary Meeting, Volume 1 p 70 1986

Avail: NTIS HC A99/MF E03

Recent advances in the resolution and stereo capability of earth imaging satellites have made it practical to produce true cartographic maps from satellite imagery. Preliminary tests with LANDSAT TM have shown that: satellite imagery can be corrected to planimetric accuracy suitable for 1:50,000 scale maps with very few control points. Elevation can be derived accurately from stereo satellite imagery by automatic computer processing. Natural planimetric features can be interpreted accurately enough for

1:50,000 scale mapping at 30 meter resolution. The results from SPOT imagery, particularly in the areas of elevation accuracy and the interpretation of cultural features where LANDSAT TM does not meet 1:50,000 scale mapping standards are updated. An operational method of producing and updating topographic base maps digitally from satellite imagery will be presented. The costs and benefits of satellite mapping, particularly for developing nations, will be discussed in detail. Author

N88-24019# Toulouse Univ. (France). Langages et Systemes Informatiques.

THE SYSTEME D'ANALYSE GEOGRAPHIQUE (SAGE) GEOGRAPHIC ANALYSIS SYSTEM Abstract Only

M. R. CAUBET and M. A. HAMEURLAIN In INPE, Latin American Symposium on Remote Sensing. 4th Brazilian Remote Sensing Symposium and 6th SELPER Plenary Meeting, Volume 1 p 86 1986

Avail: NTIS HC A99/MF E03

The design and implementation of a geographic analysis system, SAGE, is described. A classification of geographic analysis data base queries and two geographic data manipulation models are presented. Then, after establishing a data base model for geographic objects, a series of integrity constraints on the time and space elements of the geographic data base are specified and a means of ensuring the structural coherence of geographic objects is discussed. Author

N88-24020# Comision Nacional de Investigaciones Espaciales, Buenos Aires (Argentina).

SPECTRAL MEASUREMENTS FOR CORRECTING LANDSAT DATA FOR ATMOSPHERIC EFFECTS Abstract Only

A. BRIZUELA, M. A. RAED, G. HERREN, and C. MARINEZ CASADO In INPE, Latin American Symposium on Remote Sensing. 4th Brazilian Remote Sensing Symposium and 6th SELPER Plenary Meeting, Volume 1 p 92 1986

Avail: NTIS HC A99/MF E03

Target reflectance data are needed by all man and machine systems to obtain the unambiguous interpretation of LANDSAT data. In response to the need for correcting target reflectance spectral data, the capabilities of a wide range of techniques for determining and removing atmospheric parameters and effects from LANDSAT data are being evaluated. Evaluated techniques include: experimental method that includes transferring known ground reflectance to spacecraft measurements, and three empirical methods computerizing image processing techniques. The approach that was performed was the conversion of radiance data from the satellite into reflectance values from a measurement technique based on ground measurements with an Exotech Model 100 A radiometer. Two Chavez' techniques are used to correct ERTS digital data for atmospheric scattering and other associated haze effects. Another empirical method is an extension of Chavez' Regression Technique: the covariance matrix method (CMM) for estimating additive path radiance in remote sensing data. All the methods were applied to each LANDSAT image of Buenos Aires and its environment. It was concluded that in all cases, there is a big influence of path radiance with different high levels and with time. Another important conclusion was obtained: there is a high correlation between histogram minimum load and CMM empirical methods with ground data. Empirical methods are of the same order as the ground truth haze effects. Author

N88-24027# Instituto de Pesquisas Espaciais, Sao Jose dos Campos (Brazil).

TEXTURAL FEATURES FOR IMAGE CLASSIFICATION IN REMOTE SENSING Abstract Only

VITOR HAERTEL (Rio Grande do Sul Univ., Porto Alegre, Brazil) and YOSIO E. SHIMABUKURO In its Latin American Symposium on Remote Sensing. 4th Brazilian Remote Sensing Symposium and 6th SELPER Plenary Meeting, Volume 1 p 181 1986

Previously announced as N88-16181

Avail: NTIS HC A99/MF E03

Texture is an important characteristic in identifying regions of interest in an image. Several methods to quantify image texture

were reported in the literature. Experiments are described which are aimed at extracting textural features from digital images by calculating statistical properties in and around each pixel. The moving window concept is implemented and tests using LANDSAT MSS and TM imagery are presented. Author

N88-24028# Comision Nacional de Investigaciones Espaciales, Buenos Aires (Argentina).

SHAPE DETECTION IN REMOTE SENSING THROUGH GRAPH ISOMORPHISM Abstract Only

SEVERINO FERNANDEZ *In* INPE, Latin American Symposium on Remote Sensing. 4th Brazilian Remote Sensing Symposium and 6th SELPER Plenary Meeting, Volume 1 p 183 1986

Avail: NTIS HC A99/MF E03

Experiments on shape detection in remote sensing were performed using graph homeomorphism as the match criteria. The first step involved is to extract a graph from a monochromatic image, being the first approach the extraction of linear features as graph edges and intersections and points of local maximum curvature as graph nodes. This first step was performed through three consecutive algorithms: detection of edge strength and thresholding with the Vero-Massy algorithm, edge thinning and finally edge following with simultaneous graph destruction generation. This provides a description of the considered image as a set of graphs. The description is completed with the computation of the angle between graph edges incident at a common node. A candidate graph is now generated and the same description is computed. The graph matching procedure is carried out with a simplified version of a forward checking with backtracking algorithm from Haralick and Shapiro with the sum of differences between corresponding edges of prototype and candidate as a measure of graph similarity. Finally, a couple of experiments with LANDSAT images is shown. Author

N88-24064# Universidade Estadual de Paulista, Guaratingueta (Brazil). Dept. de Planejamento Regional.

IMPLANTATION OF A GEO-CARTOGRAPHICAL INFORMATION SYSTEM THROUGH MICROCOMPUTERS

[IMPLANTACAO DE UM SISTEMA DE INFORMACAO GEO-CARTOGRAFICA ATRAVES DE MICROCOMPUTADOR]

A. L. A. TEIXEIRA and L. H. O. GERARDI *In* INPE, Latin American Symposium on Remote Sensing. 4th Brazilian Remote Sensing Symposium and 6th SELPER Plenary Meeting, Volume 1 p 548-553 1986 *In* PORTUGUESE; ENGLISH summary

Avail: NTIS HC A99/MF E03

The introduction of quantitative methods as a tool for data analysis, has caused impact changes in the scientific approach to geographic problems. The growing automation of the cartographic process has changed cartography in a very significant way. Common to both cases is the problem of the enormous amount of data to be manipulated and analyzed. This volume can not be efficiently treated if more modern techniques are not used. All this considered, a geo-cartographical information system was idealized, planned, and implemented using database techniques and the microcomputer as a basic tool. Author

N88-24067# Instituto de Pesquisas Espaciais, Sao Jose dos Campos (Brazil).

STUDY OF METHODS OF POST-PROCESSING APPLIED TO A PROBLEM OF STANDARD CLASSIFICATION [ESTUDO DE METODOS DE POS-PROCESSAMENTO APLICADO A PROBLEMA DE CLASSIFICACAO DE PADROES]

LUCIANO VIEIRA DUTRA and JOSE CARLOS MOREIRA *In its* Latin American Symposium on Remote Sensing. 4th Brazilian Remote Sensing Symposium and 6th SELPER Plenary Meeting, Volume 1 p 562-568 1986 *In* PORTUGUESE; ENGLISH summary

Avail: NTIS HC A99/MF E03

In order to identify the various objects within a multispectral image, per point classification methods are normally used. This kind of method does not use the spatial information among the pixels of the images, thereby producing a higher classification error. The spatial information can be added before, within and after the

classification stage. Two methods of post-processing which take account of the spatial relationship between pixels are presented. The first one is based on a local histogram of the pixel's class. The central pixel is reclassified to the most occurring class, provided the frequency is higher than a selected threshold. The results show a fairly better classification performance and a good improvement of the visual appearance. The second method is based on a generalization of the expansion-striking concept of binary images applied to the individual classes. This method did not lead to a better performance in terms of classification precision but allowed the identification of pixels of mixed classes, which occur mainly in the border between classes, allowing a better localization of these frontiers. Author

N88-24070# Instituto de Pesquisas Espaciais, Sao Jose dos Campos (Brazil).

ANALYSIS OF THE PARAMETERS RESPONSIBLE FOR THE VARIATIONS OF THE ILLUMINATION CONDITIONS IN THE LANSAT DATA [ANALISE DOS PARAMETROS RESPONSAVEIS PELAS VARIACOES DAS CONDICAOES DE ILUMINACAO NOS DADOS LANDSAT]

R. ROSA and E. E. SANO *In its* Latin American Symposium on Remote Sensing. 4th Brazilian Remote Sensing Symposium and 6th SELPER Plenary Meeting, Volume 1 p 583-588 1986 *In* PORTUGUESE; ENGLISH summary

Avail: NTIS HC A99/MF E03

The variations in the tonality (photographic paper products) or in the digital values (computer compatible tapes (CCT) of LANDSAT data are associated with the spectral signatures of objects, atmospheric conditions, geometric measurement, and illuminations, this last is analyzed in the presented work. The parameters that influence the illumination conditions are the geometric relationships between the sensor system, the sun (solar angle of elevation and azimuth), and the surface (orientation and inclination). These parameters are defined and discussed, as well as, their implications on the LANDSAT data. B.G.

N88-24080# Instituto de Pesquisas Espaciais, Sao Jose dos Campos (Brazil).

AUTOMATIC REGISTRATION OF SATELLITE IMAGERY [REGISTRO AUTOMATICO DE IMAGENS DE SATELITE]

GILBERTO CAMARA NETO *In its* Latin American Symposium on Remote Sensing. 4th Brazilian Remote Sensing Symposium and 6th SELPER Plenary Meeting, Volume 1 p 669-671 1986 *In* PORTUGUESE; ENGLISH summary

Avail: NTIS HC A99/MF E03

Registration of satellite imagery is an important need in various application areas in remote sensing. A method is presented for registration which reduces use work to a minimum, the control points being automatically chosen. The method near tests in LANDSAT TM imagery with good results. Author

N88-24081# Instituto de Pesquisas Espaciais, Sao Jose dos Campos (Brazil).

VISUALIZATION OF DIGITAL TERRAIN MODELS [VISUALIZACAO DE MODELOS DIGITAIS DE TERRENO]

GUARACI JOSE ERTHAL, CARLOS ALBERT FELGUEIRAS, and JOAO ARGEMIRODECARVALHOPAIVA *In its* Latin American Symposium on Remote Sensing. 4th Brazilian Remote Sensing Symposium and 6th SELPER Plenary Meeting, Volume 1 p 672-674 1986 *In* PORTUGUESE; ENGLISH summary

Avail: NTIS HC A99/MF E03

The fundamental problem in displaying digital terrain models (DTM) that are tri-dimensional data, is representing them in a bi-dimensional space. Traditional approaches represent DTM data by: contour lines, grey level indexes, and perspective view of a regular grid. First results of a method for rendering tri-dimensional surfaces are presented. This method allows visualization of DTM combined with other spatial information like satellite imagery. Author

N88-24082# Instituto de Pesquisas Espaciais, Sao Jose dos Campos (Brazil).

APPLICATION OF ITS TRANSFORMATION IN COLOR ENHANCEMENT OF LANDSAT IMAGERY [APLICADAO DA TRANSFORMACAO IHS PARA REALCE DE CORES EM IMAGENS LANDSAT]

LUCIANO VIEIRA DUTRA and PAULO ROBERTO MENESES *In its* Latin American Symposium on Remote Sensing. 4th Brazilian Remote Sensing Symposium and 6th SELPER Plenary Meeting, Volume 1 p 675-681 1986 In PORTUGUESE: ENGLISH summary

Avail: NTIS HC A99/MF E03

The multispectral color composite imagery, obtained by digital processing and displayed on video monitors through the combination of the fundamental colors (red, green, and blue) consists in an efficient form of presentation. The visual or psychophysiological perception of the brain to the stimulus of particular colors, tends to combine independently the quantitative components of the fundamental colors, the intensity, (I), hue (H), and saturation (S). So it is possible to perceive each one of these attributes of color, separately. A method is presented to increase the contrast of the colors, using a transformation to the IHS coordinator which permits individual manipulation in each of these components, in order to obtain a better control about the color composite generated in the video display. The basic procedure is a manipulation of the histograms of the components (I, H, and S), in order to increase, decrease, or offset the range of possible values of the components, by linear transformations. The test of this procedure using LANDSAT-TM scene of Serra de Ramalho (BA) showed that different component manipulations resulted in different enhancements of lithologic units, formerly not distinguished in the original color composition, allowed an easier photogeologic interpretation. Author

N88-24102# Research Inst. of National Defence, Stockholm (Sweden).

TERRAIN CLASSIFICATION USING SPOT IMAGES AND THE COMPUTER SYSTEM GOP-300

MATTI SVANTESSON Sep. 1987 50 p In SWEDISH; ENGLISH summary

(FOA-C-20677-2.7; ISSN-0347-3694; ETN-88-92201) Avail: NTIS HC A03/MF A01

For the classification of multispectral images from the SPOT satellite a maximum likelihood algorithm was used. Different contextual analyses were utilized as extra features in the classification, the results of which, with only spectral information as features, was compared with the results when contextual information was used as extra features. Edge-effect is important for fixing the margins. Examples are presented. ESA

N88-25030# Institut fuer Angewandte Geodaesie, Frankfurt am Main (West Germany).

TESTS FOR THE AUTOMATIC PATTERN RECOGNITION OF BUILDING SURFACES BY THE TK 50 [VERSUCHE ZUR AUTOMATISCHEN MUSTERERKENNUNG VON GEBAEUDEFLAECHEEN DER TK 50]

JUERGEN BRENNER *In its* Reports on Cartography and Geodesy. Series 1, No. 99 p 57-77 1987 In GERMAN; ENGLISH summary

Avail: NTIS HC A08/MF A01

An essentially automatic procedure to separate features of built-up areas from the other planimetric features of the TK 50 map is presented. The features are classified by means of the object features width and area in a feature space, here two-dimensional. The procedure is based on simple raster operations: thinning, thickening, extending, and counting of pixels. The rate of wrong classifications amounts to only 3 percent. The total processing time required for 1/4 map sheet is 12 hr. The automatic vectorization of building outlines is described. ESA

N88-25038# Institut fuer Angewandte Geodaesie, Frankfurt am Main (West Germany).

RECENT DEVELOPMENTS IN SOFTWARE AND HARDWARE BY SCITEX CO. [NEUENTWICKLUNGEN IM HARD- UND SOFTWAREBEREICH BEI FIRMA SCITEX]

FERDINAND SALOMON *In its* Reports on Cartography and Geodesy. Series 1, No. 99 p 157-165 1987 In GERMAN; ENGLISH summary

Avail: NTIS HC A08/MF A01

The raster data processing applications offered by the Response 280 system of Scitex Company are being expanded in the field of user software by more sophisticated raster and vector processing modes, as interactive text positioning, DIANA (Digital Analysis) and DTM (Digital Terrain Modelling). Improved possibilities of communication achieved via direct connection of IBM/PC and or Microvax 2 of DEC are substantial hardware extensions. ESA

08

INSTRUMENTATION AND SENSORS

Includes data acquisition and camera systems and remote sensors.

A88-29286

THE ACQUISITION OF SPOT-1 HRV IMAGERY OVER SOUTHERN BRITAIN AND NORTHERN FRANCE, MAY 1986-MAY 1987

JANIS CUSHNIE (Reading, University, England) International Journal of Remote Sensing (ISSN 0143-1161), vol. 9, Jan. 1988, p. 159-167.

The number and spatial distribution of SPOT-1 HRV images acquired over southern Britain and northern France during the first commercial year of the SPOT system have been assessed in response to concern about the lack of cloud-free imagery. It is confirmed that, despite large numbers of images being acquired per scene (1 panchromatic and 12 multispectral on average over northern France; 8 panchromatic and 12 multispectral over southern Britain), most are of limited use because of cloud cover. Only 30 percent of the images collected have at least one quadrant with less than 25 percent cloud cover and 10 percent have less than 10 percent cloud cover in each quadrant. Recommendations on what can be done are presented. B.J.

A88-32850

A PC-BASED INTERACTIVE GRAPHICS SYSTEM TO PERFORM SATELLITE-DERIVED OCEANOGRAPHIC THERMAL ANALYSIS

MARCIA WEAKS, KIM BUTTLEMAN, and W. B. CAMPBELL (NOAA, National Environmental Satellite, Data and Information Service, Camp Springs, MD) IN: American Meteorological Society, International Conference on Interactive and Information Processing Systems for Meteorology, Oceanography and Hydrology, 4th, and Conference on Satellite Meteorology and Oceanography, 3rd, Anaheim, CA, Feb. 1-5, 1988, Preprints. Boston, MA, American Meteorological Society, 1988, p. J1-J8.

A project aimed at improving upon the present manual methods of satellite-based oceanographic analysis is described which is based on a combination of interactive and automated computer techniques. A suitable system configuration contains a mainframe computer to perform preprocessing functions and a PC-class microprocessor to perform image analysis and product generation. These components are described and the main outstanding development issues are discussed. C.D.

A88-33150

SPARSE-APERTURE MICROWAVE RADIOMETERS FOR EARTH REMOTE SENSING

ANDREW S. MILMAN (Michigan, Environmental Research Institute,

Ann Arbor) Radio Science (ISSN 0048-6604), vol. 23, Mar.-Apr. 1988, p. 193-205. Research supported by the Environmental Research Institute of Michigan. refs

Passive microwave instruments for remote sensing of the Earth's surface from space can measure many meteorological parameters in the absence of daylight and in the presence of clouds. Because of the large apertures that are required to achieve good spatial resolution (1-5 km) at microwave frequencies, these radiometers should be arrays of small antenna elements that are arranged so that the collecting area of the radiometer is much smaller than that of a conventional, solid scanning antenna with the same spatial resolution. Despite the various methods that might be used for combining the signals from the different array elements and the different ways the elements might be arranged, the sensitivity depends almost exclusively on the collecting area, integration time, RF bandwidth, and the system temperature. Interferometers and phased arrays have limitations on their bandwidths that depend on the size of the array; beam-forming arrays are not so limited. A cross antenna is considered in some detail as an example of a sparse-aperture radiometer. It has 5-km resolution from an 800-km orbit and significantly better sensitivity than the equivalent conically scanning parabolic antenna, while it has only 10 percent of the collecting area and no moving parts.

Author

A88-33416* National Aeronautics and Space Administration. Goddard Space Flight Center, Greenbelt, Md.

A SATELLITE INFRARED TECHNIQUE TO ESTIMATE TROPICAL CONVECTIVE AND STRATIFORM RAINFALL

ROBERT F. ADLER and ANDREW J. NEGRI (NASA, Goddard Space Flight Center, Greenbelt, MD) Journal of Applied Meteorology (ISSN 0733-3021), vol. 27, Jan. 1988, p. 30-51. refs

A new method of estimating both convective and stratiform precipitation from satellite infrared data is described. This technique defines convective cores and assigns rain rate and rain area to these features based on the infrared brightness temperature and the cloud model approach of Adler and Mack (1984). The method was tested for four south Florida cases during the second Florida Area Cumulus Experiment, and the results are presented and compared with three other satellite rain estimation schemes.

C.D.

A88-33429* National Aeronautics and Space Administration. Goddard Space Flight Center, Greenbelt, Md.

TROPICAL RAINFALL MEASURING MISSION (TRMM)

THOMAS KEATING (NASA, Goddard Space Flight Center, Greenbelt, MD) IN: EASCON '87; Proceedings of the Twentieth Annual Electronics and Aerospace Systems Conference, Washington, DC, Oct. 14-16, 1987. New York, Institute of Electrical and Electronics Engineers, Inc., 1987, p. 21-32.

By measuring rainfall in the tropics, the Tropical Rainfall Measuring Mission (TRMM) will make possible the understanding of the heat engine that drives the global weather. The TRMM mission parameters are given, and the spacecraft is described. The instruments are examined, including the precipitation radar, TRMM microwave radiometer, and Advanced Very High Frequency Radiometer. The mission life is addressed, including atmospheric data, fuel consumption, and life extension methods. The spacecraft interfaces, payload configuration, and deployment sequence are considered. The subsystems are described, including propulsion, power, command, data handling, and tracking. A Japanese Experimental Data Relay Tracking Satellite experimental package working with TRMM is briefly addressed.

C.D.

A88-33742* National Aeronautics and Space Administration. Goddard Space Flight Center, Greenbelt, Md.

A PROPOSED TROPICAL RAINFALL MEASURING MISSION (TRMM) SATELLITE

JOANNE SIMPSON, ROBERT F. ADLER (NASA, Goddard Space Flight Center, Greenbelt, MD), and GERALD R. NORTH (Texas A & M University, College Station) American Meteorological Society, Bulletin (ISSN 0003-0007), vol. 69, March 1988, p. 278-295. refs

The proposed Tropical Rainfall Measuring Mission (TRMM) satellite (presently in its third year of planning), is described. The TRMM satellite, planned for an operational duration of at least three years beginning in the mid-1990s, is intended to obtain high-quality measurements of tropical precipitation by means of information derived from a quantitative spaceborne radar, a multichannel passive microwave radiometer, and an AVHRR. The satellite's orbit will be low-altitude (320 km), for high resolution, and low-inclination (30 to 35 deg), for making it possible to visit each sampling area twice a day. Radar and passive microwave algorithms and rain-retrieval algorithms to be used in precipitation measurements are discussed together with cloud dynamical models designed to test these algorithms. I.S.

A88-33832

TECHNIQUE FOR THE INSTRUMENTED INTERPRETATION OF SPACE SCANNER IMAGERY OF THE EARTH'S CLOUD COVER [METODIKA INSTRUMENTAL'NOGO DESHIFRIROVANIYA MATERIALOV KOSMICHESKOI SKANERNOI S'EMKI OBLACHNOGO POKROVA ZEMLI]

A. I. SHAROV Geodeziya i Aerofotos'emka (ISSN 0536-101X), no. 5, 1987, p. 95-98. In Russian.

Results of the instrumented interpretation of scanner images obtained with meteorological satellites are presented. The MSP-4 synthesizing device is used to process bispectral imagery of the earth's cloud cover, and a masking technique is used to identify the structural features of cloud formations. The proposed technique is verified using data from the NOAA 6, 9, and 10 satellites. B.J.

A88-33872

CLIMATOLOGICAL INTERPRETATION OF TIME SERIES OF SATELLITE OBSERVATIONS OF THE EARTH'S RADIATION BALANCE [KLIMATOLOGICHESKAIA INTERPRETATSIIA VREMENNYKH RIADOV SPUTNIKOVYKH NABLIUDENII RADIATSIONNOGO BALANSA ZEMLI]

G. I. MARCHUK, K. IA. KONDRATEV, and V. V. KOZODEROV Akademiya Nauk SSSR, Doklady (ISSN 0002-3264), vol. 299, no. 1, 1988, p. 88-94. In Russian. refs

A method for the reliable determination of climatic-effect regions of energy active ocean zones is developed. The method involves a principal-components analysis of mean-monthly field anomalies of the outgoing long-wavelength radiation with a step of 5 deg for the whole globe. The data used include time series for observations made with NOAA (1974-1977) and Nimbus-7 (1978-1983) satellites. B.J.

A88-35154

ERS-1, EARTH RESOURCES SATELLITE-1 AND FUTURE EARTH OBSERVATION PROGRAM IN JAPAN

YUJI MIYACHI, YASUSHI HORIKAWA (National Space Development Agency of Japan, Tokyo), and YOSHIKAZU KAMIYA (National Space Development Agency of Japan, Los Angeles, CA) IN: Aerospace century XXI: Space sciences, applications, and commercial developments; Proceedings of the Thirty-third Annual AAS International Conference, Boulder, CO, Oct. 26-29, 1986. San Diego, CA, Univelt, Inc., 1987, p. 1623-1630. (AAS PAPER 86-289)

The development of the Earth Resources Satellite-1, the follow-on to the MOS-1 satellite, is discussed. The mission objectives of the ERS-1 are summarized and its sensors and spacecraft characteristics are described. The satellite orbital elements are listed. The functions of the ERS-1 sensors are stated and the developmental status is described. NASDA activities in data reception and processing relevant to the ERS-1 project and the role of NASDA in the international earth observation effort are discussed. C.D.

A88-35155

SPOT 1 - INTERNATIONAL COMMERCIALIZATION OF REMOTE SENSING

PIERRE BESCOND (Spotimage, Reston, VA) IN: Aerospace century XXI: Space sciences, applications, and commercial developments; Proceedings of the Thirty-third Annual AAS

International Conference, Boulder, CO, Oct. 26-29, 1986. San Diego, CA, Univelt, Inc., 1987, p. 1631-1636. (AAS PAPER 86-299)

The role of the Spot satellite in the French and in the international remote sensing effort is considered. The Spot satellite system and its ground segment are described, showing the functioning of the satellite as a remote sensor and the role of the ground segment in market distribution. Further innovations being made on Spot are addressed, and Spot's impact on the remote sensing industry is assessed. C.D.

A88-35159* Jet Propulsion Lab., California Inst. of Tech., Pasadena.

PRECISION POSITIONING OF EARTH ORBITING REMOTE SENSING SYSTEMS

WILLIAM G. MELBOURNE, T. P. YUNCK, and S. C. WU (California Institute of Technology, Jet Propulsion Laboratory, Pasadena) IN: Aerospace century XXI: Space sciences, applications, and commercial developments; Proceedings of the Thirty-third Annual AAS International Conference, Boulder, CO, Oct. 26-29, 1986. San Diego, CA, Univelt, Inc., 1987, p. 1677-1694. refs (AAS PAPER 86-398)

Decimeter tracking accuracy is sought for a number of precise earth sensing satellites to be flown in the 1990's. This accuracy can be achieved with techniques which use the Global Positioning System (GPS) in a differential mode. A precisely located global network of GPS ground receivers and a receiver aboard the user satellite are needed, and all techniques simultaneously estimate the user and GPS satellite states. Three basic navigation approaches include classical dynamic, wholly nondynamic, and reduced dynamic or hybrid formulations. The first two are simply special cases of the third, which promises to deliver subdecimeter accuracy for dynamically unpredictable vehicles down to the lowest orbit altitudes. The potential of these techniques for tracking and gravity field recovery will be demonstrated on NASA's Topex satellite beginning in 1991. Applications to the Shuttle, Space Station, and dedicated remote sensing platforms are being pursued. Author

A88-35162
POTENTIAL FOR EARTH OBSERVATIONS FROM THE MANNED SPACE STATION

JAMES V. TARANIK (Nevada, University, Reno) IN: Aerospace century XXI: Space sciences, applications, and commercial developments; Proceedings of the Thirty-third Annual AAS International Conference, Boulder, CO, Oct. 26-29, 1986. San Diego, CA, Univelt, Inc., 1987, p. 1725-1729. (AAS PAPER 86-426)

This paper outlines a few potential uses of the Manned Space Station for earth observations and sensor development in support of earth observations. The way the Space Station can assist in earth-based observations is briefly considered. The advantages of the Space Station for instrument development and for calibrating free-flying instruments are addressed. C.D.

A88-35395
CANADIAN LARGE-SCALE AERIAL PHOTOGRAPHIC SYSTEMS (LSP)

RAY D. SPENCER (Melbourne, University, Creswick, Australia) and R. J. HALL (Canadian Forestry Service, Edmonton, Canada) Photogrammetric Engineering and Remote Sensing (ISSN 0099-1112), vol. 54, April 1988, p. 475-482. Research supported by the Canadian Forestry Service, University of Melbourne, and University of British Columbia. refs

This paper reviews Canadian approaches for acquiring and processing large scale aerial photographs (LSP). Developments in Canada show that large scale aerial photographs (LSP) can be used as a sampling tool and so reduce the need for expensive and slow ground surveys in forest inventories. The use of LSP is a two-step process involving photo acquisition and analysis, with both steps requiring specialized equipment and techniques to ensure efficient recording, extraction, and processing of data. Canadians have pioneered two different photographic approaches

and tested various measurement-interpretation systems. One photographic approach uses twin-vertical 70-mm cameras mounted on a fixed air base; the other uses single-camera, timed-interval photography with a radar or laser altimeter and in-flight recording of tilt. The major systems for photo analysis use analytical stereo digitizers and computers to extract and process data. Author

A88-35396
DIFFERENCES IN VISIBLE AND NEAR-IR RESPONSES, AND DERIVED VEGETATION INDICES, FOR THE NOAA-9 AND NOAA-10 AVHRRS - A CASE STUDY

K. P. GALLO (NOAA, Satellite Research Laboratory, Washington, DC) and J. C. EIDENSHINK (TGS Technology, Inc., Sioux Falls, SD) Photogrammetric Engineering and Remote Sensing (ISSN 0099-1112), vol. 54, April 1988, p. 485-490. refs

This study evaluates the differences in the visible and near-IR responses of the Advanced Very High Resolution Radiometers (AVHRR) of the National Oceanic and Atmospheric Administration (NOAA)-9 and -10 satellites for coincident sample locations. The study also evaluates the differences in vegetation indices computed from those data. Data were acquired of the southeast portion of the United States for the 6 December 1986 daylight orbits of NOAA-9 and NOAA-10 satellites. The data sets were registered and 38 coincident sample locations were selected that included land and water surfaces. The data were calibrated to reflectance values with coefficients supplied by NOAA. The visible and near-IR reflectance values and the derived vegetation index values of the NOAA-9 AVHRR were usually greater than those of the NOAA-10. Visible and near-IR reflectance values exhibited trends that appeared to be related to the satellite scan angles at the examined sample locations. Linear relationships were developed between the vegetation indices of the two systems. The vegetation index values for the NOAA-9 and NOAA-10 AVHRR displayed nearly constant differences for a variety of surface features. The results suggest that, with appropriate gain and offset, the vegetation indices of the two sensor systems may be interchangeable for assessment of land surfaces. Author

A88-35968
IMAGING INSTRUMENT OF THE VEGETATION PAYLOAD (SPOT 4)

R. KRAWCZYK and G. CERUTTI-MAORI (Aerospatiale, Cannes, France) IN: Optical systems for space applications; Proceedings of the Meeting, The Hague, Netherlands, Mar. 30-Apr. 1, 1987. Bellingham, WA, Society of Photo-Optical Instrumentation Engineers, 1987, p. 125-131.

The SPOT-4 Vegetation Payload is designed for an operational global-scale survey of earth vegetation as well as for the observation of ocean areas. The push-broom imaging instrument is intended to measure ground albedo simultaneously in five spectral bands from 0.43 to 1.70 microns. A general description is given of the imaging instrument, followed by an examination of the performance of the instrument component parts. The calibration device is described, and some radiometric results are presented. B.J.

A88-36378
SPACE SHUTTLE LARGE FORMAT CAMERA PHOTOGRAPHY AND RESOURCE MANAGEMENT

JERRY D. GREER (USDA, Forest Service, Salt Lake City, UT) IN: Airborne reconnaissance XI; Proceedings of the Meeting, San Diego, CA, Aug. 17, 18, 1987. Bellingham, WA, Society of Photo-Optical Instrumentation Engineers, 1988, p. 11-21. refs

In October 1984 the Space Shuttle Challenger carrying the Large Format Camera (LFC) took 2134 photographs of the earth's land, oceans, and clouds. In this experiment, the precision cartographic LFC was used to take vertical aerial photographs on a strip of film made up of four different emulsions. An exceptionally cloudy weather system in North America and Europe caused most of primary photography sites to be obscured. Many photographs were therefore taken of secondary sites. The U.S. Department of Agriculture Forest Service participated in this experiment by

identifying many photographic test sites in the U.S. When the mission was flown, most of the National Forests selected were obscured by clouds. Author

A88-37126**REMOTE SENSING APPLICATIONS IN METEOROLOGY AND CLIMATOLOGY; PROCEEDINGS OF THE NATO ADVANCED STUDY INSTITUTE, DUNDEE, SCOTLAND, AUG. 17-SEPT. 6, 1986**

ROBIN A. VAUGHAN, ED. (Dundee, University, Scotland) Institute sponsored by NATO. Dordrecht, D. Reidel Publishing Co. (NATO ASI Series. Volume C201), 1987, 492 p. For individual items see A88-37127 to A88-37150.

The theoretical principles of remote sensing and its operational and experimental application to meteorology and climatology are examined in reviews and reports. Topics addressed include cloud formations seen by satellite; sources of variance in the upwelling radiance field; data reception, archiving, and distribution; image processing, pattern recognition, and AI; vertical sounding from satellites; the impact of satellite data on global numerical weather prediction; and satellite studies of synoptic and mesoscale atmospheric features. Consideration is given to cloud-motion analysis of cyclones within cold air masses, multispectral classification of clouds and fog, remote sensing of sea-surface winds, surface energy budgets and temperatures, and thermal inertia. Also discussed are advanced instruments being developed for ERS-1 and the Columbus polar platform of the International Space Station. T.K.

A88-37127**CLOUD FORMATIONS SEEN BY SATELLITE**

R. S. SCORER (Imperial College of Science and Technology, London, England) IN: Remote sensing applications in meteorology and climatology; Proceedings of the NATO Advanced Study Institute, Dundee, Scotland, Aug. 17-Sept. 6, 1986. Dordrecht, D. Reidel Publishing Co., 1987, p. 1-18. refs

The remote sensing of cloud formations by NOAA AVHRR and CZCS satellite instruments is surveyed. The instruments and their observing channels are listed and briefly described, with particular attention to day and night observations; intensity, absorption, and directional scattering; cloud brightness; shadows and haze; sun glint; and hot spots. Cloud formations characterized include lee waves, billows, orographic and Föhn cirrus, jet streams, warm-front instability, streets and cells, anvil and other plumes, and isolated lines such as rope clouds and ship trails. The use of archived remote-sensing images in climatological studies is illustrated for the cases of the Greenland barrier and ship trails. T.K.

A88-37129**THE PHYSICAL PRINCIPLES CONTROLLING THE REMOTE SENSING PROCESS**

M. J. DUGGIN (New York, State University, Syracuse) IN: Remote sensing applications in meteorology and climatology; Proceedings of the NATO Advanced Study Institute, Dundee, Scotland, Aug. 17-Sept. 6, 1986. Dordrecht, D. Reidel Publishing Co., 1987, p. 33-50. refs

The physical principles controlling the reflection and emission of radiation from natural and man-made surfaces are considered. Topics addressed include the interaction of the downwelling radiance field with the atmosphere, the interaction of the global irradiance field with the anisotropic reflectance, the absorbance and emissivity characteristics of clouds and of terrestrial surfaces, and the interaction of the upwelling radiance field with the sensor. The impact of these features and their interactions is examined for the bands 0.4-2.0, 3.5-4.1, and 8-12 microns. The need for sensors capable of recording radiance with high S/N in several different portions of the spectrum to discriminate cloud and land cover types is indicated. Author

A88-37130**SENSORS TO RECORD ATMOSPHERIC AND TERRESTRIAL INFORMATION - PRINCIPLES OF COLLECTION AND ANALYSIS**

M. J. DUGGIN (New York, State University, Syracuse) IN: Remote sensing applications in meteorology and climatology; Proceedings of the NATO Advanced Study Institute, Dundee, Scotland, Aug. 17-Sept. 6, 1986. Dordrecht, D. Reidel Publishing Co., 1987, p. 51-68. refs

The general principles and current status of staring and scanning sensors for satellite remote sensing of land and sea surfaces and atmospheric parameters are reviewed. The types of information obtainable in the different spectral bands are indicated; the common characteristics and specific features of sensors are listed in extensive tables and discussed; and a chronological diagram of U.S. meteorological and earth-resources satellites is provided. T.K.

A88-37132**MICROWAVE INSTRUMENTS AND METHODS**

G. E. PECKHAM (Heriot-Watt University, Edinburgh, Scotland) IN: Remote sensing applications in meteorology and climatology; Proceedings of the NATO Advanced Study Institute, Dundee, Scotland, Aug. 17-Sept. 6, 1986. Dordrecht, D. Reidel Publishing Co., 1987, p. 87-106. refs

The basic principles and current status of satellite remote sensing of the earth surface and atmosphere using active and passive microwave sensors are reviewed. Consideration is given to nadir and limb sounding of the atmosphere; radiometry of surface properties, liquid water, and integrated water vapor; scatterometry for ocean wind estimation; sea-surface altimetry; and high-resolution SAR imaging of surface features. Technological aspects examined include antennas, power sources, receivers, radiometers and calibration, spectrum analysis, and radar instrumentation. T.K.

A88-37145**CLOUD CLIMATOLOGIES FROM SPACE AND APPLICATIONS TO CLIMATE MODELLING**

A. HENDERSON-SELLERS and K. MCGUFFIE (Liverpool, University, England) IN: Remote sensing applications in meteorology and climatology; Proceedings of the NATO Advanced Study Institute, Dundee, Scotland, Aug. 17-Sept. 6, 1986. Dordrecht, D. Reidel Publishing Co., 1987, p. 359-373. refs (Contract AF-AFOSR-86-0118)

Global satellite-derived cloud climatologies are considered, and the results of an automated cloud-analysis model are presented. The zonal distribution of cloud is applied to the radiative fluxes as predicted by an energy balance model. Special-channel cloud discrimination is discussed with reference to the Landsat Thematic Mapper. Author

A88-37150**REMOTE SENSING IN THE SPACE STATION AND COLUMBUS PROGRAMMES**

D. D. HARDY (British National Space Centre, London, England) IN: Remote sensing applications in meteorology and climatology; Proceedings of the NATO Advanced Study Institute, Dundee, Scotland, Aug. 17-Sept. 6, 1986. Dordrecht, D. Reidel Publishing Co., 1987, p. 441-450.

Plans for terrestrial remote sensing from the International Space Station are reviewed, with an emphasis on ESA activities (the Columbus program). The advantages of large, long-duration (servicable) multiple-instrument platforms for remote sensing are indicated; the history of the Space Station and Columbus is briefly traced; and relevant results from the UK Space Station Utilization Study (1986) are summarized in tables. It is concluded that the two unmanned polar platforms planned for the Space Station will meet most, but not all, of the remote-sensing objectives identified in the study. It is pointed out, however, that two such platforms will overload the data-relay capacity of TDRSS and the proposed ESA DRS systems. T.K.

A88-37279#

NON-TRACKING ANTENNA SYSTEMS FOR THE ACQUISITION OF NOAA HRPT DATA

M. WEGENER, G. LENNON, D. BOWERS, J. BRANDWYK, G. WILKINS (South Australia, Flinders University, Bedford Park, Australia) et al. IN: National Space Engineering Symposium, 3rd, Canberra, Australia, June 30-July 2, 1987, Preprints of Papers. Barton, Australia/Brookfield, VT, Institution of Engineers/Brookfield Publishing Co., 1987, p. 238-240.

A concept for a NOAA HRPT receiving station using an array of yagi-type antennae instead of a tracking dish is described. It has been shown that a pointing array of antennae can provide a sufficient signal level for the reliable acquisition of NOAA HRPT data from a spatially limited area of interest. Author

A88-37286#

SPACEBORNE RADAR X-SAR FOR CIVIL APPLICATIONS

HANS MARTIN BRAUN and HELMUT KAPPEL *Dornier-Post* (English Edition) (ISSN 0012-5563), no. 1, 1988, p. 16-18.

The X-band SAR that is scheduled to fly in a joint mission with NASA's two-frequency Shuttle Imaging Radar SIR-C in 1991 is designed for simultaneous earth measurements at 1.3, 5.3, and 9.6 GHz frequencies, in order to furnish investigators with radar images having different signatures from a given target scene. In conjunction with SIR-C, X-SAR will furnish enhanced multispectral/dual-polarization data pertinent to biogeochemical cycles, hydrologic cycles, and global climate changes. Attention is given to real-time SAR signal processing capabilities. O.C.

A88-37336#

RETRIEVAL OF ATMOSPHERIC TEMPERATURE STRUCTURE FROM THE NOAA-9 SATELLITE

CHAOHUA DONG and FENGYING ZHANG (Satellite Meteorological Center, People's Republic of China) *Chinese Journal of Infrared Research* (ISSN 0258-7114), vol. 7A, no. 2, 1988, p. 125-130. In Chinese, with abstract in English.

In this paper, a statistical regression with a matching algorithm has been described to retrieve the atmospheric temperature structure from the NOAA-9 satellite. The calculated temperatures are verified by comparison with radiosondes over the China region. The study shows that the root-mean-square (rms) difference is about 2.3 C over the middle and low latitude area and about 3.0 C over the higher latitude area. The largest differences are near the ground and in the tropopause region, particularly over land with complicated topography. Author

A88-37383#

G.P.S. SURVEYING IN THE NETHERLANDS

H. J. W. VAN DER VEGT (Rijkswaterstaat, Delft, Netherlands) IN: Institute of Navigation, Technical Meeting, 1st, Colorado Springs, CO, Sept. 21-25, 1987, Proceedings. Washington, DC, Institute of Navigation, 1987, p. 49-56.

The Global Positioning System (G.P.S.) shows very promising results, which will cause enormous changes in the survey community in the next decade. Those changes will affect both the landsurveying and marine surveying activities. Some results, recently obtained at the Survey Department will be discussed, showing the possibility of integrating G.P.S. measurements in local geodetic networks. Concerning highly accurate dynamic applications, results obtained with two Sercel TR5SB receivers in a differential mode are compared with the results from an optical tracking system. The analysis shows the possibility to achieve accuracies at the decimeter level under dynamic conditions. The first preliminary results of a project aimed at the use of GPS in an airplane for photogrammetric mapping also shows accuracies at the few decimeter level. Author

A88-37384#

DEVELOPMENTS IN USE OF GPS AS RANGE TSPI

DARWIN G. ABBY (General Dynamics Services Co., Yuma, AZ) IN: Institute of Navigation, Technical Meeting, 1st, Colorado Springs, CO, Sept. 21-25, 1987, Proceedings. Washington, DC, Institute of Navigation, 1987, p. 57-61.

Techniques developed at US Army Yuma Proving Ground to evaluate GPS receiver designs and performance have been applied to demonstrate a capability to generate Time and Space Position Information (TSPI) using GPS. Flight test data collected on developmental GPS receivers is post-processed using differential GPS concepts to produce GPS based TSPI. The UPG laser tracking system is used to evaluate GPS TSPI performance. The differences between the two systems show that the accuracies of each are comparable and in the 3-5 m area. Existing capabilities and resources are described and results are presented. A concept is proven which proposes that every GPS equipped vehicle is a mobile test range. Author

A88-37391#

THE MAGNAVOX CIVIL AND MILITARY LINE OF GPS RECEIVERS - A TECHNOLOGY AND APPLICATIONS OVERVIEW

THOMAS A. STANSELL, JR. (Magnavox Advanced Products and Systems Co., Torrance, CA) IN: Institute of Navigation, Technical Meeting, 1st, Colorado Springs, CO, Sept. 21-25, 1987, Proceedings. Washington, DC, Institute of Navigation, 1987, p. 109-118. refs

Eleven different GPS receivers are described, including both military and commercial versions for land, sea, and air navigation. The receivers cover applications including geodetic land surveying, differential navigation with and without pseudolites, parachute descent navigation, and GPS integrated with an inertial navigation system. The receiver configurations range from complete packages to original equipment manufacturer modules. R.R.

A88-37416

AN UPDATE ON VISIBLE AND NEAR INFRARED CALIBRATION OF SATELLITE INSTRUMENTS

JOHN C. PRICE (USDA, Remote Sensing Research Laboratory, Beltsville, MD) *Remote Sensing of Environment* (ISSN 0034-4257), vol. 24, April 1988, p. 419-422. refs

Additions and corrections are given to the calibration of visible/near-infrared satellite instruments provided by Price (1987). The impact of the change of presentation of Channel 4 data from the Landsat multispectral scanner from six bits to seven bits is considered. It is noted that the SPOT instruments in orbit have different characteristics, particularly band central wavelength, than those previously considered by Price based on preliminary information. Instrument calibration for the Landsat Thematic Mapper and NOAA AVHRR instruments is also discussed. R.R.

A88-38411

EARTH OBSERVATION: CAPTURING THE IMAGERY - REMOTE SENSING DEPENDS ON ADVANCED RECORDING TECHNOLOGY

Space Markets (ISSN 0258-4212), Spring 1988, p. 40-43.

Problems involved in capturing earth-observation data aboard satellites and receiving and storing it on the ground are addressed, in addition to the means adopted to overcome them. Longitudinal rather than rotary-head recording are used by the SPOT data recorders, providing the benefits of fixed heads and the elimination of rapidly rotating scanners. Recent recording technologies discussed include active tape tracking, application specific integrated circuits, and high-speed word generators and error rate counters. The use of fully-automatic bit synchronization, error elimination techniques, and high density rates in ground-segment data storage is also considered. R.R.

A88-39919

COMPARATIVE ANALYSIS OF RESULTS OF PHOTOGRAPHIC OBSERVATIONS OF NATURAL OBJECTS FROM SALYUT-7 [SRAVNITEL'NYI ANALIZ REZUL'TATOV FOTOS'EMKI PRIRODNYKH OB'EKTOV SO STANTSII 'SALIUT-7']

L. A. RONZHIN and I. U. L. RESHTOGA *Geodeziia i Kartografiia* (ISSN 0016-7126), April 1988, p. 45-47. In Russian. refs

Photographs taken from space in spectral bands 10 and 40 nm wide are compared. It is shown that, in the 10-nm case, it is possible to satisfactorily identify a significant number of natural

objects, as well as to substantially enhance the contrast of objects on the background. Here, a positive effect is achieved for various natural objects, including soils, rocks, vegetation, and water bodies. B.J.

A88-40351#

SIR-B EXPERIMENTS IN JAPAN. I - SENSOR CALIBRATION EXPERIMENT

MASARU ICHINOSE, YOSHIMATSU ECHIZENYA, MITSUHIRO KAMATA, EIJI KAWAI, NORIHISA HIROMOTO et al. Radio Research Laboratory, Journal (ISSN 0033-8001), vol. 35, March 1988, p. 3-27. refs

A sensor calibration experiment was proposed as part of SIR-B experiments in Japan, together with the rice crop experiment and the ocean oil-pollution detection experiment. This sensor calibration experiment was intended (1) to establish a transfer function from image data to radar backscattering characteristics, (2) to evaluate 3-dB resolutions, (3) to verify the ability to resolve two closely-spaced targets, and (4) to clarify sidelobe structures due to range and azimuth compressions. The disused Akita Airport was chosen as the main test site for the calibration experiment on the first three objectives. This paper describes the test site, the design of the corner reflectors, and briefly predicts the results. Author

A88-40785*# National Aeronautics and Space Administration. National Space Technology Labs., Bay Saint Louis, Miss.

USING THE THERMAL INFRARED MULTISPECTRAL SCANNER (TIMS) TO ESTIMATE SURFACE THERMAL RESPONSES

J. C. LUVALL (NASA, National Space Technology Laboratories, Bay Saint Louis, MS) and H. R. HOLBO (Oregon State University, Corvallis) International Conference on Measurement of Soil and Plant Water Status, Utah State University, Logan, July 6-10, 1987, Paper. 7 p. refs

(Contract NAGW-924; NAS13-268)

A series of measurements was conducted over the H.J. Andrews, Oregon, experimental coniferous forest, using airborne thermal infrared multispectral scanner (TIMS). Flight lines overlapped, with a 28-min time difference between flight lines. Concurrent radiosonde measurements of atmospheric profiles of air temperature and moisture were used for atmospheric radiance corrections of the TIMS data. Surface temperature differences over time between flight lines were used to develop thermal response numbers (TRNs) which characterized the thermal response (in KJ/sq m/C, where K is the measured incoming solar radiation) of the different surface types. The surface types included a mature forest (canopy dominated by dense crowns of *Pseudotsuga menziesii*, with a secondary canopy of dense *Tsuga heterophylla*, and also a tall shrub layer of *Acer circinatum*) and a two-year-old clear-cut. The temperature distribution, within TIMS thermal images was found to reflect the surface type examined. The clear-cut surface had the lowest TRN, while mature Douglas fir the highest. I.S.

A88-41093

GEOGRAPHIC STUDY OF THE NORTH COAST OF SENEGAL USING MOMS-1 SATELLITE DATA [ETUDE GEOGRAPHIQUE DE LA COTE NORD DU SENEGAL A PARTIR DES DONNEES SATELLITAIRES MOMS-1]

A. T. DIAW (Institut Fondamental d'Afrique Noire, Dakar, Senegal) and G. JOLY (Institut de Geographie, Paris, France) Societe Francaise de Photogrammetrie et de Teledetection, Bulletin (ISSN 0244-6014), no. 108, 1987, p. 5-23. In French. refs

The MOMS-1 (Modular Optoelectronic Multispectral Scanner) remote sensing system was used to obtain images of the Senegal River delta and the Atlantic coast in the Lompoul region. The MOMS images have a ground resolution of 20 x 20 m. Products such as digital data stored on tape, 1:800,000 images on film, and quick-looks are produced by the MOMS system. Data processing techniques described include histogram production, mathematical transformations for smoothing, the automatic detection of landscape boundaries based on luminance values

obtained by Sobel nonlinear filtering, and the determination of ground irradiance and classification indexes. The kinematics of aeolian formations is also considered. R.R.

A88-41943

AMERICAN SOCIETY FOR PHOTOGRAMMETRY AND REMOTE SENSING AND ACSM, FALL CONVENTION, RENO, NV, OCT. 4-9, 1987, ASPRS TECHNICAL PAPERS

Convention sponsored by the American Society for Photogrammetry and Remote Sensing and ACSM. Falls Church, VA, American Society for Photogrammetry and Remote Sensing, 1987, 423 p. For individual items see A88-41944 to A88-41958.

Recent advances in remote-sensing technology and applications are examined in reviews and reports. Topics addressed include the use of Landsat TM data to assess suspended-sediment dispersion in a coastal lagoon, the use of sun incidence angle and IR reflectance levels in mapping old-growth coniferous forests, information-management systems, Large-Format-Camera soil mapping, and the economic potential of Landsat TM winter-wheat crop-condition assessment. Consideration is given to measurement of ephemeral gully erosion by airborne laser ranging, the creation of a multipurpose cadaster, high-resolution remote sensing and the news media, the role of vegetation in the global carbon cycle, PC applications in analytical photogrammetry, multispectral geological remote sensing of a suspected impact crater, fractional calculus in digital terrain modeling, and automated mapping using GP-based survey data. T.K.

A88-41956

AN APPROACH FOR EMULATING THE COLOR BALANCE OF LANDSAT MULTISPECTRAL SCANNER IMAGES WITH AVHRR DATA

BILL P. CLARK (Computer Sciences Corp., Silver Spring, MD), FRANK G. SADOWSKI (TGS Technology, Inc., Sioux Falls, SD), and A. J. JOHNSON (Central Intelligence Agency, Langley, VA) IN: American Society for Photogrammetry and Remote Sensing and ACSM, Fall Convention, Reno, NV, Oct. 4-9, 1987, ASPRS Technical Papers. Falls Church, VA, American Society for Photogrammetry and Remote Sensing, 1987, p. 331-341. (Contract USGS-14-08-0001-22521)

A mathematical procedure was developed for transforming the red and near-infrared (NIR) spectral bands of Advanced Very High Resolution Radiometer (AVHRR) data (bands 1 and 2) into three-band data space that approximates the response of Landsat Multispectral Scanner System (MSS) bands 1, 2, and 4. Color images incorporating the transformed AVHRR data emulate much of the tone and color balance of Landsat MSS color-infrared composite images. Comparative vegetative index calculations using the transformed AVHRR data and MSS data are well suited for combined visual and digital applications and can be used in multi-level sampling approaches to large-area monitoring programs. Author

A88-41976

SLAR AS A RESEARCH TOOL

G. P. DE LLOOR and P. HOOGEBOOM (Centrale Organisatie voor Toegepast-Natuurwetenschappelijk Onderzoek, The Hague, Netherlands) IN: Remote sensing for resources development and environmental management; Proceedings of the Seventh International Symposium, Enschede, Netherlands, Aug. 25-29, 1986. Volume 1. Rotterdam, A. A. Balkema, 1986, p. 115, 116. refs

In the early seventies for some time an FMI real aperture X-band SLAR with imaging on film was flown in the Netherlands. It showed many new and unexpected phenomena, in particular over the sea. It soon became clear that for a closer investigation of these phenomena an absolute and digital system is necessary. Being simple and straightforward and still giving sufficient coverage and resolution for the research purposes under consideration, a real aperture system was chosen. Its final construction and implementation required the efforts of several institutes. Radiometric and geometric errors caused by unwanted aircraft motions can now be corrected during the data processing and

08 INSTRUMENTATION AND SENSORS

resampling, resulting in a presentation of the data in a map corrected format. The radiometric accuracy of the system and its internal and external calibration are discussed. Author

A88-41985

SHUTTLE IMAGING RADAR (SIR-A) INTERPRETATION OF THE KASHGAR REGION IN WESTERN XINJIANG, CHINA
DIRK WERLE (F. G. Bercha and Associates /Ontario/, Ltd., Ottawa, Canada) IN: Remote sensing for resources development and environmental management; Proceedings of the Seventh International Symposium, Enschede, Netherlands, Aug. 25-29, 1986. Volume 1. Rotterdam, A. A. Balkema, 1986, p. 187-192. refs

A88-41990

INSERTION OF HYDROLOGICAL DECORRELATED DATA FROM PHOTOGRAPHIC SENSORS OF THE SHUTTLE IN A DIGITAL CARTOGRAPHY OF GEOPHYSICAL EXPLORATION (SPACELAB 1-METRIC CAMERA AND LARGE FORMAT CAMERA)

G. GALIBERT IN: Remote sensing for resources development and environmental management; Proceedings of the Seventh International Symposium, Enschede, Netherlands, Aug. 25-29, 1986. Volume 1. Rotterdam, A. A. Balkema, 1986, p. 251-255. refs

Microphotographic enlargements of space images from the Shuttle Metric Camera and Large Format Camera are combined with digital maps from airborne sensors to produce flight documents for different aerial geophysical surveys through various data transmission networks using the Telecom 1 and Inmarsat satellites. Two IR 2443 false-color images and one black and white XX positive first copy from the Metric Camera and two black and white 3414 positive first copies from the Large Format Camera are compared. The compression of data using a digitalization of colors and problems of storage and daily transmission from central offices to field bases are discussed. R.B.

A88-41995

SELECTION OF BANDS FOR A NEWLY DEVELOPED MULTISPECTRAL AIRBORNE REFERENCE-AIDED CALIBRATED SCANNER (MARCS)

M. A. MULDER (Landbouwhogeschool, Wageningen, Netherlands), K. SCHURER (Technisch-Fysische Dienst voor de Landbouw, Wageningen, Netherlands), A. N. DE JONG (Centrale Organisatie voor Toegepast-Natuurwetenschappelijk Onderzoek, The Hague, Netherlands), and D. DE HOOP (International Institute for Aerospace Survey and Earth Sciences, Enschede, Netherlands) IN: Remote sensing for resources development and environmental management; Proceedings of the Seventh International Symposium, Enschede, Netherlands, Aug. 25-29, 1986. Volume 1. Rotterdam, A. A. Balkema, 1986, p. 301-303. refs

The principles of design and operation of a newly developed multispectral airborne reference-aided calibrated scanner (MARCS) are described. The 16-band MARCS contains, besides an array of detectors for the measurement of radiation reflected and emitted from the land surface, a reference sensor which measures the flux of radiation coming from above (from the sun and the sky) and a device for internal calibration of the signals derived from below, i.e., the reflected and emitted radiation of the land surface. The bands have a width between 50 nm and 150 nm in the 0.3-3 micron range but become broader in the 3-10 micron range. By the choice of the wavelength bands, the MARCS is suited for the detection of features on the surface of the earth of both mineralogical and agricultural interest. Both the reference and the calibration data are recorded during the flight, while the data processing is performed off line on a ground-based system. I.S.

A88-43227

ARTIFICIAL GCPS IN AIRCRAFT AND SATELLITE SCANNER IMAGERY

N. W. T. CHISHOLM and R. L. COLLIN (University College of

Wales, Aberystwyth) International Journal of Remote Sensing (ISSN 0143-1161), vol. 9, April 1988, p. 799-821. refs

Results are presented of an experiment to determine the feasibility of providing artificial ground control points (GCPs) for controlling geometrical rectification procedures which are necessary to correct airborne scanner data and satellite imagery. These tests suggest that if proper consideration is given to the various factors governing the detectability of targets, more accurate ground control may be provided. Author

A88-44231

COMPARISON OF RADAR AND MICROWAVE RADIOMETER TECHNIQUES FOR DETERMINING PERMITTIVITY [SRAVNENIE RADIOLOKATSIONNOGO I SVCH RADIOMETRICHESKOGO METODOV OPREDELENIIA DIELEKTRICHESKOI PRONITSAEMOSTI]

V. P. IAKOVLEV and I. P. VUZMAN (Gosudarstvennyi Nauchno-Issledovatel'skii Tsentr Izucheniia Prirodnykh Resursov, Moscow, USSR) Radiofizika (ISSN 0021-3462), vol. 31, no. 4, 1988, p. 421-425. In Russian. refs

Radar and microwave radiometer methods of permittivity measurement are examined for slightly rough surfaces. The accuracies of the two methods are compared, and attention is given to the areas where the application of the two techniques are advantageous. The results are pertinent to the remote sensing of the earth's surface. B.J.

A88-44306

CLOUD AND PRECIPITATION REMOTE SENSING AT 94 GHZ

ROGER M. LHERMITTE (Miami, University, FL) IEEE Transactions on Geoscience and Remote Sensing (ISSN 0196-2892), vol. 26, May 1988, p. 207-216. refs
(Contract DAAG29-84-K-0145)

The use of short millimeter-wave Doppler radars for the observation of clouds and precipitation is discussed. Attenuation and scattering (including Mie backscattering by raindrops) of this short-wavelength radiation by hydrometers is discussed as well as the sensitivity of such radars for the observation of clouds. I.E.

A88-44449

NEW FEATURES OF THE LMK AERIAL CAMERA SYSTEM

ULRICH ZETH Jena Review (ISSN 0448-9497), vol. 32, no. 4, 1987, p. 174-176.

Extended instrument functions of the LMK aerial camera system are presented. The new features include a lens cone of 210 mm focal length, the extension of the range of forward motion compensation, and the introduction of half stop increments to reduce the jumps in the shutter speed occurring in exposure control when changing the f-stop setting. The possibility of taking simultaneous photographs with several LMK systems, the optimization of the exposure of the fiducial marks and of the data margin images, and the additional exposure of alpha-numeric auxiliary data are also discussed. R.B.

A88-44450

KARTOFLEX - AN INSTRUMENT FOR COMPUTER-AIDED PHOTOINTERPRETATION AND MAP REVISION

WERNER MARCKWARDT and ARNOLD ZEMANN Jena Review (ISSN 0448-9497), vol. 32, no. 4, 1987, p. 183-185.

A computer-aided photointerpretation and map revision instrument is examined, giving a description of the instrument equipment and its applications. The viewing unit allows for continuous (between 2.4 and 12) magnification with panoptic systems. Another panoptic system allows for 0.8 to 4 magnification. The microcomputer system contains test, orientation, area calculation, and distance calculation programs. Uses of the system and its applications for map interpretation and verification are discussed. R.B.

A88-44519

COMPARATIVE EVALUATION OF THE LARGE FORMAT CAMERA, METRIC CAMERA, AND SHUTTLE IMAGING RADAR - A DATA CONTENT

C. P. LO (Georgia, University, Athens) Photogrammetric Engineering and Remote Sensing (ISSN 0099-1112), vol. 54, June 1988, p. 731-742. Research supported by the University of Georgia. refs

LFC photography, MC photography, and SIR-A data were evaluated on their thematic contents in satisfying the requirements for topographic mapping at 1:100,000 scale. The study area of Mobile, Alabama - Pensacola, Florida was selected because of the availability of these three types of images. USGS topographic maps at 1:24,000, 1:100,000, and 1:250,000 scales were used as a standard for comparison for the completeness of linear and areal features (LAFs). It was found that the LFC photography provided nearly complete areal features and a sufficient amount of linear features for topographic mapping. The MC photography was the worst of all in revealing LAFs, although planimetrically it was the most accurate. The SIR-A data revealed an adequate amount of LAFs to complement LFC and MC photography, especially in times of poor weather conditions. It was concluded that each type of space photograph alone could not provide sufficient details for 1:100,000-scale topographic mapping, and an approach to form stereopairs of different image types was suggested.

Author

N88-20715# Instituto de Pesquisas Espaciais, Sao Jose dos Campos (Brazil).

ANALYSIS FOR ARCHITECTURE FOR IMAGE PROCESSING [ANALISE DE ARQUITETURAS PARA PROCESSAMENTO DE IMAGENS]

CELSE LUIZ MENDES, GILBERTO GAMARANETO, JOSE CLAUDIO MURA, JUAN CARLOS PINTODEGARRIDO, and RICARDO CARTAXODESTODESOUSA Aug. 1987 18 p In PORTUGUESE Presented at the 1st Brazilian Symposium Computer Architecture-Parallel Processing, Gramado, RS, 13-15 May 1987

(INPE-4294-PRE/1165) Avail: NTIS HC A03/MF A01

After a brief introduction on image processing activities at INPE, the principal characteristics of the system family SITIM are presented, followed by a presentation of procedure types most utilized in image processing. Discussed are some options already tested for augmentation on the system execution, through the use of accelerator plates and, lastly, the perspectives for future development are presented, some in the areas of accelerator plates, as systems based on parallel architecture, associated unity of advanced images.

Author

N88-21584*# Arizona Univ., Tucson. Optical Sciences Center. THE ABSOLUTE RADIOMETRIC CALIBRATION OF THE ADVANCED VERY HIGH RESOLUTION RADIOMETER Semiannual Status Report

P. N. SLATER, P. M. TILLET, and Y. DING Apr. 1988 17 p (Contract NAG5-859)

(NASA-CR-182755; NAS 1.26:182755) Avail: NTIS HC A03/MF A01 CSCL 08B

The need for independent, redundant absolute radiometric calibration methods is discussed with reference to the Thematic Mapper. Uncertainty requirements for absolute calibration of between 0.5 and 4 percent are defined based on the accuracy of reflectance retrievals at an agricultural site. It is shown that even very approximate atmospheric corrections can reduce the error in reflectance retrieval to 0.02 over the reflectance range 0 to 0.4.

Author

N88-22449# Massachusetts Inst. of Tech., Cambridge. Artificial Intelligence Lab.

RELATIVE ORIENTATION

BERTHOLD K. HORN Sep. 1987 32 p

(Contract N00014-85-K-0124; DACA76-85-C-0100)

(AD-A190385; AD-E801598; AI-M-994) Avail: NTIS HC A03/MF A01 CSCL 08B

Before corresponding points in images taken with two cameras can be used to recover distances to objects in a scene, one has to determine the position and orientation of one camera relative to the other. This is the classic photogrammetric problem of relative orientation, central to the interpretation of binocular stereo information. Iterative methods for determining relative orientation were developed long ago; without them we would not have most of the topographic maps we do today. Relative orientation is also of importance in the recovery of motion and shape from an image sequence when successive frames are widely separated in time. Workers in motion vision are rediscovering some of the methods of photogrammetry. Described here is a particularly simple iterative scheme of recovering relative orientation that, unlike existing methods, does not require a good initial guess for the baseline and the rotation. The data required is a set of pairs of corresponding rays from the two projection centers to points in the scene. It is well known that at least five pairs of rays are needed. Less appears to be known about the existence of multiple solutions and their interpretation. These issues are discussed here in detail. GRA

N88-23301# Begeleidingscommissie Remote Sensing, Delft (Netherlands).

THE RADIOMETRIC PROCESSING OF SLAR MEASURING VALUES USING THE PARES PROGRAM [DE RADIOMETRISCHE BEWERKINGEN OP SLAR MEETWAARDEN DOOR HET PARES PROGRAMMA]

H. POUWELS (National Aerospace Lab., Amsterdam, Netherlands) Aug. 1986 15 p In DUTCH

(BCRS-86-04; ETN-88-91551) Avail: NTIS HC A03/MF A01

The radiometric processing of calibration measurements using the Preprocessing Airborne Remote Sensing (PARES) program is described. The internal single-point calibration pulse with which the digital side-looking radar (SLAR) is equipped, is described. The demodulation and digitizing of the radar output are explained. The PARES program is described. The global effect of the different losses is determined using an external calibration. An absolute level can be assigned to the preprocessed images. ESA

N88-23932*# Jet Propulsion Lab., California Inst. of Tech., Pasadena.

THE SHUTTLE IMAGING RADAR B (SIR-B) EXPERIMENT REPORT

JO BEA CIMINO, BENJAMIN HOLT, and ANNIE RICHARDSON 15 Mar. 1988 223 p

(Contract NAS7-918)

(NASA-CR-182923; NAS 1.26:182923; JPL-PUBL-88-2) Avail: NTIS HC A10/MF A01 CSCL 17I

The primary objective of the SIR-B experiment was to acquire multiple-incidence-angle radar imagery of a variety of Earth's surfaces to better understand the effects of imaging geometry on radar backscatter. A complementary objective was to map extensive regions of particular interest. Under these broad objectives, many specific scientific experiments were defined by the 43 SIR-B Science Team members, including studies in the area of geology, vegetation, radar penetration, oceanography, image analysis, and calibration technique development. Approximately 20 percent of the planned digital data were collected, meeting 40 percent of the scientific objectives. This report is an overview of the SIR-B experiment and includes the science investigations, hardware design, mission scenario, mission operations, events of the actual missions, astronaut participation, data products (including auxiliary data), calibrations, and a summary of the actual coverage. Also included are several image samples.

Author

N88-24013# Instituto de Pesquisas Espaciais, Sao Jose dos Campos (Brazil).

LATIN AMERICAN SYMPOSIUM ON REMOTE SENSING. 4TH BRAZILIAN REMOTE SENSING SYMPOSIUM AND 6TH SELPER PLENARY MEETING, VOLUME 1

1986 798 p In PORTUGUESE; ENGLISH summary Symposium held in Gramado, Brazil, 10-15 Aug. 1986 Prepared in cooperation with Sociedad de Especialistas Latinoamericanos en Percepcion

08 INSTRUMENTATION AND SENSORS

Remota, Chile, and Sociedade Brasileira de Cartografia, Geodesia, Fotogrametria e Sensoriamento Remoto
Avail: NTIS HC A99/MF E03

Topics addressed include: crop cover estimation; rain penetration; forest resources in Uruguay; geometric correction of data; satellite imagery; thematic mapping; surface morphology; spatial filtering; remote sensing problems; image classifications; remote sensing; geographical information systems; computer techniques; spectral behavior of crops; tectonics; data processing; cartography; image processing; archeology; aerial photography; geological structures.

N88-24029# Instituto de Pesquisas Espaciais, Sao Jose dos Campos (Brazil).

THE MODELING OF ERROR BUDGET ANALYSIS AND TOLERANCE SPECIFICATIONS FOR BRESEX MULTIBAND LINEAR ARRAY CCD CAMERA Abstract Only

G. K. RAYALU *In its* Latin American Symposium on Remote Sensing. 4th Brazilian Remote Sensing Symposium and 6th SELPER Plenary Meeting, Volume 1 p 254 1986
Avail: NTIS HC A99/MF E03

In multispectral imaging, precise image-to-image registration is necessary to form a color composite. The accuracy to which images may be registered depends on many factors. Achieving a half-a-pixel registration error between corresponding elements of any two bands in an involved task and calls for stringent specifications on various sub-systems of a camera. An attempt is made to present what are the sources of error, how to distribute them on a RMS basis to achieve a given total registration error and derive tolerance specifications for the sub-system components and for the alignment of the BRESEX camera. The final error budget is checked for its practicability, considering various options and making full use of the available state-of-the-art technology.

Author

N88-24035# United Nations, New York, N. Y. Outer Space Affairs Div.

THE USSR SPACE SYSTEMS FOR REMOTE SENSING OF EARTH RESOURCES AND THE ENVIRONMENT (SENSOR SYSTEMS, PROCESSING TECHNIQUES, APPLICATIONS) Abstract Only

ROLF-PETER OESBERG *In* INPE, Latin American Symposium on Remote Sensing. 4th Brazilian Remote Sensing Symposium and 6th SELPER Plenary Meeting, Volume 1 p 317 1986
Avail: NTIS HC A99/MF E03

The two main techniques in present use of sensing multispectral information for different applications are photography or scanning with detector arrays from air- or space-borne platforms. The USSR remote sensing program has included manned missions on Soyuz spacecraft and Salyut orbital stations, and regular missions of Meteor and Meteor-Priroda (Meteor-Nature) operational satellites carrying multispectral sensor systems. Photography from space was acquired in the early and mid-1970s from the short-duration manned missions on Soyuz spacecraft using single-band and multiband cameras. The MKF-6 multiband camera was first flown on Soyuz-22 in 1976 and was subsequently developed further and flown on many missions, including Salyut-6 and 7. The design and technical parameters of this camera and other sensor systems that were flown on board the USSR spacecraft include the KATE-140 photographic camera on the Salyut-6 and 7 and the scanner systems MSU-M, MSU-S, MSU-SK, Fragment-2 and MSU-E on board the spacecraft Meteor and Meteor-Priroda, basic methodologies of image interpretation and processing techniques and examples of different applications. The technical parameters of these sensor systems are compared with those from other photographic and scanner systems launched or planned. Author

N88-24090# Universidade Estadual de Paulista, Guaratingueta (Brazil). Departamento de Planejamento Regional.

CURRENT STAGE OF REMOTE SENSING SYSTEM FOR CARTOGRAPHIC APPLICATION [ESTAGIO ATUAL DOS SISTEMAS DE SENSORIAMENTO REMOTO DE APLICACAO CARTOGRAFICA]

M. I. C. DEFREITAS *In* INPE, Latin American Symposium on Remote Sensing. 4th Brazilian Remote Sensing Symposium and 6th SELPER Plenary Meeting, Volume 1 p 741-753 1986 In PORTUGUESE; ENGLISH summary
Avail: NTIS HC A99/MF E03

This work is based upon the need for a better and up-to-date knowledge of existing remote sensing systems or those ready to be activated. The objective is to discuss the principal sensors and cameras with regard to their applications on cartography and photointerpretation. Initially the spatial photogrammetry (LFC, metric camera) is presented followed by the passive imaging systems (LANDSAT, MOMS, TERS, MAPSAT). Next the active imaging systems (RADAR, SLAR, SEASAT, ERS-1, RADARSAT, SIR-A, SIR-B) are shown. A comparative panel of the sensors studied with their main characteristics is presented. Among these characteristics some are mentioned: imaging mode, satellite orbit, height, circle, width of the imaged strip, resolution, possibility for stereoscopic vision, available products, and mapping applications. As a conclusion, the evolution of such systems with respect to accuracy, imaging speed, and the increasing number of different products obtainable was noted. Author

N88-24105# Technische Hogeschool, Delft (Netherlands). Dept. of Geodesy.

ADJUSTMENT IN PHOTOGRAMMETRY: METHODS, PROGRAMS AND APPLICATIONS Thesis [BLOKVEREFFENING IN DE FOTOGAMMETRIE: METHODEN, PROGRAMMATUUR EN TOEPASSINGEN]

F. DETMAR Nov. 1987 115 p In DUTCH; ENGLISH summary
(B8735130; ETN-88-92419) Avail: NTIS HC A06/MF A01

Adjustment programs and the application of nonphotogrammetric information in photogrammetry are discussed. The nonphotogrammetric data are from control objects, the Global Positioning System, and auxiliary data from horizon camera, statoscope, and the airborne profile recorder. Aerotriangulation and adjustment procedures are described with regard to the method with independent models and the method with bundles. Test procedures and error search methods such as data snooping and robust estimation are considered. Precision of the method with bundles is better than the method with independent models. For both methods the reliability measures are in good agreement with each other. The application of additional parameters is easy to manage for the bundle method in contrast with the method with independent models. Additional parameters seem not to be necessary for the method with independent models, because this method is insensitive to systematic errors. Auxiliary data only seem sufficient for small scale projects. The Global Positioning System might be used to determine terrain control point coordinates as well as to determine the projection center coordinates which can also be used as control points. ESA

N88-24387*# New Mexico Univ., Albuquerque. Technology Application Center.

REVIEW OF POWER REQUIREMENTS FOR SATELLITE REMOTE SENSING SYSTEMS

STANLEY A. MORAIN *In its* Transactions of the Fifth Symposium on Space Nuclear Power Systems p 55-63 1988
(Contract NASW-4191)

Avail: NTIS HC A99/MF A01 CSCL 22B

The space environment offers a multitude of attributes and opportunities to be used to enhance human life styles and qualities of life for all future generations, worldwide. Among the prospects having immense social as well as economic benefits are earth-observing systems capable of providing near real-time data in such areas as food and fiber production, marine fisheries, ecosystem monitoring, disaster assessment, and global environmental exchanges. The era of Space Station, the Shuttle program, the planned unmanned satellites in both high and low Earth orbit will transfer to operational status what, until now, has been largely research and development proof of concept for remotely sensing Earth's natural and cultural resources. An

important aspect of this operational status focuses on the orbital designs and power requirements needed to optimally sense any of these important areas.

Author

09

GENERAL

Includes economic analysis.

A88-32919*# Science Applications International Corp., Washington, D.C.
APPROACH AND STATUS FOR A UNIFIED NATIONAL PLAN FOR SATELLITE REMOTE SENSING RESEARCH AND DEVELOPMENT

KRISTINE BUTERA and DAVID J. OKERSON (Science Applications International Corp., Washington, DC) IN: Thematic Conference on Remote Sensing for Exploration Geology, 5th, Reno, NV, Sept. 29-Oct. 2, 1986, Proceedings. Volume 1. Ann Arbor, MI, Environmental Research Institute of Michigan, 1987, p. 325-331. NOAA-supported research. (Contract NASW-4092)

Public Law 98-365, the Land Remote-Sensing Commercialization Act of 1984, requires that the Secretary of the Department of Commerce and the Administrator of the National Aeronautics and Space Administration 'shall, within one year after the date of the Law's enactment and biennially thereafter, jointly develop and transmit to the Congress a report that includes (1) a unified national plan for remote-sensing research and development applied to the earth and its atmosphere; (2) a compilation of progress in the relevant on-going research and development activities of Federal agencies; and (3) an assessment of the state of our knowledge of the Earth and its atmosphere, the needs for additional research (including research related to operational Federal remote-sensing space programs), and opportunities available for further progress'. NASA and NOAA have organized a series of public forums to encourage interest and discussion of the national plan.

Author

A88-45110#
MISSION TO PLANET EARTH

D. JAMES BAKER (Joint Oceanographic Institution, Inc., Washington, DC) Aerospace America (ISSN 0740-722X), vol. 26, July 1988, p. 44-46.

Plans for environmental monitoring using remote-sensing satellites in the era of the International Space Station are reviewed. The role of international cooperation is stressed, considering the present Landsat, SPOT, and Marine Observation Satellite programs; ERS-1 and Topex/Poseidon; and plans for the Italian Lageos-2, the Indian Remote Sensing Satellite, and the Japanese Advanced Earth Observation Satellite. The NASA Mission to Planet Earth proposal calls for four polar-orbit and five GEO platforms (five NASA, two ESA, and two NASDA), to be in place by the year 2000, as well as dedicated spacecraft of the Earth System Explorer series in the 1990s. Payloads will monitor the geomagnetic field, atmospheric temperature and water vapor, O₃ and aerosols, outgoing radiation, precipitation, sea-surface temperature, sea ice, ocean chlorophyll, surface winds, wave height, ocean circulation, snow cover, land use, vegetation, crops, volcanic activity, and the hydrologic cycle.

T.K.

N88-21087# Executive Office of the President, Washington, D.C.
AERONAUTICS AND SPACE REPORT OF THE PRESIDENT: 1986 ACTIVITIES

1986 141 p
 Avail: NTIS HC A07/MF A01

The achievements of aeronautics and space programs in the United States for 1986 are summarized in the areas of communications: Earth atmosphere, environment, and resources;

space science; space transportation; commercial use of space; space tracking and data systems, space station; and aeronautics and space research and technology. The achievements of each of the following organizations are described: NASA, the Departments of Defense, Commerce, Energy, Interior, Agriculture, Transportation and State, the Federal Communications Commission, Environmental Protection Agency, National Science Foundation, Smithsonian Institution, Arms Control and Disarmament Agency and USIA. Appendices provide historical information on launches, satellites, manned and unmanned spacecraft, and Federal budgets for aeronautical and astronautical activities.

Author

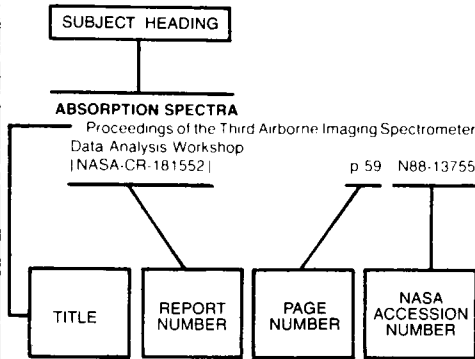
N88-24038# European Space Agency, Paris (France).
INTERNATIONAL COOPERATION IN REMOTE SENSING: THE ESA EXPERIENCE Abstract Only

VALERIE ANNE HOOD In INPE, Latin American Symposium on Remote Sensing. 4th Brazilian Remote Sensing Symposium and 6th SELPER Plenary Meeting, Volume 1 p 337 1986
 Avail: NTIS HC A99/MF E03

The active involvement of the European Space Agency (ESA) with remote sensing began with the establishment of the Earthnet program in 1978. Earthnet acquires data from the American remote sensing satellites (LANDSAT, SEASAT, HCCM, and Nimbus) from its stations in Fulcino, Kiruna, Oakhanger, and Maspalomas. Earthnet acquires remote sensing data and preprocesses them. Each member state of ESA has established a focal point who is responsible for remote sensing data distribution in their country. Regular meetings are held among the national points of contact and the other users of the data in the Earthnet coverage zone. The European Space Agency also participates in the LANDSAT Station Operators' Working Group. At a bilateral level ESA has many projects with the European Community including airborne campaigns, pilot projects, and training programs. Close contact in remote sensing is also kept with Brazil, Canada, France, United States, Japan, India, and Australia on a bilateral basis. On the meteorological side, ESA has launched Meteosats 1 and 2 and will be launching Meteosat 3 this year. An extensive promotion campaign was carried out in Europe and Africa to encourage countries to use the satellite. Training programs in meteorology and agrometeorology are conducted both by ESA alone and in cooperation with other organizations. The European Space Agency is also preparing ERS-1 and is in the process of negotiating terms for direct access with several states.

Author

Typical Subject Index Listing



The subject heading is a key to the subject content of the document. The title is used to provide a description of the subject matter. When the title is insufficiently descriptive of document content, a title extension is added, separated from the title by three hyphens. The (NASA or AIAA) accession number and the page number are included in each entry to assist the user in locating the abstract in the abstract section. If applicable, a report number is also included as an aid in identifying the document. Under any one subject heading, the accession numbers are arranged in sequence with the AIAA accession numbers appearing first.

A

ACCURACY

- G.P.S. surveying in the Netherlands p 72 A88-37383
- Mapping from LANDSAT and SPOT satellite imagery p 66 N88-24018

ADVANCED VERY HIGH RESOLUTION RADIOMETER

- Nonlinear multichannel algorithms for estimating sea surface temperature with AVHRR satellite data p 39 A88-34643
- Differences in visible and near-IR responses, and derived vegetation indices, for the NOAA-9 and NOAA-10 AVHRRs - A case study p 70 A88-35396
- Data reception, archiving and distribution --- digital image processing using AVHRR flofn on NOAA p 58 A88-37131
- An approach for emulating the color balance of Landsat multispectral scanner images with AVHRR data p 73 A88-41956
- Processing of raw digital NOAA-AVHRR data for sea- and land applications p 60 A88-41968
- Sea surface temperature studies in Norwegian coastal areas using AVHRR- and TM thermal infrared data p 44 A88-42047
- A study with NOAA-7 AVHRR-imagery in monitoring ephemeral streams in the lower catchment area of the Tana River, Kenya p 54 A88-42053
- Sea surface flow estimation from advanced very high resolution radiometer and coastal zone color scanner satellite imagery - A verification study p 44 A88-42444

- Empirical orthogonal function analysis of advanced very high resolution radiometer surface temperature patterns in Santa Barbara Channel p 45 A88-42449
- Circulation patterns in AVHRR imagery p 46 A88-43217

Statistical analysis of the near-surface distributions of chlorophyll and temperature fields on the basis of remote imagery from CZCS and AVHRR scanners p 54 A88-43666

The effect of atmospheric correction on the interpretation of multitemporal AVHRR-derived vegetation index dynamics p 11 A88-44117

Determinations of suspended sediment concentrations from multiple day Landsat and AVHRR data p 54 A88-44120

The absolute radiometric calibration of the advanced very high resolution radiometer [NASA-CR-182755] p 75 N88-21584

Calibration and processing of AVHRR data for temperature estimation [INPE-4493-PRE/1257] p 65 N88-22485

AERIAL PHOTOGRAPHY

Targeting epithermal alteration and gossans in weathered and vegetated terrains using aircraft scanners - Successful Australian case histories p 26 A88-32905

Geologic interpretation of air photos and radar imagery for hydroelectric power projects in Upper Ucayali Jungle Region of Peru p 28 A88-32922

The use of multispectral space photographs to draw up a map of land use in western Slovakia p 57 A88-33774

Canadian large-scale aerial photographic systems (LSP) p 70 A88-35395

Airphoto map control with Landsat - An alternative to the slotted templet method p 60 A88-41966

Base map production from geocoded imagery p 25 A88-41969

Monitoring of renewable resources in equatorial countries p 19 A88-42000

Inventory of decline and mortality in spruce-fir forests of the eastern U.S. with CIR photos p 7 A88-42004

A remote sensing aided inventory of fuelwood volumes in the Sahel region of west Africa - A case study of five urban zones in the Republic of Niger p 7 A88-42005

Thematic Mapping from aerial photographs for Kandi Watershed and area development project, Punjab (India) p 9 A88-42024

Assessment of desertification in the lower Nile Valley (Egypt) by an interpretation of Landsat MSS colour composites and aerial photographs p 61 A88-42025

Application of MEIS-II multispectral airborne data and CIR photography for the mapping of surficial geology and geomorphology in the Chatham area, Southwest Ontario, Canada p 34 A88-42027

Photo-interpretation of landforms and the hydrogeologic bearing in highly deformed areas, NW of the Gulf of Suez, Egypt p 34 A88-42029

Remote sensing assessment of environmental impacts caused by phosphat industry destructive influence p 19 A88-42031

A hydrological comparison of Landsat TM, Landsat MSS and black and white aerial photography p 52 A88-42041

An analysis of remote sensing for monitoring urban derelict land p 20 A88-42056

Land resource use monitoring in Romania, using aerial and space data p 21 A88-42065

Remote sensing for non-renewable resources - Satellite and airborne multiband scanners for mineral exploration p 35 A88-42068

Artificial GCPs in aircraft and satellite scanner imagery --- Ground Control Points p 74 A88-43227

Correction of spatial and temporal distortions in the photographic image input into an interactive processing system p 62 A88-43672

New features of the LMK aerial camera system p 74 A88-44449

Object-space least-squares correlation p 63 A88-44517

Estimation of reservoir submerging losses using CIR aerial photographs - Example of the Ertan hydropower station on the Yalong River in southwest China p 55 A88-45637

Geotechnical applications of three new U.S. Government remote sensing programs p 36 A88-45641

Marginal Ice Zone Experiment (MIZEX) 1984 VARAN-S data set [ETN-88-92032] p 48 N88-21625

Updating land-use of the Sao Jose dos Campos municipality through remote sensing data [INPE-4479-RPE/562] p 22 N88-23693

Latin American Symposium on Remote Sensing, 4th Brazilian Remote Sensing Symposium and 6th SELPER Plenary Meeting, volume 1 p 75 N88-24013

Remote sensing techniques in the estimation of the area cultivated with beans, corn, and castor beans in the Irecé County (Bahia State) p 15 N88-24045

Structure and dynamics of vegetation in the middle semi-arid tropics. Quixaba's Caatinga (PE): Terrain analysis of MSS/LANDSAT data p 15 N88-24049

Remote sensing and structural rupture: Application examples in the study of tectonics p 37 N88-24050

Analysis and interpretation of image lithostrucure: An application of the multiconcept in the metamorphic belt of Sul de Santana da Boa Vista (RS) p 38 N88-24051

Tornado tracks in Southwestern Brazil, Eastern Paraguay, and Northwestern Argentina p 23 N88-24071

Interpretation of MSS/LANDSAT data for evaluation of physical distribution of mangroves in Cananeia-Iguape (SP) p 16 N88-24072

Low altitude remote sensing data in the implementation of a mathematical model for the planning of urban equipment networks p 23 N88-24074

Evaluation of the mangrove area at the Piaui River (SE) through remote sensing p 16 N88-24086

The 35 mm vertical aerial photographs for mapping stands of bracinga in different age classes p 16 N88-24087

The broken anticlines, cuesta and crest homoclines, oroclinal valleys, and other forms of relief outcrops delineated with the help of remote sensing imagery p 16 N88-24089

Stereoscopic photographs, ground and aerial, of trees used in the arborization of Curitiba (PR) p 17 N88-24091

Preliminary study on the application of digital processing of TM-LANDSAT data in the mapping of apple orchards in Fraiburgo (SC) p 17 N88-24093

Characteristics of drainage determinations in aerial photographs and relief determination on different scales planialtimetric charts for three soils in the state of Sao Paulo p 17 N88-24095

Criteria for planimetric and altimetric correction of maps restituted from aerial photographs in 1:100,000 scale p 38 N88-24097

AERIAL RECONNAISSANCE

Hydrographic data from the OPTOMA (Ocean Prediction Through Observation, Modeling and Analysis) program: OPTOMA 23, 9-19 November 1986 [AD-A189868] p 49 N88-22506

AEROMAGNETISM

Structural geology and regional tectonics of the Mineral County area, Nevada, using Shuttle Imaging Radar-B and digital aeromagnetic data p 35 A88-44646

AERONAUTICAL ENGINEERING

Aeronautics and space report of the President: 1986 activities p 77 N88-21087

AEROSOLS

Particulate emissions from a mid-latitude prescribed chaparral fire p 3 A88-38805

AEROSPACE ENGINEERING

Aeronautics and space report of the President: 1986 activities p 77 N88-21087

AGRICULTURE

Preliminary investigation of Large Format Camera photography utility in soil mapping and related agricultural applications p 4 A88-41947

Application of multispectral scanning remote sensing in agricultural water management problems p 8 A88-42011

A second generation lunar agricultural system p 11 A88-43864

Assessment of crop loss from air pollutants: Meteorology-atmospheric chemistry and long range transport [PB88-146857] p 12 N88-22448

SUBJECT

- Estimation of an area cultivated with wheat from LANDSAT data through a two-phase sampling method p 14 N88-24041
- AIR POLLUTION**
Canopy reflectance of soybean as affected by chronic doses of ozone in open-top field chambers p 2 A88-35398
Assessment of crop loss from air pollutants: Meteorology-atmospheric chemistry and long range transport [PB88-146857] p 12 N88-22448
- AIR QUALITY**
Long-term air quality monitoring at the South Pole by the NOAA program Geophysical Monitoring for Climatic Change p 18 A88-36243
- AIR WATER INTERACTIONS**
A system for remote measurements of the wind stress over the ocean p 40 A88-36841
The ocean and the atmosphere p 41 A88-37143
Radiative processes affecting ocean mixed-layer heat content and their monitoring from satellite p 47 N88-20800
- AIRBORNE EQUIPMENT**
Correlation between high resolution remote sensing imagery and hydrothermal alteration, Tybo mining district, Nevada p 27 A88-32915
Exploration for mercury and lead-zinc-silver using the airborne Thematic Mapper, Almaden area, Spain p 29 A88-32939
Radiative surface temperatures of the burned and unburned areas in a tallgrass prairie p 3 A88-37418
Application of MEIS-II multispectral airborne data and CIR photography for the mapping of surficial geology and geomorphology in the Chatham area, Southwest Ontario, Canada p 34 A88-42027
Crop classification from airborne synthetic aperture radar data p 10 A88-43220
New features of the LMK aerial camera system p 74 A88-44449
An effect of coherent scattering in spaceborne and airborne SAR images p 64 A88-44651
A comparison of airborne GEMS/SAR with satellite-borne Seasat/SAR radar imagery - The value of archived multiple data sets p 64 A88-45640
Airborne resistivity mapping p 36 A88-45771
Feasibility study for a 2nd generation system for airborne maritime pollution surveillance [ETN-88-92108] p 55 N88-22466
Airborne and spaceborne radar images for geologic and environmental mapping in the Amazon rain forest, Brazil p 37 N88-24021
- AIRBORNE/SPACEBORNE COMPUTERS**
A PC-based interactive graphics system to perform satellite-derived oceanographic thermal analysis p 68 A88-32850
- AIRCRAFT INSTRUMENTS**
Selection of bands for a newly developed multispectral airborne reference-aided calibrated scanner (MARCS) p 74 A88-41995
Spruce budworm infestation detection using an airborne pushbroom scanner and Thematic Mapper data p 8 A88-42007
- ALASKA**
Influence of the Yukon River on the Bering Sea [NASA-CR-182802] p 50 N88-24126
- ALGORITHMS**
A simple atmospheric correction algorithm for Landsat Thematic Mapper satellite images p 61 A88-42054
Results of the testing of the segmentation program on RESEDA [BCRS-87-01] p 65 N88-23304
Shape detection in remote sensing through graph isomorphism p 67 N88-24028
Low altitude remote sensing data in the implementation of a mathematical model for the planning of urban equipment networks p 23 N88-24074
Research on enhancing the utilization of digital multispectral data and geographic information systems in global habitability studies [NASA-CR-182799] p 23 N88-24101
- ALPS MOUNTAINS (EUROPE)**
Discrimination of geobotanical anomalies in rugged alpine terrain using Landsat Thematic Mapper data p 32 A88-32957
- ALTIMETRY**
Tidal estimation in the Pacific with application to SEASAT altimetry [NASA-TM-100694] p 47 N88-20780
Criteria for planimetric and altimetric correction of maps restituted from aerial photographs in 1:100,000 scale p 38 N88-24097
- AMAZON REGION (SOUTH AMERICA)**
Confirmation of quantitative morphostructural analysis by seismic, aeromagnetic and geochemical data in the Amazon Basin, Brazil p 29 A88-32937

- The dispersal of the Amazon's water p 43 A88-40059
- Project CODEAMA/FUNCATE (test-area of Barreirinha-AM): Field report [INPE-4500-RPE/563] p 55 N88-22455
Detection, monitoring and analysis of some environmental effects of fires in the Amazon region through utilization of NOAA and LANDSAT satellite imagery and aircraft data [INPE-4503-TDL/326] p 13 N88-23322
- ANALOG TO DIGITAL CONVERTERS**
Tests for the automatic pattern recognition of building surfaces by the TK 50 p 68 N88-25030
- ANDES MOUNTAINS (SOUTH AMERICA)**
Discrimination and supervised classification of volcanic flows of the Puna-Altiplano, Central Andes Mountains using Landsat TM data p 31 A88-32948
- ANNUAL VARIATIONS**
Interannual Landsat-MSS reflectance variation in an urbanized temperate zone p 58 A88-37417
Examples of ice pack rigidity and mobility characteristics determined from ice motion [AD-A191163] p 50 N88-24129
- ANOMALIES**
Anomalies in the vegetation in the Alto Xingu - MT p 14 N88-24043
Remote sensing and structural rupture: Application examples in the study of tectonics p 37 N88-24050
- ANTARCTIC REGIONS**
Polynyas in the Southern Ocean p 43 A88-39284
The 1987 Airborne Antarctic Ozone Experiment: The Nimbus-7 TOMS data atlas [NASA-RP-1201] p 47 N88-20714
- ANTENNA ARRAYS**
Non-tracking antenna systems for the acquisition of NOAA HRPT Data --- High Resolution Picture Transmission p 72 A88-37279
- ANTICLINES**
The broken anticlines, cuesta and crest homoclines, oroclinal valleys, and other forms of relief outcrops delineated with the help of remote sensing imagery p 16 N88-24089
- APERTURES**
Sparse-aperture microwave radiometers for earth remote sensing p 68 A88-33150
- APPLICATIONS PROGRAMS (COMPUTERS)**
The SAGE geographic analysis system p 22 N88-24063
- ARCHAEOLOGY**
Subsurface morphology and geoarchaeology revealed by spaceborne and airborne radar p 37 N88-24022
Utilization of LANDSAT-TM, for aiding in the localization of archeological sites in the state of Sao Paulo p 38 N88-24069
- ARCHITECTURE (COMPUTERS)**
Earthscan - A range of remote sensing systems p 61 A88-41982
Analysis for architecture for image processing [INPE-4294-PRE/1165] p 75 N88-20715
- ARCTIC REGIONS**
Surface temperatures and sea ice typing for northern Baffin Bay p 42 A88-39083
Real-time environmental Arctic monitoring (R-TEAM) [AD-A189948] p 49 N88-22508
- ARID LANDS**
Operational satellite data assessment for drought/disaster early warning in Africa - Comments on GIS requirements --- Geographic Information System p 19 A88-42018
- ARTIFICIAL SATELLITES**
Aeronautics and space report of the President: 1986 activities p 77 N88-21087
Review of power requirements for satellite remote sensing systems p 76 N88-24367
- ASIA**
Ocean-atmosphere interactions in low latitude Australasia p 41 A88-37270
- ATLANTIC OCEAN**
Distribution and chemistry of suspended particles from an active hydrothermal vent site on the Mid-Atlantic Ridge at 26 deg N p 42 A88-37720
Temporal variations of particle fluxes in the deep subtropical and tropical North Atlantic - Euleian versus Lagrangian effects p 45 A88-42448
- ATMOSPHERIC ATTENUATION**
Millimeter-wave propagation in vegetation: Experiments and theory p 12 A88-44319
- ATMOSPHERIC BOUNDARY LAYER**
Modeling surface exchanges: The soil-vegetation-atmosphere continuum p 12 N88-21553
- ATMOSPHERIC CIRCULATION**
Polynyas in the Southern Ocean p 43 A88-39284

- Ocean general circulation models: Report on proceedings of a meeting of ocean and climate modelers [DE88-005530] p 49 N88-22504
- ATMOSPHERIC COMPOSITION**
Assessment of crop loss from air pollutants: Meteorology-atmospheric chemistry and long range transport [PB88-146857] p 12 N88-22448
- ATMOSPHERIC CORRECTION**
Quantitative procedure for producing color-calibrated Thematic Mapper natural-color images p 57 A88-32943
Vegetation indices and other vegetation parameters - Examples, interpretation and problems p 3 A88-38373
Relation between spectral reflectance and vegetation index p 7 A88-41998
A simple atmospheric correction algorithm for Landsat Thematic Mapper satellite images p 61 A88-42054
Radiometric correction for atmospheric and topographic effects on Landsat MSS images p 62 A88-43223
The effect of atmospheric correction on the interpretation of multitemporal AVHRR-derived vegetation index dynamics p 11 A88-44117
The absolute radiometric calibration of the advanced very high resolution radiometer [NASA-CR-182755] p 75 N88-21584
- ATMOSPHERIC EFFECTS**
Soil and atmosphere influences on the spectra of partial canopies p 11 A88-44119
Spectral measurements for correcting LANDSAT data for atmospheric effects p 66 N88-24020
Analysis of the parameters responsible for the variations of the illumination conditions in the LANDSAT data p 67 N88-24070
- ATMOSPHERIC MODELS**
The ocean and the atmosphere p 41 A88-37143
Cloud climatologies from space and applications to climate modelling p 71 A88-37145
Surface energy budget, surface temperature and thermal inertia p 58 A88-37147
Mapping frost-sensitive areas with a three-dimensional local-scale numerical model. I - Physical and numerical aspects p 4 A88-41055
Ocean general circulation models: Report on proceedings of a meeting of ocean and climate modelers [DE88-005530] p 49 N88-22504
- ATMOSPHERIC MOISTURE**
Moisture and latent heat flux variabilities in the tropical Pacific derived from satellite data p 45 A88-42445
- ATMOSPHERIC SOUNDING**
Method for rapidly estimating geophysical parameters of the ocean-atmosphere system from satellite microwave radiometry p 46 A88-43669
- ATMOSPHERIC TEMPERATURE**
Retrieval of atmospheric temperature structure from the NOAA-9 satellite p 72 A88-37336
Mass extinctions, atmospheric sulphur and climatic warming at the K/T boundary p 46 A88-43835
- AUGMENTATION**
Application of its transformation in color enhancement of LANDSAT imagery p 68 N88-24082
- AUSTRALIA**
Ocean-atmosphere interactions in low latitude Australasia p 41 A88-37270
- AUTOCORRELATION**
Using spatial autocorrelation analysis to explore the errors in maps generated from remotely sensed data p 58 A88-39097
- B**
- BACKSCATTERING**
Radar signatures of oil films floating on the sea surface and the Marangoni effect p 39 A88-33695
Comparison of unified full-wave solutions for normal incidence microwave backscatter from sea with physical optics and hybrid solutions p 42 A88-39079
SIR-B experiments in Japan. V. p 4 A88-40355
Radar backscatter characteristics of trees at 215 GHz p 11 A88-44307
Simulation of L-band and HH microwave backscattering from coniferous forest stands - A comparison with SIR-B data p 12 A88-44643
Radar penetration in the Amazonian rain forest p 15 N88-24044
- BACTERIA**
Satellite detected cyanobacteria bloom in the southwestern tropical Pacific - Implication for oceanic nitrogen fixation p 42 A88-39081

- BALTIC SEA**
Parameters of eddy structures and mushroom currents in the Baltic Sea derived from satellite imagery p 46 A88-43665
- BAND RATIOING**
The dangers of underestimating the importance of data adjustments in band ratioing p 62 A88-43225
- BARREN LAND**
An analysis of remote sensing for monitoring urban derelict land p 20 A88-42056
- BATHYMETERS**
Classification of bottom composition and bathymetry of shallow waters by passive remote sensing p 53 A88-42051
- BEARING (DIRECTION)**
Relative orientation [AD-A190385] p 75 N88-22449
- BEAUFORT SEA (NORTH AMERICA)**
Examples of ice pack rigidity and mobility characteristics determined from ice motion [AD-A191163] p 50 N88-24129
- BERING SEA**
Influence of the Yukon River on the Bering Sea [NASA-CR-182802] p 50 N88-24126
- BIOGEOCHEMISTRY**
Thermal analysis of wildfires and effects on global ecosystem cycling p 2 A88-35194
- BIOMASS**
Vegetation indices and other vegetation parameters - Examples, interpretation and problems p 3 A88-38373
Remote sensing of biomass of salt marsh vegetation in France p 3 A88-39082
Global vegetation monitoring using NOAA GAC data p 8 A88-42012
The use of SLAR and SIRA imagenes for the classification of forest types in tropical rain forests p 14 N88-24036
- BIOTITE**
An integrated study of the Alto Paranaiba Kimberlite Province, Minas Gerais, Brazil: A possible tool for diamond exploration p 37 N88-24031
- BLUE GREEN ALGAE**
Satellite detected cyanobacteria bloom in the southwestern tropical Pacific - Implication for oceanic nitrogen fixation p 42 A88-39081
- BRIGHTNESS**
Linear combinations of spectral reflectances in crop analyses p 3 A88-36170
Mapping soil and rock variation from satellite images in the Sahel p 14 N88-24023
- BRIGHTNESS DISTRIBUTION**
Spectral reflective characteristics of sea surface p 47 N88-20676
- BRIGHTNESS TEMPERATURE**
A satellite infrared technique to estimate tropical convective and stratiform rainfall p 69 A88-33416
A method for calculating the effective emissivity of a groove structure --- sea surface temperature measurement p 40 A88-35986
Snow melt on sea ice surfaces as determined from passive microwave satellite data p 42 A88-38691
- BUOYS**
Comparison of surface current determined from satellite-tracked buoy with shipboard wind data during the 4th Brazilian antarctic expedition, 10-14 March, 1986 p 49 N88-24024
Near surface current determined from INPE's satellite-tracked buoy, during 6-26 November, 1985 p 50 N88-24058
- C**
- CADAstral MAPPING**
The Systeme d'Analyse Geographique (SAGE) geographic analysis system p 66 N88-24019
The SAGE geographic analysis system p 22 N88-24063
Tests for the automatic pattern recognition of building surfaces by the TK 50 p 68 N88-25030
Recent developments in software and hardware by Scitex Co. --- computer aided mapping p 68 N88-25038
- CALIBRATING**
An update on visible and near infrared calibration of satellite instruments p 72 A88-37416
SIR-B experiments in Japan. I - Sensor calibration experiment p 73 A88-40351
Selection of bands for a newly developed multispectral airborne reference-aided calibrated scanner (MARCS) p 74 A88-41995
In flight calibration for the imaging instrument of VEGETATION payload (SPOT 4) p 10 A88-42545
- The absolute radiometric calibration of the advanced very high resolution radiometer [NASA-CR-182755] p 75 N88-21584
- CALIFORNIA**
Mesoscale variability in current meter measurements in the California Current system off northern California p 44 A88-42443
Hydrographic data from the OPTOMA (Ocean Prediction Through Observation, Modeling and Analysis) program: OPTOMA 23, 9-19 November 1986 [AD-A189868] p 49 N88-22506
- CAMERAS**
Space Shuttle Large Format Camera photography and resource management p 70 A88-36378
Preliminary investigation of Large Format Camera photography utility in soil mapping and related agricultural applications p 4 A88-41947
New features of the LMK aerial camera system p 74 A88-44449
Comparative evaluation of the Large Format Camera, Metric Camera, and Shuttle Imaging Radar - A data content p 75 A88-44519
The modeling of error budget analysis and tolerance specifications for BRESEX multiband linear array CCD camera p 76 N88-24029
- CANADIAN SHIELD**
Landsat TM data as an aid in planning and interpretation of regional geochemical surveys in the Canadian Shield p 31 A88-32950
- CANOPIES (VEGETATION)**
Effects of heavy metal induced canopy structural changes on forest canopy reflectance p 1 A88-32930
Canopy reflectance of soybean as affected by chronic doses of ozone in open-top field chambers p 2 A88-35398
Identification of terrain cover using the optimum polarimetric classifier p 3 A88-37370
Remote sensing of biomass of salt marsh vegetation in France p 3 A88-39082
Relationship between soil and leaf metal content and Landsat MSS and TM acquired canopy reflectance data p 6 A88-41986
The derivation of a simplified reflectance model for the estimation of LAI --- Leaf Area Index p 6 A88-41987
Relation between spectral reflectance and vegetation index p 7 A88-41998
Detection of environmental noises between a vegetation canopy and a radiometric sensor p 10 A88-42538
An empirical model for polarized and cross-polarized scattering from a vegetation layer p 11 A88-44116
Soil and atmosphere influences on the spectra of partial canopies p 11 A88-44119
Remote sensing of earth terrain [NASA-CR-182677] p 12 N88-20711
Modeling surface exchanges: The soil-vegetation-atmosphere continuum p 12 N88-21553
Use of energy emission for detecting the necessity of irrigation in wheat in field conditions [INPE-4461-TDL/318] p 13 N88-23315
Radar penetration in the Amazonian rain forest p 13 N88-24015
Radar penetration in the Amazonian rain forest p 15 N88-24044
Structure and dynamics of vegetation in the middle semi-arid tropics. Quixaba's Caatinga (PE): Terrain analysis of MSS/LANDSAT data p 15 N88-24049
History of wildland fires on Vandenberg Air Force Base, California [NASA-TM-100983] p 18 N88-25134
- CARBON CYCLE**
Remote sensing and the role of terrestrial vegetation in the global carbon cycle p 5 A88-41954
- CARBON DIOXIDE**
Assessment of polar climate change using satellite technology p 40 A88-36241
- CHANGE DETECTION**
A comparison between classification differencing and image differencing for land cover type change detection p 59 A88-41944
A gridding approach to detect patterns of change in coastal wetlands from digital data p 52 A88-41949
- CHAPARRAL**
Particulate emissions from a mid-latitude prescribed chaparral fire p 3 A88-38805
- CHARGE COUPLED DEVICES**
Imaging instrument of the Vegetation Payload (SPOT 4) p 70 A88-35968
- CHLOROPHYLLS**
Time evolution of surface chlorophyll patterns from cross-spectrum analysis of satellite color images p 45 A88-42446
The effect of dissolved 'yellow substance' on the quantitative retrieval of chlorophyll and total suspended sediment concentrations from remote measurements of water colour p 46 A88-43226
- Statistical analysis of the near-surface distributions of chlorophyll and temperature fields on the basis of remote imagery from CZCS and AVHRR scanners p 54 A88-43666
- CIRRUS CLOUDS**
Cloud and precipitation remote sensing at 94 GHz p 74 A88-44306
- CITIES**
Urbanization and Landsat MSS albedo change in the Windsor-Quebec corridor since 1972 p 18 A88-39094
Spatial resolution requirements for urban land cover mapping from space p 20 A88-42058
Spectral characterization of urban land covers from Thematic Mapper data p 20 A88-42059
- CLASSIFICATIONS**
The use of SLAR and SIRA imagenes for the classification of forest types in tropical rain forests p 14 N88-24036
Utilization of TM/LANDSAT images in the implanted forests mapping in the Mogi-Guaçu Region (SP-Brazil) p 14 N88-24042
Study of methods of post-processing applied to a problem of standard classification p 67 N88-24067
Research on enhancing the utilization of digital multispectral data and geographic information systems in global habitability studies [NASA-CR-182799] p 23 N88-24101
- CLASSIFIERS**
Simple classifiers of satellite data for hydrologic modelling p 52 A88-42040
- CLASSIFYING**
Comparison of classification results of original and preprocessed satellite data p 59 A88-41965
Per-field classification of a segmented SPOT simulated image p 60 A88-41970
Digital classification of forested areas using simulated TM- and SPOT- and Landsat 5/TM-data p 5 A88-41971
- CLAYS**
Spectral discrimination of zeolites and dioctahedral clays in the near-infrared p 28 A88-32926
Identification of clay minerals by feature coding of near-infrared spectra p 30 A88-32942
Pyrophyllite and kaolinite alteration - Mineral discrimination by sample reflectance measurement p 31 A88-32954
- CLIMATE CHANGE**
Assessment of polar climate change using satellite technology p 40 A88-36241
Long-term air quality monitoring at the South Pole by the NOAA program Geophysical Monitoring for Climatic Change p 18 A88-36243
Remote sensing and the role of terrestrial vegetation in the global carbon cycle p 5 A88-41954
Mass extinctions, atmospheric sulphur and climatic warming at the K/T boundary p 46 A88-43835
- CLIMATOLOGY**
Climatological interpretation of time series of satellite observations of the earth's radiation balance p 69 A88-33872
Remote sensing applications in meteorology and climatology; Proceedings of the NATO Advanced Study Institute, Dundee, Scotland, Aug. 17-Sept. 6, 1986 p 71 A88-37126
Cloud climatologies from space and applications to climate modelling p 71 A88-37145
Vegetation indices and other vegetation parameters - Examples, interpretation and problems p 3 A88-38373
- CLOUD COVER**
The acquisition of SPOT-1 HRV imagery over southern Britain and northern France, May 1986-May 1987 p 68 A88-29286
Sparse-aperture microwave radiometers for earth remote sensing p 68 A88-33150
Technique for the instrumented interpretation of space scanner imagery of the earth's cloud cover p 69 A88-33832
Cloud climatologies from space and applications to climate modelling p 71 A88-37145
Use of energy emission for detecting the necessity of irrigation in wheat in field conditions [INPE-4461-TDL/318] p 13 N88-23315
- CLOUD PHOTOGRAPHS**
Technique for the instrumented interpretation of space scanner imagery of the earth's cloud cover p 69 A88-33832
Cloud formations seen by satellite p 71 A88-37127
- CLOUDS (METEOROLOGY)**
A proposed tropical rainfall measuring mission (TRMM) satellite p 69 A88-33742
- COAL**
A satellite-based investigation of the significance of surficial deposits for surface mining operations p 36 A88-45638

COASTAL CURRENTS

- Satellite observations of tidal upwelling and mixing in the St. Lawrence estuary p 45 A88-42450
Influence of the Yukon River on the Bering Sea [NASA-CR-182802] p 50 N88-24126
- COASTAL WATER**
Quantitative analysis of distribution of suspended sediments in the Yellow River Estuary from MSS data p 50 A88-35196
Remote sensing of biomass of salt marsh vegetation in France p 3 A88-39082
Application of Landsat Thematic Mapper data to assess suspended sediment dispersion in a coastal lagoon p 51 A88-41946
The JRC program for marine coastal monitoring p 44 A88-42039
Sea surface temperature studies in Norwegian coastal areas using AVHRR- and TM thermal infrared data p 44 A88-42047
Satellite data in aquatic area research - Some ideas for future studies p 53 A88-42048
Coastal monitoring by remote sensing p 54 A88-44447
Influence of the Yukon River on the Bering Sea [NASA-CR-182802] p 50 N88-24126
- COASTAL ZONE COLOR SCANNER**
Satellite detection of bloom and pigment distributions in estuaries p 51 A88-37414
The dispersal of the Amazon's water p 43 A88-40059
Sea surface flow estimation from advanced very high resolution radiometer and coastal zone color scanner satellite imagery - A verification study p 44 A88-42444
Temporal variations of particle fluxes in the deep subtropical and tropical North Atlantic - Eulerian versus Lagrangian effects p 45 A88-42448
Statistical analysis of the near-surface distributions of chlorophyll and temperature fields on the basis of remote imagery from CZCS and AVHRR scanners p 54 A88-43666
NIMBUS-7 CZCS. Coastal Zone Color Scanner imagery for selected coastal regions. North America - Europe. South America - Africa - Antarctica. Level 2 photographic product [NASA-CR-180755] p 48 N88-22447
- COASTS**
A gridding approach to detect patterns of change in coastal wetlands from digital data p 52 A88-41949
Satellite remote sensing of the coastal environment of Bombay p 61 A88-42052
- COLOR**
Application of its transformation in color enhancement of LANDSAT imagery p 68 N88-24082
Evaluation of TM false color composites for crop discrimination p 17 N88-24096
- COLOR CODING**
Color space mapping using ternary/chromaticity diagrams - A technique for composite image interpretation p 57 A88-32932
Quantitative procedure for producing color-calibrated Thematic Mapper natural-color images p 57 A88-32943
Comparative utilization of analog and digital processes in the treatment of MSS-LANDSAT data for studying the national parks of Brazil [INPE-4011-TDL/240] p 21 N88-22456
- COLOR INFRARED PHOTOGRAPHY**
Inventory of decline and mortality in spruce-fir forests of the eastern U.S. with CIR photos p 7 A88-42004
- COLOR PHOTOGRAPHY**
Directed band ratioing for the retention of perceptually-independent topographic expression in chromaticity-enhanced imagery p 62 A88-43224
Anomalies in the vegetation in the Alto Xingu - MT p 14 N88-24043
Remote sensing techniques in the estimation of the area cultivated with beans, corn, and castor beans in the Itrec County (Bahia State) p 15 N88-24045
- COLUMBUS SPACE STATION**
Remote sensing in the Space Station and Columbus programmes p 71 A88-37150
- COMBUSTION PRODUCTS**
Thermal analysis of wildfires and effects on global ecosystem cycling p 2 A88-35194
- COMPARISON**
Groundwater sapping valleys: Experimental studies, geological controls and implications to the interpretation of valley networks on Mars [NASA-CR-182718] p 37 N88-22847
- COMPRESSION LOADS**
Geodetic measurement of deformation east of the San Andreas fault in Central California [NASA-CR-182709] p 36 N88-20754

COMPUTATION

- Calibration and processing of AVHRR data for temperature estimation [INPE-4493-PRE/1257] p 65 N88-22485
- COMPUTER AIDED MAPPING**
Computer processing of satellite data for geostructural zoning of a collisional boundary, significance and field checks - The example of Tunisia p 32 A88-35193
Quantitative description and classification of drainage patterns p 51 A88-35399
Regional geologic mapping of digitally enhanced Landsat imagery in the southcentral Alborz mountains of northern Iran p 34 A88-42017
Satellite data in aquatic area research - Some ideas for future studies p 53 A88-42048
Kartoflex - An instrument for computer-aided photointerpretation and map revision p 74 A88-44450
Integration of Landsat, DTED, and DFAD p 63 A88-44540
Coupling of satellite remote sensing to digitized topographic map to detect changes in land use [B8735129] p 23 N88-24104
Tests for the automatic pattern recognition of building surfaces by the TK 50 p 68 N88-25030
Recent developments in software and hardware by Scitex Co. --- computer aided mapping p 68 N88-25038
- COMPUTER GRAPHICS**
A PC-based interactive graphics system to perform satellite-derived oceanographic thermal analysis p 68 A88-32850
Correction of spatial and temporal distortions in the photographic image input into an interactive processing system p 62 A88-43672
Analysis for architecture for image processing [INPE-4294-PRE/1165] p 75 N88-20715
The geometric workstation, a new approach for geometric corrections of remotely sensed data p 66 N88-24017
The Systeme d'Analyse Geographique (SAGE) geographic analysis system p 66 N88-24019
Automatic registration of satellite imagery p 67 N88-24080
Visualization of digital terrain models p 67 N88-24081
- COMPUTER NETWORKS**
Global distributive computer processing systems for environmental monitoring, analysis and trend modeling in early warning and natural disaster mitigation p 19 A88-42020
- COMPUTER PROGRAMMING**
Mapping from LANDSAT and SPOT satellite imagery p 66 N88-24018
The SAGE geographic analysis system p 22 N88-24063
- COMPUTER PROGRAMS**
Geometric restoration of satellite image data [AD-A190462] p 64 N88-22450
Satellite UV image processing [AD-A190466] p 65 N88-22451
Updating of the municipal official register of real estate through a geographical information system [INPE-4459-PRE/1238] p 21 N88-22453
- COMPUTER STORAGE DEVICES**
Evaluation of regional land resources using geographic information systems based on linear quadrates p 20 A88-42063
- COMPUTER SYSTEMS PROGRAMS**
The radiometric processing of SLAR measuring values using the PARES program p 75 N88-23301
Results of the testing of the segmentation program on RESEDA [BCRS-87-01] p 65 N88-23304
- COMPUTERIZED SIMULATION**
A comparison of sampling schemes used in generating error matrices for assessing the accuracy of maps generated from remotely sensed data p 59 A88-39098
- CONFERENCES**
Thematic Conference on Remote Sensing for Exploration Geology, 5th, Reno, NV, Sept. 29-Oct. 2, 1986, Proceedings. Volumes 1 & 2 p 26 A88-32901
Remote sensing applications in meteorology and climatology; Proceedings of the NATO Advanced Study Institute, Dundee, Scotland, Aug. 17-Sept. 6, 1986 p 71 A88-37126
American Society for Photogrammetry and Remote Sensing and ACSM, Fall Convention, Reno, NV, Oct. 4-9, 1987, ASPRS Technical Papers p 73 A88-41943
Remote sensing for resources development and environmental management; Proceedings of the Seventh International Symposium, Enschede, Netherlands, Aug. 25-29, 1986. Volumes 1, 2, & 3 p 18 A88-41961

- Geotechnical applications of remote sensing and remote data transmission; Proceedings of the Symposium, Cocoa Beach, FL, Jan. 31-Feb. 1, 1986 p 35 A88-45634
Ocean general circulation models: Report on proceedings of a meeting of ocean and climate modelers [DE88-005530] p 49 N88-22504
Contributions to geodesy, photogrammetry and cartography. Series 1, number 46 --- conference [ISSN-0469-4244] p 25 N88-32729
Latin American Symposium on Remote Sensing. 4th Brazilian Remote Sensing Symposium and 6th SELPER Plenary Meeting, volume 1 p 75 N88-24013
- CONIFERS**
Optimal Thematic Mapper bands and transformations for discerning metal stress in coniferous tree canopies p 7 A88-42002
Inventory of decline and mortality in spruce-fir forests of the eastern U.S. with CIR photos p 7 A88-42004
Spruce budworm infestation detection using an airborne pushbroom scanner and Thematic Mapper data p 8 A88-42007
Simulation of L-band and HH microwave backscattering from coniferous forest stands - A comparison with SIR-B data p 12 A88-44643
- CONTINENTAL SHELVES**
Influence of the Yukon River on the Bering Sea [NASA-CR-182802] p 50 N88-24126
- COORDINATE TRANSFORMATIONS**
Transformation of Global Vegetation Index (GVI) data from the polar stereographic projection to an equatorial cylindrical projection p 58 A88-39095
- COPPER**
Spectral reflectance from lichens treated with copper p 30 A88-32945
- CORN**
Remote sensing techniques in the estimation of the area cultivated with beans, corn, and castor beans in the Itrec County (Bahia State) p 15 N88-24045
Spectral behavior of crops through analysis of LANDSAT-TM data p 15 N88-24047
Evaluation of TM false color composites for crop discrimination p 17 N88-24096
- COST EFFECTIVENESS**
Economic potential of Landsat Thematic Mapper data for crop condition assessment of winter wheat p 4 A88-41948
- CROP GROWTH**
Regional crop-forecasting with Landsat - A farmer's experience [AAS PAPER 86-401] p 2 A88-35161
The potential of numerical agronomic simulation models in remote sensing p 9 A88-42061
Assessment of crop loss from air pollutants: Meteorology-atmospheric chemistry and long range transport [PB88-146857] p 12 N88-22448
Estimation of an area cultivated with wheat from LANDSAT data through a two-phase sampling method p 14 N88-24041
Remote sensing techniques in the estimation of the area cultivated with beans, corn, and castor beans in the Itrec County (Bahia State) p 15 N88-24045
CANASATE: Sugar cane mapping by satellite p 15 N88-24046
Identification of areas cultivated with soybeans in the cerrados regions, through digital processing of satellite images: A methodological approach p 15 N88-24048
- CROP IDENTIFICATION**
Spectral signature of rice fields using Landsat-5 TM in the Mediterranean coast of Spain p 6 A88-41991
Multitemporal analysis of Landsat Multispectral Scanner (MSS) and Thematic Mapper (TM) data to map crops in the Po valley (Italy) and in Mendoza (Argentina) p 6 A88-41994
Landsat temporal-spectral profiles of crops on the South African highveld p 7 A88-41999
The use of multitemporal Landsat data for improving crop mapping accuracy p 7 A88-42003
In flight calibration for the imaging instrument of VEGETATION payload (SPOT 4) p 10 A88-42545
Crop classification from airborne synthetic aperture radar data p 10 A88-43220
Spectral behavior of crops through analysis of LANDSAT-TM data p 15 N88-24047
Identification of areas cultivated with soybeans in the cerrados regions, through digital processing of satellite images: A methodological approach p 15 N88-24048
- CROP INVENTORIES**
Contribution of remote sensing to food security and early warning systems in drought affected countries in Africa p 8 A88-42008
Double sampling for rice in Bangladesh using Landsat MSS data p 8 A88-42009

CROP VIGOR

- Economic potential of Landsat Thematic Mapper data for crop condition assessment of winter wheat p 4 A88-41948
- The derivation of a simplified reflectance model for the estimation of LAI -- Leaf Area Index p 6 A88-41987
- Contribution of remote sensing to food security and early warning systems in drought affected countries in Africa p 8 A88-42008
- Potato crop distribution and subdivision on soil type and potential water deficit - An integration of satellite imagery and environmental spatial database p 10 A88-43222
- Contrast enhancement of aerospace scanner imagery of crop fields p 11 A88-43671

CROSS POLARIZATION

- An empirical model for polarized and cross-polarized scattering from a vegetation layer p 11 A88-44116

CRUSTAL FRACTURES

- Associations among lineaments, subsurface fractures, hydrocarbon microseepage, and production in the Uinta Basin, Utah p 27 A88-32908
- Fracture patterns and production trends, Big Sandy Field, eastern Kentucky p 27 A88-32913
- Geoid anomalies across Pacific fracture zones p 24 A88-38023
- The effect of a shallow low-viscosity zone on the mantle flow, the geoid anomalies and the geoid and depth-age relationships at fracture zones p 24 A88-38024
- Magnetic lineations on the flanks of the Marquesas swell - Implications for the age of the seafloor p 44 A88-41257

D**DAMAGE ASSESSMENT**

- Determination of spectral signatures of different forest damages from varying altitudes of multispectral scanner data p 6 A88-41993
- Experiences in application of multispectral scanner-data for forest damage inventory p 8 A88-42010
- Tornado tracks in Southwestern Brazil, Eastern Paraguay, and Northwestern Argentina p 23 N88-24071

DATA ACQUISITION

- The acquisition of SPOT-1 HRV imagery over southern Britain and northern France, May 1986-May 1987 p 68 A88-29286
- Non-tracking antenna systems for the acquisition of NOAA HRPT Data --- High Resolution Picture Transmission p 72 A88-37279
- Calibration and processing of AVHRR data for temperature estimation [INPE-4493-PRE/1257] p 65 N88-22485
- Real-time environmental Arctic monitoring (R-TEAM) [AD-A189948] p 49 N88-22508

DATA BASE MANAGEMENT SYSTEMS

- Satellite data management for effective data access p 42 A88-38690

DATA BASES

- A comprehensive LRIS of the Kananaskis Valley using Landsat data --- Land-Related Information System p 21 A88-42064
- The SAGE geographic analysis system p 22 N88-24063
- Implantation of a geo-cartographical information system through microcomputers p 67 N88-24064

DATA COMPRESSION

- Processing, compression and transmission of satellite IR data for near-real-time use at sea p 41 A88-36843
- A comparative analysis of methods for compressing spectrophotometric data in the estimation of hydrological parameters p 54 A88-43673

DATA INTEGRATION

- Visual interpretation of MSS-FCC manual cartographic integration of data p 61 A88-42001
- Remote sensing and data integration: Practical solutions for resource managers p 22 N88-24034

DATA MANAGEMENT

- Satellite data management for effective data access p 42 A88-38690
- Proposals for the pre-operational use of data from the European Remote Sensing Satellite ERS-1 [BCRS-86-02] p 65 N88-23300
- Implantation of a geo-cartographical information system through microcomputers p 67 N88-24064

DATA PROCESSING

- Processing, compression and transmission of satellite IR data for near-real-time use at sea p 41 A88-36843
- Digital processing of airborne MSS data for forest cover types classification p 5 A88-41963
- Comparison of classification results of original and preprocessed satellite data p 59 A88-41965
- From satellite altimetry to ocean topography, a survey of data processing techniques [ETN-88-91841] p 48 N88-21575

- Latin American Symposium on Remote Sensing, 4th Brazilian Remote Sensing Symposium and 6th SELPER Plenary Meeting, volume 1 p 75 N88-24013
- Identification of areas cultivated with soybeans in the cerrados regions, through digital processing of satellite images: A methodological approach p 15 N88-24048

DATA RECORDERS

- Earth observation: Capturing the imagery - Remote sensing depends on advanced recording technology p 72 A88-38411

DATA SAMPLING

- A comparison of sampling schemes used in generating error matrices for assessing the accuracy of maps generated from remotely sensed data p 59 A88-39098

DATA SIMULATION

- Per-field classification of a segmented SPOT simulated image p 60 A88-41970
- Digital classification of forested areas using simulated TM- and SPOT- and Landsat 5/TM-data p 5 A88-41971
- The use of SPOT simulation data in forestry mapping p 7 A88-42006
- Comparison of SPOT-simulated and Landsat 5 TM imagery in vegetation mapping p 9 A88-42014

DATA STORAGE

- Satellite data management for effective data access p 42 A88-38690

DATA SYSTEMS

- Data reception, archiving and distribution --- digital image processing using AVHRR flofn on NOAA p 58 A88-37131
- Proposals for the pre-operational use of data from the European Remote Sensing Satellite ERS-1 [BCRS-86-02] p 65 N88-23300

DATA TRANSMISSION

- Geotechnical applications of remote sensing and remote data transmission; Proceedings of the Symposium, Cocoa Beach, FL, Jan. 31-Feb. 1, 1986 p 35 A88-45634
- Overview of remote data transmission systems p 55 A88-45643

DECIDUOUS TREES

- Shift in spectral response of nickel-loaded and control shoots of white birch p 1 A88-32928

DECISION MAKING

- Remote sensing and data integration: Practical solutions for resource managers p 22 N88-24034

DEFORMATION

- Geodetic measurement of deformation east of the San Andreas fault in Central California [NASA-CR-182709] p 36 N88-20754

DELTA

- Turbidity patterns in the delta waters of southwest Netherlands on Thematic Mapper (TM) and multispectral scanner (MSS) satellite images [BCRS-86-06] p 55 N88-23303

DEPLOYMENT

- Real-time environmental Arctic monitoring (R-TEAM) [AD-A189948] p 49 N88-22508

DESERTIFICATION

- Assessment of desertification in the lower Nile Valley (Egypt) by an interpretation of Landsat MSS colour composites and aerial photographs p 61 A88-42025

DESERTS

- Detection by side-looking radar of geological structures under thin cover sands in arid areas p 33 A88-41979
- The use of Thematic Mapper imagery for geomorphological mapping in arid and semi-arid environments p 33 A88-41992
- Monitoring geomorphological processes in desert marginal environments using multitemporal satellite imagery p 34 A88-42030
- A comparative analysis of dyke lineaments mapped from Shuttle Imaging Radar and Large Format Camera photography in hyperarid areas of the Eastern Desert, Egypt, and Red Sea Hills, Sudan p 35 A88-44647

DETECTION

- Shape detection in remote sensing through graph isomorphism p 67 N88-24028

DEVELOPING NATIONS

- Remote sensing for survey of material resources of highway engineering projects in developing countries p 20 A88-42032
- Application of remote sensing in hydromorphology for third world development - A resource development study in parts of Haryana (India) p 53 A88-42042

DIGITAL DATA

- Digital terrain model and image integration for geologic interpretation p 26 A88-32904
- Data reception, archiving and distribution --- digital image processing using AVHRR flofn on NOAA p 58 A88-37131
- Digital processing of airborne MSS data for forest cover types classification p 5 A88-41963
- SLAR as a research tool p 73 A88-41976

- Evaluation of digitally processed Landsat imagery and SIR-A imagery for geological analysis of West Java region, Indonesia p 33 A88-41983

- Insertion of hydrological decorrelated data from photographic sensors of the Shuttle in a digital cartography of geophysical exploration (Spacelab 1-Metric Camera and Large Format Camera) p 74 A88-41990

- Evaluation of combined multiple incident angle SIR-B digital data and Landsat MSS data over an urban complex p 62 A88-42055

- Use of digital terrain data in the interpretation of SPOT-1 HRV multispectral imagery p 10 A88-43221

- Application of spatial statistics to analyzing multiple remote sensing data sets p 64 A88-45639

- Calibration and processing of AVHRR data for temperature estimation [INPE-4493-PRE/1257] p 65 N88-22485

- Textural features for image classification in remote sensing p 66 N88-24027

- Visualization of digital terrain models p 67 N88-24081

- Application of its transformation in color enhancement of LANDSAT imagery p 68 N88-24082

- Preliminary study on the application of digital processing of TM-LANDSAT data in the mapping of apple orchards in Fraiburgo (SC) p 17 N88-24093

DIGITAL RADAR SYSTEMS

- Restoration techniques for SIR-B digital radar images p 57 A88-32933

DIGITAL SIMULATION

- The potential of numerical agronomic simulation models in remote sensing p 9 A88-42061

DIGITAL TECHNIQUES

- Digital elevation modeling with stereo SIR-B image data p 60 A88-41981

- Comparative utilization of analog and digital processes in the treatment of MSS-LANDSAT data for studying the national parks of Brazil [INPE-4011-TDL/240] p 21 N88-22456

- Evaluation of TM false color composites for crop discrimination p 17 N88-24096

DIPOL

- Mushroom-shaped currents (eddy dipoles) under rotation and stratification conditions p 47 N88-20678

DISPLAY DEVICES

- Restoration techniques for redisplay of LANDSAT-5 satellite imagery [INPE-4189-PRE/1076] p 64 N88-20712

DISTRIBUTED PROCESSING

- Global distributive computer processing systems for environmental monitoring, analysis and trend modeling in early warning and natural disaster mitigation p 19 A88-42020

DISTRIBUTION (PROPERTY)

- Assessment of crop loss from air pollutants: Meteorology-atmospheric chemistry and long range transport [PB88-146857] p 12 N88-22448

DIURNAL VARIATIONS

- The determination of the parameters of the diurnal thermocline using satellite and ship-based measurements p 44 A88-40834

DOPPLER NAVIGATION

- The production of distortion free SAR imagery p 57 A88-33377

DOPPLER RADAR

- Cloud and precipitation remote sensing at 94 GHz p 74 A88-44306

DRAINAGE

- Characteristics of drainage determinations in aerial photographs and relief determination on different scales planialtimetric charts for three soils in the state of Sao Paulo p 17 N88-24095
- Criteria for planimetric and altimetric correction of maps restituted from aerial photographs in 1:100,000 scale p 38 N88-24097

DRAINAGE PATTERNS

- Quantitative description and classification of drainage patterns p 51 A88-35399

DROUGHT

- Contribution of remote sensing to food security and early warning systems in drought affected countries in Africa p 8 A88-42008

- Operational satellite data assessment for drought/disaster early warning in Africa - Comments on GIS requirements --- Geographic Information System p 19 A88-42018

- Potato crop distribution and subdivision on soil type and potential water deficit - An integration of satellite imagery and environmental spatial database p 10 A88-43222

DUNES

- Shuttle imaging radar response from sand dunes and subsurface rocks of Alashan Plateau in north-central China p 33 A88-41978

- Dune fields in central Western Argentina p 38 N88-24088

E

EARLY WARNING SYSTEMS

Global distributive computer processing systems for environmental monitoring, analysis and trend modeling in early warning and natural disaster mitigation p 19 A88-42020

EARTH ALBEDO

Satellite observation of surface albedo over the Qinghai-Xinjiang plateau region p 24 A88-39518

EARTH ATMOSPHERE

Method for rapidly estimating geophysical parameters of the ocean-atmosphere system from satellite microwave radiometry p 46 A88-43669

EARTH CRUST

Mapping the Oman Ophiolite using TM data p 26 A88-32906

EARTH MANTLE

The effect of a shallow low-viscosity zone on the mantle flow, the geoid anomalies and the geoid and depth-age relationships at fracture zones p 24 A88-38024

EARTH OBSERVATIONS (FROM SPACE)

Marine Observation Satellite-1 (MOS-1) and its sensors

[AAS PAPER 86-288] p 40 A88-35153
ERS-1, Earth Resources Satellite-1 and future earth observation program in Japan

[AAS PAPER 86-289] p 69 A88-35154
Space geodesy and earthquake prediction

[AAS PAPER 86-307] p 24 A88-35156
Potential for earth observations from the manned Space Station

[AAS PAPER 86-426] p 70 A88-35162
Imaging instrument of the Vegetation Payload (SPOT 4)

Sensors to record atmospheric and terrestrial information - Principles of collection and analysis p 71 A88-37130

Microwave instruments and methods --- for sounding of earth atmosphere and surface p 71 A88-37132

Remote sensing in the Space Station and Columbus programmes p 71 A88-37150

A comparison of sampling schemes used in generating error matrices for assessing the accuracy of maps generated from remotely sensed data p 59 A88-39098

Differentiation of ecological zones in the Okavango Delta, Botswana by classification and contextual analyses of Landsat MSS data p 59 A88-39099

Comparative analysis of results of photographic observations of natural objects from Salyut-7 p 72 A88-39919

Geographic study of the north coast of Senegal using MOMS-1 satellite data p 73 A88-41093

Human settlement analysis using Shuttle Imaging Radar-A data - An evaluation p 20 A88-42057

Remote sensing technology and applications p 46 A88-44005

A comparative analysis of dyke lineaments mapped from Shuttle Imaging Radar and Large Format Camera photography in hyperarid areas of the Eastern Desert, Egypt, and Red Sea Hills, Sudan p 35 A88-44647

The 'Tsukusys' image processing system and its utilization in Thematic Mapper investigations of water quality conditions p 54 A88-45115

Evaluations of unsupervised methods for land-cover/use classifications of Landsat TM data p 64 A88-45116

Measurement of the water content of soil from space and application to the regional water balance p 55 N88-21561

Study of the dynamic topography of oceans by means of satellite altimetry p 47 N88-21567

International cooperation in remote sensing: The ESA experience p 77 N88-24038

The role of space borne imaging radars in environmental monitoring: Some shuttle imaging radar results in Asia [NASA-TM-101178] p 23 N88-24844

EARTH RADIATION BUDGET

Climatological interpretation of time series of satellite observations of the earth's radiation balance p 69 A88-33872

EARTH RESOURCES

Using the thermal infrared multispectral scanner (TIMS) to estimate surface thermal responses p 73 A88-40785

Remote sensing for resources development and environmental management; Proceedings of the Seventh International Symposium, Enschede, Netherlands, Aug. 25-29, 1986. Volumes 1, 2, & 3 p 18 A88-41961

How few data do we need - Some radical thoughts on renewable natural resources surveys p 9 A88-42060

Recording resources in rural areas p 20 A88-42062

Evaluation of regional land resources using geographic information systems based on linear quadrants p 20 A88-42063

Monitoring environmental resources through NOAA's polar orbiting satellites p 21 A88-42070

The use of metric multispectral photography in environmental and resource exploration p 21 A88-44446

Mission to planet earth p 77 A88-45110

The Joint NASA/Geosat Test Case Project p 36 A88-45642

A proposal for a project entitled assessment of forest resources in Uruguay submitted to the United Nations Industrial Development Organization (UNIDO) p 13 N88-24016

The application of satellites in connection with the environment [ETN-88-92474] p 24 N88-25020

EARTH ROTATION

Determination of Earth rotation by the combination of data from different space geodetic systems [NASA-CR-181388] p 25 N88-20713

EARTH SURFACE

Sparse-aperture microwave radiometers for earth remote sensing p 68 A88-35150

The production of distortion free SAR imagery p 57 A88-33377

The use of multispectral space photographs to draw up a map of land use in western Slovakia p 57 A88-33774

Remote sensing of snow p 50 A88-35198

Remote sensing of the earth's surface in the ultraviolet range p 32 A88-36172

Image processing for earth remote sensing p 58 A88-37287

The semivariogram in remote sensing - An introduction p 58 A88-37421

Satellite observation of surface albedo over the Qinghai-Xinjiang plateau region p 24 A88-39518

A four-layer model for the heat budget of homogeneous land surfaces p 4 A88-41028

How few data do we need - Some radical thoughts on renewable natural resources surveys p 9 A88-42060

Taking the effect of vegetation into account in the microwave-radiometer remote sensing of the earth surface on the results of remote sounding of the earth surface by microwave radiometry p 10 A88-43670

Comparison of radar and microwave radiometer techniques for determining permittivity p 74 A88-44231

A satellite-based investigation of the significance of surficial deposits for surface mining operations p 36 A88-45638

Geotechnical applications of three new U.S. Government remote sensing programs p 36 A88-45641

Airborne resistivity mapping p 36 A88-45771

Remote sensing of earth terrain [NASA-CR-182677] p 12 N88-20711

The Shuttle Imaging Radar B (SIR-B) experiment report [NASA-CR-182923] p 75 N88-23932

EARTH TIDES

Satellite observations of tidal upwelling and mixing in the St. Lawrence estuary p 45 A88-42450

EARTHNET

International cooperation in remote sensing: The ESA experience p 77 N88-24038

EARTHQUAKES

Space geodesy and earthquake prediction [AAS PAPER 86-307] p 24 A88-35156

ECOLOGY

Differentiation of ecological zones in the Okavango Delta, Botswana by classification and contextual analyses of Landsat MSS data p 59 A88-39099

ECONOMICS

Review of power requirements for satellite remote sensing systems p 76 N88-24387

ECOSYSTEMS

Monitoring the environment by remote sensing p 18 A88-33770

The use of SLAR and SIRA imagenes for the classification of forest types in tropical rain forests p 14 N88-24036

Structure and dynamics of vegetation in the middle semi-arid tropics. Quixaba's Caatinga (PE): Terrain analysis of MSS/LANDSAT data p 15 N88-24049

Interpretation of MSS/LANDSAT data for evaluation of physical distribution of mangroves in Cananea-Iguaape (SP) p 16 N88-24072

EDDY CURRENTS

Parameters of eddy structures and mushroom currents in the Baltic Sea derived from satellite imagery p 46 A88-43665

ELECTRIC POWER PLANTS

Remote sensing as a tool for assessing environmental effects of hydroelectric development in a remote river basin p 53 A88-42045

Estimation of reservoir submerging losses using CIR aerial photographs - Example of the Ertan hydropower station on the Yalong River in southwest China p 55 A88-45637

ELECTRICAL RESISTIVITY

Airborne resistivity mapping p 36 A88-45771

ELECTRIFICATION

Utilization of LANDSAT-TM imagery in the hydroenergetic inventory of the Paraba de Sul River Basin p 56 N88-24077

ELECTRO-OPTICS

Remote sensing technology and applications p 46 A88-44005

ELEVATION

Digital elevation modeling with stereo SIR-B image data p 60 A88-41981

A VHF radar to make terrain elevation models through tropical jungle p 10 A88-42760

Mapping from LANDSAT and SPOT satellite imagery p 66 N88-24018

EMISSIONITY

A method for calculating the effective emissivity of a groove structure --- sea surface temperature measurement p 40 A88-35986

ENDANGERED SPECIES

Remote sensing for wildlife management - Giant panda habitat mapping from Landsat MSS images p 2 A88-35195

ENERGY BUDGETS

Surface energy budget, surface temperature and thermal inertia p 58 A88-37147

A four-layer model for the heat budget of homogeneous land surfaces p 4 A88-41028

ENERGY SOURCES

A proposal for a project entitled assessment of forest resources in Uruguay submitted to the United Nations Industrial Development Organization (UNIDO) p 13 N88-24016

ENTHALPY

Radiative processes affecting ocean mixed-layer heat content and their monitoring from satellite p 47 N88-20800

ENTOMOLOGY

Remote-sensing methods for the monitoring and forecasting of the entomological condition of taiga forests p 2 A88-36164

ENVIRONMENT EFFECTS

Thermal analysis of wildfires and effects on global ecosystem cycling p 2 A88-35194

Assessment of crop loss from air pollutants: Meteorology-atmospheric chemistry and long range transport [PB88-146857] p 12 N88-22448

Detection, monitoring and analysis of some environmental effects of fires in the Amazon region through utilization of NOAA and LANDSAT satellite imagery and aircraft data [INPE-4503-TDL/326] p 13 N88-23322

Detection of biomass burning and smoke plumes in the Amazon region through NOAA satellite imagery p 23 N88-24085

ENVIRONMENT MANAGEMENT

Remote sensing for resources development and environmental management; Proceedings of the Seventh International Symposium, Enschede, Netherlands, Aug. 25-29, 1986. Volumes 1, 2, & 3 p 18 A88-41961

Operational satellite data assessment for drought/disaster early warning in Africa - Comments on GIS requirements --- Geographic Information System p 19 A88-42018

ENVIRONMENT POLLUTION

Particulate emissions from a mid-latitude prescribed chaparral fire p 3 A88-38805

SIR-B experiments in Japan. III - Oil-pollution experiment p 43 A88-40353

SIR-B experiments in Japan. VI. p 43 A88-40356

Remote sensing assessment of environmental impacts caused by phosphat industry destructive influence p 19 A88-42031

ENVIRONMENT PROTECTION

Coastal monitoring by remote sensing p 54 A88-44447

ENVIRONMENTAL MONITORING

Monitoring the environment by remote sensing p 18 A88-33770

Long-term air quality monitoring at the South Pole by the NOAA program Geophysical Monitoring for Climatic Change p 18 A88-36243

Global distributive computer processing systems for environmental monitoring, analysis and trend modeling in early warning and natural disaster mitigation p 19 A88-42020

Monitoring geomorphological processes in desert marginal environments using multitemporal satellite imagery p 34 A88-42030

- Remote sensing assessment of environmental impacts caused by phosphat industry destructive influence p 19 A88-42031
- Small scale erosion hazard mapping using Landsat information in the northwest of Argentina p 9 A88-42035
- Remote sensing as a tool for assessing environmental effects of hydroelectric development in a remote river basin p 53 A88-42045
- Environmental assessment for large scale civil engineering projects with data of DTM and remote sensing --- Digital Terrain Models p 53 A88-42046
- Recording resources in rural areas p 20 A88-42062
- Evaluation of regional land resources using geographic information systems based on linear quadrees p 20 A88-42063
- Land resource use monitoring in Romania, using aerial and space data p 21 A88-42065
- Monitoring environmental resources through NOAA's polar orbiting satellites p 21 A88-42070
- The use of metric multispectral photography in environmental and resource exploration p 21 A88-44446
- Coastal monitoring by remote sensing p 54 A88-44447
- Real-time environmental Arctic monitoring (R-TEAM) [AD-A189948] p 49 N88-22508
- Study of reservoir water quality utilizing remote sensing techniques: Methodological concepts p 56 N88-24076
- The role of space borne imaging radars in environmental monitoring: Some shuttle imaging radar results in Asia [NASA-TM-101178] p 23 N88-24844
- The application of satellites in connection with the environment [ETN-88-92474] p 24 N88-25020
- EQUATORIAL REGIONS**
- Monitoring of renewable resources in equatorial countries p 19 A88-42000
- ERROR ANALYSIS**
- A method for calculating the effective emissivity of a groove structure --- sea surface temperature measurement p 40 A88-35986
- Radiative surface temperatures of the burned and unburned areas in a tallgrass prairie p 3 A88-37418
- Using spatial autocorrelation analysis to explore the errors in maps generated from remotely sensed data p 58 A88-39097
- A comparison of sampling schemes used in generating error matrices for assessing the accuracy of maps generated from remotely sensed data p 59 A88-39098
- Manual interpretation of small forestlands on Landsat MSS data p 12 A88-44521
- ERRORS**
- The modeling of error budget analysis and tolerance specifications for BRESEX multiband linear array CCD camera p 76 N88-24029
- Study of methods of post-processing applied to a problem of standard classification p 67 N88-24067
- ERS-1 (ESA SATELLITE)**
- The Along-Track Scanning Radiometer with Microwave Sounder p 41 A88-37148
- Plans for ERS-1 data acquisition, processing and distribution p 41 A88-37149
- Proposals for the pre-operational use of data from the European Remote Sensing Satellite ERS-1 [BCRS-86-02] p 65 N88-23300
- Study of the plan for a national data center for the European Remote Sensing Satellite ERS-1 [BCRS-87-11] p 66 N88-23309
- ESTIMATING**
- Tidal estimation in the Pacific with application to SEASAT altimetry [NASA-TM-100694] p 47 N88-20780
- ESTUARIES**
- Quantitative analysis of distribution of suspended sediments in the Yellow River Estuary from MSS data p 50 A88-35196
- Satellite detection of bloom and pigment distributions in estuaries p 51 A88-37414
- Satellite observations of tidal upwelling and mixing in the St. Lawrence estuary p 45 A88-42450
- EUROPEAN SPACE AGENCY**
- International cooperation in remote sensing: The ESA experience p 77 N88-24038
- EUROPEAN SPACE PROGRAMS**
- Study of the plan for a national data center for the European Remote Sensing Satellite ERS-1 [BCRS-87-11] p 66 N88-23309
- International cooperation in remote sensing: The ESA experience p 77 N88-24038
- EVAPOTRANSPIRATION**
- The effect of atmospheric correction on the interpretation of multitemporal AVHRR-derived vegetation index dynamics p 11 A88-44117
- On the regional characteristics of actual evapotranspiration derived from Landsat MSS and elevation data p 54 A88-45118
- EXPERIMENT DESIGN**
- The WOCE Core Project Planning Meeting on the Gyre Dynamics Experiment --- ocean dynamics [WCP-139] p 49 N88-23358
- F**
- FARM CROPS**
- Linear combinations of spectral reflectances in crop analyses p 3 A88-36170
- Crop classification from airborne synthetic aperture radar data p 10 A88-43220
- A second generation lunar agricultural system p 11 A88-43864
- FARMLANDS**
- Processing of multirate Landsat TM data to map soil color variations related to hydrocarbon microseepage in a cropland setting - Cement, Oklahoma test site p 1 A88-32921
- FINITE ELEMENT METHOD**
- The effect of a shallow low-viscosity zone on the mantle flow, the geoid anomalies and the geoid and depth-age relationships at fracture zones p 24 A88-38024
- FIRES**
- Thermal analysis of wildfires and effects on global ecosystem cycling p 2 A88-35194
- Detection, monitoring and analysis of some environmental effects of fires in the Amazon region through utilization of NOAA and LANDSAT satellite imagery and aircraft data [INPE-4503-TDL/326] p 13 N88-23322
- Detection of biomass burning and smoke plumes in the Amazon region through NOAA satellite imagery p 23 N88-24085
- FLIR DETECTORS**
- Theoretical basis for multispectral imaging simulation p 63 A88-44532
- FLOOD DAMAGE**
- Flood damage analysis using multitemporal Landsat Thematic Mapper data p 4 A88-39090
- FLOOD PLAINS**
- Multi-temporal Landsat for land unit mapping on project scale of the Sudd-floodplain, Southern Sudan p 9 A88-42015
- Geomorphologic sector maps of Niquizanga-Mayares, province of San Juan, Argentina p 38 N88-24098
- FLOOD PREDICTIONS**
- Using Landsat to derive curve numbers for hydrologic models p 52 A88-41950
- FLOODS**
- The quantification of floodplain inundation by the use of Landsat and Metric Camera information, Belize, Central America p 53 A88-42044
- Project CODEAMA/FUNCATE (test-area of Barreirinha-AM): Field report [INPE-4500-RPE/563] p 55 N88-22455
- Evaluation of the floodable area of the canal of Sao Goncalo through TM-LANDSAT 5 imagery p 56 N88-24078
- Mapping of plant associations and the variation of surface water in the Pantanal Mato-Grossense National Park, through remote sensing techniques p 17 N88-24092
- FLOW CHARACTERISTICS**
- Remote sensing of flow characteristics of the strait of Oresund p 53 A88-42043
- FLOW DISTRIBUTION**
- Remote sensing and image processing requirements for Eulerian flow field estimations p 51 A88-39078
- Identification of shallow groundwater regions in semi-arid Brazil by remote sensing methods p 14 N88-24030
- FLUX (RATE)**
- Radiative processes affecting ocean mixed-layer heat content and their monitoring from satellite p 47 N88-20800
- FOCUSING**
- Geodetic measurement of deformation east of the San Andreas fault in Central California [NASA-CR-182709] p 36 N88-20754
- FOLIAGE**
- Millimeter-wave bistatic scattering from ground and vegetation targets p 11 A88-44308
- FOREST FIRES**
- Particulate emissions from a mid-latitude prescribed chaparral fire p 3 A88-38805
- History of wildland fires on Vandenberg Air Force Base, California [NASA-TM-100983] p 18 N88-25134
- FOREST MANAGEMENT**
- Determination of spectral signatures of different forest damages from varying altitudes of multispectral scanner data p 6 A88-41993
- Inventory of decline and mortality in spruce-fir forests of the eastern U.S. with CIR photos p 7 A88-42004
- The use of SPOT simulation data in forestry mapping p 7 A88-42006
- Experiences in application of multispectral scanner-data for forest damage inventory p 8 A88-42010
- Classification of the Riverina forests of south east Australia using co-registered Landsat MSS and SIR-B radar data p 9 A88-42013
- Utilization of TM/LANDSAT images in the implanted forests mapping in the Mogi-Guaçu Region (SP-Brazil) p 14 N88-24042
- FORESTS**
- Influence of topography on forest reflectance using Landsat Thematic Mapper and digital terrain data p 2 A88-35397
- Remote-sensing methods for the monitoring and forecasting of the entomological condition of taiga forests p 2 A88-36164
- Investigation and mapping of forests using space scanner imagery obtained in winter p 2 A88-36165
- A methodology for mapping forest latent heat flux densities using remote sensing p 3 A88-37415
- Correlation between aircraft MSS and LIDAR remotely sensed data on a forested wetland in South Carolina p 5 A88-41951
- Obtaining spectral reflectance factor measurements of stressed forest vegetation p 5 A88-41952
- Remote sensing and the role of terrestrial vegetation in the global carbon cycle p 5 A88-41954
- Digital processing of airborne MSS data for forest cover types classification p 5 A88-41963
- Digital classification of forested areas using simulated TM- and SPOT- and Landsat 5/TM-data p 5 A88-41971
- Millimeter-wave propagation in vegetation: Experiments and theory p 12 A88-44319
- Manual interpretation of small forestlands on Landsat MSS data p 12 A88-44521
- Simulation of L-band and HH microwave backscattering from coniferous forest stands - A comparison with SIR-B data p 12 A88-44643
- Remote sensing of earth terrain [NASA-CR-182677] p 12 N88-20711
- Detection, monitoring and analysis of some environmental effects of fires in the Amazon region through utilization of NOAA and LANDSAT satellite imagery and aircraft data [INPE-4503-TDL/326] p 13 N88-23322
- Radar penetration in the Amazonian rain forest p 13 N88-24015
- A proposal for a project entitled assessment of forest resources in Uruguay submitted to the United Nations Industrial Development Organization (UNIDO) p 13 N88-24016
- Airborne and spaceborne radar images for geologic and environmental mapping in the Amazon rain forest, Brazil p 37 N88-24021
- The use of SLAR and SIRA imagenes for the classification of forest types in tropical rain forests p 14 N88-24036
- Utilization of TM/LANDSAT images in the implanted forests mapping in the Mogi-Guaçu Region (SP-Brazil) p 14 N88-24042
- Anomalies in the vegetation in the Alto Xingu - MT p 14 N88-24043
- Radar penetration in the Amazonian rain forest p 15 N88-24044
- Stereoscopic photographs, ground and aerial, of trees used in the arborization of Curitiba (PR) p 17 N88-24091
- Mapping of plant associations and the variation of surface water in the Pantanal Mato-Grossense National Park, through remote sensing techniques p 17 N88-24092
- FOURIER TRANSFORMATION**
- Restoration techniques for redisplay of LANDSAT-5 satellite imagery [INPE-4189-PRE/1076] p 64 N88-20712
- FRESH WATER**
- Principles of the remote monitoring of fresh-water quality p 50 A88-34674
- The dispersal of the Amazon's water p 43 A88-40059
- FROST**
- Mapping frost-sensitive areas with a three-dimensional local-scale numerical model. I - Physical and numerical aspects p 4 A88-41055
- FRUITS**
- Preliminary study on the application of digital processing of TM-LANDSAT data in the mapping of apple orchards in Fraiburgo (SC) p 17 N88-24093

FUELS
History of wildland fires on Vandenberg Air Force Base, California [NASA-TM-100983] p 18 N88-25134

G

GAMMA RAYS
Remote sensing of snow p 50 A88-35198

GAS RECOVERY
Preliminary evaluation of remote sensing data for detection of vegetation stress related to hydrocarbon microseepage - Mist Gas Field, Oregon p 1 A88-32911

Fracture patterns and production trends, Big Sandy Field, eastern Kentucky p 27 A88-32913

GEOBOTANY

A geobotanical investigation of an exploration-sized territory p 29 A88-32931

Spectral geobotanical investigation of mineralized till sites p 29 A88-32934

Surrogate spectral reflectances of vegetation applied to geobotanical remote sensing p 1 A88-32935

Spectral reflectance from lichens treated with copper p 30 A88-32945

Remote sensing of geobotanical associations in clastic sedimentary terrane p 31 A88-32951

Discrimination of geobotanical anomalies in rugged alpine terrain using Landsat Thematic Mapper data p 32 A88-32957

Optimal Thematic Mapper bands and transformations for discerning metal stress in coniferous tree canopies p 7 A88-42002

GEOCHEMISTRY

Landsat TM data as an aid in planning and interpretation of regional geochemical surveys in the Canadian Shield p 31 A88-32950

GEODESY

Geodetic measurement of deformation east of the San Andreas Fault in Central California p 25 A88-32831

Space geodesy and earthquake prediction [AAS PAPER 86-307] p 24 A88-35156

Effect of wet tropospheric path delays on estimation of geodetic baselines in the Gulf of California using the Global Positioning System p 25 A88-41835

Determination of Earth rotation by the combination of data from different space geodetic systems [NASA-CR-181388] p 25 N88-20713

Criteria for planimetric and altimetric correction of maps restituted from aerial photographs in 1:100,000 scale p 38 N88-24097

GEODEIC SURVEYS

Geodetic measurement of deformation east of the San Andreas Fault in Central California p 25 A88-32831

Base map production from geocoded imagery p 25 A88-41969

Geodetic measurement of deformation east of the San Andreas fault in Central California [NASA-CR-182709] p 36 N88-20754

GEOELECTRICITY

Airborne resistivity mapping p 36 A88-45771

GEOGRAPHIC INFORMATION SYSTEMS

Earthscan - A range of remote sensing systems p 61 A88-41982

Operational satellite data assessment for drought/disaster early warning in Africa - Comments on GIS requirements --- Geographic Information System p 19 A88-42018

Evaluation of regional land resources using geographic information systems based on linear quadrees p 20 A88-42063

A comprehensive LRIS of the Kananaskis Valley using Landsat data --- Land-Related Information System p 21 A88-42064

The integration of remote sensing and geographic information systems p 21 A88-42069

Integration of Landsat, DTED, and DFAD p 63 A88-44540

Cartographic feature extraction with integrated SIR-B and Landsat TM images p 63 A88-44641

Updating of the municipal official register of real estate through a geographical information system [INPE-4459-PRE/1238] p 21 N88-22453

Remote sensing and data integration: Practical solutions for resource managers p 22 N88-24034

Implantation of a geo-cartographical information system through microcomputers p 67 N88-24064

Research on enhancing the utilization of digital multispectral data and geographic information systems in global habitability studies [NASA-CR-182799] p 23 N88-24101

GEOGRAPHY

The Systeme d'Analyse Geographique (SAGE) geographic analysis system p 66 N88-24019

The SAGE geographic analysis system p 22 N88-24063

GEOIDS

Geoid anomalies across Pacific fracture zones p 24 A88-38023

The effect of a shallow low-viscosity zone on the mantle flow, the geoid anomalies and the geoid and depth-age relationships at fracture zones p 24 A88-38024

Evidence from geoid data of a hotspot origin for the southern Mascarene Plateau and Mascarene Islands (Indian Ocean) p 24 A88-38902

GEOLOGICAL FAULTS

Importance of fault mapping to mineral/geothermal exploration: Relationship to fluid migration and ore formation - Northwest Washington p 28 A88-32925

Quantitative analysis of a network of faults recognized on remote-sensing images of the Mushguy area in Mongolia p 32 A88-36163

Analysis of lineaments and major fractures in Xichang-Dukou area, Sichuan province as interpreted from Landsat images p 34 A88-42022

Structural geology and regional tectonics of the Mineral County area, Nevada, using Shuttle Imaging Radar-B and digital aeromagnetic data p 35 A88-44646

Study of fracturing for groundwater research in the Sergipe state with remote sensing products p 38 N88-24052

GEOLOGICAL SURVEYS

Thematic Conference on Remote Sensing for Exploration Geology, 5th, Reno, NV, Sept. 29-Oct. 2, 1986, Proceedings, Volumes 1 & 2 p 26 A88-32901

Contribution of Landsat to a geologic expedition in the desert of North Central Sudan, Africa p 27 A88-32916

Detection of geologic features in Landsat TM imagery not revealed in Landsat MSS imagery p 30 A88-32944

Geologic spatial analysis - A new multiple data source exploration tool p 30 A88-32947

Landsat TM data as an aid in planning and interpretation of regional geochemical surveys in the Canadian Shield p 31 A88-32950

Pattern recognition and geological interpretation of SIR-B images of Central Australia p 31 A88-32956

Potential of Landsat Thematic Mapper image for crystalline rock type discrimination - Gregory Rift, Kenya p 32 A88-35192

Computer processing of satellite data for geostructural zoning of a collisional boundary, significance and field checks - The example of Tunisia p 32 A88-35193

Regional geologic mapping of digitally enhanced Landsat imagery in the southcentral Alborz mountains of northern Iran p 34 A88-42017

Geological analysis of the satellite lineaments of the Vistula Delta Plain, Zulawy Wislane, Poland p 34 A88-42021

Application of remote sensing in the field of experimental tectonics p 34 A88-42023

Application of MEIS-II multispectral airborne data and CIR photography for the mapping of surficial geology and geomorphology in the Chatham area, Southwest Ontario, Canada p 34 A88-42027

Remote sensing methods in geological research of the Lublin coal basin, SE Poland p 34 A88-42028

Detecting and mapping of different volcanic stages and other geomorphic features by Landsat images in 'Katakekaumene', Western Turkey p 35 A88-42033

A methodology for integrating satellite imagery and field observations for hydrological regionalisation in Alpine catchments p 52 A88-42038

GEOLOGY

Groundwater sapping valleys: Experimental studies, geological controls and implications to the interpretation of valley networks on Mars [NASA-CR-182718] p 37 N88-22847

GEOMETRIC RECTIFICATION (IMAGERY)

Artificial GCPs in aircraft and satellite scanner imagery --- Ground Control Points p 74 A88-43227

Dependence of image grey values on topography in SIR-B images p 63 A88-44649

GEOMETRICAL OPTICS

Radar backscatter characteristics of trees at 215 GHz p 11 A88-44307

GEOMETRY

The geometric workstation, a new approach for geometric corrections of remotely sensed data p 66 N88-24017

GEOMORPHOLOGY

Multispectral geologic remote sensing of a suspected impact crater near Al Madafi, Saudi Arabia p 33 A88-41955

The use of Thematic Mapper imagery for geomorphological mapping in arid and semi-arid environments p 33 A88-41992

Comparison between interpretation of images of different nature p 34 A88-42019

Monitoring geomorphological processes in desert marginal environments using multitemporal satellite imagery p 34 A88-42030

A remote sensing methodological approach for applied geomorphology mapping in plain areas p 35 A88-42034

Project CODEAMA/FUNCATE (test-area) of Barreirinha-AM): Field report [INPE-4500-RPE/563] p 55 N88-22455

Airborne and spaceborne radar images for geologic and environmental mapping in the Amazon rain forest, Brazil p 37 N88-24021

Subsurface morphology and geochronology revealed by spaceborne and airborne radar p 37 N88-24022

Utilization of LANDSAT-TM, for aiding in the localization of archeological sites in the state of Sao Paulo p 38 N88-24069

The breaked anticlines, cuesta and crest homoclines, ortocinal valleys, and other forms of relief outcrops delineated with the help of remote sensing imagery p 16 N88-24089

Geomorphologic sector maps of Niquizanga-Mayares, province of San Juan, Argentina p 38 N88-24098

GEOPHYSICAL FLUIDS

Discrimination and supervised classification of volcanic flows of the Puna-Altiplano, Central Andes Mountains using Landsat TM data p 31 A88-32948

Distribution and chemistry of suspended particles from an active hydrothermal vent site on the Mid-Atlantic Ridge at 26 deg N p 42 A88-37720

The effect of a shallow low-viscosity zone on the mantle flow, the geoid anomalies and the geoid and depth-age relationships at fracture zones p 24 A88-38024

GEOPHYSICS

Integration of SIR-B imagery with geological and geophysical data in Australia p 27 A88-32912

An integrated study of the Alto Paranaiba Kimberlite Province, Minas Gerais, Brazil: A possible tool for diamond exploration p 37 N88-24031

GEOSAT SATELLITES

The Joint NASA/Geosat Test Case Project p 36 A88-45642

GEO THERMAL RESOURCES

Importance of fault mapping to mineral/geothermal exploration: Relationship to fluid migration and ore formation - Northwest Washington p 28 A88-32925

Digital analysis of stereo pairs for the detection of anomalous signatures in geothermal fields p 61 A88-42037

GLOBAL AIR POLLUTION

Thermal analysis of wildfires and effects on global ecosystem cycling p 2 A88-35194

GLOBAL POSITIONING SYSTEM

Precision positioning of earth orbiting remote sensing systems [AAS PAPER 86-398] p 70 A88-35159

G.P.S. surveying in the Netherlands p 72 A88-37383

Developments in use of GPS as range TSPI --- Time and Space Position Information p 72 A88-37384

The Magnavox civil and military line of GPS receivers - A technology and applications overview p 72 A88-37391

Effect of wet tropospheric path delays on estimation of geodetic baselines in the Gulf of California using the Global Positioning System p 25 A88-41835

Adjustment in photogrammetry: Methods, programs and applications [B8735130] p 76 N88-24105

GOES SATELLITES

A satellite infrared technique to estimate tropical convective and stratiform rainfall p 69 A88-33416

GOLD

A comparison of lineaments interpreted from remotely sensed data and airborne magnetics and their relationship to gold deposits in central Nova Scotia p 29 A88-32936

Thematic Mapper applied to alteration zone mapping for gold exploration in south-east Spain p 29 A88-32938

An integrated approach to the use of Landsat TM data for gold exploration in west central Nevada p 30 A88-32941

GRAPHS (CHARTS)

The semivariogram in remote sensing - An introduction p 58 A88-37421

Shape detection in remote sensing through graph isomorphism p 67 N88-24028

GRASSES

Millimeter-wave multipath measurements on snow cover p 54 A88-44311

GRASSLANDS

Radiative surface temperatures of the burned and unburned areas in a tallgrass prairie p 3 A88-37418

- Mapping of plant associations and the variation of surface water in the Pantanal Mato-Grossense National Park, through remote sensing techniques p 17 N88-24092
- GRAY SCALE**
Dependence of image grey values on topography in SIR-B images p 63 A88-44649
Visualization of digital terrain models p 67 N88-24081
- GRAZING INCIDENCE**
Millimeter-wave multipath measurements on snow cover p 54 A88-44311
- GREAT LAKES (NORTH AMERICA)**
Toward an integrated system for satellite remote sensing of water quality in the Great Lakes p 52 A88-41957
- GROUND BASED CONTROL**
Artificial GCPs in aircraft and satellite scanner imagery --- Ground Control Points p 74 A88-43227
- GROUND TRUTH**
SIR-B experiments in Japan. II - Rice crop experiment p 4 A88-40352
Structural information of the landscape as ground truth for the interpretation of satellite imagery p 59 A88-41962
Double sampling for rice in Bangladesh using Landsat MSS data p 8 A88-42009
Evaluation of an estimation system for an irrigated area in a tropical region through TM-LANDSAT imagery p 16 N88-24075
Evaluation of the mangrove area at the Piaui River (SE) through remote sensing p 16 N88-24086
Stereoscopic photographs, ground and aerial, of trees used in the arborization of Curitiba (PR) p 17 N88-24091
- GROUND WATER**
Saline salt and water surface mapping on the basis of data from the Gyunesh-84 remote-sensing experiment p 51 A88-36166
Spring mound and aioun mapping from Landsat TM imagery in south-central Tunisia p 52 A88-42026
Lineaments: Significance, criteria for determination, and varied effects on ground-water systems - A case history in the use of remote sensing p 55 A88-45636
Groundwater sapping valleys: Experimental studies, geological controls and implications to the interpretation of valley networks on Mars [NASA-CR-182718] p 37 N88-22847
Identification of shallow groundwater regions in semi-arid Brazil by remote sensing methods p 14 N88-24030
Study of fracturing for groundwater research in the Sergipe state with remote sensing products p 38 N88-24052
- GYRES**
The WOCE Core Project Planning Meeting on the Gyre Dynamics Experiment --- ocean dynamics [WCP-139] p 49 N88-23358
- H**
- HABITATS**
Remote sensing for wildlife management - Giant panda habitat mapping from Landsat MSS images p 2 A88-35195
Research on enhancing the utilization of digital multispectral data and geographic information systems in global habitability studies [NASA-CR-182799] p 23 N88-24101
- HEAT FLUX**
On the regional characteristics of actual evapotranspiration derived from Landsat MSS and elevation data p 54 A88-45118
- HEAT TRANSMISSION**
Digital analysis of stereo pairs for the detection of anomalous signatures in geothermal fields p 61 A88-42037
- HEAVY ELEMENTS**
Effects of heavy metal induced canopy structural changes on forest canopy reflectance p 1 A88-32930
- HEURISTIC METHODS**
Low altitude remote sensing data in the implementation of a mathematical model for the planning of urban equipment networks p 23 N88-24074
- HIGH RESOLUTION**
The acquisition of SPOT-1 HRV imagery over southern Britain and northern France, May 1986-May 1987 p 68 A88-29286
Correlation between high resolution remote sensing imagery and hydrothermal alteration, Tybo mining district, Nevada p 27 A88-32915
- HIGH TEMPERATURE FLUIDS**
Distribution and chemistry of suspended particles from an active hydrothermal vent site on the Mid-Atlantic Ridge at 26 deg N p 42 A88-37720
- HIGHWAYS**
Remote sensing for survey of material resources of highway engineering projects in developing countries p 20 A88-42032
- HISTORIES**
History of wildland fires on Vandenberg Air Force Base, California [NASA-TM-100983] p 18 N88-25134
- HYDROCARBON FUEL PRODUCTION**
Fracture patterns and production trends, Big Sandy Field, eastern Kentucky p 27 A88-32913
After exploration, what? - Case histories of seven diverse production, development and distribution applications of remote sensing p 28 A88-32918
- HYDROCARBON POISONING**
Preliminary evaluation of remote sensing data for detection of vegetation stress related to hydrocarbon microseepage - Mist Gas Field, Oregon p 1 A88-32911
- HYDROCARBONS**
Processing of multitemporal Landsat TM data to map soil color variations related to hydrocarbon microseepage in a cropland setting - Cement, Oklahoma test site p 1 A88-32921
The South Alamurynian ring structure - A new promising area to search for hydrocarbon deposits p 32 A88-36162
- HYDROELECTRIC POWER STATIONS**
Geologic interpretation of air photos and radar imagery for hydroelectric power projects in Upper Ucayali Jungle Region of Peru p 28 A88-32922
Utilization of LANDSAT-TM imagery in the hydroenergetic inventory of the Paraíba de Sul River Basin p 56 N88-24077
- HYDROELECTRICITY**
Remote sensing as a tool for assessing environmental effects of hydroelectric development in a remote river basin p 53 A88-42045
Estimation of reservoir submerging losses using CIR aerial photographs - Example of the Ertan hydropower station on the Yalong River in southwest China p 55 A88-45637
- HYDROGEOLOGY**
Spring mound and aioun mapping from Landsat TM imagery in south-central Tunisia p 52 A88-42026
Photo-interpretation of landforms and the hydrogeologic bearing in highly deformed areas, NW of the Gulf of Suez, Egypt p 34 A88-42029
- HYDROGRAPHY**
Insertion of hydrological decolorated data from photographic sensors of the Shuttle in a digital cartography of geophysical exploration (Spacelab 1-Metric Camera and Large Format Camera) p 74 A88-41990
Hydrographic data from the OPTOMA (Ocean Prediction Through Observation, Modeling and Analysis) program: OPTOMA 23, 9-19 November 1986 [AD-A189868] p 49 N88-22506
Hydrographic observations in the northwestern Weddell Sea Marginal Ice Zone during March 1986 [PB88-173240] p 55 N88-23359
- HYDROLOGY**
Remote sensing and image processing requirements for Eulerian flow field estimations p 51 A88-39078
Rangeland runoff curve numbers as determined from Landsat MSS data p 51 A88-39089
Using Landsat to derive curve numbers for hydrologic models p 52 A88-41950
A methodology for integrating satellite imagery and field observations for hydrological regionalisation in Alpine catchments p 52 A88-42038
A hydrological comparison of Landsat TM, Landsat MSS and black and white aerial photography p 52 A88-42041
Application of remote sensing in hydromorphology for third world development - A resource development study in parts of Haryana (India) p 53 A88-42042
A study with NOAA-7 AVHRR-imagery in monitoring ephemeral streams in the lower catchment area of the Tana River, Kenya p 54 A88-42053
A comparative analysis of methods for compressing spectrophotometric data in the estimation of hydrological parameters p 54 A88-43673
Lineaments: Significance, criteria for determination, and varied effects on ground-water systems - A case history in the use of remote sensing p 55 A88-45636
Overview of remote data transmission systems p 55 A88-45643
Project CODEAMA/FUNCATE (test-area of Barreirinha-AM): Field report [INPE-4500-RPE/563] p 55 N88-22455
Evaluation of the floodable area of the canal of Sao Goncalo through TM-LANDSAT 5 imagery p 56 N88-24078
- HYDROLOGY MODELS**
Simple classifiers of satellite data for hydrologic modelling p 52 A88-42040
- HYDROMETEOROLOGY**
The dispersal of the Amazon's water p 43 A88-40059
- HYDROTHERMAL SYSTEMS**
Correlation between high resolution remote sensing imagery and hydrothermal alteration, Tybo mining district, Nevada p 27 A88-32915
Thematic Mapper data applied to mapping hydrothermal alteration in south west New Mexico p 28 A88-32923
- HYPERVELOCITY IMPACT**
Multispectral geologic remote sensing of a suspected impact crater near Al Madafi, Saudi Arabia p 33 A88-41955
- I**
- ICE ENVIRONMENTS**
Real-time environmental Arctic monitoring (R-TEAM) [AD-A189948] p 49 N88-22508
- ICE MAPPING**
Satellite and aircraft passive microwave observations during the Marginal Ice Zone Experiment in 1984 p 45 A88-42447
Marginal Ice Zone Experiment (MIZEX) 1984 VARAN-S data set [ETN-88-92032] p 48 N88-21625
- ICE REPORTING**
A model of satellite radar altimeter return from ice sheets p 46 A88-43218
Ice conditions along the Ohio River as observed on LANDSAT images, 1972-1985 [AD-A191172] p 57 N88-25018
- IGNEOUS ROCKS**
Mapping the Oman Ophiolite using TM data p 26 A88-32906
- ILLUMINANCE**
Analysis of the parameters responsible for the variations of the illumination conditions in the LANDSAT data p 67 N88-24070
- IMAGE ANALYSIS**
Color space mapping using ternary/chromaticity diagrams - A technique for composite image interpretation p 57 A88-32932
Quantitative procedure for producing color-calibrated Thematic Mapper natural-color images p 57 A88-32943
Quantitative analysis of a network of faults recognized on remote-sensing images of the Mushugai area in Mongolia p 32 A88-36163
New aspects of the interpretation of space radar images p 58 A88-36171
Differentiation of ecological zones in the Okavango Delta, Botswana by classification and contextual analyses of Landsat MSS data p 59 A88-39099
Structural information of the landscape as ground truth for the interpretation of satellite imagery p 59 A88-41962
Space photomaps - Their compilation and peculiarities of geographical application p 60 A88-41967
Per-field classification of a segmented SPOT simulated image p 60 A88-41970
Spatial feature extraction from radar imagery p 60 A88-41974
Geological analysis of Seasat SAR and SIR-B data in Haiti p 33 A88-41980
Shuttle imaging radar (SIR-A) interpretation of the Kashgar region in western Xinjiang, China p 74 A88-41985
Determination of spectral signatures of different forest damages from varying altitudes of multispectral scanner data p 6 A88-41993
Comparison between interpretation of images of different nature p 34 A88-42019
Analysis of lineaments and major fractures in Xichang-Dukou area, Sichuan province as interpreted from Landsat images p 34 A88-42022
Analysis of Landsat multispectral-multitemporal images for geologic-lithologic map of the Bangladesh Delta p 35 A88-42049
Textural features for image classification in remote sensing p 66 N88-24027
Interpretation of MSS/LANDSAT data for evaluation of physical distribution of mangroves in Cananea-Iguape (SP) p 16 N88-24072
An update on remote measurement of soil moisture over vegetation using infrared temperature measurements: A FIFE perspective [NASA-CR-182926] p 18 N88-24109
- IMAGE CONTRAST**
Contrast enhancement of aerospace scanner imagery of crop fields p 11 A88-43671
- IMAGE CORRELATORS**
Object-space least-squares correlation p 63 A88-44517

IMAGE ENHANCEMENT

Assessment of digital enhancement techniques using Landsat TM data in mapping geologic lineaments, with application to the Mactaquac headpond area, southern New Brunswick p 31 A88-32949
 Enhancement of SPOT image resolution using an intensity-hue-saturation transformation p 59 A88-41958

Regional geologic mapping of digitally enhanced Landsat imagery in the southcentral Alborz mountains of northern Iran p 34 A88-42017
 Directed band ratioing for the retention of perceptually-independent topographic expression in chromaticity-enhanced imagery p 62 A88-43224
 The dangers of underestimating the importance of data adjustments in band ratioing p 62 A88-43225

IMAGE PROCESSING

Targeting epithermal alteration and gossans in weathered and vegetated terrains using aircraft scanners - Successful Australian case histories p 26 A88-32905

Integration of SIR-B imagery with geological and geophysical data in Australia p 27 A88-32912

Spot 1 - International commercialization of remote sensing [AAS PAPER 86-299] p 69 A88-35155
 Regional crop-forecasting with Landsat - A farmer's experience [AAS PAPER 86-401] p 2 A88-35161

Computer processing of satellite data for geostructural zoning of a collisional boundary, significance and field checks - The example of Tunisia p 32 A88-35193
 Data reception, archiving and distribution --- digital image processing using AVHRR float on NOAA p 58 A88-37131

Image processing for earth remote sensing p 58 A88-37287

Remote sensing and image processing requirements for Eulerian flow field estimations p 51 A88-39078
 Geographic study of the north coast of Senegal using MOMS-1 satellite data p 73 A88-41093

Image optimization versus classification - An application oriented comparison of different methods by use of Thematic Mapper data p 59 A88-41964
 Processing of raw digital NOAA-AVHRR data for sea- and land applications p 60 A88-41968
 Spatial feature extraction from radar imagery p 60 A88-41974

Digital elevation modeling with stereo SIR-B image data p 60 A88-41981
 Earthscan - A range of remote sensing systems p 61 A88-41982

Evaluation of digitally processed Landsat imagery and SIR-A imagery for geological analysis of West Java region, Indonesia p 33 A88-41983
 Object-space least-squares correlation p 63 A88-44517

Integration of Landsat, DTED, and DFAD p 63 A88-44540

The 'Tsukusys' image processing system and its utilization in Thematic Mapper investigations of water quality conditions p 54 A88-45115

Analysis for architecture for image processing [INPE-4294-PRE/1165] p 75 N88-20715

Satellite UV image processing [AD-A190466] p 65 N88-22451
 Method for restoration and resampling of TM sensor imagery [INPE-4491-PRE/1255] p 65 N88-22454

Calibration and processing of AVHRR data for temperature estimation [INPE-4493-PRE/1257] p 65 N88-22485

The radiometric processing of SLAR measuring values using the PARES program [BCRS-86-04] p 75 N88-23301

Results of the testing of the segmentation program on RESEDA [BCRS-87-01] p 65 N88-23304

Latin American Symposium on Remote Sensing, 4th Brazilian Remote Sensing Symposium and 6th SELPER Plenary Meeting, volume 1 p 75 N88-24013

Textural features for image classification in remote sensing p 66 N88-24027

The USSR space systems for remote sensing of earth resources and the environment (sensor systems, processing techniques, applications) p 76 N88-24035

Study of methods of post-processing applied to a problem of standard classification p 67 N88-24067

Interpretation of MSS/LANDSAT data for evaluation of physical distribution of mangroves in Cananea-Iguape (SP) p 66 N88-24072

Automatic registration of satellite imagery p 67 N88-24080

Application of its transformation in color enhancement of LANDSAT imagery p 68 N88-24082

Preliminary study on the application of digital processing of TM-LANDSAT data in the mapping of apple orchards in Fraiburgo (SC) p 17 N88-24093

Evaluation of TM false color composites for crop discrimination p 17 N88-24096

Terrain classification using SPOT images and the computer system GOP-300 [FOA-C-20677-2.7] p 68 N88-24102

Adjustment in photogrammetry: Methods, programs and applications [BB735130] p 76 N88-24105

IMAGE RECONSTRUCTION

Restoration techniques for SIR-B digital radar images p 57 A88-32933

Correction of spatial and temporal distortions in the photographic image input into an interactive processing system p 62 A88-43672

Application of spatial statistics to analyzing multiple remote sensing data sets p 64 A88-45639

Restoration techniques for redisplay of LANDSAT-5 satellite imagery [INPE-4189-PRE/1076] p 64 N88-20712

Geometric restoration of satellite image data [AD-A190462] p 64 N88-22450

IMAGE RESOLUTION

Enhancement of SPOT image resolution using an intensity-hue-saturation transformation p 59 A88-41958

IMAGING RADAR

Investigation of the usefulness of speckle analysis in imaging radar systems [BCRS-86-05] p 65 N88-23302

The role of space borne imaging radars in environmental monitoring: Some shuttle imaging radar results in Asia [NASA-TM-101178] p 23 N88-24844

IMAGING SPECTROMETERS

Correlation between high resolution remote sensing imagery and hydrothermal alteration, Tybo mining district, Nevada p 27 A88-32915

IMAGING TECHNIQUES

Remote sensing of the earth's surface in the ultraviolet range p 32 A88-36172

Method for restoration and resampling of TM sensor imagery [INPE-4491-PRE/1255] p 65 N88-22454

Comparative utilization of analog and digital processes in the treatment of MSS-LANDSAT data for studying the national parks of Brazil [INPE-4011-TDL/240] p 21 N88-22456

Latin American Symposium on Remote Sensing, 4th Brazilian Remote Sensing Symposium and 6th SELPER Plenary Meeting, volume 1 p 75 N88-24013

The geometric workstation, a new approach for geometric corrections of remotely sensed data p 66 N88-24017

Subsurface morphology and geoarchaeology revealed by spaceborne and airborne radar p 37 N88-24022

Mapping soil and rock variation from satellite images in the Sahel p 14 N88-24023

Textural features for image classification in remote sensing p 66 N88-24027

Shape detection in remote sensing through graph isomorphism p 67 N88-24028

The modeling of error budget analysis and tolerance specifications for BRESEX multiband linear array CCD camera p 76 N88-24029

Study of methods of post-processing applied to a problem of standard classification p 67 N88-24067

Analysis of the parameters responsible for the variations of the illumination conditions in the LANDSAT data p 67 N88-24070

Automatic registration of satellite imagery p 67 N88-24080

Application of its transformation in color enhancement of LANDSAT imagery p 68 N88-24082

Evaluation of TM false color composites for crop discrimination p 17 N88-24096

INDIAN OCEAN

Evidence from geoid data of a hotspot origin for the southern Mascarene Plateau and Mascarene Islands (Indian Ocean) p 24 A88-38902

INERTIA

Surface energy budget, surface temperature and thermal inertia p 58 A88-37147

INFORMATION RETRIEVAL

Satellite data management for effective data access p 42 A88-38690

INFRARED ABSORPTION

Use of calibration targets in the measurement of 2.22-micron mineral absorption features in Thematic Mapper data p 29 A88-32927

INFRARED IMAGERY

Identification of clay minerals by feature coding of near-infrared spectra p 30 A88-32942

Processing, compression and transmission of satellite IR data for near-real-time use at sea p 41 A88-36843

Surface currents off the west coast of Ireland studied from satellite images p 43 A88-39085

An approach for emulating the color balance of Landsat multispectral scanner images with AVHRR data p 73 A88-41956

Global vegetation monitoring using NOAA GAC data p 8 A88-42012

Assessment of TM thermal infrared band contribution in land cover/land use multispectral classification p 61 A88-42016

Theoretical basis for multispectral imaging simulation p 63 A88-44532

Thermal modeling and IR scene generation p 63 A88-44534

An update on remote measurement of soil moisture over vegetation using infrared temperature measurements: A FIFE perspective [NASA-CR-182926] p 18 N88-24109

INFRARED PHOTOGRAPHY

Application of MEIS-II multispectral airborne data and CIR photography for the mapping of surficial geology and geomorphology in the Chatham area, Southwest Ontario, Canada p 34 A88-42027

INFRARED RADIATION

The application of a vegetation index in correcting the infrared reflectance for soil background p 6 A88-41988

INFRARED RADIOMETERS

The effect of atmospheric correction on the interpretation of multitemporal AVHRR-derived vegetation index dynamics p 11 A88-44117

INFRARED REFLECTION

Remote sensing of leaf water status p 4 A88-40784

INFRARED SCANNERS

Using the thermal infrared multispectral scanner (TIMS) to estimate surface thermal responses p 73 A88-40785

INFRARED SPECTRA

Preliminary measurements of spectral signatures of tropical and temperate plants in the thermal infrared p 1 A88-32909

Spectral discrimination of zeolites and dioctahedral clays in the near-infrared p 28 A88-32926

A satellite infrared technique to estimate tropical convective and stratiform rainfall p 69 A88-33416

Measurement of the water content of soil from space and application to the regional water balance p 55 N88-21561

INFRARED SPECTROSCOPY

Spectral signatures of soils and terrain conditions using lasers and spectrometers p 6 A88-41997

INLAND WATERS

Determinations of suspended sediment concentrations from multiple day Landsat and AVHRR data p 54 A88-44120

INTERNATIONAL COOPERATION

International cooperation in remote sensing: The ESA experience p 77 N88-24038

INVENTORIES

Utilization of LANDSAT-TM imagery in the hydroenergetic inventory of the Paraiba de Sul River Basin p 56 N88-24077

ION EMISSION

Particulate emissions from a mid-latitude prescribed chaparral fire p 3 A88-38805

IRRIGATION

Use of energy emission for detecting the necessity of irrigation in wheat in field conditions [INPE-4461-TDL/318] p 13 N88-23315

Evaluation of an estimation system for an irrigated area in a tropical region through TM-LANDSAT imagery p 16 N88-24075

ITERATIVE SOLUTION

Relative orientation [AD-A190385] p 75 N88-22449

J

JET FLOW

Mushroom-shaped currents (eddy dipoles) under rotation and stratification conditions p 47 N88-20678

L

LABORATORY EQUIPMENT

Kartoflex - An instrument for computer-aided photointerpretation and map revision p 74 A88-44450

LAGOONS

Application of Landsat Thematic Mapper data to assess suspended sediment dispersion in a coastal lagoon p 51 A88-41946

LAKES

Satellite data in aquatic area research - Some ideas for future studies p 53 A88-42048

LAND ICE

The role of remote sensing in the study of polar ice sheets p 48 N88-21570

LAND MANAGEMENT

Thematic Mapping by satellite - A new tool for planning and management p 60 A88-41973

Thematic Mapping from aerial photographs for Kandi Watershed and area development project, Punjab (India) p 9 A88-42024

Small scale erosion hazard mapping using Landsat information in the northwest of Argentina p 9 A88-42035

Recording resources in rural areas p 20 A88-42062

LAND USE

The use of multispectral space photographs to draw up a map of land use in western Slovakia p 57 A88-33774

Urbanization and Landsat MSS albedo change in the Windsor-Quebec corridor since 1972 p 18 A88-39094

A comparison between classification differencing and image differencing for land cover type change detection p 59 A88-41944

Shuttle imaging radar (SIR-A) interpretation of the Kashgar region in western Xinjiang, China p 74 A88-41985

Assessment of TM thermal infrared band contribution in land cover/land use multispectral classification p 61 A88-42016

An analysis of remote sensing for monitoring urban derelict land p 20 A88-42056

Human settlement analysis using Shuttle Imaging Radar-A data - An evaluation p 20 A88-42057

Spatial resolution requirements for urban land cover mapping from space p 20 A88-42058

Spectral characterization of urban land covers from Thematic Mapper data p 20 A88-42059

Land resource use monitoring in Romania, using aerial and space data p 21 A88-42065

Updating of the municipal official register of real estate through a geographical information system [INPE-4459-PRE/1238] p 21 N88-22453

Comparative utilization of analog and digital processes in the treatment of MSS-LANDSAT data for studying the national parks of Brazil p 21 N88-22456

Orbital remote sensing: An instrument for monitoring urban growth [INPE-4456-PRE/1287] p 22 N88-22833

Applications of multitemporal compositions obtained from LANDSAT data in the study of urban growth [INPE-4480-PRE/1246] p 22 N88-23692

Updating land-use of the Sao Jose dos Campos municipality through remote sensing data [INPE-4479-RPE/562] p 22 N88-23693

Landuse and landform studies of the Mahanadi River Delta with the help of satellite MSS band p 56 N88-24033

Remote sensing techniques in the estimation of the area cultivated with beans, corn, and castor beans in the Itrec County (Bahia State) p 15 N88-24045

CANASATE: Sugar cane mapping by satellite p 15 N88-24046

Utilization of LANDSAT-TM imagery in the hydroenergetic inventory of the Paraiba de Sul River Basin p 56 N88-24077

Preliminary study on the application of digital processing of TM-LANDSAT data in the mapping of apple orchards in Fraiburgo (SC) p 17 N88-24093

Research on enhancing the utilization of digital multispectral data and geographic information systems in global habitability studies [NASA-CR-182799] p 23 N88-24101

Coupling of satellite remote sensing to digitized topographic map to detect changes in land use [B8735129] p 23 N88-24104

LANDFORMS

Photo-interpretation of landforms and the hydrogeologic bearing in highly deformed areas, NW of the Gulf of Suez, Egypt p 34 A88-42029

LANDSAT SATELLITES

Landsat structural analysis of the Rhine Valley and the Jura Mountain area, Western Europe p 26 A88-32903

Contribution of Landsat to a geologic expedition in the desert of North Central Sudan, Africa p 27 A88-32916

Regional crop-forecasting with Landsat - A farmer's experience [AAS PAPER 86-401] p 2 A88-35161

Interannual Landsat-MSS reflectance variation in an urbanized temperate zone p 58 A88-37417

Comparison of measured suspended sediment concentrations with suspended sediment concentrations estimated from Landsat MSS data p 51 A88-39080

An approach for emulating the color balance of Landsat multispectral scanner images with AVHRR data p 73 A88-41956

Airphoto map control with Landsat - An alternative to the slotted template method p 60 A88-41966

Classification of land features, using Landsat MSS data in a mountainous terrain p 19 A88-41972

Evaluation of digitally processed Landsat imagery and SIR-A imagery for geological analysis of West Java region, Indonesia p 33 A88-41983

Multitemporal analysis of Landsat Multispectral Scanner (MSS) and Thematic Mapper (TM) data to map crops in the Po valley (Italy) and in Mendoza (Argentina) p 6 A88-41994

Landsat temporal-spectral profiles of crops on the South African highveld p 7 A88-41999

The use of multitemporal Landsat data for improving crop mapping accuracy p 7 A88-42003

A remote sensing aided inventory of fuelwood volumes in the Sahel region of west Africa - A case study of five urban zones in the Republic of Niger p 7 A88-42005

Classification of the Riverina forests of south east Australia using co-registered Landsat MSS and SIR-B radar data p 9 A88-42013

Multi-temporal Landsat for land unit mapping on project scale of the Sudd-floodplain, Southern Sudan p 9 A88-42015

The quantification of floodplain inundation by the use of Landsat and Metric Camera information, Belize, Central America p 53 A88-42044

Analysis of Landsat multispectral-multitemporal images for geologic-lithologic map of the Bangladesh Delta p 35 A88-42049

Satellite remote sensing of the coastal environment of Bombay p 61 A88-42052

A simple atmospheric correction algorithm for Landsat Thematic Mapper satellite images p 61 A88-42054

Evaluation of combined multiple incident angle SIR-B digital data and Landsat MSS data over an urban complex p 62 A88-42055

How few data do we need - Some radical thoughts on renewable natural resources surveys p 9 A88-42060

Manual interpretation of small forestlands on Landsat MSS data p 12 A88-44521

Evaluations of unsupervised methods for land-cover/use classifications of Landsat TM data p 64 A88-45116

On the regional characteristics of actual evapotranspiration derived from Landsat MSS and elevation data p 54 A88-45118

Applications of multitemporal compositions obtained from LANDSAT data in the study of urban growth [INPE-4480-PRE/1246] p 22 N88-23692

Mapping soil and rock variation from satellite images in the Sahel p 14 N88-24023

LASER SPECTROSCOPY

Spectral signatures of soils and terrain conditions using lasers and spectrometers p 6 A88-41997

LATENT HEAT

Moisture and latent heat flux variabilities in the tropical Pacific derived from satellite data p 45 A88-42445

LEAF AREA INDEX

Relationship between soil and leaf metal content and Landsat MSS and TM acquired canopy reflectance data p 6 A88-41986

The derivation of a simplified reflectance model for the estimation of LAI --- Leaf Area Index p 6 A88-41987

LEAST SQUARES METHOD

Object-space least-squares correlation p 63 A88-44517

LEAVES

Preliminary measurements of spectral signatures of tropical and temperate plants in the thermal infrared p 1 A88-32909

Remote sensing of leaf water status p 4 A88-40784

LEGUMINOUS PLANTS

Remote sensing techniques in the estimation of the area cultivated with beans, corn, and castor beans in the Itrec County (Bahia State) p 15 N88-24045

LICHENS

Spectral reflectance from lichens treated with copper p 30 A88-32945

LIGHT SCATTERING

Evaluation of the possibility of determining concentrations of variable components of ocean water from averaged spectra of the diffuse optical reflection coefficient p 40 A88-36160

An empirical model for polarized and cross-polarized scattering from a vegetation layer p 11 A88-44116

LIMNOLOGY

Comparison of measured suspended sediment concentrations with suspended sediment concentrations estimated from Landsat MSS data p 51 A88-39080

Toward an integrated system for satellite remote sensing of water quality in the Great Lakes p 52 A88-41957

Determinations of suspended sediment concentrations from multiple day Landsat and AVHRR data p 54 A88-44120

LITHOLOGY

Discrimination of lithologic units, alteration patterns and major structural blocks in the Tonopah, Nevada area using Thematic Mapper data p 27 A88-32907

Influence of mineral coatings and vegetation on TM imagery over Tertiary Caldera lithologies basin and range province, western U.S. p 32 A88-41945

Analysis of Landsat multispectral-multitemporal images for geologic-lithologic map of the Bangladesh Delta p 35 A88-42049

Analysis and interpretation of image lithostrucure: An application of the multiconcept in the metamorphic belt of Sul de Santana da Boa Vista (RS) p 38 N88-24051

Lithostrucure interpretation of Chapda do Cachimbo (Pa-Am-Mt), based on radar and LANDSAT imagery p 39 N88-24100

LITHOSPHERE

Geoid anomalies across Pacific fracture zones p 24 A88-38023

Evidence from geoid data of a hotspot origin for the southern Mascarene Plateau and Mascarene Islands (Indian Ocean) p 24 A88-38902

LONG RANGE WEATHER FORECASTING

Sea ice observations and models p 48 N88-21572

LONG TERM EFFECTS

Long-term air quality monitoring at the South Pole by the NOAA program Geophysical Monitoring for Climatic Change p 18 A88-36243

Urbanization and Landsat MSS albedo change in the Windsor-Quebec corridor since 1972 p 18 A88-39094

Sea ice observations and models p 48 N88-21572

LUNAR BASES

A second generation lunar agricultural system p 11 A88-43864

M

MAGNETIC ANOMALIES

Magnetic lineations on the flanks of the Marquesas swell - Implications for the age of the seafloor p 44 A88-41257

MAN ENVIRONMENT INTERACTIONS

Remote sensing and the role of terrestrial vegetation in the global carbon cycle p 5 A88-41954

Remote sensing assessment of environmental impacts caused by phosphat industry destructive influence p 19 A88-42031

Coastal monitoring by remote sensing p 54 A88-44447

MANNED SPACE FLIGHT

Aeronautics and space report of the President: 1986 activities p 77 N88-21087

MAPPING

Correlation between aircraft MSS and LIDAR remotely sensed data on a forested wetland in South Carolina p 5 A88-41951

Airborne resistivity mapping p 36 A88-45771

The 1987 Airborne Antarctic Ozone Experiment: The Nimbus-7 TOMS data atlas [NASA-RP-1201] p 47 N88-20714

Geometric restoration of satellite image data [AD-A190462] p 64 N88-22450

Contributions to geodesy, photogrammetry and cartography. Series 1, number 46 --- conference [ISSN-0469-4244] p 25 N88-23279

Updating land-use of the Sao Jose dos Campos municipality through remote sensing data [INPE-4479-RPE/562] p 22 N88-23693

A proposal for a project entitled assessment of forest resources in Uruguay submitted to the United Nations Industrial Development Organization (UNIDO) p 13 N88-24016

The geometric workstation, a new approach for geometric corrections of remotely sensed data p 66 N88-24017

Mapping from LANDSAT and SPOT satellite imagery p 66 N88-24018

Airborne and spaceborne radar images for geologic and environmental mapping in the Amazon rain forest, Brazil p 37 N88-24021

Mapping soil and rock variation from satellite images in the Sahel p 14 N88-24023

Remote sensing and data integration: Practical solutions for resource managers p 22 N88-24034

Utilization of TM/LANDSAT images in the implanted forests mapping in the Mogi-Guacu Region (SP-Brazil) p 14 N88-24042

CANASATE: Sugar cane mapping by satellite p 15 N88-24046

Structure and dynamics of vegetation in the middle semi-arid tropics, Quixaba's Caatinga (PE): Terrain analysis of MSS/LANDSAT data p 15 N88-24049

- Study of fracturing for groundwater research in the Sergipe state with remote sensing products p 38 N88-24052
- Implantation of a geo-cartographical information system through microcomputers p 67 N88-24064
- Detection of biomass burning and smoke plumes in the Amazon region through NOAA satellite imagery p 23 N88-24085
- The 35 mm vertical aerial photographs for mapping stands of bracing in different age classes p 16 N88-24087
- The breaked anticlines, cuesta and crest homoclines, orotinal valleys, and other forms of relief outcrops delineated with the help of remote sensing imagery p 16 N88-24089
- Current stage of remote sensing system for cartographic application p 76 N88-24090
- Mapping of plant associations and the variation of surface water in the Pantanal Mato-Grossense National Park, through remote sensing techniques p 17 N88-24092
- Characteristics of drainage determinations in aerial photographs and relief determination on different scales planialtimetric charts for three soils in the state of Sao Paulo p 17 N88-24095
- Criteria for planimetric and altimetric correction of maps restituted from aerial photographs in 1:100,000 scale p 38 N88-24097
- Geomorphologic sector maps of Niquizanga-Mayares, province of San Juan, Argentina p 38 N88-24098
- Research on enhancing the utilization of digital multispectral data and geographic information systems in global habitability studies [NASA-CR-182799] p 23 N88-24101
- MAPS**
- Relative orientation [AD-A190385] p 75 N88-22449
- Contributions to geodesy, photogrammetry and cartography, Series 1, number 46 --- conference [ISSN-0469-4244] p 25 N88-23279
- MARANGONI CONVECTION**
- Radar signatures of oil films floating on the sea surface and the Marangoni effect p 39 A88-33695
- MARINE CHEMISTRY**
- Distribution and chemistry of suspended particles from an active hydrothermal vent site on the Mid-Atlantic Ridge at 26 deg N p 42 A88-37720
- Satellite detected cyanobacteria bloom in the southwestern tropical Pacific - Implication for oceanic nitrogen fixation p 42 A88-39081
- MARINE ENVIRONMENTS**
- Range variations of the tropospheric propagation of ultrashort radio waves above the sea p 39 A88-33920
- Evaluation of the possibility of determining concentrations of variable components of ocean water from averaged spectra of the diffuse optical reflection coefficient p 40 A88-36160
- New aspects of the interpretation of space radar images p 58 A88-36171
- The JRC program for marine coastal monitoring p 44 A88-42039
- Real-time environmental Arctic monitoring (R-TEAM) [AD-A189948] p 49 N88-22508
- MARINE METEOROLOGY**
- A system for remote measurements of the wind stress over the ocean p 40 A88-36841
- The ocean and the atmosphere p 41 A88-37143
- Remote sensing of sea-surface winds p 41 A88-37144
- Ocean-atmosphere interactions in low latitude Australasia p 41 A88-37270
- An evaluation of the performance of the ECMWF operational system in analyzing and forecasting easterly wave disturbances over Africa and the tropical Atlantic p 43 A88-39746
- Moisture and latent heat flux variabilities in the tropical Pacific derived from satellite data p 45 A88-42445
- MARITIME SATELLITES**
- Mesoscale variability in current meter measurements in the California Current system off northern California p 44 A88-42443
- MARKETING**
- Regional crop-forecasting with Landsat - A farmer's experience [AAS PAPER 86-401] p 2 A88-35161
- MARS SURFACE**
- Groundwater sapping valleys: Experimental studies, geological controls and implications to the interpretation of valley networks on Mars [NASA-CR-182718] p 37 N88-22847
- MARSHLANDS**
- Remote sensing of biomass of salt marsh vegetation in France p 3 A88-39082
- Satellite remote sensing of the coastal environment of Bombay p 61 A88-42052

MATHEMATICAL MODELS

- Low altitude remote sensing data in the implementation of a mathematical model for the planning of urban equipment networks p 23 N88-24074
- Visualization of digital terrain models p 67 N88-24081

- An update on remote measurement of soil moisture over vegetation using infrared temperature measurements: A FIFE perspective [NASA-CR-182926] p 18 N88-24109
- MAXIMUM LIKELIHOOD ESTIMATES**
- Evaluations of unsupervised methods for land-cover/use classifications of Landsat TM data p 64 A88-45116

MEDICAL EQUIPMENT

- Low altitude remote sensing data in the implementation of a mathematical model for the planning of urban equipment networks p 23 N88-24074

MELTING

- Snow melt on sea ice surfaces as determined from passive microwave satellite data p 42 A88-38691

MESOMETEOROLOGY

- Use of radar and satellite imagery for the measurement and short-term prediction of rainfall in the United Kingdom p 51 A88-37136

MESOSCALE PHENOMENA

- Diagnostic study of the Fram Strait marginal ice zone during summer from 1983 and 1984 Marginal Ice Zone Experiment Lagrangian observations p 39 A88-33694

- Mapping frost-sensitive areas with a three-dimensional local-scale numerical model. I - Physical and numerical aspects p 4 A88-41055

- Mesoscale variability in current meter measurements in the California Current system off northern California p 44 A88-42443

METALS

- Effects of heavy metal induced canopy structural changes on forest canopy reflectance p 1 A88-32930

- Optimal Thematic Mapper bands and transformations for discerning metal stress in coniferous tree canopies p 7 A88-42002

METEORITE CRATERS

- Multispectral geologic remote sensing of a suspected impact crater near Al Madafi, Saudi Arabia p 33 A88-41955

METEOROLOGICAL PARAMETERS

- On the regional characteristics of actual evapotranspiration derived from Landsat MSS and elevation data p 54 A88-45118

- Use of energy emission for detecting the necessity of irrigation in wheat in field conditions [INPE-4461-TDL/318] p 13 N88-23315

METEOROLOGICAL RADAR

- Use of radar and satellite imagery for the measurement and short-term prediction of rainfall in the United Kingdom p 51 A88-37136

METEOROLOGICAL RESEARCH AIRCRAFT

- Satellite and aircraft passive microwave observations during the Marginal Ice Zone Experiment in 1984 p 45 A88-42447

METEOROLOGICAL SATELLITES

- Tropical rainfall measuring mission (TRMM) [AAS PAPER 86-306] p 39 A88-35058

- Passive microwave data for snow and ice research - Planned products from the DMSP SSM/I system p 40 A88-35199

- Cloud formations seen by satellite p 71 A88-37127

- Ocean-atmosphere interactions in low latitude Australasia p 41 A88-37270

- The determination of the parameters of the diurnal thermocline using satellite and ship-based measurements p 44 A88-40834

METEOROLOGICAL SERVICES

- Remote sensing applications in meteorology and climatology; Proceedings of the NATO Advanced Study Institute, Dundee, Scotland, Aug. 17-Sept. 6, 1986 p 71 A88-37126

METRIC PHOTOGRAPHY

- The quantification of floodplain inundation by the use of Landsat and Metric Camera information, Belize, Central America p 53 A88-42044

- The use of metric multispectral photography in environmental and resource exploration p 21 A88-44446

- New features of the LMK aerial camera system p 74 A88-44449

MICHIGAN

- Surface expression of subsurface structures in the Michigan Basin p 29 A88-32929

MICROCLIMATOLOGY

- Mapping frost-sensitive areas with a three-dimensional local-scale numerical model. I - Physical and numerical aspects p 4 A88-41055

MICROCOMPUTERS

- Implantation of a geo-cartographical information system through microcomputers p 67 N88-24064

MICROMETEOROLOGY

- An update on remote measurement of soil moisture over vegetation using infrared temperature measurements: A FIFE perspective [NASA-CR-182926] p 18 N88-24109

MICROWAVE IMAGERY

- Passive microwave data for snow and ice research - Planned products from the DMSP SSM/I system p 40 A88-35199

- SIR-B experiments in Japan. V. p 4 A88-40355

- Theoretical basis for multispectral imaging simulation p 63 A88-44532

MICROWAVE INTERFEROMETERS

- Active two-element microwave interferometry of the sea surface p 41 A88-37679

MICROWAVE RADIOMETERS

- Sparse-aperture microwave radiometers for earth remote sensing p 68 A88-33150

- A proposed tropical rainfall measuring mission (TRMM) satellite p 69 A88-33742

- The Along-Track Scanning Radiometer with Microwave Sounder p 41 A88-37148

- Spaceborne radar X-SAR for civil applications p 72 A88-37286

- Snow melt on sea ice surfaces as determined from passive microwave satellite data p 42 A88-38691

- Satellite and aircraft passive microwave observations during the Marginal Ice Zone Experiment in 1984 p 45 A88-42447

- Radiometric investigation of the sea-wave breaking process p 46 A88-43664

- Method for rapidly estimating geophysical parameters of the ocean-atmosphere system from satellite microwave radiometry p 46 A88-43669

- Taking the effect of vegetation into account in the microwave-radiometer remote sensing of the earth surface on the results of remote sounding of the earth surface by microwave radiometry p 10 A88-43670

- Comparison of radar and microwave radiometer techniques for determining permittivity p 74 A88-44231

MICROWAVE SCATTERING

- Comparison of unified full-wave solutions for normal incidence microwave backscatter from sea with physical optics and hybrid solutions p 42 A88-39079

- Simulation of L-band and HH microwave backscattering from coniferous forest stands - A comparison with SIR-B data p 12 A88-44643

MICROWAVE SENSORS

- Microwave instruments and methods --- for sounding of earth atmosphere and surface p 71 A88-37132

MICROWAVE SOUNDING

- Passive microwave data for snow and ice research - Planned products from the DMSP SSM/I system p 40 A88-35199

MIDLATITUDE ATMOSPHERE

- Particulate emissions from a mid-latitude prescribed chaparral fire p 3 A88-38805

MIE SCATTERING

- Cloud and precipitation remote sensing at 94 GHz p 74 A88-44306

MILLIMETER WAVES

- Cloud and precipitation remote sensing at 94 GHz p 74 A88-44306

- Radar backscatter characteristics of trees at 215 GHz p 11 A88-44307

- Millimeter-wave bistatic scattering from ground and vegetation targets p 11 A88-44308

- Millimeter-wave multipath measurements on snow cover p 54 A88-44311

- Millimeter-wave propagation in vegetation: Experiments and theory p 12 A88-44319

MINERAL DEPOSITS

- Application of remote sensing to tectonic and metallogenic studies in NE Africa p 28 A88-32924

- Use of calibration targets in the measurement of 2.22-micron mineral absorption features in Thematic Mapper data p 29 A88-32927

- A geobotanical investigation of an exploration-sized territory p 29 A88-32931

- Influence of mineral coatings and vegetation on TM imagery over Tertiary Caldera lithologies basin and range province, western U.S. p 32 A88-41945

MINERAL EXPLORATION

- Thematic Conference on Remote Sensing for Exploration Geology, 5th, Reno, NV, Sept. 29-Oct. 2, 1986, Proceedings, Volumes 1 & 2 p 26 A88-32901

- Targeting epithermal alteration and gossans in weathered and vegetated terrains using aircraft scanners - Successful Australian case histories p 26 A88-32905
- Mapping the Oman Ophiolite using TM data p 26 A88-32906
- Rock discrimination and alteration mapping for mineral exploration using the Carr Boyd/Geoscan airborne multispectral scanner p 27 A88-32914
- Correlation between high resolution remote sensing imagery and hydrothermal alteration, Tybo mining district, Nevada p 27 A88-32915
- Thematic Mapper data applied to mapping hydrothermal alteration in south west New Mexico p 28 A88-32923
- Application of remote sensing to tectonic and metallogenic studies in NE Africa p 28 A88-32924
- Importance of fault mapping to mineral/geothermal exploration: Relationship to fluid migration and ore formation - Northwest Washington p 28 A88-32925
- Shift in spectral response of nickel-loaded and control shoots of white birch p 1 A88-32928
- Spectral geobotanical investigation of mineralized till sites p 29 A88-32934
- A comparison of lineaments interpreted from remotely sensed data and airborne magnetics and their relationship to gold deposits in central Nova Scotia p 29 A88-32936
- Thematic Mapper applied to alteration zone mapping for gold exploration in south-east Spain p 29 A88-32938
- Exploration for mercury and lead-zinc-silver using the airborne Thematic Mapper, Almaden area, Spain p 29 A88-32939
- The use of Thematic Mapper imagery for mineral exploration in the sedimentary terrain of the Spring Mountains, Nevada p 30 A88-32940
- An integrated approach to the use of Landsat TM data for gold exploration in west central Nevada p 30 A88-32941
- Identification of clay minerals by feature coding of near-infrared spectra p 30 A88-32942
- Use of digitally processed laboratory reflectance spectra for the definition of probable microseepage - Induced mineralogic variations, Lisbon Valley, Utah p 30 A88-32946
- Geologic spatial analysis - A new multiple data source exploration tool p 30 A88-32947
- Remote sensing of geobotanical associations in clastic sedimentary terrane p 31 A88-32951
- Integration of remote sensing and other geo-data for ore exploration - A SW-Iberian case study p 31 A88-32952
- Pyrophyllite and kaolinite alteration - Mineral discrimination by sample reflectance measurement p 31 A88-32954
- The South Alamyrynian ring structure - A new promising area to search for hydrocarbon deposits p 32 A88-36162
- An evaluation of potential uranium deposit area by Landsat data analysis in Officer Basin, South-Western part of Australia p 35 A88-42036
- Remote sensing for non-renewable resources - Satellite and airborne multiband scanners for mineral exploration p 35 A88-42068
- A satellite-based investigation of the significance of surficial deposits for surface mining operations p 36 A88-45638
- An integrated study of the Alto Paranaiba Kimberlite Province, Minas Gerais, Brazil: A possible tool for diamond exploration p 37 A88-24031
- Lithostructural interpretation of Chapda do Cachimbo (Pa-Am-Mt), based on radar and LANDSAT imagery p 39 A88-24100
- MINERALOGY**
- Detecting and mapping of different volcanic stages and other geomorphic features by Landsat images in 'Katakekaumene', Western Turkey p 35 A88-42033
- MINES**
- Criteria for planimetric and altimetric correction of maps restituted from aerial photographs in 1:100,000 scale p 38 A88-24097
- MINES (EXCAVATIONS)**
- Case studies on the application of remote sensing data to geotechnical investigations in Ontario, Canada p 35 A88-45635
- MOBILITY**
- Examples of ice pack rigidity and mobility characteristics determined from ice motion [AD-A191163] p 50 A88-24129
- MODELS**
- Modeling surface exchanges: The soil-vegetation-atmosphere continuum p 12 A88-21553
- The Systeme d'Analyse Geographique (SAGE) geographic analysis system p 66 A88-24019
- MOISTURE**
- Use of calibration targets in the measurement of 2.22-micron mineral absorption features in Thematic Mapper data p 29 A88-32927
- MOISTURE CONTENT**
- Remote sensing of leaf water status p 4 A88-40784
- Use of energy emission for detecting the necessity of irrigation in wheat in field conditions [INPE-4461-TDL/318] p 13 A88-23315
- MONITORS**
- Real-time environmental Arctic monitoring (R-TEAM) [AD-A189948] p 49 A88-22508
- MOORING**
- Real-time environmental Arctic monitoring (R-TEAM) [AD-A189948] p 49 A88-22508
- MORPHOLOGY**
- Study of fracturing for groundwater research in the Sergipe state with remote sensing products p 38 A88-24052
- Dune fields in central Western Argentina p 38 A88-24088
- MOUNTAINS**
- Landsat structural analysis of the Rhine Valley and the Jura Mountain area, Western Europe p 26 A88-32903
- Classification of land features, using Landsat MSS data in a mountainous terrain p 19 A88-41972
- MULTISENSOR APPLICATIONS**
- Cartographic feature extraction with integrated SIR-B and Landsat TM images p 63 A88-44641
- A demonstration of stereophotogrammetry with combined SIR-B and Landsat TM images p 63 A88-44650
- MULTISPECTRAL BAND SCANNERS**
- A near infrared vegetation index formed with airborne multispectral scanner data p 1 A88-32910
- Integration of SIR-B imagery with geological and geophysical data in Australia p 27 A88-32912
- Rock discrimination and alteration mapping for mineral exploration using the Carr Boyd/Geoscan airborne multispectral scanner p 27 A88-32914
- Detection of geologic features in Landsat TM imagery not revealed in Landsat MSS imagery p 30 A88-32944
- Remote sensing for wildlife management - Giant panda habitat mapping from Landsat MSS images p 2 A88-35195
- Quantitative analysis of distribution of suspended sediments in the Yellow River Estuary from MSS data p 50 A88-35196
- Interannual Landsat-MSS reflectance variation in an urbanized temperate zone p 58 A88-37417
- Comparison of measured suspended sediment concentrations with suspended sediment concentrations estimated from Landsat MSS data p 51 A88-39080
- Differentiation of ecological zones in the Okavango Delta, Botswana by classification and contextual analyses of Landsat MSS data p 59 A88-39099
- Using the thermal infrared multispectral scanner (TIMS) to estimate surface thermal responses p 73 A88-40785
- Geographic study of the north coast of Senegal using MOMS-1 satellite data p 73 A88-41093
- An approach for emulating the color balance of Landsat multispectral scanner images with AVHRR data p 73 A88-41956
- Digital processing of airborne MSS data for forest cover types classification p 5 A88-41963
- Classification of land features, using Landsat MSS data in a mountainous terrain p 19 A88-41972
- Relationship between soil and leaf metal content and Landsat MSS and TM acquired canopy reflectance data p 6 A88-41986
- Determination of spectral signatures of different forest damages from varying altitudes of multispectral scanner data p 6 A88-41993
- Multitemporal analysis of Landsat Multispectral Scanner (MSS) and Thematic Mapper (TM) data to map crops in the Po valley (Italy) and in Mendoza (Argentina) p 6 A88-41994
- Selection of bands for a newly developed multispectral airborne reference-aided calibrated scanner (MARCS) p 74 A88-41995
- Visual interpretation of MSS-FCC manual cartographic integration of data p 61 A88-42001
- Optimal Thematic Mapper bands and transformations for discerning metal stress in coniferous tree canopies p 7 A88-42002
- The use of multitemporal Landsat data for improving crop mapping accuracy p 7 A88-42003
- Double sampling for rice in Bangladesh using Landsat MSS data p 8 A88-42009
- Experiences in application of multispectral scanner-data for forest damage inventory p 8 A88-42010
- Application of multispectral scanning remote sensing in agricultural water management problems p 8 A88-42011
- Classification of the Riverina forests of south east Australia using co-registered Landsat MSS and SIR-B radar data p 9 A88-42013
- A hydrological comparison of Landsat TM, Landsat MSS and black and white aerial photography p 52 A88-42041
- Evaluation of combined multiple incident angle SIR-B digital data and Landsat MSS data over an urban complex p 62 A88-42055
- How few data do we need - Some radical thoughts on renewable natural resources surveys p 9 A88-42060
- Remote sensing for non-renewable resources - Satellite and airborne multiband scanners for mineral exploration p 35 A88-42068
- Manual interpretation of small forestlands on Landsat MSS data p 12 A88-44521
- NIMBUS-7 CZCS, Coastal Zone Color Scanner imagery for selected coastal regions. North America - Europe, South America - Africa - Antarctica. Level 2 photographic product [NASA-CR-180755] p 48 A88-22447
- Turbidity patterns in the delta waters of southwest Netherlands on Thematic Mapper (TM) and multispectral scanner (MSS) satellite images [BCRS-86-06] p 55 A88-23303
- Applications of multitemporal composites obtained from LANDSAT data in the study of urban growth [INPE-4480-PRE/1246] p 22 A88-23692
- MULTISPECTRAL PHOTOGRAPHY**
- The use of multispectral space photographs to draw up a map of land use in western Slovakia p 57 A88-33774
- Multispectral geologic remote sensing of a suspected impact crater near Al Madafi, Saudi Arabia p 33 A88-41955
- Assessment of TM thermal infrared band contribution in land cover/land use multispectral classification p 61 A88-42016
- Use of digital terrain data in the interpretation of SPOT-1 HRV multispectral imagery p 10 A88-43221
- Radiometric correction for atmospheric and topographic effects on Landsat MSS images p 62 A88-43223
- Directed band ratioing for the retention of perceptually-independent topographic expression in chromaticity-enhanced imagery p 62 A88-43224
- The use of metric multispectral photography in environmental and resource exploration p 21 A88-44446
- Theoretical basis for multispectral imaging simulation p 63 A88-44532
- Study of methods of post-processing applied to a problem of standard classification p 67 A88-24067
- MULTISTATIC RADAR**
- Millimeter-wave bistatic scattering from ground and vegetation targets p 11 A88-44308
- N**
- NASA PROGRAMS**
- Geotechnical applications of three new U.S. Government remote sensing programs p 36 A88-45641
- The Joint NASA/Geosat Test Case Project p 36 A88-45642
- NASA SPACE PROGRAMS**
- Approach and status for a unified national plan for satellite remote sensing research and development p 77 A88-32919
- Remote sensing in the Space Station and Columbus programmes p 71 A88-37150
- Aeronautics and space report of the President: 1986 activities p 77 A88-21087
- NATURAL GAS**
- Fracture patterns and production trends, Big Sandy Field, eastern Kentucky p 27 A88-32913
- NATURAL GAS EXPLORATION**
- Surface expression of subsurface structures in the Michigan Basin p 29 A88-32929
- Remote sensing and surface geochemical study of Railroad Valley, Nye County, Nevada - Detailed grid study p 31 A88-32953
- NAVIGATION**
- Ice conditions along the Ohio River as observed on LANDSAT images, 1972-1985 [AD-A191172] p 57 A88-25018
- NAVIGATION AIDS**
- The Magnavox civil and military line of GPS receivers - A technology and applications overview p 72 A88-37391
- NEAR INFRARED RADIATION**
- A near infrared vegetation index formed with airborne multispectral scanner data p 1 A88-32910

- Spectral discrimination of zeolites and dioctahedral clays in the near-infrared p 28 A88-32926
 Identification of clay minerals by feature coding of near-infrared spectra p 30 A88-32942
 An update on visible and near infrared calibration of satellite instruments p 72 A88-37416

NEARSHORE WATER

- Surface currents off the west coast of Ireland studied from satellite images p 43 A88-39085
 Remote sensing of flow characteristics of the strait of Oresund p 53 A88-42043

NETHERLANDS

- Study of the plan for a national data center for the European Remote Sensing Satellite ERS-1 [BCRS-87-11] p 66 N88-23309

NICKEL

- Shift in spectral response of nickel-loaded and control shoots of white birch p 1 A88-32928

NIMBUS 7 SATELLITE

- Passive microwave data for snow and ice research - Planned products from the DMSP SSM/I system p 40 A88-35199

- The 1987 Airborne Antarctic Ozone Experiment: The Nimbus-7 TOMS data atlas [NASA-RP-1201] p 47 N88-20714

- NIMBUS-7 CZCS. Coastal Zone Color Scanner imagery for selected coastal regions. North America - Europe. South America - Africa - Antarctica. Level 2 photographic product [NASA-CR-180755] p 48 N88-22447

NITROGEN

- Satellite detected cyanobacteria bloom in the southwestern tropical Pacific - Implication for oceanic nitrogen fixation p 42 A88-39081

NOAA SATELLITES

- Differences in visible and near-IR responses, and derived vegetation indices, for the NOAA-9 and NOAA-10 AVHRRs - A case study p 70 A88-35396

- Ocean-atmosphere interactions in low latitude Australasia p 41 A88-37270

- Non-tracking antenna systems for the acquisition of NOAA HRPT Data --- High Resolution Picture Transmission p 72 A88-37279

- Retrieval of atmospheric temperature structure from the NOAA-9 satellite p 72 A88-37336

- Vegetation indices and other vegetation parameters - Examples, interpretation and problems p 3 A88-38373

- Processing of raw digital NOAA-AVHRR data for sea- and land applications p 60 A88-41968

- Monitoring environmental resources through NOAA's polar orbiting satellites p 21 A88-42070

NOAA 7 SATELLITE

- A study with NOAA-7 AVHRR-imagery in monitoring ephemeral streams in the lower catchment area of the Tana River, Kenya p 54 A88-42053

NOISE MEASUREMENT

- Detection of environmental noises between a vegetation canopy and a radiometric sensor p 10 A88-42538

O**OCEAN BOTTOM**

- Geoid anomalies across Pacific fracture zones p 24 A88-38023

- Evidence from geoid data of a hotspot origin for the southern Mascarene Plateau and Mascarene Islands (Indian Ocean) p 24 A88-38902

- Magnetic lineations on the flanks of the Marquesas swell - Implications for the age of the seafloor p 44 A88-41257

OCEAN CURRENTS

- Diagnostic study of the Fram Strait marginal ice zone during summer from 1983 and 1984 Marginal Ice Zone Experiment Lagrangian observations p 39 A88-33694

- Satellite observations and the numerical simulation of the interaction between a synoptic eddy and a frontal zone in the ocean p 40 A88-36159

- Surface currents off the west coast of Ireland studied from satellite images p 43 A88-39085

- Mesoscale variability in current meter measurements in the California Current system off northern California p 44 A88-42443

- Sea surface flow estimation from advanced very high resolution radiometer and coastal zone color scanner satellite imagery - A verification study p 44 A88-42444

- Temporal variations of particle fluxes in the deep subtropical and tropical North Atlantic - Eulerian versus Lagrangian effects p 45 A88-42448

- Circulation patterns in AVHRR imagery p 46 A88-43217

- Parameters of eddy structures and mushroom currents in the Baltic Sea derived from satellite imagery p 46 A88-43665

- Mushroom-shaped currents (eddy dipoles) under rotation and stratification conditions p 47 N88-20678

- Ocean general circulation models: Report on proceedings of a meeting of ocean and climate modelers [DE88-005530] p 49 N88-22504

- Hydrographic data from the OPTOMA (Ocean Prediction Through Observation, Modeling and Analysis) program: OPTOMA 23, 9-19 November 1986 [AD-A189868] p 49 N88-22506

- The WOCE Core Project Planning Meeting on the Gyre Dynamics Experiment --- ocean dynamics [WCP-139] p 49 N88-23358

- Near surface current determined from INPE's satellite-tracked buoy, during 6-26 November, 1985 p 50 N88-24058

OCEAN DATA ACQUISITIONS SYSTEMS

- Basic networks of TOGA: Determination of thermal profiles by XBT and of sea level by tide gage p 48 N88-21568

- From satellite altimetry to ocean topography, a survey of data processing techniques [ETN-88-91841] p 48 N88-21575

- Hydrographic data from the OPTOMA (Ocean Prediction Through Observation, Modeling and Analysis) program: OPTOMA 23, 9-19 November 1986 [AD-A189868] p 49 N88-22506

OCEAN DYNAMICS

- Satellite observations and the numerical simulation of the interaction between a synoptic eddy and a frontal zone in the ocean p 40 A88-36159

- Study of the dynamic topography of oceans by means of satellite altimetry p 47 N88-21567

- Hydrographic data from the OPTOMA (Ocean Prediction Through Observation, Modeling and Analysis) program: OPTOMA 23, 9-19 November 1986 [AD-A189868] p 49 N88-22506

- The WOCE Core Project Planning Meeting on the Gyre Dynamics Experiment --- ocean dynamics [WCP-139] p 49 N88-23358

OCEAN MODELS

- The ocean and the atmosphere p 41 A88-37143

- Sea ice observations and models p 48 N88-21572

- Ocean general circulation models: Report on proceedings of a meeting of ocean and climate modelers [DE88-005530] p 49 N88-22504

OCEAN SURFACE

- Radar signatures of oil films floating on the sea surface and the Marangoni effect p 39 A88-33695

- Marine Observation Satellite-1 (MOS-1) and its sensors [AAS PAPER 86-288] p 40 A88-35153

- Active two-element microwave interferometry of the sea surface p 41 A88-37679

- Snow melt on sea ice surfaces as determined from passive microwave satellite data p 42 A88-38691

- Comparison of unified full-wave solutions for normal incidence microwave backscatter from sea with physical optics and hybrid solutions p 42 A88-39079

- SIR-B experiments in Japan. VI. p 43 A88-40356

- Possibility of replacing complex values of permittivity with real values --- for ocean surface remote sensing p 44 A88-41398

- Sea surface flow estimation from advanced very high resolution radiometer and coastal zone color scanner satellite imagery - A verification study p 44 A88-42444

- Time evolution of surface chlorophyll patterns from cross-spectrum analysis of satellite color images p 45 A88-42446

- Statistical analysis of the near-surface distributions of chlorophyll and temperature fields on the basis of remote imagery from CZCS and AVHRR scanners p 54 A88-43666

- Spectral reflective characteristics of sea surface p 47 N88-20676

- From satellite altimetry to ocean topography, a survey of data processing techniques [ETN-88-91841] p 48 N88-21575

- NIMBUS-7 CZCS. Coastal Zone Color Scanner imagery for selected coastal regions. North America - Europe. South America - Africa - Antarctica. Level 2 photographic product [NASA-CR-180755] p 48 N88-22447

OCEAN TEMPERATURE

- Statistical analysis of the near-surface distributions of chlorophyll and temperature fields on the basis of remote imagery from CZCS and AVHRR scanners p 54 A88-43666

- Mass extinctions, atmospheric sulphur and climatic warming at the K/T boundary p 46 A88-43835

- Radiative processes affecting ocean mixed-layer heat content and their monitoring from satellite p 47 N88-20800

OCEANOGRAPHIC PARAMETERS

- The Along-Track Scanning Radiometer with Microwave Sounder p 41 A88-37148

- Plans for ERS-1 data acquisition, processing and distribution p 41 A88-37149

- Surface temperatures and sea ice typing for northern Baffin Bay p 42 A88-39083

- SLAR as a research tool p 73 A88-41976

- Method for rapidly estimating geophysical parameters of the ocean-atmosphere system from satellite microwave radiometry p 46 A88-43669

- Hydrographic data from the OPTOMA (Ocean Prediction Through Observation, Modeling and Analysis) program: OPTOMA 23, 9-19 November 1986 [AD-A189868] p 49 N88-22506

OCEANOGRAPHY

- Topex/Poseidon - A contribution to the world climate research program [AAS PAPER 86-306] p 39 A88-35058

- Satellite data management for effective data access p 42 A88-38690

- Basic networks of TOGA: Determination of thermal profiles by XBT and of sea level by tide gage p 48 N88-21568

- Definition and implementation study for the Varan-S radar [CNES-CT/DRT/TIT/RL-143-T] p 48 N88-22267

- Ocean general circulation models: Report on proceedings of a meeting of ocean and climate modelers [DE88-005530] p 49 N88-22504

- Hydrographic data from the OPTOMA (Ocean Prediction Through Observation, Modeling and Analysis) program: OPTOMA 23, 9-19 November 1986 [AD-A189868] p 49 N88-22506

- Investigation of the imaging of ocean surface waves using a synthetic aperture radar [SER-A-WISS-ABHANDL-84] p 49 N88-23357

- The WOCE Core Project Planning Meeting on the Gyre Dynamics Experiment --- ocean dynamics [WCP-139] p 49 N88-23358

OCEANS

- Mapping the Oman Ophiolite using TM data p 26 A88-32906

OHIO RIVER (US)

- Ice conditions along the Ohio River as observed on LANDSAT images, 1972-1985 [AD-A191172] p 57 N88-25018

OIL EXPLORATION

- Thematic Conference on Remote Sensing for Exploration Geology, 5th, Reno, NV, Sept. 29-Oct. 2, 1986. Proceedings. Volumes 1 & 2 p 26 A88-32901

- Application of synthetic aperture radar (SAR) to southern Papua New Guinea fold belt exploration p 26 A88-32902

- Associations among lineaments, subsurface fractures, hydrocarbon microseepage, and production in the Uinta Basin, Utah p 27 A88-32908

- Contribution of Landsat to a geologic expedition in the desert of North Central Sudan, Africa p 27 A88-32916

- After exploration, what? - Case histories of seven diverse production, development and distribution applications of remote sensing p 28 A88-32918

- Lineaments of the northern Denver Basin and their paleotectonic and hydrocarbon significance p 28 A88-32920

- Surface expression of subsurface structures in the Michigan Basin p 29 A88-32929

OIL FIELDS

- Associations among lineaments, subsurface fractures, hydrocarbon microseepage, and production in the Uinta Basin, Utah p 27 A88-32908

- Preliminary evaluation of remote sensing data for detection of vegetation stress related to hydrocarbon microseepage - Mist Gas Field, Oregon p 1 A88-32911

OIL SLICKS

- Radar signatures of oil films floating on the sea surface and the Marangoni effect p 39 A88-33695

- SIR-B experiments in Japan. III - Oil-pollution experiment p 43 A88-40353

- SIR-B experiments in Japan. VI. p 43 A88-40356

ONBOARD EQUIPMENT

- Definition and implementation study for the Varan-S radar [CNES-CT/DRT/TIT/RL-143-T] p 48 N88-22267

OPTICAL DATA PROCESSING

- The dangers of underestimating the importance of data adjustments in band ratioing p 62 A88-43225

OPTICAL MEASURING INSTRUMENTS

- Kartoflex - An instrument for computer-aided photointerpretation and map revision p 74 A88-44450

OPTICAL RADAR

- Correlation between aircraft MSS and LIDAR remotely sensed data on a forested wetland in South Carolina p 5 A88-41951

OPTIMIZATION

- Image optimization versus classification - An application oriented comparison of different methods by use of Thematic Mapper data p 59 A88-41964

ORCHARDS

- Preliminary study on the application of digital processing of TM-LANDSAT data in the mapping of apple orchards in Fraiburgo (SC) p 17 N88-24093

OROGRAPHY

- Regional geologic mapping of digitally enhanced Landsat imagery in the southcentral Alborz mountains of northern Iran p 34 A88-42017

ORTHOGRAPHY

- Integration of Landsat, DTED, and DFAD p 63 A88-44540

OZONE

- Canopy reflectance of soybean as affected by chronic doses of ozone in open-top field chambers p 2 A88-35398

- Assessment of crop loss from air pollutants: Meteorology-atmospheric chemistry and long range transport [PB88-146857] p 12 N88-22448

OZONE DEPLETION

- The 1987 Airborne Antarctic Ozone Experiment: The Nimbus-7 TOMS data atlas [NASA-RP-1201] p 47 N88-20714

P**PACIFIC OCEAN**

- Geoid anomalies across Pacific fracture zones p 24 A88-38023

- Mesoscale variability in current meter measurements in the California Current system off northern California p 44 A88-42443

- Moisture and latent heat flux variabilities in the tropical Pacific derived from satellite data p 45 A88-42445

- Empirical orthogonal function analysis of advanced very high resolution radiometer surface temperature patterns in Santa Barbara Channel p 45 A88-42449

- Tidal estimation in the Pacific with application to SEASAT altimetry [NASA-TM-100694] p 47 N88-20780

PAMPAS

- A remote sensing methodological approach for applied geomorphology mapping in plain areas p 35 A88-42034

PAPUA NEW GUINEA

- Application of synthetic aperture radar (SAR) to southern Papua New Guinea fold belt exploration p 26 A88-32902

PARALLEL PROCESSING (COMPUTERS)

- Analysis for architecture for image processing [INPE-4294-PRE/1165] p 75 N88-20715

PARKS

- Comparative utilization of analog and digital processes in the treatment of MSS-LANDSAT data for studying the national parks of Brazil [INPE-4011-TDL/240] p 21 N88-22456

PARTICULATE SAMPLING

- Temporal variations of particle fluxes in the deep subtropical and tropical North Atlantic - Eulerian versus Lagrangian effects p 45 A88-42448

PATTERN RECOGNITION

- Pattern recognition and geological interpretation of SIR-B images of Central Australia p 31 A88-32956

- Quantitative description and classification of drainage patterns p 51 A88-35399

- Spatial feature extraction from radar imagery p 60 A88-41974

- Tests for the automatic pattern recognition of building surfaces by the TK 50 p 68 N88-25030

PATTERN REGISTRATION

- The modeling of error budget analysis and tolerance specifications for BRESEX multiband linear array CCD camera p 76 N88-24029

- Automatic registration of satellite imagery p 67 N88-24080

PENETRATION

- Subsurface morphology and geoarchaeology revealed by spaceborne and airborne radar p 37 N88-24022

PERFORMANCE PREDICTION

- A statistical model for prediction of precision and accuracies of radar scattering coefficient measurements derived from SAR data p 62 A88-42771

PERIDOTITE

- An integrated study of the Alto Paranaiba Kimberlite Province, Minas Gerais, Brazil: A possible tool for diamond exploration p 37 N88-24031

PERMEABILITY

- Study of fracturing for groundwater research in the Sergipe state with remote sensing products p 38 N88-24052

PERMITTIVITY

- Possibility of replacing complex values of permittivity with real values --- for ocean surface remote sensing p 44 A88-41398

- Comparison of radar and microwave radiometer techniques for determining permittivity p 74 A88-44231

PETROLOGY

- Detecting and mapping of different volcanic stages and other geomorphic features by Landsat images in 'Katakekaumene', Western Turkey p 35 A88-42033

PHOSPHATES

- Remote sensing assessment of environmental impacts caused by phosphat industry destructive influence p 19 A88-42031

PHOTO GEOLOGY

- Digital terrain model and image integration for geologic interpretation p 26 A88-32904

- Discrimination of lithologic units, alteration patterns and major structural blocks in the Tonopah, Nevada area using Thematic Mapper data p 27 A88-32907

- Integration of SIR-B imagery with geological and geophysical data in Australia p 27 A88-32912

- Fracture patterns and production trends, Big Sandy Field, eastern Kentucky p 27 A88-32913

- Contribution of Landsat to a geologic expedition in the desert of North Central Sudan, Africa p 27 A88-32916

- Detection of geologic features in Landsat TM imagery not revealed in Landsat MSS imagery p 30 A88-32944

- Use of digitally processed laboratory reflectance spectra for the definition of probable microseepage - Induced mineralogical variations, Lisbon Valley, Utah p 30 A88-32946

- Integration of remote sensing and other geo-data for ore exploration - A SW-Iberian case study p 31 A88-32952

- Pyrophyllite and kaolinite alteration - Mineral discrimination by sample reflectance measurement p 31 A88-32954

- Pattern recognition and geological interpretation of SIR-B images of Central Australia p 31 A88-32956

- Discrimination of geobotanical anomalies in rugged alpine terrain using Landsat Thematic Mapper data p 32 A88-32957

- Application of aerospace remote sensing to geological investigations in Nevada and California [AAS PAPER 86-400] p 32 A88-35160

- The use of space data to study Precambrian structures p 32 A88-36161

- The South Alamyrian ring structure - A new promising area to search for hydrocarbon deposits p 32 A88-36162

- Quantitative analysis of a network of faults recognized on remote-sensing images of the Mushugai area in Mongolia p 32 A88-36163

- Synthetic geological map obtained by remote sensing - An application to Palawan Island p 33 A88-41975

- Detection by side-looking radar of geological structures under thin cover sands in arid areas p 33 A88-41979

- Geological analysis of Seasat SAR and SIR-B data in Haiti p 33 A88-41980

- Evaluation of digitally processed Landsat imagery and SIR-A imagery for geological analysis of West Java region, Indonesia p 33 A88-41983

- The use of Thematic Mapper imagery for geomorphological mapping in arid and semi-arid environments p 33 A88-41992

- Geological analysis of the satellite lineaments of the Vistula Delta Plain, Zulawy Wislane, Poland p 34 A88-42021

- Analysis of lineaments and major fractures in Xichang-Dukou area, Sichuan province as interpreted from Landsat images p 34 A88-42022

- Application of remote sensing in the field of experimental tectonics p 34 A88-42023

- Application of MEIS-II multispectral airborne data and CIR photography for the mapping of surficial geology and geomorphology in the Chatham area, Southwest Ontario, Canada p 34 A88-42027

- Remote sensing methods in geological research of the Lublin coal basin, SE Poland p 34 A88-42028

- Monitoring geomorphological processes in desert marginal environments using multitemporal satellite imagery p 34 A88-42030

- An evaluation of potential uranium deposit area by Landsat data analysis in Officer Basin, South-Western part of Australia p 35 A88-42036

- Analysis of Landsat multispectral-multitemporal images for geologic-lithologic map of the Bangladesh Delta p 35 A88-42049

- Lineaments: Significance, criteria for determination, and varied effects on ground-water systems - A case history in the use of remote sensing p 55 A88-45636

PHOTOGRAMMETRY

- American Society for Photogrammetry and Remote Sensing and ACSM, Fall Convention, Reno, NV, Oct. 4-9, 1987, ASPRS Technical Papers p 73 A88-41943

- Object-space least-squares correlation p 63 A88-44517

- A demonstration of stereophotogrammetry with combined SIR-B and Landsat TM images p 63 A88-44650

- Relative orientation [AD-A190385] p 75 N88-22449

- Stereoscopic photographs, ground and aerial, of trees used in the arborization of Curitiba (PR) p 17 N88-24091

- Adjustment in photogrammetry: Methods, programs and applications [B8735130] p 76 N88-24105

PHOTOGRAPHIC EQUIPMENT

- Canadian large-scale aerial photographic systems (LSP) p 70 A88-35395

PHOTOGRAPHIC MEASUREMENT

- Canadian large-scale aerial photographic systems (LSP) p 70 A88-35395

PHOTOGRAPHIC PROCESSING

- Correction of spatial and temporal distortions in the photographic image input into an interactive processing system p 62 A88-43672

PHOTOGRAPHY

- The USSR space systems for remote sensing of earth resources and the environment (sensor systems, processing techniques, applications) p 76 N88-24035

PHOTOINTERPRETATION

- Digital terrain model and image integration for geologic interpretation p 26 A88-32904

- Targeting epithermal alteration and gossans in weathered and vegetated terrains using aircraft scanners - Successful Australian case histories p 26 A88-32905

- Discrimination of lithologic units, alteration patterns and major structural blocks in the Tonopah, Nevada area using Thematic Mapper data p 27 A88-32907

- Geologic interpretation of air photos and radar imagery for hydroelectric power projects in Upper Ucayali Jungle Region of Peru p 28 A88-32922

- Canadian large-scale aerial photographic systems (LSP) p 70 A88-35395

- A comparison between classification differencing and image differencing for land cover type change detection p 59 A88-41944

- Structural information of the landscape as ground truth for the interpretation of satellite imagery p 59 A88-41962

- A remote sensing aided inventory of fuelwood volumes in the Sahel region of west Africa - A case study of five urban zones in the Republic of Niger p 7 A88-42005

- Multi-temporal Landsat for land unit mapping on project scale of the Sudd-floodplain, Southern Sudan p 9 A88-42015

- Assessment of TM thermal infrared band contribution in land cover/land use multispectral classification p 61 A88-42016

- Comparison between interpretation of images of different nature p 34 A88-42019

- Assessment of desertification in the lower Nile Valley (Egypt) by an interpretation of Landsat MSS colour composites and aerial photographs p 61 A88-42025

- Photo-interpretation of landforms and the hydrogeologic bearing in highly deformed areas, NW of the Gulf of Suez, Egypt p 34 A88-42029

- Digital analysis of stereo pairs for the detection of anomalous signatures in geothermal fields p 61 A88-42037

- Simple classifiers of satellite data for hydrologic modelling p 52 A88-42040

- Kartoflex - An instrument for computer-aided photointerpretation and map revision p 74 A88-44450

- Comparative utilization of analog and digital processes in the treatment of MSS-LANDSAT data for studying the national parks of Brazil [INPE-4011-TDL/240] p 21 N88-22456

- Updating land-use of the Sao Jose dos Campos municipality through remote sensing data [INPE-4479-RPE/562] p 22 N88-23693

- An integrated study of the Alto Paranaiba Kimberlite Province, Minas Gerais, Brazil: A possible tool for diamond exploration p 37 N88-24031

- Anomalies in the vegetation in the Alto Xingu - MT p 14 N88-24043

- Remote sensing and structural rupture: Application examples in the study of tectonics p 37 N88-24050

- Analysis and interpretation of image lithostructure: An application of the multiconcept in the metamorphic belt of Sul de Santana da Boa Vista (RS) p 38 N88-24051

- Application of its transformation in color enhancement of LANDSAT imagery p 68 N88-24082
The 35 mm vertical aerial photographs for mapping stands of bracinga in different age classes p 16 N88-24087
Stereoscopic photographs, ground and aerial, of trees used in the arborization of Curitiba (PR) p 17 N88-24091
Characteristics of drainage determinations in aerial photographs and relief determination on different scales planialtimetric charts for three soils in the state of Sao Paulo p 17 N88-24095
Lithostructural interpretation of Chapda do Cachimbo (Pa-Am-Mt), based on radar and LANDSAT imagery p 39 N88-24100
- PHOTOMAPPING**
Color space mapping using ternary/chromaticity diagrams - A technique for composite image interpretation p 57 A88-32932
Alternatives for mapping from satellite imagery [IAF PAPER 86-76] p 59 A88-41298
A gridding approach to detect patterns of change in coastal wetlands from digital data p 52 A88-41949
Airphoto map control with Landsat - An alternative to the slotted templet method p 60 A88-41966
Space photomaps - Their compilation and peculiarities of geographical application p 60 A88-41967
Base map production from geocoded imagery p 25 A88-41969
Insertion of hydrological decorrelated data from photographic sensors of the Shuttle in a digital cartography of geophysical exploration (Spacelab 1-Metric Camera and Large Format Camera) p 74 A88-41990
The use of SPOT simulation data in forestry mapping p 7 A88-42006
Multi-temporal Landsat for land unit mapping on project scale of the Sudd-floodplain, Southern Sudan p 9 A88-42015
Detecting and mapping of different volcanic stages and other geomorphic features by Landsat images in 'Katakekaumene', Western Turkey p 35 A88-42033
The quantification of floodplain inundation by the use of Landsat and Metric Camera information, Belize, Central America p 53 A88-42044
Spatial resolution requirements for urban land cover mapping from space p 20 A88-42058
Artificial GCPs in aircraft and satellite scanner imagery --- Ground Control Points p 74 A88-43227
Cartographic feature extraction with integrated SIR-B and Landsat TM images p 63 A88-44641
- PHOTOSYNTHESIS**
Relation between spectral reflectance and vegetation index p 7 A88-41998
- PHYTOPLANKTON**
Mass extinctions, atmospheric sulphur and climatic warming at the K/T boundary p 46 A88-43835
- PIPELINES**
Case studies on the application of remote sensing data to geotechnical investigations in Ontario, Canada p 35 A88-45635
- PIXELS**
Evaluations of unsupervised methods for land-cover/use classifications of Landsat TM data p 64 A88-45116
Textural features for image classification in remote sensing p 66 N88-24027
Study of methods of post-processing applied to a problem of standard classification p 67 N88-24067
- PLAINS**
A remote sensing methodological approach for applied geomorphology mapping in plain areas p 35 A88-42034
- PLANNING**
Identification of areas cultivated with soybeans in the cerrados regions, through digital processing of satellite images: A methodological approach p 15 N88-24048
- PLANT DISEASES**
Spruce budworm infestation detection using an airborne pushbroom scanner and Thematic Mapper data p 8 A88-42007
- PLANT STRESS**
Preliminary measurements of spectral signatures of tropical and temperate plants in the thermal infrared p 1 A88-32909
Preliminary evaluation of remote sensing data for detection of vegetation stress related to hydrocarbon microseepage - Mist Gas Field, Oregon p 1 A88-32911
Shift in spectral response of nickel-loaded and control shoots of white birch p 1 A88-32928
Canopy reflectance of soybean as affected by chronic doses of ozone in open-top field chambers p 2 A88-35398
Obtaining spectral reflectance factor measurements of stressed forest vegetation p 5 A88-41952
- Optimal Thematic Mapper bands and transformations for discerning metal stress in coniferous tree canopies p 7 A88-42002
- PLANTS (BOTANY)**
The potential of numerical agronomic simulation models in remote sensing p 9 A88-42061
The 35 mm vertical aerial photographs for mapping stands of bracinga in different age classes p 16 N88-24087
Mapping of plant associations and the variation of surface water in the Pantanal Mato-Grossense National Park, through remote sensing techniques p 17 N88-24092
- PLATEAUS**
Shuttle imaging radar response from sand dunes and subsurface rocks of Alashan Plateau in north-central China p 33 A88-41978
- PLATES (TECTONICS)**
Space geodesy and earthquake prediction [AAS PAPER 86-307] p 24 A88-35156
Geoid anomalies across Pacific fracture zones p 24 A88-38023
Geoid roughness and long-wavelength segmentation of the South Atlantic spreading ridge p 24 A88-40688
- PLUMES**
The dispersal of the Amazon's water p 43 A88-40059
Detection of biomass burning and smoke plumes in the Amazon region through NOAA satellite imagery p 23 N88-24085
- POINTS (MATHEMATICS)**
Automatic registration of satellite imagery p 67 N88-24080
- POLAR CAPS**
The role of remote sensing in the study of polar ice sheets p 48 N88-21570
Elements of sea ice dynamics and thermodynamics p 48 N88-21571
- POLAR METEOROLOGY**
Assessment of polar climate change using satellite technology p 40 A88-36241
- POLAR REGIONS**
The 1987 Airborne Antarctic Ozone Experiment: The Nimbus-7 TOMS data atlas [NASA-PP-1201] p 47 N88-20714
Sea ice observations and models p 48 N88-21572
- POLARIMETRY**
Identification of terrain cover using the optimum polarimetric classifier p 3 A88-37370
- POLLUTION MONITORING**
Feasibility study for a 2nd generation system for airborne maritime pollution surveillance [ETN-88-92108] p 55 N88-22466
- POLLUTION TRANSPORT**
The JRC program for marine coastal monitoring p 44 A88-42039
Assessment of crop loss from air pollutants: Meteorology-atmospheric chemistry and long range transport [PB88-146857] p 12 N88-22448
Detection, monitoring and analysis of some environmental effects of fires in the Amazon region through utilization of NOAA and LANDSAT satellite imagery and aircraft data [INPE-4503-TDL/326] p 13 N88-23322
- POSEIDON SATELLITE**
Topex/Poseidon - A contribution to the world climate research program [AAS PAPER 86-306] p 39 A88-35058
- POSITION (LOCATION)**
Real-time environmental Arctic monitoring (R-TEAM) [AD-A189948] p 49 N88-22508
- POSITION SENSING**
Developments in use of GPS as range TSPI --- Time and Space Position Information p 72 A88-37384
- PRECAMBRIAN PERIOD**
The use of space data to study Precambrian structures p 32 A88-36161
- PRECIPITATES**
Distribution and chemistry of suspended particles from an active hydrothermal vent site on the Mid-Atlantic Ridge at 26 deg N p 42 A88-37720
- PRECIPITATION PARTICLE MEASUREMENT**
Tropical rainfall measuring mission (TRMM) p 69 A88-33429
- PREPROCESSING**
Comparison of classification results of original and preprocessed satellite data p 59 A88-41965
- PROBABILITY DENSITY FUNCTIONS**
Identification of terrain cover using the optimum polarimetric classifier p 3 A88-37370
- PRODUCTIVITY**
Interpretation of MSS/LANDSAT data for evaluation of physical distribution of mangroves in Cananea-Iguape (SP) p 16 N88-24072
- Research on enhancing the utilization of digital multispectral data and geographic information systems in global habitability studies [NASA-CR-182799] p 23 N88-24101
- PROJECT PLANNING**
Proposals for the pre-operational use of data from the European Remote Sensing Satellite ERS-1 [BCRS-86-02] p 65 N88-23300
Study of the plan for a national data center for the European Remote Sensing Satellite ERS-1 [BCRS-87-11] p 66 N88-23309
- PROJECTIVE GEOMETRY**
Transformation of Global Vegetation Index (GVI) data from the polar stereographic projection to an equatorial cylindrical projection p 58 A88-39095
- PUSHBROOM SENSOR MODES**
Spruce budworm infestation detection using an airborne pushbroom scanner and Thematic Mapper data p 8 A88-42007
- Q**
- QUERY LANGUAGES**
The SAGE geographic analysis system p 22 N88-24063
- R**
- RADAR ANTENNAS**
Millimeter-wave multipath measurements on snow cover p 54 A88-44311
- RADAR CROSS SECTIONS**
Radar backscatter characteristics of trees at 215 GHz p 11 A88-44307
- RADAR DATA**
Crop classification from airborne synthetic aperture radar data p 10 A88-43220
Proposals for the pre-operational use of data from the European Remote Sensing Satellite ERS-1 [BCRS-86-02] p 65 N88-23300
- RADAR DETECTION**
Detection by side-looking radar of geological structures under thin cover sands in arid areas p 33 A88-41979
- RADAR ECHOES**
New aspects of the interpretation of space radar images p 58 A88-36171
- RADAR GEOLOGY**
Application of synthetic aperture radar (SAR) to southern Papua New Guinea fold belt exploration p 26 A88-32902
Fracture patterns and production trends, Big Sandy Field, eastern Kentucky p 27 A88-32913
Application of aerospace remote sensing to geological investigations in Nevada and California [AAS PAPER 86-400] p 32 A88-35160
- RADAR IMAGERY**
Application of synthetic aperture radar (SAR) to southern Papua New Guinea fold belt exploration p 26 A88-32902
Geologic interpretation of air photos and radar imagery for hydroelectric power projects in Upper Ucayali Jungle Region of Peru p 28 A88-32922
Restoration techniques for SIR-B digital radar images p 57 A88-32933
The production of distortion free SAR imagery p 57 A88-33377
Application of aerospace remote sensing to geological investigations in Nevada and California [AAS PAPER 86-400] p 32 A88-35160
Spaceborne radar X-SAR for civil applications p 72 A88-37286
Image processing for earth remote sensing p 58 A88-37287
SIR-B experiments in Japan. I - Sensor calibration experiment p 73 A88-40351
SIR-B experiments in Japan. II - Rice crop experiment p 4 A88-40352
SIR-B experiments in Japan. V. p 4 A88-40355
SIR-B experiments in Japan. VI. p 43 A88-40356
Spatial feature extraction from radar imagery p 60 A88-41974
Shuttle imaging radar response from sand dunes and subsurface rocks of Alashan Plateau in north-central China p 33 A88-41978
Remote sensing methods in geological research of the Lublin coal basin, SE Poland p 34 A88-42028
Human settlement analysis using Shuttle Imaging Radar-A data - An evaluation p 20 A88-42057
Structural geology and regional tectonics of the Mineral County area, Nevada, using Shuttle Imaging Radar-B and digital aeromagnetic data p 35 A88-44646
SIR-B stereo-radargrammetry of Australia p 63 A88-44648

- Dependence of image grey values on topography in SIR-B images p 63 A88-44649
- A comparison of airborne GEMS/SAR with satellite-borne Seasat/SAR radar imagery - The value of archived multiple data sets p 64 A88-45640
- Results of the testing of the segmentation program on RESEDA [BCRS-87-01] p 65 N88-23304
- Investigation of the imaging of ocean surface waves using a synthetic aperture radar [SER-A-WISS-ABHANDL-84] p 49 N88-23357
- The Shuttle Imaging Radar B (SIR-B) experiment report [NASA-CR-182923] p 75 N88-23932
- Radar penetration in the Amazonian rain forest p 13 N88-24015
- Airborne and spaceborne radar images for geologic and environmental mapping in the Amazon rain forest, Brazil p 37 N88-24021
- Subsurface morphology and geoarchaeology revealed by spaceborne and airborne radar p 37 N88-24022
- The use of SLAR and SIRA imagenes for the classification of forest typen in tropical rain forests p 14 N88-24036
- Radar penetration in the Amazonian rain forest p 15 N88-24044
- Analysis and interpretation of image lithostructure: An application of the multiconcept in the metamorphic belt of Sul de Santana da Boa Vista (RS) p 38 N88-24051
- Interpretation of MSS/LANDSAT data for evaluation of physical distribution of mangroves in Cananea-Iguape (SP) p 16 N88-24072
- Lithostructural interpretation of Chapda do Cachimbo (Pa-Am-Mt), based on radar and LANDSAT imagery p 39 N88-24100
- RADAR MAPS**
- Satellite radars for geologic mapping in tropical regions p 27 A88-32917
- Importance of fault mapping to mineral/geothermal exploration: Relationship to fluid migration and ore formation - Northwest Washington p 28 A88-32925
- The production of distortion free SAR imagery p 57 A88-33377
- Synthetic geological map obtained by remote sensing - An application to Palawan Island p 33 A88-41975
- A VHF radar to make terrain elevation models through tropical jungle p 10 A88-42760
- Shuttle radar mapping with diverse incidence angles in the rainforest of Borneo p 12 A88-44644
- Marginal Ice Zone Experiment (MIZEX) 1984 VARAN-S data set [ETN-88-92032] p 48 N88-21625
- Geometric restoration of satellite image data [AD-A190462] p 64 N88-22450
- RADAR MEASUREMENT**
- A satellite infrared technique to estimate tropical convective and stratiform rainfall p 69 A88-33416
- Comparison of radar and microwave radiometer techniques for determining permittivity p 74 A88-44231
- Millimeter-wave multipath measurements on snow cover p 54 A88-44311
- RADAR SCATTERING**
- Radar signatures of oil films floating on the sea surface and the Marangoni effect p 39 A88-33695
- SIR-B experiments in Japan. I - Sensor calibration experiment p 73 A88-40351
- Evaluation of combined multiple incident angle SIR-B digital data and Landsat MSS data over an urban complex p 62 A88-42055
- A statistical model for prediction of precision and accuracies of radar scattering coefficient measurements derived from SAR data p 62 A88-42771
- Radar backscatter characteristics of trees at 215 GHz p 11 A88-44307
- Millimeter-wave bistatic scattering from ground and vegetation targets p 11 A88-44308
- An effect of coherent scattering in spaceborne and airborne SAR images p 64 A88-44651
- RADAR SIGNATURES**
- Radar signatures of oil films floating on the sea surface and the Marangoni effect p 39 A88-33695
- RADIANCE**
- Factors affecting feature differentiation - The impact and source of variance in the upwelling radiance field p 58 A88-37128
- The physical principles controlling the remote sensing process p 71 A88-37129
- Calibration and processing of AVHRR data for temperature estimation [INPE-4493-PRE/1257] p 65 N88-22485
- RADIATIVE TRANSFER**
- Mapping frost-sensitive areas with a three-dimensional local-scale numerical model. I - Physical and numerical aspects p 4 A88-41055
- Classification of bottom composition and bathymetry of shallow waters by passive remote sensing p 53 A88-42051
- Soil and atmosphere influences on the spectra of partial canopies p 11 A88-44119
- RADIO ALTIMETERS**
- Precision positioning of earth orbiting remote sensing systems [AAS PAPER 86-398] p 70 A88-35159
- A model of satellite radar altimeter return from ice sheets p 46 A88-43218
- RADIO RECEIVERS**
- Sparse-aperture microwave radiometers for earth remote sensing p 68 A88-33150
- G.P.S. surveying in the Netherlands p 72 A88-37383
- The Magnavox civil and military line of GPS receivers - A technology and applications overview p 72 A88-37391
- RADIOMETERS**
- Marine Observation Satellite-1 (MOS-1) and its sensors [AAS PAPER 86-288] p 40 A88-35153
- A method for calculating the effective emissivity of a groove structure --- sea surface temperature measurement p 40 A88-35986
- Detection of environmental noises between a vegetation canopy and a radiometric sensor p 10 A88-42538
- RADIOMETRIC CORRECTION**
- Radiometric correction for atmospheric and topographic effects on Landsat MSS images p 62 A88-43223
- The radiometric processing of SLAR measuring values using the PARES program [BCRS-86-04] p 75 N88-23301
- RADIOMETRIC RESOLUTION**
- Empirical orthogonal function analysis of advanced very high resolution radiometer surface temperature patterns in Santa Barbara Channel p 45 A88-42449
- Statistical analysis of the near-surface distributions of chlorophyll and temperature fields on the basis of remote imagery from CZCS and AVHRR scanners p 54 A88-43666
- Restoration techniques for redisplay of LANDSAT-5 satellite imagery [INPE-4189-PRE/1076] p 64 N88-20712
- Method for restoration and resampling of TM sensor imagery [INPE-4491-PRE/1255] p 65 N88-22454
- RADIOSONDES**
- Retrieval of atmospheric temperature structure from the NOAA-9 satellite p 72 A88-37336
- RAIN**
- A satellite infrared technique to estimate tropical convective and stratiform rainfall p 69 A88-33416
- Tropical rainfall measuring mission (TRMM) p 69 A88-33429
- A proposed tropical rainfall measuring mission (TRMM) satellite p 69 A88-33742
- Use of radar and satellite imagery for the measurement and short-term prediction of rainfall in the United Kingdom p 51 A88-37136
- Cloud and precipitation remote sensing at 94 GHz p 74 A88-44306
- Airborne and spaceborne radar images for geologic and environmental mapping in the Amazon rain forest, Brazil p 37 N88-24021
- RAIN FORESTS**
- Shuttle radar mapping with diverse incidence angles in the rainforest of Borneo p 12 A88-44644
- RANDOM PROCESSES**
- Factors affecting feature differentiation - The impact and source of variance in the upwelling radiance field p 58 A88-37128
- RANGEFINDING**
- Developments in use of GPS as range TSPI --- Time and Space Position Information p 72 A88-37384
- RANGELANDS**
- Rangeland runoff curve numbers as determined from Landsat MSS data p 51 A88-39089
- RAYLEIGH SCATTERING**
- The physical principles controlling the remote sensing process p 71 A88-37129
- REAL TIME OPERATION**
- The 1987 Airborne Antarctic Ozone Experiment: The Nimbus-7 TOMS data atlas [NASA-RP-1201] p 47 N88-20714
- Real-time environmental Arctic monitoring (R-TEAM) [AD-A189948] p 49 N88-22508
- REFLECTANCE**
- Relationship between soil and leaf metal content and Landsat MSS and TM acquired canopy reflectance data p 6 A88-41986
- The derivation of a simplified reflectance model for the estimation of LAI --- Leaf Area Index p 6 A88-41987
- The application of a vegetation index in correcting the infrared reflectance for soil background p 6 A88-41988
- Spectral measurements for correcting LANDSAT data for atmospheric effects p 66 N88-24020
- The use of SLAR and SIRA imagenes for the classification of forest typen in tropical rain forests p 14 N88-24036
- Analysis of the parameters responsible for the variations of the illumination conditions in the LANSAT data p 67 N88-24070
- REFLECTED WAVES**
- The physical principles controlling the remote sensing process p 71 A88-37129
- REGRESSION ANALYSIS**
- Spectral measurements for correcting LANDSAT data for atmospheric effects p 66 N88-24020
- Estimation of an area cultivated with wheat from LANDSAT data through a two-phase sampling method p 14 N88-24041
- Evaluation of an estimation system for an irrigated area in a tropical region through TM-LANDSAT imagery p 16 N88-24075
- REMOTE SENSING**
- The acquisition of SPOT-1 HRV imagery over southern Britain and northern France, May 1986-May 1987 p 68 A88-29286
- Thematic Conference on Remote Sensing for Exploration Geology, 5th, Reno, NV, Sept. 29-Oct. 2, 1986, Proceedings, Volumes 1 & 2 p 26 A88-32901
- Correlation between high resolution remote sensing imagery and hydrothermal alteration, Tybo mining district, Nevada p 27 A88-32915
- After exploration, what? - Case histories of seven diverse production, development and distribution applications of remote sensing p 28 A88-32918
- Approach and status for a unified national plan for satellite remote sensing research and development p 77 A88-32919
- Application of remote sensing to tectonic and metallogenic studies in NE Africa p 28 A88-32924
- Spectral geobotanical investigation of mineralized till sites p 29 A88-32934
- Surrogate spectral reflectances of vegetation applied to geobotanical remote sensing p 1 A88-32935
- A comparison of lineaments interpreted from remotely sensed data and airborne magnetics and their relationship to gold deposits in central Nova Scotia p 29 A88-32936
- Confirmation of quantitative morphostructural analysis by seismic, aeromagnetic and geochemical data in the Amazon Basin, Brazil p 29 A88-32937
- Identification of clay minerals by feature coding of near-infrared spectra p 30 A88-32942
- Spectral reflectance from lichens treated with copper p 30 A88-32945
- Use of digitally processed laboratory reflectance spectra for the definition of probable microseepage - Induced mineralogic variations, Lisbon Valley, Utah p 30 A88-32946
- Geologic spatial analysis - A new multiple data source exploration tool p 30 A88-32947
- Remote sensing of geobotanical associations in clastic sedimentary terrane p 31 A88-32951
- Integration of remote sensing and other geo-data for ore exploration - A SW-iberian case study p 31 A88-32952
- Remote sensing and surface geochemical study of Railroad Valley, Nye County, Nevada - Detailed grid study p 31 A88-32953
- Pyrophyllite and kaolinite alteration - Mineral discrimination by sample reflectance measurement p 31 A88-32954
- Sparse-aperture microwave radiometers for earth remote sensing p 68 A88-33150
- The production of distortion free SAR imagery p 57 A88-33377
- Diagnostic study of the Fram Strait marginal ice zone during summer from 1983 and 1984 Marginal Ice Zone Experiment Lagrangian observations p 39 A88-33694
- Monitoring the environment by remote sensing p 18 A88-33770
- Principles of the remote monitoring of fresh-water quality p 50 A88-34674
- Spot 1 - International commercialization of remote sensing [AAS PAPER 86-299] p 69 A88-35155
- Precision positioning of earth orbiting remote sensing systems [AAS PAPER 86-398] p 70 A88-35159
- Application of aerospace remote sensing to geological investigations in Nevada and California [AAS PAPER 86-400] p 32 A88-35160
- Remote sensing for wildlife management - Giant panda habitat mapping from Landsat MSS images p 2 A88-35195

- Remote sensing of snow p 50 A88-35198
 Canadian large-scale aerial photographic systems (LSP) p 70 A88-35395
 Differences in visible and near-IR responses, and derived vegetation indices, for the NOAA-9 and NOAA-10 AVHRRs - A case study p 70 A88-35396
 Canopy reflectance of soybean as affected by chronic doses of ozone in open-top field chambers p 2 A88-35398
 Quantitative description and classification of drainage patterns p 51 A88-35399
 Remote-sensing methods for the monitoring and forecasting of the entomological condition of taiga forests p 2 A88-36164
 Remote sensing of the earth's surface in the ultraviolet range p 32 A88-36172
 A system for remote measurements of the wind stress over the ocean p 40 A88-36841
 Remote sensing applications in meteorology and climatology; Proceedings of the NATO Advanced Study Institute, Dundee, Scotland, Aug. 17-Sept. 6, 1986 p 71 A88-37126
 Factors affecting feature differentiation - The impact and source of variance in the upwelling radiance field p 58 A88-37128
 The physical principles controlling the remote sensing process p 71 A88-37129
 Data reception, archiving and distribution --- digital image processing using AVHRR Ilofin on NOAA p 58 A88-37131
 The ocean and the atmosphere p 41 A88-37143
 Surface energy budget, surface temperature and thermal inertia p 58 A88-37147
 Plans for ERS-1 data acquisition, processing and distribution p 41 A88-37149
 Remote sensing in the Space Station and Columbus programmes p 71 A88-37150
 Spaceborne radar X-SAR for civil applications p 72 A88-37286
 Image processing for earth remote sensing p 58 A88-37287
 Identification of terrain cover using the optimum polarimetric classifier p 3 A88-37370
 A methodology for mapping forest latent heat flux densities using remote sensing p 3 A88-37415
 Radiative surface temperatures of the burned and unburned areas in a tallgrass prairie p 3 A88-37418
 The semivariogram in remote sensing - An introduction p 58 A88-37421
 Active two-element microwave interferometry of the sea surface p 41 A88-37679
 Earth observation: Capturing the imagery - Remote sensing depends on advanced recording technology p 72 A88-38411
 Remote sensing and image processing requirements for Eulerian flow field estimations p 51 A88-39078
 Remote sensing of biomass of salt marsh vegetation in France p 3 A88-39082
 Methodology for an operational monitoring of remotely-sensed sea surface temperatures in Indonesia p 43 A88-39084
 Using spatial autocorrelation analysis to explore the errors in maps generated from remotely sensed data p 58 A88-39097
 A comparison of sampling schemes used in generating error matrices for assessing the accuracy of maps generated from remotely sensed data p 59 A88-39098
 Differentiation of ecological zones in the Okavango Delta, Botswana by classification and contextual analyses of Landsat MSS data p 59 A88-39099
 Comparative analysis of results of photographic observations of natural objects from Salyut-7 p 72 A88-39919
 SIR-B experiments in Japan. I - Sensor calibration experiment p 73 A88-40351
 SIR-B experiments in Japan. II - Rice crop experiment p 4 A88-40352
 SIR-B experiments in Japan. V. p 4 A88-40355
 Remote sensing of leaf water status p 4 A88-40784
 Using the thermal infrared multispectral scanner (TIMS) to estimate surface thermal responses p 73 A88-40785
 Alternatives for mapping from satellite imagery [IAF PAPER 86-76] p 59 A88-41298
 Possibility of replacing complex values of permittivity with real values --- for ocean surface remote sensing p 44 A88-41398
 American Society for Photogrammetry and Remote Sensing and ACSM, Fall Convention, Reno, NV, Oct. 4-9, 1987, ASPRS Technical Papers p 73 A88-41943
 A comparison between classification differencing and image differencing for land cover type change detection p 59 A88-41944
 Correlation between aircraft MSS and LIDAR remotely sensed data on a forested wetland in South Carolina p 5 A88-41951
 Obtaining spectral reflectance factor measurements of stressed forest vegetation p 5 A88-41952
 Remote sensing and the role of terrestrial vegetation in the global carbon cycle p 5 A88-41954
 Toward an integrated system for satellite remote sensing of water quality in the Great Lakes p 52 A88-41957
 Remote sensing for resources development and environmental management; Proceedings of the Seventh International Symposium, Enschede, Netherlands, Aug. 25-29, 1986. Volumes 1, 2, & 3 p 18 A88-41961
 Synthetic geological map obtained by remote sensing - An application to Palawan Island p 33 A88-41975
 Earthscan - A range of remote sensing systems p 61 A88-41982
 Monitoring of renewable resources in equatorial countries p 19 A88-42000
 A remote sensing aided inventory of fuelwood volumes in the Sahel region of west Africa - A case study of five urban zones in the Republic of Niger p 7 A88-42005
 Contribution of remote sensing to food security and early warning systems in drought affected countries in Africa p 8 A88-42008
 Double sampling for rice in Bangladesh using Landsat MSS data p 8 A88-42009
 Application of multispectral scanning remote sensing in agricultural water management problems p 8 A88-42011
 Remote sensing methods in geological research of the Lublin coal basin, SE Poland p 34 A88-42028
 Remote sensing assessment of environmental impacts caused by phosphat industry destructive influence p 19 A88-42031
 Remote sensing for survey of material resources of highway engineering projects in developing countries p 20 A88-42032
 A remote sensing methodological approach for applied geomorphology mapping in plain areas p 35 A88-42034
 Digital analysis of stereo pairs for the detection of anomalous signatures in geothermal fields p 61 A88-42037
 Application of remote sensing in hydromorphology for third world development - A resource development study in parts of Haryana (India) p 53 A88-42042
 Remote sensing of flow characteristics of the strait of Oresund p 53 A88-42043
 Environmental assessment for large scale civil engineering projects with data of DTM and remote sensing --- Digital Terrain Models p 53 A88-42046
 Satellite data in aquatic area research - Some ideas for future studies p 53 A88-42048
 Determination of spectral signature of natural water by optical airborne and shipborne instruments p 44 A88-42050
 Classification of bottom composition and bathymetry of shallow waters by passive remote sensing p 53 A88-42051
 Satellite remote sensing of the coastal environment of Bombay p 61 A88-42052
 An analysis of remote sensing for monitoring urban derelict land p 20 A88-42056
 How few data do we need - Some radical thoughts on renewable natural resources surveys p 9 A88-42060
 The potential of numerical agronomic simulation models in remote sensing p 9 A88-42061
 The integration of remote sensing and geographic information systems p 21 A88-42069
 Detection of environmental noises between a vegetation canopy and a radiometric sensor p 10 A88-42538
 Crop classification from airborne synthetic aperture radar data p 10 A88-43220
 The dangers of underestimating the importance of data adjustments in band ratioing p 62 A88-43225
 The effect of dissolved 'yellow substance' on the quantitative retrieval of chlorophyll and total suspended sediment concentrations from remote measurements of water colour p 46 A88-43226
 Statistical analysis of the near-surface distributions of chlorophyll and temperature fields on the basis of remote imagery from CZCS and AVHRR scanners p 54 A88-43666
 Taking the effect of vegetation into account in the microwave-radiometer remote sensing of the earth surface on the results of remote sounding of the earth surface by microwave radiometry p 10 A88-43670
 Contrast enhancement of aerospace scanner imagery of crop fields p 11 A88-43671
 A comparative analysis of methods for compressing spectrophotometric data in the estimation of hydrological parameters p 54 A88-43673
 Remote sensing technology and applications p 46 A88-44005
 An empirical model for polarized and cross-polarized scattering from a vegetation layer p 11 A88-44116
 Soil and atmosphere influences on the spectra of partial canopies p 11 A88-44119
 Comparison of radar and microwave radiometer techniques for determining permittivity p 74 A88-44231
 Cloud and precipitation remote sensing at 94 GHz p 74 A88-44306
 Millimeter-wave propagation in vegetation: Experiments and theory p 12 A88-44319
 Coastal monitoring by remote sensing p 54 A88-44447
 Object-space least-squares correlation p 63 A88-44517
 Simulation of L-band and HH microwave backscattering from coniferous forest stands - A comparison with SIR-B data p 12 A88-44643
 Shuttle radar mapping with diverse incidence angles in the rainforest of Borneo p 12 A88-44644
 Structural geology and regional tectonics of the Mineral County area, Nevada, using Shuttle Imaging Radar-B and digital aeromagnetic data p 35 A88-44646
 A comparative analysis of dyke lineaments mapped from Shuttle Imaging Radar and Large Format Camera photography in hyperarid areas of the Eastern Desert, Egypt, and Red Sea Hills, Sudan p 35 A88-44647
 SIR-B stereo-radargrammetry of Australia p 63 A88-44648
 Mission to planet earth p 77 A88-45110
 The 'T'sukusys' image processing system and its utilization in Thematic Mapper investigations of water quality conditions p 54 A88-45115
 Geotechnical applications of remote sensing and remote data transmission; Proceedings of the Symposium, Cocoa Beach, FL, Jan. 31-Feb. 1, 1986 p 35 A88-45634
 Case studies on the application of remote sensing data to geotechnical investigations in Ontario, Canada p 35 A88-45635
 Lineaments: Significance, criteria for determination, and varied effects on ground-water systems - A case history in the use of remote sensing p 55 A88-45636
 Application of spatial statistics to analyzing multiple remote sensing data sets p 64 A88-45639
 Geotechnical applications of three new U.S. Government remote sensing programs p 36 A88-45641
 Overview of remote data transmission systems p 55 A88-45643
 Airborne resistivity mapping p 36 A88-45771
 Remote sensing of earth terrain [NASA-CR-182677] p 12 N88-20711
 Determination of Earth rotation by the combination of data from different space geodetic systems [NASA-CR-181388] p 25 N88-20713
 The role of remote sensing in the study of polar ice sheets p 48 N88-21570
 Development of remote sensing techniques capable of delineating soils as an aid to soil survey [NASA-CR-182610] p 13 N88-22452
 Orbital remote sensing: An instrument for monitoring urban growth [INPE-4456-PRE/1287] p 22 N88-22833
 Study of the plan for a national data center for the European Remote Sensing Satellite ERS-1 [BCRS-87-11] p 66 N88-23309
 Use of energy emission for detecting the necessity of irrigation in wheat in field conditions [INPE-4461-TDL/318] p 13 N88-23315
 Detection, monitoring and analysis of some environmental effects of fires in the Amazon region through utilization of NOAA and LANDSAT satellite imagery and aircraft data [INPE-4503-TDL/326] p 13 N88-23322
 Applications of multitemporal compositions obtained from LANDSAT data in the study of urban growth [INPE-4480-PRE/1246] p 22 N88-23692
 The geometric workstation, a new approach for geometric corrections of remotely sensed data p 66 N88-24017
 Shape detection in remote sensing through graph isomorphism p 67 N88-24028
 Satellite remote sensing of turbidity and sediment concentration in Lagoa dos Patos p 56 N88-24032
 International cooperation in remote sensing: The ESA experience p 77 N88-24038
 Estimation of an area cultivated with wheat from LANDSAT data through a two-phase sampling method p 14 N88-24041
 Remote sensing techniques in the estimation of the area cultivated with beans, corn, and castor beans in the Irecé County (Bahia State) p 15 N88-24045
 Terrain classification using SPOT images and the computer system GOP-300 [FOA-C-20677-2.7] p 68 N88-24102

- An update on remote measurement of soil moisture over vegetation using infrared temperature measurements: A FIFE perspective
[NASA-CR-182926] p 18 N88-24109
- Review of power requirements for satellite remote sensing systems p 76 N88-24387
- The application of satellites in connection with the environment
[ETN-88-92474] p 24 N88-25020
- REMOTE SENSORS**
- Marine Observation Satellite-1 (MOS-1) and its sensors
[AAS PAPER 86-288] p 40 A88-35153
- Sensors to record atmospheric and terrestrial information - Principles of collection and analysis
p 71 A88-37130
- Microwave instruments and methods --- for sounding of earth atmosphere and surface p 71 A88-37132
- Feasibility study for a 2nd generation system for airborne maritime pollution surveillance
[ETN-88-92108] p 55 N88-22466
- RESEARCH AND DEVELOPMENT**
- Approach and status for a unified national plan for satellite remote sensing research and development
p 77 A88-32919
- RESEARCH MANAGEMENT**
- Aeronautics and space report of the President: 1986 activities p 77 N88-21087
- RESEARCH PROJECTS**
- The Joint NASA/Geosat Test Case Project
p 36 A88-45642
- RESERVOIRS**
- Estimation of reservoir submerging losses using CIR aerial photographs - Example of the Ertan hydropower station on the Yalong River in southwest China
p 55 A88-45637
- Study of reservoir water quality utilizing remote sensing techniques: Methodological concepts
p 56 N88-24076
- Utilization of LANDSAT-TM imagery in the hydroenergetic inventory of the Paraíba de Sul River Basin
p 56 N88-24077
- RESOURCES MANAGEMENT**
- Space Shuttle Large Format Camera photography and resource management p 70 A88-36378
- Monitoring of renewable resources in equatorial countries p 19 A88-42000
- Remote sensing for survey of material resources of highway engineering projects in developing countries
p 20 A88-42032
- Application of remote sensing in hydromorphology for third world development - A resource development study in parts of Haryana (India) p 53 A88-42042
- Remote sensing for non-renewable resources - Satellite and airborne multiband scanners for mineral exploration
p 35 A88-42068
- The integration of remote sensing and geographic information systems p 21 A88-42069
- Monitoring environmental resources through NOAA's polar orbiting satellites p 21 A88-42070
- The Joint NASA/Geosat Test Case Project
p 36 A88-45642
- Orbital remote sensing: An instrument for monitoring urban growth
[INPE-4456-PRE/1287] p 22 N88-22833
- A proposal for a project entitled assessment of forest resources in Uruguay submitted to the United Nations Industrial Development Organization (UNIDO)
p 13 N88-24016
- Remote sensing and data integration: Practical solutions for resource managers p 22 N88-24034
- Identification of areas cultivated with soybeans in the cerrados regions, through digital processing of satellite images: A methodological approach p 15 N88-24048
- Research on enhancing the utilization of digital multispectral data and geographic information systems in global habitability studies
[NASA-CR-182799] p 23 N88-24101
- RICE**
- Flood damage analysis using multitemporal Landsat Thematic Mapper data p 4 A88-39090
- SIR-B experiments in Japan. II - Rice crop experiment
p 4 A88-40352
- SIR-B experiments in Japan. V. p 4 A88-40355
- Double sampling for rice in Bangladesh using Landsat MSS data p 8 A88-42009
- RIDGES**
- Geoid roughness and long-wavelength segmentation of the South Atlantic spreading ridge p 24 A88-40688
- RING STRUCTURES**
- The South Alamyrynian ring structure - A new promising area to search for hydrocarbon deposits
p 32 A88-36162
- RIVERS**
- Landuse and landform studies of the Mahanadi River Delta with the help of satellite MSS band
p 56 N88-24033
- Geomorphologic sector maps of Niquizanga-Mayares, province of San Juan, Argentina p 38 N88-24098
- Influence of the Yukon River on the Bering Sea
[NASA-CR-182802] p 50 N88-24126
- ROCKS**
- Potential of Landsat Thematic Mapper image for crystalline rock type discrimination - Gregory Rift, Kenya
p 32 A88-35192
- ROTATING FLUIDS**
- Mushroom-shaped currents (eddy dipoles) under rotation and stratification conditions p 47 N88-20678
- ROUGHNESS**
- Relating L-band scatterometer data with soil moisture content and roughness p 5 A88-41984
- RURAL AREAS**
- Double sampling for rice in Bangladesh using Landsat MSS data p 8 A88-42009
- RURAL LAND USE**
- Recording resources in rural areas p 20 A88-42062
- S**
- SALINITY**
- Saline salt and water surface mapping on the basis of data from the Gyunesh-84 remote-sensing experiment
p 51 A88-36166
- Hydrographic observations in the northwestern Weddell Sea Marginal Ice Zone during March 1986
[PB88-173240] p 55 N88-23359
- Influence of the Yukon River on the Bering Sea
[NASA-CR-182802] p 50 N88-24126
- SALYUT SPACE STATION**
- Comparative analysis of results of photographic observations of natural objects from Salyut-7
p 72 A88-39919
- The USSR space systems for remote sensing of earth resources and the environment (sensor systems, processing techniques, applications) p 76 N88-24035
- SAMPLING**
- Evaluation of an estimation system for an irrigated area in a tropical region through TM-LANDSAT imagery
p 16 N88-24075
- SAN ANDREAS FAULT**
- Geodetic measurement of deformation east of the San Andreas Fault in Central California p 25 A88-32831
- Geodetic measurement of deformation east of the San Andreas fault in Central California
[NASA-CR-182709] p 36 N88-20754
- SANDS**
- Detection by side-looking radar of geological structures under thin cover sands in arid areas p 33 A88-41979
- SATELLITE ALTIMETRY**
- Geoid roughness and long-wavelength segmentation of the South Atlantic spreading ridge p 24 A88-40688
- Study of the dynamic topography of oceans by means of satellite altimetry p 47 N88-21567
- From satellite altimetry to ocean topography, a survey of data processing techniques
[ETN-88-91841] p 48 N88-21575
- SATELLITE COMMUNICATION**
- Real-time environmental Arctic monitoring (R-TEAM)
[AD-A189948] p 49 N88-22508
- SATELLITE DESIGN**
- Definition and identification study for the Varan-S radar
[CNES-CT/DRT/TIT/RL-143-T] p 48 N88-22267
- SATELLITE IMAGERY**
- The acquisition of SPOT-1 HRV imagery over southern Britain and northern France, May 1986-May 1987
p 68 A88-29286
- A PC-based interactive graphics system to perform satellite-derived oceanographic thermal analysis
p 68 A88-32850
- Landsat structural analysis of the Rhine Valley and the Jura Mountain area, Western Europe p 26 A88-32903
- Satellite radars for geologic mapping in tropical regions p 27 A88-32917
- Technique for the instrumented interpretation of space scanner imagery of the earth's cloud cover
p 69 A88-33832
- Principles of the remote monitoring of fresh-water quality p 50 A88-34674
- Spot 1 - International commercialization of remote sensing
[AAS PAPER 86-299] p 69 A88-35155
- Application of aerospace remote sensing to geological investigations in Nevada and California
[AAS PAPER 86-400] p 32 A88-35160
- Potential of Landsat Thematic Mapper image for crystalline rock type discrimination - Gregory Rift, Kenya
p 32 A88-35192
- Computer processing of satellite data for geostructural zoning of a collisional boundary, significance and field checks - The example of Tunisia p 32 A88-35193
- Remote sensing for wildlife management - Giant panda habitat mapping from Landsat MSS images
p 2 A88-35195
- Differences in visible and near-IR responses, and derived vegetation indices, for the NOAA-9 and NOAA-10 AVHRRs - A case study p 70 A88-35396
- Influence of topography on forest reflectance using Landsat Thematic Mapper and digital terrain data
p 2 A88-35397
- Quantitative description and classification of drainage patterns p 51 A88-35399
- Imaging instrument of the Vegetation Payload (SPOT 4) p 70 A88-35968
- The use of space data to study Precambrian structures p 32 A88-36161
- The South Alamyrynian ring structure - A new promising area to search for hydrocarbon deposits
p 32 A88-36162
- Saline salt and water surface mapping on the basis of data from the Gyunesh-84 remote-sensing experiment
p 51 A88-36166
- Linear combinations of spectral reflectances in crop analyses p 3 A88-36170
- New aspects of the interpretation of space radar images p 58 A88-36171
- Assessment of polar climate change using satellite technology p 40 A88-36241
- Cloud formations seen by satellite p 71 A88-37127
- Use of radar and satellite imagery for the measurement and short-term prediction of rainfall in the United Kingdom p 51 A88-37136
- Cloud climatologies from space and applications to climate modelling p 71 A88-37145
- Interannual Landsat-MSS reflectance variation in an urbanized temperate zone p 58 A88-37417
- Earth observation: Capturing the imagery - Remote sensing depends on advanced recording technology
p 72 A88-38411
- Satellite detected cyanobacteria bloom in the southwestern tropical Pacific - Implication for oceanic nitrogen fixation p 42 A88-39081
- Surface currents off the west coast of Ireland studied from satellite images p 43 A88-39085
- Rangeland runoff curve numbers as determined from Landsat MSS data p 51 A88-39089
- Flood damage analysis using multitemporal Landsat Thematic Mapper data p 4 A88-39090
- Urbanization and Landsat MSS albedo change in the Windsor-Quebec corridor since 1972 p 18 A88-39094
- Transformation of Global Vegetation Index (GVI) data from the polar stereographic projection to an equatorial cylindrical projection p 58 A88-39095
- Using spatial autocorrelation analysis to explore the errors in maps generated from remotely sensed data
p 58 A88-39097
- Differentiation of ecological zones in the Okavango Delta, Botswana by classification and contextual analyses of Landsat MSS data p 59 A88-39099
- Polynyas in the Southern Ocean p 43 A88-39284
- An evaluation of the performance of the ECMWF operational system in analyzing and forecasting easterly wave disturbances over Africa and the tropical Atlantic
p 43 A88-39746
- The dispersal of the Amazon's water
p 43 A88-40059
- Alternatives for mapping from satellite imagery
[IAF PAPER 86-76] p 59 A88-41298
- American Society for Photogrammetry and Remote Sensing and ACSM, Fall Convention, Reno, NV, Oct. 4-9, 1987, ASPRS Technical Papers p 73 A88-41943
- Influence of mineral coatings and vegetation on TM imagery over Tertiary Caldera lithologies basin and range province, western U.S. p 32 A88-41945
- Application of Landsat Thematic Mapper data to assess suspended sediment dispersion in a coastal lagoon
p 51 A88-41946
- Economic potential of Landsat Thematic Mapper data for crop condition assessment of winter wheat
p 4 A88-41948
- Using Landsat to derive curve numbers for hydrologic models p 52 A88-41950
- An approach for emulating the color balance of Landsat multispectral scanner images with AVHRR data
p 73 A88-41956
- Toward an integrated system for satellite remote sensing of water quality in the Great Lakes p 52 A88-41957
- Enhancement of SPOT image resolution using an intensity-hue-saturation transformation
p 59 A88-41958
- Remote sensing for resources development and environmental management; Proceedings of the Seventh International Symposium, Enschede, Netherlands, Aug. 25-29, 1986. Volumes 1, 2, & 3 p 18 A88-41961

- Structural information of the landscape as ground truth for the interpretation of satellite imagery p 59 A88-41962
- Image optimization versus classification - An application oriented comparison of different methods by use of Thematic Mapper data p 59 A88-41964
- Comparison of classification results of original and preprocessed satellite data p 59 A88-41965
- Space photomaps - Their compilation and peculiarities of geographical application p 60 A88-41967
- Earthscan - A range of remote sensing systems p 61 A88-41982
- Evaluation of digitally processed Landsat imagery and SIR-A imagery for geological analysis of West Java region, Indonesia p 33 A88-41983
- Monitoring of renewable resources in equatorial countries p 19 A88-42000
- Visual interpretation of MSS-FCC manual cartographic integration of data p 61 A88-42001
- Comparison of SPOT-simulated and Landsat 5 TM imagery in vegetation mapping p 9 A88-42014
- Regional geologic mapping of digitally enhanced Landsat imagery in the southcentral Alborz mountains of northern Iran p 34 A88-42017
- Operational satellite data assessment for drought/disaster early warning in Africa - Comments on GIS requirements --- Geographic Information System p 19 A88-42018
- Comparison between interpretation of images of different nature p 34 A88-42019
- Geological analysis of the satellite lineaments of the Vistula Delta Plain, Zulawy Wislane, Poland p 34 A88-42021
- Analysis of lineaments and major fractures in Xichang-Dukou area, Sichuan province as interpreted from Landsat images p 34 A88-42022
- Application of remote sensing in the field of experimental tectonics p 34 A88-42023
- Assessment of desertification in the lower Nile Valley (Egypt) by an interpretation of Landsat MSS colour composites and aerial photographs p 61 A88-42025
- Spring mound and aouin mapping from Landsat TM imagery in south-central Tunisia p 52 A88-42026
- Photo-interpretation of landforms and the hydrogeologic bearing in highly deformed areas, NW of the Gulf of Suez, Egypt p 34 A88-42029
- Monitoring geomorphological processes in desert marginal environments using multitemporal satellite imagery p 34 A88-42030
- Detecting and mapping of different volcanic stages and other geomorphic features by Landsat images in 'Katakakekaumene', Western Turkey p 35 A88-42033
- Small scale erosion hazard mapping using Landsat information in the northwest of Argentina p 9 A88-42035
- An evaluation of potential uranium deposit area by Landsat data analysis in Officer Basin, South-Western part of Australia p 35 A88-42036
- A methodology for integrating satellite imagery and field observations for hydrological regionalisation in Alpine catchments p 52 A88-42038
- The JRC program for marine coastal monitoring p 44 A88-42039
- Simple classifiers of satellite data for hydrologic modelling p 52 A88-42040
- A hydrological comparison of Landsat TM, Landsat MSS and black and white aerial photography p 52 A88-42041
- Remote sensing of flow characteristics of the strait of Oresund p 53 A88-42043
- The quantification of floodplain inundation by the use of Landsat and Metric Camera information, Belize, Central America p 53 A88-42044
- Remote sensing as a tool for assessing environmental effects of hydroelectric development in a remote river basin p 53 A88-42045
- Satellite data in aquatic area research - Some ideas for future studies p 53 A88-42048
- Analysis of Landsat multispectral-multitemporal images for geologic-lithologic map of the Bangladesh Delta p 35 A88-42049
- Determination of spectral signature of natural water by optical airborne and shipborne instruments p 44 A88-42050
- Satellite remote sensing of the coastal environment of Bombay p 61 A88-42052
- A study with NOAA-7 AVHRR-imagery in monitoring ephemeral streams in the lower catchment area of the Tana River, Kenya p 54 A88-42053
- A simple atmospheric correction algorithm for Landsat Thematic Mapper satellite images p 61 A88-42054
- An analysis of remote sensing for monitoring urban derelict land p 20 A88-42056
- Spatial resolution requirements for urban land cover mapping from space p 20 A88-42058
- Recording resources in rural areas p 20 A88-42062
- A comprehensive LRIS of the Kananaskis Valley using Landsat data --- Land-Related Information System p 21 A88-42064
- Land resource use monitoring in Romania, using aerial and space data p 21 A88-42065
- Remote sensing for non-renewable resources - Satellite and airborne multiband scanners for mineral exploration p 35 A88-42068
- Monitoring environmental resources through NOAA's polar orbiting satellites p 21 A88-42070
- Sea surface flow estimation from advanced very high resolution radiometer and coastal zone color scanner satellite imagery - A verification study p 44 A88-42444
- Time evolution of surface chlorophyll patterns from cross-spectrum analysis of satellite color images p 45 A88-42446
- Empirical orthogonal function analysis of advanced very high resolution radiometer surface temperature patterns in Santa Barbara Channel p 45 A88-42449
- Satellite observations of tidal upwelling and mixing in the St. Lawrence estuary p 45 A88-42450
- In flight calibration for the imaging instrument of VEGETATION payload (SPOT 4) p 10 A88-42545
- Circulation patterns in AVHRR imagery p 46 A88-43217
- Use of digital terrain data in the interpretation of SPOT-1 HRV multispectral imagery p 10 A88-43221
- Potato crop distribution and subdivision on soil type and potential water deficit - An integration of satellite imagery and environmental spatial database p 10 A88-43222
- Radiometric correction for atmospheric and topographic effects on Landsat MSS images p 62 A88-43223
- Artificial GCPs in aircraft and satellite scanner imagery --- Ground Control Points p 74 A88-43227
- Parameters of eddy structures and mushroom currents in the Baltic Sea derived from satellite imagery p 46 A88-43665
- Method for rapidly estimating geophysical parameters of the ocean-atmosphere system from satellite microwave radiometry p 46 A88-43669
- Contrast enhancement of aerospace scanner imagery of crop fields p 11 A88-43671
- Determinations of suspended sediment concentrations from multiple day Landsat and AVHRR data p 54 A88-44120
- Comparative evaluation of the Large Format Camera, Metric Camera, and Shuttle Imaging Radar - A data content p 75 A88-44519
- Manual interpretation of small forestlands on Landsat MSS data p 12 A88-44521
- An effect of coherent scattering in spaceborne and airborne SAR images p 64 A88-44651
- A satellite-based investigation of the significance of surficial deposits for surface mining operations p 36 A88-45638
- Overview of remote data transmission systems p 55 A88-45643
- Restoration techniques for redisplay of LANDSAT-5 satellite imagery [INPE-4189-PRE/1076] p 64 N88-20712
- Analysis for architecture for image processing [INPE-4294-PRE/1165] p 75 N88-20715
- Geometric restoration of satellite image data [AD-A190462] p 64 N88-22450
- Satellite UV image processing [AD-A190466] p 65 N88-22451
- Project CODEAMA/FUNCATE (test-area of Barreirinha-AM): Field report [INPE-4500-RPE/563] p 55 N88-22455
- Comparative utilization of analog and digital processes in the treatment of MSS-LANDSAT data for studying the national parks of Brazil [INPE-4011-TDL/240] p 21 N88-22456
- Calibration and processing of AVHRR data for temperature estimation [INPE-4493-PRE/1257] p 65 N88-22485
- Detection, monitoring and analysis of some environmental effects of fires in the Amazon region through utilization of NOAA and LANDSAT satellite imagery and aircraft data [INPE-4503-TDL/326] p 13 N88-23322
- Updating land-use of the Sao Jose dos Campos municipality through remote sensing data [INPE-4479-RPE/562] p 22 N88-23693
- Latin American Symposium on Remote Sensing, 4th Brazilian Remote Sensing Symposium and 6th SELPER Plenary Meeting, volume 1 p 75 N88-24013
- Mapping from LANDSAT and SPOT satellite imagery p 66 N88-24018
- Spectral measurements for correcting LANDSAT data for atmospheric effects p 66 N88-24020
- Mapping soil and rock variation from satellite images in the Sahel p 14 N88-24023
- An integrated study of the Alto Paranaiba Kimberlite Province, Minas Gerais, Brazil: A possible tool for diamond exploration p 37 N88-24031
- Satellite remote sensing of turbidity and sediment concentration in Lagoa dos Patos p 56 N88-24032
- Estimation of an area cultivated with wheat from LANDSAT data through a two-phase sampling method p 14 N88-24041
- Utilization of TM/LANDSAT images in the implanted forests mapping in the Mogi-Guaçu Region (SP-Brazil) p 14 N88-24042
- Anomalies in the vegetation in the Alto Xingu - MT p 14 N88-24043
- Remote sensing techniques in the estimation of the area cultivated with beans, corn, and castor beans in the Irece County (Bahia State) p 15 N88-24045
- CANASATE: Sugar cane mapping by satellite p 15 N88-24046
- Spectral behavior of crops through analysis of LANDSAT-TM data p 15 N88-24047
- Identification of areas cultivated with soybeans in the cerrados regions, through digital processing of satellite images: A methodological approach p 15 N88-24048
- Structure and dynamics of vegetation in the middle semi-arid tropics, Quixaba's Caatinga (PE): Terrain analysis of MSS/LANDSAT data p 15 N88-24049
- Study of fracturing for groundwater research in the Sergipe state with remote sensing products p 38 N88-24052
- Analysis of the parameters responsible for the variations of the illumination conditions in the LANDSAT data p 67 N88-24070
- Tornado tracks in Southwestern Brazil, Eastern Paraguay, and Northwestern Argentina p 23 N88-24071
- Interpretation of MSS/LANDSAT data for evaluation of physical distribution of mangroves in Cananea-Iguaçu (SP) p 16 N88-24072
- Evaluation of an estimation system for an irrigated area in a tropical region through TM-LANDSAT imagery p 16 N88-24075
- Study of reservoir water quality utilizing remote sensing techniques: Methodological concepts p 56 N88-24076
- Utilization of LANDSAT-TM imagery in the hydroenergetic inventory of the Paraba de Sul River Basin p 56 N88-24077
- Evaluation of the floodable area of the canal of Sao Goncalo through TM-LANDSAT 5 imagery p 56 N88-24078
- Automatic registration of satellite imagery p 67 N88-24080
- Visualization of digital terrain models p 67 N88-24081
- Application of its transformation in color enhancement of LANDSAT imagery p 68 N88-24082
- Detection of biomass burning and smoke plumes in the Amazon region through NOAA satellite imagery p 23 N88-24085
- Evaluation of the mangrove area at the Piaui River (SE) through remote sensing p 16 N88-24086
- Dune fields in central Western Argentina p 38 N88-24088
- The broken anticlines, cuesta and crest homoclines, oroclinal valleys, and other forms of relief outcrops delineated with the help of remote sensing imagery p 16 N88-24089
- Mapping of plant associations and the variation of surface water in the Pantanal Mato-Grossense National Park, through remote sensing techniques p 17 N88-24092
- Evaluation of TM false color composites for crop discrimination p 17 N88-24096
- Lithostructural interpretation of Chapda do Cachimbo (Pa-Am-Mt), based on radar and LANDSAT imagery p 39 N88-24100
- Research on enhancing the utilization of digital multispectral data and geographic information systems in global habitability studies [NASA-CR-182799] p 23 N88-24101
- Terrain classification using SPOT images and the computer system GOP-300 [FOA-C-20677-2.7] p 68 N88-24102
- Coupling of satellite remote sensing to digitized topographic map to detect changes in land use [B8735129] p 23 N88-24104
- Influence of the Yukon River on the Bering Sea [NASA-CR-182802] p 50 N88-24126
- Ice conditions along the Ohio River as observed on LANDSAT images, 1972-1985 [AD-A191172] p 57 N88-25018

SATellite OBSERVATION

- Satellite radars for geologic mapping in tropical regions p 27 A88-32917
- Effects of heavy metal induced canopy structural changes on forest canopy reflectance p 1 A88-32930

- Climatological interpretation of time series of satellite observations of the earth's radiation balance p 69 A88-33872
- Topex/Poseidon - A contribution to the world climate research program [AAS PAPER 86-306] p 39 A88-35058
- Quantitative analysis of distribution of suspended sediments in the Yellow River Estuary from MSS data p 50 A88-35196
- Satellite observations and the numerical simulation of the interaction between a synoptic eddy and a frontal zone in the ocean p 40 A88-36159
- Data reception, archiving and distribution --- digital image processing using AVHRR flofn on NOAA p 58 A88-37131
- Ocean-atmosphere interactions in low latitude Australasia p 41 A88-37270
- The effect of a shallow low-viscosity zone on the mantle flow, the geoid anomalies and the geoid and depth-age relationships at fracture zones p 24 A88-38024
- Satellite data management for effective data access p 42 A88-38690
- Comparison of measured suspended sediment concentrations with suspended sediment concentrations estimated from Landsat MSS data p 51 A88-39080
- Satellite observation of surface albedo over the Qinghai-Xinzang plateau region p 24 A88-39518
- The determination of the parameters of the diurnal thermocline using satellite and ship-based measurements p 44 A88-40834
- Geographic study of the north coast of Senegal using MOMS-1 satellite data p 73 A88-41093
- Comparison of classification results of original and preprocessed satellite data p 59 A88-41965
- Contribution of remote sensing to food security and early warning systems in drought affected countries in Africa p 8 A88-42008
- Global vegetation monitoring using NOAA GAC data p 8 A88-42012
- Moisture and latent heat flux variabilities in the tropical Pacific derived from satellite data p 45 A88-42445
- Satellite and aircraft passive microwave observations during the Marginal Ice Zone Experiment in 1984 p 45 A88-42447
- Mission to planet earth p 77 A88-45110
- Geotechnical applications of remote sensing and remote data transmission; Proceedings of the Symposium, Cocoa Beach, FL, Jan. 31-Feb. 1, 1986 p 35 A88-45634
- Radiative processes affecting ocean mixed-layer heat content and their monitoring from satellite p 47 A88-20800
- The role of remote sensing in the study of polar ice sheets p 48 A88-21570
- Elements of sea ice dynamics and thermodynamics p 48 A88-21571
- Turbidity patterns in the delta waters of southwest Netherlands on Thematic Mapper (TM) and multispectral scanner (MSS) satellite images [BCRS-86-06] p 55 A88-23303
- The application of satellites in connection with the environment [ETN-88-92474] p 24 A88-25020
- SATELLITE SOUNDING**
- Monitoring the environment by remote sensing p 18 A88-33770
- Nonlinear multichannel algorithms for estimating sea surface temperature with AVHRR satellite data p 39 A88-34643
- Factors affecting feature differentiation - The impact and source of variance in the upwelling radiance field p 58 A88-37128
- Microwave instruments and methods --- for sounding of earth atmosphere and surface p 71 A88-37132
- The ocean and the atmosphere p 41 A88-37143
- Remote sensing of sea-surface winds p 41 A88-37144
- Plans for ERS-1 data acquisition, processing and distribution p 41 A88-37149
- Retrieval of atmospheric temperature structure from the NOAA-9 satellite p 72 A88-37336
- Satellite detection of bloom and pigment distributions in estuaries p 51 A88-37414
- Classification of bottom composition and bathymetry of shallow waters by passive remote sensing p 53 A88-42051
- The potential of numerical agronomic simulation models in remote sensing p 9 A88-42061
- SATELLITE TRACKING**
- Precision positioning of earth orbiting remote sensing systems [AAS PAPER 86-398] p 70 A88-35159
- SATELLITE TRANSMISSION**
- Processing, compression and transmission of satellite IR data for near-real-time use at sea p 41 A88-36843
- Earth observation: Capturing the imagery - Remote sensing depends on advanced recording technology p 72 A88-38411
- SATELLITE-BORNE INSTRUMENTS**
- A PC-based interactive graphics system to perform satellite-derived oceanographic thermal analysis p 68 A88-32850
- A proposed tropical rainfall measuring mission (TRMM) satellite p 69 A88-33742
- ERS-1, Earth Resources Satellite-1 and future earth observation program in Japan [AAS PAPER 86-289] p 69 A88-35154
- Remote sensing of snow p 50 A88-35198
- Sensors to record atmospheric and terrestrial information - Principles of collection and analysis p 71 A88-37130
- The Along-Track Scanning Radiometer with Microwave Sounder p 41 A88-37148
- Retrieval of atmospheric temperature structure from the NOAA-9 satellite p 72 A88-37336
- An update on visible and near infrared calibration of satellite instruments p 72 A88-37416
- Vegetation indices and other vegetation parameters - Examples, interpretation and problems p 3 A88-38373
- Polynyas in the Southern Ocean p 43 A88-39284
- In flight calibration for the imaging instrument of VEGETATION payload (SPOT 4) p 10 A88-42545
- A model of satellite radar altimeter return from ice sheets p 46 A88-43218
- Remote sensing technology and applications p 46 A88-44005
- SATELLITE-BORNE PHOTOGRAPHY**
- The use of multispectral space photographs to draw up a map of land use in western Slovakia p 57 A88-33774
- Investigation and mapping of forests using space scanner imagery obtained in winter p 2 A88-36165
- Space Shuttle Large Format Camera photography and resource management p 70 A88-36378
- Comparative analysis of results of photographic observations of natural objects from Salyut-7 p 72 A88-39919
- Preliminary investigation of Large Format Camera photography utility in soil mapping and related agricultural applications p 4 A88-41947
- SAUDI ARABIA**
- Multispectral geologic remote sensing of a suspected impact crater near Al Madafi, Saudi Arabia p 33 A88-41955
- SCATTERING COEFFICIENTS**
- A statistical model for prediction of precision and accuracies of radar scattering coefficient measurements derived from SAR data p 62 A88-42771
- SCATTEROMETERS**
- Spaceborne radar X-SAR for civil applications p 72 A88-37286
- Relating L-band scatterometer data with soil moisture content and roughness p 5 A88-41984
- SCENE ANALYSIS**
- Quantitative procedure for producing color-calibrated Thematic Mapper natural-color images p 57 A88-32943
- Thermal modeling and IR scene generation p 63 A88-44534
- SEA BREEZE**
- Remote sensing of sea-surface winds p 41 A88-37144
- SEA ICE**
- Diagnostic study of the Fram Strait marginal ice zone during summer from 1983 and 1984 Marginal Ice Zone Experiment Lagrangian observations p 39 A88-33694
- Passive microwave data for snow and ice research - Planned products from the DMSP SSM/I system p 40 A88-35199
- Snow melt on sea ice surfaces as determined from passive microwave satellite data p 42 A88-38691
- Surface temperatures and sea ice typing for northern Baffin Bay p 42 A88-39083
- Polynyas in the Southern Ocean p 43 A88-39284
- A model of satellite radar altimeter return from ice sheets p 46 A88-43218
- Elements of sea ice dynamics and thermodynamics p 48 A88-21571
- Sea ice observations and models p 48 A88-21572
- Hydrographic observations in the northwestern Weddell Sea Marginal Ice Zone during March 1986 [PB88-173240] p 55 A88-23359
- Examples of ice pack rigidity and mobility characteristics determined from ice motion [AD-A191163] p 50 A88-24129
- SEA ROUGHNESS**
- A method for calculating the effective emissivity of a groove structure --- sea surface temperature measurement p 40 A88-35986
- Radiometric investigation of the sea-wave breaking process p 46 A88-43664
- SEA SURFACE TEMPERATURE**
- A PC-based interactive graphics system to perform satellite-derived oceanographic thermal analysis p 68 A88-32850
- Nonlinear multichannel algorithms for estimating sea surface temperature with AVHRR satellite data p 39 A88-34643
- A method for calculating the effective emissivity of a groove structure --- sea surface temperature measurement p 40 A88-35986
- Processing, compression and transmission of satellite IR data for near-real-time use at sea p 41 A88-36843
- Plans for ERS-1 data acquisition, processing and distribution p 41 A88-37149
- Surface temperatures and sea ice typing for northern Baffin Bay p 42 A88-39083
- Methodology for an operational monitoring of remotely-sensed sea surface temperatures in Indonesia p 43 A88-39084
- The determination of the parameters of the diurnal thermocline using satellite and ship-based measurements p 44 A88-40834
- Sea surface temperature studies in Norwegian coastal areas using AVHRR- and TM thermal infrared data p 44 A88-42047
- Empirical orthogonal function analysis of advanced very high resolution radiometer surface temperature patterns in Santa Barbara Channel p 45 A88-42449
- Circulation patterns in AVHRR imagery p 46 A88-43217
- Influence of the Yukon River on the Bering Sea [NASA-CR-182802] p 50 A88-24126
- SEA WATER**
- Evaluation of the possibility of determining concentrations of variable components of ocean water from averaged spectra of the diffuse optical reflection coefficient p 40 A88-36160
- Polynyas in the Southern Ocean p 43 A88-39284
- Determination of spectral signature of natural water by optical airborne and shipborne instruments p 44 A88-42050
- Temporal variations of particle fluxes in the deep subtropical and tropical North Atlantic - Eulerian versus Lagrangian effects p 45 A88-42448
- The effect of dissolved 'yellow substance' on the quantitative retrieval of chlorophyll and total suspended sediment concentrations from remote measurements of water colour p 46 A88-43226
- SEAS**
- Hydrographic observations in the northwestern Weddell Sea Marginal Ice Zone during March 1986 [PB88-173240] p 55 A88-23359
- SEASAT SATELLITES**
- Image processing for earth remote sensing p 58 A88-37287
- Geological analysis of Seasat SAR and SIR-B data in Haiti p 33 A88-41980
- Tidal estimation in the Pacific with application to SEASAT altimetry [NASA-TM-100694] p 47 A88-20780
- SEDIMENTARY ROCKS**
- The use of Thematic Mapper imagery for mineral exploration in the sedimentary terrain of the Spring Mountains, Nevada p 30 A88-32940
- Remote sensing of geobotanical associations in clastic sedimentary terrane p 31 A88-32951
- SEDIMENTS**
- Quantitative analysis of distribution of suspended sediments in the Yellow River Estuary from MSS data p 50 A88-35196
- Comparison of measured suspended sediment concentrations with suspended sediment concentrations estimated from Landsat MSS data p 51 A88-39080
- Application of Landsat Thematic Mapper data to assess suspended sediment dispersion in a coastal lagoon p 51 A88-41946
- The effect of dissolved 'yellow substance' on the quantitative retrieval of chlorophyll and total suspended sediment concentrations from remote measurements of water colour p 46 A88-43226
- Determinations of suspended sediment concentrations from multiple day Landsat and AVHRR data p 54 A88-44120
- Satellite remote sensing of turbidity and sediment concentration in Lagoa dos Patos p 56 A88-24032
- SEGMENTS**
- Results of the testing of the segmentation program on RESEDA [BCRS-87-01] p 65 A88-23304
- Automatic registration of satellite imagery p 67 A88-24080

SEISMIC WAVES

Geodetic measurement of deformation east of the San Andreas fault in Central California [NASA-CR-182709] p 36 N88-20754

SEISMOLOGY

Space geodesy and earthquake prediction [AAS PAPER 86-307] p 24 A88-35156

SHALLOW WATER

Classification of bottom composition and bathymetry of shallow waters by passive remote sensing p 53 A88-42051

SHAPES

Shape detection in remote sensing through graph isomorphism p 67 N88-24028

SHEAR STRAIN

Geodetic measurement of deformation east of the San Andreas fault in Central California [NASA-CR-182709] p 36 N88-20754

SHORT WAVE RADIO TRANSMISSION

Range variations of the tropospheric propagation of ultrashort radio waves above the sea p 39 A88-33920

SHUTTLE IMAGING RADAR

Integration of SIR-B imagery with geological and geophysical data in Australia p 27 A88-32912
Restoration techniques for SIR-B digital radar images p 57 A88-32933

Pattern recognition and geological interpretation of SIR-B images of Central Australia p 31 A88-32956
Spaceborne radar X-SAR for civil applications p 72 A88-37286

SIR-B experiments in Japan. I - Sensor calibration experiment p 73 A88-40351
SIR-B experiments in Japan. II - Rice crop experiment p 4 A88-40352

SIR-B experiments in Japan. III - Oil-pollution experiment p 43 A88-40353
SIR-B experiments in Japan. V. p 4 A88-40355
SIR-B experiments in Japan. VI. p 43 A88-40356

Shuttle imaging radar response from sand dunes and subsurface rocks of Alashan Plateau in north-central China p 33 A88-41978
Detection by side-looking radar of geological structures under thin cover sands in arid areas p 33 A88-41979

Geological analysis of Seasat SAR and SIR-B data in Haiti p 33 A88-41980
Digital elevation modeling with stereo SIR-B image data p 60 A88-41981

Evaluation of digitally processed Landsat imagery and SIR-A imagery for geological analysis of West Java region, Indonesia p 33 A88-41983
Shuttle imaging radar (SIR-A) interpretation of the Kashgar region in western Xinjiang, China p 74 A88-41985

Classification of the Riverina forests of south east Australia using co-registered Landsat MSS and SIR-B radar data p 9 A88-42013

Evaluation of combined multiple incident angle SIR-B digital data and Landsat MSS data over an urban complex p 62 A88-42055

Human settlement analysis using Shuttle Imaging Radar-A data - An evaluation p 20 A88-42057
Comparative evaluation of the Large Format Camera, Metric Camera, and Shuttle Imaging Radar - A data content p 75 A88-44519

Cartographic feature extraction with integrated SIR-B and Landsat TM images p 63 A88-44641
Simulation of L-band and HH microwave backscattering from coniferous forest stands - A comparison with SIR-B data p 12 A88-44643

Shuttle radar mapping with diverse incidence angles in the rainforest of Borneo p 12 A88-44644
A comparative analysis of dyke lineaments mapped from Shuttle Imaging Radar and Large Format Camera photography in hyperarid areas of the Eastern Desert, Egypt, and Red Sea Hills, Sudan p 35 A88-44647

SIR-B stereo-radargrammetry of Australia p 63 A88-44648
A demonstration of stereophotogrammetry with combined SIR-B and Landsat TM images p 63 A88-44650

Geotechnical applications of three new U.S. Government remote sensing programs p 36 A88-45641

The Shuttle Imaging Radar B (SIR-B) experiment report [NASA-CR-182923] p 75 N88-23932

Subsurface morphology and geochronology revealed by spaceborne and airborne radar p 37 N88-24022

The role of space borne imaging radars in environmental monitoring: Some shuttle imaging radar results in Asia [NASA-TM-101178] p 23 N88-24844

SIDE-LOOKING RADAR

SLAR as a research tool p 73 A88-41976
Detection by side-looking radar of geological structures under thin cover sands in arid areas p 33 A88-41979

A comparison of airborne GEMS/SAR with satellite-borne Seasat/SAR radar imagery - The value of archived multiple data sets p 64 A88-45640

Geotechnical applications of three new U.S. Government remote sensing programs p 36 A88-45641

Marginal Ice Zone Experiment (MIZEX) 1984 VARAN-S data set [ETN-88-92032] p 48 N88-21625

Definition and implementation study for the Varan-S radar [CNES-CT/DRT/TIT/RL-143-T] p 48 N88-22267

The radiometric processing of SLAR measuring values using the PARES program [BCRS-86-04] p 75 N88-23301

Investigation of the usefulness of speckle analysis in imaging radar systems [BCRS-86-05] p 65 N88-23302

SIGNAL PROCESSING

Analysis for architecture for image processing [INPE-4294-PRE/1165] p 75 N88-20715

Near surface current determined from INPE's satellite-tracked buoy, during 6-26 November, 1985 p 50 N88-24058

SIGNATURE ANALYSIS

Spectral signature of rice fields using Landsat-5 TM in the Mediterranean coast of Spain p 6 A88-41991

Determination of spectral signatures of different forest damages from varying altitudes of multispectral scanner data p 6 A88-41993

SIMULATION

Theoretical basis for multispectral imaging simulation p 63 A88-44532

SITE SELECTION

Utilization of LANDSAT-TM, for aiding in the localization of archeological sites in the state of Sao Paulo p 38 N88-24069

SMOKE

Detection of biomass burning and smoke plumes in the Amazon region through NOAA satellite imagery p 23 N88-24085

SNOW

Remote sensing of snow p 50 A88-35198
Passive microwave data for snow and ice research - Planned products from the DMSP SSM/I system p 40 A88-35199

SNOW COVER

Snow melt on sea ice surfaces as determined from passive microwave satellite data p 42 A88-38691

Millimeter-wave multipath measurements on snow cover [AD-A191172] p 57 N88-25018

SOFTWARE ENGINEERING

Implantation of a geo-cartographical information system through microcomputers p 67 N88-24064

SOIL EROSION

Thematic Mapping from aerial photographs for Kandi Watershed and area development project, Punjab (India) p 9 A88-42024

Small scale erosion hazard mapping using Landsat information in the northwest of Argentina p 9 A88-42035

SOIL MAPPING

Processing of multirate Landsat TM data to map soil color variations related to hydrocarbon microseepage in a cropland setting - Cement, Oklahoma test site p 1 A88-32921

Thematic Mapper data applied to mapping hydrothermal alteration in south west New Mexico p 28 A88-32923

Spectral discrimination of zeolites and dioctahedral clays in the near-infrared p 28 A88-32926

Remote sensing and surface geochemical study of Railroad Valley, Nye County, Nevada - Detailed grid study p 31 A88-32953

Mapping frost-sensitive areas with a three-dimensional local-scale numerical model. I - Physical and numerical aspects p 4 A88-41055

Preliminary investigation of Large Format Camera photography utility in soil mapping and related agricultural applications p 4 A88-41947

Relating L-band scatterometer data with soil moisture content and roughness p 5 A88-41984

The application of a vegetation index in correcting the infrared reflectance for soil background p 6 A88-41988

Multitemporal analysis of Thematic Mapper data for soil survey in Southern Tunisia p 6 A88-41989

Spectral signatures of soils and terrain conditions using lasers and spectrometers p 6 A88-41997

Multi-temporal Landsat for land unit mapping on project scale of the Sudd-floodplain, Southern Sudan p 9 A88-42015

Development of remote sensing techniques capable of delineating soils as an aid to soil survey [NASA-CR-182610] p 13 N88-22452

SOIL MOISTURE

A four-layer model for the heat budget of homogeneous land surfaces p 4 A88-41028

Relating L-band scatterometer data with soil moisture content and roughness p 5 A88-41984

Measurement of the water content of soil from space and application to the regional water balance p 55 N88-21561

An update on remote measurement of soil moisture over vegetation using infrared temperature measurements: A FIFE perspective [NASA-CR-182926] p 18 N88-24109

SOIL SCIENCE

Relationship between soil and leaf metal content and Landsat MSS and TM acquired canopy reflectance data p 6 A88-41986

SOILS

Linear combinations of spectral reflectances in crop analyses p 3 A88-36170

Soil and atmosphere influences on the spectra of partial canopies p 11 A88-44119

Modeling surface exchanges: The soil-vegetation-atmosphere continuum p 12 N88-21553

Development of remote sensing techniques capable of delineating soils as an aid to soil survey [NASA-CR-182610] p 13 N88-22452

Mapping soil and rock variation from satellite images in the Sahel p 14 N88-24023

Identification of shallow groundwater regions in semi-arid Brazil by remote sensing methods p 14 N88-24030

Characteristics of drainage determinations in aerial photographs and relief determination on different scales planialtimetric charts for three soils in the state of Sao Paulo p 17 N88-24095

SOLAR RADIATION

Landsat temporal-spectral profiles of crops on the South African highveld p 7 A88-41999

Classification of bottom composition and bathymetry of shallow waters by passive remote sensing p 53 A88-42051

Radiative processes affecting ocean mixed-layer heat content and their monitoring from satellite p 47 N88-20800

SOLID SUSPENSIONS

Determination of spectral signature of natural water by optical airborne and shipborne instruments p 44 A88-42050

SOYBEANS

Spectral behavior of crops through analysis of LANDSAT-TM data p 15 N88-24047

Identification of areas cultivated with soybeans in the cerrados regions, through digital processing of satellite images: A methodological approach p 15 N88-24048

Evaluation of TM false color composites for crop discrimination p 17 N88-24096

SOYUZ SPACECRAFT

The USSR space systems for remote sensing of earth resources and the environment (sensor systems, processing techniques, applications) p 76 N88-24035

SPACE BASED RADAR

The role of space borne imaging radars in environmental monitoring: Some shuttle imaging radar results in Asia [NASA-TM-101178] p 23 N88-24844

SPACE COLONIES

A second generation lunar agricultural system p 11 A88-43864

SPACE COMMERCIALIZATION

Approach and status for a unified national plan for satellite remote sensing research and development p 77 A88-32919

SPACE PROGRAMS

Aeronautics and space report of the President: 1986 activities p 77 N88-21087

SPACE SHUTTLE PAYLOADS

Space Shuttle Large Format Camera photography and resource management p 70 A88-36378

Insertion of hydrological decoupled data from photographic sensors of the Shuttle in a digital cartography of geophysical exploration (Spacelab 1-Metric Camera and Large Format Camera) p 74 A88-41990

The Shuttle Imaging Radar B (SIR-B) experiment report [NASA-CR-182923] p 75 N88-23932

SPACE STATIONS

Potential for earth observations from the manned Space Station [AAS PAPER 86-426] p 70 A88-35162

SPACEBORNE EXPERIMENTS

Airborne and spaceborne radar images for geologic and environmental mapping in the Amazon rain forest, Brazil p 37 N88-24021

SPACEBORNE PHOTOGRAPHY

- Color space mapping using ternary/chromaticity diagrams - A technique for composite image interpretation p 57 A88-32932
- Space photomaps - Their compilation and peculiarities of geographical application p 60 A88-41967
- Insertion of hydrological decorrelated data from photographic sensors of the Shuttle in a digital cartography of geophysical exploration (Spacelab 1-Metric Camera and Large Format Camera) p 74 A88-41990
- Correction of spatial and temporal distortions in the photographic image input into an interactive processing system p 62 A88-43672

SPACECRAFT INSTRUMENTS

- Earth observation: Capturing the imagery - Remote sensing depends on advanced recording technology p 72 A88-38411
- Insertion of hydrological decorrelated data from photographic sensors of the Shuttle in a digital cartography of geophysical exploration (Spacelab 1-Metric Camera and Large Format Camera) p 74 A88-41990
- NIMBUS-7 CZCS. Coastal Zone Color Scanner imagery for selected coastal regions. North America - Europe. South America - Africa - Antarctica. Level 2 photographic product [NASA-CR-180755] p 48 A88-22447

SPACECRAFT PERFORMANCE

- Tropical rainfall measuring mission (TRMM) p 69 A88-33429

SPACECRAFT POWER SUPPLIES

- Review of power requirements for satellite remote sensing systems p 76 A88-24387

SPAIN

- Thematic Mapper applied to alteration zone mapping for gold exploration in south-east Spain p 29 A88-32938

SPATIAL DISTRIBUTION

- Anomalies in the vegetation in the Alto Xingu - MT p 14 A88-24043

SPATIAL RESOLUTION

- Spatial resolution requirements for urban land cover mapping from space p 20 A88-42058
- Method for restoration and resampling of TM sensor imagery [INPE-4491-PRE/1255] p 65 A88-22454

SPECKLE PATTERNS

- Investigation of the usefulness of speckle analysis in imaging radar systems [BCRS-86-05] p 65 A88-23302

SPECTRAL BANDS

- Selection of bands for a newly developed multispectral airborne reference-aided calibrated scanner (MARCS) p 74 A88-41995
- The dangers of underestimating the importance of data adjustments in band ratioing p 62 A88-43225

SPECTRAL METHODS

- Spectral characterization of urban land covers from Thematic Mapper data p 20 A88-42059
- Development of remote sensing techniques capable of delineating soils as an aid to soil survey [NASA-CR-182610] p 13 A88-22452

SPECTRAL REFLECTANCE

- Preliminary measurements of spectral signatures of tropical and temperate plants in the thermal infrared p 1 A88-32909
- A near infrared vegetation index formed with airborne multispectral scanner data p 1 A88-32910
- Shift in spectral response of nickel-loaded and control shoots of white birch p 1 A88-32928
- Spectral geobotanical investigation of mineralized till sites p 29 A88-32934
- Surrogate spectral reflectances of vegetation applied to geobotanical remote sensing p 1 A88-32935
- Spectral reflectance from lichens treated with copper p 30 A88-32945
- Use of digitally processed laboratory reflectance spectra for the definition of probable microseepage - Induced mineralogic variations, Lisbon Valley, Utah p 30 A88-32946
- Influence of topography on forest reflectance using Landsat Thematic Mapper and digital terrain data p 2 A88-35397
- Canopy reflectance of soybean as affected by chronic doses of ozone in open-top field chambers p 2 A88-35398
- Evaluation of the possibility of determining concentrations of variable components of ocean water from averaged spectra of the diffuse optical reflection coefficient p 40 A88-36160
- Linear combinations of spectral reflectances in crop analyses p 3 A88-36170
- Interannual Landsat-MSS reflectance variation in an urbanized temperate zone p 58 A88-37417
- Active two-element microwave interferometry of the sea surface p 41 A88-37679

Remote sensing of leaf water status

- p 4 A88-40784
- Obtaining spectral reflectance factor measurements of stressed forest vegetation p 5 A88-41952
- Relation between spectral reflectance and vegetation index p 7 A88-41998
- Determination of spectral signature of natural water by optical airborne and shipborne instruments p 44 A88-42050
- Potato crop distribution and subdivision on soil type and potential water deficit - An integration of satellite imagery and environmental spatial database p 10 A88-43222
- Spectral reflective characteristics of sea surface p 47 A88-20676

SPECTRAL RESOLUTION

- Processing of raw digital NOAA-AVHRR data for sea- and land applications p 60 A88-41968

SPECTRAL SIGNATURES

- Preliminary measurements of spectral signatures of tropical and temperate plants in the thermal infrared p 1 A88-32909
- Color space mapping using ternary/chromaticity diagrams - A technique for composite image interpretation p 57 A88-32932
- Spectral signature of rice fields using Landsat-5 TM in the Mediterranean coast of Spain p 6 A88-41991
- Determination of spectral signatures of different forest damages from varying altitudes of multispectral scanner data p 6 A88-41993
- Spectral signatures of soils and terrain conditions using lasers and spectrometers p 6 A88-41997
- Digital analysis of stereo pairs for the detection of anomalous signatures in geothermal fields p 61 A88-42037
- Determination of spectral signature of natural water by optical airborne and shipborne instruments p 44 A88-42050
- Analysis of the parameters responsible for the variations of the illumination conditions in the LANDSAT data p 67 A88-24070

SPECTROPHOTOMETRY

- A comparative analysis of methods for compressing spectrophotometric data in the estimation of hydrological parameters p 54 A88-43673

SPECTRUM ANALYSIS

- Spectral discrimination of zeolites and dioctahedral clays in the near-infrared p 28 A88-32926
- Development of remote sensing techniques capable of delineating soils as an aid to soil survey [NASA-CR-182610] p 13 A88-22452
- Spectral measurements for correcting LANDSAT data for atmospheric effects p 66 A88-24020
- Utilization of LANDSAT-TM, for aiding in the localization of archeological sites in the state of Sao Paulo p 38 A88-24069
- Study of reservoir water quality utilizing remote sensing techniques: Methodological concepts p 56 A88-24076

SPOT (FRENCH SATELLITE)

- Spot 1 - International commercialization of remote sensing [AAS PAPER 86-299] p 69 A88-35155
- Imaging instrument of the Vegetation Payload (SPOT 4) p 70 A88-35968
- Enhancement of SPOT image resolution using an intensity-hue-saturation transformation p 59 A88-41958
- Per-field classification of a segmented SPOT simulated image p 60 A88-41970
- Digital classification of forested areas using simulated TM- and SPOT- and Landsat 5/TM-data p 5 A88-41971
- The use of SPOT simulation data in forestry mapping p 7 A88-42006
- Comparison of SPOT-simulated and Landsat 5 TM imagery in vegetation mapping p 9 A88-42014
- In flight calibration for the imaging instrument of VEGETATION payload (SPOT 4) p 10 A88-42545
- Use of digital terrain data in the interpretation of SPOT-1 HRV multispectral imagery p 10 A88-43221
- Terrain classification using SPOT images and the computer system GOP-300 [FOA-C-20677-2.7] p 68 A88-24102

SPRINGS (WATER)

- Spring mound and aoum mapping from Landsat TM imagery in south-central Tunisia p 52 A88-42026

STATISTICAL ANALYSIS

- Retrieval of atmospheric temperature structure from the NOAA-9 satellite p 72 A88-37336
- A statistical model for prediction of precision and accuracies of radar scattering coefficient measurements derived from SAR data p 62 A88-42771
- Application of spatial statistics to analyzing multiple remote sensing data sets p 64 A88-45639

STRUCTURAL PROPERTIES (GEOLOGY)

- Remote sensing techniques in the estimation of the area cultivated with beans, corn, and castor beans in the Itrec County (Bahia State) p 15 A88-24045
- Characteristics of drainage determinations in aerial photographs and relief determination on different scales planialtimetric charts for three soils in the state of Sao Paulo p 17 A88-24095

STATISTICAL DISTRIBUTIONS

- Evaluation of an estimation system for an irrigated area in a tropical region through TM-LANDSAT imagery p 16 A88-24075
- Evaluation of the floodable area of the canal of Sao Goncalo through TM-LANDSAT 5 imagery p 56 A88-24078
- The 35 mm vertical aerial photographs for mapping stands of bracinga in different age classes p 16 A88-24087
- Preliminary study on the application of digital processing of TM-LANDSAT data in the mapping of apple orchards in Fraiburgo (SC) p 17 A88-24093

STEREOPHOTOGRAPHY

- Digital elevation modeling with stereo SIR-B image data p 60 A88-41981
- Digital analysis of stereo pairs for the detection of anomalous signatures in geothermal fields p 61 A88-42037
- A demonstration of stereophotogrammetry with combined SIR-B and Landsat TM images p 63 A88-44650
- Relative orientation [AD-A190385] p 75 A88-22449
- Stereoscopic photographs, ground and aerial, of trees used in the arborization of Curitiba (PR) p 17 A88-24091

STEREOSCOPY

- SIR-B stereo-radargrammetry of Australia p 63 A88-44648

STRAITS

- Remote sensing of flow characteristics of the strait of Oresund p 53 A88-42043

STRATIFIED FLOW

- Mushroom-shaped currents (eddy dipoles) under rotation and stratification conditions p 47 A88-20678

STREAMS

- A study with NOAA-7 AVHRR-imagery in monitoring ephemeral streams in the lower catchment area of the Tana River, Kenya p 54 A88-42053

STRIP MINING

- A satellite-based investigation of the significance of surficial deposits for surface mining operations p 36 A88-45638

STRUCTURAL ANALYSIS

- Landsat structural analysis of the Rhine Valley and the Jura Mountain area, Western Europe p 26 A88-32903
- Remote sensing and structural rupture: Application examples in the study of tectonics p 37 A88-24050
- Analysis and interpretation of image lithostructure: An application of the multiconcept in the metamorphic belt of Sul de Santana da Boa Vista (RS) p 38 A88-24051
- Study of fracturing for groundwater research in the Sergipe state with remote sensing products p 38 A88-24052
- Lithostructural interpretation of Chapada do Cachimbo (Pa-Am-Mt), based on radar and LANDSAT imagery p 39 A88-24100

STRUCTURAL BASINS

- Lineaments of the northern Denver Basin and their paleotectonic and hydrocarbon significance p 28 A88-32920
- Surface expression of subsurface structures in the Michigan Basin p 29 A88-32929
- Evidence from geoid data of a hotspot origin for the southern Mascarene Plateau and Mascarene Islands (Indian Ocean) p 24 A88-38902

STRUCTURAL PROPERTIES (GEOLOGY)

- Associations among lineaments, subsurface fractures, hydrocarbon microseepage, and production in the Uinta Basin, Utah p 27 A88-32908
- Lineaments of the northern Denver Basin and their paleotectonic and hydrocarbon significance p 28 A88-32920
- Importance of fault mapping to mineral/geothermal exploration: Relationship to fluid migration and ore formation - Northwest Washington p 28 A88-32925
- A comparison of lineaments interpreted from remotely sensed data and airborne magnetics and their relationship to gold deposits in central Nova Scotia p 29 A88-32936
- Confirmation of quantitative morphostructural analysis by seismic, aeromagnetic and geochemical data in the Amazon Basin, Brazil p 29 A88-32937
- Geologic spatial analysis - A new multiple data source exploration tool p 30 A88-32947

- Assessment of digital enhancement techniques using Landsat TM data in mapping geologic lineaments, with application to the Mactaquac headpond area, southern New Brunswick p 31 A88-32949
- Computer processing of satellite data for geostructural zoning of a collisional boundary, significance and field checks - The example of Tunisia p 32 A88-35193
- The use of space data to study Precambrian structures p 32 A88-36161
- Quantitative analysis of a network of faults recognized on remote-sensing images of the Mushugai area in Mongolia p 32 A88-36163
- Geological analysis of the satellite lineaments of the Vistula Delta Plain, Zulawy Wislane, Poland p 34 A88-42021
- Analysis of lineaments and major fractures in Xichang-Dukou area, Sichuan province as interpreted from Landsat images p 34 A88-42022
- Application of remote sensing in the field of experimental tectonics p 34 A88-42023
- Remote sensing methods in geological research of the Lublin coal basin, SE Poland p 34 A88-42028
- Structural geology and regional tectonics of the Mineral County area, Nevada, using Shuttle Imaging Radar-B and digital aeromagnetic data p 35 A88-44646
- A comparative analysis of dyke lineaments mapped from Shuttle Imaging Radar and Large Format Camera photography in hyperarid areas of the Eastern Desert, Egypt, and Red Sea Hills, Sudan p 35 A88-44647
- Subsurface morphology and geochronology revealed by spaceborne and airborne radar p 37 N88-24022
- An integrated study of the Alto Paranaiba Kimberlite Province, Minas Gerais, Brazil: A possible tool for diamond exploration p 37 N88-24031
- Landuse and landform studies of the Mahanadi River Delta with the help of satellite MSS band p 56 N88-24033
- Remote sensing and structural rupture: Application examples in the study of tectonics p 37 N88-24050
- Analysis and interpretation of image lithostructure: An application of the multiconcept in the metamorphic belt of Sul de Santana da Boa Vista (RS) p 38 N88-24051
- Dune fields in central Western Argentina p 38 N88-24088
- The broken anticlines, cuesta and crest homoclines, oroclinal valleys, and other forms of relief outcrops delineated with the help of remote sensing imagery p 16 N88-24089
- Lithostructural interpretation of Chapda do Cachimbo (Pa-Am-Mt), based on radar and LANDSAT imagery p 39 N88-24100
- SUBMERGING**
- Estimation of reservoir submerging losses using CIR aerial photographs - Example of the Ertan hydropower station on the Yalong River in southwest China p 55 A88-45637
- SUGAR CANE**
- CANASATE: Sugar cane mapping by satellite p 15 N88-24046
- Spectral behavior of crops through analysis of LANDSAT-TM data p 15 N88-24047
- Evaluation of TM false color composites for crop discrimination p 17 N88-24096
- SULFUR**
- Mass extinctions, atmospheric sulphur and climatic warming at the K/T boundary p 46 A88-43835
- SULFUR DIOXIDES**
- Assessment of crop loss from air pollutants: Meteorology-atmospheric chemistry and long range transport [PB88-146857] p 12 N88-22448
- SUPERHIGH FREQUENCIES**
- SLAR as a research tool p 73 A88-41976
- SURFACE PROPERTIES**
- Analysis of the parameters responsible for the variations of the illumination conditions in the LANDSAT data p 67 N88-24070
- SURFACE ROUGHNESS**
- Comparison of unified full-wave solutions for normal incidence microwave backscatter from sea with physical optics and hybrid solutions p 42 A88-39079
- Geoid roughness and long-wavelength segmentation of the South Atlantic spreading ridge p 24 A88-40688
- SURFACE ROUGHNESS EFFECTS**
- An empirical model for polarized and cross-polarized scattering from a vegetation layer p 11 A88-44116
- SURFACE TEMPERATURE**
- Surface energy budget, surface temperature and thermal inertia p 58 A88-37147
- A methodology for mapping forest latent heat flux densities using remote sensing p 3 A88-37415
- Radiative surface temperatures of the burned and unburned areas in a tallgrass prairie p 3 A88-37418
- Using the thermal infrared multispectral scanner (TIMS) to estimate surface thermal responses p 73 A88-40785
- Radiative processes affecting ocean mixed-layer heat content and their monitoring from satellite p 47 N88-20800
- Identification of shallow groundwater regions in semi-arid Brazil by remote sensing methods p 14 N88-24030
- SURFACE WATER**
- Influence of the Yukon River on the Bering Sea [NASA-CR-182802] p 50 N88-24126
- SURFACE WAVES**
- Investigation of the imaging of ocean surface waves using a synthetic aperture radar [SER-A-WISS-ABHANDL-64] p 49 N88-23357
- SURVEYS**
- Study of reservoir water quality utilizing remote sensing techniques: Methodological concepts p 56 N88-24076
- SUSPENDING (MIXING)**
- Distribution and chemistry of suspended particles from an active hydrothermal vent site on the Mid-Atlantic Ridge at 26 deg N p 42 A88-37720
- SYNCHRONOUS SATELLITES**
- Sensors to record atmospheric and terrestrial information - Principles of collection and analysis p 71 A88-37130
- SYNOPTIC METEOROLOGY**
- Remote sensing of snow p 50 A88-35198
- SYNTHETIC APERTURE RADAR**
- Application of synthetic aperture radar (SAR) to southern Papua New Guinea fold belt exploration p 26 A88-32902
- The production of distortion free SAR imagery p 57 A88-33377
- Spaceborne radar X-SAR for civil applications p 72 A88-37286
- Image processing for earth remote sensing p 58 A88-37287
- SIR-B experiments in Japan. III - Oil-pollution experiment p 43 A88-40353
- SIR-B experiments in Japan. VI. Synthetic geological map obtained by remote sensing - An application to Palawan Island p 33 A88-41975
- Geological analysis of Seasat SAR and SIR-B data in Haiti p 33 A88-41980
- A statistical model for prediction of precision and accuracies of radar scattering coefficient measurements derived from SAR data p 62 A88-42771
- Crop classification from airborne synthetic aperture radar data p 10 A88-43220
- Comparative evaluation of the Large Format Camera, Metric Camera, and Shuttle Imaging Radar - A data content p 75 A88-44519
- Shuttle radar mapping with diverse incidence angles in the rainforest of Borneo p 12 A88-44644
- Dependence of image grey values on topography in SIR-B images p 63 A88-44649
- An effect of coherent scattering in spaceborne and airborne SAR images p 64 A88-44651
- A comparison of airborne GEMS/SAR with satellite-borne Seasat/SAR radar imagery - The value of archived multiple data sets p 64 A88-45640
- Investigation of the imaging of ocean surface waves using a synthetic aperture radar [SER-A-WISS-ABHANDL-64] p 49 N88-23357
- The role of space borne imaging radars in environmental monitoring: Some shuttle imaging radar results in Asia [NASA-TM-101178] p 23 N88-24844
- SYSTEMS INTEGRATION**
- The integration of remote sensing and geographic information systems p 21 A88-42069
- T**
- TECHNOLOGY ASSESSMENT**
- Overview of remote data transmission systems p 55 A88-45643
- Current stage of remote sensing system for cartographic application p 76 N88-24090
- TECTONICS**
- Geodetic measurement of deformation east of the San Andreas Fault in Central California p 25 A88-32831
- Discrimination of lithologic units, alteration patterns and major structural blocks in the Tonopah, Nevada area using Thematic Mapper data p 27 A88-32907
- Lineaments of the northern Denver Basin and their paleotectonic and hydrocarbon significance p 28 A88-32920
- Application of remote sensing to tectonic and metallogenic studies in NE Africa p 28 A88-32924
- Computer processing of satellite data for geostructural zoning of a collisional boundary, significance and field checks - The example of Tunisia p 32 A88-35193
- Comparison between interpretation of images of different nature p 34 A88-42019
- Application of remote sensing in the field of experimental tectonics p 34 A88-42023
- Structural geology and regional tectonics of the Mineral County area, Nevada, using Shuttle Imaging Radar-B and digital aeromagnetic data p 35 A88-44646
- Remote sensing and structural rupture: Application examples in the study of tectonics p 37 N88-24050
- TELEMTRY**
- Overview of remote data transmission systems p 55 A88-45643
- Geometric restoration of satellite image data [AD-A190462] p 64 N88-22450
- TEMPERATE REGIONS**
- Interannual Landsat-MSS reflectance variation in an urbanized temperate zone p 58 A88-37417
- TEMPERATURE**
- Calibration and processing of AVHRR data for temperature estimation [INPE-4493-PRE/1257] p 65 N88-22485
- TEMPERATURE DISTRIBUTION**
- Using the thermal infrared multispectral scanner (TIMS) to estimate surface thermal responses p 73 A88-40785
- Hydrographic observations in the northwestern Weddell Sea Marginal Ice Zone during March 1986 [PB88-173240] p 55 N88-23359
- TEMPERATURE MEASUREMENT**
- The Along-Track Scanning Radiometer with Microwave Sounder p 41 A88-37148
- Methodology for an operational monitoring of remotely-sensed sea surface temperatures in Indonesia p 43 A88-39084
- Sea surface temperature studies in Norwegian coastal areas using AVHRR- and TM thermal infrared data p 44 A88-42047
- TEMPERATURE PROFILES**
- Basic networks of TOGA: Determination of thermal profiles by XBT and of sea level by tide gage p 48 N88-21568
- TEMPORAL DISTRIBUTION**
- Multitemporal analysis of Thematic Mapper data for soil survey in Southern Tunisia p 68 A88-41989
- TEMPORAL RESOLUTION**
- Multitemporal analysis of Landsat Multispectral Scanner (MSS) and Thematic Mapper (TM) data to map crops in the Po valley (Italy) and in Mendoza (Argentina) p 6 A88-41994
- Applications of multitemporal compositions obtained from LANDSAT data in the study of urban growth [INPE-4480-PRE/1246] p 22 N88-23692
- TERRADYNAMICS**
- Geoid roughness and long-wavelength segmentation of the South Atlantic spreading ridge p 24 A88-40688
- TERRAIN**
- Digital terrain model and image integration for geologic interpretation p 26 A88-32904
- Visualization of digital terrain models p 67 N88-24081
- Terrain classification using SPOT images and the computer system GOP-300 [FOA-C-20677-2.7] p 68 N88-24102
- TERRAIN ANALYSIS**
- Influence of topography on forest reflectance using Landsat Thematic Mapper and digital terrain data p 2 A88-35397
- Identification of terrain cover using the optimum polarimetric classifier p 3 A88-37370
- Structural information of the landscape as ground truth for the interpretation of satellite imagery p 59 A88-41962
- Classification of land features, using Landsat MSS data in a mountainous terrain p 19 A88-41972
- Digital elevation modeling with stereo SIR-B image data p 60 A88-41981
- Evaluation of digitally processed Landsat imagery and SIR-A imagery for geological analysis of West Java region, Indonesia p 33 A88-41983
- Shuttle imaging radar (SIR-A) interpretation of the Kashgar region in western Xinjiang, China p 74 A88-41985
- Spectral signatures of soils and terrain conditions using lasers and spectrometers p 6 A88-41997
- Environmental assessment for large scale civil engineering projects with data of DTM and remote sensing --- Digital Terrain Models p 53 A88-42046
- A VHF radar to make terrain elevation models through tropical jungle p 10 A88-42760
- Use of digital terrain data in the interpretation of SPOT-1 HRV multispectral imagery p 10 A88-43221
- Thermal modeling and IR scene generation p 63 A88-44534
- Remote sensing of earth terrain [NASA-CR-182677] p 12 N88-20711
- Study of fracturing for groundwater research in the Sergipe state with remote sensing products p 38 N88-24052

TEXTURES

- Textural features for image classification in remote sensing p 66 N88-24027
 Remote sensing and structural rupture: Application examples in the study of tectonics p 37 N88-24050

THEMATIC MAPPERS (LANDSAT)

- Digital terrain model and image integration for geologic interpretation p 26 A88-32904
 Discrimination of lithologic units, alteration patterns and major structural blocks in the Tonopah, Nevada area using Thematic Mapper data p 27 A88-32907
 Integration of SIR-B imagery with geological and geophysical data in Australia p 27 A88-32912
 Processing of multirate Landsat TM data to map soil color variations related to hydrocarbon microseepage in a cropland setting - Cement, Oklahoma test site p 1 A88-32921
 Thematic Mapper data applied to mapping hydrothermal alteration in south west New Mexico p 28 A88-32923
 Use of calibration targets in the measurement of 2.22-micron mineral absorption features in Thematic Mapper data p 29 A88-32927
 A geobotanical investigation of an exploration-sized territory p 29 A88-32931
 Thematic Mapper applied to alteration zone mapping for gold exploration in south-east Spain p 29 A88-32938
 The use of Thematic Mapper imagery for mineral exploration in the sedimentary terrain of the Spring Mountains, Nevada p 30 A88-32940
 An integrated approach to the use of Landsat TM data for gold exploration in west central Nevada p 30 A88-32941
 Quantitative procedure for producing color-calibrated Thematic Mapper natural-color images p 57 A88-32943
 Detection of geologic features in Landsat TM imagery not revealed in Landsat MSS imagery p 30 A88-32944
 Discrimination and supervised classification of volcanic flows of the Puna-Altiplano, Central Andes Mountains using Landsat TM data p 31 A88-32948
 Assessment of digital enhancement techniques using Landsat TM data in mapping geologic lineaments, with application to the Mactaquac headpond area, southern New Brunswick p 31 A88-32949
 Landsat TM data as an aid in planning and interpretation of regional geochemical surveys in the Canadian Shield p 31 A88-32950
 Discrimination of geobotanical anomalies in rugged alpine terrain using Landsat Thematic Mapper data p 32 A88-32957
 Application of aerospace remote sensing to geological investigations in Nevada and California [AAS PAPER 86-400] p 32 A88-35160
 Potential of Landsat Thematic Mapper image for crystalline rock type discrimination - Gregory Rift, Kenya p 32 A88-35192
 Influence of topography on forest reflectance using Landsat Thematic Mapper and digital terrain data p 2 A88-35397
 Flood damage analysis using multitemporal Landsat Thematic Mapper data p 4 A88-39090
 Application of Landsat Thematic Mapper data to assess suspended sediment dispersion in a coastal lagoon p 51 A88-41946
 Economic potential of Landsat Thematic Mapper data for crop condition assessment of winter wheat p 4 A88-41948
 Image optimization versus classification - An application oriented comparison of different methods by use of Thematic Mapper data p 59 A88-41964
 Digital classification of forested areas using simulated TM- and SPOT- and Landsat 5/TM-data p 5 A88-41971
 Thematic Mapping by satellite - A new tool for planning and management p 60 A88-41973
 Relationship between soil and leaf metal content and Landsat MSS and TM acquired canopy reflectance data p 6 A88-41986
 Multitemporal analysis of Thematic Mapper data for soil survey in Southern Tunisia p 6 A88-41989
 Spectral signature of rice fields using Landsat-5 TM in the Mediterranean coast of Spain p 6 A88-41991
 The use of Thematic Mapper imagery for geomorphological mapping in arid and semi-arid environments p 33 A88-41992
 Multitemporal analysis of Landsat Multispectral Scanner (MSS) and Thematic Mapper (TM) data to map crops in the Po valley (Italy) and in Mendoza (Argentina) p 6 A88-41994
 Optimal Thematic Mapper bands and transformations for discerning metal stress in coniferous tree canopies p 7 A88-42002

- Spruce budworm infestation detection using an airborne pushbroom scanner and Thematic Mapper data p 8 A88-42007
 Comparison of SPOT-simulated and Landsat 5 TM imagery in vegetation mapping p 9 A88-42014
 Assessment of TM thermal infrared band contribution in land cover/land use multispectral classification p 61 A88-42016
 A hydrological comparison of Landsat TM, Landsat MSS and black and white aerial photography p 52 A88-42041
 Sea surface temperature studies in Norwegian coastal areas using AVHRR- and TM thermal infrared data p 44 A88-42047
 Spectral characterization of urban land covers from Thematic Mapper data p 20 A88-42059
 Integration of Landsat, DTED, and DFAD p 63 A88-44540
 Cartographic feature extraction with integrated SIR-B and Landsat TM images p 63 A88-44641
 A demonstration of stereophotogrammetry with combined SIR-B and Landsat TM images p 63 A88-44650
 The 'Tsukusys' image processing system and its utilization in Thematic Mapper investigations of water quality conditions p 54 A88-45115
 Method for restoration and resampling of TM sensor imagery [INPE-4491-PRE/1255] p 65 N88-22454
 Turbidity patterns in the delta waters of southwest Netherlands on Thematic Mapper (TM) and multispectral scanner (MSS) satellite images [BCRS-86-06] p 55 N88-23303
 Evaluation of an estimation system for an irrigated area in a tropical region through TM-LANDSAT imagery p 16 N88-24075
- THEMATIC MAPPING**
 Thematic Conference on Remote Sensing for Exploration Geology, 5th, Reno, NV, Sept. 29-Oct. 2, 1986, Proceedings, Volumes 1 & 2 p 26 A88-32901
 Mapping the Oman Ophiolite using TM data p 26 A88-32906
 Rock discrimination and alteration mapping for mineral exploration using the Carr Boyd/Geoscan airborne multispectral scanner p 27 A88-32914
 Exploration for mercury and lead-zinc-silver using the airborne Thematic Mapper, Almaden area, Spain p 29 A88-32939
 The use of multispectral space photographs to draw up a map of land use in western Slovakia p 57 A88-33774
 Investigation and mapping of forests using space scanner imagery obtained in winter p 2 A88-36165
 Saline salt and water surface mapping on the basis of data from the Gyunesh-84 remote-sensing experiment p 51 A88-36166
 A methodology for mapping forest latent heat flux densities using remote sensing p 3 A88-37415
 Using spatial autocorrelation analysis to explore the errors in maps generated from remotely sensed data p 58 A88-39097
 A comparison of sampling schemes used in generating error matrices for assessing the accuracy of maps generated from remotely sensed data p 59 A88-39098
 Influence of mineral coatings and vegetation on TM imagery over Tertiary Caldera lithologies basin and range province, western U.S. p 32 A88-41945
 Space photomaps - Their compilation and peculiarities of geographical application p 60 A88-41967
 The use of Thematic Mapper imagery for geomorphological mapping in arid and semi-arid environments p 33 A88-41992
 Visual interpretation of MSS-FCC manual cartographic integration of data p 61 A88-42001
 Application of multispectral scanning remote sensing in agricultural water management problems p 8 A88-42011
 Thematic Mapping from aerial photographs for Kandi Watershed and area development project, Punjab (India) p 9 A88-42024
 Satellite remote sensing of the coastal environment of Bombay p 61 A88-42052
 Human settlement analysis using Shuttle Imaging Radar-A data - An evaluation p 20 A88-42057
 A comprehensive LRLIS of the Kananaskis Valley using Landsat data --- Land-Related Information System p 21 A88-42064
 Comparative evaluation of the Large Format Camera, Metric Camera, and Shuttle Imaging Radar - A data content p 75 A88-44519
 Latin American Symposium on Remote Sensing, 4th Brazilian Remote Sensing Symposium and 6th SELPER Plenary Meeting, volume 1 p 75 N88-24013

- Utilization of TM/LANDSAT images in the implanted forests mapping in the Mogi-Guaçu Region (SP-Brazil) p 14 N88-24042
 Utilization of LANDSAT-TM, for aiding in the localization of archeological sites in the state of Sao Paulo p 38 N88-24069
 Interpretation of MSS/LANDSAT data for evaluation of physical distribution of mangroves in Cananea-Iguaçu (SP) p 16 N88-24072
 Utilization of LANDSAT-TM imagery in the hydroenergetic inventory of the Paraíba de Sul River Basin p 56 N88-24077
 Evaluation of the mangrove area at the Piauí River (SE) through remote sensing p 16 N88-24086
 Evaluation of TM false color composites for crop discrimination p 17 N88-24096
- THERMAL ANALYSIS**
 A PC-based interactive graphics system to perform satellite-derived oceanographic thermal analysis p 68 A88-32850
 Thermal analysis of wildfires and effects on global ecosystem cycling p 2 A88-35194
- THERMAL MAPPING**
 Using the thermal infrared multispectral scanner (TIMS) to estimate surface thermal responses p 73 A88-40785
- THERMAL RADIATION**
 Radiative surface temperatures of the burned and unburned areas in a tallgrass prairie p 3 A88-37418
- THERMAL SIMULATION**
 Thermal modeling and IR scene generation p 63 A88-44534
- THERMOCLINES**
 The determination of the parameters of the diurnal thermocline using satellite and ship-based measurements p 44 A88-40834
- THERMODYNAMICS**
 Elements of sea ice dynamics and thermodynamics p 48 N88-21571
- TIDES**
 Tidal estimation in the Pacific with application to SEASAT altimetry [NASA-TM-100694] p 47 N88-20780
- TIMBER IDENTIFICATION**
 The use of SPOT simulation data in forestry mapping p 7 A88-42006
- TIMBER INVENTORY**
 Inventory of decline and mortality in spruce-fir forests of the eastern U.S. with CIR photos p 7 A88-42004
 A remote sensing aided inventory of fuelwood volumes in the Sahel region of west Africa - A case study of five urban zones in the Republic of Niger p 7 A88-42005
 Experiences in application of multispectral scanner-data for forest damage inventory p 8 A88-42010
- TIMBER VIGOR**
 Remote-sensing methods for the monitoring and forecasting of the entomological condition of taiga forests p 2 A88-36164
- TIME DEPENDENCE**
 Developments in use of GPS as range TSPI --- Time and Space Position Information p 72 A88-37384
- TIME SERIES ANALYSIS**
 Climatological interpretation of time series of satellite observations of the earth's radiation balance p 69 A88-33872
 Comparison of surface current determined from satellite-tracked buoy with shipboard wind data during the 4th Brazilian antarctic expedition, 10-14 March, 1986 p 49 N88-24024
- TOPEX**
 Topex/Poseidon - A contribution to the world climate research program [AAS PAPER 86-306] p 39 A88-35058
 Precision positioning of earth orbiting remote sensing systems [AAS PAPER 86-398] p 70 A88-35159
- TOPOGRAPHY**
 Influence of topography on forest reflectance using Landsat Thematic Mapper and digital terrain data p 2 A88-35397
 Geoid roughness and long-wavelength segmentation of the South Atlantic spreading ridge p 24 A88-40688
 Base map production from geocoded imagery p 25 A88-41969
 Environmental assessment for large scale civil engineering projects with data of DTM and remote sensing --- Digital Terrain Models p 53 A88-42046
 Radiometric correction for atmospheric and topographic effects on Landsat MSS images p 62 A88-43223
 Directed band rationing for the retention of perceptually-independent topographic expression in chromaticity-enhanced imagery p 62 A88-43224
 Dependence of image grey values on topography in SIR-B images p 63 A88-44649
 Study of the dynamic topography of oceans by means of satellite altimetry p 47 N88-21567

From satellite altimetry to ocean topography, a survey of data processing techniques [ETN-88-91841] p 48 N88-21575
 Criteria for planimetric and altimetric correction of maps restituted from aerial photographs in 1:100,000 scale p 38 N88-24097
 Recent developments in software and hardware by Scitex Co. --- computer aided mapping p 68 N88-25038

TORNADOES

Tornado tracks in Southwestern Brazil, Eastern Paraguay, and Northwestern Argentina p 23 N88-24071

TOTAL OZONE MAPPING SPECTROMETER

The 1987 Airborne Antarctic Ozone Experiment: The Nimbus-7 TOMS data atlas [NASA-RP-1201] p 47 N88-20714

TRACKING (POSITION)

Comparison of surface current determined from satellite-tracked buoy with shipboard wind data during the 4th Brazilian antarctic expedition, 10-14 March, 1986 p 49 N88-24024
 Near surface current determined from INPE's satellite-tracked buoy, during 6-26 November, 1985 p 50 N88-24058

TRACKING NETWORKS

Precision positioning of earth orbiting remote sensing systems [AAS PAPER 86-398] p 70 A88-35159

TRAJECTORIES

Comparison of surface current determined from satellite-tracked buoy with shipboard wind data during the 4th Brazilian antarctic expedition, 10-14 March, 1986 p 49 N88-24024
 Tornado tracks in Southwestern Brazil, Eastern Paraguay, and Northwestern Argentina p 23 N88-24071

TRANSFER FUNCTIONS

Method for restoration and resampling of TM sensor imagery [INPE-4491-PRE/1255] p 65 N88-22454

TRANSFORMATIONS (MATHEMATICS)

Application of its transformation in color enhancement of LANDSAT imagery p 68 N88-24082

TRANSORBITAL RADIO PROPAGATION

Range variations of the tropospheric propagation of ultrashort radio waves above the sea p 39 A88-33920

TREES (MATHEMATICS)

Evaluation of regional land resources using geographic information systems based on linear quadratrees p 20 A88-42063

TREES (PLANTS)

Preliminary measurements of spectral signatures of tropical and temperate plants in the thermal infrared p 1 A88-32909
 Radar backscatter characteristics of trees at 215 GHz p 11 A88-44307
 Millimeter-wave bistatic scattering from ground and vegetation targets p 11 A88-44308
 Utilization of TM/LANDSAT images in the implanted forests mapping in the Mogi-Guaçu Region (SP-Brazil) p 14 N88-24042
 Interpretation of MSS/LANDSAT data for evaluation of physical distribution of mangroves in Cananeia-Iguape (SP) p 16 N88-24072
 Evaluation of the mangrove area at the Piauí River (SE) through remote sensing p 16 N88-24086
 Stereoscopic photographs, ground and aerial, of trees used in the arborization of Curitiba (PR) p 17 N88-24091

TRIANGULATION

Adjustment in photogrammetry: Methods, programs and applications [B8735130] p 76 N88-24105

TROPICAL METEOROLOGY

A satellite infrared technique to estimate tropical convective and stratiform rainfall p 69 A88-33416
 Tropical rainfall measuring mission (TRMM) p 69 A88-33429

TROPICAL REGIONS

Satellite radars for geologic mapping in tropical regions p 27 A88-32917
 A proposed tropical rainfall measuring mission (TRMM) satellite p 69 A88-33742
 Methodology for an operational monitoring of remotely-sensed sea surface temperatures in Indonesia p 43 A88-39084
 Temporal variations of particle fluxes in the deep subtropical and tropical North Atlantic - Eulerian versus Lagrangian effects p 45 A88-42448
 A VHF radar to make terrain elevation models through tropical jungle p 10 A88-42760
 Basic networks of TOGA: Determination of thermal profiles by XBT and of sea level by tide gauge p 48 N88-21568

TROPICAL STORMS

An evaluation of the performance of the ECMWF operational system in analyzing and forecasting easterly wave disturbances over Africa and the tropical Atlantic p 43 A88-39746

TROPOSPHERE

Effect of wet tropospheric path delays on estimation of geodetic baselines in the Gulf of California using the Global Positioning System p 25 A88-41835

TROPOSPHERIC WAVES

Range variations of the tropospheric propagation of ultrashort radio waves above the sea p 39 A88-33920

TURBIDITY

Quantitative analysis of distribution of suspended sediments in the Yellow River Estuary from MSS data p 50 A88-35196
 Satellite detection of bloom and pigment distributions in estuaries p 51 A88-37414
 Turbidity patterns in the delta waters of southwest Netherlands on Thematic Mapper (TM) and multispectral scanner (MSS) satellite images [BCRS-86-06] p 55 N88-23303
 Satellite remote sensing of turbidity and sediment concentration in Lagoa dos Patos p 56 N88-24032

TURBULENT MIXING

Radiative processes affecting ocean mixed-layer heat content and their monitoring from satellite p 47 N88-20800

U

U.S.S.R. SPACE PROGRAM

The USSR space systems for remote sensing of earth resources and the environment (sensor systems, processing techniques, applications) p 76 N88-24035

ULTRAHIGH FREQUENCIES

Relating L-band scatterometer data with soil moisture content and roughness p 5 A88-41984

ULTRAVIOLET PHOTOMETRY

Satellite UV image processing [AD-A190466] p 65 N88-22451

ULTRAVIOLET SPECTROMETERS

Satellite UV image processing [AD-A190466] p 65 N88-22451

ULTRAVIOLET SPECTROSCOPY

Remote sensing of the earth's surface in the ultraviolet range p 32 A88-36172

UNDERWATER OPTICS

Evaluation of the possibility of determining concentrations of variable components of ocean water from averaged spectra of the diffuse optical reflection coefficient p 40 A88-36160

URANIUM

An evaluation of potential uranium deposit area by Landsat data analysis in Officer Basin, South-Western part of Australia p 35 A88-42036

URBAN DEVELOPMENT

Orbital remote sensing: An instrument for monitoring urban growth [INPE-4456-PRE/1287] p 22 N88-22833
 Applications of multitemporal compositions obtained from LANDSAT data in the study of urban growth [INPE-4480-PRE/1246] p 22 N88-23692

URBAN PLANNING

Orbital remote sensing: An instrument for monitoring urban growth [INPE-4456-PRE/1287] p 22 N88-22833
 Low altitude remote sensing data in the implementation of a mathematical model for the planning of urban equipment networks p 23 N88-24074

URBAN RESEARCH

Using Landsat to derive curve numbers for hydrologic models p 52 A88-41950
 An analysis of remote sensing for monitoring urban derelict land p 20 A88-42056

USER REQUIREMENTS

The SAGE geographic analysis system p 22 N88-24063

V

VALLEYS

Landsat structural analysis of the Rhine Valley and the Jura Mountain area, Western Europe p 26 A88-32903
 Groundwater sapping valleys: Experimental studies, geological controls and implications to the interpretation of valley networks on Mars [NASA-CR-182718] p 37 N88-22847

VEGETATION

Targeting epithermal alteration and gossans in weathered and vegetated terrains using aircraft scanners - Successful Australian case histories p 26 A88-32905

Vegetation indices and other vegetation parameters - Examples, interpretation and problems p 3 A88-38373

SIR-B experiments in Japan. II - Rice crop experiment p 4 A88-40352

A four-layer model for the heat budget of homogeneous land surfaces p 4 A88-41028

Influence of mineral coatings and vegetation on TM imagery over Tertiary Caldera lithologies basin and range province, western U.S. p 32 A88-41945

Obtaining spectral reflectance factor measurements of stressed forest vegetation p 5 A88-41952

Comparison of SPOT-simulated and Landsat 5 TM imagery in vegetation mapping p 9 A88-42014

Millimeter-wave propagation in vegetation: Experiments and theory p 12 A88-44319

Subsurface morphology and geoarchaeology revealed by spaceborne and airborne radar p 37 N88-24022

Anomalies in the vegetation in the Alto Xingu - MT p 14 N88-24043

An update on remote measurement of soil moisture over vegetation using infrared temperature measurements: A FIFE perspective [NASA-CR-182926] p 18 N88-24109

VEGETATION GROWTH

Surrogate spectral reflectances of vegetation applied to geobotanical remote sensing p 1 A88-32935

A study with NOAA-7 AVHRR-imagery in monitoring ephemeral streams in the lower catchment area of the Tana River, Kenya p 54 A88-42053

VEGETATIVE INDEX

A near infrared vegetation index formed with airborne multispectral scanner data p 1 A88-32910

Differences in visible and near-IR responses, and derived vegetation indices, for the NOAA-9 and NOAA-10 AVHRRs - A case study p 70 A88-35396

Transformation of Global Vegetation Index (GVI) data from the polar stereographic projection to an equatorial cylindrical projection p 58 A88-39095

The application of a vegetation index in correcting the infrared reflectance for soil background p 6 A88-41988

Spectral signature of rice fields using Landsat-5 TM in the Mediterranean coast of Spain p 6 A88-41991

Multitemporal analysis of Landsat Multispectral Scanner (MSS) and Thematic Mapper (TM) data to map crops in the Po valley (Italy) and in Mendoza (Argentina) p 6 A88-41994

Relation between spectral reflectance and vegetation index p 7 A88-41998

Landsat temporal-spectral profiles of crops on the South African highveld p 7 A88-41999

Global vegetation monitoring using NOAA GAC data p 8 A88-42012

Classification of the Riverina forests of south east Australia using co-registered Landsat MSS and SIR-B radar data p 9 A88-42013

Taking the effect of vegetation into account in the microwave-radiometer remote sensing of the earth surface on the results of remote sounding of the earth surface by microwave radiometry p 10 A88-43670

The effect of atmospheric correction on the interpretation of multitemporal AVHRR-derived vegetation index dynamics p 11 A88-44117

VERTICAL MOTION

Factors affecting feature differentiation - The impact and source of variance in the upwelling radiance field p 58 A88-37128

VERY HIGH FREQUENCIES

A VHF radar to make terrain elevation models through tropical jungle p 10 A88-42760

VIDEO DATA

Non-tracking antenna systems for the acquisition of NOAA HRPT Data --- High Resolution Picture Transmission p 72 A88-37279

VISIBLE SPECTRUM

The acquisition of SPOT-1 HRV imagery over southern Britain and northern France, May 1986-May 1987 p 68 A88-29286

Differences in visible and near-IR responses, and derived vegetation indices, for the NOAA-9 and NOAA-10 AVHRRs - A case study p 70 A88-35396

An update on visible and near infrared calibration of satellite instruments p 72 A88-37416

VOLCANOLOGY

Discrimination and supervised classification of volcanic flows of the Puna-Altiplano, Central Andes Mountains using Landsat TM data p 31 A88-32948

VORTICES

Satellite observations and the numerical simulation of the interaction between a synoptic eddy and a frontal zone in the ocean p 40 A88-36159

Mushroom-shaped currents (eddy dipoles) under rotation and stratification conditions p 47 A88-20678

VORTICITY

- An evaluation of the performance of the ECMWF operational system in analyzing and forecasting easterly wave disturbances over Africa and the tropical Atlantic
p 43 A88-39746

W

WASTE DISPOSAL

- Case studies on the application of remote sensing data to geotechnical investigations in Ontario, Canada
p 35 A88-45635

WASTE WATER

- Case studies on the application of remote sensing data to geotechnical investigations in Ontario, Canada
p 35 A88-45635

WATER BALANCE

- Measurement of the water content of soil from space and application to the regional water balance
p 55 N88-21561

WATER CIRCULATION

- Satellite observations and the numerical simulation of the interaction between a synoptic eddy and a frontal zone in the ocean
p 40 A88-36159
- Remote sensing of flow characteristics of the strait of Oresund
p 53 A88-42043
- Circulation patterns in AVHRR imagery
p 46 A88-43217

- On the regional characteristics of actual evapotranspiration derived from Landsat MSS and elevation data
p 54 A88-45118

WATER COLOR

- Satellite detection of bloom and pigment distributions in estuaries
p 51 A88-37414
- Time evolution of surface chlorophyll patterns from cross-spectrum analysis of satellite color images
p 45 A88-42446
- The effect of dissolved 'yellow substance' on the quantitative retrieval of chlorophyll and total suspended sediment concentrations from remote measurements of water colour
p 46 A88-43226

WATER FLOW

- Evaluation of the floodable area of the canal of Sao Goncalo through TM-LANDSAT 5 imagery
p 56 N88-24078

WATER MANAGEMENT

- Thematic Mapping by satellite - A new tool for planning and management
p 60 A88-41973
- Shuttle imaging radar (SIR-A) interpretation of the Kashgar region in western Xinjiang, China
p 74 A88-41985
- Application of multispectral scanning remote sensing in agricultural water management problems
p 8 A88-42011
- Coastal monitoring by remote sensing
p 54 A88-44447

WATER POLLUTION

- SIR-B experiments in Japan. I - Sensor calibration experiment
p 73 A88-40351
- The JRC program for marine coastal monitoring
p 44 A88-42039
- The 'Tsukusys' image processing system and its utilization in Thematic Mapper investigations of water quality conditions
p 54 A88-45115
- Feasibility study for a 2nd generation system for airborne maritime pollution surveillance
[ETN-88-92108]
p 55 N88-22466
- Study of reservoir water quality utilizing remote sensing techniques: Methodological concepts
p 56 N88-24076

WATER QUALITY

- Principles of the remote monitoring of fresh-water quality
p 50 A88-34674
- Toward an integrated system for satellite remote sensing of water quality in the Great Lakes
p 52 A88-41957
- The 'Tsukusys' image processing system and its utilization in Thematic Mapper investigations of water quality conditions
p 54 A88-45115
- Satellite remote sensing of turbidity and sediment concentration in Lagoa dos Patos
p 56 N88-24032
- Study of reservoir water quality utilizing remote sensing techniques: Methodological concepts
p 56 N88-24076

WATER RESOURCES

- Application of remote sensing in hydromorphology for third world development - A resource development study in parts of Haryana (India)
p 53 A88-42042
- Environmental assessment for large scale civil engineering projects with data of DTM and remote sensing - Digital Terrain Models
p 53 A88-42046

WATER RUNOFF

- Rangeland runoff curve numbers as determined from Landsat MSS data
p 51 A88-39089
- Using Landsat to derive curve numbers for hydrologic models
p 52 A88-41950

- A methodology for integrating satellite imagery and field observations for hydrological regionalisation in Alpine catchments
p 52 A88-42038
- Groundwater sapping valleys: Experimental studies, geological controls and implications to the interpretation of valley networks on Mars
[NASA-CR-182718]
p 37 N88-22847

WATER VAPOR

- On the regional characteristics of actual evapotranspiration derived from Landsat MSS and elevation data
p 54 A88-45118

WATER WAVES

- Radiometric investigation of the sea-wave breaking process
p 46 A88-43664
- Study of the dynamic topography of oceans by means of satellite altimetry
p 47 N88-21567
- Investigation of the imaging of ocean surface waves using a synthetic aperture radar
[SER-A-WISS-ABHANDL-84]
p 49 N88-23357

WATERSHEDS

- A methodology for mapping forest latent heat flux densities using remote sensing
p 3 A88-37415
- Thematic Mapping from aerial photographs for Kandi Watershed and area development project, Punjab (India)
p 9 A88-42024

WAVE PROPAGATION

- Range variations of the tropospheric propagation of ultrashort radio waves above the sea
p 39 A88-33920
- Effect of wet tropospheric path delays on estimation of geodetic baselines in the Gulf of California using the Global Positioning System
p 25 A88-41835
- Millimeter-wave propagation in vegetation: Experiments and theory
p 12 A88-44319

WAVE REFLECTION

- The physical principles controlling the remote sensing process
p 71 A88-37129

WEATHER FORECASTING

- Use of radar and satellite imagery for the measurement and short-term prediction of rainfall in the United Kingdom
p 51 A88-37136
- An evaluation of the performance of the ECMWF operational system in analyzing and forecasting easterly wave disturbances over Africa and the tropical Atlantic
p 43 A88-39746

WETLANDS

- A gridding approach to detect patterns of change in coastal wetlands from digital data
p 52 A88-41949
- Correlation between aircraft MSS and LIDAR remotely sensed data on a forested wetland in South Carolina
p 5 A88-41951

WHEAT

- Economic potential of Landsat Thematic Mapper data for crop condition assessment of winter wheat
p 4 A88-41948
- Use of energy emission for detecting the necessity of irrigation in wheat in field conditions
[INPE-4461-TDL/318]
p 13 N88-23315
- Estimation of an area cultivated with wheat from LANDSAT data through a two-phase sampling method
p 14 N88-24041

WILDERNESS

- History of wildland fires on Vandenberg Air Force Base, California
[NASA-TM-100983]
p 18 N88-25134

WILDLIFE

- Remote sensing for wildlife management - Giant panda habitat mapping from Landsat MSS images
p 2 A88-35195

WIND EFFECTS

- Use of energy emission for detecting the necessity of irrigation in wheat in field conditions
[INPE-4461-TDL/318]
p 13 N88-23315

WIND MEASUREMENT

- Remote sensing of sea-surface winds
p 41 A88-37144
- Comparison of surface current determined from satellite-tracked buoy with shipboard wind data during the 4th Brazilian antarctic expedition, 10-14 March, 1986
p 49 N88-24024

WIND VELOCITY MEASUREMENT

- A system for remote measurements of the wind stress over the ocean
p 40 A88-36841

WINTER

- Investigation and mapping of forests using space scanner imagery obtained in winter
p 2 A88-36165

WORKSTATIONS

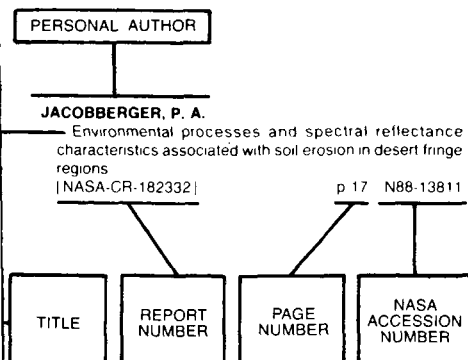
- The geometric workstation, a new approach for geometric corrections of remotely sensed data
p 66 N88-24017

Z

ZEOLITES

- Spectral discrimination of zeolites and dioctahedral clays in the near-infrared
p 28 A88-32926

Typical Personal Author Index Listing



Listings in this index are arranged alphabetically by personal author. The title of the document provides the user with a brief description of the subject matter. The report number helps to indicate the type of document listed (e.g., NASA report, translation, NASA contractor report). The page and accession numbers are located beneath and to the right of the title. Under any one author's name the accession numbers are arranged in sequence with the AIAA accession numbers appearing first.

A

ABBOTT, MARK R.
Time evolution of surface chlorophyll patterns from cross-spectrum analysis of satellite color images p 45 A88-42446

ABBY, DARWIN G.
Developments in use of GPS as range TSPI p 72 A88-37384

ABRAHAO, ADRIANA
Updating of the municipal official register of real estate through a geographical information system [INPE-4459-PRE/1238] p 21 N88-22453

ABRAMS, MICHAEL
Mapping the Oman Ophiolite using TM data p 26 A88-32906

ADA, LAWALLY
A remote sensing aided inventory of fuelwood volumes in the Sahel region of west Africa - A case study of five urban zones in the Republic of Niger p 7 A88-42005

ADLER, ROBERT F.
A satellite infrared technique to estimate tropical convective and stratiform rainfall p 69 A88-33416
A proposed tropical rainfall measuring mission (TRMM) satellite p 69 A88-33742

AKIYAMA, TSUYOSHI
Flood damage analysis using multitemporal Landsat Thematic Mapper data p 4 A88-39090

ALLAN, J. A.
How few data do we need - Some radical thoughts on renewable natural resources surveys p 9 A88-42060

ALLAN, R. J.
Ocean-atmosphere interactions in low latitude Australasia p 41 A88-37270

ALLEWIJN, R.
A methodology for integrating satellite imagery and field observations for hydrological regionalisation in Alpine catchments p 52 A88-42038

ALONSO, EDUARDO M. B.
Comparison of surface current determined from satellite-tracked buoy with shipboard wind data during the 4th Brazilian antarctic expedition, 10-14 March, 1986 p 49 N88-24024
Near surface current determined from INPE's satellite-tracked buoy, during 6-26 November, 1985 p 50 N88-24058

ALPERS, WERNER
Radar signatures of oil films floating on the sea surface and the Marangoni effect p 39 A88-33695

ALTSCHULLER, A. P.
Assessment of crop loss from air pollutants: Meteorology-atmospheric chemistry and long range transport [PB88-146857] p 12 N88-22448

AMAMOO-OTCHERE, E.
Visual interpretation of MSS-FCC manual cartographic integration of data p 61 A88-42001

AMBROSIA, VINCENT G.
Thermal analysis of wildfires and effects on global ecosystem cycling p 2 A88-35194
Particulate emissions from a mid-latitude prescribed chaparral fire p 3 A88-38805

AMBROSIUS, B. A. C.
From satellite altimetry to ocean topography, a survey of data processing techniques [ETN-88-91841] p 48 N88-21575

AMORETTILISBOA, NELSON
Analysis and interpretation of image lithostructure: An application of the multiconcept in the metamorphic belt of Sul de Santana da Boa Vista (RS) p 38 N88-24051

ANDERSON, MARK R.
Snow melt on sea ice surfaces as determined from passive microwave satellite data p 42 A88-38691

ANGULOFILHO, R.
Characteristics of drainage determinations in aerial photographs and relief determination on different scales planialtimetric charts for three soils in the state of Sao Paulo p 17 N88-24095

ANTONIODEOLIVO, ACIOLI
Low altitude remote sensing data in the implementation of a mathematical model for the planning of urban equipment networks p 23 N88-24074

ANTROP, M.
Structural information of the landscape as ground truth for the interpretation of satellite imagery p 59 A88-41962

ARCHINAL, BRENT ALLEN
Determination of Earth rotation by the combination of data from different space geodetic systems [NASA-CR-181388] p 25 N88-20713

ARDANUY, PHILIP E.
The 1987 Airborne Antarctic Ozone Experiment: The Nimbus-7 TOMS data atlas [NASA-RP-1201] p 47 N88-20714

ARGEMIRODECARVALHOPAIVA, JOAO
Visualization of digital terrain models p 67 N88-24081

ARGIALAS, DEMETRE P.
Quantitative description and classification of drainage patterns p 51 A88-35399

ARIUNAA, Z.
Quantitative analysis of a network of faults recognized on remote-sensing images of the Mushugai area in Mongolia p 32 A88-36163

ASRAR, G.
Radiative surface temperatures of the burned and unburned areas in a tallgrass prairie p 3 A88-37418

AVISSAR, R.
Mapping frost-sensitive areas with a three-dimensional local-scale numerical model. I - Physical and numerical aspects p 4 A88-41055

AZZALI, S.
Multitemporal analysis of Landsat Multispectral Scanner (MSS) and Thematic Mapper (TM) data to map crops in the Po valley (Italy) and in Mendoza (Argentina) p 6 A88-41994

B

BABINSKI, NELSON ADAO
Confirmation of quantitative morphostructural analysis by seismic, aeromagnetic and geochemical data in the Amazon Basin, Brazil p 29 A88-32937

BAGHERI, SIMA
Regional geologic mapping of digitally enhanced Landsat imagery in the southcentral Alborz mountains of northern Iran p 34 A88-42017

BAHAR, E.
Comparison of unified full-wave solutions for normal incidence microwave backscatter from sea with physical optics and hybrid solutions p 42 A88-39079

BAKER, D. JAMES
Mission to planet earth p 77 A88-45110

BANERJEE, RANJIT KUMAR
Landuse and landform studies of the Mahanadi River Delta with the help of satellite MSS band p 56 N88-24033

BANNINGER, C.
Effects of heavy metal induced canopy structural changes on forest canopy reflectance p 1 A88-32930
Discrimination of geobotanical anomalies in rugged alpine terrain using Landsat Thematic Mapper data p 32 A88-32957
Relationship between soil and leaf metal content and Landsat MSS and TM acquired canopy reflectance data p 6 A88-41986
Optimal Thematic Mapper bands and transformations for discerning metal stress in coniferous tree canopies p 7 A88-42002

BANON, GERALD JEAN FRANCIS
Restoration techniques for redisplay of LANDSAT-5 satellite imagery [INPE-4189-PRE/1076] p 64 N88-20712

BARRICK, D. E.
Comparison of unified full-wave solutions for normal incidence microwave backscatter from sea with physical optics and hybrid solutions p 42 A88-39079

BARRIOT, JEAN PIERRE
Evidence from geoid data of a hotspot origin for the southern Mascarene Plateau and Mascarene Islands (Indian Ocean) p 24 A88-38902

BARRY, ROGER G.
Passive microwave data for snow and ice research - Planned products from the DMSP SSM/I system p 40 A88-35199

BARSOTTIDELIMA, UBIRAJARA MAURICIO
Applications of multitemporal composites obtained from LANDSAT data in the study of urban growth [INPE-4480-PRE/1246] p 22 N88-23692

BARTALEV, S. A.
Correction of spatial and temporal distortions in the photographic image input into an interactive processing system p 62 A88-43672

BARYKIN, A. S.
Contrast enhancement of aerospace scanner imagery of crop fields p 11 A88-43671

BATEMAN, D. A.
Plans for ERS-1 data acquisition, processing and distribution p 41 A88-37149

BAUMGARDNER, MARION F.
Assessment of TM thermal infrared band contribution in land cover/land use multispectral classification p 61 A88-42016

BAYER, ROGER
Evidence from geoid data of a hotspot origin for the southern Mascarene Plateau and Mascarene Islands (Indian Ocean) p 24 A88-38902

BAYLIS, P. E.
Data reception, archiving and distribution p 58 A88-37131

BECK, R.
Thematic Mapping by satellite - A new tool for planning and management p 60 A88-41973

BECKER, ALEX
Airborne resistivity mapping p 36 A88-45771

BECKETT, P. J.
Shift in spectral response of nickel-loaded and control shoots of white birch p 1 A88-32928
Surrogate spectral reflectances of vegetation applied to geobotanical remote sensing p 1 A88-32935
Spectral reflectance from lichens treated with copper p 30 A88-32945

BEDFORD, KEITH W.
Determinations of suspended sediment concentrations from multiple day Landsat and AVHRR data p 54 A88-44120

BEKKERING, J. A.
The JRC program for marine coastal monitoring p 44 A88-42039

- BELLAVIA, G.**
Spatial feature extraction from radar imagery p 60 A88-41974
- BELTRAME, LAWSON**
Satellite remote sensing of turbidity and sediment concentration in Lagoa dos Patos p 56 N88-24032
- BELWARD, ALAN**
Mapping soil and rock variation from satellite images in the Sahel p 14 N88-24023
Satellite remote sensing of turbidity and sediment concentration in Lagoa dos Patos p 56 N88-24032
- BELWARD, ALAN S.**
The use of multitemporal Landsat data for improving crop mapping accuracy p 7 A88-42003
- BENARD, F.**
Synthetic geological map obtained by remote sensing - An application to Palawan Island p 33 A88-41975
- BERGER, Z.**
Landsat structural analysis of the Rhine Valley and the Jura Mountain area, Western Europe p 26 A88-32903
- BERHE, SEIFE M.**
Application of remote sensing to tectonic and metallogenic studies in NE Africa p 28 A88-32924
- BERKHOUT, J. A. A.**
The potential of numerical agronomic simulation models in remote sensing p 9 A88-42061
- BERLIN, GRAYDON L.**
Restoration techniques for SIR-B digital radar images p 57 A88-32933
Quantitative procedure for producing color-calibrated Thematic Mapper natural-color images p 57 A88-32943
- BERNSTEIN, ROBERT L.**
Empirical orthogonal function analysis of advanced very high resolution radiometer surface temperature patterns in Santa Barbara Channel p 45 A88-42449
- BESCOND, PIERRE**
Spot 1 - International commercialization of remote sensing [AAS PAPER 86-299] p 69 A88-35155
- BIANCO, CARLOS**
Utilization of LANDSAT-TM imagery in the hydroenergetic inventory of the Paraiba de Sul River Basin p 56 N88-24077
- BILHAM, ROGER**
Space geodesy and earthquake prediction [AAS PAPER 86-307] p 24 A88-35156
- BIRNIE, R. W.**
Remote sensing of geobotanical associations in clastic sedimentary terrane p 31 A88-32951
- BLODGET, H. W.**
Multispectral geologic remote sensing of a suspected impact crater near Al Madafi, Saudi Arabia p 33 A88-41955
- BLOEMER, H. H. L.**
Global distributive computer processing systems for environmental monitoring, analysis and trend modeling in early warning and natural disaster mitigation p 19 A88-42020
- BLOEMER, HUBERTUS L.**
Operational satellite data assessment for drought/disaster early warning in Africa - Comments on GIS requirements p 19 A88-42018
- BLOM, RONALD G.**
Directed band ratioing for the retention of perceptually-independent topographic expression in chromaticity-enhanced imagery p 62 A88-43224
- BLOOM, ARTHUR L.**
A demonstration of stereophotogrammetry with combined SIR-B and Landsat TM images p 63 A88-44650
- BLUEMEL, K.**
Vegetation indices and other vegetation parameters - Examples, interpretation and problems p 3 A88-38373
- BOCCONCELLI, ALESSANDRO**
Real-time environmental Arctic monitoring (R-TEAM) [AD-A189948] p 49 N88-22508
- BODECHTEL, J.**
Integration of remote sensing and other geo-data for ore exploration - A SW-Iberian case study p 31 A88-32952
- BOELY, T.**
Methodology for an operational monitoring of remotely-sensed sea surface temperatures in Indonesia p 43 A88-39084
- BOGART, LOWELL E.**
Importance of fault mapping to mineral/geothermal exploration: Relationship to fluid migration and ore formation - Northwest Washington p 28 A88-32925
- BOLLETTINARI, G.**
Comparison between interpretation of images of different nature p 34 A88-42019
- BONDI, HERMANN**
The application of satellites in connection with the environment [ETN-88-92474] p 24 N88-25020
- BONN, FERDINAND**
Urbanization and Landsat MSS albedo change in the Windsor-Quebec corridor since 1972 p 18 A88-39094
- BONNEVILLE, ALAIN**
Evidence from geoid data of a hotspot origin for the southern Mascarene Plateau and Mascarene Islands (Indian Ocean) p 24 A88-38902
- BOREL, CHRISTOPH C.**
Radar backscatter characteristics of trees at 215 GHz p 11 A88-44307
- BORENGASSER, MARCUS X.**
Structural geology and regional tectonics of the Mineral County area, Nevada, using Shuttle Imaging Radar-B and digital aeromagnetic data p 35 A88-44646
- BOUWMANS, J. M. M.**
Application of multispectral scanning remote sensing in agricultural water management problems p 8 A88-42011
- BOWERS, D.**
Non-tracking antenna systems for the acquisition of NOAA HRPT Data p 72 A88-37279
- BOYLE, TIMOTHY**
Differentiation of ecological zones in the Okavango Delta, Botswana by classification and contextual analyses of Landsat MSS data p 59 A88-39099
- BRANDT, CYNTHIA**
Associations among lineaments, subsurface fractures, hydrocarbon microseepage, and production in the Uinta Basin, Utah p 27 A88-32908
- BRANDWYK, J.**
Non-tracking antenna systems for the acquisition of NOAA HRPT Data p 72 A88-37279
- BRASS, JAMES A.**
Thermal analysis of wildfires and effects on global ecosystem cycling p 2 A88-35194
Particulate emissions from a mid-latitude prescribed chaparral fire p 3 A88-38805
- BRAUN, HANS MARTIN**
Spaceborne radar X-SAR for civil applications p 72 A88-37286
- BREED, C. S.**
Shuttle imaging radar response from sand dunes and subsurface rocks of Alashan Plateau in north-central China p 33 A88-41978
- BREIDO, M. D.**
Correction of spatial and temporal distortions in the photographic image input into an interactive processing system p 62 A88-43672
- BRENNECKE, JUERGEN**
Tests for the automatic pattern recognition of building surfaces by the TK 50 p 68 N88-25030
- BRICKEY, DAVID W.**
The use of Thematic Mapper imagery for mineral exploration in the sedimentary terrain of the Spring Mountains, Nevada p 30 A88-32940
- BRIVIO, P. A.**
Digital analysis of stereo pairs for the detection of anomalous signatures in geothermal fields p 61 A88-42037
- BRIZUELA, A.**
Spectral measurements for correcting LANDSAT data for atmospheric effects p 66 N88-24020
- BROWN, OTIS B.**
Processing, compression and transmission of satellite IR data for near-real-time use at sea p 41 A88-36843
- BROWNING, K. A.**
Use of radar and satellite imagery for the measurement and short-term prediction of rainfall in the United Kingdom p 51 A88-37136
- BRUCE, BILL**
Remote sensing and data integration: Practical solutions for resource managers p 22 N88-24034
- BRUENING, CLAUS**
Investigation of the imaging of ocean surface waves using a synthetic aperture radar [SER-A-WISS-ABHANDL-84] p 49 N88-23357
- BRUMFIELD, J. O.**
Global distributive computer processing systems for environmental monitoring, analysis and trend modeling in early warning and natural disaster mitigation p 19 A88-42020
- BRUNNER, JAKE**
Thematic Mapper data applied to mapping hydrothermal alteration in south west New Mexico p 28 A88-32923
- BUGAEVA, G. V.**
New aspects of the interpretation of space radar images p 58 A88-36171
- BULLARD, RICHARD K.**
Recording resources in rural areas p 20 A88-42062
- BURTELL, S. G.**
Remote sensing and surface geochemical study of Railroad Valley, Nye County, Nevada - Detailed grid study p 31 A88-32953
- BUSINGER, J. A.**
A system for remote measurements of the wind stress over the ocean p 40 A88-36841
- BUTERA, KRISTINE**
Approach and status for a unified national plan for satellite remote sensing research and development p 77 A88-32919
- BUTTLEMAN, KIM**
A PC-based interactive graphics system to perform satellite-derived oceanographic thermal analysis p 68 A88-32850
- BYCHKOVA, I. A.**
Parameters of eddy structures and mushroom currents in the Baltic Sea derived from satellite imagery p 46 A88-43665

C

- CAI, WU SHEN**
Remote sensing for wildlife management - Giant panda habitat mapping from Landsat MSS images p 2 A88-35195
- CAMARGOLAMPARELLI, RUBENS AUGUSTO**
Use of energy emission for detecting the necessity of irrigation in wheat in field conditions [INPE-4461-TDL/318] p 13 N88-23315
- CAMPBELL, W. B.**
A PC-based interactive graphics system to perform satellite-derived oceanographic thermal analysis p 68 A88-32850
- CAMPBELL, W. J.**
Marginal Ice Zone Experiment (MIZEX) 1984 VARAN-S data set [ETN-88-92032] p 48 N88-21625
- CAMPBELL, WILLIAM J.**
Satellite and aircraft passive microwave observations during the Marginal Ice Zone Experiment in 1984 p 45 A88-42447
- CANOBA, CARLOS**
A remote sensing methodological approach for applied geomorphology mapping in plain areas p 35 A88-42034
- CAPPELLETTI, CARLOS A.**
Estimation of an area cultivated with wheat from LANDSAT data through a two-phase sampling method p 14 N88-24041
- CARDOSODELIMA, MARIO IVAN**
Lithostructural interpretation of Chapda do Cachimbo (Pa-Am-Mt), based on radar and LANDSAT imagery p 39 N88-24100
- CARGILL, GEORGE**
Pyrophyllite and kaolinite alteration - Mineral discrimination by sample reflectance measurement p 31 A88-32954
- CARLSON, TOBY N.**
An update on remote measurement of soil moisture over vegetation using infrared temperature measurements: A FIFE perspective [NASA-CR-182926] p 18 N88-24109
- CARPER, W. JOSEPH**
Enhancement of SPOT image resolution using an intensity-hue-saturation transformation p 59 A88-41958
- CARR, JAMES R.**
Application of spatial statistics to analyzing multiple remote sensing data sets p 64 A88-45639
- CARTAXOMODESTODESOUZA, RICARDO**
Analysis for architecture for image processing [INPE-4294-PRE/1165] p 75 N88-20715
- CARTWRIGHT, DAVID E.**
Tidal estimation in the Pacific with application to SEASAT altimetry [NASA-TM-100694] p 47 N88-20780
- CASADO, C. MARINEZ**
Spectral measurements for correcting LANDSAT data for atmospheric effects p 66 N88-24020
- CASE, DAVID W.**
Obtaining spectral reflectance factor measurements of stressed forest vegetation p 5 A88-41952
- CASELLES, V.**
Spectral signature of rice fields using Landsat-5 TM in the Mediterranean coast of Spain p 6 A88-41991
- CASEY, D. J.**
Shuttle radar mapping with diverse incidence angles in the rainforest of Borneo p 12 A88-44644
- CASTLE, JOHN R. VANDE**
Toward an integrated system for satellite remote sensing of water quality in the Great Lakes p 52 A88-41957
- CAUBET, M. R.**
The Systeme d'Analyse Geographique (SAGE) geographic analysis system p 66 N88-24019

- CAUBET, R.**
The SAGE geographic analysis system
p 22 N88-24063
- CAZENAVE, ANNY**
Geoid anomalies across Pacific fracture zones
p 24 A88-38023
- CELSODECARVALHO, VITOR**
Structure and dynamics of vegetation in the middle semi-arid tropics. Quixaba's Caatinga (PE): Terrain analysis of MSS/LANDSAT data
p 15 N88-24049
- CERUTTI-MAORI, G.**
Imaging instrument of the Vegetation Payload (SPOT 4)
p 70 A88-35968
In flight calibration for the imaging instrument of VEGETATION payload (SPOT 4)
p 10 A88-42545
- CHANDRA, J. J.**
Assessment of digital enhancement techniques using Landsat TM data in mapping geologic lineaments, with application to the Mactaquac headpond area, southern New Brunswick
p 31 A88-32949
- CHANG, A. T. C.**
Remote sensing of snow
p 50 A88-35198
- CHARBONNEAU, LISE**
Interannual Landsat-MSS reflectance variation in an urbanized temperate zone
p 58 A88-37417
Urbanization and Landsat MSS albedo change in the Windsor-Quebec corridor since 1972
p 18 A88-39094
- CHARNOCK, H.**
The ocean and the atmosphere
p 41 A88-37143
- CHATURVEDI, ARVIND**
An integrated study of the Alto Paranaiba Kimberlite Province, Minas Gerais, Brazil: A possible tool for diamond exploration
p 37 N88-24031
- CHAVEZ, PAT S., JR.**
Restoration techniques for SIR-B digital radar images
p 57 A88-32933
Quantitative procedure for producing color-calibrated Thematic Mapper natural-color images
p 57 A88-32943
- CHEN, SHERRY C.**
Evaluation of an estimation system for an irrigated area in a tropical region through TM-LANDSAT imagery
p 16 N88-24075
- CHEN, SHERRY CHOU**
Spectral behavior of crops through analysis of LANDSAT-TM data
p 15 N88-24047
- CHEN, YEONG-KUAN**
A comparison between classification differencing and image differencing for land cover type change detection
p 59 A88-41944
Digital processing of airborne MSS data for forest cover types classification
p 5 A88-41963
- CHERNYI, I. V.**
Radiometric investigation of the sea-wave breaking process
p 46 A88-43664
- CHIAO, KUO-MU**
A comparison between classification differencing and image differencing for land cover type change detection
p 59 A88-41944
Digital processing of airborne MSS data for forest cover types classification
p 5 A88-41963
- CHIDLEY, T. R. E.**
Simple classifiers of satellite data for hydrologic modelling
p 52 A88-42040
- CHISHOLM, N. W. T.**
Artificial GCPs in aircraft and satellite scanner imagery
p 74 A88-43227
- CHOUDHURY, B. J.**
A four-layer model for the heat budget of homogeneous land surfaces
p 4 A88-41028
- CHOW, CHAO-FU**
A comparison between classification differencing and image differencing for land cover type change detection
p 59 A88-41944
- CHUKHLANTSEV, A. A.**
Taking the effect of vegetation into account in the microwave-radiometer remote sensing of the earth surface on the results of remote sounding of the earth surface by microwave radiometry
p 10 A88-43670
- CICIVIZZO, VITALINA PAGLIUCA**
Utilization of LANDSAT-TM, for aiding in the localization of archeological sites in the state of Sao Paulo
p 38 N88-24069
- CIESLA, W. M.**
Inventory of decline and mortality in spruce-fir forests of the eastern U.S. with CIR photos
p 7 A88-42004
- CIMINO, J.**
Dependence of image grey values on topography in SIR-B images
p 63 A88-44649
- CIMINO, JO BEA**
The Shuttle Imaging Radar B (SIR-B) experiment report
[NASA-CR-182923]
p 75 N88-23932
- CLARK, BILL P.**
An approach for emulating the color balance of Landsat multispectral scanner images with AVHRR data
p 73 A88-41956
- CLEM, KEITH**
Associations among lineaments, subsurface fractures, hydrocarbon microseepage, and production in the Uinta Basin, Utah
p 27 A88-32908
- CLEMENTEICK, NILO**
Analysis and interpretation of image lithostructure: An application of the multiconcept in the metamorphic belt of Sul de Santana da Boa Vista (RS)
p 38 N88-24051
- CLEVERS, J. G. P. W.**
The derivation of a simplified reflectance model for the estimation of LAI
p 6 A88-41987
The application of a vegetation index in correcting the infrared reflectance for soil background
p 6 A88-41988
- COATES, D.**
Thematic Mapper applied to alteration zone mapping for gold exploration in south-east Spain
p 29 A88-32938
- COFER, WESLEY R., III**
Particulate emissions from a mid-latitude prescribed chaparral fire
p 3 A88-38805
- COLEMAN, T. L.**
Development of remote sensing techniques capable of delineating soils as an aid to soil survey
[NASA-CR-182610]
p 13 N88-22452
- COLIJN, A. W.**
A comprehensive LRIS of the Kananaskis Valley using Landsat data
p 21 A88-42064
- COLLADO, D. A.**
Multitemporal analysis of Landsat Multispectral Scanner (MSS) and Thematic Mapper (TM) data to map crops in the Po valley (Italy) and in Mendoza (Argentina)
p 6 A88-41994
- COLLIN, R. L.**
Artificial GCPs in aircraft and satellite scanner imagery
p 74 A88-43227
- COLLINS, W. C.**
Simple classifiers of satellite data for hydrologic modelling
p 52 A88-42040
- COLLINS, W. G.**
Classification of land features, using Landsat MSS data in a mountainous terrain
p 19 A88-41972
The use of SPOT simulation data in forestry mapping
p 7 A88-42006
An analysis of remote sensing for monitoring urban derelict land
p 20 A88-42056
- COLUZZI, MICHAEL EUGENE**
Millimeter-wave bistatic scattering from ground and vegetation targets
p 11 A88-44308
- COMISO, JOSEFINO C.**
Polynyas in the Southern Ocean
p 43 A88-39284
- CONGALTON, RUSSELL G.**
A methodology for mapping forest latent heat flux densities using remote sensing
p 3 A88-37415
Using spatial autocorrelation analysis to explore the errors in maps generated from remotely sensed data
p 58 A88-39097
A comparison of sampling schemes used in generating error matrices for assessing the accuracy of maps generated from remotely sensed data
p 59 A88-39098
- COOPER, CHARLES M.**
Comparison of measured suspended sediment concentrations with suspended sediment concentrations estimated from Landsat MSS data
p 51 A88-39080
- COOPER, D. I.**
Radiative surface temperatures of the burned and unburned areas in a tallgrass prairie
p 3 A88-37418
- CORNILLON, PETER**
Processing, compression and transmission of satellite IR data for near-real-time use at sea
p 41 A88-36843
- CORONA, F. V.**
Landsat structural analysis of the Rhine Valley and the Jura Mountain area, Western Europe
p 26 A88-32903
- COURTILLOT, VINCENT**
Geoid roughness and long-wavelength segmentation of the South Atlantic spreading ridge
p 24 A88-40688
- COURTIN, G. M.**
Shift in spectral response of nickel-loaded and control shoots of white birch
p 1 A88-32928
Surrogate spectral reflectances of vegetation applied to geobotanical remote sensing
p 1 A88-32935
Spectral reflectance from lichens treated with copper
p 30 A88-32945
- CRACKNELL, A. P.**
Surface currents off the west coast of Ireland studied from satellite images
p 43 A88-39085
- CRAWFORD, MICHAEL F.**
Preliminary evaluation of remote sensing data for detection of vegetation stress related to hydrocarbon microseepage - Mist Gas Field, Oregon
p 1 A88-32911
- CRIPPEN, ROBERT E.**
Directed band ratioing for the retention of perceptually-independent topographic expression in chromaticity-enhanced imagery
p 62 A88-43224
The dangers of underestimating the importance of data adjustments in band ratioing
p 62 A88-43225
- CURE, WILLIAM W.**
Canopy reflectance of soybean as affected by chronic doses of ozone in open-top field chambers
p 2 A88-35398
- CURRAN, PAUL J.**
The semivariogram in remote sensing - An introduction
p 58 A88-37421
- CUSHNIE, JANIS**
The acquisition of SPOT-1 HRV imagery over southern Britain and northern France, May 1986-May 1987
p 68 A88-29286

D

- DACOSTAPEREIRA, MARCOS**
Detection, monitoring and analysis of some environmental effects of fires in the Amazon region through utilization of NOAA and LANDSAT satellite imagery and aircraft data
[INPE-4503-TDL/326]
p 13 N88-23322
- DAELS, L.**
Assessment of desertification in the lower Nile Valley (Egypt) by an interpretation of Landsat MSS colour composites and aerial photographs
p 61 A88-42025
- DALLEMAND, JEAN FRANCOIS**
Spectral behavior of crops through analysis of LANDSAT-TM data
p 15 N88-24047
- DAMEN, M. C. J.**
Remote sensing for resources development and environmental management; Proceedings of the Seventh International Symposium, Enschede, Netherlands, Aug. 25-29, 1986. Volumes 1, 2, & 3
p 18 A88-41961
- DANDONNEAU, YVES**
Satellite detected cyanobacteria bloom in the southwestern tropical Pacific - Implication for oceanic nitrogen fixation
p 42 A88-39081
- DANIEL DANIELSKA, BARBARA**
Geological analysis of the satellite lineaments of the Vistula Delta Plain, Zulawy Wislane, Poland
p 34 A88-42021
Remote sensing methods in geological research of the Lublin coal basin, SE Poland
p 34 A88-42028
- DANIELS, J. L.**
Rock discrimination and alteration mapping for mineral exploration using the Carr Boyd/Geoscan airborne multispectral scanner
p 27 A88-32914
- DANTASBITENCOURTPEREIRA, MARISA**
Study of reservoir water quality utilizing remote sensing techniques: Methodological concepts
p 56 N88-24076
- DASILVA, CARLOS L., JR.**
Comparison of surface current determined from satellite-tracked buoy with shipboard wind data during the 4th Brazilian antarctic expedition, 10-14 March, 1986
p 49 N88-24024
- DAUS, STEVEN J.**
A remote sensing aided inventory of fuelwood volumes in the Sahel region of west Africa - A case study of five urban zones in the Republic of Niger
p 7 A88-42005
- DE HOOP, D.**
Selection of bands for a newly developed multispectral airborne reference-aided calibrated scanner (MARCS)
p 74 A88-41995
- DE JONG, A. N.**
Selection of bands for a newly developed multispectral airborne reference-aided calibrated scanner (MARCS)
p 74 A88-41995
- DE LOOR, G. P.**
SLAR as a research tool
p 73 A88-41976
- DE MIRANDA, FERNANDO PELLON**
Confirmation of quantitative morphostructural analysis by seismic, aeromagnetic and geochemical data in the Amazon Basin, Brazil
p 29 A88-32937
- DE WULF, ROBERT R.**
Remote sensing for wildlife management - Giant panda habitat mapping from Landsat MSS images
p 2 A88-35195
- DEAN, KENNESON G.**
Influence of the Yukon River on the Bering Sea
[NASA-CR-182802]
p 50 N88-24126
- DEFEO, N. J.**
Remote sensing of geobotanical associations in clastic sedimentary terrane
p 31 A88-32951
- DEFRANCA, G. V.**
Characteristics of drainage determinations in aerial photographs and relief determination on different scales planialtimetric charts for three soils in the state of Sao Paulo
p 17 N88-24095

DEFREITAS, M. I. C.

Current stage of remote sensing system for cartographic application p 76 N88-24090

DEHANDSCHUTTER, J.

Application of remote sensing in the field of experimental tectonics p 34 A88-42023

DELFINODAVILAMASCARENHAS, NELSON

Method for restoration and resampling of TM sensor imagery [INPE-4491-PRE/1255] p 65 N88-22454

DELIMA, ANGELA MARIA

Evaluation of TM false color composites for crop discrimination p 17 N88-24096

DELLWIG, LOUIS F.

A comparison of airborne GEMS/SAR with satellite-borne Seasat/SAR radar imagery - The value of archived multiple data sets p 64 A88-45640

DELOUDESNEVESDEOLIVEIRAKURKDJIAN, MARIA

Low altitude remote sensing data in the implementation of a mathematical model for the planning of urban equipment networks p 23 N88-24074

DELOURDESBUENOTRINIDADE, MARIA

Anomalies in the vegetation in the Alto Xingu - MT p 14 N88-24043

DELOURDES N. DEO. KURKDJIAN, MARIA

Updating land-use of the Sao Jose dos Campos municipality through remote sensing data [INPE-4479-RPE/562] p 22 N88-23693

DELOURDES N. O. KURKDJIAN, MARIA

Orbital remote sensing: An instrument for monitoring urban growth [INPE-4456-PRE/1287] p 22 N88-22833

DELOURDESNEVESDEO. KURKDJIAN, MARIA

Applications of multitemporal compositions obtained from LANDSAT data in the study of urban growth [INPE-4480-PRE/1246] p 22 N88-23692

DELSOL, F.

An evaluation of the performance of the ECMWF operational system in analyzing and forecasting easterly wave disturbances over Africa and the tropical Atlantic p 43 A88-39746

DEMETRIO, V. A.

Characteristics of drainage determinations in aerial photographs and relief determination on different scales planimetric charts for three soils in the state of Sao Paulo p 17 N88-24095

DEMOURAABDON, MYRIAN

Evaluation of the mangrove area at the Piaui River (SE) through remote sensing p 16 N88-24086

DENMAN, KENNETH L.

Time evolution of surface chlorophyll patterns from cross-spectrum analysis of satellite color images p 45 A88-42446

DENNER, WARREN W.

Examples of ice pack rigidity and mobility characteristics determined from ice motion [AD-A191163] p 50 N88-24129

DEOLIVEIRASCHUCK, MARISA T. G.

Analysis and interpretation of image lithostructure: An application of the multiconcept in the metamorphic belt of Sul de Santana da Boa Vista (RS) p 38 N88-24051

DERENYI, E.

Assessment of digital enhancement techniques using Landsat TM data in mapping geologic lineaments, with application to the Mactaquac headpond area, southern New Brunswick p 31 A88-32949

DETMAR, F.

Adjustment in photogrammetry: Methods, programs and applications [B8735130] p 76 N88-24105

DEUSER, W. G.

Temporal variations of particle fluxes in the deep subtropical and tropical North Atlantic - Eulerian versus Lagrangian effects p 45 A88-42448

DIAW, A. T.

Geographic study of the north coast of Senegal using MOMS-1 satellite data p 73 A88-41093

DING, Y.

The absolute radiometric calibration of the advanced very high resolution radiometer [NASA-CR-182755] p 75 N88-21584

DIRKS, R. W. J.

Classification of bottom composition and bathymetry of shallow waters by passive remote sensing p 53 A88-42051

DISPERATI, ATTILIO ANTONIO

The 35 mm vertical aerial photographs for mapping stands of bracing in different age classes p 16 N88-24087

Stereoscopic photographs, ground and aerial, of trees used in the arborization of Curitiba (PR) p 17 N88-24091

DIXON, TIMOTHY H.

Effect of wet tropospheric path delays on estimation of geodetic baselines in the Gulf of California using the Global Positioning System p 25 A88-41835

DOCOUTO, HILTON T. Z.

Utilization of TM/LANDSAT images in the implanted forests mapping in the Mogi-Guacu Region (SP-Brazil) p 14 N88-24042

DOIRON, SCOTT D.

The 1987 Airborne Antarctic Ozone Experiment: The Nimbus-7 TOMS data atlas [NASA-RP-1201] p 47 N88-20714

DOLGOPOLOV, B. IA.

Saline salt and water surface mapping on the basis of data from the Gyunesh-84 remote-sensing experiment p 51 A88-36166

DOMIK, G.

SIR-B stereo-radargrammetry of Australia p 63 A88-44648

Dependence of image grey values on topography in SIR-B images p 63 A88-44649

DONG, CHAOHUA

Retrieval of atmospheric temperature structure from the NOAA-9 satellite p 72 A88-37336

DONGUY, J. R.

Basic networks of TOGA: Determination of thermal profiles by XBT and of sea level by tide gage p 48 N88-21568

DOSANJOSFERREIRAPINTO, SERGIO

Project CODEAMA/FUNCATE (test-area of Barreirinha-AM): Field report [INPE-4500-RPE/563] p 55 N88-22455

DOW, D. D.

A gridding approach to detect patterns of change in coastal wetlands from digital data p 52 A88-41949

DOWNEY, I. D.

Circulation patterns in AVHRR imagery p 46 A88-43217

DOWNEY, JOE S.

Lineaments: Significance, criteria for determination, and varied effects on ground-water systems - A case history in the use of remote sensing p 55 A88-45636

DOWNING, J. P.

Ocean general circulation models: Report on proceedings of a meeting of ocean and climate modelers [DE88-005530] p 49 N88-22504

DRAYTON, R. S.

Simple classifiers of satellite data for hydrologic modeling p 52 A88-42040

DREWRY, DAVID J.

The role of remote sensing in the study of polar ice sheets p 48 N88-21570

DRISCOLL, MAVIS

The effect of a shallow low-viscosity zone on the mantle flow, the geoid anomalies and the geoid and depth-age relationships at fracture zones p 24 A88-38024

DUGGIN, M. J.

Factors affecting feature differentiation - The impact and source of variance in the upwelling radiance field p 58 A88-37128

The physical principles controlling the remote sensing process p 71 A88-37129

Sensors to record atmospheric and terrestrial information - Principles of collection and analysis p 71 A88-37130

DULL, C. W.

Inventory of decline and mortality in spruce-fir forests of the eastern U.S. with CIR photos p 7 A88-42004

DUPAS, FRANCISCO A.

Criteria for planimetric and altimetric correction of maps restituted from aerial photographs in 1:100,000 scale p 38 N88-24097

DUPOUY, CECILE

Satellite detected cyanobacteria bloom in the southwestern tropical Pacific - Implication for oceanic nitrogen fixation p 42 A88-39081

DURAND, J. M.

Influence of topography on forest reflectance using Landsat Thematic Mapper and digital terrain data p 2 A88-35397

DURANPINTO, JOAQUIM HENRIQUE

Comparative utilization of analog and digital processes in the treatment of MSS-LANDSAT data for studying the national parks of Brazil [INPE-4011-TDL/240] p 21 N88-22456

DURY, S. J.

The use of SPOT simulation data in forestry mapping p 7 A88-42006

DUSSEAULT, M. M.

Application of MEIS-II multispectral airborne data and CIR photography for the mapping of surficial geology and geomorphology in the Chatham area, Southwest Ontario, Canada p 34 A88-42027

DUTRA, LUCIANO VIEIRA

Study of methods of post-processing applied to a problem of standard classification p 67 N88-24067

Application of its transformation in color enhancement of LANDSAT imagery p 68 N88-24082

DYER, ROBERT C.

Tornado tracks in Southwestern Brazil, Eastern Paraguay, and Northwestern Argentina p 23 N88-24071

DZHAFAROV, E. M.

Saline salt and water surface mapping on the basis of data from the Gyunesh-84 remote-sensing experiment p 51 A88-36166

E

EAST, JACK R.

Millimeter-wave bistatic scattering from ground and vegetation targets p 11 A88-44308

ECCLES, DAVE

The Along-Track Scanning Radiometer with Microwave Sounder p 41 A88-37148

ECHIZENYA, YOSHIMATSU

SIR-B experiments in Japan. I - Sensor calibration experiment p 73 A88-40351

SIR-B experiments in Japan. II - Rice crop experiment p 4 A88-40352

EDEN, PAUL

Processing, compression and transmission of satellite IR data for near-real-time use at sea p 41 A88-36843

EHLERS, MANFRED

Cartographic feature extraction with integrated SIR-B and Landsat TM images p 63 A88-44641

EHMANN, WILLIAM J.

Spectral discrimination of zeolites and dioctahedral clays in the near-infrared p 28 A88-32926

EIDENSHINK, J. C.

Differences in visible and near-IR responses, and derived vegetation indices, for the NOAA-9 and NOAA-10 AVHRRs - A case study p 70 A88-35396

ELGY, J.

Spatial feature extraction from radar imagery p 60 A88-41974

ELIASON, JAY R.

Geologic spatial analysis - A new multiple data source exploration tool p 30 A88-32947

ELLIS, JAMES M.

Application of synthetic aperture radar (SAR) to southern Papua New Guinea fold belt exploration p 26 A88-32902

ELVIDGE, CHRISTOPHER D.

A near infrared vegetation index formed with airborne multispectral scanner data p 1 A88-32910

Use of calibration targets in the measurement of 2.22-micron mineral absorption features in Thematic Mapper data p 29 A88-32927

ENGBRETSON, RONALD E.

Examples of ice pack rigidity and mobility characteristics determined from ice motion [AD-A191163] p 50 N88-24129

ENGMAN, E. T.

Rangeland runoff curve numbers as determined from Landsat MSS data p 51 A88-39089

EPEMA, G. F.

Multitemporal analysis of Thematic Mapper data for soil survey in Southern Tunisia p 6 A88-41989

EPP, H.

Spruce budworm infestation detection using an airborne pushbroom scanner and Thematic Mapper data p 8 A88-42007

ERTHAL, GUARACI JOSE

Visualization of digital terrain models p 67 N88-24081

ESPELAND, RICHARD H.

Millimeter-wave propagation in vegetation: Experiments and theory p 12 A88-44319

ESPINDOLA, CARMEN REGINA S.

Evaluation of the mangrove area at the Piaui River (SE) through remote sensing p 16 N88-24086

EVANS, DAVID

Processing, compression and transmission of satellite IR data for near-real-time use at sea p 41 A88-36843

EVANS, ROBERT

Processing, compression and transmission of satellite IR data for near-real-time use at sea p 41 A88-36843

F

FARAGO, T.

A comparative analysis of methods for compressing spectrophotometric data in the estimation of hydrological parameters p 54 A88-43673

FAUST, NICKOLAS L.

Integration of Landsat, DTED, and DFAD p 63 A88-44540

FEDER, ALLEN M.

After exploration, what? - Case histories of seven diverse production, development and distribution applications of remote sensing p 28 A88-32918

- FEDOROV, K. N.**
The determination of the parameters of the diurnal thermocline using satellite and ship-based measurements p 44 A88-40834
Mushroom-shaped currents (eddy dipoles) under rotation and stratification conditions p 47 N88-20678
- FELDMAN, S. C.**
Correlation between high resolution remote sensing imagery and hydrothermal alteration, Tybo mining district, Nevada p 27 A88-32915
- FELGUEIRAS, CARLOS ALBERT**
Visualization of digital terrain models p 67 N88-24081
- FERANEC, J.**
The use of multispectral space photographs to draw up a map of land use in western Slovakia p 57 A88-33774
- FERNANDEZ, SEVERINO**
Shape detection in remote sensing through graph isomorphism p 67 N88-24028
- FERRARI, MASSIMO**
Potential of Landsat Thematic Mapper image for crystalline rock type discrimination - Gregory Rift, Kenya p 32 A88-35192
- FIEDLER, RUDOLPH**
Image processing for earth remote sensing p 58 A88-37287
- FIEDLER, JUDITH**
A second generation lunar agricultural system p 11 A88-43864
- FIELDING, E. J.**
Discrimination and supervised classification of volcanic flows of the Puna-Altiplano, Central Andes Mountains using Landsat TM data p 31 A88-32948
- FIELDING, ERIC J.**
A demonstration of stereophotogrammetry with combined SIR-B and Landsat TM images p 63 A88-44650
- FILHO, AUGUSTO PAIVA**
Utilization of LANDSAT-TM imagery in the hydroenergetic inventory of the Paraiba de Sul River Basin p 56 N88-24077
- FILHO, MARIO VALERIO**
Evaluation of an estimation system for an irrigated area in a tropical region through TM-LANDSAT imagery p 16 N88-24075
- FILHO, PEDRO HERNANDEZ**
A proposal for a project entitled assessment of forest resources in Uruguay submitted to the United Nations Industrial Development Organization (UNIDO) p 13 N88-24016
Anomalies in the vegetation in the Alto Xingu - MT p 14 N88-24043
- FILY, MICHEL**
Diagnostic study of the Fram Strait marginal ice zone during summer from 1983 and 1984 Marginal Ice Zone Experiment Lagrangian observations p 39 A88-33694
- FITZWATER, M. A.**
Comparison of unified full-wave solutions for normal incidence microwave backscatter from sea with physical optics and hybrid solutions p 42 A88-39079
- FONSECA, LEILA MARIA GARCIA**
Restoration techniques for redisplay of LANDSAT-5 satellite imagery [INPE-4189-PRE/1076] p 64 N88-20712
- FOODY, G. M.**
Crop classification from airborne synthetic aperture radar data p 10 A88-43220
- FORD, J. P.**
Satellite radars for geologic mapping in tropical regions p 27 A88-32917
Shuttle radar mapping with diverse incidence angles in the rainforest of Borneo p 12 A88-44644
- FORD, JOHN**
Radar penetration in the Amazonian rain forest p 13 N88-24015
- FORD, JOHN P.**
Airborne and spaceborne radar images for geologic and environmental mapping in the Amazon rain forest, Brazil p 37 N88-24021
Radar penetration in the Amazonian rain forest p 15 N88-24044
- FORESTI, CELINA**
Applications of multitemporal compositions obtained from LANDSAT data in the study of urban growth [INPE-4480-PRE/1246] p 22 N88-23692
- FORSTER, B. C.**
Evaluation of combined multiple incident angle SIR-B digital data and Landsat MSS data over an urban complex p 62 A88-42055
- FORTESCUE, JOHN A. C.**
Landsat TM data as an aid in planning and interpretation of regional geochemical surveys in the Canadian Shield p 31 A88-32950
- FOSTER, J. L.**
Remote sensing of snow p 50 A88-35198
- FOWLER, GARY W.**
A statistical model for prediction of precision and accuracies of radar scattering coefficient measurements derived from SAR data p 62 A88-42771
- FOX, LAWRENCE, III**
Remote sensing and the role of terrestrial vegetation in the global carbon cycle p 5 A88-41954
- FRANCE, M. J.**
A hydrological comparison of Landsat TM, Landsat MSS and black and white aerial photography p 52 A88-42041
- FRASER, S. J.**
Targeting epithermal alteration and gossans in weathered and vegetated terrains using aircraft scanners - Successful Australian case histories p 26 A88-32905
- FROIDEVAUX, CLAUDE M.**
Contribution of Landsat to a geologic expedition in the desert of North Central Sudan, Africa p 27 A88-32916
- FU, XIU-YEN**
A demonstration of stereophotogrammetry with combined SIR-B and Landsat TM images p 63 A88-44650
- FUKUE, K.**
Global vegetation monitoring using NOAA GAC data p 8 A88-42012
- FUKUE, KIYONARI**
Evaluations of unsupervised methods for land-cover/use classifications of Landsat TM data p 64 A88-45116
- FUNG, A. K.**
An empirical model for polarized and cross-polarized scattering from a vegetation layer p 11 A88-44116

G

- GABELL, A. R.**
Targeting epithermal alteration and gossans in weathered and vegetated terrains using aircraft scanners - Successful Australian case histories p 26 A88-32905
- GAD, A.**
Assessment of desertification in the lower Nile Valley (Egypt) by an interpretation of Landsat MSS colour composites and aerial photographs p 61 A88-42025
- GAGNE, JACQUES A.**
Satellite observations of tidal upwelling and mixing in the St. Lawrence estuary p 45 A88-42450
- GAHEGAN, MARK**
Evaluation of regional land resources using geographic information systems based on linear quadrates p 20 A88-42063
- GALIBERT, G.**
Insertion of hydrological decorrallated data from photographic sensors of the Shuttle in a digital cartography of geophysical exploration (Spacelab 1-Metric Camera and Large Format Camera) p 74 A88-41990
- GALIMORE, REGINALD N.**
The 1987 Airborne Antarctic Ozone Experiment: The Nimbus-7 TOMS data atlas [NASA-RP-1201] p 47 N88-20714
- GALLO, K. P.**
Differences in visible and near-IR responses, and derived vegetation indices, for the NOAA-9 and NOAA-10 AVHRRs - A case study p 70 A88-35396
- GALLOTTIFLORENZANO, TERESA**
Updating land-use of the Sao Jose dos Campos municipality through remote sensing data [INPE-4479-RPE/562] p 22 N88-23693
- GAMARANETO, GILBERTO**
Analysis for architecture for image processing [INPE-4294-PRE/1165] p 75 N88-20715
- GAN-OUCHIR, ZH.**
Quantitative analysis of a network of faults recognized on remote-sensing images of the Mushugai area in Mongolia p 32 A88-36163
- GANDIA, S.**
Spectral signature of rice fields using Landsat-5 TM in the Mediterranean coast of Spain p 6 A88-41991
- GANZORIG, M.**
Quantitative analysis of a network of faults recognized on remote-sensing images of the Mushugai area in Mongolia p 32 A88-36163
- GARCIAFONSECA, LEILA MARIA**
Method for restoration and resampling of TM sensor imagery [INPE-4491-PRE/1255] p 65 N88-22454
- GARRARD, G. R.**
Exploration for mercury and lead-zinc-silver using the airborne Thematic Mapper, Almaden area, Spain p 29 A88-32939
- GARVIN, J. B.**
Multispectral geologic remote sensing of a suspected impact crater near Al Madafi, Saudi Arabia p 33 A88-41955
- GASCARD, J. C.**
Elements of sea ice dynamics and thermodynamics p 48 N88-21571
- GASCARD, JEAN-CLAUDE**
Diagnostic study of the Fram Strait marginal ice zone during summer from 1983 and 1984 Marginal Ice Zone Experiment Lagrangian observations p 39 A88-33694
- GASTELLU-ETCHEGORRY, J. P.**
Methodology for an operational monitoring of remotely-sensed sea surface temperatures in Indonesia p 43 A88-39084
- GATTO, LAWRENCE W.**
Ice conditions along the Ohio River as observed on LANDSAT images, 1972-1985 [AD-A191172] p 57 N88-25018
- GAUTIER, CATHERINE**
Radiative processes affecting ocean mixed-layer heat content and their monitoring from satellite p 47 N88-20800
- GEOKHLANIAN, T. KH.**
New aspects of the interpretation of space radar images p 58 A88-36171
- GEORGE, H.**
Application of MEIS-II multispectral airborne data and CIR photography for the mapping of surficial geology and geomorphology in the Chatham area, Southwest Ontario, Canada p 34 A88-42027
- GERARDI, L. H. O.**
Implantation of a geo-cartographical information system through microcomputers p 67 N88-24064
- GETULIOMVIEIRA, ERNESTO**
Evaluation of the mangrove area at the Piaui River (SE) through remote sensing p 16 N88-24086
- GIBERT, DOMINIQUE**
Geoid roughness and long-wavelength segmentation of the South Atlantic spreading ridge p 24 A88-40688
- GILBERT, A.**
Spectral signature of rice fields using Landsat-5 TM in the Mediterranean coast of Spain p 6 A88-41991
- GINZBURG, A. I.**
The determination of the parameters of the diurnal thermocline using satellite and ship-based measurements p 44 A88-40834
Mushroom-shaped currents (eddy dipoles) under rotation and stratification conditions p 47 N88-20678
- GITEL'SON, A. A.**
Principles of the remote monitoring of fresh-water quality p 50 A88-34674
- GLASS, CHARLES E.**
Application of spatial statistics to analyzing multiple remote sensing data sets p 64 A88-45639
- GLINER, A. R.**
Range variations of the tropospheric propagation of ultrashort radio waves above the sea p 39 A88-33920
- GLOERSEN, PER**
Satellite and aircraft passive microwave observations during the Marginal Ice Zone Experiment in 1984 p 45 A88-42447
- GODOYJUNIOR, MOACIR**
Updating of the municipal official register of real estate through a geographical information system [INPE-4459-PRE/1238] p 21 N88-22453
- GOETZ, ALEXANDER F. H.**
Remote sensing for non-renewable resources - Satellite and airborne multiband scanners for mineral exploration p 35 A88-42068
- GOMARASCA, M. A.**
Digital analysis of stereo pairs for the detection of anomalous signatures in geothermal fields p 61 A88-42037
- GONCALVES, MARLEY**
Satellite remote sensing of turbidity and sediment concentration in Lagoa dos Patos p 56 N88-24032
- GOODENOUGH, DAVID G.**
The integration of remote sensing and geographic information systems p 21 A88-42069
- GOOSSENS, ROLAND E.**
Remote sensing for wildlife management - Giant panda habitat mapping from Landsat MSS images p 2 A88-35195
- GORDON, ARNOLD L.**
Polynyas in the Southern Ocean p 43 A88-39284
- GOUCHER, G.**
Assessment of digital enhancement techniques using Landsat TM data in mapping geologic lineaments, with application to the Mactaquac headpond area, southern New Brunswick p 31 A88-32949
- GRATTON, YVES**
Satellite observations of tidal upwelling and mixing in the St. Lawrence estuary p 45 A88-42450
- GRAY, A. L.**
An effect of coherent scattering in spaceborne and airborne SAR images p 64 A88-44651
- GRAY, J. L.**
An analysis of remote sensing for monitoring urban derelict land p 20 A88-42056

GREEN, A. A.

Targeting epithermal alteration and gossans in weathered and vegetated terrains using aircraft scanners - Successful Australian case histories p 26 A88-32905

GREER, JERRY D.

Space Shuttle Large Format Camera photography and resource management p 70 A88-36378

GRIFFITH, J. H.

Fracture patterns and production trends, Big Sandy Field, eastern Kentucky p 27 A88-32913

GROSKOPF, NORMAN

Pyrophyllite and kaolinite alteration - Mineral discrimination by sample reflectance measurement p 31 A88-32954

GROSS, M. F.

Remote sensing of biomass of salt marsh vegetation in France p 3 A88-39082

GUERETTE, JACQUES

Remote sensing and data integration: Practical solutions for resource managers p 22 N88-24034

GUERO, MAMANE

A remote sensing aided inventory of fuelwood volumes in the Sahel region of west Africa - A case study of five urban zones in the Republic of Niger p 7 A88-42005

GULAI, ABDISHAKOUR A.

Contribution of remote sensing to food security and early warning systems in drought affected countries in Africa p 8 A88-42008

GUO, HUADONG

Shuttle imaging radar response from sand dunes and subsurface rocks of Alashan Plateau in north-central China p 33 A88-41978

GUYMER, T. H.

Remote sensing of sea-surface winds p 41 A88-37144

H

HAACK, BARRY N.

Double sampling for rice in Bangladesh using Landsat MSS data p 8 A88-42009

HADDOCK, THOMAS F.

Millimeter-wave bistatic scattering from ground and vegetation targets p 11 A88-44308

HAERTEL, VITOR

Textural features for image classification in remote sensing p 66 N88-24027

HAJEK, M.

The use of multispectral space photographs to draw up a map of land use in western Slovakia p 57 A88-33774

HALL, D. K.

Remote sensing of snow p 50 A88-35198

HALL, DOROTHY K.

Assessment of polar climate change using satellite technology p 40 A88-36241

HALL, R. J.

Canadian large-scale aerial photographic systems (LSP) p 70 A88-35395

HALSEY, J. H.

Fracture patterns and production trends, Big Sandy Field, eastern Kentucky p 27 A88-32913

HAMEURLAIN, A.

The SAGE geographic analysis system p 22 N88-24063

HAMEURLAIN, M. A.

The Systeme d'Analyse Geographique (SAGE) geographic analysis system p 66 N88-24019

HANSON, BRADFORD C.

A comparison of airborne GEMS/SAR with satellite-borne Seasat/SAR radar imagery - The value of archived multiple data sets p 64 A88-45640

HARDING, A. E.

Exploration for mercury and lead-zinc-silver using the airborne Thematic Mapper, Almaden area, Spain p 29 A88-32939

HARDY, D. D.

Remote sensing in the Space Station and Columbus programmes p 71 A88-37150

HARDY, J. R.

Transformation of Global Vegetation Index (GVI) data from the polar stereographic projection to an equatorial cylindrical projection p 58 A88-39095

HARRIS, J.

A comparison of lineaments interpreted from remotely sensed data and airborne magnetics and their relationship to gold deposits in central Nova Scotia p 29 A88-32936

HARRIS, T. R.

Radiative surface temperatures of the burned and unburned areas in a tallgrass prairie p 3 A88-37418

HARTMANN, C.

Evaluation of the floodable area of the canal of Sao Goncalo through TM-LANDSAT 5 imagery p 56 N88-24078

HASKELL, A.

Plans for ERS-1 data acquisition, processing and distribution p 41 A88-37149

HAVERTZ, MICHAEL J.

Associations among lineaments, subsurface fractures, hydrocarbon microseepage, and production in the Uinta Basin, Utah p 27 A88-32908

HAWKINS, R. H.

Rangeland runoff curve numbers as determined from Landsat MSS data p 51 A88-39089

HAYDN, R.

Integration of remote sensing and other geo-data for ore exploration - A SW-Iberian case study p 31 A88-32952

HAYES, DALLAS T.

Millimeter-wave multipath measurements on snow cover p 54 A88-44311

HEAGLE, ALLEN S.

Canopy reflectance of soybean as affected by chronic doses of ozone in open-top field chambers p 2 A88-35398

HECKLEY, W. A.

An evaluation of the performance of the ECMWF operational system in analyzing and forecasting easterly wave disturbances over Africa and the tropical Atlantic p 43 A88-39746

HEDGES, P. D.

The use of SPOT simulation data in forestry mapping p 7 A88-42006
A hydrological comparison of Landsat TM, Landsat MSS and black and white aerial photography p 52 A88-42041

HELAVA, U. V.

Object-space least-squares correlation p 63 A88-44517

HEMLEBEN, C.

Temporal variations of particle fluxes in the deep subtropical and tropical North Atlantic - Eulerian versus Lagrangian effects p 45 A88-42448

HENDERSON-SELLERS, A.

Cloud climatologies from space and applications to climate modelling p 71 A88-37145

HERMAN, JOHN D.

Surface expression of subsurface structures in the Michigan Basin p 29 A88-32929

HERREN, G.

Spectral measurements for correcting LANDSAT data for atmospheric effects p 66 N88-24020

HEWITT, DAVID

Mapping soil and rock variation from satellite images in the Sahel p 14 N88-24023

HEYADA, JAN R.

Directed band ratioing for the retention of perceptually-independent topographic expression in chromaticity-enhanced imagery p 62 A88-43224

HICKSON, DIANA E.

History of wildland fires on Vandenberg Air Force Base, California [NASA-TM-100983] p 18 N88-25134

HIDEKIYANASSE, HORACIO

Low altitude remote sensing data in the implementation of a mathematical model for the planning of urban equipment networks p 23 N88-24074

HIROMOTO, NORIHISA

SIR-B experiments in Japan. I - Sensor calibration experiment p 73 A88-40351

HOCK, JOAN C.

Monitoring environmental resources through NOAA's polar orbiting satellites p 21 A88-42070

HODGSON, MICHAEL E.

Correlation between aircraft MSS and LIDAR remotely sensed data on a forested wetland in South Carolina p 5 A88-41951

HODGSON, R. A.

Remote sensing and surface geochemical study of Railroad Valley, Nye County, Nevada - Detailed grid study p 31 A88-32953

HOEKMAN, D. H.

Results of the testing of the segmentation program on RESEDA [BCRS-87-01] p 65 N88-23304

HOGAN, PATRICK D.

Satellite data management for effective data access p 42 A88-38690

HOGG, JAMES

Evaluation of regional land resources using geographic information systems based on linear quadrates p 20 A88-42063

HOLBO, H. R.

Using the thermal infrared multispectral scanner (TIMS) to estimate surface thermal responses p 73 A88-40785

HOLLINGSWORTH, A.

An evaluation of the performance of the ECMWF operational system in analyzing and forecasting easterly wave disturbances over Africa and the tropical Atlantic p 43 A88-39746

HOLT, BENJAMIN

The Shuttle Imaging Radar B (SIR-B) experiment report [NASA-CR-182923] p 75 N88-23932

HONEY, F. R.

Rock discrimination and alteration mapping for mineral exploration using the Carr Boyd/Geoscan airborne multispectral scanner p 27 A88-32914

HOOD, VALERIE ANNE

International cooperation in remote sensing: The ESA experience p 77 N88-24038

HOOGBOOM, P.

SLAR as a research tool p 73 A88-41976

HOPPIN, RICHARD A.

Evaluation of digitally processed Landsat imagery and SIR-A imagery for geological analysis of West Java region, Indonesia p 33 A88-41983

HORIKAWA, YASUSHI

Marine Observation Satellite-1 (MOS-1) and its sensors [AAS PAPER 86-288] p 40 A88-35153

ERS-1, Earth Resources Satellite-1 and future earth observation program in Japan [AAS PAPER 86-289] p 69 A88-35154

HORN, BERTHOLD K.

Relative orientation [AD-A190385] p 75 N88-22449

HOSHI, TAKASHI

The 'Tsukusys' image processing system and its utilization in Thematic Mapper investigations of water quality conditions p 54 A88-45115

On the regional characteristics of actual evapotranspiration derived from Landsat MSS and elevation data p 54 A88-45118

HOSOMURA, T.

Global vegetation monitoring using NOAA GAC data p 8 A88-42012

HSU, L. C.

Influence of mineral coatings and vegetation on TM imagery over Tertiary Caldera lithologies basin and range province, western U.S. p 32 A88-41945

HUANG, W. G.

Surface currents off the west coast of Ireland studied from satellite images p 43 A88-39085

HUCKERBY, J. A.

Thematic Mapper applied to alteration zone mapping for gold exploration in south-east Spain p 29 A88-32938

HUDNALL, W. H.

Preliminary investigation of Large Format Camera photography utility in soil mapping and related agricultural applications p 4 A88-41947

HUEHNERFUSS, HEINRICH

Radar signatures of oil films floating on the sea surface and the Marangoni effect p 39 A88-33695

HUETE, A. R.

Soil and atmosphere influences on the spectra of partial canopies p 11 A88-44119

HUNTINGTON, J. F.

Targeting epithermal alteration and gossans in weathered and vegetated terrains using aircraft scanners - Successful Australian case histories p 26 A88-32905

HURTAJ, J. J.

Subsurface morphology and geoarchaeology revealed by spaceborne and airborne radar p 37 N88-24022

HURTAJ, JAMES J.

Airborne and spaceborne radar images for geologic and environmental mapping in the Amazon rain forest, Brazil p 37 N88-24021

HUSBY, D. M.

Hydrographic observations in the northwestern Weddell Sea Marginal Ice Zone during March 1986 [PB88-173240] p 55 N88-23359

HYATT, E. C.

An analysis of remote sensing for monitoring urban derelict land p 20 A88-42056

I

IAKOVLEV, V. P.

Comparison of radar and microwave radiometer techniques for determining permittivity p 74 A88-44231

IAROSHCHUK, E. V.

Satellite observations and the numerical simulation of the interaction between a synoptic eddy and a frontal zone in the ocean p 40 A88-36159

- ICHINOSE, MASARU**
SIR-B experiments in Japan. I - Sensor calibration experiment p 73 A88-40351
SIR-B experiments in Japan. II - Rice crop experiment p 4 A88-40352
- SIR-B experiments in Japan. V. p 4 A88-40355
- IGUCHI, TOSHIO**
SIR-B experiments in Japan. VI. p 43 A88-40356
- IMHOFF, MARC L.**
The role of space borne imaging radars in environmental monitoring: Some shuttle imaging radar results in Asia [NASA-TM-101178] p 23 N88-24844
- INOMATA, HIDEYUKI**
SIR-B experiments in Japan. III - Oil-pollution experiment p 43 A88-40353
SIR-B experiments in Japan. VI. p 43 A88-40356
- IRSYAM, MAHSUM**
Monitoring of renewable resources in equatorial countries p 19 A88-42000
- ISACKS, B. L.**
Discrimination and supervised classification of volcanic flows of the Puna-Altiplano, Central Andes Mountains using Landsat TM data p 31 A88-32948
- ISAEV, A. S.**
Remote-sensing methods for the monitoring and forecasting of the entomological condition of taiga forests p 2 A88-36164
- ISHIDA, TOMOYUKI**
The 'Tsukusys' image processing system and its utilization in Thematic Mapper investigations of water quality conditions p 54 A88-45115
- ISKANDAR, L. L.**
Photo-interpretation of landforms and the hydrogeologic bearing in highly deformed areas, NW of the Gulf of Suez, Egypt p 34 A88-42029
- IVANOV, A. V.**
Active two-element microwave interferometry of the sea surface p 41 A88-37679
- J**
- JACKSON, R. D.**
Soil and atmosphere influences on the spectra of partial canopies p 11 A88-44119
- JADHAV, A. S.**
Application of remote sensing in hydromorphology for third world development - A resource development study in parts of Haryana (India) p 53 A88-42042
- JAETHN, SIGMUND**
The use of metric multispectral photography in environmental and resource exploration p 21 A88-44446
- JANG, BAOLIN**
Analysis of lineaments and major fractures in Xichang-Dukou area, Sichuan province as interpreted from Landsat images p 34 A88-42022
- JEANNIN, PIERRE-FRANCOIS**
Diagnostic study of the Fram Strait marginal ice zone during summer from 1983 and 1984 Marginal Ice Zone Experiment Lagrangian observations p 39 A88-33694
- JENSEN, JOHN R.**
Application of Landsat Thematic Mapper data to assess suspended sediment dispersion in a coastal lagoon p 51 A88-41946
Correlation between aircraft MSS and LIDAR remotely sensed data on a forested wetland in South Carolina p 5 A88-41951
- JOHN, KARL-HEINZ**
The use of metric multispectral photography in environmental and resource exploration p 21 A88-44446
- JOHNSON, A. I.**
Geotechnical applications of remote sensing and remote data transmission; Proceedings of the Symposium, Cocoa Beach, FL, Jan. 31-Feb. 1, 1986 p 35 A88-45634
- JOHNSON, A. J.**
An approach for emulating the color balance of Landsat multispectral scanner images with AVHRR data p 73 A88-41956
- JOHNSON, J. E.**
Hydrographic data from the OPTOMA (Ocean Prediction Through Observation, Modeling and Analysis) program: OPTOMA 23, 9-19 November 1986 [AD-A189868] p 49 N88-22506
- JOLY, G.**
Geographic study of the north coast of Senegal using MOMS-1 satellite data p 73 A88-41093
- JONES, A. R.**
The use of Thematic Mapper imagery for geomorphological mapping in arid and semi-arid environments p 33 A88-41992
Monitoring geomorphological processes in desert marginal environments using multitemporal satellite imagery p 34 A88-42030
- Use of digital terrain data in the interpretation of SPOT-1 HRV multispectral imagery p 10 A88-43221
- JONES, ARWYN RHYS**
Spring mound and aoum mapping from Landsat TM imagery in south-central Tunisia p 52 A88-42026
- JONES, V. T.**
Remote sensing and surface geochemical study of Railroad Valley, Nye County, Nevada - Detailed grid study p 31 A88-32953
- JONSSON, L.**
Remote sensing of flow characteristics of the strait of Oresund p 53 A88-42043
- K**
- KADRO, A.**
Determination of spectral signatures of different forest damages from varying altitudes of multispectral scanner data p 6 A88-41993
Experiences in application of multispectral scanner-data for forest damage inventory p 8 A88-42010
- KAHRU, M. M.**
Statistical analysis of the near-surface distributions of chlorophyll and temperature fields on the basis of remote imagery from CZCS and AVHRR scanners p 54 A88-43666
- KAMATA, MITSUHIRO**
SIR-B experiments in Japan. I - Sensor calibration experiment p 73 A88-40351
SIR-B experiments in Japan. II - Rice crop experiment p 4 A88-40352
- KAMIYA, YOSHIKAZU**
Marine Observation Satellite-1 (MOS-1) and its sensors [AAS PAPER 86-288] p 40 A88-35153
ERS-1, Earth Resources Satellite-1 and future earth observation program in Japan [AAS PAPER 86-289] p 69 A88-35154
- KAPPEL, HELMUT**
Spaceborne radar X-SAR for civil applications p 72 A88-37286
- KARTERIS, MICHAEL A.**
Manual interpretation of small forestlands on Landsat MSS data p 12 A88-44521
- KASISCHKE, ERIC S.**
A statistical model for prediction of precision and accuracies of radar scattering coefficient measurements derived from SAR data p 62 A88-42771
- KATO, YUICHI**
Environmental assessment for large scale civil engineering projects with data of DTM and remote sensing p 53 A88-42046
- KAUFMANN, HERMANN**
Image optimization versus classification - An application oriented comparison of different methods by use of Thematic Mapper data p 59 A88-41964
- KAWAI, EIJI**
SIR-B experiments in Japan. I - Sensor calibration experiment p 73 A88-40351
- KAWATA, YOSHIYUKI**
Radiometric correction for atmospheric and topographic effects on Landsat MSS images p 62 A88-43223
- KAZARYAN, V. V.**
Spectral reflective characteristics of sea surface p 47 N88-20676
- KEATING, THOMAS**
Tropical rainfall measuring mission (TRMM) p 69 A88-33429
- KEPPER, JOHN C.**
Discrimination of lithologic units, alteration patterns and major structural blocks in the Tonopah, Nevada area using Thematic Mapper data p 27 A88-32907
- KERGOMARD, CLAUDE**
Diagnostic study of the Fram Strait marginal ice zone during summer from 1983 and 1984 Marginal Ice Zone Experiment Lagrangian observations p 39 A88-33694
- KESIK, A. B.**
Application of MEIS-II multispectral airborne data and CIR photography for the mapping of surficial geology and geomorphology in the Chatham area, Southwest Ontario, Canada p 34 A88-42027
- KIBITLEWSKI, STANISLAW**
Geological analysis of the satellite lineaments of the Vistula Delta Plain, Zulawy Wislane, Poland p 34 A88-42021
Remote sensing methods in geological research of the Lublin coal basin, SE Poland p 34 A88-42028
- KIEFER, RALPH W.**
Enhancement of SPOT image resolution using an intensity-hue-saturation transformation p 59 A88-41958
Regional geologic mapping of digitally enhanced Landsat imagery in the southcentral Alborz mountains of northern Iran p 34 A88-42017
- KING, THOMAS A.**
Color space mapping using ternary/chromaticity diagrams - A technique for composite image interpretation p 57 A88-32932
- KJERFVE, BJORN**
Application of Landsat Thematic Mapper data to assess suspended sediment dispersion in a coastal lagoon p 51 A88-41946
- KLEMAS, V.**
Quantitative analysis of distribution of suspended sediments in the Yellow River Estuary from MSS data p 50 A88-35196
Remote sensing of biomass of salt marsh vegetation in France p 3 A88-39082
- KOBRICK, M.**
SIR-B stereo-radargrammetry of Australia p 63 A88-44648
- KOCHEL, R. CRAIG**
Groundwater sapping valleys: Experimental studies, geological controls and implications to the interpretation of valley networks on Mars [NASA-CR-182718] p 37 N88-22847
- KOEPP, JOERG**
Feasibility study for a 2nd generation system for airborne maritime pollution surveillance [ETN-88-92108] p 55 N88-22466
- KOIDE, K.**
An evaluation of potential uranium deposit area by Landsat data analysis in Officer Basin, South-Western part of Australia p 35 A88-42036
- KOLM, KENNETH E.**
Lineaments: Significance, criteria for determination, and varied effects on ground-water systems - A case history in the use of remote sensing p 55 A88-45636
- KOMHYR, W. D.**
Long-term air quality monitoring at the South Pole by the NOAA program Geophysical Monitoring for Climatic Change p 18 A88-36243
- KONDRAT'EV, K. IA.**
Climatological interpretation of time series of satellite observations of the earth's radiation balance p 69 A88-33872
Principles of the remote monitoring of fresh-water quality p 50 A88-34674
- KONECNY, G.**
Alternatives for mapping from satellite imagery [IAF PAPER 86-76] p 59 A88-41298
- KONG, J. A.**
Identification of terrain cover using the optimum polarimetric classifier p 3 A88-37370
Remote sensing of earth terrain [NASA-CR-182677] p 12 N88-20711
- KOOPMANS, B. N.**
Detection by side-looking radar of geological structures under thin cover sands in arid areas p 33 A88-41979
A comparative analysis of dyke lineaments mapped from Shuttle Imaging Radar and Large Format Camera photography in hyperarid areas of the Eastern Desert, Egypt, and Red Sea Hills, Sudan p 35 A88-44647
- KORANY, E. A.**
Photo-interpretation of landforms and the hydrogeologic bearing in highly deformed areas, NW of the Gulf of Suez, Egypt p 34 A88-42029
- KOROVIN, V. P.**
Spectral reflective characteristics of sea surface p 47 N88-20676
- KOSTYANOV, A. G.**
Mushroom-shaped currents (eddy dipoles) under rotation and stratification conditions p 47 N88-20678
- KOTLAREK, THOMAS L.**
Satellite data management for effective data access p 42 A88-38690
- KOZODEROV, V. V.**
Climatological interpretation of time series of satellite observations of the earth's radiation balance p 69 A88-33872
- KRABILL, WILLIAM**
Correlation between aircraft MSS and LIDAR remotely sensed data on a forested wetland in South Carolina p 5 A88-41951
- KRAVTSOVA, V. I.**
Investigation and mapping of forests using space scanner imagery obtained in winter p 2 A88-36165
- KRAWCZYK, R.**
Imaging instrument of the Vegetation Payload (SPOT 4) p 70 A88-35968
In flight calibration for the imaging instrument of VEGETATION payload (SPOT 4) p 10 A88-42545
- KRIVONozHKIN, S. N.**
Range variations of the tropospheric propagation of ultrashort radio waves above the sea p 39 A88-33920
- KRUEGER, ARLIN J.**
The 1987 Airborne Antarctic Ozone Experiment: The Nimbus-7 TOMS data atlas [NASA-PP-1201] p 47 N88-20714

KRUG, THELMA

- Remote sensing techniques in the estimation of the area cultivated with beans, corn, and castor beans in the Irece County (Bahia State) p 15 N88-24045
 Preliminary study on the application of digital processing of TM-LANDSAT data in the mapping of apple orchards in Fraiburgo (SC) p 17 N88-24093

KRUSE, SARAH E.

- Magnetic lineations on the flanks of the Marquesas swell - Implications for the age of the seafloor p 44 A88-41257

KUGLER, BARBARA

- Comparison of classification results of original and preprocessed satellite data p 59 A88-41965

KUNTZ, S.

- Experiences in application of multispectral scanner-data for forest damage inventory p 8 A88-42010

KUSAKA, TAKASHI

- Radiometric correction for atmospheric and topographic effects on Landsat MSS images p 62 A88-43223

KUX, HERMANN J. H.

- Mapping of plant associations and the variation of surface water in the Pantanal Mato-Grossense National Park, through remote sensing techniques p 17 N88-24092

L

LAGERLOEF, GARY S. E.

- Empirical orthogonal function analysis of advanced very high resolution radiometer surface temperature patterns in Santa Barbara Channel p 45 A88-42449

LAGO, BERNARD

- Geoid anomalies across Pacific fracture zones p 24 A88-38023

LAMB, FRANK G.

- Regional crop-forecasting with Landsat - A farmer's experience [AAS PAPER 86-401] p 2 A88-35161

LAMMERS, UVE H. W.

- Millimeter-wave multipath measurements on snow cover p 54 A88-44311

LAMPARELLI, R. A. C.

- Evaluation of the floodable area of the canal of Sao Goncalo through TM-LANDSAT 5 imagery p 56 N88-24078

LANGERAAR, W. D.

- Airphoto map control with Landsat - An alternative to the slotted template method p 60 A88-41966

LANNELONGUE, N.

- Marginal Ice Zone Experiment (MIZEX) 1984 VARAN-S data set [ETN-88-92032] p 48 N88-21625
 Definition and implementation study for the Varan-S radar [CNES-CT/DRT/TIT/RL-143-T] p 48 N88-22267

LAO, K. Q.

- Theoretical basis for multispectral imaging simulation p 63 A88-44532

LAPITAN, R. L.

- Radiative surface temperatures of the burned and unburned areas in a tallgrass prairie p 3 A88-37418

LARGE, WILLIAM G.

- A system for remote measurements of the wind stress over the ocean p 40 A88-36841

LARKO, DAVID E.

- The 1987 Airborne Antarctic Ozone Experiment: The Nimbus-7 TOMS data atlas [NASA-PP-1201] p 47 N88-20714

LATHROP, RICHARD G., JR.

- Toward an integrated system for satellite remote sensing of water quality in the Great Lakes p 52 A88-41957

LAVERTY, IAN

- Base map production from geocoded imagery p 25 A88-41969
 Mapping from LANDSAT and SPOT satellite imagery p 66 N88-24018

LAWRENCE, PAUL M.

- Pyrophyllite and kaolinite alteration - Mineral discrimination by sample reflectance measurement p 31 A88-32954

LEACH, JOSEPH H. J.

- A satellite-based investigation of the significance of surficial deposits for surface mining operations p 36 A88-45638

LEAODEMORAESNOVO, EVELYN MARCIA

- Updating land-use of the Sao Jose dos Campos municipality through remote sensing data [INPE-4479-RPE/562] p 22 N88-23693

LEBERL, F.

- SIR-B stereo-radiogrammetry of Australia p 63 A88-44648
 Dependence of image grey values on topography in SIR-B images p 63 A88-44649

LEE, DAVID CHUNG LIANG

- A proposal for a project entitled assessment of forest resources in Uruguay submitted to the United Nations Industrial Development Organization (UNIDO) p 13 N88-24016

LEE, DEBORAH H.

- Determinations of suspended sediment concentrations from multiple day Landsat and AVHRR data p 54 A88-44120

LEE, KEENAN

- Lineaments of the northern Denver Basin and their paleotectonic and hydrocarbon significance p 28 A88-32920

LEFEBVRE, MICHEL

- Topex/Poseidon - A contribution to the world climate research program [AAS PAPER 86-306] p 39 A88-35058

LEGGETT, NICKOLAUS

- A second generation lunar agricultural system p 11 A88-43864

LEGUZAMON, S.

- Multitemporal analysis of Landsat Multispectral Scanner (MSS) and Thematic Mapper (TM) data to map crops in the Po valley (Italy) and in Mendoza (Argentina) p 6 A88-41994

LEMKE, P.

- Sea ice observations and models p 48 N88-21572

LENNON, G.

- Non-tracking antenna systems for the acquisition of NOAA HRPT Data p 72 A88-37279

LEPRIEUR, C. E.

- Influence of topography on forest reflectance using Landsat Thematic Mapper and digital terrain data p 2 A88-35397

LETT, RAYMOND E.

- Pyrophyllite and kaolinite alteration - Mineral discrimination by sample reflectance measurement p 31 A88-32954

LEVASSEUR, J. E.

- Remote sensing of biomass of salt marsh vegetation in France p 3 A88-39082

LEVENTUEV, V. P.

- Evaluation of the possibility of determining concentrations of variable components of ocean water from averaged spectra of the diffuse optical reflection coefficient p 40 A88-36160

LEVINE, JOEL S.

- Particulate emissions from a mid-latitude prescribed chaparral fire p 3 A88-38805

LEWIS, A. J.

- Shuttle imaging radar response from sand dunes and subsurface rocks of Alashan Plateau in north-central China p 33 A88-41978

LEWIS, JAMES K.

- Examples of ice pack rigidity and mobility characteristics determined from ice motion [AD-A191163] p 50 N88-24129

LEWIS, JOHN E.

- Surface temperatures and sea ice typing for northern Baffin Bay p 42 A88-39083

LHERMITTE, ROGER M.

- Cloud and precipitation remote sensing at 94 GHz p 74 A88-44306

LI, YINHAI

- Satellite observation of surface albedo over the Qinghai-Xinjiang plateau region p 24 A88-39518

LILLESAND, THOMAS M.

- Toward an integrated system for satellite remote sensing of water quality in the Great Lakes p 52 A88-41957
 Enhancement of SPOT image resolution using an intensity-hue-saturation transformation p 59 A88-41958

LIMADALGE, JULIO CESAR

- Updating land-use of the Sao Jose dos Campos municipality through remote sensing data [INPE-4479-RPE/562] p 22 N88-23693

LIN, HUI

- Estimation of reservoir submerging losses using CIR aerial photographs - Example of the Ertan hydropower station on the Yalong River in southwest China p 55 A88-45637

LISOWSKI, MICHAEL

- Geodetic measurement of deformation east of the San Andreas Fault in Central California p 25 A88-32831
 Geodetic measurement of deformation east of the San Andreas fault in Central California [NASA-CR-182709] p 36 N88-20754

LIU, BINGGUANG

- Analysis of lineaments and major fractures in Xichang-Dukou area, Sichuan province as interpreted from Landsat images p 34 A88-42022

LIU, H. L.

- An empirical model for polarized and cross-polarized scattering from a vegetation layer p 11 A88-44116

LIU, W. TIMOTHY

- Moisture and latent heat flux variabilities in the tropical Pacific derived from satellite data p 45 A88-42445

LIU, WEN-YAO

- Quantitative analysis of distribution of suspended sediments in the Yellow River Estuary from MSS data p 50 A88-35196

LO, C. P.

- Human settlement analysis using Shuttle Imaging Radar-A data - An evaluation p 20 A88-42057
 Comparative evaluation of the Large Format Camera, Metric Camera, and Shuttle Imaging Radar - A data content p 75 A88-44519

LOBANOV, V. B.

- Satellite observations and the numerical simulation of the interaction between a synoptic eddy and a frontal zone in the ocean p 40 A88-36159

LODWICK, G. D.

- A comprehensive LRIS of the Kananaskis Valley using Landsat data p 21 A88-42064

LOEFER, G. R.

- Theoretical basis for multispectral imaging simulation p 63 A88-44532

LOWRY, RAYMOND T.

- A VHF radar to make terrain elevation models through tropical jungle p 10 A88-42760

LU, DEFU

- Analysis of lineaments and major fractures in Xichang-Dukou area, Sichuan province as interpreted from Landsat images p 34 A88-42022

LUCAS, R. D.

- Geometric restoration of satellite image data [AD-A190462] p 64 N88-22450

LUGASKI, THOMAS P.

- Discrimination of lithologic units, alteration patterns and major structural blocks in the Tonopah, Nevada area using Thematic Mapper data p 27 A88-32907

LUVALL, J. C.

- Using the thermal infrared multispectral scanner (TIMS) to estimate surface thermal responses p 73 A88-40785

LYNNE, G. J.

- Integration of SIR-B imagery with geological and geophysical data in Australia p 27 A88-32912
 Pattern recognition and geological interpretation of SIR-B images of Central Australia p 31 A88-32956

LYON, JOHN G.

- Quantitative description and classification of drainage patterns p 51 A88-35399
 Determinations of suspended sediment concentrations from multiple day Landsat and AVHRR data p 54 A88-44120

LYON, RONALD J. P.

- Identification of clay minerals by feature coding of near-infrared spectra p 30 A88-32942

M

MACDONALD, JOHN S.

- Discrimination of lithologic units, alteration patterns and major structural blocks in the Tonopah, Nevada area using Thematic Mapper data p 27 A88-32907

MACKAY, HALKARD E., JR.

- Correlation between aircraft MSS and LIDAR remotely sensed data on a forested wetland in South Carolina p 5 A88-41951

MACKINNON, JOHN R.

- Remote sensing for wildlife management - Giant panda habitat mapping from Landsat MSS images p 2 A88-35195

MAGEE, R.

- Thematic Mapper applied to alteration zone mapping for gold exploration in south-east Spain p 29 A88-32938

MAGEE, ROBERT W.

- Thematic Mapper data applied to mapping hydrothermal alteration in south west New Mexico p 28 A88-32923

MAGILL, KAREN

- Application of Landsat Thematic Mapper data to assess suspended sediment dispersion in a coastal lagoon p 51 A88-41946

MAHRER, Y.

- Mapping frost-sensitive areas with a three-dimensional local-scale numerical model. I - Physical and numerical aspects p 4 A88-41055

MALLETT, C. W.

- A satellite-based investigation of the significance of surficial deposits for surface mining operations p 36 A88-45638

MAMEDOV, E. A.

- Saline salt and water surface mapping on the basis of data from the Gyunesh-84 remote-sensing experiment p 51 A88-36166

- MANNSTEIN, H.**
Surface energy budget, surface temperature and thermal inertia p 58 A88-37147
- MANTOVANI, F.**
Comparison between interpretation of images of different nature p 34 A88-42019
- MARCHUK, G. I.**
Climatological interpretation of time series of satellite observations of the earth's radiation balance p 69 A88-33872
- MARCKWARDT, WERNER**
Kartoflex - An instrument for computer-aided photointerpretation and map revision p 74 A88-44450
- MAREK, KARL-HEINZ**
The use of metric multispectral photography in environmental and resource exploration p 21 A88-44446
- MARINO, CARLO MARIA**
Computer processing of satellite data for geostructural zoning of a collisional boundary, significance and field checks - The example of Tunisia p 32 A88-35193
- MARK, DAVID J.**
Determinations of suspended sediment concentrations from multiple day Landsat and AVHRR data p 54 A88-44120
- MARR, RICHARD A.**
Millimeter-wave multipath measurements on snow cover p 54 A88-44311
- MARTINI, PAULO ROBERTO**
Project CODEAMA/FUNCATE (test-area of Barreirinha-AM): Field report [INPE-4500-RPE/563] p 55 N88-22455
- MARTINKO, EDWARD A.**
Research on enhancing the utilization of digital multispectral data and geographic information systems in global habitability studies [NASA-CR-182799] p 23 N88-24101
- MARTY, JEAN-CHARLES**
Geoid anomalies across Pacific fracture zones p 24 A88-38023
- MARUYAMA, Y.**
An evaluation of potential uranium deposit area by Landsat data analysis in Officer Basin, South-Western part of Australia p 35 A88-42036
- MASCARENHAS, NELSON DELFINO DAVILA**
Restoration techniques for redisplay of LANDSAT-5 satellite imagery [INPE-4189-PRE/1076] p 64 N88-20712
- MASUKO, HARUNOBU**
SIR-B experiments in Japan. III - Oil-pollution experiment p 43 A88-40353
- MATHESON, WILMA**
Differentiation of ecological zones in the Okavango Delta, Botswana by classification and contextual analyses of Landsat MSS data p 59 A88-39099
- MATOSDEMEDEIROS, VALDER**
Calibration and processing of AVHRR data for temperature estimation [INPE-4493-PRE/1257] p 65 N88-22485
- MATUMAE, YOSHIKI**
Evaluations of unsupervised methods for land-cover/use classifications of Landsat TM data p 64 A88-45116
- MAY, GEORGE**
Economic potential of Landsat Thematic Mapper data for crop condition assessment of winter wheat p 4 A88-41948
- MAYR, W.**
SIR-B stereo-radargrammetry of Australia p 63 A88-44648
- MCCRIDE, J. H.**
Discrimination and supervised classification of volcanic flows of the Puna-Altiplano, Central Andes Mountains using Landsat TM data p 31 A88-32948
- MCCLAIN, CHARLES R.**
The dispersal of the Amazon's water p 43 A88-40059
- MCCOY, ROGER**
Associations among lineaments, subsurface fractures, hydrocarbon microseepage, and production in the Uinta Basin, Utah p 27 A88-32908
- MCCRERY, L. R.**
Inventory of decline and mortality in spruce-fir forests of the eastern U.S. with CIR photos p 7 A88-42004
- MCGEACHY, C.**
Earthscan - A range of remote sensing systems p 61 A88-41982
- MCGREGOR, KENT M.**
Using Landsat to derive curve numbers for hydrologic models p 52 A88-41950
- MCGUFFIE, K.**
Cloud climatologies from space and applications to climate modelling p 71 A88-37145
- MCINTOSH, ROBERT E.**
Radar backscatter characteristics of trees at 215 GHz p 11 A88-44307
- MCKEON, JOHN B.**
Processing of multitemporal Landsat TM data to map soil color variations related to hydrocarbon microseepage in a cropland setting - Cement, Oklahoma test site p 1 A88-32921
- MCROY, C. PETER**
Influence of the Yukon River on the Bering Sea [NASA-CR-182802] p 50 N88-24126
- MEKHTIEV, A. SH.**
Saline salt and water surface mapping on the basis of data from the Gyunesh-84 remote-sensing experiment p 51 A88-36166
- MELBOURNE, WILLIAM G.**
Precision positioning of earth orbiting remote sensing systems [AAS PAPER 86-398] p 70 A88-35159
- MELIA, J.**
Spectral signature of rice fields using Landsat-5 TM in the Mediterranean coast of Spain p 6 A88-41991
- MENDES, CELSO LUIZ**
Analysis for architecture for image processing [INPE-4294-PRE/1165] p 75 N88-20715
- MENDONCA, FRANCISCO JOSE**
CANASATE: Sugar cane mapping by satellite p 15 N88-24046
- MENENTI, M.**
Multitemporal analysis of Landsat Multispectral Scanner (MSS) and Thematic Mapper (TM) data to map crops in the Po valley (Italy) and in Mendoza (Argentina) p 6 A88-41994
- MENESES, PAULO ROBERTO**
Application of its transformation in color enhancement of LANDSAT imagery p 68 N88-24082
- MEPHAM, M. P.**
A comprehensive LRIS of the Kananaskis Valley using Landsat data p 21 A88-42064
- MERCHANT, JAMES W.**
Research on enhancing the utilization of digital multispectral data and geographic information systems in global habitability studies [NASA-CR-182799] p 23 N88-24101
- MERCIER DE L'EPINAY, B.**
Geological analysis of Seasat SAR and SIR-B data in Haiti p 33 A88-41980
- MERIN, IRA S.**
Use of digitally processed laboratory reflectance spectra for the definition of probable microseepage - Induced mineralogical variations, Lisbon Valley, Utah p 30 A88-32946
- MERTZ, GORDON**
Satellite observations of tidal upwelling and mixing in the St. Lawrence estuary p 45 A88-42450
- MIELKE, M. E.**
Inventory of decline and mortality in spruce-fir forests of the eastern U.S. with CIR photos p 7 A88-42004
- MILLER, K. G.**
Remote sensing of geobotanical associations in clastic sedimentary terrane p 31 A88-32951
- MILLER, N. L.**
An integrated approach to the use of Landsat TM data for gold exploration in west central Nevada p 30 A88-32941
- MILLER, S. T.**
The quantification of floodplain inundation by the use of Landsat and Metric Camera information, Belize, Central America p 53 A88-42044
- MILLINGTON, A. C.**
Monitoring geomorphological processes in desert marginal environments using multitemporal satellite imagery p 34 A88-42030
- MILLINGTON, ANDREW**
Spring mound and aicun mapping from Landsat TM imagery in south-central Tunisia p 52 A88-42026
- MILMAN, ANDREW S.**
Sparse-aperture microwave radiometers for earth remote sensing p 68 A88-33150
- MILTON, N. M.**
Preliminary measurements of spectral signatures of tropical and temperate plants in the thermal infrared p 1 A88-32909
- MINSTER, J. F.**
Study of the dynamic topography of oceans by means of satellite altimetry p 47 N88-21567
- MINTZER, OLIN W.**
Quantitative description and classification of drainage patterns p 51 A88-35399
- MIYACHI, YUJI**
Marine Observation Satellite-1 (MOS-1) and its sensors [AAS PAPER 86-288] p 40 A88-35153
ERS-1, Earth Resources Satellite-1 and future earth observation program in Japan [AAS PAPER 86-289] p 69 A88-35154
- MOLINAMARINO, LUIS CARLOS**
The use of SLAR and SIRA imagenes for the classification of forest types in tropical rain forests p 14 N88-24036
- MOLNIA, BRUCE F.**
Geotechnical applications of three new U.S. Government remote sensing programs p 36 A88-45641
- MONTEITH, J. L.**
A four-layer model for the heat budget of homogeneous land surfaces p 4 A88-41028
- MONTGOMERY, O. L.**
Development of remote sensing techniques capable of delineating soils as an aid to soil survey [NASA-CR-182610] p 13 N88-22452
- MOOERS, CHRISTOPHER N.**
Hydrographic data from the OPTOMA (Ocean Prediction Through Observation, Modeling and Analysis) program: OPTOMA 23, 9-19 November 1986 [AD-A189868] p 49 N88-22506
- MOOERS, CHRISTOPHER N. K.**
Mesoscale variability in current meter measurements in the California Current system off northern California p 44 A88-42443
- MOORE, J. MCM.**
Thematic Mapper applied to alteration zone mapping for gold exploration in south-east Spain p 29 A88-32938
- MOORE, JOHN MCMAHON**
Thematic Mapper data applied to mapping hydrothermal alteration in south west New Mexico p 28 A88-32923
- MORAIN, STANLEY A.**
Review of power requirements for satellite remote sensing systems p 76 N88-24387
- MOREIRA, JOSE CARLOS**
Study of methods of post-processing applied to a problem of standard classification p 67 N88-24067
- MORRICE, J. G.**
Potato crop distribution and subdivision on soil type and potential water deficit - An integration of satellite imagery and environmental spatial database p 10 A88-43222
- MORRIS, CHARLES**
Passive microwave data for snow and ice research - Planned products from the DMSP SSM/I system p 40 A88-35199
- MOUAT, D. A.**
An integrated approach to the use of Landsat TM data for gold exploration in west central Nevada p 30 A88-32941
- MUEKSCH, M. C.**
Detection of environmental noises between a vegetation canopy and a radiometric sensor p 10 A88-42538
- MUENCH, R. D.**
Hydrographic observations in the northwestern Weddell Sea Marginal Ice Zone during March 1986 [PB88-173240] p 55 N88-23359
- MUIRHEAD, KEITH**
The Along-Track Scanning Radiometer with Microwave Sounder p 41 A88-37148
- MULARZ, S. C.**
Remote sensing assessment of environmental impacts caused by phosphat industry destructive influence p 19 A88-42031
- MULDERS, M. A.**
Selection of bands for a newly developed multispectral airborne reference-aided calibrated scanner (MARCS) p 74 A88-41995
- MULLER-KARGER, F. E.**
Temporal variations of particle fluxes in the deep subtropical and tropical North Atlantic - Eulerian versus Lagrangian effects p 45 A88-42448
- MULLER-KARGER, FRANK E.**
The dispersal of the Amazon's water p 43 A88-40059
- MULLER, C.**
Synthetic geological map obtained by remote sensing - An application to Palawan Island p 33 A88-41975
- MURA, JOSE CLAUDIO**
Analysis for architecture for image processing [INPE-4294-PRE/1165] p 75 N88-20715
- MYERS, DONALD E.**
Application of spatial statistics to analyzing multiple remote sensing data sets p 64 A88-45639
- MYERS, J. S.**
An integrated approach to the use of Landsat TM data for gold exploration in west central Nevada p 30 A88-32941

NAKAMURA, KENJI

SIR-B experiments in Japan. III - Oil-pollution experiment p 43 A88-40353

NAKAMURA, MASAHARU

Environmental assessment for large scale civil engineering projects with data of DTM and remote sensing p 53 A88-42046

NANDA, R. L.

Remote sensing for survey of material resources of highway engineering projects in developing countries p 20 A88-42032

NARAYANAN, RAM MOHAN

Radar backscatter characteristics of trees at 215 GHz p 11 A88-44307

NARRACOTT, A. S.

Transformation of Global Vegetation Index (GVI) data from the polar stereographic projection to an equatorial cylindrical projection p 58 A88-39095

NASU, M.

An evaluation of potential uranium deposit area by Landsat data analysis in Officer Basin, South-Western part of Australia p 35 A88-42036

NEEDHAM, SCOTT E.

Operational satellite data assessment for drought/disaster early warning in Africa - Comments on GIS requirements p 19 A88-42018

NEGRI, ANDREW J.

A satellite infrared technique to estimate tropical convective and stratiform rainfall p 69 A88-33416

NETO, GILBERTO CAMARA

Automatic registration of satellite imagery p 67 N88-24080

NICHOLS, THOMAS C., JR.

Lineaments: Significance, criteria for determination, and varied effects on ground-water systems - A case history in the use of remote sensing p 55 A88-45636

NIEROPEREIRA, MADALENA

Applications of multitemporal compositions obtained from LANDSAT data in the study of urban growth [INPE-4480-PRE/1246] p 22 N88-23692

Updating land-use of the Sao Jose dos Campos municipality through remote sensing data [INPE-4479-RPE/562] p 22 N88-23693

NIEUWENHUIS, G. J. A.

Application of multispectral scanning remote sensing in agricultural water management problems p 8 A88-42011

NIL'SON, T. A.

Linear combinations of spectral reflectances in crop analyses p 3 A88-36170

NING, CARLOS HO SHIH

Calibration and processing of AVHRR data for temperature estimation [INPE-4493-PRE/1257] p 65 N88-22485

NOGUEIRADONASCIMENTO, NELIO

Project CODEAMA/FUNCATE (test-area of Barreirinha-AM): Field report [INPE-4500-RPE/563] p 55 N88-22455

NOOREN, G. J. L.

Results of the testing of the segmentation program on RESEDA [BCRS-87-01] p 65 N88-23304

NORTH, GERALD R.

A proposed tropical rainfall measuring mission (TRMM) satellite p 69 A88-33742

NOVAES, RENE ANTONIO

A proposal for a project entitled assessment of forest resources in Uruguay submitted to the United Nations Industrial Development Organization (UNIDO) p 13 N88-24016

NOVAK, L. M.

Identification of terrain cover using the optimum polarimetric classifier p 3 A88-37370

NOVAKOVSKII, B. A.

Space photomaps - Their compilation and peculiarities of geographical application p 60 A88-41967

NOVELLI, YARA SCHAEFFER

Evaluation of the mangrove area at the Piaui River (SE) through remote sensing p 16 N88-24086

NOVO, EVLYN M. LEAO

Evaluation of an estimation system for an irrigated area in a tropical region through TM-LANDSAT imagery p 16 N88-24075

NUSSEER, SARAH M.

Canopy reflectance of soybean as affected by chronic doses of ozone in open-top field chambers p 2 A88-35398

O

OESBERG, ROLF-PETER

The USSR space systems for remote sensing of earth resources and the environment (sensor systems, processing techniques, applications) p 76 N88-24035

OHARA, TOMOYUKI

Project CODEAMA/FUNCATE (test-area of Barreirinha-AM): Field report [INPE-4500-RPE/563] p 55 N88-22455

OHASHI, T.

Remote sensing and surface geochemical study of Railroad Valley, Nye County, Nevada - Detailed grid study p 31 A88-32953

OKADA, K.

Remote sensing and surface geochemical study of Railroad Valley, Nye County, Nevada - Detailed grid study p 31 A88-32953

OKERSON, DAVID J.

Approach and status for a unified national plan for satellite remote sensing research and development p 77 A88-32919

OKUYAMA, TOSHIYUKI

SIR-B experiments in Japan. III - Oil-pollution experiment p 43 A88-40353

OLTMANS, S. J.

Long-term air quality monitoring at the South Pole by the NOAA program Geophysical Monitoring for Climatic Change p 18 A88-36243

ORTEGA GIRONES, E.

Exploration for mercury and lead-zinc-silver using the airborne Thematic Mapper, Almaden area, Spain p 29 A88-32939

OSHIMA, TAICHI

Environmental assessment for large scale civil engineering projects with data of DTM and remote sensing p 53 A88-42046

OTANEL, J.

The use of multispectral space photographs to draw up a map of land use in western Slovakia p 57 A88-33774

OZANER, F. SANCAR

Detecting and mapping of different volcanic stages and other geomorphic features by Landsat images in 'Katakekaumene', Western Turkey p 35 A88-42033

P

PACHECOSSANTOS, ARMANDO

A proposal for a project entitled assessment of forest resources in Uruguay submitted to the United Nations Industrial Development Organization (UNIDO) p 13 N88-24016

PAINE, S. H.

A comprehensive LRIS of the Kananaskis Valley using Landsat data p 21 A88-42064

PARSONS, BARRY

The effect of a shallow low-viscosity zone on the mantle flow, the geoid anomalies and the geoid and depth-age relationships at fracture zones p 24 A88-38024

PARTINGTON, K. C.

A model of satellite radar altimeter return from ice sheets p 46 A88-43218

PASCAUD, P. N.

The geometric workstation, a new approach for geometric corrections of remotely sensed data p 66 N88-24017

PATEL, VIPUL

Satellite remote sensing of turbidity and sediment concentration in Lagoa dos Patos p 56 N88-24032

PATERSON, W. MURRAY

Remote sensing as a tool for assessing environmental effects of hydroelectric development in a remote river basin p 53 A88-42045

PAUKEN, ROBERT J.

Fracture patterns and production trends, Big Sandy Field, eastern Kentucky p 27 A88-32913

PAULSON, RICHARD W.

Overview of remote data transmission systems p 55 A88-45643

PAVLOV, A. M.

Mushroom-shaped currents (eddy dipoles) under rotation and stratification conditions p 47 N88-20678

PECKHAM, G. E.

Microwave instruments and methods p 71 A88-37132

PEDERSEN, J. P.

Sea surface temperature studies in Norwegian coastal areas using AVHRR- and TM thermal infrared data p 44 A88-42047

PELLEMANS, A. H. J. M.

Investigation of the usefulness of speckle analysis in imaging radar systems [BCRS-86-05] p 65 N88-23302

PELLETIER, R. E.

Preliminary investigation of Large Format Camera photography utility in soil mapping and related agricultural applications p 4 A88-41947

A gridding approach to detect patterns of change in coastal wetlands from digital data p 52 A88-41949

PENN, LANNING M.

The 1987 Airborne Antarctic Ozone Experiment: The Nimbus-7 TOMS data atlas [NASA-RP-1201] p 47 N88-20714

PERBOS, J.

Marginal Ice Zone Experiment (MIZEX) 1984 VARAN-S data set [ETN-88-92032] p 48 N88-21625

PEREIRA, M. C.

Detection of biomass burning and smoke plumes in the Amazon region through NOAA satellite imagery p 23 N88-24085

PEREIRADACUNHA, ROBERTO

Radar penetration in the Amazonian rain forest p 13 N88-24015

Anomalies in the vegetation in the Alto Xingu - MT p 14 N88-24043

Radar penetration in the Amazonian rain forest p 15 N88-24044

PERRIER, A. D.

Modeling surface exchanges: The soil-vegetation-atmosphere continuum p 12 N88-21553

PERRY, S. L.

Lineaments of the northern Denver Basin and their paleotectonic and hydrocarbon significance p 28 A88-32920

PETER, KATHY D.

Lineaments: Significance, criteria for determination, and varied effects on ground-water systems - A case history in the use of remote sensing p 55 A88-45636

PETIT, MICHEL

Satellite detected cyanobacteria bloom in the southwestern tropical Pacific - Implication for oceanic nitrogen fixation p 42 A88-39081

PETERSSON, C. B.

Geotechnical applications of remote sensing and remote data transmission; Proceedings of the Symposium, Cocoa Beach, FL, Jan. 31-Feb. 1, 1986 p 35 A88-45634

PEYRON, J. L.

Influence of topography on forest reflectance using Landsat Thematic Mapper and digital terrain data p 2 A88-35397

PFEIFFER, BERTHOLD

Image optimization versus classification - An application oriented comparison of different methods by use of Thematic Mapper data p 59 A88-41964

PIERCE, LARS L.

A methodology for mapping forest latent heat flux densities using remote sensing p 3 A88-37415

PINTO, SERGIO DOSANJOS F.

Evaluation of an estimation system for an irrigated area in a tropical region through TM-LANDSAT imagery p 16 N88-24075

PINTODEGARRIDO, JUAN CARLOS

Analysis for architecture for image processing [INPE-4294-PRE/1165] p 75 N88-20715

PLACE, MICHAEL C.

Use of digitally processed laboratory reflectance spectra for the definition of probable microseepage - Induced mineralogical variations, Lisbon Valley, Utah p 30 A88-32946

PLOURDE, F.

Digital elevation modeling with stereo SIR-B image data p 60 A88-41981

POLIAKOV, V. M.

Method for rapidly estimating geophysical parameters of the ocean-atmosphere system from satellite microwave radiometry p 46 A88-43669

PONZONI, FLAVIO JORGE

A proposal for a project entitled assessment of forest resources in Uruguay submitted to the United Nations Industrial Development Organization (UNIDO) p 13 N88-24016

POPKOV, V. I.

The South Alamyrynian ring structure - A new promising area to search for hydrocarbon deposits p 32 A88-36162

POPOLIZIO, ELISEO

A remote sensing methodological approach for applied geomorphology mapping in plain areas p 35 A88-42034

POPOV, V. P.

Contrast enhancement of aerospace scanner imagery of crop fields p 11 A88-43671

POUWELS, H.

The radiometric processing of SLAR measuring values using the PARES program [BCRS-86-04] p 75 N88-23301

PRANGSMA, G. J.

Processing of raw digital NOAA-AVHRR data for sea- and land applications p 60 A88-41968

PRICE, JOHN C.

An update on visible and near infrared calibration of satellite instruments p 72 A88-37416

- PRINCZ, J. G.**
An effect of coherent scattering in spaceborne and airborne SAR images p 64 A88-44651
- PROVESI, JOSE ROBERTO**
Preliminary study on the application of digital processing of TM-LANDSAT data in the mapping of apple orchards in Fraiburgo (SC) p 17 N88-24093
- PRUETT, FRANK D.**
Application of synthetic aperture radar (SAR) to southern Papua New Guinea fold belt exploration p 26 A88-32902
- Q**
- QUARMBY, N.**
Monitoring geomorphological processes in desert marginal environments using multitemporal satellite imagery p 34 A88-42030
- R**
- RABINOVICH, A. A.**
The South Alamyrian ring structure - A new promising area to search for hydrocarbon deposits p 32 A88-36162
- RAED, M. A.**
Spectral measurements for correcting LANDSAT data for atmospheric effects p 66 N88-24020
- RAITALA, JOUKO T.**
Satellite data in aquatic area research - Some ideas for future studies p 53 A88-42048
- RAMPINO, MICHAEL R.**
Mass extinctions, atmospheric sulphur and climatic warming at the K/T boundary p 46 A88-43835
- RAMSEY, ELIJAH W., III**
Application of Landsat Thematic Mapper data to assess suspended sediment dispersion in a coastal lagoon p 51 A88-41946
- RANEY, R. K.**
An effect of coherent scattering in spaceborne and airborne SAR images p 64 A88-44651
- RANGO, A.**
Rangeland runoff curve numbers as determined from Landsat MSS data p 51 A88-39089
- RAYALU, G. K.**
The modeling of error budget analysis and tolerance specifications for BRESEX multiband linear array CCD camera p 76 N88-24029
- READDY, LEIGH A.**
Importance of fault mapping to mineral/geothermal exploration: Relationship to fluid migration and ore formation - Northwest Washington p 28 A88-32925
- REALMUTO, VINCENT J.**
Color space mapping using ternary/chromaticity diagrams - A technique for composite image interpretation p 57 A88-32932
- REBILLARD, PH.**
Geological analysis of Seasat SAR and SIR-B data in Haiti p 33 A88-41980
The geometric workstation, a new approach for geometric corrections of remotely sensed data p 66 N88-24017
- REED, R.**
Spruce budworm infestation detection using an airborne pushbroom scanner and Thematic Mapper data p 8 A88-42007
- REED, R. J.**
An evaluation of the performance of the ECMWF operational system in analyzing and forecasting easterly wave disturbances over Africa and the tropical Atlantic p 43 A88-39746
- REIFF, J.**
Proposals for the pre-operational use of data from the European Remote Sensing Satellite ERS-1 [BCRS-86-02] p 65 N88-23300
- RESHTOGA, IU. L.**
Comparative analysis of results of photographic observations of natural objects from Salyut-7 p 72 A88-39919
- RIAPOLOV, V. IA.**
Remote-sensing methods for the monitoring and forecasting of the entomological condition of taiga forests p 2 A88-36164
- RIBEIRODOSSANTOS, ATHOS**
Remote sensing and structural rupture: Application examples in the study of tectonics p 37 N88-24050
- RICHARDS, J. A.**
Classification of the Riverina forests of south east Australia using co-registered Landsat MSS and SIR-B radar data p 9 A88-42013
- RICHARDSON, ANNIE**
The Shuttle Imaging Radar B (SIR-B) experiment report [NASA-CR-182923] p 75 N88-23932
- RICHARDSON, PHILIP L.**
The dispersal of the Amazon's water p 43 A88-40059
- RIDLEY, J. K.**
A model of satellite radar altimeter return from ice sheets p 46 A88-43218
- RIENECKER, MICHELE M.**
Mesoscale variability in current meter measurements in the California Current system off northern California p 44 A88-42443
- RIGGIN, PHILIP J.**
Particulate emissions from a mid-latitude prescribed chaparral fire p 3 A88-38805
- RIJKS, H.**
Thematic Mapping by satellite - A new tool for planning and management p 60 A88-41973
- RIKIMARU, ATSUSHI**
Environmental assessment for large scale civil engineering projects with data of DTM and remote sensing p 53 A88-42046
- RINGROSE, SUSAN**
Differentiation of ecological zones in the Okavango Delta, Botswana by classification and contextual analyses of Landsat MSS data p 59 A88-39099
- RIPPLE, WILLIAM J.**
Remote sensing of leaf water status p 4 A88-40784
- RITCHIE, J. C.**
Rangeland runoff curve numbers as determined from Landsat MSS data p 51 A88-39089
- RITCHIE, JERRY C.**
Comparison of measured suspended sediment concentrations with suspended sediment concentrations estimated from Landsat MSS data p 51 A88-39080
- ROBERTODOSSANTOS, JOAO**
The 35 mm vertical aerial photographs for mapping stands of bracinga in different age classes p 16 N88-24087
- ROBINS, ROBERT E.**
Geometric restoration of satellite image data [AD-A190462] p 64 N88-22450
- ROBINSON, E.**
Long-term air quality monitoring at the South Pole by the NOAA program Geophysical Monitoring for Climatic Change p 18 A88-36243
- ROBINSON, ELIZABETH M.**
The effect of a shallow low-viscosity zone on the mantle flow, the geoid anomalies and the geoid and depth-age relationships at fracture zones p 24 A88-38024
- ROCK, BARRETT N.**
A near infrared vegetation index formed with airborne multispectral scanner data p 1 A88-32910
- RODERJAN, CARLOS VELLOZO**
Stereoscopic photographs, ground and aerial, of trees used in the arborization of Curitiba (PR) p 17 N88-24091
- RODHAINÉ, B. A.**
Long-term air quality monitoring at the South Pole by the NOAA program Geophysical Monitoring for Climatic Change p 18 A88-36243
- RONZHIN, L. A.**
Comparative analysis of results of photographic observations of natural objects from Salyut-7 p 72 A88-39919
- ROOZEKRANS, J. N.**
Processing of raw digital NOAA-AVHRR data for sea- and land applications p 60 A88-41968
- ROSA, R.**
Analysis of the parameters responsible for the variations of the illumination conditions in the LANSAT data p 67 N88-24070
Evaluation of the floodable area of the canal of Sao Goncalo through TM-LANDSAT 5 imagery p 56 N88-24078
- ROSA, ROBERTO**
Evaluation of an estimation system for an irrigated area in a tropical region through TM-LANDSAT imagery p 16 N88-24075
- ROSACARNEIRO, PAULO JORGE**
Identification of areas cultivated with soybeans in the cerrados regions, through digital processing of satellite images: A methodological approach p 15 N88-24048
- ROSE, DENNIS ROSS**
Base map production from geocoded imagery p 25 A88-41969
- ROSENBERG, NORMAN**
Satellite UV image processing [AD-A190466] p 65 N88-22451
- ROSENTHAL, DANIEL ALFREDO**
Spectral behavior of crops through analysis of LANDSAT-TM data p 15 N88-24047
- ROSOT, NELSON CARLOS**
The 35 mm vertical aerial photographs for mapping stands of bracinga in different age classes p 16 N88-24087
- ROYER, ALAIN**
Interannual Landsat-MSS reflectance variation in an urbanized temperate zone p 58 A88-37417
Urbanization and Landsat MSS albedo change in the Windsor-Quebec corridor since 1972 p 18 A88-39094
- RUDORFF, BERNARDO F. T.**
Remote sensing techniques in the estimation of the area cultivated with beans, corn, and castor beans in the Itrec County (Bahia State) p 15 N88-24045
- S**
- SABINS, F. F.**
Satellite radars for geologic mapping in tropical regions p 27 A88-32917
- SADOWSKI, FRANK G.**
An approach for emulating the color balance of Landsat multispectral scanner images with AVHRR data p 73 A88-41956
- SADURSKI, ANDRZEJ**
Geological analysis of the satellite lineaments of the Vistula Delta Plain, Zulawy Wislane, Poland p 34 A88-42021
- SAFAR, J.**
The use of multispectral space photographs to draw up a map of land use in western Slovakia p 57 A88-33774
- SAKATA, T.**
Global vegetation monitoring using NOAA GAC data p 8 A88-42012
- SAKATA, TOSHIBUMI**
Evaluations of unsupervised methods for land-cover/use classifications of Landsat TM data p 64 A88-45116
- SALAKHETDINOVA, E. P.**
Investigation and mapping of forests using space scanner imagery obtained in winter p 2 A88-36165
- SALISBURY, JOHN W.**
Preliminary measurements of spectral signatures of tropical and temperate plants in the thermal infrared p 1 A88-32909
- SALOMON, FERDINAND**
Recent developments in software and hardware by Scitex Co. p 68 N88-25038
- SANCHEZ, BRAULIO V.**
Tidal estimation in the Pacific with application to SEASAT altimetry [NASA-TM-100694] p 47 N88-20780
- SANO, E. E.**
Analysis of the parameters responsible for the variations of the illumination conditions in the LANSAT data p 67 N88-24070
Evaluation of the floodable area of the canal of Sao Goncalo through TM-LANDSAT 5 imagery p 56 N88-24078
- SANTIADOBARROS, MARIA SUELENA**
Low altitude remote sensing data in the implementation of a mathematical model for the planning of urban equipment networks p 23 N88-24074
- SANTOS, AUXILIADORA MARIA**
Evaluation of the mangrove area at the Piaui River (SE) through remote sensing p 16 N88-24086
- SARMA, S. V. KAMESWARA**
Identification of shallow groundwater regions in semi-arid Brazil by remote sensing methods p 14 N88-24030
- SATAKE, MAKOTO**
SIR-B experiments in Japan. V. p 4 A88-40355
- SAUBER, JEANNE**
Geodetic measurement of deformation east of the San Andreas Fault in Central California p 25 A88-32831
- SAUBER, JEANNE M.**
Geodetic measurement of deformation east of the San Andreas fault in Central California [NASA-CR-182709] p 36 N88-20754
- SAULL, R. J.**
The effect of atmospheric correction on the interpretation of multitemporal AVHRR-derived vegetation index dynamics p 11 A88-44117
- SAUSEN, TANIA MARIA**
Utilization of LANDSAT-TM, for aiding in the localization of archeological sites in the state of Sao Paulo p 38 N88-24069
Study of reservoir water quality utilizing remote sensing techniques: Methodological concepts p 56 N88-24076
Utilization of LANDSAT-TM imagery in the hydroenergetic inventory of the Paraiba de Sul River Basin p 56 N88-24077
- SAVORSKII, V. P.**
Method for rapidly estimating geophysical parameters of the ocean-atmosphere system from satellite microwave radiometry p 46 A88-43669

SAYAGO, JOSE MANUEL

Small scale erosion hazard mapping using Landsat information in the northwest of Argentina p 9 A88-42035

SCHABER, G. G.

Shuttle imaging radar response from sand dunes and subsurface rocks of Alashan Plateau in north-central China p 33 A88-41978

SCHARDT, M.

Digital classification of forested areas using simulated TM- and SPOT- and Landsat 5/TM-data p 5 A88-41971

SCHMIDT, ARLEN D.

A VHF radar to make terrain elevation models through tropical jungle p 10 A88-42760

SCHOBER, JOSEF

Feasibility study for a 2nd generation system for airborne maritime pollution surveillance [ETN-88-92108] p 55 N88-22466

SCHREIER, H.

Spectral signatures of soils and terrain conditions using lasers and spectrometers p 6 A88-41997

SCHRUMPF, BARRY J.

Remote sensing of leaf water status p 4 A88-40784

SCHUELER, C. F.

Remote sensing technology and applications p 46 A88-44005

SCHURER, K.

Selection of bands for a newly developed multispectral airborne reference-aided calibrated scanner (MARCS) p 74 A88-41995

SCHWALLER, MATHEW R.

A geobotanical investigation of an exploration-sized territory p 29 A88-32931

SCHWERING, FELIX K.

Millimeter-wave propagation in vegetation: Experiments and theory p 12 A88-44319

SCOGGINS, RANDY K.

Thermal modeling and IR scene generation p 63 A88-44534

SCORER, R. S.

Cloud formations seen by satellite p 71 A88-37127

SEARS, STEWART K.

Remote sensing as a tool for assessing environmental effects of hydroelectric development in a remote river basin p 53 A88-42045

SEBACHER, DANIEL I.

Particulate emissions from a mid-latitude prescribed chaparral fire p 3 A88-38805

SECHRIST, FRANK S.

The 1987 Airborne Antarctic Ozone Experiment: The Nimbus-7 TOMS data atlas [NASA-RP-1201] p 47 N88-20714

SEGAL, DONALD B.

Use of digitally processed laboratory reflectance spectra for the definition of probable microseepage - Induced mineralogic variations, Lisbon Valley, Utah p 30 A88-32946

SELIVANOV, V. A.

Remote sensing of the earth's surface in the ultraviolet range p 32 A88-36172

SERAFINI, MARIA C.

Estimation of an area cultivated with wheat from LANDSAT data through a two-phase sampling method p 14 N88-24041

SESOREN, A.

Analysis of Landsat multispectral-multitemporal images for geologic-lithologic map of the Bangladesh Delta p 35 A88-42049

SETTLE, J. J.

Use of digital terrain data in the interpretation of SPOT-1 HRV multispectral imagery p 10 A88-43221

SETTLE, MARK

Processing of multirate Landsat TM data to map soil color variations related to hydrocarbon microseepage in a cropland setting - Cement, Oklahoma test site p 1 A88-32921

SETZER, A. W.

Detection of biomass burning and smoke plumes in the Amazon region through NOAA satellite imagery p 23 N88-24085

SETZER, ALBERTO W.

Evaluation of the mangrove area at the Piaui River (SE) through remote sensing p 16 N88-24086

SHARKOV, E. A.

Radiometric investigation of the sea-wave breaking process p 46 A88-43664

SHAROV, A. I.

Technique for the instrumented interpretation of space scanner imagery of the earth's cloud cover p 69 A88-33832

SHEEHAN, CYNTHIA A.

After exploration, what? - Case histories of seven diverse production, development and distribution applications of remote sensing p 28 A88-32918

SHERRY, CHOU CHEN

Evaluation of TM false color composites for crop discrimination p 17 N88-24096

SHERWOOD, C. R.

Ocean general circulation models: Report on proceedings of a meeting of ocean and climate modelers [DE88-005530] p 49 N88-22504

SHEVTSOV, B. M.

Range variations of the tropospheric propagation of ultrashort radio waves above the sea p 39 A88-33920

SHIEH, HANN-CHIN

Digital processing of airborne MSS data for forest cover types classification p 5 A88-41963

SHIMABUKURO, YOSIO E.

Textural features for image classification in remote sensing p 66 N88-24027

SHIMODA, H.

Global vegetation monitoring using NOAA GAC data p 8 A88-42012

SHIMODA, HARUHISA

Evaluations of unsupervised methods for land-cover/use classifications of Landsat TM data p 64 A88-45116

SHIN, R. T.

Identification of terrain cover using the optimum polarimetric classifier p 3 A88-37370

SHUTKO, A. M.

Taking the effect of vegetation into account in the microwave-radiometer remote sensing of the earth surface on the results of remote sounding of the earth surface by microwave radiometry p 10 A88-43670

SILVA, DAGOBERTO

Mapping of plant associations and the variation of surface water in the Pantanal Mato-Grossense National Park, through remote sensing techniques p 17 N88-24092

SILVEIRAESPINDOLA, CARMEN REGINA

Interpretation of MSS/LANDSAT data for evaluation of physical distribution of mangroves in Cananea-Iguape (SP) p 16 N88-24072

SIMARD, R.

Digital terrain model and image integration for geologic interpretation p 26 A88-32904
Digital elevation modeling with stereo SIR-B image data p 60 A88-41981

SIMONETT, DAVID S.

Simulation of L-band and HH microwave backscattering from coniferous forest stands - A comparison with SIR-B data p 12 A88-44643

SIMPSON, JOANNE

A proposed tropical rainfall measuring mission (TRMM) satellite p 69 A88-33742

SINGH, B. DIDAR

Thematic Mapping from aerial photographs for Kandi Watershed and area development project, Punjab (India) p 9 A88-42024

SINGH, KANWARJIT

Thematic Mapping from aerial photographs for Kandi Watershed and area development project, Punjab (India) p 9 A88-42024

SINGH, S. M.

Transformation of Global Vegetation Index (GVI) data from the polar stereographic projection to an equatorial cylindrical projection p 58 A88-39095
Relation between spectral reflectance and vegetation index p 7 A88-41998

The effect of atmospheric correction on the interpretation of multitemporal AVHRR-derived vegetation index dynamics p 11 A88-44117

SINGHROY, V.

Spectral geobotanical investigation of mineralized till sites p 29 A88-32934

SINGHROY, VERN H.

Landsat TM data as an aid in planning and interpretation of regional geochemical surveys in the Canadian Shield p 31 A88-32950

SINGHROY, VERNON H.

Case studies on the application of remote sensing data to geotechnical investigations in Ontario, Canada p 35 A88-45635

SKIDMORE, A. K.

Classification of the Riverina forests of south east Australia using co-registered Landsat MSS and SIR-B radar data p 9 A88-42013

SLANEY, R.

Digital terrain model and image integration for geologic interpretation p 26 A88-32904

SLATER, P. N.

The absolute radiometric calibration of the advanced very high resolution radiometer [NASA-CR-182755] p 75 N88-21584

SLOBODA, S.

The use of multispectral space photographs to draw up a map of land use in western Slovakia p 57 A88-33774

SLOGGETT, D. R.

Earthscan - A range of remote sensing systems p 61 A88-41982

SMIT, G. SICCO

Remote sensing for resources development and environmental management; Proceedings of the Seventh International Symposium, Enschede, Netherlands, Aug. 25-29, 1986, Volumes 1, 2, & 3 p 18 A88-41961

SMITH, ROBERT L.

Mesoscale variability in current meter measurements in the California Current system off northern California p 44 A88-42443

SNEED, JIM

Application of Landsat Thematic Mapper data to assess suspended sediment dispersion in a coastal lagoon p 51 A88-41946

SOEISOLO, INDROYONO

Evaluation of digitally processed Landsat imagery and SIR-A imagery for geological analysis of West Java region, Indonesia p 33 A88-41983

SOLEWICZ, REINALDO

Comparison of surface current determined from satellite-tracked buoy with shipboard wind data during the 4th Brazilian antarctic expedition, 10-14 March, 1986 p 49 N88-24024

SOLOMON, SEAN C.

Geodetic measurement of deformation east of the San Andreas Fault in Central California p 25 A88-32831
Geodetic measurement of deformation east of the San Andreas fault in Central California [NASA-CR-182709] p 36 N88-20754

SONDHEIM, MARK

Base map production from geocoded imagery p 25 A88-41969

SOUZASAMPAIO, OSVALDO

Study of fracturing for groundwater research in the Sergipe state with remote sensing products p 38 N88-24052

SPATZ, D. M.

Influence of mineral coatings and vegetation on TM imagery over Tertiary Caldera lithologies basin and range province, western U.S. p 32 A88-41945

SPENCER, RAY D.

Canadian large-scale aerial photographic systems (LSP) p 70 A88-35395

SPITZER, D.

Determination of spectral signature of natural water by optical airborne and shipborne instruments p 44 A88-42050

Classification of bottom composition and bathymetry of shallow waters by passive remote sensing p 53 A88-42051

SPRINGER, J.

Spectral geobotanical investigation of mineralized till sites p 29 A88-32934

STAKENBERG, J. H. T.

Per-field classification of a segmented SPOT simulated image p 60 A88-41970

STANSELL, THOMAS A., JR.

The Magnavox civil and military line of GPS receivers - A technology and applications overview p 72 A88-37391

STANTON-GRAY, R.

Spectral geobotanical investigation of mineralized till sites p 29 A88-32934

STANTON-GRAY, ROBERTA

Landsat TM data as an aid in planning and interpretation of regional geochemical surveys in the Canadian Shield p 31 A88-32950

STEELE, L. P.

Long-term air quality monitoring at the South Pole by the NOAA program Geophysical Monitoring for Climatic Change p 18 A88-36244

STEFFEN, KONRAD

Surface temperatures and sea ice typing for northern Baffin Bay p 42 A88-39088

STEPHENS, SCOTT A.

Effect of wet tropospheric path delays on estimation of geodetic baselines in the Gulf of California using the Global Positioning System p 25 A88-4183

STEVENSON, MERRITT R.

Comparison of surface current determined from satellite-tracked buoy with shipboard wind data during the 4th Brazilian antarctic expedition, 10-14 March, 1986 p 49 N88-24024

Near surface current determined from INPE satellite-tracked buoy, during 6-26 November, 1985 p 50 N88-2405

STEWART, ROBERT H.

Topex/Poseidon - A contribution to the world climate research program [AAS PAPER 86-306] p 39 A88-3505

STEYAERT, LOUIS T.

Operational satellite data assessment for drought/disaster early warning in Africa - Comments on GIS requirements p 19 A88-4201

- STIBIG, H.-J.**
Digital classification of forested areas using simulated TM- and SPOT- and Landsat 5/TM-data
p 5 A88-41971
- STOW, DOUGLAS A.**
Remote sensing and image processing requirements for Eulerian flow field estimations
p 51 A88-39078
- STRONKHORST, J.**
Turbidity patterns in the delta waters of southwest Netherlands on Thematic Mapper (TM) and multispectral scanner (MSS) satellite images
[BCRS-86-06]
p 55 N88-23303
- STUART, JOHN D.**
Remote sensing and the role of terrestrial vegetation in the global carbon cycle
p 5 A88-41954
- STUART, NEIL**
Evaluation of regional land resources using geographic information systems based on linear quadrees
p 20 A88-42063
- STUMPF, RICHARD P.**
Satellite detection of bloom and pigment distributions in estuaries
p 51 A88-37414
- SUBRAMANYAN, V.**
Satellite remote sensing of the coastal environment of Bombay
p 61 A88-42052
- SUITZ, TAKESHI**
SIR-B experiments in Japan. II - Rice crop experiment
p 4 A88-40352
- SUN, GUO-QING**
Simulation of L-band and HH microwave backscattering from coniferous forest stands - A comparison with SIR-B data
p 12 A88-44643
- SUVIRES, GRACIELA M.**
Dune fields in central Western Argentina
p 38 N88-24088
The broken anticlines, cuesta and crest homoclines, oroclinal valleys, and other forms of relief outcrops delineated with the help of remote sensing imagery
p 16 N88-24089
Geomorphologic sector maps of Niquizanga-Mayares, province of San Juan, Argentina
p 38 N88-24098
- SUYO RIVERA, EPIFANIO**
Geologic interpretation of air photos and radar imagery for hydroelectric power projects in Upper Ucayali Jungle Region of Peru
p 28 A88-32922
- SVANTESSON, MATTI**
Terrain classification using SPOT images and the computer system GOP-300
[FOA-C-20677-2.7]
p 68 N88-24102
- SVEJKOVSKY, JAN**
Sea surface flow estimation from advanced very high resolution radiometer and coastal zone color scanner satellite imagery - A verification study
p 44 A88-42444
- SWART, P. J. F.**
Relating L-band scatterometer data with soil moisture content and roughness
p 5 A88-41984
- SWARTZ, A. A.**
Identification of terrain cover using the optimum polarimetric classifier
p 3 A88-37370
- T**
- TAHERKIA, H.**
Classification of land features, using Landsat MSS data in a mountainous terrain
p 19 A88-41972
- TANAKA, KEIKO**
Calibration and processing of AVHRR data for temperature estimation
[INPE-4493-PRE/1257]
p 65 N88-22485
- TAPPER, G. O.**
Shift in spectral response of nickel-loaded and control shoots of white birch
p 1 A88-32928
Surrogate spectral reflectances of vegetation applied to geobotanical remote sensing
p 1 A88-32935
- TARANIK, J. V.**
Correlation between high resolution remote sensing imagery and hydrothermal alteration, Tybo mining district, Nevada
p 27 A88-32915
Influence of mineral coatings and vegetation on TM imagery over Tertiary Caldera lithologies basin and range province, western U.S.
p 32 A88-41945
- TARANIK, JAMES V.**
Application of aerospace remote sensing to geological investigations in Nevada and California
[AAS PAPER 86-400]
p 32 A88-35160
Potential for earth observations from the manned Space Station
[AAS PAPER 86-426]
p 70 A88-35162
Structural geology and regional tectonics of the Mineral County area, Nevada, using Shuttle Imaging Radar-B and digital aeromagnetic data
p 35 A88-44646
- TASSAN, S.**
The effect of dissolved 'yellow substance' on the quantitative retrieval of chlorophyll and total suspended sediment concentrations from remote measurements of water colour
p 46 A88-43226
- TAUCH, RUEDIGER**
Comparison of classification results of original and preprocessed satellite data
p 59 A88-41965
- TAVARESDEMATOS, JUERCIO**
Study of fracturing for groundwater research in the Sergipe state with remote sensing products
p 38 N88-24052
- TAYLOR, G. R.**
Integration of SIR-B imagery with geological and geophysical data in Australia
p 27 A88-32912
Pattern recognition and geological interpretation of SIR-B images of Central Australia
p 31 A88-32956
- TAYLOR, JOHN**
Mapping soil and rock variation from satellite images in the Sahel
p 14 N88-24023
Satellite remote sensing of turbidity and sediment concentration in Lagoa dos Patos
p 56 N88-24032
- TAYLOR, JOHN C.**
The use of multitemporal Landsat data for improving crop mapping accuracy
p 7 A88-42003
- TEILLET, P. M.**
The absolute radiometric calibration of the advanced very high resolution radiometer
[NASA-CR-182755]
p 75 N88-21584
- TEILLET, PHILIPPE M.**
Interannual Landsat-MSS reflectance variation in an urbanized temperate zone
p 58 A88-37417
- TEIXEIRA, A. L. A.**
Implantation of a geo-cartographical information system through microcomputers
p 67 N88-24064
- THETFORD, WARREN**
Economic potential of Landsat Thematic Mapper data for crop condition assessment of winter wheat
p 4 A88-41948
- THIESSEN, RICHARD L.**
Geologic spatial analysis - A new multiple data source exploration tool
p 30 A88-32947
- TIBALDI, ALESSANDRO**
Potential of Landsat Thematic Mapper image for crystalline rock type discrimination - Gregory Rift, Kenya
p 32 A88-35192
Computer processing of satellite data for geostructural zoning of a collisional boundary, significance and field checks - The example of Tunisia
p 32 A88-35193
- TKACH, STEVEN J.**
Contribution of Landsat to a geologic expedition in the desert of North Central Sudan, Africa
p 27 A88-32916
A geobotanical investigation of an exploration-sized territory
p 29 A88-32931
- TODD, WILLIAM J.**
Spatial resolution requirements for urban land cover mapping from space
p 20 A88-42058
- TOMASONI, R.**
Digital analysis of stereo pairs for the detection of anomalous signatures in geothermal fields
p 61 A88-42037
- TOMMERVIK, H.**
Comparison of SPOT-simulated and Landsat 5 TM imagery in vegetation mapping
p 9 A88-42014
- TONN, W.**
Vegetation indices and other vegetation parameters - Examples, interpretation and problems
p 3 A88-38373
- TORII, KIYOSHI**
The 'Tsukusys' image processing system and its utilization in Thematic Mapper investigations of water quality conditions
p 54 A88-45115
- TOUTIN, T.**
Digital elevation modeling with stereo SIR-B image data
p 60 A88-41981
- TOWNSEND, T. E.**
Detection of geologic features in Landsat TM imagery not revealed in Landsat MSS imagery
p 30 A88-32944
- TOWNSHEND, J. R. G.**
Monitoring geomorphological processes in desert marginal environments using multitemporal satellite imagery
p 34 A88-42030
- TRALLI, DAVID M.**
Effect of wet tropospheric path delays on estimation of geodetic baselines in the Gulf of California using the Global Positioning System
p 25 A88-41835
- TREFRY, JOHN H.**
Distribution and chemistry of suspended particles from an active hydrothermal vent site on the Mid-Atlantic Ridge at 26 deg N
p 42 A88-37720
- TROCINE, ROBERT P.**
Distribution and chemistry of suspended particles from an active hydrothermal vent site on the Mid-Atlantic Ridge at 26 deg N
p 42 A88-37720
- TURNER, B.**
Landsat temporal-spectral profiles of crops on the South African highveld
p 7 A88-41999
- TYLER, MARY A.**
Satellite detection of bloom and pigment distributions in estuaries
p 51 A88-37414
- U**
- UCHIDA, SATOSHI**
On the regional characteristics of actual evapotranspiration derived from Landsat MSS and elevation data
p 54 A88-45118
- UENO, SUEO**
Radiometric correction for atmospheric and topographic effects on Landsat MSS images
p 62 A88-43223
- UIMANOVA, L. N.**
The use of space data to study Precambrian structures
p 32 A88-36161
- ULABY, FAWWAZ T.**
Millimeter-wave bistatic scattering from ground and vegetation targets
p 11 A88-44308
- V**
- VAILLANT, D.**
Marginal Ice Zone Experiment (MIZEX) 1984 VARAN-S data set
[ETN-88-92032]
p 48 N88-21625
Definition and implementation study for the Varan-S radar
[CNES-CT/DRT/TIT/RL-143-T]
p 48 N88-22267
- VALDES ALATAMIRA, JOSE A.**
Assessment of TM thermal infrared band contribution in land cover/land use multispectral classification
p 61 A88-42016
- VALENZUELA, CARLOS R.**
Assessment of TM thermal infrared band contribution in land cover/land use multispectral classification
p 61 A88-42016
- VALERIANO, DALTON DEM.**
Evaluation of the mangrove area at the Piaui River (SE) through remote sensing
p 16 N88-24086
- VALERIANO, DALTON DEMORISSON**
Preliminary study on the application of digital processing of TM-LANDSAT data in the mapping of apple orchards in Fraiburgo (SC)
p 17 N88-24093
- VAN DEN BRINK, J. W.**
Thematic Mapping by satellite - A new tool for planning and management
p 60 A88-41973
A study with NOAA-7 AVHRR-imagery in monitoring ephemeral streams in the lower catchment area of the Tana River, Kenya
p 54 A88-42053
- VAN DER VEGT, H. J. W.**
G.P.S. surveying in the Netherlands
p 72 A88-37383
- VAN DEVENTER, TAHERA E.**
Millimeter-wave bistatic scattering from ground and vegetation targets
p 11 A88-44308
- VAN GILS, H. A. M. J.**
Multi-temporal Landsat for land unit mapping on project scale of the Sudd-floodplain, Southern Sudan
p 9 A88-42015
- VAN KONIJNENBURG, R.**
Monitoring of renewable resources in equatorial countries
p 19 A88-42000
- VANGELDORP, G. H. M.**
From satellite altimetry to ocean topography, a survey of data processing techniques
[ETN-88-91841]
p 48 N88-21575
- VANOUPINES, P. I. G. M.**
A simple atmospheric correction algorithm for Landsat Thematic Mapper satellite images
p 61 A88-42054
- VANSWOL, R. W.**
Study of the plan for a national data center for the European Remote Sensing Satellite ERS-1
[BCRS-87-11]
p 66 N88-23309
- VAUGHAN, R. A.**
Circulation patterns in AVHRR imagery
p 46 A88-43217
- VAUGHAN, ROBIN A.**
Remote sensing applications in meteorology and climatology; Proceedings of the NATO Advanced Study Institute, Dundee, Scotland, Aug. 17-Sept. 6, 1986
p 71 A88-37126
- VENEZIANI, PAULO**
Study of fracturing for groundwater research in the Sergipe state with remote sensing products
p 38 N88-24052
- VERGO, NORMA**
Spectral discrimination of zeolites and dioctahedral clays in the near-infrared
p 28 A88-32926

- VERHEIJ, L. F.**
Coupling of satellite remote sensing to digitized topographic map to detect changes in land use [B8735129] p 23 N88-24104
- VERMILLION, C. H.**
The role of space borne imaging radars in environmental monitoring: Some shuttle imaging radar results in Asia [NASA-TM-101178] p 23 N88-24844
- VERSTAPPEN, H. TH.**
Remote sensing for resources development and environmental management; Proceedings of the Seventh International Symposium, Enschede, Netherlands, Aug. 25-29, 1986. Volumes 1, 2, & 3 p 18 A88-41961
- VETTORAZZI, CARLOS A.**
Utilization of TM/LANDSAT images in the implanted forests mapping in the Mogi-Guacu Region (SP-Brazil) p 14 N88-24042
- VICKERS, ROGER S.**
A VHF radar to make terrain elevation models through tropical jungle p 10 A88-42760
- VIDAL-MADJAR, DANIEL**
Measurement of the water content of soil from space and application to the regional water balance p 55 N88-21561
- VIJAYKUMAR, NANDAMUDI LANKALAPALLI**
Low altitude remote sensing data in the implementation of a mathematical model for the planning of urban equipment networks p 23 N88-24074
- VIKTOROV, S. V.**
Parameters of eddy structures and mushroom currents in the Baltic Sea derived from satellite imagery p 46 A88-43665
- VIOLETTE, EDMOND J.**
Millimeter-wave propagation in vegetation: Experiments and theory p 12 A88-44319
- VIXO, DARCY L.**
After exploration, what? - Case histories of seven diverse production, development and distribution applications of remote sensing p 28 A88-32918
- VLASOV, A. A.**
Possibility of replacing complex values of permittivity with real values p 44 A88-41398
- VOIGT, THOMAS**
Coastal monitoring by remote sensing p 54 A88-44447
- VOLK, P.**
Integration of remote sensing and other geo-data for ore exploration - A SW-Iberian case study p 31 A88-32952
- VOLK, TYLER**
Mass extinctions, atmospheric sulphur and climatic warming at the K/T boundary p 46 A88-43835
- VOZMAN, I. P.**
Comparison of radar and microwave radiometer techniques for determining permittivity p 74 A88-44231

W

- WACKERMAN, CHRISTOPHER C.**
A statistical model for prediction of precision and accuracies of radar scattering coefficient measurements derived from SAR data p 62 A88-42771
- WADA, H.**
An evaluation of potential uranium deposit area by Landsat data analysis in Officer Basin, South-Western part of Australia p 35 A88-42036
- WAITES, JANE E.**
Surface expression of subsurface structures in the Michigan Basin p 29 A88-32929
- WAKKER, K. F.**
From satellite altimetry to ocean topography, a survey of data processing techniques [ETN-88-91841] p 48 N88-21575
- WALTON, CHARLES C.**
Nonlinear multichannel algorithms for estimating sea surface temperature with AVHRR satellite data p 39 A88-34643
- WEAKS, MARCIA**
A PC-based interactive graphics system to perform satellite-derived oceanographic thermal analysis p 68 A88-32850
- WEAVER, RONALD**
Passive microwave data for snow and ice research - Planned products from the DMSP SSM/I system p 40 A88-35199
- WEGENER, M.**
Ocean-atmosphere interactions in low latitude Australasia p 41 A88-37270
Non-tracking antenna systems for the acquisition of NOAA HRPT Data p 72 A88-37279
- WEISS, DIETRICH**
Coastal monitoring by remote sensing p 54 A88-44447

- WELCH, R.**
Cartographic feature extraction with integrated SIR-B and Landsat TM images p 63 A88-44641
- WERLE, DIRK**
Shuttle imaging radar (SIR-A) interpretation of the Kashgar region in western Xinjiang, China p 74 A88-41985
- WERNAND, M. R.**
Determination of spectral signature of natural water by optical airborne and shipborne instruments p 44 A88-42050
- WESTMAN, WALTER E.**
Monitoring the environment by remote sensing p 18 A88-33770
- WHEELER, DOUGLAS J.**
Spectral characterization of urban land covers from Thematic Mapper data p 20 A88-42059
- WILKINS, G.**
Non-tracking antenna systems for the acquisition of NOAA HRPT Data p 72 A88-37279
- WILLIAMS, DARREL L.**
Obtaining spectral reflectance factor measurements of stressed forest vegetation p 5 A88-41952
- WINSTEAD, EDWARD L.**
Particulate emissions from a mid-latitude prescribed chaparral fire p 3 A88-38805
- WITTMANN, PAUL A.**
Hydrographic data from the OPTOMA (Ocean Prediction Through Observation, Modeling and Analysis) program: OPTOMA 23, 9-19 November 1986 [AD-A189868] p 49 N88-22506
- WOOD, J. W.**
The production of distortion free SAR imagery p 57 A88-33377
- WOODGATE, P. W.**
Classification of the Riverina forests of south east Australia using co-registered Landsat MSS and SIR-B radar data p 9 A88-42013
- WRIGHT, G. G.**
Potato crop distribution and subdivision on soil type and potential water deficit - An integration of satellite imagery and environmental spatial database p 10 A88-43222
- WRIGLEY, ROBERT C.**
Spatial resolution requirements for urban land cover mapping from space p 20 A88-42058
- WU, S. C.**
Precision positioning of earth orbiting remote sensing systems [AAS PAPER 86-398] p 70 A88-35159
- WYATT, B. K.**
Use of digital terrain data in the interpretation of SPOT-1 HRV multispectral imagery p 10 A88-43221
- WYATT, BARRY**
Mapping soil and rock variation from satellite images in the Sahel p 14 N88-24023

X

- XU, RUISONG**
Analysis of lineaments and major fractures in Xichang-Dukou area, Sichuan province as interpreted from Landsat images p 34 A88-42022

Y

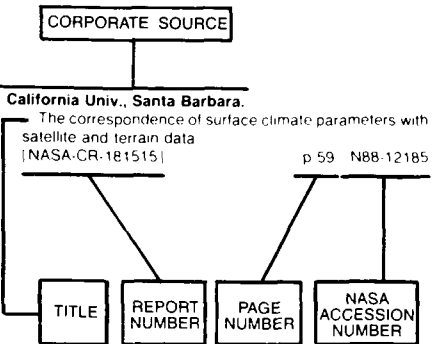
- YAMAGATA, YOSHIKI**
Flood damage analysis using multitemporal Landsat Thematic Mapper data p 4 A88-39090
- YAMAGUCHI, RYOUJI**
Evaluations of unsupervised methods for land-cover/use classifications of Landsat TM data p 64 A88-45116
- YAMAGUCHI, YASUSHI**
Identification of clay minerals by feature coding of near-infrared spectra p 30 A88-32942
- YAMAZAKI, YOSHIHIRO**
Calibration and processing of AVHRR data for temperature estimation [INPE-4493-PRE/1257] p 65 N88-22485
- YANG, HSIEN-MIN**
Application of spatial statistics to analyzing multiple remote sensing data sets p 64 A88-45639
- YATH, Y. A.**
Multi-temporal Landsat for land unit mapping on project scale of the Sudd-floodplain, Southern Sudan p 9 A88-42015
- YAZDANI, R.**
Assessment of digital enhancement techniques using Landsat TM data in mapping geologic lineaments, with application to the Mactaquac headpond area, southern New Brunswick p 31 A88-32949
- YEN, CHIEH-CHENG J.**
Determinations of suspended sediment concentrations from multiple day Landsat and AVHRR data p 54 A88-44120

- YOSHIKADO, SHIN**
SIR-B experiments in Japan. II - Rice crop experiment p 4 A88-40352
SIR-B experiments in Japan. V. p 4 A88-40355
- YOUNG, STEPHEN**
Associations among lineaments, subsurface fractures, hydrocarbon microseepage, and production in the Uinta Basin, Utah p 27 A88-32908
- YUEH, H. A.**
Identification of terrain cover using the optimum polarimetric classifier p 3 A88-37370
- YUNCK, T. P.**
Precision positioning of earth orbiting remote sensing systems [AAS PAPER 86-398] p 70 A88-35159

Z

- ZANDBERGEN, R. C. A.**
From satellite altimetry to ocean topography, a survey of data processing techniques [ETN-88-91841] p 48 N88-21575
- ZEGHERU, N.**
Land resource use monitoring in Romania, using aerial and space data p 21 A88-42065
- ZEMANN, ARNOLD**
Kartoflex - An instrument for computer-aided photointerpretation and map revision p 74 A88-44450
- ZETH, ULRICH**
New features of the LMK aerial camera system p 74 A88-44449
- ZEVENBERGEN, A. W.**
Rangeland runoff curve numbers as determined from Landsat MSS data p 51 A88-39089
- ZHANG, FENGYING**
Retrieval of atmospheric temperature structure from the NOAA-9 satellite p 72 A88-37336
- ZHANG, WENHUA**
Analysis of lineaments and major fractures in Xichang-Dukou area, Sichuan province as interpreted from Landsat images p 34 A88-42022
- ZHANG, ZHIMIN**
A method for calculating the effective emissivity of a groove structure p 40 A88-35986
- ZHONG, QIANG**
Satellite observation of surface albedo over the Qinghai-Xinjiang plateau region p 24 A88-39518
- ZILIOI, E.**
Digital analysis of stereo pairs for the detection of anomalous signatures in geothermal fields p 61 A88-42037

Typical Corporate Source Index Listing



Listings in this index are arranged alphabetically by corporate source. The title of the document is used to provide a brief description of the subject matter. The page number and the accession number are included in each entry to assist the user in locating the abstract in the abstract section. If applicable, a report number is also included as an aid in identifying the document.

A

Alabama A & M Univ., Huntsville.
Development of remote sensing techniques capable of delineating soils as an aid to soil survey
[NASA-CR-182610] p 13 N88-22452

Alaska Univ., Fairbanks.
Influence of the Yukon River on the Bering Sea
[NASA-CR-182802] p 50 N88-24126

Analytic Sciences Corp., Reading, Mass.
The effect of a shallow low-viscosity zone on the mantle flow, the geoid anomalies and the geoid and depth-age relationships at fracture zones p 24 A88-38024

Arizona Univ., Tucson.
Radiative surface temperatures of the burned and unburned areas in a tallgrass prairie p 3 A88-37418
The absolute radiometric calibration of the advanced very high resolution radiometer
[NASA-CR-182755] p 75 N88-21584

Army Cold Regions Research and Engineering Lab., Hanover, N.H.
Ice conditions along the Ohio River as observed on LANDSAT images, 1972-1985
[AD-A191172] p 57 N88-25018

B

Begeleidingscommissie Remote Sensing, Delft (Netherlands).
Proposals for the pre-operational use of data from the European Remote Sensing Satellite ERS-1
[BCRS-86-02] p 65 N88-23300
The radiometric processing of SLAR measuring values using the PARES program
[BCRS-86-04] p 75 N88-23301
Investigation of the usefulness of speckle analysis in imaging radar systems
[BCRS-86-05] p 65 N88-23302

Turbidity patterns in the delta waters of southwest Netherlands on Thematic Mapper (TM) and multispectral scanner (MSS) satellite images
[BCRS-86-06] p 55 N88-23303
Results of the testing of the segmentation program on RESEDA
[BCRS-87-01] p 65 N88-23304
Study of the plan for a national data center for the European Remote Sensing Satellite ERS-1
[BCRS-87-11] p 66 N88-23309

Bohan (Walter A.) Co., Park Ridge, Ill.
NIMBUS-7 CZCS. Coastal Zone Color Scanner imagery for selected coastal regions. North America - Europe. South America - Africa - Antarctica. Level 2 photographic product
[NASA-CR-180755] p 48 N88-22447

BP Mineracao Ltda., Rio de Janeiro (Brazil).
Tornado tracks in Southwestern Brazil, Eastern Paraguay, and Northwestern Argentina p 23 N88-24071

C

California Univ., Berkeley.
Monitoring the environment by remote sensing p 18 A88-33770
A methodology for mapping forest latent heat flux densities using remote sensing p 3 A88-37415

California Univ., La Jolla.
Snow melt on sea ice surfaces as determined from passive microwave satellite data p 42 A88-38691
Time evolution of surface chlorophyll patterns from cross-spectrum analysis of satellite color images p 45 A88-42446

California Univ., Santa Barbara.
The dangers of underestimating the importance of data adjustments in band ratioing p 62 A88-43225
Simulation of L-band and HH microwave backscattering from coniferous forest stands - A comparison with SIR-B data p 12 A88-44643

Centre National d'Etudes des Telecommunications, Issy-les-Moulineaux (France).
Measurement of the water content of soil from space and application to the regional water balance p 55 N88-21561

Centre National d'Etudes Spatiales, Toulouse (France).
Study of the dynamic topography of oceans by means of satellite altimetry p 47 N88-21567
Marginal Ice Zone Experiment (MIZE) 1984 VARAN-S data set p 48 N88-21625
[ETN-88-92032] p 48 N88-21625
Definition and implementation study for the Varan-S radar
[CNES-CT/DRT/TIT/RL-143-T] p 48 N88-22267

Chevron Oil Field Research Co., La Habra, Calif.
Satellite radars for geologic mapping in tropical regions p 27 A88-32917

Colorado Univ., Boulder.
Space geodesy and earthquake prediction
[AAS PAPER 86-307] p 24 A88-35156
Correlation between aircraft MSS and LIDAR remotely sensed data on a forested wetland in South Carolina p 5 A88-41951
Remote sensing for non-renewable resources - Satellite and airborne multiband scanners for mineral exploration p 35 A88-42068

Colespan, Inc., Boulder, Colo.
Passive microwave data for snow and ice research - Planned products from the DMSF SSM/I system p 40 A88-35199

Columbia Univ., New York, N.Y.
Polynyas in the Southern Ocean p 43 A88-39284

Comision Nacional de Investigaciones Espaciales, Buenos Aires (Argentina).
Spectral measurements for correcting LANDSAT data for atmospheric effects p 66 N88-24020
Shape detection in remote sensing through graph isomorphism p 67 N88-24028

Cornell Univ., Ithaca, N.Y.
Discrimination and supervised classification of volcanic flows of the Puna-Altiplano, Central Andes Mountains using Landsat TM data p 31 A88-32948
A demonstration of stereophotogrammetry with combined SIR-B and Landsat TM images p 63 A88-44650

D

Dartmouth Coll., Hanover, N.H.
Remote sensing of geobotanical associations in clastic sedimentary terrane p 31 A88-32951

Delaware Univ., Newark.
Remote sensing of biomass of salt marsh vegetation in France p 3 A88-39082

Domier-Werke G.m.b.H., Friedrichshafen (West Germany).
Feasibility study for a 2nd generation system for airborne maritime pollution surveillance
[ETN-88-92108] p 55 N88-22466

E

Empresa Brasileiro de Pesquisa Agropecuaria, Planaltina.
Identification of areas cultivated with soybeans in the cerrados regions, through digital processing of satellite images: A methodological approach p 15 N88-24048

Environmental Protection Agency, Research Triangle Park, N.C.
Assessment of crop loss from air pollutants: Meteorology-atmospheric chemistry and long range transport
[PB88-146857] p 12 N88-22448

European Space Agency, Paris (France).
International cooperation in remote sensing: The ESA experience p 77 N88-24038

Executive Office of the President, Washington, D. C.
Aeronautics and space report of the President: 1986 activities p 77 N88-21087

F

Fundacao Univ. do Rio Grande (Brazil).
Evaluation of the floodable area of the canal of Sao Goncalo through TM-LANDSAT 5 imagery p 56 N88-24078

G

Geological Survey, Baton Rouge, La.
A comparison of airborne GEMS/SAR with satellite-borne Seasat/SAR radar imagery - The value of archived multiple data sets p 64 A88-45640

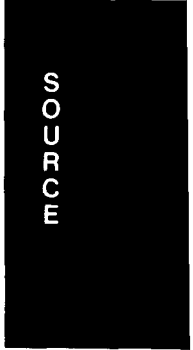
Geological Survey, Menlo Park, Calif.
Geodetic measurement of deformation east of the San Andreas Fault in Central California p 25 A88-32831
Geodetic measurement of deformation east of the San Andreas fault in Central California
[NASA-CR-182709] p 36 N88-20754

Geological Survey, Reston, Va.
Preliminary measurements of spectral signatures of tropical and temperate plants in the thermal infrared p 1 A88-32909

Geological Survey, Tacoma, Wash.
Satellite and aircraft passive microwave observations during the Marginal Ice Zone Experiment in 1984 p 45 A88-42447

Georgia Univ., Athens.
Cartographic feature extraction with integrated SIR-B and Landsat TM images p 63 A88-44641

Gregory Geoscience Ltd., Ottawa (Ontario).
Remote sensing and data integration: Practical solutions for resource managers p 22 N88-24034



IBGE/DRN/BA SEPLAN, Salvador (Brazil).

Lithostructural interpretation of Chapda do Cachimbo (Pa-Am-Mt), based on radar and LANDSAT imagery p 39 N88-24100

Indian Association for the Cultivation of Science, Calcutta.

Landuse and landform studies of the Mahanadi River Delta with the help of satellite MSS band p 56 N88-24033

Institut Français de Recherche pour l'Exploitation de la Mer, Brest (France).

Basic networks of TOGA: Determination of thermal profiles by XBT and of sea level by tide gage p 48 N88-21568

Institut fuer Angewandte Geodaesie, Frankfurt am Main (West Germany).

Contributions to geodesy, photogrammetry and cartography. Series 1, number 46 [ISSN-0469-4244] p 25 N88-23279
Tests for the automatic pattern recognition of building surfaces by the TK 50 p 68 N88-25030
Recent developments in software and hardware by Scitex Co. p 68 N88-25038

Institut National de la Recherche Agronomique, Paris (France).

Modeling surface exchanges: The soil-vegetation-atmosphere continuum p 12 N88-21553

Institute of Ocean Sciences, Sidney (British Columbia).

Time evolution of surface chlorophyll patterns from cross-spectrum analysis of satellite color images p 45 A88-42446

Instituto de Economia e Pesquisas, Aracaju (Brazil).

Study of fracturing for groundwater research in the Sergipe state with remote sensing products p 38 N88-24052

Instituto de Pesquisas Espaciais, Sao Jose dos Campos (Brazil).

Restoration techniques for redisplay of LANDSAT-5 satellite imagery [INPE-4189-PRE/1076] p 64 N88-20712

Analysis for architecture for image processing [INPE-4294-PRE/1165] p 75 N88-20715

Updating of the municipal official register of real estate through a geographical information system [INPE-4459-PRE/1238] p 21 N88-22453

Method for restoration and resampling of TM sensor imagery [INPE-4491-PRE/1255] p 65 N88-22454

Project CODEAMA/FUNCATE (test-area of Barreirinha-AM): Field report [INPE-4500-RPE/563] p 55 N88-22455

Comparative utilization of analog and digital processes in the treatment of MSS-LANDSAT data for studying the national parks of Brazil [INPE-4011-TDL/240] p 21 N88-22456

Calibration and processing of AVHRR data for temperature estimation [INPE-4493-PRE/1257] p 65 N88-22485

Orbital remote sensing: An instrument for monitoring urban growth [INPE-4456-PRE/1287] p 22 N88-22833

Use of energy emission for detecting the necessity of irrigation in wheat in field conditions [INPE-4461-TDL/318] p 13 N88-23315

Detection, monitoring and analysis of some environmental effects of fires in the Amazon region through utilization of NOAA and LANDSAT satellite imagery and aircraft data [INPE-4503-TDL/326] p 13 N88-23322

Applications of multitemporal compositions obtained from LANDSAT data in the study of urban growth [INPE-4480-PRE/1246] p 22 N88-23692

Updating land-use of the Sao Jose dos Campos municipality through remote sensing data [INPE-4479-RPE/562] p 22 N88-23693

Latin American Symposium on Remote Sensing. 4th Brazilian Remote Sensing Symposium and 6th SELPER Plenary Meeting, volume 1 p 75 N88-24013

A proposal for a project entitled assessment of forest resources in Uruguay submitted to the United Nations Industrial Development Organization (UNIDO) p 13 N88-24016

Comparison of surface current determined from satellite-tracked buoy with shipboard wind data during the 4th Brazilian antarctic expedition, 10-14 March, 1986 p 49 N88-24024

Textural features for image classification in remote sensing p 66 N88-24027

The modeling of error budget analysis and tolerance specifications for BRESEX multiband linear array CCD camera p 76 N88-24029

Anomalies in the vegetation in the Alto Xingu - MT p 14 N88-24043

Remote sensing techniques in the estimation of the area cultivated with beans, corn, and castor beans in the Irecê County (Bahia State) p 15 N88-24045

CANASATE: Sugar cane mapping by satellite p 15 N88-24046

Spectral behavior of crops through analysis of LANDSAT-TM data p 15 N88-24047

Structure and dynamics of vegetation in the middle semi-arid tropics. Quixaba's Caatinga (PE): Terrain analysis of MSS/LANDSAT data p 15 N88-24049

Remote sensing and structural rupture: Application examples in the study of tectonics p 37 N88-24050

Near surface current determined from INPE's satellite-tracked buoy, during 6-26 November, 1985 p 50 N88-24058

Study of methods of post-processing applied to a problem of standard classification p 67 N88-24067

Utilization of LANDSAT-TM, for aiding in the localization of archeological sites in the state of Sao Paulo p 38 N88-24069

Analysis of the parameters responsible for the variations of the illumination conditions in the LANDSAT data p 67 N88-24070

Interpretation of MSS/LANDSAT data for evaluation of physical distribution of mangroves in Cananea-Iguape (SP) p 16 N88-24072

Low altitude remote sensing data in the implementation of a mathematical model for the planning of urban equipment networks p 23 N88-24074

Evaluation of an estimation system for an irrigated area in a tropical region through TM-LANDSAT imagery p 16 N88-24075

Study of reservoir water quality utilizing remote sensing techniques: Methodological concepts p 56 N88-24076

Evaluation of the floodable area of the canal of Sao Goncalo through TM-LANDSAT 5 imagery p 56 N88-24078

Automatic registration of satellite imagery p 67 N88-24080

Visualization of digital terrain models p 67 N88-24081

Application of its transformation in color enhancement of LANDSAT imagery p 68 N88-24082

Detection of biomass burning and smoke plumes in the Amazon region through NOAA satellite imagery p 23 N88-24085

Evaluation of the mangrove area at the Piaui River (SE) through remote sensing p 16 N88-24086

Mapping of plant associations and the variation of surface water in the Pantanal Mato-Grossense National Park, through remote sensing techniques p 17 N88-24092

Preliminary study on the application of digital processing of TM-LANDSAT data in the mapping of apple orchards in Fraiburgo (SC) p 17 N88-24093

Evaluation of TM false color composites for crop discrimination p 17 N88-24096

J**Jet Propulsion Lab., California Inst. of Tech., Pasadena.**

Mapping the Oman Ophiolite using TM data p 26 A88-32906

A near infrared vegetation index formed with airborne multispectral scanner data p 1 A88-32910

Satellite radars for geologic mapping in tropical regions p 27 A88-32917

Use of calibration targets in the measurement of 2.22-micron mineral absorption features in Thematic Mapper data p 29 A88-32927

Precision positioning of earth orbiting remote sensing systems [AAS PAPER 86-398] p 70 A88-35159

Passive microwave data for snow and ice research - Planned products from the DMSP SSM/I system p 40 A88-35199

Satellite data management for effective data access p 42 A88-38690

Effect of wet tropospheric path delays on estimation of geodetic baselines in the Gulf of California using the Global Positioning System p 25 A88-41835

Satellite data in aquatic area research - Some ideas for future studies p 53 A88-42048

Remote sensing for non-renewable resources - Satellite and airborne multiband scanners for mineral exploration p 35 A88-42068

Moisture and latent heat flux variabilities in the tropical Pacific derived from satellite data p 45 A88-42445

Time evolution of surface chlorophyll patterns from cross-spectrum analysis of satellite color images p 45 A88-42446

Directed band ratioing for the retention of perceptually-independent topographic expression in chromaticity-enhanced imagery p 62 A88-43224

The dangers of underestimating the importance of data adjustments in band ratioing p 62 A88-43225

Shuttle radar mapping with diverse incidence angles in the rainforest of Borneo p 12 A88-44644

SIR-B stereo-radargrammetry of Australia p 63 A88-44648

Dependence of image grey values on topography in SIR-B images p 63 A88-44649

The Shuttle Imaging Radar B (SIR-B) experiment report [NASA-CR-182923] p 75 N88-23932

Radar penetration in the Amazonian rain forest p 13 N88-24015

Airborne and spaceborne radar images for geologic and environmental mapping in the Amazon rain forest, Brazil p 37 N88-24021

Radar penetration in the Amazonian rain forest p 15 N88-24044

Joint Publications Research Service, Arlington, Va.

Spectral reflective characteristics of sea surface p 47 N88-20676

Mushroom-shaped currents (eddy dipoles) under rotation and stratification conditions p 47 N88-20678

K**Kansas State Univ., Manhattan.**

Radiative surface temperatures of the burned and unburned areas in a tallgrass prairie p 3 A88-37418

Kansas Univ., Lawrence.

A comparison of airborne GEMS/SAR with satellite-borne Seasat/SAR radar imagery - The value of archived multiple data sets p 64 A88-45640

Research on enhancing the utilization of digital multispectral data and geographic information systems in global habitability studies [NASA-CR-182799] p 23 N88-24101

L**Laboratoire d'Océanographie Dynamique et de Climatologie, Paris (France).**

Elements of sea ice dynamics and thermodynamics p 48 N88-21571

Lamont-Doherty Geological Observatory, Palisades, N.Y.

Space geodesy and earthquake prediction [AAS PAPER 86-307] p 24 A88-35156

Lockheed Missiles and Space Co., Sunnyvale, Calif.

Spatial resolution requirements for urban land cover mapping from space p 20 A88-42058

Louisiana State Univ., Baton Rouge.

Preliminary investigation of Large Format Camera photography utility in soil mapping and related agricultural applications p 4 A88-41947

M**MacDonald, Dettwiler and Associates Ltd., Richmond (British Columbia).**

Mapping from LANDSAT and SPOT satellite imagery p 66 N88-24018

Maryland Univ., Cambridge.

The dispersal of the Amazon's water p 43 A88-40059

Temporal variations of particle fluxes in the deep subtropical and tropical North Atlantic - Eulerian versus Lagrangian effects p 45 A88-42448

Massachusetts Inst. of Tech., Cambridge.

Geodetic measurement of deformation east of the San Andreas Fault in Central California p 25 A88-32831

Identification of terrain cover using the optimum polarimetric classifier p 3 A88-37370

Remote sensing of earth terrain [NASA-CR-182677] p 12 N88-20711

Geodetic measurement of deformation east of the San Andreas fault in Central California [NASA-CR-182709] p 36 N88-20754

Relative orientation [AD-A190385] p 75 N88-22449

Massachusetts Inst. of Tech., Lexington.

Identification of terrain cover using the optimum polarimetric classifier p 3 A88-37370

Max-Planck-Inst. fuer Meteorologie, Hamburg (West Germany).

Sea ice observations and models p 48 N88-21572

Investigation of the imaging of ocean surface waves using a synthetic aperture radar [SER-A-WISS-ABHANDL-84] p 49 N88-23357

- Millersville Univ., Pa.**
Remote sensing of geobotanical associations in clastic sedimentary terrane p 31 A88-32951
- Mineracao Taboca S.A., Manaus (Brazil).**
Criteria for planimetric and altimetric correction of maps restituted from aerial photographs in 1:100,000 scale p 38 N88-24097

N

- National Aeronautics and Space Administration. Ames Research Center, Moffett Field, Calif.**
An integrated approach to the use of Landsat TM data for gold exploration in west central Nevada p 30 A88-32941
Monitoring the environment by remote sensing p 18 A88-33770
Thermal analysis of wildfires and effects on global ecosystem cycling p 2 A88-35194
Particulate emissions from a mid-latitude prescribed chaparral fire p 3 A88-38805
Spatial resolution requirements for urban land cover mapping from space p 20 A88-42058
- National Aeronautics and Space Administration. Goddard Inst. for Space Studies, New York, N.Y.**
Mass extinctions, atmospheric sulphur and climatic warming at the K/T boundary p 46 A88-43835
- National Aeronautics and Space Administration. Goddard Space Flight Center, Greenbelt, Md.**
A satellite infrared technique to estimate tropical convective and stratiform rainfall p 69 A88-33416
Tropical rainfall measuring mission (TRMM) p 69 A88-33429
A proposed tropical rainfall measuring mission (TRMM) satellite p 69 A88-33742
Remote sensing of snow p 50 A88-35198
Assessment of polar climate change using satellite technology p 40 A88-36241
Polynyas in the Southern Ocean p 43 A88-39284
The dispersal of the Amazon's water p 43 A88-40059
A four-layer model for the heat budget of homogeneous land surfaces p 4 A88-41028
Obtaining spectral reflectance factor measurements of stressed forest vegetation p 5 A88-41952
Multispectral geologic remote sensing of a suspected impact crater near Al Madafi, Saudi Arabia p 33 A88-41955
Satellite and aircraft passive microwave observations during the Marginal Ice Zone Experiment in 1984 p 45 A88-42447
The 1987 Airborne Antarctic Ozone Experiment: The Nimbus-7 TOMS data atlas [NASA-PP-1201] p 47 N88-20714
Tidal estimation in the Pacific with application to SEASAT altimetry [NASA-TM-100694] p 47 N88-20780
The role of space borne imaging radars in environmental monitoring: Some shuttle imaging radar results in Asia [NASA-TM-101178] p 23 N88-24844
- National Aeronautics and Space Administration. John C. Stennis Space Center, Bay Saint Louis, Miss.**
Preliminary investigation of Large Format Camera photography utility in soil mapping and related agricultural applications p 4 A88-41947
A gridding approach to detect patterns of change in coastal wetlands from digital data p 52 A88-41949
Remote sensing technology and applications p 46 A88-44005
- National Aeronautics and Space Administration. John F. Kennedy Space Center, Cocoa Beach, Fla.**
History of wildland fires on Vandenberg Air Force Base, California [NASA-TM-100983] p 18 N88-25134
- National Aeronautics and Space Administration. Langley Research Center, Hampton, Va.**
Particulate emissions from a mid-latitude prescribed chaparral fire p 3 A88-38805
- National Aeronautics and Space Administration. National Space Technology Labs., Bay Saint Louis, Miss.**
Using the thermal infrared multispectral scanner (TIMS) to estimate surface thermal responses p 73 A88-40785
- National Aeronautics and Space Administration. Wallops Flight Facility, Wallops Island, Va.**
Correlation between aircraft MSS and LIDAR remotely sensed data on a forested wetland in South Carolina p 5 A88-41951
- National Center for Atmospheric Research, Boulder, Colo.**
A system for remote measurements of the wind stress over the ocean p 40 A88-36841

- National Marine Fisheries Service, Monterey, Calif.**
Hydrographic observations in the northwestern Weddell Sea Marginal Ice Zone during March 1986 [PB88-173240] p 55 N88-23359
- Naval Postgraduate School, Monterey, Calif.**
Hydrographic data from the OPTOMA (Ocean Prediction Through Observation, Modeling and Analysis) program: OPTOMA 23, 9-19 November 1986 [AD-A189868] p 49 N88-22506
- Nevada Univ., Reno.**
Correlation between high resolution remote sensing imagery and hydrothermal alteration, Tybo mining district, Nevada p 27 A88-32915
An integrated approach to the use of Landsat TM data for gold exploration in west central Nevada p 30 A88-32941
- New Mexico Univ., Albuquerque.**
Review of power requirements for satellite remote sensing systems p 76 N88-24387
- New York Univ., New York.**
Mass extinctions, atmospheric sulphur and climatic warming at the K/T boundary p 46 A88-43835
- Northwest Research Associates, Inc., Bellevue, Wash.**
Geometric restoration of satellite image data [AD-A190462] p 64 N88-22450
Satellite UV image processing [AD-A190466] p 65 N88-22451

O

- Ohio State Univ., Columbus.**
Determination of Earth rotation by the combination of data from different space geodetic systems [NASA-CR-181388] p 25 N88-20713
- Oregon State Univ., Corvallis.**
Remote sensing of leaf water status p 4 A88-40784
Using the thermal infrared multispectral scanner (TIMS) to estimate surface thermal responses p 73 A88-40785
- Oxford Univ. (England).**
The effect of a shallow low-viscosity zone on the mantle flow, the geoid anomalies and the geoid and depth-age relationships at fracture zones p 24 A88-38024

P

- Pacific Northwest Labs., Richland, Wash.**
Ocean general circulation models: Report on proceedings of a meeting of ocean and climate modelers [DE88-005530] p 49 N88-22504
- Paraiba Univ., Joao Pessoa (Brazil).**
Identification of shallow groundwater regions in semi-arid Brazil by remote sensing methods p 14 N88-24030
- Pennsylvania State Univ., University Park.**
An update on remote measurement of soil moisture over vegetation using infrared temperature measurements: A FIFE perspective [NASA-CR-182926] p 18 N88-24109
- Purdue Univ., West Lafayette, Ind.**
An integrated study of the Alto Paranaiba Kimberlite Province, Minas Gerais, Brazil: A possible tool for diamond exploration p 37 N88-24031

R

- Rennes Univ. (France).**
Remote sensing of biomass of salt marsh vegetation in France p 3 A88-39082
- Research Inst. of National Defence, Stockholm (Sweden).**
Terrain classification using SPOT images and the computer system GOP-300 [FOA-C-20677-2.7] p 68 N88-24102
- Rio Grande do Sul Univ., Porto Alegre (Brazil).**
Analysis and interpretation of image lithostructure: An application of the multiconcept in the metamorphic belt of Sul de Santana da Boa Vista (RS) p 38 N88-24051

S

- San Diego State Univ., Calif.**
Remote sensing and image processing requirements for Eulerian flow field estimations p 51 A88-39078
- Sao Paulo Univ. (Brazil).**
Utilization of TM/LANDSAT images in the implanted forests mapping in the Mogi-Guaçu Region (SP-Brazil) p 14 N88-24042

- Characteristics of drainage determinations in aerial photographs and relief determination on different scales planialtimetric charts for three soils in the state of Sao Paulo p 17 N88-24095
- Science Applications International Corp., Bellevue, Wash.**
Hydrographic observations in the northwestern Weddell Sea Marginal Ice Zone during March 1986 [PB88-173240] p 55 N88-23359
- Science Applications International Corp., College Station, Tex.**
Examples of ice pack rigidity and mobility characteristics determined from ice motion [AD-A191163] p 50 N88-24129
- Science Applications International Corp., Washington, D.C.**
Approach and status for a unified national plan for satellite remote sensing research and development p 77 A88-32919
- Science Applications Research, Lanham, Md.**
Obtaining spectral reflectance factor measurements of stressed forest vegetation p 5 A88-41952
- Scott Polar Research Inst., Cambridge (England).**
The role of remote sensing in the study of polar ice sheets p 48 N88-21570
- Scripps Institution of Oceanography, La Jolla, Calif.**
Radiative processes affecting ocean mixed-layer heat content and their monitoring from satellite p 47 N88-20800

- Silsoe Coll., Bedford (England).**
Mapping soil and rock variation from satellite images in the Sahel p 14 N88-24023
Satellite remote sensing of turbidity and sediment concentration in Lagoa dos Patos p 56 N88-24032
- Sociedad Colombiana de Fotogrametria y Percepcion Remota, Bogota.**
The use of SLAR and SIRA imagenes for the classification of forest types in tropical rain forests p 14 N88-24036
- Sociedad de Especialistas Latinoamericanos en Percepcion Remota (Chile).**
Latin American Symposium on Remote Sensing. 4th Brazilian Remote Sensing Symposium and 6th SELPER Plenary Meeting, volume 1 p 75 N88-24013
- Sociedade Brasileira de Cartografia, Geodesia, Fotogrametria e Sensoriamento Remoto.**
Latin American Symposium on Remote Sensing. 4th Brazilian Remote Sensing Symposium and 6th SELPER Plenary Meeting, volume 1 p 75 N88-24013
- Societe Europeenne de Propulsion, Bordeaux (France).**
The geometric workstation, a new approach for geometric corrections of remotely sensed data p 66 N88-24017
- South Carolina Univ., Columbia.**
Correlation between aircraft MSS and LIDAR remotely sensed data on a forested wetland in South Carolina p 5 A88-41951
- ST Systems Corp., Hampton, Va.**
Particulate emissions from a mid-latitude prescribed chaparral fire p 3 A88-38805
- Stanford Univ., Calif.**
The effect of a shallow low-viscosity zone on the mantle flow, the geoid anomalies and the geoid and depth-age relationships at fracture zones p 24 A88-38024

T

- Technische Hogeschool, Delft (Netherlands).**
From satellite altimetry to ocean topography, a survey of data processing techniques [ETN-88-91841] p 48 N88-21575
Coupling of satellite remote sensing to digitized topographic map to detect changes in land use [B8735129] p 23 N88-24104
Adjustment in photogrammetry: Methods, programs and applications [B8735130] p 76 N88-24105
- Technische Hogeschool, Eindhoven (Netherlands).**
The application of satellites in connection with the environment [ETN-88-92474] p 24 N88-25020
- Technological Marketing Analysis Corp., San Francisco, Calif.**
Subsurface morphology and geoarchaeology revealed by spaceborne and airborne radar p 37 N88-24022
- Texas A&M Univ., College Station.**
A proposed tropical rainfall measuring mission (TRMM) satellite p 69 A88-33742
- Texas Univ., Arlington.**
An empirical model for polarized and cross-polarized scattering from a vegetation layer p 11 A88-44116
- THEMAG Egenharia Ltda., Sao Paulo (Brazil).**
Utilization of LANDSAT-TM imagery in the hydroenergetic inventory of the Paraiba de Sul River Basin p 56 N88-24077

Thessaloniki Univ. (Greece).

Manual interpretation of small forestlands on Landsat
MSS data p 12 A88-44521

Toulouse Univ. (France).

The Systeme d'Analyse Geographique (SAGE)
geographic analysis system p 66 N88-24019
The SAGE geographic analysis system
p 22 N88-24063

Tuebingen Univ. (West Germany).

Temporal variations of particle fluxes in the deep
subtropical and tropical North Atlantic - Eulerian versus
Lagrangian effects p 45 A88-42448

U

United Nations, New York, N. Y.

The USSR space systems for remote sensing of earth
resources and the environment (sensor systems,
processing techniques, applications) p 76 N88-24035

Universidad Nacional de Lujan (Argentina).

Estimation of an area cultivated with wheat from
LANDSAT data through a two-phase sampling method
p 14 N88-24041

Universidad Nacional de San Juan (Argentina).

Dune fields in central Western Argentina
p 38 N88-24088

The breaked anticlines, cuesta and crest homoclines,
ortoclinal valleys, and other forms of relief outcrops
delineated with the help of remote sensing imagery
p 16 N88-24089

Geomorphologic sector maps of Niquizanga-Mayares,
province of San Juan, Argentina p 38 N88-24098

**Universidade Estadual de Paulista, Guaratingueta
(Brazil).**

Implantation of a geo-cartographical information system
through microcomputers p 67 N88-24064

Current stage of remote sensing system for cartographic
application p 76 N88-24090

Universidade Federal de Parana, Curitiba (Brazil).

The 35 mm vertical aerial photographs for mapping
stands of bracatinga in different age classes
p 16 N88-24087

Stereoscopic photographs, ground and aerial, of trees
used in the arborization of Curitiba (PR)
p 17 N88-24091

University of Southern Illinois, Carbondale.

Groundwater sapping valleys: Experimental studies,
geological controls and implications to the interpretation
of valley networks on Mars
[NASA-CR-182718] p 37 N88-22847

V

Vexcell Corp., Boulder, Colo.

SIR-B stereo-radargrammetry of Australia
p 63 A88-44648

Dependence of image grey values on topography in
SIR-B images p 63 A88-44649

W

Woods Hole Oceanographic Institution, Mass.

The dispersal of the Amazon's water
p 43 A88-40059

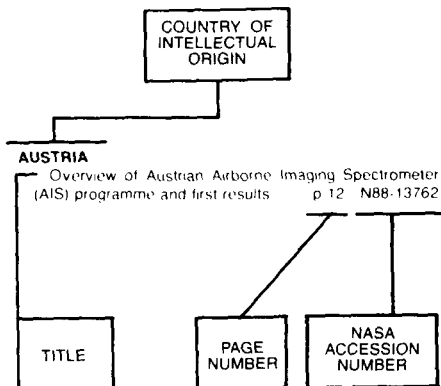
Temporal variations of particle fluxes in the deep
subtropical and tropical North Atlantic - Eulerian versus
Lagrangian effects p 45 A88-42448

Real-time environmental Arctic monitoring (R-TEAM)
[AD-A189948] p 49 N88-22508

World Climate Programme, Geneva (Switzerland).

The WOCE Core Project Planning Meeting on the Gyre
Dynamics Experiment
[WCP-139] p 49 N88-23358

Typical Foreign Technology Index Listing



Listings in this index are arranged alphabetically by country of intellectual origin. The title of the document is used to provide a brief description of the subject matter. The page number and the accession number are included in each entry to assist the user in locating the citation in the abstract section. If applicable, a report number is also included as an aid in identifying the document.

A

ARGENTINA

- A remote sensing methodological approach for applied geomorphology mapping in plain areas p 35 A88-42034
- Small scale erosion hazard mapping using Landsat information in the northwest of Argentina p 9 A88-42035
- Spectral measurements for correcting LANDSAT data for atmospheric effects p 66 N88-24020
- Shape detection in remote sensing through graph isomorphism p 67 N88-24028
- Estimation of an area cultivated with wheat from LANDSAT data through a two-phase sampling method p 14 N88-24041
- Dune fields in central Western Argentina p 38 N88-24088
- The broken anticlines, cuesta and crest homoclines, oroclinal valleys, and other forms of relief outcrops delineated with the help of remote sensing imagery p 16 N88-24089

AUSTRALIA

- Targeting epithermal alteration and gossans in weathered and vegetated terrains using aircraft scanners - Successful Australian case histories p 26 A88-32905
- Integration of SIR-B imagery with geological and geophysical data in Australia p 27 A88-32912
- Rock discrimination and alteration mapping for mineral exploration using the Carr Boyd/Geoscan airborne multispectral scanner p 27 A88-32914
- Pattern recognition and geological interpretation of SIR-B images of Central Australia p 31 A88-32956
- Canadian large-scale aerial photographic systems (LSP) p 70 A88-35395
- Ocean-atmosphere interactions in low latitude Australasia p 41 A88-37270
- Non-tracking antenna systems for the acquisition of NOAA HRPT Data p 72 A88-37279

- Classification of the Riverina forests of south east Australia using co-registered Landsat MSS and SIR-B radar data p 9 A88-42013
- Evaluation of combined multiple incident angle SIR-B digital data and Landsat MSS data over an urban complex p 62 A88-42055
- A satellite-based investigation of the significance of surficial deposits for surface mining operations p 36 A88-45638

AUSTRIA

- Effects of heavy metal induced canopy structural changes on forest canopy reflectance p 1 A88-32930
- Discrimination of geobotanical anomalies in rugged alpine terrain using Landsat Thematic Mapper data p 32 A88-32957
- Relationship between soil and leaf metal content and Landsat MSS and TM acquired canopy reflectance data p 6 A88-41986
- Optimal Thematic Mapper bands and transformations for discerning metal stress in coniferous tree canopies p 7 A88-42002

B

BELGIUM

- Remote sensing for wildlife management - Giant panda habitat mapping from Landsat MSS images p 2 A88-35195
- Structural information of the landscape as ground truth for the interpretation of satellite imagery p 59 A88-41962
- Application of remote sensing in the field of experimental tectonics p 34 A88-42023
- Assessment of desertification in the lower Nile Valley (Egypt) by an interpretation of Landsat MSS colour composites and aerial photographs p 61 A88-42025
- A simple atmospheric correction algorithm for Landsat Thematic Mapper satellite images p 61 A88-42054

BOTSWANA

- Differentiation of ecological zones in the Okavango Delta, Botswana by classification and contextual analyses of Landsat MSS data p 59 A88-39099

BRAZIL

- Confirmation of quantitative morphostructural analysis by seismic, aeromagnetic and geochemical data in the Amazon Basin, Brazil p 29 A88-32937
- Restoration techniques for redisplay of LANDSAT-5 satellite imagery [INPE-4189-PRE/1076] p 64 N88-20712
- Analysis for architecture for image processing [INPE-4294-PRE/1165] p 75 N88-20715
- Updating of the municipal official register of real estate through a geographical information system [INPE-4459-PRE/1238] p 21 N88-22453
- Method for restoration and resampling of TM sensor imagery [INPE-4461-PRE/1255] p 65 N88-22454
- Project CODEAMA/FUNCATE (test-area of Barreirinha-AM): Field report [INPE-4500-RPE/563] p 55 N88-22455
- Comparative utilization of analog and digital processes in the treatment of MSS-LANDSAT data for studying the national parks of Brazil [INPE-4011-TDL/240] p 21 N88-22456
- Calibration and processing of AVHRR data for temperature estimation [INPE-4493-PRE/1257] p 65 N88-22485
- Orbital remote sensing: An instrument for monitoring urban growth [INPE-4456-PRE/1287] p 22 N88-22833
- Use of energy emission for detecting the necessity of irrigation in wheat in field conditions [INPE-4461-TDL/318] p 13 N88-23315
- Detection, monitoring and analysis of some environmental effects of fires in the Amazon region through utilization of NOAA and LANDSAT satellite imagery and aircraft data [INPE-4503-TDL/326] p 13 N88-23322
- Applications of multitemporal composites obtained from LANDSAT data in the study of urban growth [INPE-4480-PRE/1246] p 22 N88-23692

- Updating land-use of the Sao Jose dos Campos municipality through remote sensing data [INPE-4479-RPE/562] p 22 N88-23693
- Latin American Symposium on Remote Sensing. 4th Brazilian Remote Sensing Symposium and 6th SELPER Plenary Meeting, volume 1 p 75 N88-24013
- Radar penetration in the Amazonian rain forest p 13 N88-24015
- A proposal for a project entitled assessment of forest resources in Uruguay submitted to the United Nations Industrial Development Organization (UNIDO) p 13 N88-24016
- Comparison of surface current determined from satellite-tracked buoy with shipboard wind data during the 4th Brazilian antarctic expedition, 10-14 March, 1986 p 49 N88-24024
- Textural features for image classification in remote sensing p 66 N88-24027
- The modeling of error budget analysis and tolerance specifications for BRESEX multiband linear array CCD camera p 76 N88-24029
- Identification of shallow groundwater regions in semi-arid Brazil by remote sensing methods p 14 N88-24030
- International cooperation in remote sensing: The ESA experience p 77 N88-24038
- Utilization of TM/LANDSAT images in the implanted forests mapping in the Mogi-Guaçu Region (SP-Brazil) p 14 N88-24042
- Anomalies in the vegetation in the Alto Xingu - MT p 14 N88-24043
- Radar penetration in the Amazonian rain forest p 15 N88-24044
- Remote sensing techniques in the estimation of the area cultivated with beans, corn, and castor beans in the Irecê County (Bahia State) p 15 N88-24045
- CANASATE: Sugar cane mapping by satellite p 15 N88-24046
- Spectral behavior of crops through analysis of LANDSAT-TM data p 15 N88-24047
- Identification of areas cultivated with soybeans in the cerrados regions, through digital processing of satellite images: A methodological approach p 15 N88-24048
- Structure and dynamics of vegetation in the middle semi-arid tropics, Quixaba's Caatinga (PE): Terrain analysis of MSS/LANDSAT data p 15 N88-24049
- Remote sensing and structural rupture: Application examples in the study of tectonics p 37 N88-24050
- Analysis and interpretation of image lithostructure: An application of the multiconcept in the metamorphic belt of Sul de Santana da Boa Vista (RS) p 38 N88-24051
- Study of fracturing for groundwater research in the Sergipe state with remote sensing products p 38 N88-24052
- Near surface current determined from INPE's satellite-tracked buoy, during 6-26 November, 1985 p 50 N88-24058
- The SAGE geographic analysis system p 22 N88-24063
- Implantation of a geo-cartographical information system through microcomputers p 67 N88-24064
- Study of methods of post-processing applied to a problem of standard classification p 67 N88-24067
- Utilization of LANDSAT-TM, for aiding in the localization of archeological sites in the state of Sao Paulo p 38 N88-24069
- Analysis of the parameters responsible for the variations of the illumination conditions in the LANSAT data p 67 N88-24070
- Tornado tracks in Southwestern Brazil, Eastern Paraguay, and Northwestern Argentina p 23 N88-24071
- Interpretation of MSS/LANDSAT data for evaluation of physical distribution of mangroves in Cananea-Iguape (SP) p 16 N88-24072
- Low altitude remote sensing data in the implementation of a mathematical model for the planning of urban equipment networks p 23 N88-24074
- Evaluation of an estimation system for an irrigated area in a tropical region through TM-LANDSAT imagery p 16 N88-24075

- Study of reservoir water quality utilizing remote sensing techniques: Methodological concepts p 56 N88-24076
- Utilization of LANDSAT-TM imagery in the hydroenergetic inventory of the Paraba de Sul River Basin p 56 N88-24077
- Evaluation of the floodable area of the canal of Sao Goncalo through TM-LANDSAT 5 imagery p 56 N88-24078
- Automatic registration of satellite imagery p 67 N88-24080
- Visualization of digital terrain models p 67 N88-24081
- Application of its transformation in color enhancement of LANDSAT imagery p 68 N88-24082
- Detection of biomass burning and smoke plumes in the Amazon region through NOAA satellite imagery p 23 N88-24085
- Evaluation of the mangrove area at the Piaui River (SE) through remote sensing p 16 N88-24086
- The 35 mm vertical aerial photographs for mapping stands of bracatinga in different age classes p 16 N88-24087
- Current stage of remote sensing system for cartographic application p 76 N88-24090
- Stereoscopic photographs, ground and aerial, of trees used in the arborization of Curitiba (PR) p 17 N88-24091
- Mapping of plant associations and the variation of surface water in the Pantanal Mato-Grossense National Park, through remote sensing techniques p 17 N88-24092
- Preliminary study on the application of digital processing of TM-LANDSAT data in the mapping of apple orchards in Fraiburgo (SC) p 17 N88-24093
- Characteristics of drainage determinations in aerial photographs and relief determination on different scales planialtimetric charts for three soils in the state of Sao Paulo p 17 N88-24095
- Evaluation of TM false color composites for crop discrimination p 17 N88-24096
- Criteria for planimetric and altimetric correction of maps restituted from aerial photographs in 1:100,000 scale p 38 N88-24097
- Lithostructural interpretation of Chapada do Cachimbo (Pa-Am-Mt), based on radar and LANDSAT imagery p 39 N88-24100

C

CANADA

- Digital terrain model and image integration for geologic interpretation p 26 A88-32904
- Shift in spectral response of nickel-loaded and control shoots of white birch p 1 A88-32928
- Spectral geobotanical investigation of mineralized till sites p 29 A88-32934
- Surrogate spectral reflectances of vegetation applied to geobotanical remote sensing p 1 A88-32935
- A comparison of lineaments interpreted from remotely sensed data and airborne magnetics and their relationship to gold deposits in central Nova Scotia p 29 A88-32936
- Spectral reflectance from lichens treated with copper p 30 A88-32945
- Assessment of digital enhancement techniques using Landsat TM data in mapping geologic lineaments, with application to the Mactaquac headpond area, southern New Brunswick p 31 A88-32949
- Landsat TM data as an aid in planning and interpretation of regional geochemical surveys in the Canadian Shield p 31 A88-32950
- Pyrophyllite and kaolinite alteration - Mineral discrimination by sample reflectance measurement p 31 A88-32954
- Interannual Landsat-MSS reflectance variation in an urbanized temperate zone p 58 A88-37417
- Urbanization and Landsat MSS albedo change in the Windsor-Quebec corridor since 1972 p 18 A88-39094
- Base map production from geocoded imagery p 25 A88-41969
- Digital elevation modeling with stereo SIR-B image data p 60 A88-41981
- Shuttle imaging radar (SIR-A) interpretation of the Kashgar region in western Xinjiang, China p 74 A88-41985
- Spectral signatures of soils and terrain conditions using lasers and spectrometers p 6 A88-41997
- Spruce budworm infestation detection using an airborne pushbroom scanner and Thematic Mapper data p 8 A88-42007
- Application of MEIS-II multispectral airborne data and CIR photography for the mapping of surficial geology and geomorphology in the Chatham area, Southwest Ontario, Canada p 34 A88-42027

D-2

- Remote sensing as a tool for assessing environmental effects of hydroelectric development in a remote river basin p 53 A88-42045
- A comprehensive LRIS of the Kananaskis Valley using Landsat data p 21 A88-42064
- The integration of remote sensing and geographic information systems p 21 A88-42069
- Time evolution of surface chlorophyll patterns from cross-spectrum analysis of satellite color images p 45 A88-42446
- Satellite observations of tidal upwelling and mixing in the St. Lawrence estuary p 45 A88-42450
- An effect of coherent scattering in spaceborne and airborne SAR images p 64 A88-44651
- Case studies on the application of remote sensing data to geotechnical investigations in Ontario, Canada p 35 A88-45635
- Mapping from LANDSAT and SPOT satellite imagery p 66 N88-24018
- Remote sensing and data integration: Practical solutions for resource managers p 22 N88-24034

CHINA, PEOPLE'S REPUBLIC OF

- Retrieval of atmospheric temperature structure from the NOAA-9 satellite p 72 A88-37336
- Satellite observation of surface albedo over the Qinghai-Xinzing plateau region p 24 A88-39518
- Shuttle imaging radar response from sand dunes and subsurface rocks of Alashan Plateau in north-central China p 33 A88-41978
- Analysis of lineaments and major fractures in Xichang-Dukou area, Sichuan province as interpreted from Landsat images p 34 A88-42022
- Estimation of reservoir submerging losses using CIR aerial photographs - Example of the Ertan hydropower station on the Yalong River in southwest China p 55 A88-45637

COLOMBIA

- The use of SLAR and SIRA imagenes for the classification of forest types in tropical rain forests p 14 N88-24036

CZECHOSLOVAKIA

- The use of multispectral space photographs to draw up a map of land use in western Slovakia p 57 A88-33774

E

ESTONIA

- Linear combinations of spectral reflectances in crop analyses p 3 A88-36170
- Statistical analysis of the near-surface distributions of chlorophyll and temperature fields on the basis of remote imagery from CZCS and AVHRR scanners p 54 A88-43666

F

FRANCE

- Diagnostic study of the Fram Strait marginal ice zone during summer from 1983 and 1984 Marginal Ice Zone Experiment Lagrangian observations p 39 A88-33694
- Influence of topography on forest reflectance using Landsat Thematic Mapper and digital terrain data p 2 A88-35397
- Imaging instrument of the Vegetation Payload (SPOT 4) p 70 A88-35968
- Geoid anomalies across Pacific fracture zones p 24 A88-38023
- Evidence from geoid data of a hotspot origin for the southern Mascarene Plateau and Mascarene Islands (Indian Ocean) p 24 A88-38902
- Satellite detected cyanobacteria bloom in the southwestern tropical Pacific - Implication for oceanic nitrogen fixation p 42 A88-39081
- Geoid roughness and long-wavelength segmentation of the South Atlantic spreading ridge p 24 A88-40688
- Synthetic geological map obtained by remote sensing - An application to Palawan Island p 33 A88-41975
- Geological analysis of Seasat SAR and SIR-B data in Haiti p 33 A88-41980
- Insertion of hydrological decolored data from photographic sensors of the Shuttle in a digital cartography of geophysical exploration (Spacelab 1-Metric Camera and Large Format Camera) p 74 A88-41990
- In flight calibration for the imaging instrument of VEGETATION payload (SPOT 4) p 10 A88-42545
- Modeling surface exchanges: The soil-vegetation-atmosphere continuum p 12 N88-21553
- Measurement of the water content of soil from space and application to the regional water balance p 55 N88-21561
- Study of the dynamic topography of oceans by means of satellite altimetry p 47 N88-21567

- Basic networks of TOGA: Determination of thermal profiles by XBT and of sea level by tide gage p 48 N88-21568
- Elements of sea ice dynamics and thermodynamics p 48 N88-21571
- Marginal Ice Zone Experiment (MIZEX) 1984 VARAN-S data set [ETN-88-92032] p 48 N88-21625
- Definition and implementation study for the Varan-S radar [CNES-CT/DRT/TIT/RL-143-T] p 48 N88-22267
- The geometric workstation, a new approach for geometric corrections of remotely sensed data p 66 N88-24017
- The Systeme d'Analyse Geographique (SAGE) geographic analysis system p 66 N88-24019

G

GERMANY DEMOCRATIC REPUBLIC

- The use of metric multispectral photography in environmental and resource exploration p 21 A88-44446
- Coastal monitoring by remote sensing p 54 A88-44447
- New features of the LMK aerial camera system p 74 A88-44449
- Kartoflex - An instrument for computer-aided photointerpretation and map revision p 74 A88-44450

GERMANY, FEDERAL REPUBLIC OF

- Integration of remote sensing and other geo-data for ore exploration - A SW-Iberian case study p 31 A88-32952
- Radar signatures of oil films floating on the sea surface and the Marangoni effect p 39 A88-33695
- Surface energy budget, surface temperature and thermal inertia p 58 A88-37147
- Spaceborne radar X-SAR for civil applications p 72 A88-37286
- Image processing for earth remote sensing p 58 A88-37287
- Vegetation indices and other vegetation parameters - Examples, interpretation and problems p 3 A88-38373
- Alternatives for mapping from satellite imagery [IAF PAPER 86-76] p 59 A88-41298
- Image optimization versus classification - An application oriented comparison of different methods by use of Thematic Mapper data p 59 A88-41964
- Comparison of classification results of original and preprocessed satellite data p 59 A88-41965
- Digital classification of forested areas using simulated TM- and SPOT- and Landsat 5/TM-data p 5 A88-41971
- Determination of spectral signatures of different forest damages from varying altitudes of multispectral scanner data p 6 A88-41993
- Contribution of remote sensing to food security and early warning systems in drought affected countries in Africa p 8 A88-42008
- Experiences in application of multispectral scanner-data for forest damage inventory p 8 A88-42010
- Detection of environmental noises between a vegetation canopy and a radiometric sensor p 10 A88-42538
- Sea ice observations and models p 48 N88-21572
- Feasibility study for a 2nd generation system for airborne maritime pollution surveillance [ETN-88-92108] p 55 N88-22466
- Contributions to geodesy, photogrammetry and cartography. Series 1, number 46 [ISSN-0469-4244] p 25 N88-23279
- Investigation of the imaging of ocean surface waves using a synthetic aperture radar [SER-A-WISS-ABHANDL-84] p 49 N88-23357
- Tests for the automatic pattern recognition of building surfaces by the TK 50 p 68 N88-25030
- Recent developments in software and hardware by Scitex Co. p 68 N88-25038

GREECE

- Manual interpretation of small forestlands on Landsat MSS data p 12 A88-44521

H

HUNGARY

- A comparative analysis of methods for compressing spectrophotometric data in the estimation of hydrological parameters p 54 A88-43673

INDIA

- Thematic Mapping from aerial photographs for Kandi Watershed and area development project, Punjab (India) p 9 A88-42024
- Application of remote sensing in hydromorphology for third world development - A resource development study in parts of Haryana (India) p 53 A88-42042
- Satellite remote sensing of the coastal environment of Bombay p 61 A88-42052
- Landuse and landform studies of the Mahanadi River Delta with the help of satellite MSS band p 56 N88-24033

INDONESIA

- Methodology for an operational monitoring of remotely-sensed sea surface temperatures in Indonesia p 43 A88-39084

INTERNATIONAL ORGANIZATION

- The Along-Track Scanning Radiometer with Microwave Sounder p 41 A88-37148
- An evaluation of the performance of the ECMWF operational system in analyzing and forecasting easterly wave disturbances over Africa and the tropical Atlantic p 43 A88-39746
- Airphoto map control with Landsat - An alternative to the slotted templet method p 60 A88-41966
- Per-field classification of a segmented SPOT simulated image p 60 A88-41970
- Visual interpretation of MSS-FCC manual cartographic integration of data p 61 A88-42001
- The JRC program for marine coastal monitoring p 44 A88-42039
- The effect of dissolved 'yellow substance' on the quantitative retrieval of chlorophyll and total suspended sediment concentrations from remote measurements of water colour p 46 A88-43226

ITALY

- Potential of Landsat Thematic Mapper image for crystalline rock type discrimination - Gregory Rift, Kenya p 32 A88-35192
- Computer processing of satellite data for geostructural zoning of a collisional boundary, significance and field checks - The example of Tunisia p 32 A88-35193
- Comparison between interpretation of images of different nature p 34 A88-42019
- Digital analysis of stereo pairs for the detection of anomalous signatures in geothermal fields p 61 A88-42037

J**JAPAN**

- Marine Observation Satellite-1 (MOS-1) and its sensors [AAS PAPER 86-288] p 40 A88-35153
- ERS-1, Earth Resources Satellite-1 and future earth observation program in Japan [AAS PAPER 86-289] p 69 A88-35154
- Flood damage analysis using multitemporal Landsat Thematic Mapper data p 4 A88-39090
- SIR-B experiments in Japan. I - Sensor calibration experiment p 73 A88-40351
- SIR-B experiments in Japan. II - Rice crop experiment p 4 A88-40352
- SIR-B experiments in Japan. III - Oil-pollution experiment p 43 A88-40353
- SIR-B experiments in Japan. V. p 4 A88-40355
- SIR-B experiments in Japan. VI. p 43 A88-40356
- Global vegetation monitoring using NOAA GAC data p 8 A88-42012
- An evaluation of potential uranium deposit area by Landsat data analysis in Officer Basin, South-Western part of Australia p 35 A88-42036
- Environmental assessment for large scale civil engineering projects with data of DTM and remote sensing p 53 A88-42046
- Radiometric correction for atmospheric and topographic effects on Landsat MSS images p 62 A88-43223
- The 'Tsukusys' image processing system and its utilization in Thematic Mapper investigations of water quality conditions p 54 A88-45115
- Evaluations of unsupervised methods for land-cover/use classifications of Landsat TM data p 64 A88-45116
- On the regional characteristics of actual evapotranspiration derived from Landsat MSS and elevation data p 54 A88-45118

M**MEXICO**

- Assessment of TM thermal infrared band contribution in land cover/land use multispectral classification p 61 A88-42016

MONGOLIA

- Quantitative analysis of a network of faults recognized on remote-sensing images of the Mushugai area in Mongolia p 32 A88-36163

N**NETHERLANDS**

- G.P.S. surveying in the Netherlands p 72 A88-37383
- Rangeland runoff curve numbers as determined from Landsat MSS data p 51 A88-39089
- Remote sensing for resources development and environmental management; Proceedings of the Seventh International Symposium, Enschede, Netherlands, Aug. 25-29, 1986. Volumes 1, 2, & 3 p 18 A88-41961
- Processing of raw digital NOAA-AVHRR data for sea- and land applications p 60 A88-41968
- Thematic Mapping by satellite - A new tool for planning and management p 60 A88-41973
- SLAR as a research tool p 73 A88-41976
- Detection by side-looking radar of geological structures under thin cover sands in arid areas p 33 A88-41979
- Relating L-band scatterometer data with soil moisture content and roughness p 5 A88-41984
- The derivation of a simplified reflectance model for the estimation of LAI p 6 A88-41987
- The application of a vegetation index in correcting the infrared reflectance for soil background p 6 A88-41988
- Multitemporal analysis of Thematic Mapper data for soil survey in Southern Tunisia p 6 A88-41989
- Multitemporal analysis of Landsat Multispectral Scanner (MSS) and Thematic Mapper (TM) data to map crops in the Po valley (Italy) and in Mendoza (Argentina) p 6 A88-41994
- Selection of bands for a newly developed multispectral airborne reference-aided calibrated scanner (MARCS) p 74 A88-41995
- Monitoring of renewable resources in equatorial countries p 19 A88-42000
- Application of multispectral scanning remote sensing in agricultural water management problems p 8 A88-42011
- A methodology for integrating satellite imagery and field observations for hydrological regionalisation in Alpine catchments p 52 A88-42038
- Analysis of Landsat multispectral-multitemporal images for geologic-lithologic map of the Bangladesh Delta p 35 A88-42049
- Determination of spectral signature of natural water by optical airborne and shipborne instruments p 44 A88-42050
- Classification of bottom composition and bathymetry of shallow waters by passive remote sensing p 53 A88-42051
- A study with NOAA-7 AVHRR-imagery in monitoring ephemeral streams in the lower catchment area of the Tana River, Kenya p 54 A88-42053
- The potential of numerical agronomic simulation models in remote sensing p 9 A88-42061
- A comparative analysis of dyke lineaments mapped from Shuttle Imaging Radar and Large Format Camera photography in hyperarid areas of the Eastern Desert, Egypt, and Red Sea Hills, Sudan p 35 A88-44647
- From satellite altimetry to ocean topography, a survey of data processing techniques p 48 N88-21575
- Proposals for the pre-operational use of data from the European Remote Sensing Satellite ERS-1 [BCRS-86-02] p 65 N88-23300
- The radiometric processing of SLAR measuring values using the PARES program [BCRS-86-04] p 75 N88-23301
- Investigation of the usefulness of speckle analysis in imaging radar systems [BCRS-86-05] p 65 N88-23302
- Turbidity patterns in the delta waters of southwest Netherlands on Thematic Mapper (TM) and multispectral scanner (MSS) satellite images [BCRS-86-06] p 55 N88-23303
- Results of the testing of the segmentation program on RESEDA [BCRS-87-01] p 65 N88-23304
- Study of the plan for a national data center for the European Remote Sensing Satellite ERS-1 [BCRS-87-11] p 66 N88-23309
- Coupling of satellite remote sensing to digitized topographic map to detect changes in land use [B8735129] p 23 N88-24104
- Adjustment in photogrammetry: Methods, programs and applications [B8735130] p 76 N88-24105

- The application of satellites in connection with the environment [ETN-88-92474] p 24 N88-25020

NIGER

- A remote sensing aided inventory of fuelwood volumes in the Sahel region of west Africa - A case study of five urban zones in the Republic of Niger p 7 A88-42005

NIGERIA

- Remote sensing for survey of material resources of highway engineering projects in developing countries p 20 A88-42032

NORWAY

- Comparison of SPOT-simulated and Landsat 5 TM imagery in vegetation mapping p 9 A88-42014
- Sea surface temperature studies in Norwegian coastal areas using AVHRR- and TM thermal infrared data p 44 A88-42047

O**OTHER**

- Photo-interpretation of landforms and the hydrogeologic bearing in highly deformed areas, NW of the Gulf of Suez, Egypt p 34 A88-42029

P**PERU**

- Geologic interpretation of air photos and radar imagery for hydroelectric power projects in Upper Ucayali Jungle Region of Peru p 28 A88-32922

POLAND

- Geological analysis of the satellite lineaments of the Vistula Delta Plain, Zulawy Wislane, Poland p 34 A88-42021
- Remote sensing methods in geological research of the Lublin coal basin, SE Poland p 34 A88-42028
- Remote sensing assessment of environmental impacts caused by phosphat industry destructive influence p 19 A88-42031

R**ROMANIA (RUMANIA)**

- Land resource use monitoring in Romania, using aerial and space data p 21 A88-42065

S**SENEGAL**

- Geographic study of the north coast of Senegal using MOMS-1 satellite data p 73 A88-41093

SOMALIA

- Multi-temporal Landsat for land unit mapping on project scale of the Sudd-floodplain, Southern Sudan p 9 A88-42015

SOUTH AFRICA, REPUBLIC OF

- Landsat temporal-spectral profiles of crops on the South African highveld p 7 A88-41999

SPAIN

- Spectral signature of rice fields using Landsat-5 TM in the Mediterranean coast of Spain p 6 A88-41991
- Geomorphologic sector maps of Niquizanga-Mayares, province of San Juan, Argentina p 38 N88-24098

SWEDEN

- Remote sensing of flow characteristics of the strait of Oresund p 53 A88-42043
- Terrain classification using SPOT images and the computer system GOP-300 [FOA-C-20677-2.7] p 68 N88-24102

SWITZERLAND

- Earth observation: Capturing the imagery - Remote sensing depends on advanced recording technology p 72 A88-38411
- Surface temperatures and sea ice typing for northern Baffin Bay p 42 A88-39083
- The WOCE Core Project Planning Meeting on the Gyre Dynamics Experiment [WCP-139] p 49 N88-23358

T**TAIWAN**

- A comparison between classification differencing and image differencing for land cover type change detection p 59 A88-41944
- Digital processing of airborne MSS data for forest cover types classification p 5 A88-41963

TURKEY

- Detecting and mapping of different volcanic stages and other geomorphic features by Landsat images in 'Katakekaumene', Western Turkey p 35 A88-42033

U

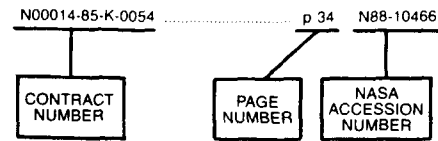
U.S.S.R.

- Technique for the instrumented interpretation of space scanner imagery of the earth's cloud cover p 69 A88-33832
- Climatological interpretation of time series of satellite observations of the earth's radiation balance p 69 A88-33872
- Range variations of the tropospheric propagation of ultrashort radio waves above the sea p 39 A88-33920
- Principles of the remote monitoring of fresh-water quality p 50 A88-34674
- Satellite observations and the numerical simulation of the interaction between a synoptic eddy and a frontal zone in the ocean p 40 A88-36159
- Evaluation of the possibility of determining concentrations of variable components of ocean water from averaged spectra of the diffuse optical reflection coefficient p 40 A88-36160
- The use of space data to study Precambrian structures p 32 A88-36161
- The South Alamyrynian ring structure - A new promising area to search for hydrocarbon deposits p 32 A88-36162
- Remote-sensing methods for the monitoring and forecasting of the entomological condition of taiga forests p 2 A88-36164
- Investigation and mapping of forests using space scanner imagery obtained in winter p 2 A88-36165
- Saline salt and water surface mapping on the basis of data from the Gyunesh-84 remote-sensing experiment p 51 A88-36166
- New aspects of the interpretation of space radar images p 58 A88-36171
- Remote sensing of the earth's surface in the ultraviolet range p 32 A88-36172
- Active two-element microwave interferometry of the sea surface p 41 A88-37679
- Comparative analysis of results of photographic observations of natural objects from Salyut-7 p 72 A88-39919
- The determination of the parameters of the diurnal thermocline using satellite and ship-based measurements p 44 A88-40834
- Possibility of replacing complex values of permittivity with real values p 44 A88-41398
- Space photomaps - Their compilation and peculiarities of geographical application p 60 A88-41967
- Radiometric investigation of the sea-wave breaking process p 46 A88-43664
- Parameters of eddy structures and mushroom currents in the Baltic Sea derived from satellite imagery p 46 A88-43665
- Method for rapidly estimating geophysical parameters of the ocean-atmosphere system from satellite microwave radiometry p 46 A88-43669
- Taking the effect of vegetation into account in the microwave-radiometer remote sensing of the earth surface on the results of remote sounding of the earth surface by microwave radiometry p 10 A88-43670
- Contrast enhancement of aerospace scanner imagery of crop fields p 11 A88-43671
- Correction of spatial and temporal distortions in the photographic image input into an interactive processing system p 62 A88-43672
- Comparison of radar and microwave radiometer techniques for determining permittivity p 74 A88-44231
- Spectral reflective characteristics of sea surface p 47 A88-20676
- Mushroom-shaped currents (eddy dipoles) under rotation and stratification conditions p 47 A88-20678
- UNITED KINGDOM**
- The acquisition of SPOT-1 HRV imagery over southern Britain and northern France, May 1986-May 1987 p 68 A88-29286
- Thematic Mapper data applied to mapping hydrothermal alteration in south west New Mexico p 28 A88-32923
- Application of remote sensing to tectonic and metallogenic studies in NE Africa p 28 A88-32924
- Thematic Mapper applied to alteration zone mapping for gold exploration in south-east Spain p 29 A88-32938
- Exploration for mercury and lead-zinc-silver using the airborne Thematic Mapper, Almaden area, Spain p 29 A88-32939
- The production of distortion free SAR imagery p 57 A88-33377
- A method for calculating the effective emissivity of a groove structure p 40 A88-35986
- Remote sensing applications in meteorology and climatology; Proceedings of the NATO Advanced Study Institute, Dundee, Scotland, Aug. 17-Sept. 6, 1986 p 71 A88-37126
- Cloud formations seen by satellite p 71 A88-37127

- Data reception, archiving and distribution p 58 A88-37131
- Microwave instruments and methods p 71 A88-37132
- Use of radar and satellite imagery for the measurement and short-term prediction of rainfall in the United Kingdom p 51 A88-37136
- The ocean and the atmosphere p 41 A88-37143
- Remote sensing of sea-surface winds p 41 A88-37144
- Cloud climatologies from space and applications to climate modelling p 71 A88-37145
- Plans for ERS-1 data acquisition, processing and distribution p 41 A88-37149
- Remote sensing in the Space Station and Columbus programmes p 71 A88-37150
- The semivariogram in remote sensing - An introduction p 58 A88-37421
- Surface currents off the west coast of Ireland studied from satellite images p 43 A88-39085
- Transformation of Global Vegetation Index (GVI) data from the polar stereographic projection to an equatorial cylindrical projection p 58 A88-39095
- Classification of land features, using Landsat MSS data in a mountainous terrain p 19 A88-41972
- Spatial feature extraction from radar imagery p 60 A88-41974
- Earthscan - A range of remote sensing systems p 61 A88-41982
- The use of Thematic Mapper imagery for geomorphological mapping in arid and semi-arid environments p 33 A88-41992
- Relation between spectral reflectance and vegetation index p 7 A88-41998
- The use of multitemporal Landsat data for improving crop mapping accuracy p 7 A88-42003
- The use of SPOT simulation data in forestry mapping p 7 A88-42006
- Spring mound and aioun mapping from Landsat TM imagery in south-central Tunisia p 52 A88-42026
- Monitoring geomorphological processes in desert marginal environments using multitemporal satellite imagery p 34 A88-42030
- Simple classifiers of satellite data for hydrologic modelling p 52 A88-42040
- A hydrological comparison of Landsat TM, Landsat MSS and black and white aerial photography p 52 A88-42041
- The quantification of floodplain inundation by the use of Landsat and Metric Camera information, Belize, Central America p 53 A88-42044
- An analysis of remote sensing for monitoring urban derelict land p 20 A88-42056
- How few data do we need - Some radical thoughts on renewable natural resources surveys p 9 A88-42060
- Recording resources in rural areas p 20 A88-42062
- Evaluation of regional land resources using geographic information systems based on linear quadrates p 20 A88-42063
- Circulation patterns in AVHRR imagery p 46 A88-43217
- A model of satellite radar altimeter return from ice sheets p 46 A88-43218
- Crop classification from airborne synthetic aperture radar data p 10 A88-43220
- Use of digital terrain data in the interpretation of SPOT-1 HRV multispectral imagery p 10 A88-43221
- Potato crop distribution and subdivision on soil type and potential water deficit - An integration of satellite imagery and environmental spatial database p 10 A88-43222
- Artificial GCPs in aircraft and satellite scanner imagery p 74 A88-43227
- The effect of atmospheric correction on the interpretation of multitemporal AVHRR-derived vegetation index dynamics p 11 A88-44117
- The role of remote sensing in the study of polar ice sheets p 48 A88-21570
- Mapping soil and rock variation from satellite images in the Sahel p 14 A88-24023
- Satellite remote sensing of turbidity and sediment concentration in Lagoa dos Patos p 56 A88-24032

CONTRACT NUMBER INDEX

Typical Contract Number Index Listing



Listings in this index are arranged alphanumerically by contract number. Under each contract number, the accession numbers denoting documents that have been produced as a result of research done under the contract are arranged in ascending order with the AIAA accession numbers appearing first. The accession number denotes the number by which the citation is identified in the abstract section. Preceding the accession number is the page number on which the citation may be found.

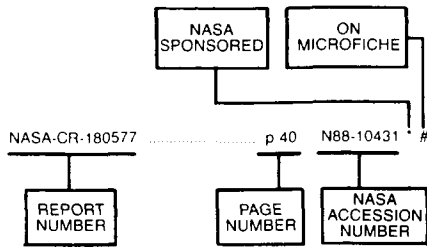
AF-AFOSR-86-0118	p 71	A88-37145
BMFT-01-QS-0730	p 31	A88-32952
BMFT-01-QS-86174	p 39	A88-33695
CNES-85-1257	p 2	A88-35397
CNEXO-83/7202	p 3	A88-39082
CNRS-ASP-PNEDC-950057	p 39	A88-33694
CNRS-ATP-85-430510	p 39	A88-33694
CNRS-ATP-86-430010	p 39	A88-33694
CNRS-508533	p 2	A88-35397
DAAG29-84-K-0145	p 74	A88-44306
DAAG29-85-K-0227	p 11	A88-44307
DACA76-85-C-0100	p 75	N88-22449
DE-AC06-76RL-01830	p 30	A88-32947
	p 49	N88-22504
DE-AC09-76SR-00001	p 5	A88-41951
DFG-WA-124/12-1	p 39	A88-33695
EEC-CLI-083-F	p 39	A88-33694
F19628-87-C-0003	p 64	N88-22450
	p 65	N88-22451
JPL-954946	p 64	A88-45640
JPL-956887	p 12	A88-44643
JPL-956926	p 63	A88-44650
JPL-956937	p 31	A88-32951
JPL-957516	p 63	A88-44641
JPL-957549	p 63	A88-44648
	p 63	A88-44649
MOESC-80129032	p 62	A88-43223
VAGW-1028	p 42	A88-38691
VAGW-374	p 3	A88-39082
VAGW-455	p 62	A88-43225
VAGW-641	p 40	A88-35199
VAGW-707	p 37	N88-22847
VAGW-814	p 46	A88-44005
VAGW-924	p 4	A88-40784
	p 73	A88-40785
VAG13-3	p 13	N88-22452
VAG5-177	p 62	A88-43225
VAG5-270	p 12	N88-20711
VAG5-389	p 3	A88-37418
VAG5-415	p 24	A88-38024
VAG5-799	p 24	A88-35156
VAG5-814	p 25	A88-32831
	p 36	N88-20754
VAG5-859	p 75	N88-21584
VAG5-919	p 18	N88-24109
VAG9-115	p 11	A88-44116
ASA ORDER L-61130-C	p 35	A88-44646
ASA ORDER W-15969	p 40	A88-36841
ASW-4049	p 31	A88-32951
ASW-4050	p 27	A88-32915
ASW-4092	p 77	A88-32919

NASW-4191	p 76	N88-24387
NAS10-10285	p 18	N88-25134
NAS13-268	p 73	A88-40785
NASS-28767	p 31	A88-32948
	p 63	A88-44650
NASS-28769	p 50	N88-24126
NASS-29079	p 48	N88-22447
NAS7-918	p 75	N88-23932
NCA2-13B	p 3	A88-37415
NERC-F60/G6/12	p 58	A88-39095
	p 7	A88-41998
	p 11	A88-44117
NERC-GR/3/5096	p 58	A88-37421
NGL-17-004-024	p 23	N88-24101
NGT-17-002-801	p 3	A88-37418
NGT-21-002-822	p 45	A88-42448
NGT-33-010-801	p 63	A88-44650
NGT5-0103	p 36	N88-20754
NOAA-NA-80AAD00120	p 44	A88-42444
NOAA-NA-81AAD00095	p 54	A88-44120
NOAA-NA-84AAD00065	p 52	A88-41957
NOAA-NA-84AAD00079	p 54	A88-44120
NOAA-NA-85WCC06144	p 42	A88-37720
NSERC-A-5252	p 58	A88-37417
	p 18	A88-39094
NSERC-A-8643	p 58	A88-37417
	p 18	A88-39094
NSF ATM-84-14181	p 4	A88-41055
NSF ATM-84-21396	p 43	A88-39746
NSF ATM-86-16662	p 4	A88-41055
NSF EAR-83-06349	p 24	A88-38024
NSF EAR-86-10036	p 24	A88-35156
NSF OCE-76-21280	p 45	A88-42448
NSF OCE-78-19813	p 45	A88-42448
NSF OCE-80-24130	p 45	A88-42448
NSF OCE-81-09928	p 51	A88-37414
NSF OCE-81-17002	p 45	A88-42448
NSF OCE-82-14791	p 47	N88-20800
NSF OCE-82-19588	p 45	A88-42448
NSF OCE-83-10407	p 51	A88-37414
NSF OCE-84-17909	p 45	A88-42448
NSF OCE-85-01955	p 45	A88-42448
NSF OCE-86-09526	p 44	A88-41257
NSG-5265	p 25	N88-20713
N00014-81-C-0062	p 41	A88-36843
N00014-85-K-0124	p 75	N88-22449
N00014-86-C-0135	p 49	N88-22508
N00014-86-K-0752	p 47	N88-20800
N00014-87-C-0173	p 50	N88-24129
N00014-87-K-0177	p 42	A88-39079
N0014-85-F-031	p 40	A88-36841
USGS-14-08-0001-22521	p 73	A88-41956

CONTRACT

REPORT NUMBER INDEX

Typical Report Number Index Listing

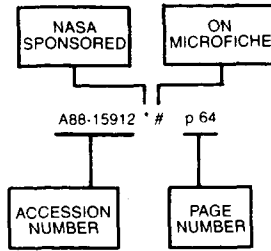


Listings in this index are arranged alphanumerically by report number. The page number indicates the page on which the citation is located. The accession number denotes the number by which the citation is identified. An asterisk (*) indicates that the item is a NASA report. A pound sign (#) indicates that the item is available on microfiche.

NASA-CR-180577	p 40	N88-10431 #	ETN-88-91560	p 66	N88-23309 #	PNL-SA-15557	p 49	N88-22504 #
			ETN-88-91841	p 48	N88-21575 #			
			ETN-88-92030	p 48	N88-22267 #	REPT-375	p 25	N88-20713 * #
			ETN-88-92032	p 48	N88-21625 #	REPT-88B0061	p 47	N88-20780 * #
			ETN-88-92108	p 55	N88-22466 #	REPT-88B0107	p 47	N88-20714 * #
			ETN-88-92201	p 68	N88-24102 #			
			ETN-88-92209	p 49	N88-23358 #	SAIC-87/1869	p 50	N88-24129 #
			ETN-88-92386	p 25	N88-23279 #			
			ETN-88-92418	p 23	N88-24104 #	SER-A-WISS-ABHANDL-84	p 49	N88-23357
			ETN-88-92419	p 76	N88-24105 #			
			ETN-88-92474	p 24	N88-25020 #	WCP-139	p 49	N88-23358 #
						WHOI-87-50	p 49	N88-22508 #
FOA-C-20677-2.7	p 68	N88-24102 #				WMO/TD-192	p 49	N88-23358 #
GWWS-405	p 55	N88-23303 #						
			IAF PAPER 86-76	p 59	A88-41298			
			INPE-4011-TDL/240	p 21	N88-22456 #			
			INPE-4189-PRE/1076	p 64	N88-20712 #			
			INPE-4294-PRE/1165	p 75	N88-20715 #			
			INPE-4456-PRE/1287	p 22	N88-22833 #			
			INPE-4459-PRE/1238	p 21	N88-22453 #			
			INPE-4461-TDL/318	p 13	N88-23315 #			
			INPE-4479-RPE/562	p 22	N88-23693 #			
			INPE-4480-PRE/1246	p 22	N88-23692 #			
			INPE-4491-PRE/1255	p 65	N88-22454 #			
			INPE-4493-PRE/1257	p 65	N88-22485 #			
			INPE-4500-RPE/563	p 55	N88-22455 #			
			INPE-4503-TDL/326	p 13	N88-23322 #			
			ISSN-0347-3694	p 68	N88-24102 #			
			ISSN-0469-4244	p 25	N88-23279 #			
			JPL-PUBL-88-2	p 75	N88-23932 * #			
			NAS 1.15:100694	p 47	N88-20780 * #			
			NAS 1.15:100983	p 18	N88-25134 * #			
			NAS 1.15:101178	p 23	N88-24844 * #			
			NAS 1.26:180755	p 48	N88-22447 * #			
			NAS 1.26:181388	p 25	N88-20713 * #			
			NAS 1.26:182610	p 13	N88-22452 * #			
			NAS 1.26:182677	p 12	N88-20711 * #			
			NAS 1.26:182709	p 36	N88-20754 * #			
			NAS 1.26:182718	p 37	N88-22847 * #			
			NAS 1.26:182755	p 75	N88-21584 * #			
			NAS 1.26:182799	p 23	N88-24101 * #			
			NAS 1.26:182802	p 50	N88-24126 * #			
			NAS 1.26:182923	p 75	N88-23932 * #			
			NAS 1.26:182926	p 18	N88-24109 * #			
			NAS 1.61:1201	p 47	N88-20714 * #			
			NASA-CR-180755	p 48	N88-22447 * #			
			NASA-CR-181388	p 25	N88-20713 * #			
			NASA-CR-182610	p 13	N88-22452 * #			
			NASA-CR-182677	p 12	N88-20711 * #			
			NASA-CR-182709	p 36	N88-20754 * #			
			NASA-CR-182718	p 37	N88-22847 * #			
			NASA-CR-182755	p 75	N88-21584 * #			
			NASA-CR-182799	p 23	N88-24101 * #			
			NASA-CR-182802	p 50	N88-24126 * #			
			NASA-CR-182923	p 75	N88-23932 * #			
			NASA-CR-182926	p 18	N88-24109 * #			
			NASA-RP-1201	p 47	N88-20714 * #			
			NASA-TM-100694	p 47	N88-20780 * #			
			NASA-TM-100983	p 18	N88-25134 * #			
			NASA-TM-101178	p 23	N88-24844 * #			
			NLR-TR-86104-L	p 65	N88-23304 #			
			NLR-TR-87055-L	p 66	N88-23309 #			
			NOAA-TM-NMFS-SWFC-106	p 55	N88-23359 #			
			NPS-68-88-001	p 49	N88-22506 #			
			NWRA-CR-R019	p 64	N88-22450 #			
			NWRA-CR-87-R016	p 65	N88-22451 #			
			PB88-146857	p 12	N88-22448 #			
			PB88-173240	p 55	N88-23359 #			
AAS PAPER 86-288	p 40	A88-35153						
AAS PAPER 86-289	p 69	A88-35154						
AAS PAPER 86-299	p 69	A88-35155						
AAS PAPER 86-306	p 39	A88-35058						
AAS PAPER 86-307	p 24	A88-35156 *						
AAS PAPER 86-398	p 70	A88-35159 *						
AAS PAPER 86-400	p 32	A88-35160						
AAS PAPER 86-401	p 2	A88-35161						
AAS PAPER 86-426	p 70	A88-35162						
ACARS-123187	p 13	N88-22452 * #						
AD-A189868	p 49	N88-22506 #						
AD-A189948	p 49	N88-22508 #						
AD-A190385	p 75	N88-22449 #						
AD-A190462	p 64	N88-22450 #						
AD-A190466	p 65	N88-22451 #						
AD-A191163	p 50	N88-24129 #						
AD-A191172	p 57	N88-25018 #						
AD-E801598	p 75	N88-22449 #						
AFGL-TR-87-0270	p 64	N88-22450 #						
AFGL-TR-87-0271	p 65	N88-22451 #						
AI-M-994	p 75	N88-22449 #						
BCRS-86-02	p 65	N88-23300 #						
BCRS-86-04	p 75	N88-23301 #						
BCRS-86-05	p 65	N88-23302 #						
BCRS-86-06	p 55	N88-23303 #						
BCRS-87-01	p 65	N88-23304 #						
BCRS-87-11	p 66	N88-23309 #						
BIO-1	p 18	N88-25134 * #						
B8735129	p 23	N88-24104 #						
B8735130	p 76	N88-24105 #						
CNES-CT/DRT/TIT/RL-143-T	p 48	N88-22267 #						
CONF-8707147-SUMM	p 49	N88-22504 #						
CRREL-SR-88-1	p 57	N88-25018 #						
DE88-005530	p 49	N88-22504 #						
EPA-600/D-87-366	p 12	N88-22448 #						
ETN-88-91470	p 49	N88-23357						
ETN-88-91549	p 65	N88-23300 #						
ETN-88-91551	p 75	N88-23301 #						
ETN-88-91552	p 65	N88-23302 #						
ETN-88-91553	p 55	N88-23303 #						
ETN-88-91554	p 65	N88-23304 #						

ACCESSION NUMBER INDEX

Typical Accession Number Index Listing



Listings in this index are arranged alphanumerically by accession number. The page number listed to the right indicates the page on which the citation is located. An asterisk (*) indicates that the item is a NASA report. A pound sign (#) indicates that the item is available on microfiche.

A88-29286	p 68	A88-32953	# p 31	A88-41948	p 4	A88-42036	p 35
A88-32831	* p 25	A88-32954	# p 31	A88-41949	* p 52	A88-42037	p 61
A88-32850	p 68	A88-32956	# p 31	A88-41950	p 52	A88-42038	p 52
A88-32901	p 26	A88-32957	# p 32	A88-41951	* p 5	A88-42039	p 44
A88-32902	# p 26	A88-33150	p 68	A88-41952	* p 5	A88-42040	p 52
A88-32903	# p 26	A88-33377	p 57	A88-41954	p 5	A88-42041	p 52
A88-32904	# p 26	A88-33416	* p 69	A88-41955	* p 33	A88-42042	p 53
A88-32905	* p 26	A88-33429	* p 69	A88-41956	p 73	A88-42043	p 53
A88-32906	* # p 26	A88-33694	p 39	A88-41957	p 52	A88-42044	p 53
A88-32907	# p 27	A88-33695	p 39	A88-41958	p 59	A88-42045	p 53
A88-32908	# p 27	A88-33742	* p 69	A88-41961	p 18	A88-42046	p 53
A88-32909	* # p 1	A88-33770	* p 18	A88-41962	p 59	A88-42047	p 44
A88-32910	* # p 1	A88-33774	p 57	A88-41963	p 5	A88-42048	* p 53
A88-32911	# p 1	A88-33832	p 69	A88-41964	p 59	A88-42049	p 35
A88-32912	# p 27	A88-33872	p 69	A88-41965	p 59	A88-42050	p 44
A88-32913	# p 27	A88-33920	p 39	A88-41966	p 60	A88-42051	p 53
A88-32914	# p 27	A88-34643	# p 39	A88-41967	p 60	A88-42052	p 61
A88-32915	* # p 27	A88-34674	p 50	A88-41968	p 60	A88-42053	p 54
A88-32916	# p 27	A88-35058	p 39	A88-41969	p 25	A88-42054	p 61
A88-32917	* # p 27	A88-35153	p 40	A88-41970	p 60	A88-42055	p 62
A88-32918	# p 28	A88-35154	p 69	A88-41971	p 5	A88-42056	p 20
A88-32919	* # p 77	A88-35155	p 69	A88-41972	p 19	A88-42057	p 20
A88-32920	# p 28	A88-35156	* p 24	A88-41973	p 60	A88-42058	* p 20
A88-32921	# p 1	A88-35159	* p 70	A88-41974	p 60	A88-42059	p 20
A88-32922	# p 28	A88-35160	p 32	A88-41975	p 33	A88-42060	p 9
A88-32923	# p 28	A88-35161	p 2	A88-41976	p 73	A88-42061	p 9
A88-32924	# p 28	A88-35162	p 70	A88-41978	p 33	A88-42062	p 20
A88-32925	# p 28	A88-35192	p 32	A88-41979	p 33	A88-42063	p 20
A88-32926	# p 28	A88-35193	p 32	A88-41980	p 33	A88-42064	p 21
A88-32927	* # p 29	A88-35194	* p 2	A88-41981	p 60	A88-42065	p 21
A88-32928	# p 1	A88-35195	p 2	A88-41982	p 61	A88-42068	* p 35
A88-32929	# p 29	A88-35196	p 50	A88-41983	p 33	A88-42069	p 21
A88-32930	# p 1	A88-35198	* p 50	A88-41984	p 5	A88-42070	p 21
A88-32931	# p 29	A88-35199	* p 40	A88-41985	p 74	A88-42443	p 44
A88-32932	# p 57	A88-35395	p 70	A88-41986	p 6	A88-42444	p 44
A88-32933	# p 57	A88-35396	p 70	A88-41987	p 6	A88-42445	* p 45
A88-32934	# p 29	A88-35397	p 2	A88-41988	p 6	A88-42446	* p 45
A88-32935	# p 1	A88-35398	p 2	A88-41989	p 6	A88-42447	* # p 45
A88-32936	# p 29	A88-35399	p 51	A88-41990	p 74	A88-42448	* # p 45
A88-32937	# p 29	A88-35968	p 70	A88-41991	p 6	A88-42449	p 45
A88-32938	# p 29	A88-35986	p 40	A88-41992	p 33	A88-42450	p 45
A88-32939	# p 29	A88-36159	p 40	A88-41993	p 6	A88-42538	p 10
A88-32940	# p 30	A88-36160	p 40	A88-41994	p 6	A88-42545	p 10
A88-32941	* # p 30	A88-36161	p 32	A88-41995	p 74	A88-42760	p 10
A88-32942	# p 30	A88-36162	p 32	A88-41997	p 6	A88-42771	p 62
A88-32943	# p 57	A88-36163	p 32	A88-41998	p 7	A88-43217	p 46
A88-32944	# p 30	A88-36164	p 2	A88-41999	p 7	A88-43218	p 46
A88-32945	# p 30	A88-36165	p 2	A88-42000	p 19	A88-43220	p 10
A88-32946	# p 30	A88-36166	p 51	A88-42001	p 61	A88-43221	p 10
A88-32947	# p 30	A88-36170	p 3	A88-42002	p 7	A88-43222	p 10
A88-32948	* # p 31	A88-36171	p 58	A88-42003	p 7	A88-43223	p 62
A88-32949	# p 31	A88-36172	p 32	A88-42004	p 7	A88-43224	* p 62
A88-32950	# p 31	A88-36241	* # p 40	A88-42005	p 7	A88-43225	* p 62
A88-32951	* # p 31	A88-36243	# p 18	A88-42006	p 7	A88-43226	p 46
A88-32952	# p 31	A88-36378	p 70	A88-42007	p 8	A88-43227	p 74
				A88-42008	p 8	A88-43664	p 46
				A88-42009	p 8	A88-43665	p 46
				A88-42010	p 8	A88-43666	p 54
				A88-42011	p 8	A88-43669	p 46
				A88-42012	p 8	A88-43670	p 10
				A88-42013	p 9	A88-43671	p 11
				A88-42014	p 9	A88-43672	p 62
				A88-42015	p 9	A88-43673	p 54
				A88-42016	p 61	A88-43835	* p 46
				A88-42017	p 34	A88-43864	p 11
				A88-42018	p 19	A88-44005	* # p 46
				A88-42019	p 34	A88-44116	* # p 11
				A88-42020	p 19	A88-44117	p 11
				A88-42021	p 34	A88-44119	p 11
				A88-42022	p 34	A88-44120	p 54
				A88-42023	p 34	A88-44231	p 74
				A88-42024	p 9	A88-44306	p 74
				A88-42025	p 61	A88-44307	p 11
				A88-42026	p 52	A88-44308	p 11
				A88-42027	p 34	A88-44311	# p 54
				A88-42028	p 34	A88-44319	# p 12
				A88-42029	p 34	A88-44446	p 21
				A88-42030	p 34	A88-44447	p 54
				A88-42031	p 19	A88-44449	p 74
				A88-42032	p 20	A88-44450	p 74
				A88-42033	p 35	A88-44517	p 63
				A88-42034	p 35	A88-44519	p 75
				A88-42035	p 9	A88-44521	p 12
A88-36841	* p 40						
A88-36843	p 41						
A88-37126	p 71						
A88-37127	p 71						
A88-37128	p 58						
A88-37129	p 71						
A88-37130	p 71						
A88-37131	p 58						
A88-37132	p 71						
A88-37136	p 51						
A88-37143	p 41						
A88-37144	p 41						
A88-37145	p 71						
A88-37147	p 58						
A88-37148	p 41						
A88-37149	p 41						
A88-37150	p 71						
A88-37270	# p 41						
A88-37279	# p 72						
A88-37286	# p 72						
A88-37287	# p 58						
A88-37336	# p 72						
A88-37370	* p 3						
A88-37383	# p 72						
A88-37384	# p 72						
A88-37391	# p 72						
A88-37414	p 51						
A88-37415	* p 3						
A88-37416	p 72						
A88-37417	p 58						
A88-37418	* p 3						
A88-37421	p 58						
A88-37679	p 41						
A88-37720	p 42						
A88-38023	p 24						
A88-38024	* p 24						
A88-38373	# p 3						
A88-38411	p 72						
A88-38690	* p 42						
A88-38691	* p 42						
A88-38805	* p 3						
A88-38902	p 24						
A88-39078	p 51						
A88-39079	p 42						
A88-39080	p 51						
A88-39081	p 42						
A88-39082	* p 3						
A88-39083	p 42						
A88-39084	p 43						
A88-39085	p 43						
A88-39089	p 51						
A88-39090	p 4						
A88-39094	p 18						
A88-39095	p 58						
A88-39097	p 58						
A88-39098	p 59						
A88-39099	p 59						
A88-39284	* p 43						
A88-39518	# p 24						
A88-39746	# p 43						
A88-39919	p 72						
A88-40059	* p 43						
A88-40351	# p 73						
A88-40352	# p 4						
A88-40353	# p 43						
A88-40355	# p 4						
A88-40356	# p 43						
A88-40688	p 24						
A88-40784	* # p 4						
A88-40785	* # p 73						
A88-40834	p 44						
A88-41028	* # p 4						
A88-41055	p 4						
A88-41093	p 73						
A88-41257	p 44						
A88-41298	p 59						
A88-41398	p 44						
A88-41835	* p 25						
A88-41943	p 73						
A88-41944	p 59						
A88-41945	p 32						
A88-41946	p 51						
A88-41947	* p 4						

A88-44532

A88-44532 # p 63
 A88-44534 # p 63
 A88-44540 # p 63
 A88-44641 * # p 63
 A88-44643 * # p 12
 A88-44644 * # p 12
 A88-44646 * # p 35
 A88-44647 # p 35
 A88-44648 * # p 63
 A88-44649 * # p 63
 A88-44650 * # p 63
 A88-44651 # p 64
 A88-45110 # # p 77
 A88-45115 # p 54
 A88-45116 # p 64
 A88-45118 # p 54
 A88-45634 # p 35
 A88-45635 # p 35
 A88-45636 # p 55
 A88-45637 # p 55
 A88-45638 # p 36
 A88-45639 # p 64
 A88-45640 * # p 64
 A88-45641 # p 36
 A88-45642 # p 36
 A88-45643 # p 55
 A88-45771 # p 36

 N88-20676 # # p 47
 N88-20678 # # p 47
 N88-20711 # # p 12
 N88-20712 # # p 64
 N88-20713 * # # p 25
 N88-20714 * # # p 47
 N88-20715 # # p 75
 N88-20754 * # # p 36
 N88-20780 * # # p 47
 N88-20800 # # p 47
 N88-21087 # # p 77
 N88-21553 # # p 12
 N88-21561 # # p 55
 N88-21567 # # p 47
 N88-21568 # # p 48
 N88-21570 # # p 48
 N88-21571 # # p 48
 N88-21572 # # p 48
 N88-21575 # # p 48
 N88-21584 * # # p 75
 N88-21625 # # p 48
 N88-22267 # # p 48
 N88-22447 * # # p 48
 N88-22448 # # p 12
 N88-22449 # # p 75
 N88-22450 # # p 64
 N88-22451 # # p 65
 N88-22452 * # # p 13
 N88-22453 # # p 21
 N88-22454 # # p 65
 N88-22455 # # p 55
 N88-22456 # # p 21
 N88-22466 # # p 55
 N88-22485 # # p 65
 N88-22504 # # p 49
 N88-22506 # # p 49
 N88-22508 # # p 49
 N88-22833 # # p 22
 N88-22847 * # # p 37
 N88-23279 # # p 25
 N88-23300 # # p 65
 N88-23301 # # p 75
 N88-23302 # # p 65
 N88-23303 # # p 55
 N88-23304 # # p 65
 N88-23309 # # p 66
 N88-23315 # # p 13
 N88-23322 # # p 13
 N88-23357 # # p 49
 N88-23358 # # p 49
 N88-23359 # # p 55
 N88-23692 # # p 22
 N88-23693 # # p 22
 N88-23932 * # # p 75
 N88-24013 # # p 75
 N88-24015 # # p 13
 N88-24016 # # p 13
 N88-24017 # # p 66
 N88-24018 # # p 66
 N88-24019 # # p 66
 N88-24020 # # p 66
 N88-24021 * # # p 37
 N88-24022 # # p 37
 N88-24023 # # p 14
 N88-24024 # # p 49
 N88-24027 # # p 66
 N88-24028 # # p 67
 N88-24029 # # p 76

 N88-24030 # # p 14
 N88-24031 # # p 37
 N88-24032 # # p 56
 N88-24033 # # p 56
 N88-24034 # # p 22
 N88-24035 # # p 76
 N88-24036 # # p 14
 N88-24038 # # p 77
 N88-24041 # # p 14
 N88-24042 # # p 14
 N88-24043 # # p 14
 N88-24044 * # # p 15
 N88-24045 # # p 15
 N88-24046 # # p 15
 N88-24047 # # p 15
 N88-24048 # # p 15
 N88-24049 # # p 15
 N88-24050 # # p 37
 N88-24051 # # p 38
 N88-24052 # # p 38
 N88-24058 # # p 50
 N88-24063 # # p 22
 N88-24064 # # p 67
 N88-24067 # # p 67
 N88-24069 # # p 38
 N88-24070 # # p 67
 N88-24071 # # p 23
 N88-24072 # # p 16
 N88-24074 # # p 23
 N88-24075 # # p 16
 N88-24076 # # p 56
 N88-24077 # # p 56
 N88-24078 # # p 56
 N88-24080 # # p 67
 N88-24081 # # p 67
 N88-24082 # # p 68
 N88-24085 # # p 23
 N88-24086 # # p 16
 N88-24087 # # p 16
 N88-24088 # # p 38
 N88-24089 # # p 16
 N88-24090 # # p 76
 N88-24091 # # p 17
 N88-24092 # # p 17
 N88-24093 # # p 17
 N88-24095 # # p 17
 N88-24096 # # p 17
 N88-24097 # # p 38
 N88-24098 # # p 38
 N88-24100 # # p 39
 N88-24101 * # # p 23
 N88-24102 # # p 68
 N88-24104 # # p 23
 N88-24105 # # p 76
 N88-24109 * # # p 18
 N88-24126 * # # p 50
 N88-24129 # # p 50
 N88-24387 * # # p 76
 N88-24844 * # # p 23
 N88-25018 # # p 57
 N88-25020 # # p 24
 N88-25030 # # p 68
 N88-25038 # # p 68
 N88-25134 * # # p 18

AVAILABILITY OF CITED PUBLICATIONS

IAA ENTRIES (A88-10000 Series)

Publications announced in *IAA* are available from the AIAA Technical Information Service as follows: Paper copies of accessions are available at \$10.00 per document (up to 50 pages), additional pages \$0.25 each. Microfiche⁽¹⁾ of documents announced in *IAA* are available at the rate of \$4.00 per microfiche on demand. Standing order microfiche are available at the rate of \$1.45 per microfiche for *IAA* source documents and \$1.75 per microfiche for AIAA meeting papers.

Minimum air-mail postage to foreign countries is \$2.50. All foreign orders are shipped on payment of pro-forma invoices.

All inquiries and requests should be addressed to: Technical Information Service, American Institute of Aeronautics and Astronautics, 555 West 57th Street, New York, NY 10019. Please refer to the accession number when requesting publications.

STAR ENTRIES (N88-10000 Series)

One or more sources from which a document announced in *STAR* is available to the public is ordinarily given on the last line of the citation. The most commonly indicated sources and their acronyms or abbreviations are listed below. If the publication is available from a source other than those listed, the publisher and his address will be displayed on the availability line or in combination with the corporate source line.

Avail: NTIS. Sold by the National Technical Information Service. Prices for hard copy (HC) and microfiche (MF) are indicated by a price code preceded by the letters HC or MF in the *STAR* citation. Current values for the price codes are given in the tables on NTIS PRICE SCHEDULES.

Documents on microfiche are designated by a pound sign (#) following the accession number. The pound sign is used without regard to the source or quality of the microfiche.

Initially distributed microfiche under the NTIS SRIM (Selected Research in Microfiche) is available at greatly reduced unit prices. For this service and for information concerning subscription to NASA printed reports, consult the NTIS Subscription Section, Springfield, Va. 22161.

NOTE ON ORDERING DOCUMENTS: When ordering NASA publications (those followed by the * symbol), use the N accession number. NASA patent applications (only the specifications are offered) should be ordered by the US-Patent-Appl-SN number. Non-NASA publications (no asterisk) should be ordered by the AD, PB, or other *report number* shown on the last line of the citation, not by the N accession number. It is also advisable to cite the title and other bibliographic identification.

Avail: SOD (or GPO). Sold by the Superintendent of Documents, U.S. Government Printing Office, in hard copy. The current price and order number are given following the availability line. (NTIS will fill microfiche requests, as indicated above, for those documents identified by a # symbol.)

(1) A microfiche is a transparent sheet of film, 105 by 148 mm in size containing as many as 60 to 98 pages of information reduced to micro images (not to exceed 26.1 reduction).

- Avail: BLL (formerly NLL): British Library Lending Division, Boston Spa, Wetherby, Yorkshire, England. Photocopies available from this organization at the price shown. (If none is given, inquiry should be addressed to the BLL.)
- Avail: DOE Depository Libraries. Organizations in U.S. cities and abroad that maintain collections of Department of Energy reports, usually in microfiche form, are listed in *Energy Research Abstracts*. Services available from the DOE and its depositories are described in a booklet, *DOE Technical Information Center - Its Functions and Services* (TID-4660), which may be obtained without charge from the DOE Technical Information Center.
- Avail: ESDU. Pricing information on specific data, computer programs, and details on ESDU topic categories can be obtained from ESDU International Ltd. Requesters in North America should use the Virginia address while all other requesters should use the London address, both of which are on the page titled ADDRESSES OF ORGANIZATIONS.
- Avail: Fachinformationszentrum, Karlsruhe. Sold by the Fachinformationszentrum Energie, Physik, Mathematik GMBH, Eggenstein Leopoldshafen, Federal Republic of Germany, at the price shown in deutschmarks (DM).
- Avail: HMSO. Publications of Her Majesty's Stationery Office are sold in the U.S. by Pendragon House, Inc. (PHI), Redwood City, California. The U.S. price (including a service and mailing charge) is given, or a conversion table may be obtained from PHI.
- Avail: NASA Public Document Rooms. Documents so indicated may be examined at or purchased from the National Aeronautics and Space Administration, Public Documents Room (Room 126), 600 Independence Ave., S.W., Washington, D.C. 20546, or public document rooms located at each of the NASA research centers, the NASA Space Technology Laboratories, and the NASA Pasadena Office at the Jet Propulsion Laboratory.
- Avail: Univ. Microfilms. Documents so indicated are dissertations selected from *Dissertation Abstracts* and are sold by University Microfilms as xerographic copy (HC) and microfilm. All requests should cite the author and the Order Number as they appear in the citation.
- Avail: US Patent and Trademark Office. Sold by Commissioner of Patents and Trademarks, U.S. Patent and Trademark Office, at the standard price of \$1.50 each, postage free. (See discussion of NASA patents and patent applications below.)
- Avail: (US Sales Only). These foreign documents are available to users within the United States from the National Technical Information Service (NTIS). They are available to users outside the United States through the International Nuclear Information Service (INIS) representative in their country, or by applying directly to the issuing organization.
- Avail: USGS. Originals of many reports from the U.S. Geological Survey, which may contain color illustrations, or otherwise may not have the quality of illustrations preserved in the microfiche or facsimile reproduction, may be examined by the public at the libraries of the USGS field offices whose addresses are listed in this Introduction. The libraries may be queried concerning the availability of specific documents and the possible utilization of local copying services, such as color reproduction.
- Avail: Issuing Activity, or Corporate Author, or no indication of availability. Inquiries as to the availability of these documents should be addressed to the organization shown in the citation as the corporate author of the document.

PUBLIC COLLECTIONS OF NASA DOCUMENTS

DOMESTIC: NASA and NASA-sponsored documents and a large number of aerospace publications are available to the public for reference purposes at the library maintained by the American Institute of Aeronautics and Astronautics, Technical Information Service, 555 West 57th Street, 12th Floor, New York, New York 10019.

EUROPEAN: An extensive collection of NASA and NASA-sponsored publications is maintained by the British Library Lending Division, Boston Spa, Wetherby, Yorkshire, England for public access. The British Library Lending Division also has available many of the non-NASA publications cited in *STAR*. European requesters may purchase facsimile copy or microfiche of NASA and NASA-sponsored documents, those identified by both the symbols # and • from ESA – Information Retrieval Service European Space Agency, 8-10 rue Mario-Nikis, 75738 CEDEX 15, France.

FEDERAL DEPOSITORY LIBRARY PROGRAM

In order to provide the general public with greater access to U.S. Government publications, Congress established the Federal Depository Library Program under the Government Printing Office (GPO), with 50 regional depositories responsible for permanent retention of material, inter-library loan, and reference services. At least one copy of nearly every NASA and NASA-sponsored publication, either in printed or microfiche format, is received and retained by the 50 regional depositories. A list of the regional GPO libraries, arranged alphabetically by state, appears on the inside back cover. These libraries are *not* sales outlets. A local library can contact a Regional Depository to help locate specific reports, or direct contact may be made by an individual.

STANDING ORDER SUBSCRIPTIONS

NASA SP-7041 and its supplements are available from the National Technical Information Service (NTIS) on standing order subscription as PB 88-903800 at the price of \$15.50 domestic and \$31.00 foreign. Standing order subscriptions do not terminate at the end of a year, as do regular subscriptions, but continue indefinitely unless specifically terminated by the subscriber.

ADDRESSES OF ORGANIZATIONS

American Institute of Aeronautics and
Astronautics
Technical Information Service
555 West 57th Street, 12th Floor
New York, New York 10019

British Library Lending Division,
Boston Spa, Wetherby, Yorkshire,
England

Commissioner of Patents and
Trademarks
U.S. Patent and Trademark Office
Washington, D.C. 20231

Department of Energy
Technical Information Center
P.O. Box 62
Oak Ridge, Tennessee 37830

ESA-Information Retrieval Service
ESRIN
Via Galileo Galilei
00044 Frascati (Rome) Italy

ESDU International, Ltd.
1495 Chain Bridge Road
McLean, Virginia 22101

ESDU International, Ltd.
251-259 Regent Street
London, W1R 7AD, England

Fachinformationszentrum Energie, Physik,
Mathematik GMBH
7514 Eggenstein Leopoldshafen
Federal Republic of Germany

Her Majesty's Stationery Office
P.O. Box 569, S.E. 1
London, England

NASA Scientific and Technical Information
Facility
P.O. Box 8757
B.W.I. Airport, Maryland 21240

National Aeronautics and Space
Administration
Scientific and Technical Information
Division (NTT-1)
Washington, D.C. 20546

National Technical Information Service
5285 Port Royal Road
Springfield, Virginia 22161

Pendragon House, Inc.
899 Broadway Avenue
Redwood City, California 94063

Superintendent of Documents
U.S. Government Printing Office
Washington, D.C. 20402

University Microfilms
A Xerox Company
300 North Zeeb Road
Ann Arbor, Michigan 48106

University Microfilms, Ltd.
Tylers Green
Londorf, England

U.S. Geological Survey Library
National Center - MS 950
12201 Sunrise Valley Drive
Reston, Virginia 22092

U.S. Geological Survey Library
2255 North Gemini Drive
Flagstaff, Arizona 86001

U.S. Geological Survey
345 Middlefield Road
Menlo Park, California 94025

U.S. Geological Survey Library
Box 25046
Denver Federal Center, MS914
Denver, Colorado 80225

NTIS PRICE SCHEDULES

(Effective January 1, 1988)

Schedule A STANDARD PRICE DOCUMENTS AND MICROFICHE

PRICE CODE	NORTH AMERICAN PRICE	FOREIGN PRICE
A01	\$ 6.95	\$13.90
A02	9.95	19.90
A03	12.95	25.90
A04-A05	14.95	29.90
A06-A09	19.95	39.90
A10-A13	25.95	51.90
A14-A17	32.95	65.90
A18-A21	38.95	77.90
A22-A25	44.95	89.90
A99	*	*
NO1	49.50	89.90
NO2	48.00	80.00

Schedule E EXCEPTION PRICE DOCUMENTS AND MICROFICHE

PRICE CODE	NORTH AMERICAN PRICE	FOREIGN PRICE
E01	\$ 8.50	17.00
E02	11.00	22.00
E03	12.00	24.00
E04	14.50	29.00
E05	16.50	33.00
E06	19.00	38.00
E07	21.50	43.00
E08	24.00	48.00
E09	26.50	53.00
E10	29.00	58.00
E11	31.50	63.00
E12	34.00	68.00
E13	36.50	73.00
E14	39.50	79.00
E15	43.00	86.00
E16	47.00	94.00
E17	51.00	102.00
E18	55.00	110.00
E19	61.00	122.00
E20	71.00	142.00
E99	*	*

* Contact NTIS for price quote.

IMPORTANT NOTICE

NTIS Shipping and Handling Charges

U.S., Canada, Mexico — ADD \$3.00 per TOTAL ORDER

All Other Countries — ADD \$4.00 per TOTAL ORDER

Exceptions — Does NOT apply to:

ORDERS REQUESTING NTIS RUSH HANDLING
ORDERS FOR SUBSCRIPTION OR STANDING ORDER PRODUCTS ONLY

NOTE: Each additional delivery address on an order
requires a separate shipping and handling charge.

1. Report No. NASA SP-7041 (59)	2. Government Accession No.	3. Recipient's Catalog No.	
4. Title and Subtitle EARTH RESOURCES A Continuing Bibliography with Indexes (Issue 59)		5. Report Date November, 1988	
		6. Performing Organization Code	
7. Author(s)		8. Performing Organization Report No.	
		10. Work Unit No.	
9. Performing Organization Name and Address National Aeronautics and Space Administration Washington, DC 20546		11. Contract or Grant No.	
		13. Type of Report and Period Covered	
12. Sponsoring Agency Name and Address		14. Sponsoring Agency Code	
15. Supplementary Notes			
16. Abstract This bibliography lists 518 reports, articles and other documents introduced into the NASA scientific and technical information system between July 1 and September 30, 1988. Emphasis is placed on the use of remote sensing and geophysical instrumentation in spacecraft and aircraft to survey and inventory natural resources and urban areas. Subject matter is grouped according to agriculture and forestry, environmental changes and cultural resources, geodesy and cartography, geology and mineral resources, hydrology and water management, data processing and distribution systems, instrumentation and sensors, and economic analysis.			
17. Key Words (Suggested by Author(s)) Bibliographies Earth Resources Remote Sensors		18. Distribution Statement Unclassified - Unlimited	
19. Security Classif. (of this report) Unclassified	20. Security Classif. (of this page) Unclassified	21. No. of Pages 146	22. Price * A07/HC

FEDERAL REGIONAL DEPOSITORY LIBRARIES

ALABAMA

AUBURN UNIV. AT MONTGOMERY LIBRARY
Documents Department
Montgomery, AL 36193
(205) 271-9650

UNIV. OF ALABAMA LIBRARY
Documents Dept.-Box S
University, AL 35486
(205) 348-6046

ARIZONA

DEPT. OF LIBRARY, ARCHIVES AND PUBLIC RECORDS
Third Floor—State Cap.
1700 West Washington
Phoenix, AZ 85007
(602) 255-4121

UNIVERSITY OF ARIZONA LIB.
Government Documents Dept.
Tucson, AZ 85721
(602) 621-6433

ARKANSAS

ARKANSAS STATE LIBRARY
One Capitol Mall
Little Rock, AR 72201
(501) 371-2326

CALIFORNIA

CALIFORNIA STATE LIBRARY
Govt. Publications Section
P.O. Box 2037
Sacramento, CA 95809
(916) 324-4863

COLORADO

UNIV OF COLORADO LIB.
Government Pub. Division
Campus Box 184
Boulder, CO 80309
(303) 492-8834

DENVER PUBLIC LIBRARY

Govt. Pub. Department
1357 Broadway
Denver, CO 80203
(303) 571-2131

CONNECTICUT

CONNECTICUT STATE LIBRARY
Government Documents Unit
231 Capitol Avenue
Hartford, CT 06106
(203) 566-7029

FLORIDA

UNIV. OF FLORIDA LIBRARIES
Library West
Documents Department
Gainesville, FL 32611
(904) 392-0367

GEORGIA

UNIV. OF GEORGIA LIBRARIES
Government Reference Dept.
Athens, GA 30602
(404) 542-8949

HAWAII

UNIV. OF HAWAII LIBRARY
Govt. Documents Collection
2550 The Mall
Honolulu, HI 96822
(808) 948-8230

IDAHO

UNIV. OF IDAHO LIBRARY
Documents Section
Moscow, ID 83843
(208) 885-6344

ILLINOIS

ILLINOIS STATE LIBRARY
Information Services Branch
Centennial Building
Springfield, IL 62756
(217) 782-5185

INDIANA

INDIANA STATE LIBRARY
Serials Documents Section
140 North Senate Avenue
Indianapolis, IN 46204
(317) 232-3686

IOWA

UNIV. OF IOWA LIBRARIES
Govt. Documents Department
Iowa City, IA 52242
(319) 353-3318

KANSAS

UNIVERSITY OF KANSAS
Doc. Collect.—Spencer Lib.
Lawrence, KS 66045-2800
(913) 864-4662

KENTUCKY

UNIV. OF KENTUCKY LIBRARIES
Govt. Pub. Department
Lexington, KY 40506-0039
(606) 257-3139

LOUISIANA

LOUISIANA STATE UNIVERSITY
Middleton Library
Govt. Docs. Dept.
Baton Rouge, LA 70803
(504) 388-2570

LOUISIANA TECHNICAL UNIV. LIBRARY

Documents Department
Ruston, LA 71272-0046
(318) 257-4962

MAINE

UNIVERSITY OF MAINE
Raymond H. Fogler Library
Tri-State Regional Documents
Depository
Orono, ME 04469
(207) 581-1680

MARYLAND

UNIVERSITY OF MARYLAND
McKeldin Lib.—Doc. Div.
College Park, MD 20742
(301) 454-3034

MASSACHUSETTS

BOSTON PUBLIC LIBRARY
Government Docs. Dept.
Boston, MA 02117
(617) 536-5400 ext.226

MICHIGAN

DETROIT PUBLIC LIBRARY
Sociology Department
5201 Woodward Avenue
Detroit, MI 48202-4093
(313) 833-1409

MICHIGAN STATE LIBRARY

P.O. Box 30007
Lansing, MI 48909
(517) 373-1593

MINNESOTA

UNIVERSITY OF MINNESOTA
Government Pubs. Division
409 Wilson Library
309 19th Avenue South
Minneapolis, MN 55455
(612) 373-7870

MISSISSIPPI

UNIV. OF MISSISSIPPI LIB.
Documents Department
University, MS 38677
(601) 232-5857

MONTANA

UNIV. OF MONTANA
Mansfield Library
Documents Division
Missoula, MT 59812
(406) 243-6700

NEBRASKA

UNIVERSITY OF NEBRASKA - LINCOLN
Love Library
Documents Department
Lincoln, NE 68588-0410
(402) 472-2562

NEVADA

UNIVERSITY OF NEVADA LIB.
Govt. Pub. Department
Reno, NV 89557-0044
(702) 784-6579

NEW JERSEY

NEWARK PUBLIC LIBRARY
5 Washington Street
Newark, NJ 07101-0630
(201) 733-7812

NEW MEXICO

UNIVERSITY OF NEW MEXICO
Zimmerman Library
Government Pub. Dept.
Albuquerque, NM 87131
(505) 277-5441

NEW MEXICO STATE LIBRARY

Reference Department
325 Don Gaspar Avenue
Santa Fe, NM 87503
(505) 827-3826

NEW YORK

NEW YORK STATE LIBRARY
Empire State Plaza
Albany, NY 12230
(518) 474-5563

NORTH CAROLINA

UNIVERSITY OF NORTH CAROLINA AT CHAPEL HILL
Davis Library
BA/SS Documents Division
Chapel Hill, NC 27515
(919) 962-1151

NORTH DAKOTA

UNIVERSITY OF NORTH DAKOTA
Chester Fritz Library
Documents Department
Grand Forks, ND 58202
(701) 777-4629
In cooperation with North
Dakota State Univ. Library

OHIO

STATE LIBRARY OF OHIO
Documents Department
65 South Front Street
Columbus, OH 43266-0334
(614) 462-7051

OKLAHOMA

OKLAHOMA DEPT. OF LIB.
Government Documents
200 NE 18th Street
Oklahoma City, OK 73105
(405) 521-2502, ext. 252

OKLAHOMA STATE UNIV. LIB.
Documents Department
Stillwater, OK 74078
(405) 624-6546

OREGON

PORTLAND STATE UNIV. LIB.
Documents Department
P.O. Box 1151
Portland, OR 97207
(503) 229-3673

PENNSYLVANIA

STATE LIBRARY OF PENN.
Government Pub. Section
P.O. Box 1601
Harrisburg, PA 17105
(717) 787-3752

TEXAS

TEXAS STATE LIBRARY
Public Services Department
P.O. Box 12927—Cap. Sta.
Austin, TX 78711
(512) 475-2996

TEXAS TECH. UNIV. LIBRARY

Govt. Documents Department
Lubbock, TX 79409
(806) 742-2268

UTAH

UTAH STATE UNIVERSITY
Merrill Library, U.M.C. 30
Logan, UT 84322
(801) 750-2682

VIRGINIA

UNIVERSITY OF VIRGINIA
Alderman Lib.—Public Doc.
Charlottesville, VA 22903-2498
(804) 924-3133

WASHINGTON

WASHINGTON STATE LIBRARY
Documents Section
Olympia, WA 98504
(206) 753-4027

WEST VIRGINIA

WEST VIRGINIA UNIV. LIB.
Documents Department
Morgantown, WV 26506-6069
(304) 293-3640

WISCONSIN

MILWAUKEE PUBLIC LIBRARY
814 West Wisconsin Avenue
Milwaukee, WI 53233
(414) 278-3065

ST. HIST LIB. OF WISCONSIN

Government Pub. Section
816 State Street
Madison, WI 53706
(608) 262-4347

WYOMING

WYOMING STATE LIBRARY
Supreme Ct. & Library Bld.
Cheyenne, WY 82002
(307) 777-5919

National Aeronautics and
Space Administration
Code NTT-4

Washington, D.C.
20546-0001

Official Business
Penalty for Private Use, \$300

SPECIAL FOURTH-CLASS RATE
POSTAGE & FEES PAID
NASA
Permit No. G-27

NASA

**POSTMASTER: If Undeliverable (Section 158
Postal Manual) Do Not Return**
